DEVELOPMENT OF SMALL MOLECULE CREBBP BROMODOMAIN LIGANDS USING MEDICINAL CHEMISTRY-BASED APPROACHES



Thesis submitted for the degree of:

DPhil in Organic Chemistry

Mustafa Moroglu

Keble College, University of Oxford

Supervisor: Prof. Stuart J. Conway



To Anne,

Thank you for your unwavering support.

Department of Chemistry

DECLARATION OF AUTHORSHIP

Name: Mustafa Moroglu **Candidate number: 831360**

College: Keble College **Supervisor: Prof. Stuart Conway**

Title of thesis:

Development of small molecule CREBBP bromodomain ligands using medicinal chemistry-based approaches

I have read and understood the University's disciplinary regulations concerning conduct in examinations and, in particular, the regulations on plagiarism (*The University Student Handbook* Section 8.8; available at https://www.ox.ac.uk/students/academic/student-handbook).	☑
I have read and understood the Education Committee's information and guidance on academic good practice and plagiarism at https://www.ox.ac.uk/students/academic/guidance/skills?wssl=1.	☑
The thesis I am submitting is entirely my own work except where otherwise indicated.	☑
It has not been submitted, either partially or in full, either for this Honour School or qualification or for another Honour School or qualification of this University (except where the Special Regulations for the subject permit this), or for a qualification at any other institution.	☑
I have clearly indicated the presence of all material I have quoted from other sources, including any diagrams, charts, tables or graphs.	☑
I have clearly indicated the presence of all paraphrased material with appropriate references.	☑
I have acknowledged appropriately any assistance I have received in addition to that provided by my supervisor.	☑
I have not copied from the work of any other candidate.	☑
I have not used the services of any agency providing specimen, model or ghostwritten work in the preparation of this thesis. (See also section 2.4 of Statute XI on University Discipline under which members of the University are prohibited from providing material of this nature for candidates in examinations at this University or elsewhere: http://www.admin.ox.ac.uk/statutes/352-051a.shtml).	☑
I agree to retain an electronic copy of this work until the publication of my final examination result, except where submission in hand-written format is permitted.	☑
I agree to make any such electronic copy available to the examiners should it be necessary to confirm my word count or to check for plagiarism.	☑

Candidate's signature: …….. Date: ……..

Development of small molecule CREBBP bromodomain ligands using medicinal chemistry-based approaches

Lysine acetylation is a post-translational modification that is recognised by epigenetic "reader" modules known as bromodomains. These proteins play important roles in many cellular processes, and the development of selective bromodomain ligands has been of recent clinical interest. Of the 46 human bromodomain-containing proteins, much research has focused on the BET family. Consequently, there have been remarkably few selective ligands reported for the remaining bromodomain families, despite their involvement in many fundamental biological processes.

The Conway group were the first to report ligands with sub-micromolar affinity for the CREBBP bromodomain. However, these ligands showed only moderate selectivity over the BET family of bromodomains. This work explores medicinal chemistry-based approaches to develop CREBBP bromodomain ligands, using protein-ligand X-ray crystallography to enable structure-guided drug design. Here, we report the improvement of affinity and selectivity for the previously reported inhibitor **(*R*)11** through; (i) bioisosteric modifications to remove unfavourable enthalpic contributions to binding; and (ii) macrocyclic drug design to favour the CREBBP bromodomain binding mode. These improved ligands were also incorporated into (iii) PROTACs to develop full-length CREBBP degraders as a proof-of-concept for this target. In collaboration with Prof. Dario Neri's group (ETH Zurich), we use (iv) DNA-encoded chemical library technology to identify novel CREBBP bromodomain fragments and scaffolds. This work has provided valuable insight in the development of selective inhibitors for the CREBBP bromodomain and sets the foundations for applying new technologies to identify novel inhibitors and degraders for this target protein.

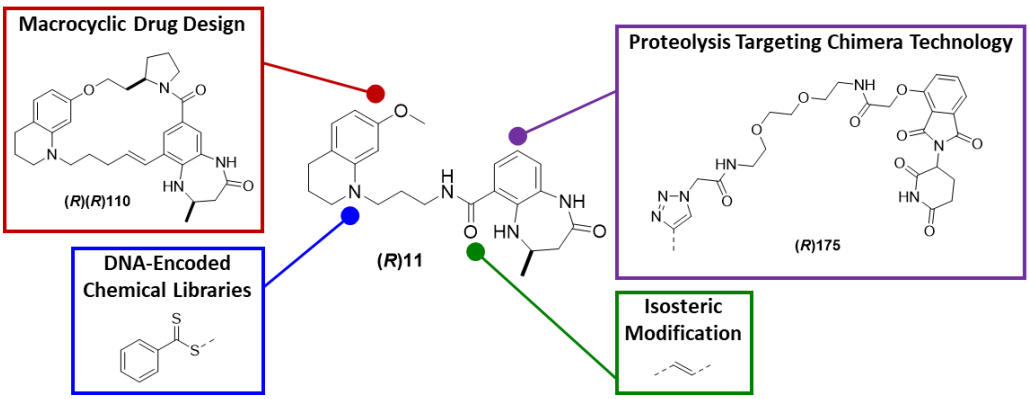


Figure 1 Medicinal chemistry-based approaches used to develop previously reported CREBBP ligand **(*R*)11**.

Table of Contents

Abstract ..... **v**

Acknowledgements ..... **xi**

Abbreviations ..... **xiv**

Chapter 1: Introduction **1**

1.1 Epigenetics **2**

1.1.1 Chromatin structure and Post-translational modifications 2

1.1.2 Histone writers, erasers and readers 3

1.1.3 Epigenetic drugs 4

1.2 Bromodomains **5**

1.2.1 Bromodomain structure 6

1.2.2 Bromodomains as drug targets 7

1.3 CREBBP bromodomain **8**

1.3.1 CREBBP and EP300 8

1.3.2 CREBBP bromodomain structure 10

1.3.3 CREBBP bromodomain ligands 11

1.4 Recent medicinal chemistry-based approaches for small molecule drug discovery **14**

1.4.1 Macrocyclic drug design 14

1.4.1.1 Improvement of affinity and selectivity 15

1.4.1.2 Modulation of physicochemical properties 17

1.4.1.3 Conformational analysis for macrocyclic drug design 18

1.4.2 Small molecule PROTAC technology 21

1.4.2.1 Early PROTAC publications 22

1.4.2.2 PROTAC degradation of BET proteins 23

1.4.3 DNA-encoded chemical libraries 26

1.4.3.1 Types of DNA-encoded chemical libraries 26

1.4.3.2 Ligand discovery using DNA-encoded chemical libraries 28

1.5 Project aim **30**

Chapter 2: Amide bioisosteres to improve CREBBP bromodomain affinity and selectivity **31**

2.1 Introduction and aims **32**

2.2 Synthesis of amide bioisosteric analogues **33**

2.3 Biological evaluation of the bioisosteric analogues **35**

2.3.1 Intramolecular hydrogen bond analysis by ^{1}H NMR 35

2.3.2 Affinity data for CREBBP bromodomain 36

2.3.3 Selectivity data against BRD4(1) bromodomain 37

2.3.4 X-ray crystallography of ligand (*R*)48 39

2.3.5 *In vitro* cell data for ligand (*R*)48 41

2.4 Conclusion **42**

Chapter 3: Macrocycles as CREBBP bromodomain ligands – first generation **43**

3.1 Introduction and aims **44**

3.2 Computational design **46**

3.2.1 Macrocycle library design 46

3.2.2 Molecular docking of the macrocycle library 47

3.3 Synthesis of target macrocycles **49**

3.3.1 Synthetic strategy: Ring closing metathesis macrocyclisation 49

3.3.1.1 Retrosynthetic Analysis 49

*3.3.1.2 Synthesis of fragment **61*** 49

*3.3.1.3 Synthesis of THBD fragment **(R)62*** 50

*3.3.1.4 Synthesis of THBD fragment **(R)63*** 51

*3.3.1.5 Synthesis of macrocycle **(R)60*** 52

3.3.2 Synthetic strategy: S_N2 macrocyclisation 55

3.3.2.1 Retrosynthetic Analysis 55

*3.3.2.2 Synthesis of fragment **78*** 55

*3.3.2.3 Synthesis of THBD fragment **(R)79*** 56

*3.3.2.4 Synthesis of macrocycle **(R)77*** 56

3.4 Synthesis of acyclic analogue of (*R*)96 ..... **59**

3.5 Biophysical evaluation of CREBBP bromodomain binding affinity **60**

3.6 Conclusion **61**

Chapter 4: Macrocycles as CREBBP bromodomain ligands – second generation **63**

4.1 Introduction and aims **64**

4.2 Synthesis-led design of macrocycle series **66**

4.3 Computational analysis of the macrocycle series **67**

4.3.1 BRD4(1) macrocycle 22 69

4.3.2 Acyclic CREBBP bromodomain ligands 71

4.3.3 Macrocycle series 1 – Aliphatic linker 73

4.3.4 Macrocycle series 2 – Triazole linker 75

4.3.5 Macrocycle series 3 – Amide linker 77

4.4 Synthesis of the macrocycle series **79**

4.4.1 Late-stage intermediate 116 80

4.4.2 Macrocycle series 1 81

*4.4.2.1 Macrocycle **(R)104** – S_N2 displacement macrocyclisation* 81

*4.4.2.2 Macrocycle **(R)105** – S_N2 displacement macrocyclisation* 83

4.4.3 Macrocycle series 2 85

*4.4.3.1 Macrocycle **(R)106** – S_N2 displacement macrocyclisation* 85

*4.4.3.2 Macrocycle **(R)106** – Ru-catalysed azide-alkyne cycloaddition macrocyclisation* 87

*4.4.3.3 Macrocycle **(R)107** – Cu-catalysed azide-alkyne cycloaddition macrocyclisation* 88

4.4.4 Macrocycle series 3 89

*4.4.4.1 Macrocycle **(R)108** – Macrolactamisation* 89

*4.4.4.2 Macrocycle **(R)109** – Macrolactamisation* 90

*4.4.4.3 Macrocycle **(R)(R)110** – Macrolactamisation* 90

4.4.5 Acyclic analogues of macrocycle series 92

4.5 Biophysical evaluation of the macrocycle series **94**

4.5.1 CREBBP bromodomain binding affinity 94

4.5.2 BRD4(1) binding affinity 98

4.5.3 Conformational analysis 100

4.5.3.1 Small molecule X-ray crystal structures 100

4.5.3.2 ^{1}H NMR of macrocycle series 3 101

4.6 Conclusion **103**

Chapter 5: Development of PROTACs for the degradation of CREBBP **105**

5.1 Introduction and aims **106**

5.2 PROTAC drug-design **107**

5.3 CREBBP bromodomain SAR for linker attachment **109**

5.3.1 Syntheses of CREBBP bromodomain ligands 109
5.3.2 CREBBP bromodomain binding affinity 111
5.4 PROTAC approach using ligand (*R*)160 ..... **113**
5.4.1 Synthetic preparation of CREBBP PROTACs 113
5.4.2 CREBBP bromodomain binding affinity 115
5.5 Conclusion **116**
Chapter 6: Use of an ESAC library to identify novel CREBBP bromodomain ligands **117**
6.1 Introduction and aims **118**
6.2 Binding affinity of fragment pairs using known CREBBP bromodomain ligands **119**
6.2.1 Syntheses of fragment pairs 120
6.2.2 CREBBP bromodomain binding affinities 122
6.3 ESAC library screening against the CREBBP bromodomain **124**
6.3.1 Fragment hit identification using ESAC library 124
6.3.2 CREBBP bromodomain binding affinity 126
6.4 Affinity determination of 'off-LNA' CREBBP bromodomain ligands **127**
6.4.1 Synthesis of 'off-LNA' CREBBP bromodomain ligands 127
6.4.2 CREBBP bromodomain binding affinity 128
6.5 Investigation of alternative THBD fragments **129**
6.5.1 Synthesis of THBD fragments (*R*)202 and (*S*)202 129
6.5.2 CREBBP bromodomain binding affinity 130
6.6 Conclusion **131**
Chapter 7: Conclusions and future work **133**
7.1 Conclusions **134**
7.2 Future work **136**
Chapter 8: Experimental Section **137**
8.1 General Experimental **138**
8.1.1 Computational methods 138
8.1.2 Biochemical and biophysical methods 138
8.1.3 Synthetic methods 141
8.2 Procedures **144**

8.2.1 Chapter 2 - Amide bioisosteres 144
8.2.2 Chapter 3 - First Generation Macrocycles 149
8.2.3 Chapter 4 - Second Generation Macrocycles 170
8.2.4 Chapter 6 - ESAC Library 214

References 225

Appendices 232

Acknowledgements

I would like to start by thanking my supervisor Prof. Stuart J. Conway – I have thoroughly enjoyed my DPhil project and this is credit to the support and guidance you have provided me throughout (**Figure 2**). It has been a real pleasure to work for you and I wish the group great success for the future. To my industrial mentors Dr Matthew Selby, Dr James Reuberson and Dr Will Pitt, thanks for arranging my placement to UCB, I gained a lot from our discussions over the course of the DPhil.

I would like to also thank everyone I have collaborated with during my DPhil. Prof. Panagis Filippakopoulos and Dr Sarah Picaud (Structural Genomics Consortium) who have provided me with protein X-ray crystal structures, which was very helpful for the progress of my project. Prof. Ester Hammond and Dr Ania Skwarska for their contributions toward the CREBBP biological data. Prof. Dario Neri and Marco Catalano (ETH Zurich) for screening their DNA-encoded library against the CREBBP bromodomain. Dr James Clayton, Dr Matthias Schiedel, Corentine Laurin, Joseph Bluck, Margarida Espadinha and Katrina Andrews (University of Oxford) for their contributions towards the respective projects discussed in this thesis. Dr David Staunton for his advice and training on ITC. Prof. Timothy Claridge, Dr Nader Amin and the NMR stuff for their helpful discussions and excellent service. Dr Kirsten Christensen for acquiring my macrocyclic crystal structures. Dr Elisabetta Chiarparin and Dr Rodrigo Carbajo for their helpful discussions on 1D NMR elucidation of macrocyclic conformations in solution. Thank you for your contributions – it has been great working with you all.

Thanks to Prof. Martin Smith and Prof. Darren Dixon, and the associated funding bodies, for providing me a place on the Synthesis for Biology and Medicine CDT. I extend these thanks to my peers from the SBM Cohort 2015.

Throughout my time at Oxford, the Conway group has been a supportive and welcoming environment. This is thanks to the fantastic group members, both past and present. I would like to begin giving thanks to all the great Post-Docs I have worked with during my DPhil. Anthony – thank you for teaching me protein expression and purification. Your dedication to Science is second to none, and your willingness to help everyone in the group was refreshing to see. Lingbing – thank you for letting me share a third of your fumehood when I was on rotation (and for the record, Sue is not my best friend!). Amélie – Thank you for settling my nerves when I first joined the group. I am still waiting for my macrocycle bike t-shirt you promised me! James – thank you for all your contributions to the CREBBP project. You are the human form of Google and always got a good story to tell (…at least about Ann Arbor!). Ewen –

you kept the group running like a well-oiled machine! I loved all our video game chats and thank you for getting me into skateboarding. I'm sure we will have some skating sessions in London soon! Maze – I admire your scientific thinking and I have learnt so much from our discussions. Thanks for showing me Bodrums (the best Kebab place in Oxford) and I'm sure we will watch Tottenham win the Champions League together soon. Debs – Thanks for being an amazing fumehood neighbour! (did you steal my swan neck adaptor?). Please don't suggest pyjamas for my leaving present. Pietro a.k.a. el deficator fantasma(?!) a.k.a. Ferrero Rocher Bandit – thanks for putting on the occasional pyrotechnics display in your fumehood. Remember, eat burgers at Five Fingers and not at Wembley Stadium.

I have had the pleasure to work with some amazing DPhil students. Amy – I've loved every moment working with you! From hearing your lunch time gossip in the Rex Richards building; eating free pizza from the DTC; getting you a fake potato; not sharing the Champagne with Nick; beating you at Teddy Hall Relay/Super Mario Party/table football; starting the Gareth Southgate chant in the pub; finding out your initials spell ARS; and so much more! Best of luck for the future and I know we will remain friends for a long time! (I've ran out of Kleenex, so I hope you aren't crying reading this!). Coco – Your drunk speech at St. Hilda's got me to join the group and I am very thankful of that. The Enchufla on Magdalen Bridge will probably remain the best Salsa move I will ever do in my life. Remember, I will still be your friend even if you are bald from your hair catching fire on the Bunsen burner. Please don't leak all the embarrassing photos you have taken of me over the last four years! I wish you all the best for your Post Doc in America! Joe – From sharing a fumehood with you on rotation, to sharing a room at ACS, its been a pleasure to work with you! I still think back to you falling into that lake in Florida!

Thank you to Alex, Michael, Charles and Chris for making me feel welcomed when I first joined the group. Sarah – I enjoyed all our football and running chats, and thanks for helping me get a free Fitbit! See Dr Larissa – Thanks for keeping G12 in shipshape and for sharing your Chiffon cake recipe with me. The G12 mysteries stopped happening since you left, so I think I know who the culprit was. (You still owe me £10.50 for my lab services). Catherine – Our muffin reviews were amazing, even if no one gave two Kefs about it. Send my regards to Georgina and Big Nige. I still don't forgive you for pushing in front of me in Café Baba. Holly – Thanks for telling everyone who joins the group that I am the nicest boy in the Conway group. I REALLY appreciate that. (I'm being sarcastic for the record :p). Jess – A100daysJessandMus. JessandMus100times. JESSANDMUSFOREVERANDEVER100YEARS. www.JessandMusAdventures.com. Remember to drink gout tea everyday, no matter what the FDA says, it will make the contagious gout disappear.* Adam – Thanks for keeping a close eye on me through your HPLC peep hole. You kept the

*This statement has not been evaluated by the Food and Drug Administration. Gout tea is not intended to diagnose, treat, cure, or prevent any disease.

tunes in G12 lit; with Drake, George Ezra, and the occasional Miley Cyrus rap. (Also, I've never met anyone who loves the song "Cats in the Cradle" as much as you do!?). The group is in safe hands with you as the Social/Welfare Sec. and your secret of boosting Instagram likes using the Conway group account is safe with me! Darius – I hope you end up loving column chromatography more than me (impossible). Katrina – I couldn't have wished for anyone better to take on the CREBBP project. You are going to absolutely smash the DPhil. (Also, try not to kill Marco). Reece – thanks for all the work you did on rotation! I'm sure we will work with each other again and you are always invited round for pizza and to lose at Mario Kart! Giulia – Thanks for all the great memories! I will remember how you "hated" every reaction, but were ok once you listened to "Friday, I'm in Love". Margarida – Thank you for all your hard work on the CREBBP project, even though you threatened to kill me every day. I look forward to sending you more photos of me drinking cocktails when you are working in the lab.

Thanks to all the Part II and rotation students I have worked with throughout the DPhil. Jesse Moses – You were a great friend and are sorely missed. Thanks for destroying me at FIFA. Bea and Steph – Thanks for the lab chat and creating the most annoying fumehood game. Leila and Ed – I apologise for letting Leila snake Ed on so many occasions. Elliot – My acknowledgement prediction is that Liverpool will get relegated next year and Tottenham will do the treble. James Tilden – I hope you get a bin next to your fumehood in your PhD. I'm still very impressed with your longest "Yeah Boiiiiii" ever attempts.

Thanks to Stuart, James, Ewen, Jess, Larissa, Katrina, Marco and Debs for proof-reading my thesis.

A huge thanks to Indigo Lily Dean (and her family!) for her support over the last 8 years of University studies – we are always laughing and having fun together, I love all the memories we have made! I give thanks to my parents, Öncel and Stuart, and my siblings Medar, Sultana, Thomas and Shantel. I couldn't have wished for a more loving and supportive family, and I am lucky to have you all in my life. I would also like to thank my Nene – thanks for taking care of me and cooking me so much delicious food!



Figure 2 Example of the support and guidance provided by Prof. Stuart J. Conway.

Abbreviations

ADDP	1,1'-(Azodicarbonyl)dipiperidine
ADME	Absorption, distribution, metabolism and excretion
AGP	Alpha-1-acid glycoprotein
ALK	Anaplastic lymphoma kinase
AMP	Adenosine monophosphate
AR	Androgen receptor
BCL6	B-cell lymphoma 6
BET	Bromodomain and extra terminal domain
BnBr	Benzyl bromide
Boc	*tert*-Butyloxycarbonyl
CMBP	(Cyanomethylene)tributylphosphorane
COSY	Homonuclear correlation spectroscopy
CREBBP	Cyclic AMP response element binding protein (CREB) binding protein
CuAAC	Copper-catalysed azide-alkyne cycloaddition
DEAD	Diethyl azodicarboxylate
DHQ	Dihydroquinoxalinone
DIAD	Diisopropyl azodicarboxylate
DIPEA	*N,N*-Diisopropylethylamine
DMF	*N,N*-Dimethylformamide
DMSO	Dimethyl sulfoxide
DNA	Deoxyribonucleic acid
EP300	E1A Binding protein p300
ESAC	Encoded self-assembling chemical
Et_2O	Diethyl ether
EtOAc	Ethyl acetate
EtOH	Ethanol
FDA	Food and Drug Administration
FP	Fluorescence polarisation
h	Hour(s)
HAT	Histone acetyltransferase
HCT116	Human colorectal cancer cells
HDAC	Histone deacetylase

HEPES	4-(2-Hydroxyethyl)-1-piperazineethanesulfonic acid
HMBC	Heteronuclear multiple bond correlation
HPLC	High performance liquid chromatography
HRMS	High resolution mass spectrometry
HSQC	Heteronuclear single quantum correlation
HTDS	High-throughput DNA sequencing
HTS	High-throughput screen
IAP1	Inhibitor of apoptosis protein 1
IC_{50}	Half maximal inhibitory concentration
IMAC	Immobilised metal affinity chromatography
IPA	Isopropanol
IPTG	Isopropyl β-D-1-thiogalactopyranoside
ITC	Isothermal titration calorimetry
KAc	ε-*N*-Acetylated lysine
KAT	Lysine acetyltransferase
K_d	Dissociation constant
K_i	Inhibitory constant
LNA	Locked nucleic acid
LRMS	Low resolution mass spectrometry
MD	Molecular dynamics
MDM2	Mouse double minute 2 homolog
MeCN	Acetonitrile
MeI	Iodomethane
MeOH	Methanol
min	Minute(s)
mp	Melting point
MsCl	Methanesulfonyl chloride
NEt_3	Triethylamine
NIS	*N*-Iodosuccinimide
NMP	*N*-Methyl-2-pyrrolidone
NMR	Nuclear magnetic resonance
NOE	Nuclear Overhauser effect
PCR	Polymerase chain reaction
PDB	Protein data bank

PEG	Polyethylene glycol
PHD	Plant homeodomain
PK	Pharmacokinetic
PPI	Protein-protein interaction
ppm	Parts per million
PROTAC	Proteolysis-targeting chimeras
PTM	Post-translational modification
PyBOP	Benzotriazol-1-yl-oxytripyrrolidinophosphonium hexafluorophosphate
QM	Quantum mechanics
RCM	Ring closing metathesis
R_f	Retention factor
RMSD	Root-mean-square deviation
rpm	Revolutions per minute
rt	Room temperature
RuAAC	Ruthenium-catalysed azide-alkyne cycloaddition
SAR	Structure-activity relationship
SDS-PAGE	Sodium dodecyl sulfate polyacrylamide gel electrophoresis
S_EAr	Electrophilic aromatic substitution
SEC	Size exclusion chromatography
sEH	Soluble epoxide hydrolase
SGC	Structural Genomics Consortium
S_NAr	Nucleophilic aromatic substitution
TFA	Trifluoroacetic acid
THBD	Tetrahydrobenzodiazepinone
THF	Tetrahydrofuran
THQ	Tetrahydroquinoline
TIPS	Triisopropylsilyl
TLC	Thin layer chromatography
TPSA	Topological polar surface area
TRIM24	Tripartite motif-containing 24
UV	Ultraviolet
VHL	Von Hippel-Lindau

Chapter 1

Introduction

1.1 Epigenetics

In 1942, Conrad Waddington coined the term 'epigenetics' to refer to the changes in phenotype, without changes to the genotype.[1] Today, epigenetics is defined as the dynamic and reversible modification of DNA packaging, which leads to stable heritable differences in gene expression without alteration in the DNA sequence.[2] The epigenetic phenomena are controlled by the events of post-translational modifications (PTMs) that occur on histone proteins, which lead to alteration of chromatin structure.[3] These modifications control the accessibility to DNA of transcriptional machinery, dictating the gene sequences that are expressed. However, many of the biological responses caused by the alteration of the chromatin structure are unknown, making this an exciting area for research and drug discovery.

1.1.1 Chromatin structure and Post-translational modifications

The nucleosome is the first level of condensation of the genetic material into chromatin, and comprises DNA supercoiled twice around a histone octamer; which is formed of a $(H3\text{-}H4)_2$ tetramer and H2A-H2B dimers.[4] Chromatin can either assume a compact conformation (heterochromatin) or an open conformation (euchromatin), in which gene expression is silenced or activated, respectively.[5] The conformation of the chromatin, and hence the DNA accessibility to transcriptional machinery, is an important epigenetic determinant of function and is dependent on the dynamic modification of the histone proteins. This includes the PTMs on both the genetic information (i.e. DNA methylation) and on the histone. Examples of histone PTMs include, but are not limited to; acetylation, methylation, ubiquitination of lysine residues; methylation of arginine residues and the phosphorylation of serine and threonine residues (**Figure 1.1**).[6] The PTMs can occur within the folded histone domains or on the histone tails, and act as docking sites for proteins that regulate chromatin structure and function. Examples of these functions include nucleosome remodelling, promotion of gene transcription, and DNA repair and replication.[7]

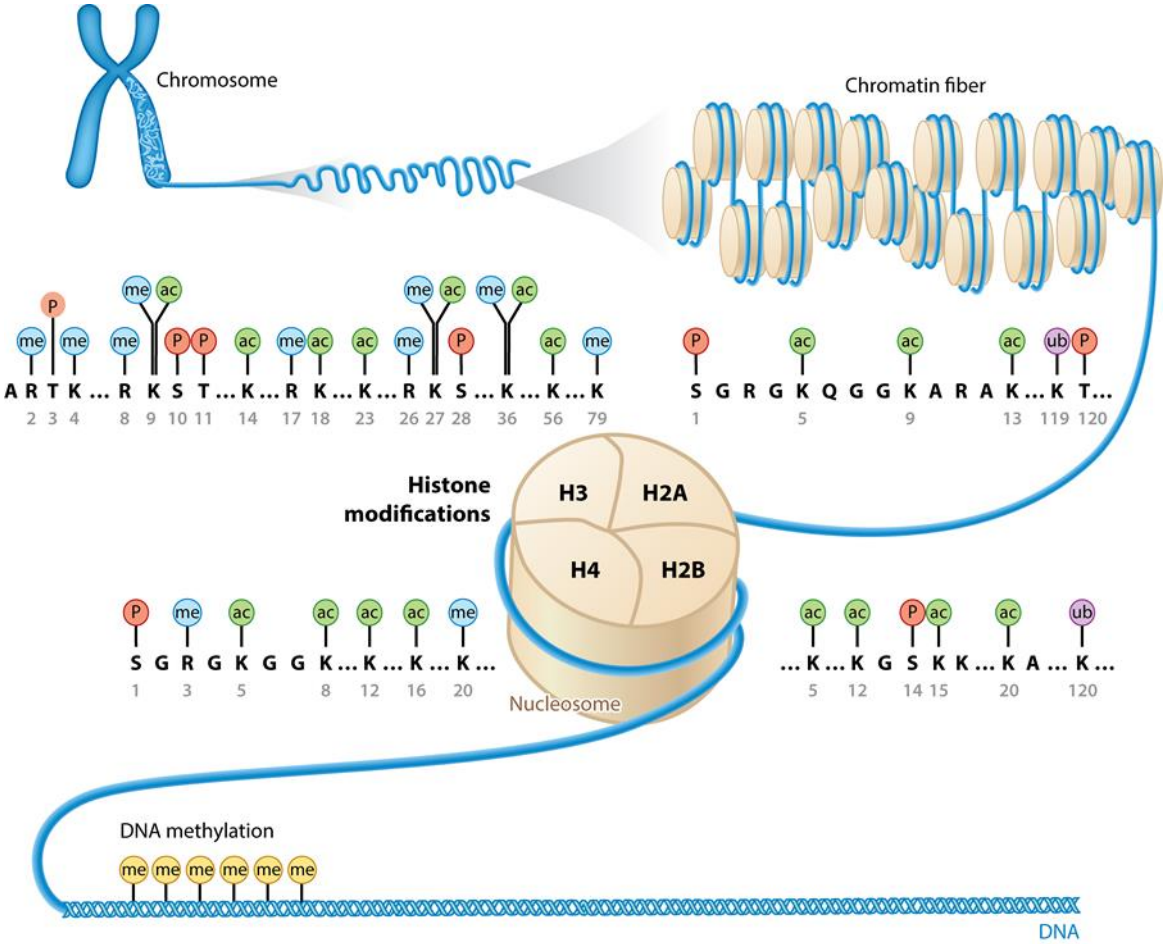


Figure 1.1 Overview of chromosome structure and post-translational modifications. DNA is compacted into nucleosomes and subsequently into chromatin fibres. Histones tail modifications include acetylation (ac), methylation (me), phosphorylation (P) and ubiquitination (ub). Adapted with permission from Z. Chen *et al*.[6]

1.1.2 Histone writers, erasers and readers

The dynamic process of histone PTMs that regulate gene expression has been referred to as the 'histone code'.[8] This term describes the enzymes that either catalyse the addition of PTMs as "writers", remove PTMs as "erasers" and the proteins that mediate PTM recognition as "readers". Lysine acetylation is one of the most abundant histone PTMs and has led to the intense study of its associated writers (histone acetyltransferases, HATs) and erasers (histone deacetylases, HDACs) as targets in drug discovery, for their roles in cancer, inflammation and other diseases states.[5] This thesis will focus on reader proteins, known as bromodomains, which recognise acetylated lysine PTMs, with particular attention on recent drug discovery efforts for the elucidation of their role in human biology and pathology.

1.1.3 Epigenetic drugs

The major advantage of using epigenetic proteins as drug targets is their ability to mediate altered gene expression driven by upstream signals. This enables the indirect targeting of proteins which are normally considered 'undruggable', including oncogenic transcription factors, to modulate a particular disease state.[5] In the last 15 years, there have been four drugs which target epigenetic modifiers that have been approved for clinical use. These include azacitidine (**1**) and decitabine (**2**) (DNA methyltransferase inhibitors), for the treatment of myelodysplastic syndrome, and vorinostat (**3**) and romidepsin (**4**) (HDAC inhibitors), for the treatment of relapsed cutaneous T-cell lymphoma (**Figure 1.2**).[9] In addition, it has been reported that around 1% of all FDA approved drugs show some epigenetic activity in cancer.[10] This recent progress of drug development demonstrates the targeting of epigenetic proteins as a promising approach to treat disease states such as cancer.

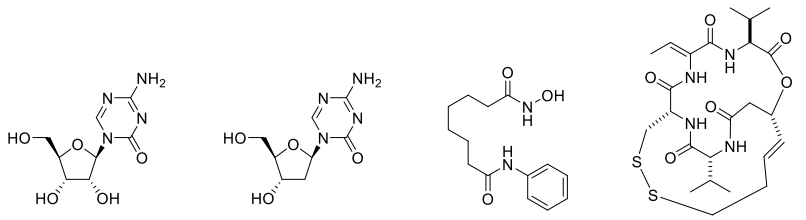


Figure 1.2 Approved drugs in the clinic targeting epigenetic modifiers.[9]

1.2 Bromodomains

Bromodomains, first discovered in the *Drosophila* protein brahma, are epigenetic readers that recognise ε-*N*-acetylated lysine (KAc) residues and consequently mediate protein-protein interactions (PPIs).[11,12] They are typically found in diverse multidomain proteins, which often contain other reader domains (e.g. methyl-lysine recognition domains known as PHD fingers) or catalytic domains (e.g. HATs). In the human proteome, there are 61 bromodomain modules that are found in 46 different bromodomain-containing proteins.[13] Based on their sequence and structural homology similarities, human bromodomains are classified into eight major families (**Figure 1.3**).[12]

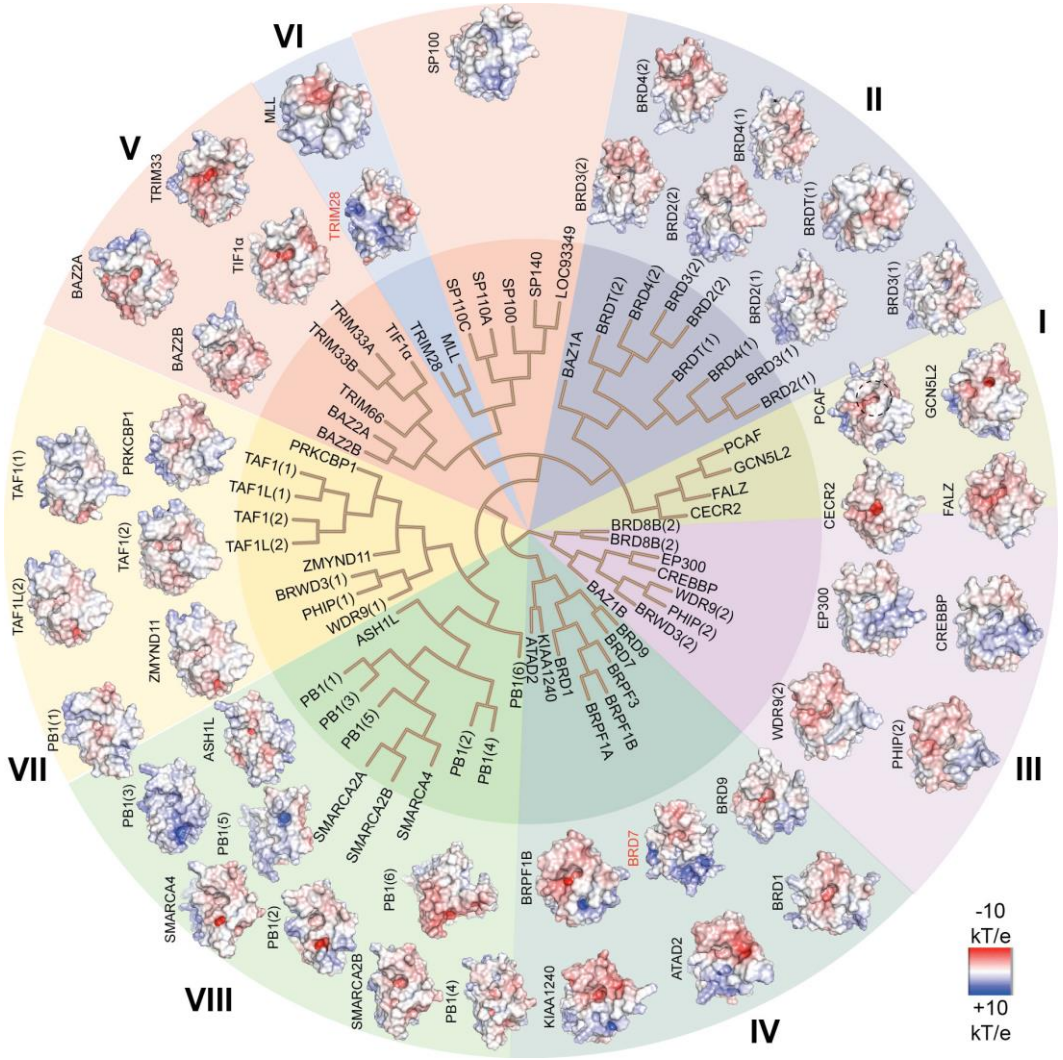


Figure 1.3 Structure-based phylogenetic tree of the human bromodomain family. All bromodomain structures are shown with KAc pocket facing up. With permission from T. Fujisawa *et al*.[12]

1.2.1 Bromodomain structure

Bromodomains consists of ~110 amino acid residues that are arranged into a left-handed bundle of four α-helices (α_z, α_a, α_b and α_c). This tertiary structure is conserved for all bromodomains. The hydrophobic pocket for KAc recognition is formed from a loop between α_b and α_c (BC loop) and a longer loop between α_z and α_a (ZA loop) (**Figure 1.4**). Asparagine and tyrosine residues, found on the BC and ZA loops, respectively, are important for KAc recognition and are conserved for the majority of bromodomains. In addition, there are four or five water molecules that are typically found at the bottom of the KAc binding site, another conserved feature which has been consistently observed in many bromodomain X-ray crystal structures.[5] The small binding site and highly conserved structure of bromodomains makes the identification of selective ligands challenging for these targets.

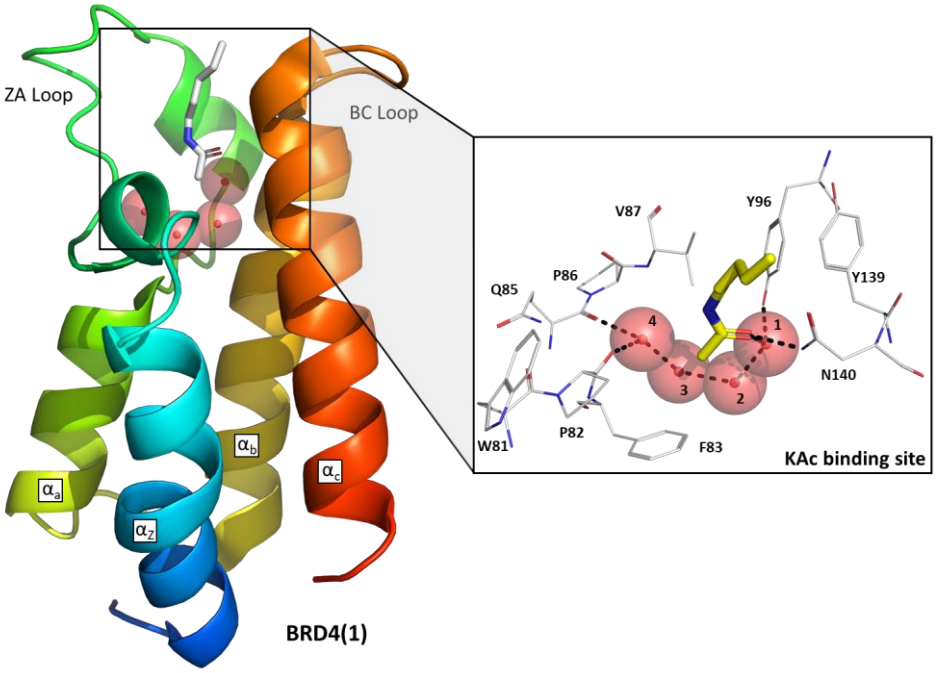


Figure 1.4 Structure of BRD4(1) bound to diacetylated histone peptide ligand H4K12acK16ac (PDB:3UVX). Four α-helices (labelled α_z, α_a, α_b and α_c) joined together by ZA and BC loop to form the KAc binding pocket. A focused view of the binding pocket shows the conserved residues N140 and Y96 forming direct and water-mediated hydrogen bonding interactions with the KAc ligand, respectively.

1.2.2 Bromodomains as drug targets

There has been great success recently in the discovery of small-molecule bromodomain ligands. These compounds have favourable, drug/lead-like properties, that inhibit bromodomain modules from mediating PPIs. This has been particularly true for the bromodomain and extra terminal (BET) family of bromodomains, which comprises four proteins; BRD2; BRD3; BRD4 and BRDT, each possessing two bromodomain. In 2010, (+)JQ1 (**5**)[14] and I-BET762 (**6**),[15] were published as the first high affinity pan-selective BET ligands (**Figure 1.5**). Since these landmark publications, many tool compounds have shown robust preclinical activity for the BET family, linking them to key oncogenic transcriptional networks. This success has led to the development of advanced BET ligands which are currently in clinical trials for both oncology and non-oncology (e.g. diabetes) indications.[16]

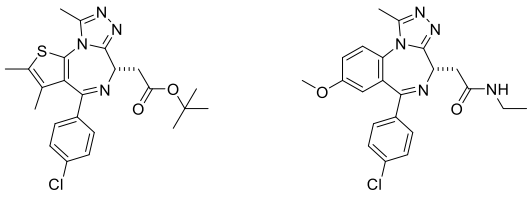


Figure 1.5 Chemical structures of selective BET inhibitors (+)JQ1[14] and I-BET762.[15]

The development of advanced BET ligands for clinical trials has stimulated enormous interest in other bromodomain proteins as drug targets. However, unlike the BET family which show a profound biological effect in cellular studies, the advancement of other bromodomain targets has been slower in some cases, due to their weaker phenotypes. This has led to the immature understanding of cellular function, and the relevance of these proteins in disease states. Consequently, ligands must be highly selective over the BET family to avoid incorrectly attributing a biological response to the targeted bromodomain. Nevertheless, achieving high selectivity is a major challenge in this field due to the highly conserved structural features of bromodomain proteins.

1.3 CREBBP bromodomain

1.3.1 CREBBP and EP300

Cyclic AMP response element binding protein (CREB) binding protein (CREBBP) and E1A binding protein p300 (EP300) are paralogous lysine acetyltransferases (KATs).[17] They function as transcription co-factors for several proteins, including oncoproteins (e.g. myb) and tumour suppressor proteins (e.g. p53). CREBBP and EP300 each comprise nine domains; NRID; C/H1; KIX; bromodomain; PHD; KAT; ZZ; TAZ2 and NCBD, sharing a 61% overall sequence homology (**Figure 1.6**).[18] Despite the acetyltransferase domain regions (which includes the bromodomain) having an 86% amino acid residue similarity, CREBBP and EP300 serve distinct, non-overlapping, functions.[19]

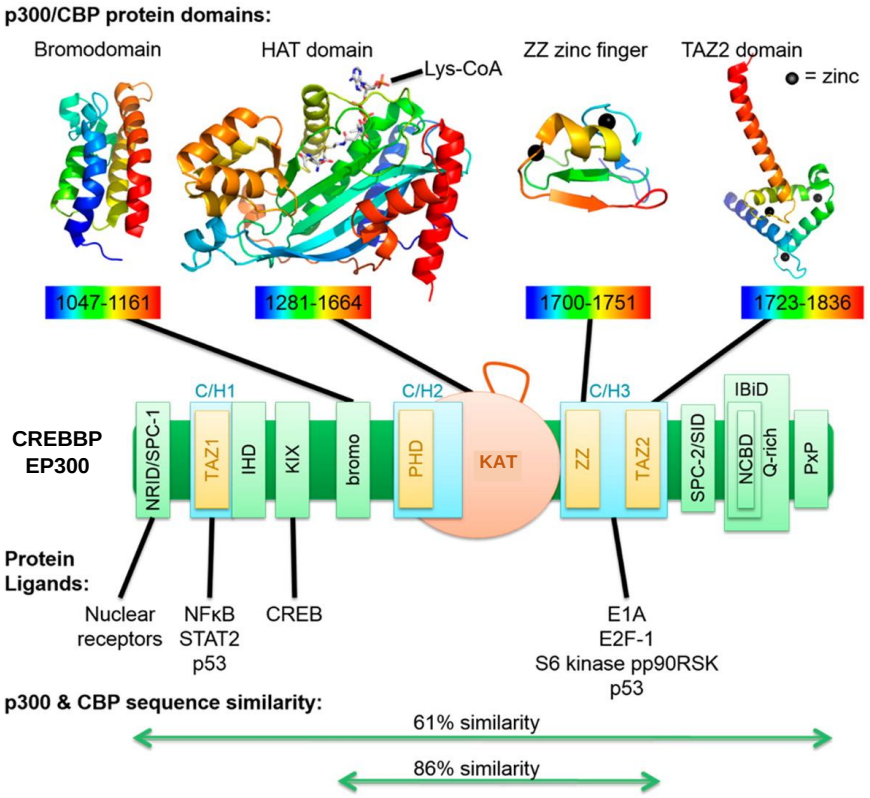


Figure 1.6 Domain structure of CREBBP and EP300, with protein structures for the bromodomain (PDB: 3I3J), catalytic KAT domain (PDB: 3BIY), ZZ zinc finger (PDB: 1TOT) and TAZ2 domain (PDB 3IO2). CREBBP and EP300 bromodomains show very high similarity. High sequence similarity is also observed from the bromodomain to the C/H 3 region. Adapted with permission from B. M. Dancy *et al*.[18] Copyright 2015 American Chemical Society.

Over 400 different proteins interact with CREBBP/EP300 in the human protein-protein interactome, mediating several signalling pathway responses that include DNA damage and cellular stress.[18,20] For example, CREBBP/EP300 activates the non-histone protein p53 by acetylation of its C-terminal lysine

residues, which leads to interaction with the bromodomain to promote a positive feedback mechanism. However, the p53 transcription factor is implicated in several diseases including cancer, Alzheimer's disease, Parkinson's disease, diabetes, atherosclerosis, multiple sclerosis and myocardial ischemia.[5] As the direct inhibition of p53 has proven to be challenging, the inhibition of its interaction with CREBBP and EP300 could help prevent these disease states, making the multidomain proteins attractive targets for drug discovery.[17]

The relevance of CREBBP/EP300 as oncological targets were first shown using inhibitors of their KAT activity, demonstrating *in vivo* tumour suppression in mice. However, these compounds were shown to lack affinity and specificity.[21] Nevertheless, this work has prompted research towards the development of small molecule probes for the individual domains of CREBBP/EP300, including the KAT,[22] KIX,[23] TAZ1,[24] and bromodomain.[25] These molecules will enable the dissection of the specific role of the individual domains within the context of the whole protein function. Prompted by the success of the BET bromodomains and their pre-clinical advancement, dual CREBBP and EP300 bromodomain inhibitors have since been developed. This thesis will focus on the development of high affinity and selective CREBBP/EP300 bromodomain ligands, and will refer to dual bromodomain inhibitors as CREBBP bromodomain ligands.

1.3.2 CREBBP bromodomain structure

The CREBBP/EP300 bromodomains have a similar ZA loop length as the BET family of bromodomains, with similar residues in the binding site (**Figure 1.7**).[26] These shared features make achieving high selectivity against the BET family a challenging task for ligand discovery. However, the CREBBP/EP300 bromodomains contains two additional water molecules in the ZA channel, and an arginine residue outside the KAc pocket that enables charged interactions with ligands. In addition, tryptophan 81 in the BET family of bromodomains, which forms part of the ZA channel known as the WPF shelf (**Figure 1.4**), is replaced by a smaller leucine residue for the CREBBP/EP300 bromodomains, resulting in a different topology. These unique structural features of the CREBBP/EP300 bromodomain provides a good handle for developing selective ligands.

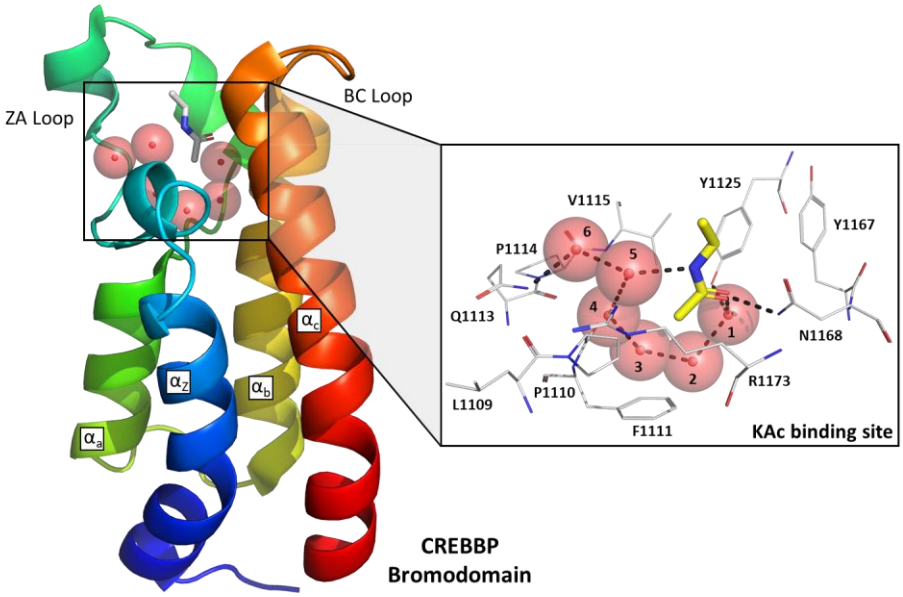


Figure 1.7 Structure of CREBBP bromodomain bound to acetylated lysine (PDB:3P1C). Four α-helices (labelled α_z, α_a, α_b and α_c) joined together by ZA and BC loop to form the KAc binding pocket. A focused view of the binding pocket shows the conserved residues N1168 and Y1125 forming direct and water-mediated hydrogen bonding interactions with the KAc ligand respectively. Notable differences observed between BRD4(1) and CREBBP bromodomain is the LPF shelf, and residue R1173 located outside the KAc pocket.

1.3.3 CREBBP bromodomain ligands

In 2006, Zhou and co-workers identified the first CREBBP bromodomain ligand using an NMR-based screen, reporting ligand MS7972 (**7**) to have low micromolar affinity (K_d = 19.6 μM).[27] After this discovery, they performed another NMR-based screen on a library of 100,000 compounds and a structure-activity relationship (SAR) study led to the identification of the azabenzene ligand ischemin (**8**) (K_d = 19.0 μM).[28] Continuing their pioneering work, Zhou and co-workers used molecular dynamics (MD) and NMR studies to develop cyclic peptide **9** for the CREBBP bromodomain with an IC_{50} = 8 μM (**Figure 1.8**).[29]

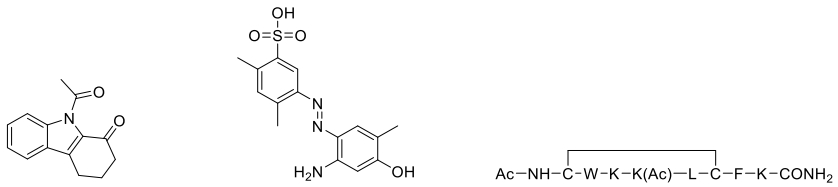


Figure 1.8 Chemical structures of early CREBBP bromodomain inhibitors.

The Conway group published the first sub-micromolar ligand, **(*R*)10**, for the CREBBP bromodomain with a K_d = 390 nM.[25] They identified that the dihydroquinoxalinone (DHQ) headgroup acts as a KAc mimic, with the lactam forming hydrogen bonding interactions with residue N1168 in the KAc binding pocket. The headgroup is attached to a tetrahydroquinoline (THQ) moiety through an amide linker, which forms cation-π interaction with residue R1173 in an induced fit pocket and hydrophobic interactions with the LPF shelf (**Figure 1.9A**). However, it was identified that the DHQ headgroup was susceptible to oxidation and racemisation, and it was evident from the protein-ligand X-ray crystal structure of **(*R*)10** that there was unoccupied space in the KAc binding pocket.

Through MD studies, it was identified that a tetrahydrobenzodiazepinone (THBD) headgroup would be a suitable KAc mimic to replace the DHQ group, occupying a larger area of the KAc pocket (**Figure 1.9B**). This led to the development of ligand **(*R*)11**, which gave a K_d = 490 nM.[30] Despite the THBD headgroup resulting in a weaker affinity to the CREBBP bromodomain, this headgroup was more stable to oxidation and racemisation than the DHQ headgroup. In addition, enantiomer **(*S*)11** showed no detectable binding to the CREBBP bromodomain, providing a valuable negative control.

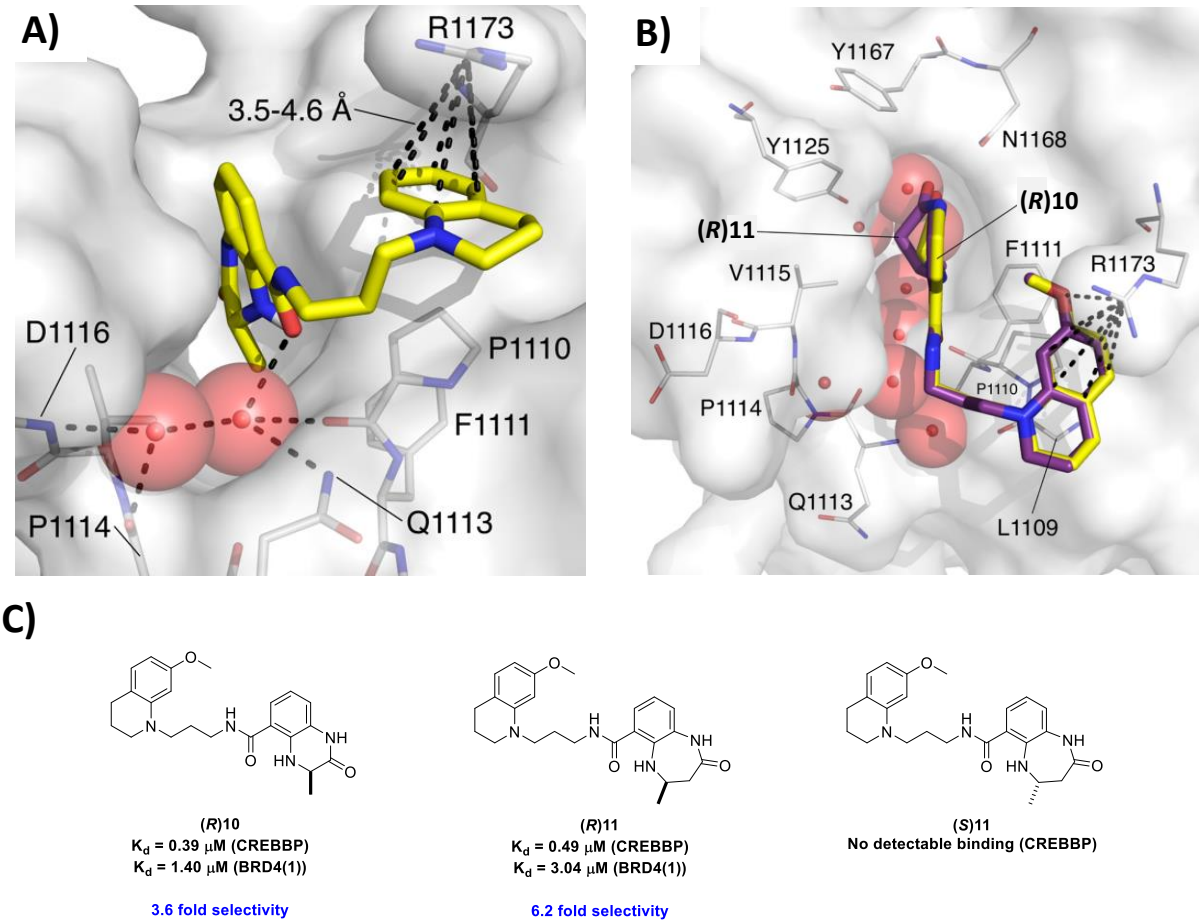


Figure 1.9 Protein-ligand X-ray structures of (A) **(*R*)10** (PDB:4NYX, carbon:yellow) and (B) **(*R*)11** (carbon:purple) bound to the CREBBP bromodomain. X-ray structures show cation-π interaction with the THQ moiety and residue R1173. Ligand **(*R*)11** occupies are larger space in the KAc pocket than ligand **(*R*)10**. (C) Chemical structures of CREBBP bromodomain ligands **(*R*)10** and **(*R*)11**, and negative control **(*S*)11**. Adapted with permission from Prof. Stuart Conway.

Ligands **(*R*)10** and **(*R*)11** were amongst the first reported high affinity CREBBP bromodomain ligands, however both ligands only showed moderate selectivity over the BET family (**Figure 1.9C**).

In recent years, high affinity and selective inhibitors for the CREBBP bromodomain have been reported by Genentech and Constellation Pharmaceuticals. Initial work led to the development of CREBBP bromodomain inhibitor CPI-637 (**(*R*)12**), which shared the same THBD KAc mimic as ligand **(*R*)11**, but had a pyrazole moiety which formed interactions with residue R1173. Ligand **(*R*)12** gave an IC_{50} = 30 nM for the CREBBP bromodomain, with a >360-fold selectivity against BRD4(1), however, off-target activity was observed against the non-BET bromodomain BRD9 (IC_{50} = 730 nM).[31] Following the publication of inhibitor **(*R*)12**, Genentech and Constellation Pharmaceuticals reported the pyrazolopiperidine ligands GNE-272 (**13**)[32] (IC_{50} = 20 nM) and GNE-049 (**14**)[33] (IC_{50} = 1.1 nM) as high affinity, and selective inhibitors of the CREBBP bromodomain (**Figure 1.10**). These ligands showed favourable metabolic

stability and bioavailability, with good cellular activity, making them suitable for *in vivo* studies.[16] Furthermore, GNE-049 (**14**) has nearly 4,000-fold selectivity over BRD4(1) and demonstrated good *in vitro* and *in vivo* activity in preclinical models for castration-resistant prostate cancer.[33]

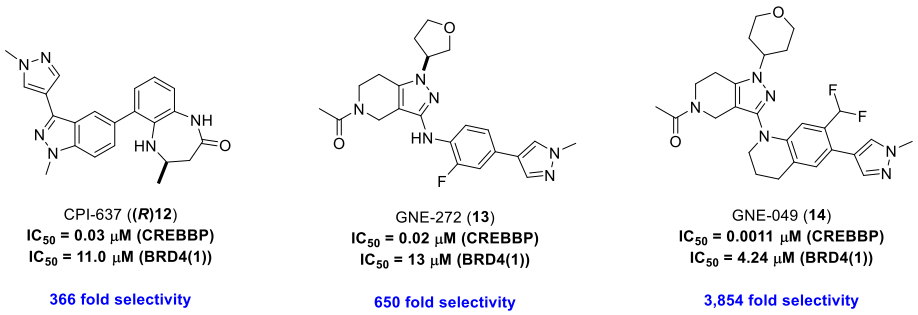


Figure 1.10 Chemical structures of CREBBP bromodomain inhibitors reported by Genentech and Constellation Pharmaceuticals.

CellCentric has identified the lead CCS1477 (**15**) as a CREBBP bromodomain ligand which is currently in phase I/IIa clinical trials for the treatment of metastatic prostate cancer (**Figure 1.11**).[34] This makes the CREBBP bromodomain the second bromodomain target, after the BET family, to reach the clinical trials. However, the clinical development of CCS1477 (**15**) underscores the selectivity challenge for drug development in this area, showing 170-fold selectivity for the CREBBP bromodomain over BRD4(1).[16] This selectivity difference may not be large enough to cleanly differentiate between the two bromodomain targets at pharmacologically active doses. Nevertheless, the recent development of CREBBP bromodomain inhibitors states the importance and relevance of this target for drug discovery, highlighting the need for more selective CREBBP bromodomain ligands.

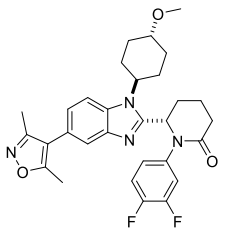


Figure 1.11 Chemical structure of phase I/IIa CREBBP bromodomain ligand CC1477 (**15**).

1.4 Recent medicinal chemistry-based approaches for small molecule drug discovery

In recent years, the identification of drug-like compounds in the pharmaceutical industry has relied on high-throughput screens (HTS), cross-screening of known drugs, and the use of fragment-based lead generation.[35] These techniques are often coupled with protein-crystallography, which enables structure-based drug discovery to guide medicinal chemistry efforts. Academic groups have become an increasingly important source of new targets and chemical probes, leading to several collaborative programmes between academia and industry. Examples include the development of technologies such as proteolysis-targeting chimeras (PROTACs) and DNA-encoded libraries, which are now both routinely used in the pharmaceutical industry for drug development. This section will review some recent advancements in medicinal chemistry-based approaches, which are used for the identification of small molecule inhibitors, as well as for the improvement of affinity and target selectivity.

1.4.1 Macrocyclic drug design

Macrocycles are defined as a ring system composed of 12 or more atoms.[36–38] Historically, their use as drug candidates originated from natural product sources and were often directly used as therapeutics. These include known drugs such as erythromycin (**16**) (antibiotic), cyclosporine (**17**) (immunosuppressant), epothilone B (**18**) (anticancer) and amphotericin B (**19**) (antifungal) (**Figure 1.12**).[37] However, macrocycles were largely under-explored and poorly exploited drug discovery for many years. This was due to macrocycles not being compliant to many of the rules set by medicinal chemists, often lying outside drug-like space, with their preparations being synthetically challenging.

In recent years, synthetic macrocycles have become an increasingly attractive modality for pharmaceutical drug discovery projects. This is due to the ability of macrocycles to span large surface areas, while remaining conformationally pre-organised, making them suitable for targets displaying shallow surfaces and difficult to drug binding sites, such as PPIs.[39] This section will discuss the use of macrocyclisation strategies in drug discovery to improve affinity, selectivity and physicochemical properties compared to their acyclic counterparts, with particular focus on non-peptidic small molecule inhibitors.

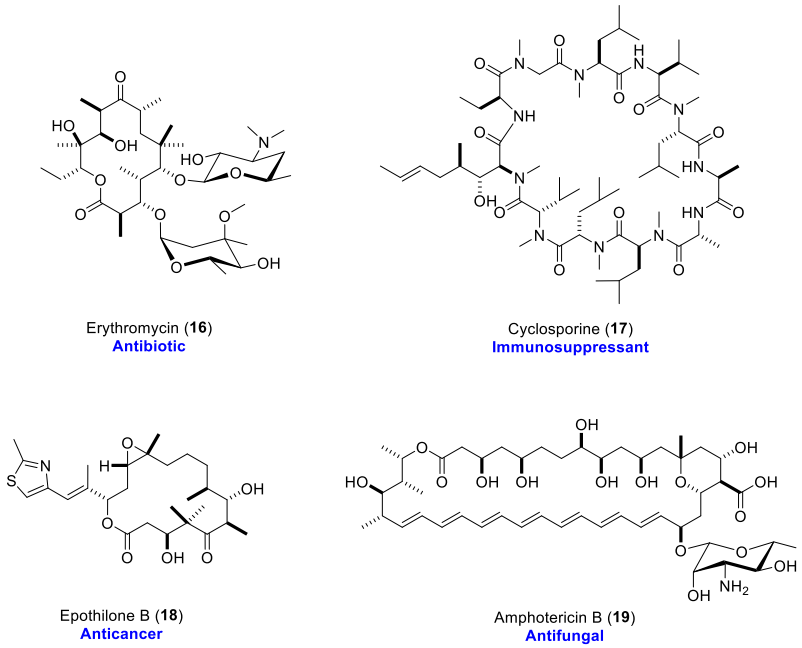


Figure 1.12 Chemical structures of naturally occurring macrocycles with their associated therapeutic applications.[37]

1.4.1.1 Improvement of affinity and selectivity

The improvement in the affinity seen in macrocyclic structures, compared to their acyclic counterparts, is mainly due to the propensity of macrocycles to adopt a solution-state conformation that has a greater similarity to the protein-bound structure. This conformational constraint minimises the internal entropic penalty associated with the ligand changing conformationally from the unbound to the bound state.[38] With regards to the Gibbs free energy of reversible binding equation (**Equation 1.1**), a more negative ΔG results in an improvement in binding affinity (ln*K*). This is typically achieved by the displacement of water molecules, as well as strong hydrogen-bonding and van der Waals interactions in the protein-ligand complex, leading to an increase in the entropic (Δ*S*) and enthalpic (Δ*H*) terms, respectively. The result of ligand conformational constraints, such as macrocyclisations, will reduce the overall motion of a bound complex, compared against the acyclic analogues. This strengthens the intermolecular interactions (i.e. hydrogen-bonds) and increases enthalpic contributions.

$$\Delta \mathrm{G} = \Delta H - \mathrm{T}\Delta S = -\mathrm{RT}\ln K \qquad \textbf{(1.1)}$$

ΔG = Gibbs free energy change on binding; Δ*H* = Enthalpy change; T = Temperature; Δ*S* = Entropy change; R = Gas constant (8.13 $Jmol^{-1}K^{-1}$); K = Binding constant.

There have been several publications in recent years that demonstrate the use of macrocyclic drug design to increase affinity to their respective targets. A representative example is the BRD4(1) macrocyclic inhibitor reported by the biopharmaceutical company AbbVie Inc.[40] Their efforts began

with an NMR-based screen which identified phenylpyridazinone fragment (**20**) (K_i = 160 µM). A structure-based drug design approach led to the development of potent BRD4(1) acyclic ligand **21** (EC_{50} = 39 nM) (**Figure 1.13A**). From the X-ray protein-ligand structure of **21** bound to BRD4(1), it was observed that the aliphatic side chain was in close proximity to the difluoro-phenyl ring system (**Figure 1.13B**). These sites were tethered together to form macrocyclic analogue **22** (**Figure 1.13C**), which saw a 6-fold increase in affinity (EC_{50} = 6.5 nM), and improved cellular potency, when compared to the acyclic analogue **21**.

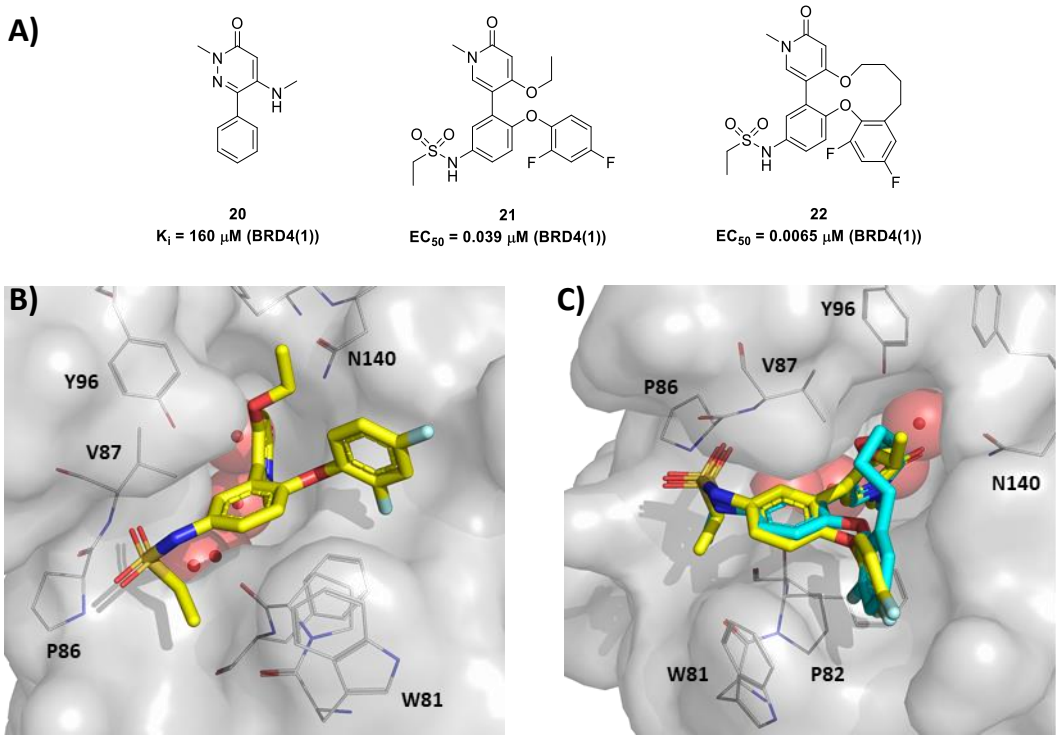


Figure 1.13 (A) Chemical structures of BRD4(1) inhibitors **21** and **22** based on phenylpyridazinone fragment **20**. Protein-ligand X-ray crystal structures of inhibitors (B) **21** (PDB: 5UEW, carbon:yellow) and (C) **22** (PDB: 5UEX, carbon:cyan) bound to BRD4(1). X-ray structures showed the ether moiety was close in space to difluoro-ring, with sufficient space to accommodate a macrocycle.[40]

Macrocyclisation strategies have also enabled selectivity between closely related target proteins. For instance, a macrocyclic structure could preferentially bind to the desired target, however, due to conformational ring constraints, it may not be able to adopt the alternative binding mode of the 'undesired' target. An example of this was reported by Breslin *et al.* for their development of macrocyclic anaplastic lymphoma kinase (ALK) inhibitors.[41] Based on X-ray crystallography, they observed that their acyclic ALK inhibitors, such as ligand **23**, adopted a U-shaped binding conformation, therefore they rationalised that a macrocyclisation approach could lead to an increased potency by locking the inhibitor scaffold into the bioactive conformation. Their hypothesis was proven to be correct, with macrocycle **24** showing a 7-fold increase in potency compared to the acyclic analogue **23**.

Selectivity was determined using an IR tyrosine kinase enzyme assay, as ALK is a member of this superfamily. An >18-fold selectivity difference for ALK over IR was observed for macrocycle **24** when compared against its acyclic counterpart **23** (**Figure 1.14**).

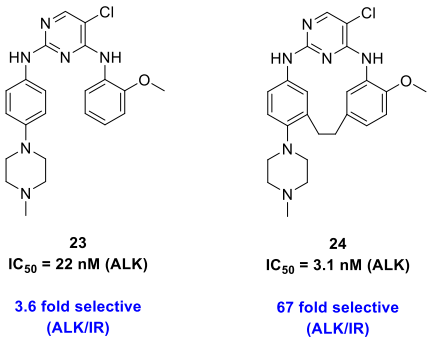


Figure 1.14 Chemical structures of ALK inhibitors with affinity and selectivity profiles.[41]

Although there are reports of macrocycles improving selectivity profiles of inhibitors, there are relatively few examples of how macrocycle strategies directly affect the intrinsic selectivity profiles of acyclic scaffolds.[38]

1.4.1.2 Modulation of physicochemical properties

Based on classical molecular descriptors used in medicinal chemistry, the macrocycle drug class violate most criteria set for good pharmacokinetic (PK) – absorption, distribution, metabolism and excretion (ADME) properties. For example, Lipinski's 'rule of five' are strict guidelines that medicinal chemists rigorously follow in most pharmaceutical companies, and are applied to achieve good oral bioavailability in drug development projects.[42] Typically, macrocycles have molecular weights (ranging between 500–900 g mol^{-1}) and hydrogen-bond donors & acceptors which are beyond the accepted Lipinski's 'rule of five'. In addition, their topological polar surface area (TPSA) are often unfavourable for accepted drug-like properties.[43] Despite these violations, macrocycles are consistently reported to have good solubility, cell permeability, metabolic stability and bioavailability.[37]

One factor that enables macrocycles to have good pharmacological properties is their ability to adopt conformations which shield multiple polar groups from the surrounding solvent. This is achieved through intramolecular interactions, such as hydrogen bonding. This allows the macrocycles to present a mostly 'non-polar' surface when in hydrophobic environments (i.e. passing through cell membranes). This is often referred to as the 'chameleonic behaviour' of macrocycles.[44] For this reason, traditional 2D descriptors, including TPSA and hydrogen-bond donors & acceptors, fail to predict if chameleonic

compounds beyond the rule of five space will have good cell permeability and oral absorption. Consequently, there have been recent efforts to use 3D molecular descriptors, including 3D polar surface area (3D PSA), to give a better insight into what determines drug-like properties for this chemical space.[45]

The above point is nicely represented in the publication of Sebastiano *et al*. who used protein-ligand crystal structures to demonstrate how the conformational differences in chameleonic compound can affect their 3D PSA.[45] For the case of telithromycin (**25**), a large difference in 3D PSA was observed for its conformations when bound to two different strains of bacterial 50S ribosomal subunit proteins (represented as Min and Max in **Figure 1.15**). The bulky pyridyl group in telithromycin (**25**) can dictate the difference in PSA by either folding over the polar macrocyclic core (Min SA 3D PSA), or leaving it exposed (Max SA 3D PSA). The flexibility of macrocyclic structures to interchange between these intramolecular interactions is what ultimately determines good cellular permeability and solubility.

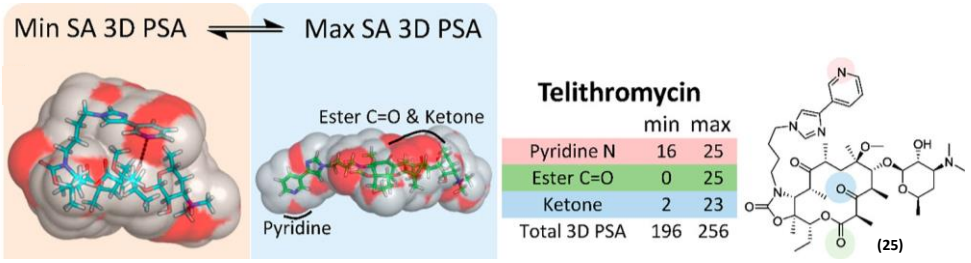


Figure 1.15 Conformational changes in telithromycin (**25**) in crystal structures that display minimum (PDB: 1YIJ) and maximum (PDB: 1P9X) solvent accessible 3D PSA. The table shows the difference in PSA for the selected functional groups in the Min and Max telithromycin structures. Adapted with permission from Sebastiano *et al*.[45] Copyright 2018 American Chemical Society.

1.4.1.3 Conformational analysis for macrocyclic drug design

As discussed in Section 1.4.1.1, the pre-organisation of macrocycles to adopt the bioactive conformation in solution reduces free energy penalties, leading to improved affinities.[39] For most drug discovery projects, the rationale to constrain an acyclic ligand into a macrocyclic structure is often derived from protein-ligand X-ray structure analysis. However, X-ray crystallography only provides a static 'snapshot' of the final protein-ligand complex, with no information to quantify the amount of ligand strain incurred to adopt the observed binding mode.

In recent years, there have been a number of publications that have used 1D NMR for conformational analysis of macrocycles to enhance structure-based drug design. This is because NMR chemical shifts and *J*-couplings are sensitive to both local electronic environments and molecular dynamics, encoding

3D information about free ligand conformations.[39] McCoull *et al.* used NMR conformational analysis to evaluate to what extent free molecules in solution were adopting the bioactive conformation for inhibitors against B-cell lymphoma 6 (BCL6) protein.[46] For acyclic analogue **26**, they were able to determine two main conformations in a relative population of 40:60, however, neither of the solution conformations were able to fully adopt the bioactive conformer (**Figure 1.16A**). In comparison, macrocycle **27** had two main solutional conformations in a relative population of 79:18, with the most populated conformer (79%) showing a nearly perfect match with the bioactive conformer (**Figure 1.16B**). The high propensity of macrocycle **27** to adopt the bioactive conformation in solution explains the 128-fold improvement in affinity when compared to acyclic ligand **26**(IC_{50} = 2.9 nM *vs* IC_{50} = 370 nM, respectively).

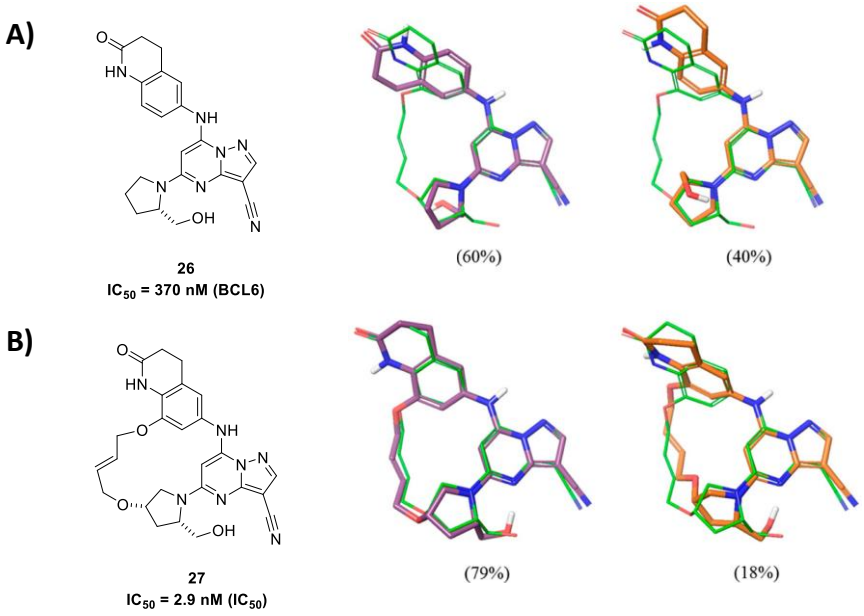


Figure 1.16 1D NMR conformation analysis showing relative conformational populations of (A) **26** and (B) **27**. The bioactive conformation of **27** (PDB: 5N1Z, carbon:green) is shown for comparison. Adapted with permission from McCoull *et al*.[46] Copyright 2017 American Chemical Society.

Conformational analysis using 1D NMR can additionally be used to support SAR and drug design for series which share similar scaffolds. This is exemplified by Johannes *et al*. who reported macrocyclic Mcl-1 inhibitors (**28**).[47] Upon screening different linker chains, they were able to observe that a difference in ~1ppm for a particular chemical shift, ('conformational signature' – hydrogen atom highlighted in pink), that could enable the differentiation between the bioactive and non-bioactive conformations (**Figure 1.17**). Understanding 1D NMR signatures of free macrocyclic ligands can provide a quick analytical marker for conformational flexibility and molecular shape in solution, helping guide macrocyclic drug design.[39]

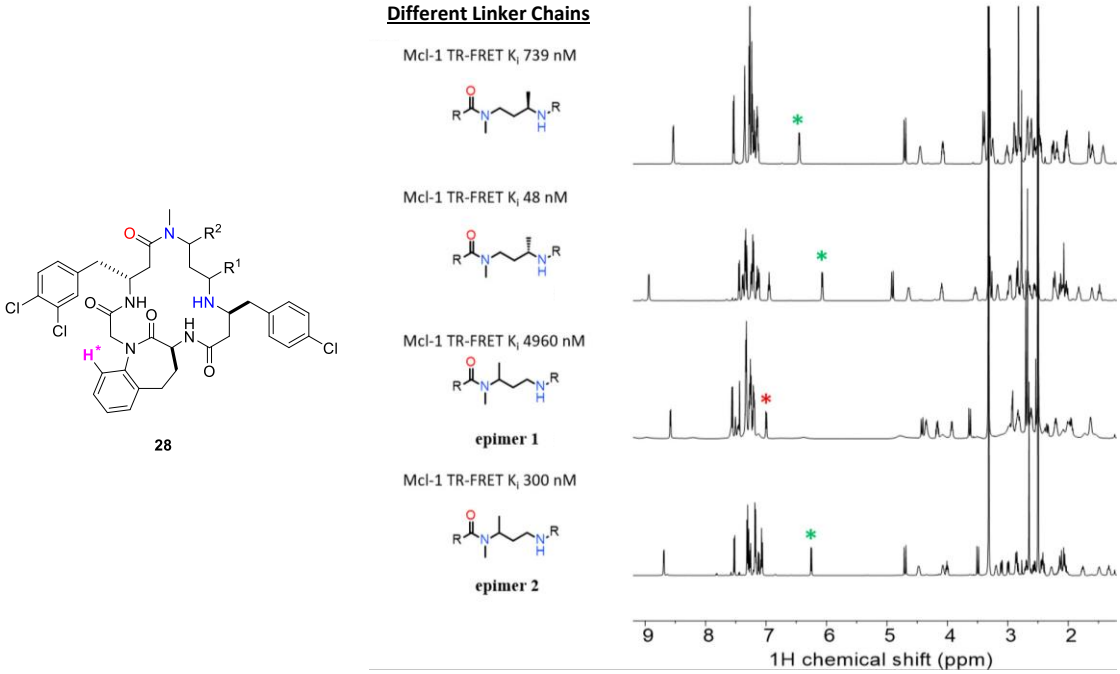


Figure 1.17 ^{1}H NMR spectra (DMSO-d_6) of macrocyclic Mcl-1 inhibitors with its conformational signals (hydrogen atom marked with asterisk) highlighting bioactive (green) and non-bioactive (red) conformations. Adapted with permission from Balazs *et al*.[39] Copyright 2019 American Chemical Society.

1.4.2 Small molecule PROTAC technology

Small molecule inhibitors are the main therapy used in the clinic to target intracellular proteins, functioning through the occupation of a protein's active site, leading to the inhibition of its function. However, there are still some problems associated with their use as drugs. These therapies are unsuitable for proteins without active sites, such as transcription factors and non-enzymatic proteins, which are often classed as 'undruggable' targets.[48] Furthermore, small molecule inhibitors are typically required at high drug doses to elicit therapeutic responses, which can lead to undesirable off-target effects. In addition, the long-term targeting of a protein can lead to its over-expression, resulting in the intracellular protein accumulation that prevents complete target inhibition. These limitations can obstruct clinical effectiveness of small molecule inhibitors.

A potential way to overcome some of the limitations associated with small molecule inhibitors is through the use of induced protein degradation.[49] This approach involves a transient binding event of a target protein using small molecule inhibitors, that results in a ubiquitination event to signals for the protein's degradation. After the degradation of the protein, the small molecule inhibitor can catalytically continue another cycle of protein degradation, enabling 'sub-stoichiometric' drug doses. Furthermore, this approach can target 'undruggable' proteins, as the inhibitors only require a brief interaction with the protein of interest to signal its degradation.

PROTACs are a recent technological development which has been used to induce protein degradation. They are heterobifunctional compounds which comprise three components; a ligand for the target protein; a ligand to recruit the E3 ubiquitin ligase; and a linker that connects the two ligands.[48] This results in the formation of a ligase:PROTAC:target ternary complex which causes a polyubiquitination event to occur on the protein of interest, through the use of a recruited E2 ubiquitin-conjugating enzyme, promoting its degradation (**Figure 1.18**). Several publications have reported PROTACs to induce degradation of various types of proteins such as kinases, nuclear receptors and transcription factors.[48] This has led to great interest in the pharmaceutical industry. Arvinas are the first company to develop PROTAC drug candidates that have reached clinical trials, with phase I studies currently on-going for their treatment of metastatic castration-resistant prostate cancer and metastatic breast cancer, respectively.[50,51] This section will give an overview of early PROTAC development, and their use in the bromodomain field.

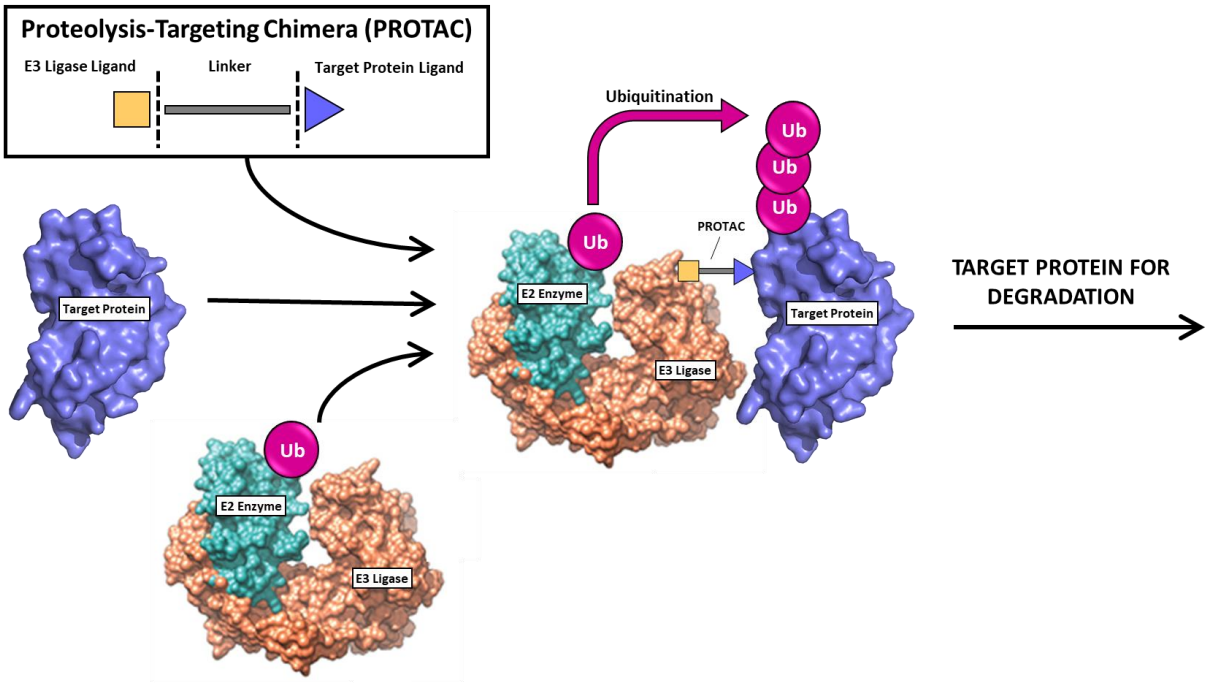
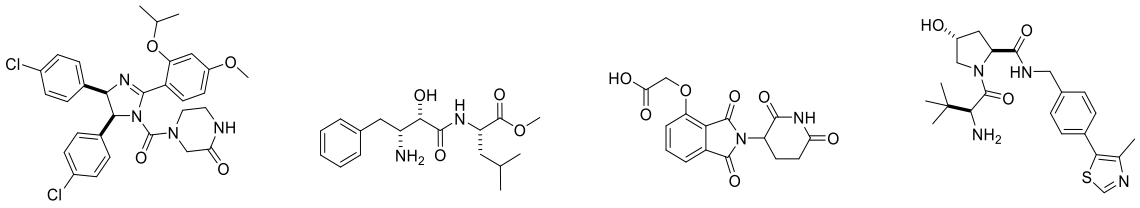


Figure 1.18 Degradation of a target protein using PROTAC technology. E3 ubiquitin ligase and the target protein are recruited by the PROTAC, bringing the proteins into close proximity for the E2 ubiquitin-conjugating enzyme to transfer ubiquitin to the surface of the target protein. The poly-ubiquitination of the target protein signals for its degradation.[52]

1.4.2.1 Early PROTAC publications

In 2001, the first PROTACs were reported for the degradation of MetAP-2 using the recruitment of the E3 ubiquitin ligase β-TRCP.[53] The PROTACs used in this publication contained a phosphopeptide as the E3 ubiquitin ligase ligand, however, poor cell permeability limited their utility as chemical probes. This led to the development of cell permeable peptide ligands as PROTACs to recruit the von Hippel-Lindau (VHL) E3 ubiquitin ligase.[54] However, there were several limitations with using peptides in PROTACs, an artefact of their high molecular weights, low affinities and poor metabolic stabilities.

To overcome the issues of peptide ligands in PROTAC development, small molecule E3 ubiquitin ligase inhibitors have been used for their recruitment. To date, there have been four small molecule E3 ligase ligands that have been successfully reported for their use in PROTACs (**Figure 1.19**). Mouse double minute 2 homolog (MDM2) inhibitor **29** was incorporated into the first non-peptidic small molecule PROTAC, used for the degradation of the androgen receptor (AR) to treat prostate tumour cell.[52] In addition, inhibitor of apoptosis protein 1 (IAP1) ligands were incorporated into several small molecule PROTACs, although off-target effects and self-degradation of IAP1 has limited their use in the field.[48,55] However, the majority of PROTAC publications in recent years have made use of cereblon, or VHL, E3 ligase inhibitors, (such as thalidomide-based ligand **31** and thiazole **32**, respectively), describing their use in the degradation of the several proteins, including the BET family of bromodomains.

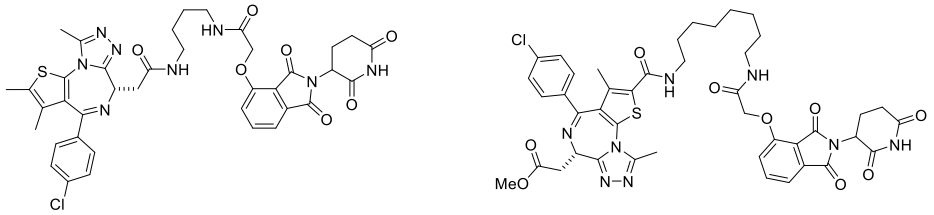


29 30 31 32

Figure 1.19 Chemical structures of the four E3 ubiquitin ligase binding site inhibitors reported for their use in PROTACs.[48]

1.4.2.2 PROTAC degradation of BET proteins

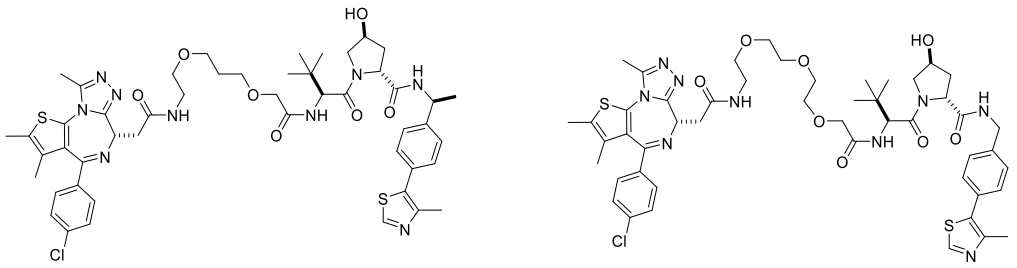
Winter *et al*. published the first BET PROTAC, dBET1 (**33**), which comprised of BET inhibitor (+)JQ1 (**5**) connected to the cereblon inhibitor **31**.[56] They performed *in vitro* cell assays which showed depletion of BRD4 after 1 h, followed by partial recovery of BRD4 after 24 h. This sparked several reports of thalidomide-based PROTACs for BET degradation, as well as alternative linking strategies to connect to ligand (+)JQ1 (**5**), as shown in PROTAC dBET23 (**34**) (**Figure 1.20**).[57]



dBET1 (**33**) dBET23 (**34**)

Figure 1.20 Chemical structures of known BET PROTACs with a cereblon ligand component.[56,57]

Arvinas reported the BET PROTAC ARV-771 (**35**), containing a VHL ligand as the E3 ligase component.[58] This showed rapid BRD2/3/4 degradation in castration-resistant prostate cancer cell lines. Ciulli and co-workers reported the PROTAC MZ1 (**36**), which also contained the VHL ligand, to show selective degradation of BRD4 over the other BET bromodomains. This was interesting as the PROTAC contained the pan-selective inhibitor (+)JQ1 (**5**).[59] Furthermore, the main difference in the structures of the independently reported PROTACs ARV-771 (**35**) and MZ1 (**36**) were the linker lengths (**Figure 1.21**). This observation revealed the importance of the linker component for determining the selectivity of target degradation, as it effects the formation of the ligase:PROTAC:target ternary complex.



ARV-771 (**35**) MZ1 (**36**)

Figure 1.21 Chemical structures of known BET PROTACs with a VHL ligand component.[58,59]

The X-ray crystal structures of ligase:PROTAC:target ternary complexes have since been determined, containing the BET bromodomain BRD4(1) with E3 ubiquitin ligases, cereblon (**Figure 1.22A**) and VHL (**Figure 1.22B**) , respectively.[57,60] These structures have enabled the design of new PROTACs with better selectivity for BRD4 degradation, using computational protein-protein docking calculations to identify low energy binding complexes between BRD4(1) and the E3 ligase proteins.[60] The comparison of the cereblon and VHL crystal structures with BRD4(1) identified that unique cell surface interactions were being made in their respective ternary complexes (**Figure 1.22C**). The differing surface complementarities, between the E3 ligases and target proteins, may provide the explanation for the varying degradation efficacies that are observed when alternative E3 ubiquitin ligase inhibitors are employed in PROTAC development. However, the prediction of the surface complementarity for novel targets is a challenging task, and PROTAC design is typically based on empirical results.

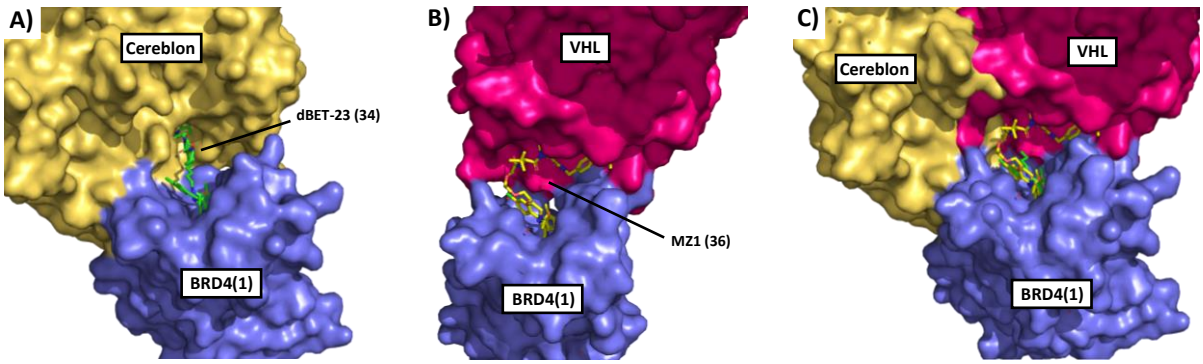


Figure 1.22 X-Ray crystal structures of ligase:PROTAC:target ternary complexes, highlighting difference in surface complementarities between BRD4(1) (surface:blue) and E3 ubiquitin ligases (A) cereblon (PDB: 6BOY, surface:yellow)[57] and (B) VHL (PDB: 5T35, surface:pink).[60] (C) Overlaid X-ray structures of both cereblon and VHL ternary complexes with BRD4(1).

Pre-clinical *in vitro* models with pan-BET PROTACs have been shown to inhibit growth of tumours more effectively than using the corresponding pan-BET inhibitor alone.[61] Furthermore, *in vivo* experiments in mice have demonstrated BET degraders to be well tolerated and to have low toxicities. Despite the impressive *in vitro* and *in vivo* pre-clinical activity demonstrated by the BET PROTACs, none have advanced for clinical development.[48] Nevertheless, the publication of the first BET PROTAC was reported less than five years ago, with this field showing great promise to provide new types of therapies for treating human cancers and other disease states.

1.4.3 DNA-encoded chemical libraries

In 1985, George P. Smith proposed the use of filamentous phage viruses as tools to display polypeptides on their surfaces. This idea led to the development of a viral entity which features a functional display property ('phenotype'), attached to its corresponding genetic information ('genotype').[62,63] This technology was successful applied in antibody phage display libraries and was used in the discovery of antibody Humira™, a multimillion-pound drug for the treatment of autoimmune diseases.[64] In 1992, Sydney Brenner and Richard A. Lerner postulated that the use of DNA alone could function as amplifiable bar codes to encode molecular entities (**Figure 1.23A**).[65] This approach led to the emergence of DNA-encoded libraries for affinity-based screening of up to one billion organic molecules against proteins of interest.[63] The identity and relative affinities of individual compounds can then be determined by polymerase chain reaction (PCR) procedures, followed by high-throughput DNA sequencing (HTDS) (**Figure 1.23B**).[62] This section will provide an overview of the different types of DNA-encoded libraries, as well as published examples of their applications.

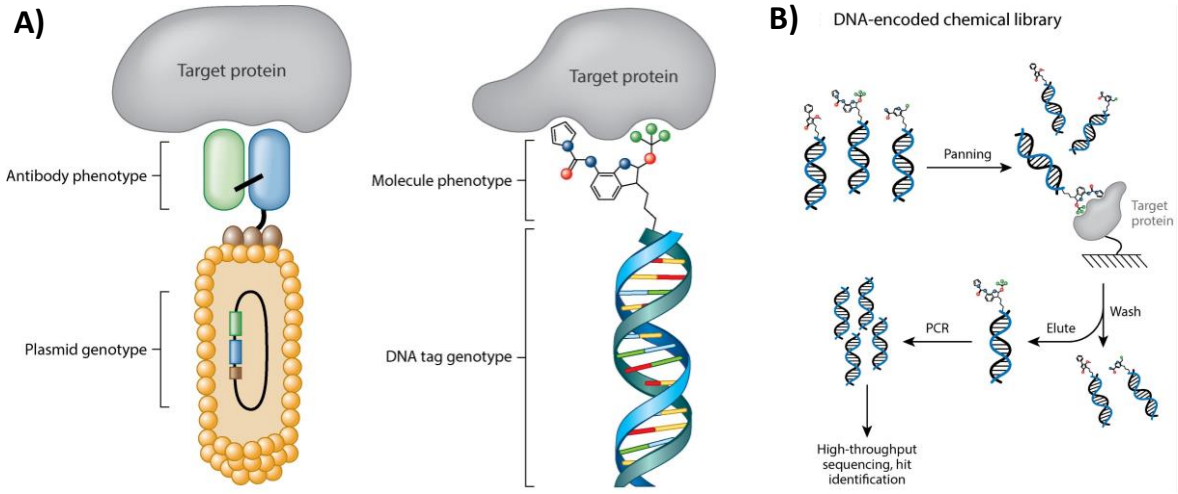


Figure 1.23 Schematic representation of (A) antibody phage display libraries and DNA-encoded chemical libraries and (B) and screening procedures with DNA-encoded chemical libraries. Large collections of organic molecules with DNA tags are screened in an affinity capture procedure. Enriched molecules can then be identified by PCR amplification followed by high-throughput DNA sequencing. Adapted with permission from Dario *et al*.[62]

1.4.3.1 Types of DNA-encoded chemical libraries

The advancement of DNA synthesis and amplification have enabled the facile creation and identification of individual chemical entities in large libraries. There are two types of DNA-encoded chemical libraries, 'single-pharmacophore' and 'dual-pharmacophore' libraries (**Figure 1.24**).[62]

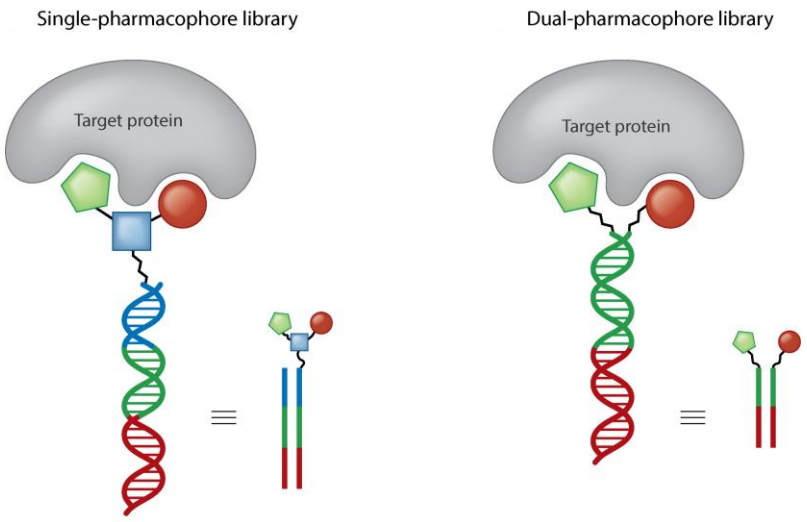


Figure 1.24 Schematic of single-pharmacophore and dual-pharmacophore libraries. Adapted with permission from Dario *et al*.[62]

For single-pharmacophore libraries, individual molecules are attached to distinctive DNA fragments, typically coupled to one of the complementary DNA strands. These libraries can consist of up to one billion different molecules and are constructed using split and pool synthesis procedures. For example, once the split DNA fragments are reacted with new and unique chemical moieties, creating structurally different pharmacophores, a ligation step attaches a new double-stranded DNA fragment to encode for the particular chemical reaction (**Figure 1.25**).[62] The DNA fragments are then pooled together for the process to be repeated.

In the case of dual-pharmacophore libraries, (also referred as encoded self-assembling chemical (ESAC) libraries), both DNA complementary strand are individually coupled to fragment-type molecules, creating two sub-libraries. In this setting, a single DNA strand which contains an abasic site, ('sub-library A'), is encoded with an oligonucleotide bar code. A second DNA strand ('sub-library B') recognises the abasic region of the 'sub-library A' DNA strand. A Klenow polymerisation step, which enables the synthesis of double stranded DNA from single stranded templates, encodes the 'sub-library A' bar code onto the 'sub-library B' DNA strand (**Figure 1.25**).[62] This enables the unambiguous identification of DNA strand combinations within the library.

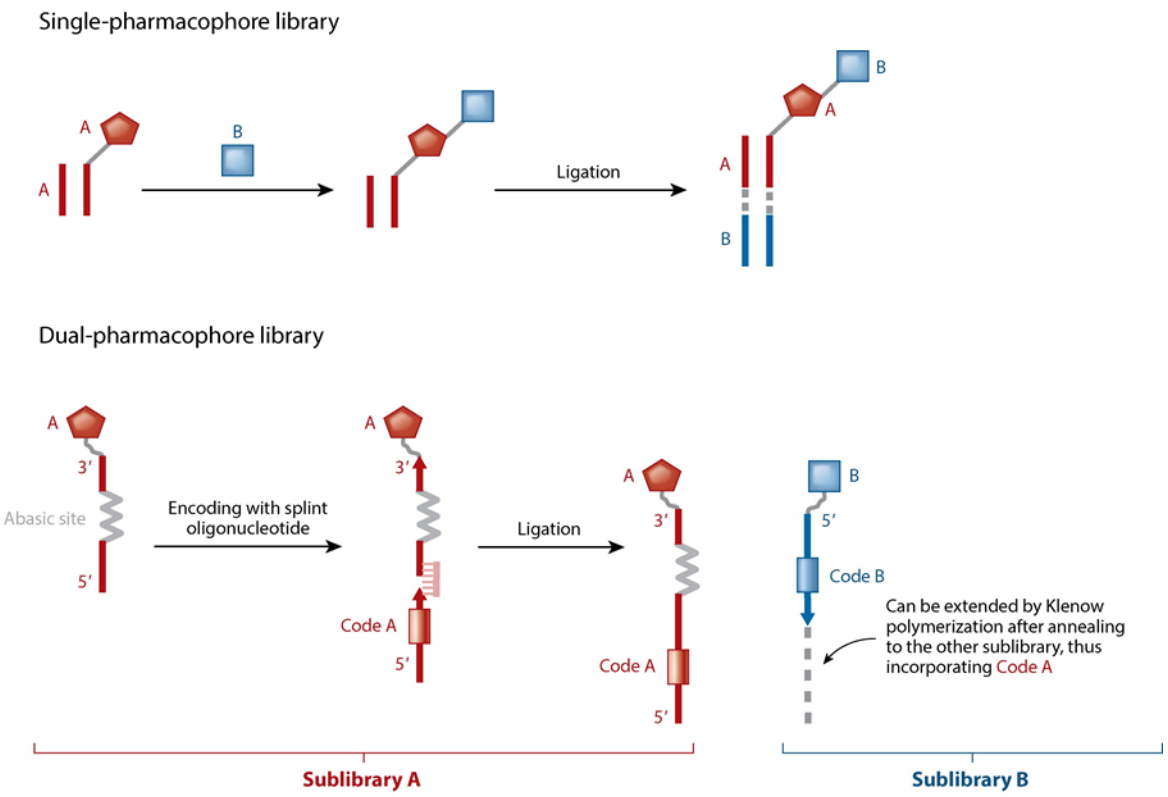
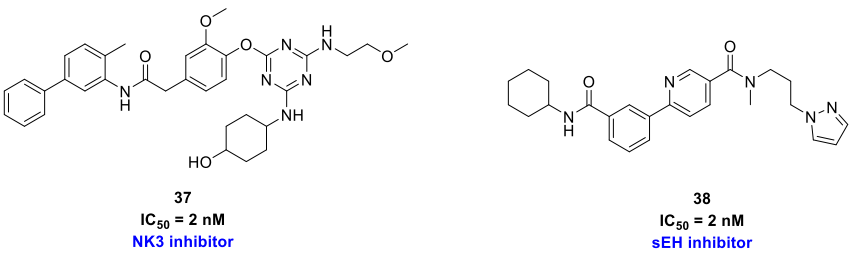


Figure 1.25 Schematic representation of encoding strategy for single-pharmacophore and dual-pharmacophore chemical libraries. Adapted with permission from Dario *et al*.[62]

1.4.3.2 Ligand discovery using DNA-encoded chemical libraries

Over the last decade, DNA-encoded chemical libraries have been routinely used in academia and industry to identify novel ligands for several different targets. GlaxoSmithKline constructed a 41 million single-pharmacophore DNA-encoded library (made from 3-sets of building blocks) that was based on a central 1,3,5-triazine scaffold. With this screen, they were able to identify inhibitor **37** as an antagonist for Neurokinin 3 with a (IC_{50} = 2 nM).[66] The biotechnology company X-Chem used a 334-million membered library (made from 3-sets of building blocks) to identify potent inhibitor **38** against soluble epoxide hydrolase (sEH), an important target involved in cardiovascular diseases (**Figure 1.26**).[67]



37
IC_{50} = 2 nM
NK3 inhibitor

38
IC_{50} = 2 nM
sEH inhibitor

Figure 1.26 Chemical structures of ligands identified through DNA-encoded chemical libraries.[66,67]

ESAC libraries have also been applied for drug discovery efforts in recent years. Wichert *et al*. reported the use of the same 100,000 membered DNA-encoded fragment library to identify high affinity ligands to target carbonic anhydrase IX and alpha-1-acid glycoprotein (AGP) proteins, respectively.[68,69] Furthermore, ESAC libraries have also been used in the identification of covalent inhibitors.[70] However, a challenge associated with ESAC technology is the identification of suitable connecting linkers to join individual fragments together when testing their 'off-DNA' binding. The fragments must be connected so that they are still able to interact with the associated regions of the target protein, without compromising the synergistic gain in affinity. Most reported examples use diamine linkers to connect the two individual fragments together *via* amide couplings, often maintaining high affinity for the protein target. Nevertheless, linker optimisation remains empirical at present.[63]

1.5 Project aim

As outlined in Section 1.3.3, the Conway group reported ligands **(*R*)10** and **(*R*)11** as one of the first high affinity CREBBP bromodomain ligands. However, their moderate selectivity over the BET family limited their applicability as chemical probes. The main focus of this thesis will be to apply medicinal chemistry-based techniques to improve affinity and selectivity of this ligand series. This will be achieved through 'traditional' approaches, such as bioisosteric modifications (Chapter 2), and more recent approaches, such as macrocyclic drug design (Chapter 3 & 4). In addition, this series of CREBBP bromodomain ligands will be used to develop PROTACs for the degradation of full-length CREBBP, providing a proof-of-concept for this target (Chapter 5). Finally, in a collaboration with Prof. Dario Neri's group (ETH Zurich), ESAC technology will be used to screen a library of fragments against the CREBBP bromodomain for the identification of novel ligands (Chapter 6).

Chapter 2

Amide bioisosteres to improve CREBBP bromodomain affinity and selectivity

2.1 Introduction and aims

The development of ligand **(*R*)10** to **(*R*)11**, discussed in Section 1.3.3, identified the THBD headgroup to be more stable when compared against the DHQ headgroup. In addition, enantiomer **(*S*)11** has no detectable binding to the CREBBP bromodomain, which provides a valuable negative control. However, when compared to **(*R*)10**, ligand **(*R*)11** did not show an improvement in affinity. This result was unexpected, as the THBD headgroup occupies a larger area space than the DHQ headgroup in the binding pocket, and therefore should have more van der Waal interactions to increase the binding enthalpy (Δ*H*) and the overall Gibbs free energy of binding.

It was previously shown for ligand **(*R*)10** that the intramolecular hydrogen bond, between aniline N-H of the headgroup and the carbonyl oxygen of the linker amide, is crucial for ligand binding, as it stabilises the bioactive conformation of the ligand.[25] Interestingly, the intramolecular hydrogen bond was not present for ligand **(*R*)11** when bound to the CREBBP bromodomain (**Figure 2.1A**). However, this intramolecular hydrogen bond was present in the small molecule X-ray structure of ligand **(*R*)11** (See Appendix E). It was postulated that if ligand **(*R*)11** has to break the intramolecular hydrogen bond to accommodate the bioactive conformation, this would have an unfavourable effect on the binding enthalpy (Δ*H*). To remove the intramolecular hydrogen bond, but without losing the structural pre-organisation present in the amide bond, it was rationalised that an *E*-alkene would be a suitable isosteric modification.[71] Furthermore, analogues with varying bond orders (single bond, *Z*-double bond and triple bond) would be prepared to study the effect that linker geometry and conformational flexibility have towards the binding affinity of the CREBBP bromodomain (**Figure 2.1B**).

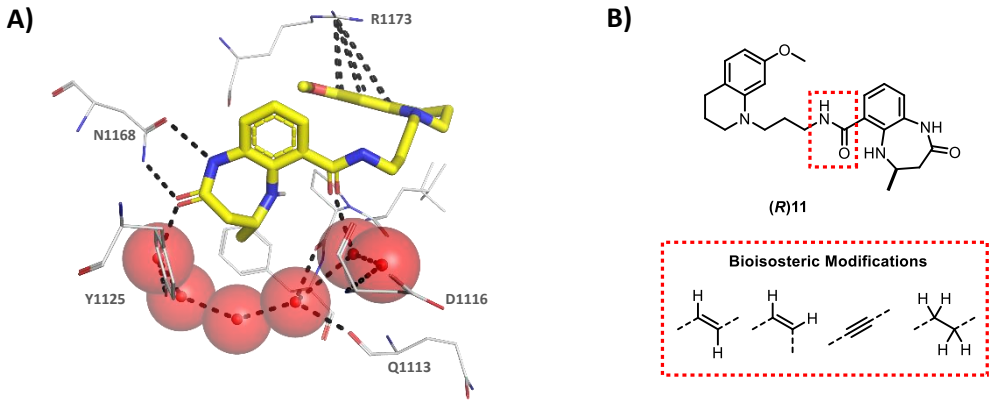
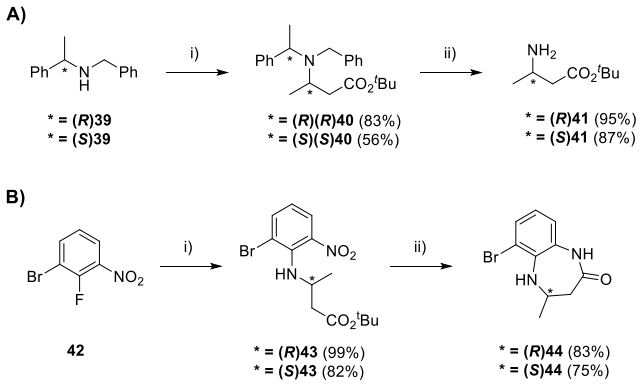


Figure 2.1 (A) Hydrogen bonding network present in the co-crystal structure of **(*R*)11** and CREBBP bromodomain, highlighting the absence of the intramolecular hydrogen bond between the amide carbonyl and aniline hydrogen. (B) Bioisosteric modification of the amide bond to study the effect of hydrogen bonding, geometry and conformational flexibility on binding affinity.

2.2 Synthesis of amide bioisosteric analogues

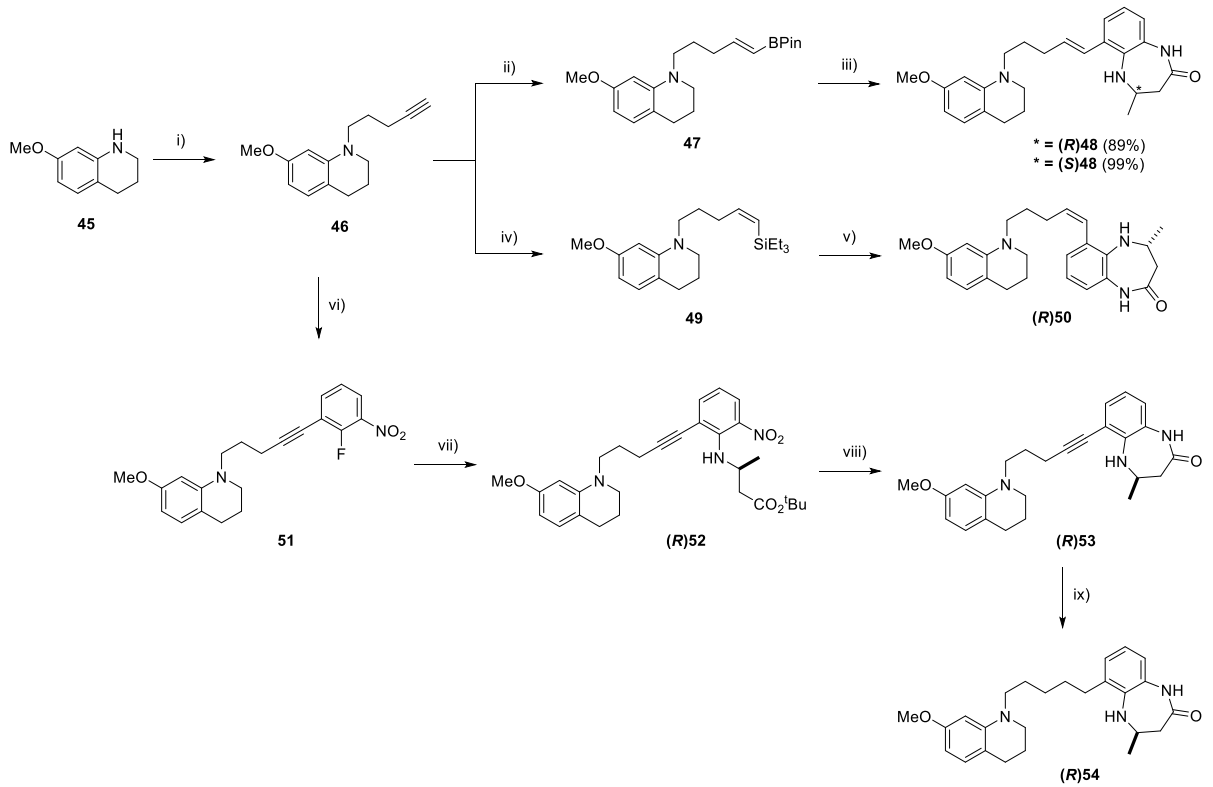
The synthetic approach to prepare the bioisosteric analogues used cross-coupling reactions to link the THBD headgroups and THQ fragments together. This allowed the facile synthesis of all the desired analogues. The synthesis of the THBD headgroups, **(*R*)44** and **(*S*)44**, used enantiopure chiral amines **(*R*)41** and **(*S*)41** prepared from chiral lithium amide methodology developed by Davies *et al.*[72] (**Scheme 2.1A**). The chiral amines were reacted in an S_NAr reaction with commercially available starting material **42**, to afford aniline intermediates **(*R*)43** and **(*S*)43**, respectively. These intermediates were then reacted with iron and acetic acid in a two-step procedure to yield the desired THBD headgroups (**Scheme 2.1B**).



Scheme 2.1 (A) Synthesis of the β-amino acid ester derivatives **(*R*)41** and **(*S*)41**. *Reagents and conditions:* (i) ^{n}BuLi, THF, −78 °C, 30 min, then *tert* butyl crotonate, THF, −78 °C, 5 h; (ii) **(*R*)(*R*)40**/**(*S*)(*S*)40**, H_2, $Pd(OH)_2$/C, MeOH/H_2O, AcOH, 20 h; (B) Synthesis of THBD headgroups **(*R*)44 and (*S*)44**. *Reagents and conditions*: (i) **(*R*)41**/**(*S*)41**, DIPEA, DMF, 85 °C, 14 h; (ii) **(*R*)43**/**(*S*)43**, TFA, CH_2Cl_2, rt, 2 h, then Fe, AcOH, 100 °C, 4 h.

The THQ fragments were prepared by alkylation of **45** to yield alkyne **46** (**Scheme 2.2**). This approach enabled a divergent synthesis, as alkyne **46** could be used as a common intermediate to prepare precursors for the different cross-coupling reaction. Alkyne **46** was reacted in a hydroboration with pinocolborane to yield the borate ester **47**, prepared with a catalytic amount of Schwartz's reagent to afford high *E*-selectivity.[73] The borate ester **47** was then reacted in a Suzuki-Miyaura cross-coupling with **(*R*)44** and **(*S*)44** to give enantiomers **(*R*)48** and **(*S*)48** with *E*-double bond stereochemistry, respectively. To achieve the *Z*-double bond geometry, a ruthenium catalyzed hydrosilylation of **46** was employed to afford silane **49**.[74] Intermediate **49** was then used in a boro-desilylation with BCl_3, forming a borate intermediate *in situ*, which was subsequently reacted in a Suzuki-Miyaura cross-coupling with **(*R*)44** to yield *Z*-alkene **(*R*)50**. Initial attempts to prepare the alkyne analogue **(*R*)53** used a Heck alkynylation with alkyne **46** and THBD fragment **(*R*)44**. However, this approach resulted in an undesired Larock-indole formation as the major product, a result of having an aniline adjacent to the alkyne

moiety in the presence of a palladium catalyst. To avoid this side reaction, alkyne **46** was reacted in a Sonogashira coupling with starting material **42** to afford internal alkyne **51**. This intermediate was then reacted in an S_NAr reaction with chiral amine **(*R*)41**, followed by THBD headgroup formation, to yield the desired alkyne analogue **(*R*)53**. The single bond analogue **(*R*)54** was prepared through the hydrogenation of the alkyne in compound **(*R*)53**. All bioisosteric analogues were synthesised by Dr James Clayton in the group of Prof. Stuart Conway (University of Oxford).



Scheme 2.2 Synthesis of THBD analogues **(*R*)48**, **(*S*)48**, **(*R*)50**, **(*R*)53** and **(*R*)54**. *Reagents and conditions*: (i) **45**, pent-4-yn-1-yl methanesulfonate, KI, DIPEA, DMF, μλ, 100 °C, 1 h, 62%; (ii) **46**, HBPin, Cp_2ZrClH, DCE, 60 °C, 20 h, 72%; (iii) **(*R*)44**/**(*S*)44**, **47**, $Pd(PPh_3)_2Cl_2$, K_2CO_3, 1,4-dioxane, H_2O, 100 °C; (iv) **46**, Grubbs 1st generation catalyst, $HSiEt_3$, Tol, 40 °C, 2 h, 69%; (v) **49**, 1 M BCl_3 in heptane, CH_2Cl_2, 0 °C, 16 h, then **(*R*)44**, $Pd(Amphos)_2Cl_2$, K_2CO_3, toluene, THF, EtOH, H_2O, 100 °C, 80% over two steps; (vi) **42**, **46**, $Pd(OAc)_2$, Cu(I)I, PPh_3, NEt_3, 100 °C, 44%; (vii) **(*R*)41X**, **51**, DIPEA, DMF, 85 °C, 14 h, 66%; (viii) **(*R*)52**, TFA, CH_2Cl_2, rt, 2 h, then Fe, AcOH, 100 °C, 30 min, 44%; (ix) **(*R*)53**, H_2, 10% Pd/C, EtOH, rt, 3 h, 78%.

2.3 Biological evaluation of the bioisosteric analogues

2.3.1 Intramolecular hydrogen bond analysis by ^{1}H NMR

^{1}H NMR can be used to observe the presence and strength of an intramolecular hydrogen bond in solution. This is achieved by the observation of the chemical shift difference for the given hydrogen atom when the NMR solvent is changed from $CDCl_3$ to DMSO-d_6. The chemical shift of hydrogen atoms that are not engaged in intramolecular hydrogen bonds typically show a Δ_{ppm} $CDCl_3$→DMSO-d_6 = 2–4 ppm, as their environment is predominantly dictated by the surrounding solvent. However, hydrogen atoms that are involved in an intramolecular hydrogen bond typically show Δ_{ppm} $CDCl_3$→DMSO-d_6 < 1 ppm, as their environment is less affected by the surrounding solvent. This analysis was applied to compounds **(*R*)11** and **(*R*)48**. For **(*R*)11**, the signals for the amide and lactam protons shifted downfield (Δ_{ppm} = 2.23 ppm and 2.35 ppm, respectively), but the proton of the secondary aniline showed only a small change in chemical shift (Δ_{ppm} = −0.12 ppm) (**Figure 2.2A**). This is consistent with the secondary aniline being involved in an intramolecular hydrogen bond for ligand **(*R*)11**. In contrast, both the lactam and secondary aniline from **(*R*)48** have a notable chemical shift change (Δ_{ppm} = 2.05 ppm and 1.12 ppm, respectively), indicating no intramolecular hydrogen bond engagement, which was expected for the *E*-alkene (**Figure 2.2B**). In conclusion, this ^{1}H NMR analysis showed the intramolecular hydrogen bond was removed following the isosteric modification to ligand **(*R*)48**. This study was performed by Dr Matthias Schiedel in the group of Prof. Stuart Conway (University of Oxford).

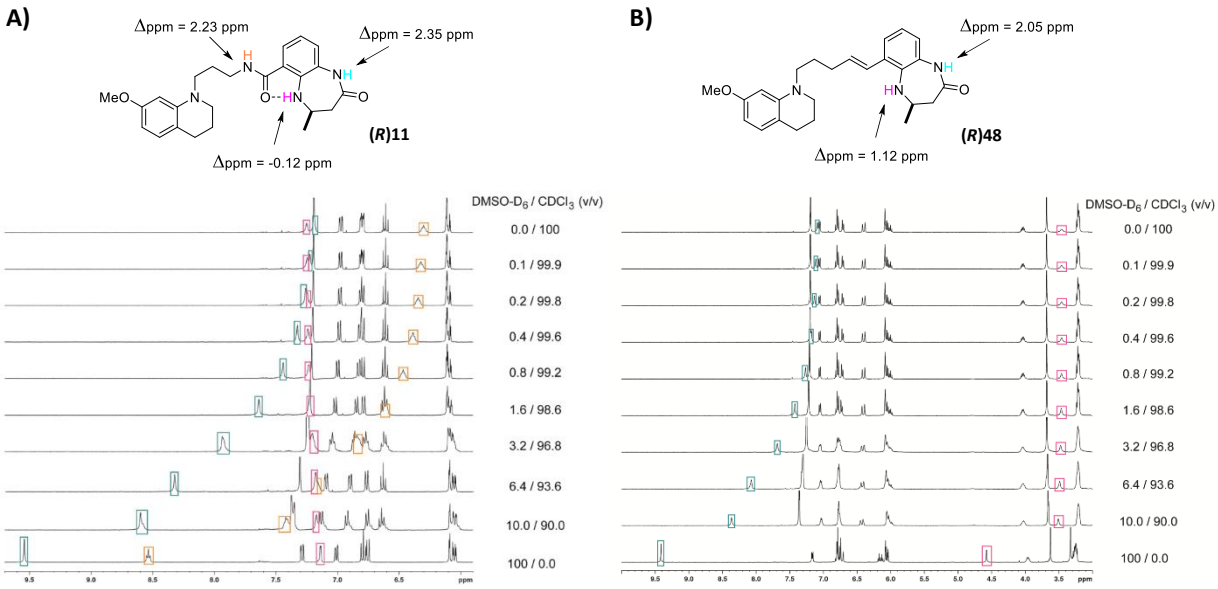
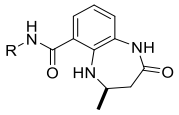
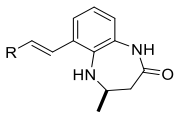
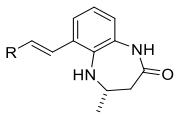
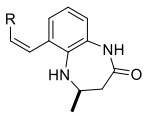
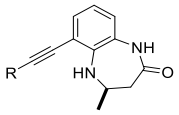
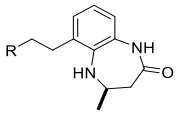


Figure 2.2 Study to observe the internal hydrogen bond (proton shown in red) in solution for (A) **(*R*)11** and (B) **(*R*)48**. ^{1}H NMR spectra of the compounds dissolved in different mixtures of $CDCl_3$ and DMSO-d_6. All experiments were performed at a compound concentration of 2 mg/mL.

2.3.2 Affinity data for CREBBP bromodomain

The analogues prepared in Section 2.2 were evaluated by isothermal titration calorimetry (ITC) to determine their K_d values for the CREBBP bromodomain (**Table 2.1**). The *E*-alkene isostere **(*R*)48**, showed a 5-fold increase in binding affinity for the CREBBP bromodomain (K_d = 96 nM). Enantiomer **(*S*)48** showed no detectable binding and provides a valuable negative control. Interestingly, the *Z*-alkene and triple bond analogues **(*R*)50**, and **(*R*)53**, also showed low nanomolar affinity (K_d = 329 nM and K_d = 171 nM, respectively), indicating these alternative geometries are still accommodated in the binding pocket of the CREBBP bromodomain. Compound **(*R*)54**, which has a fully saturated linker, gave no detectable binding and emphasised that a degree of conformational rigidity is important for maintaining affinity.

Table 2.1 Affinity data for amide analogues against the CREBBP bromodomain. ITC traces are shown in Appendix C1 and BromoScan data in Appendix D. R = 3-(7-methoxy-3,4-dihydroquinolin-1(2H)-yl)propyl.

	Compounds	ITC K_d/μM CREBBP	BromoScan K_d/μM CREBBP
(*R*)11		0.490 ± 0.16	0.330
(*R*)48		0.096 ± 0.03	0.180
(*S*)48		n.b.	n.b.
(*R*)50		0.329 ± 0.08	n.t.
(*R*)53		0.171 ± 0.04	n.t.
(*R*)54		n.b.	n.t.

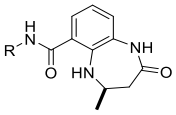
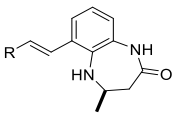
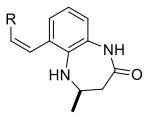
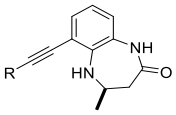
n.b.: no binding; n.t.: not tested.

A BromoScan assay was used as an orthogonal approach to assess the binding affinity to the CREBBP bromodomain. This data was consistent with the ITC results, showing an increased affinity for ligand **(*R*)48** (K_d = 170–190 nM), when compared to ligand **(*R*)11** (K_d = 260–400 nM).

2.3.3 Selectivity data against BRD4(1) bromodomain

As mentioned in Section 1.3.3, ligands **(*R*)10** and **(*R*)11** only showed moderate selectivity over BRD4(1) (K_d = 1.40 μM and K_d = 3.04 μM, respectively), and achieving high selectivity against the BET family of bromodomain has been a major challenge in the field.[75] ITC studies with BRD4(1) were used to determine the selectivity profile of the amide bioisosteric analogues. It was observed that the *Z*-alkene analogue **(*R*)50** had a 2-fold increase in affinity to BRD4(1), compared to the amide ligand **(*R*)11**. We were pleased to observe that *E*-alkene isostere **(*R*)48** and alkyne analogue **(*R*)53** showed no detectable binding to BRD4(1) by ITC. These results underlines the crucial role this region has on the selectivity against BRD4(1) (**Table 2.2**).

Table 2.2 Affinity data for amide analogues against the BRD4(1) bromodomain. ITC traces are shown in Appendix C2 and Ligand observed ^{1}H NMR binding data in Appendix D3. R = 3-(7-methoxy-3,4-dihydroquinolin-1(2H)-yl)propyl.

	Compounds	ITC K_d/μM BRD4(1)	NMR K_d/μM (BRD4(1))
(*R*)11		3.04 ± 0.79	5.80 ± 0.99
(*R*)48		n.b.	10.3 ± 1.89
(*R*)50		1.41 ± 0.21	2.03± 0.41
(*R*)53		n.b	n.t.

n.b.: no binding; n.t.: not tested.

In an attempt to quantify the selectivity of analogue **(*R*)48** for the CREBBP bromodomain over BRD4(1), the use of an orthogonal ligand-observed ^{1}H NMR-based binding assay was investigated. As the ITC studies showed ligands **(*R*)11** and **(*R*)50** were able to bind to BRD4(1), these ligands were included as positive controls. The binding of these compounds to BRD4(1) was followed by observing the signal reduction of the methyl group found on the THBD headgroup upon addition of the protein (See Appendix D3). Ligand **(*R*)48** was determined to have a K_d = 10.3 μM for BRD4(1), indicating >100-fold selectivity for the CREBBP bromodomain over BRD4(1). In addition, compound **(*R*)11** (K_d = 5.80 μM) and **(*R*)50** (K_d = 2.03 μM) were consistent with the K_d values obtained from ITC (K_d = 3.04 μM and

K_d = 1.41 µM, respectively). This NMR study was performed in collaboration with Corentine Laurin in the group of Prof. Stuart Conway (University of Oxford).

To further assess the selectivity of **(*R*)48**, a BromoScan assay was used to determine K_d values against a phylogenetically-diverse panel of 12 bromodomains (**Figure 2.3**). This assay showed ligand **(*R*)48** to be selective for the CREBBP and EP300 bromodomains, displaying no binding for the remaining bromodomains at concentrations of up to 1 µM. The same assay showed enantiomer **(*S*)48** to have no binding to any of the bromodomain tested at concentrations of up to 1 µM. The selectivity data showed ligand **(*R*)48** to be suitable for use in cellular settings to probe the effect of inhibiting the CREBBP and EP300 bromodomain function.

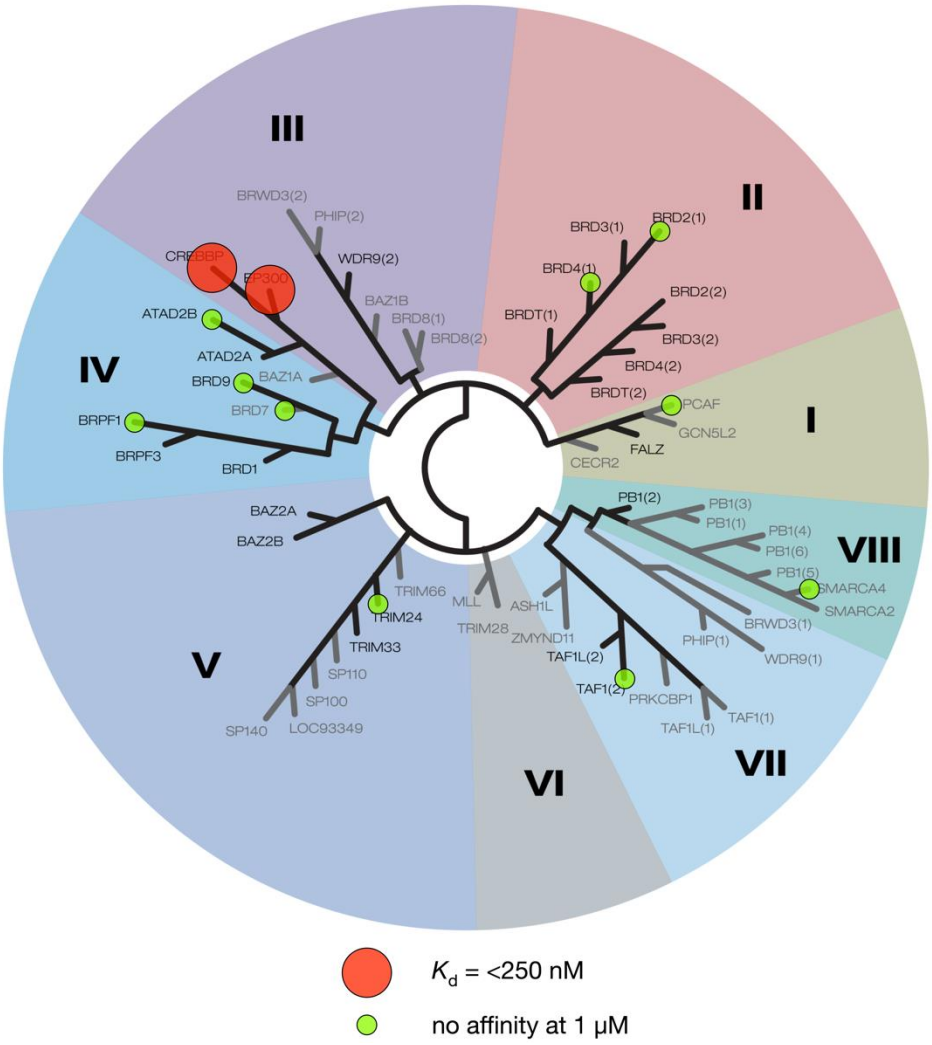


Figure 2.3 A representation of the bromoKdELECT data for **(*R*)48**. Binding was observed for the CREBBP and EP300 bromodomain. No binding was seen for any other bromodomains at concentrations up to 1 µM.

2.3.4 X-ray crystallography of ligand (*R*)48

Dr Sarah Picaud and Prof. Panagis Filippakopoulos (SGC, Oxford) were able to obtain a protein-ligand crystal structure of **(*R*)48** bound to the CREBBP bromodomain. The resulting structure had a unit cell of seven proteins to seven ligands (**Figure 2.4A**). The THBD headgroup showed a binding mode similar to the crystal structure observed for **(*R*)11** (**Figure 2.1A**), forming hydrogen bonding interactions with the N1168 residue inside the binding pocket. Surprisingly, the THQ moiety had formed an interaction with the R1173 residue of a neighboring CREBBP bromodomain. This revealed an unprecedented dimerisation of two CREBBP bromodomain proteins binding to two of the ligands (**Figure 2.4B**).

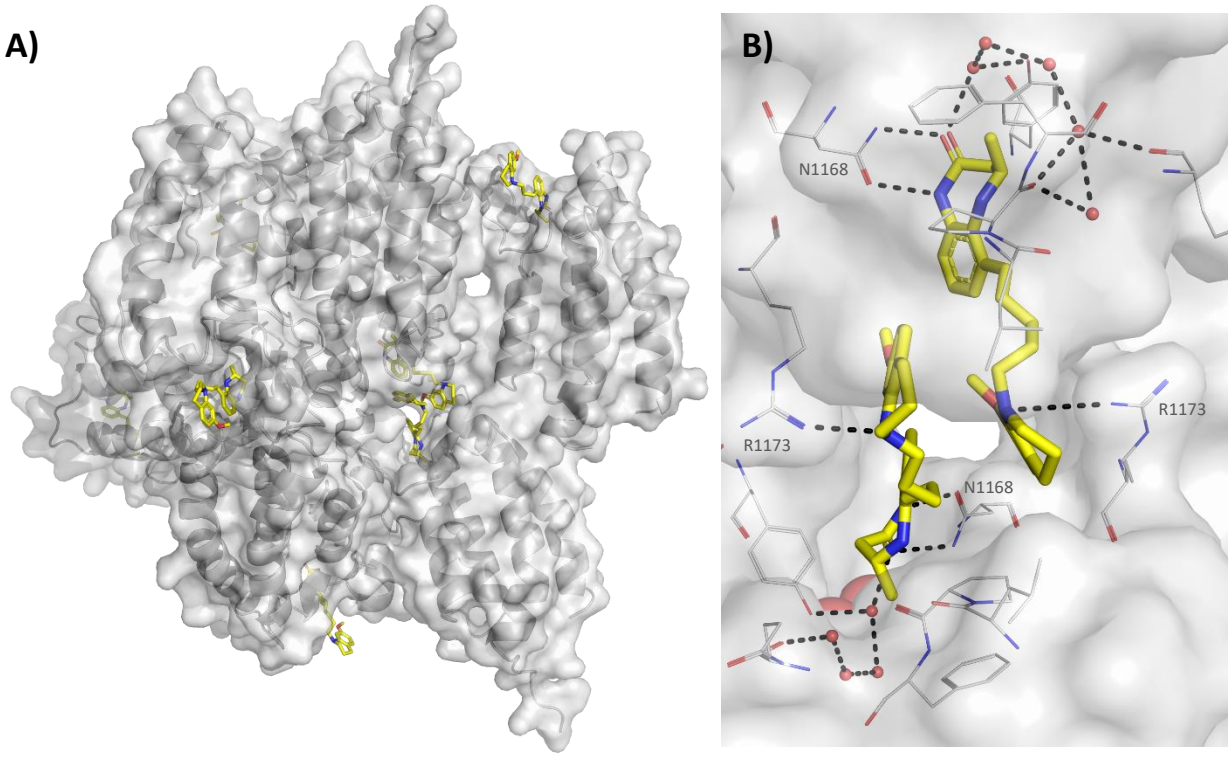


Figure 2.4 (A) X-Ray crystal structure of **(*R*)11** with CREBBP bromodomain which shows a 7:7 ligand to protein ratio. (B) A closer view shows dimeric interactions between the CREBBP bromodomains containing two ligands. R1173 residues are observed to have interactions with the THQ moiety of a ligand from the neighbouring bromodomain.

Size Exclusion Chromatography (SEC) was used to study whether **(*R*)48** induces the dimerisation of two CREBBP bromodomains in the solution state, or if this observation is a crystallographic artefact. SEC has been widely reported in the literature for the verification of bivalent bromodomain ligands.[76,77] The SEC experiment did not indicate that a dimerisation event was occurring in solution (Appendix D4). It is suspected that the observed dimerisation is due to a crystallographic artefact.

To predict the likely monomeric binding mode for **(*R*)48**, MD simulations were performed by Joseph Bluck in the groups of Prof. Stuart Conway (University of Oxford) and Prof. Phil Biggin (University of Oxford). It was predicted that in the presence of a single CREBBP bromodomain, **(*R*)48** would reform the cation-π interaction between the THQ moiety and residue R1173 (**Figure 2.5**). This computationally generated binding mode was shown to be consistent with the observed poses seen in the co-crystal structure of **(*R*)10**[25] and **(*R*)11** (**Figure 2.1**) with the CREBBP bromodomain. We therefore assume that **(*R*)48** binds in a similar fashion in solution.

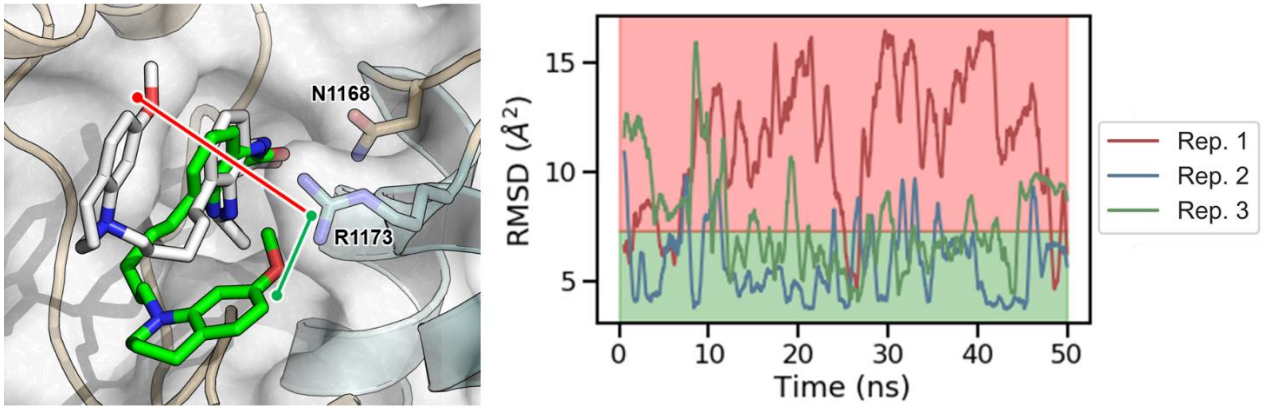


Figure 2.5 Recovery of the electrostatic interaction with R1173 through MD simulations. The distance between R1173 and the π-system of **(*R*)48** drops to below 7 Å during equilibrium MD simulations, where the initial pose (carbon:white) settles during MD to the predicted binding mode (carbon:green). Simulations were carried out in triplicate.

2.3.5 *In vitro* cell data for ligand (*R*)48

With high affinity for the CREBBP bromodomain (K_d = 96 nM), high selectivity over BRD4(1), and no effects on a phylogenetically-diverse panel of bromodomains, ligand **(*R*)48** was determined to be suitable for probing the CREBBP bromodomain function in cells. Upon treatment of human colorectal cancer cells (HCT116) with **(*R*)48** (10 μM), the expression of the transcription factor c-Myc was reduced after 6 h, with more substantial effects observed after 16 h and 24 h (**Figure 2.6A**). These effects were observed on the level of c-Myc RNA, confirming that the CREBBP/EP300 bromodomain inhibitions affects c-Myc at the transcriptional level. Treatment of the HCT116 cells with **(*S*)48** (10 μM) showed no effect on c-Myc expression after 24 h (**Figure 2.6B**). This supports the hypothesis that these effects occur through the selective inhibition of CREBBP/EP300 function. This study was performed by Dr Ania Skwarska in the group of Prof. Ester Hammond (University of Oxford).

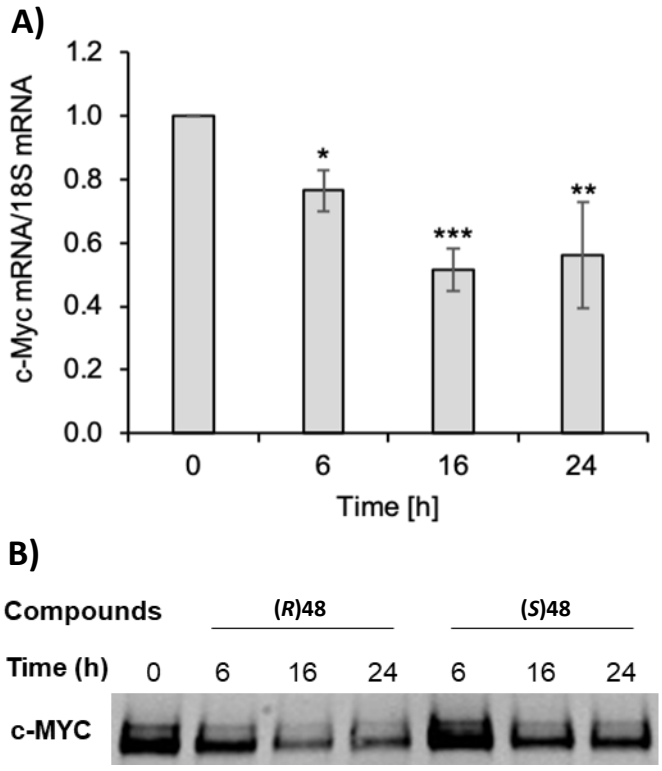


Figure 2.6 Treatment of HCT116 cells with **(*R*)48** shows reduced c-Myc expression. (A) Quantative-PCR was used to determine c-Myc mRNA levels compared to 18S mRNA. Data were analysed using one-way ANOVA. *P<0.05; **P<0.01; ***P<0.001. (B) Western blots showing the reduction of c-Myc levels when HCT116 cells are treated with **(*R*)48**, but no reduction of c-Myc after the treatment with **(*S*)48**.

2.4 Conclusion

The loss in potency observed in the development of ligand **(*R*)10** to **(*R*)11** was postulated to be due to an energy barrier associated with breaking an intramolecular hydrogen bond formed in solution upon protein binding. This hypothesis was validated through ^{1}H NMR and ITC experiments (both solution state) with ligand **(*R*)48** showing an increased binding affinity to the CREBBP bromodomain. In addition, the *Z*-alkene, single and triple bond compounds, **(*R*)50**, **(*R*)54** and **(*R*)53** respectively, gave valuable insight to the effect that these geometries have on the binding affinity. For the CREBBP bromodomain, ligands **(*R*)50** and **(*R*)53** saw an increase in affinity compared to **(*R*)11**, but **(*R*)54** gave no detectable binding. This indicated that some conformational restraint is required for the binding affinity. This region was also shown to be crucial for selectivity over the BET family of bromodomain, which was not previously known. *Z*-Alkene **(*R*)50** had an increased affinity for BRD4(1) compared to **(*R*)11**, however, ITC studies showed no detectable binding for **(*R*)48** and **(*R*)53**. To assess the selectivity profile of **(*R*)48**, ^{1}H NMR-based binding assay determined a >100-fold difference in affinity between the CREBBP bromodomain and BRD4(1). A BromoScan assay determined ligand **(*R*)48** to be selective for the CREBBP/EP300 bromodomains at a concentration of 1 µM when screened against a phylogenetically-diverse panel of 12 bromodomains.

Acyclic ligand **(*R*)48** provides the basis for a good CREBBP bromodomain probe. However, its selectivity profile against the BET family may not be high enough to distinguish CREBBP function at pharmacological doses. Approaches to improve affinity; selectivity and physicochemical properties, would enable the identification of a powerful tool molecule to probe the role of CREBBP in an *in vivo* setting.

Chapter 3

Macrocycles as CREBBP bromodomain ligands – first generation

3.1 Introduction and aims

The term 'chemical probe' has been defined as "… *a selective small-molecule modulator of a protein's function that allows the user to ask mechanistic and phenotypic questions about its molecular target in biochemical, cell-based or animal studies.*"[78] A critical view of the probes published in the bromodomain field is that, although most of these probes display a high selectivity for a sub-set of bromodomains, they retain a lower, yet significant, affinity for different bromodomains families.[79] This is particularly true for the BET family of bromodomains (BRD2, BRD3, BRD4 and BRDT), as even partial inhibition can lead to phenotypic responses, masking the phenotype attributed to the target bromodomain. A recent Nature Communication article stated that due to the high sequence homology of the known 61 human bromodomains, and the sharing of a common mechanism for KAc recognition, the task of achieving absolute selectivity for a single bromodomain is very challenging.[75] Consequently, the identification of a selective ligand for the CREBBP bromodomain is a sought-after probe in the epigenetic field. As discussed in Section 1.3.3, the previously reported CREBBP bromodomain ligands, **(*R*)10** and **(*R*)11**, only have a moderate selectivity over BRD4(1). The work in Section 2.3.3 identified that ligand **(*R*)48** has >100-fold selectivity against BRD4(1), however, the diastereomer **(*R*)50** retained affinity for BRD4(1). This highlights that there is a great subtlety in achieving selectivity for this family of related ligands.

To gain a better insight in to how we might design CREBBP bromodomain ligands that are selective over the BET family of bromodomains, Dr Sarah Picaud and Prof. Panagis Filippakopoulos (SGC, Oxford) obtained a protein-ligand co-crystal structure of **(*R*)11** bound to the BRD4(1) bromodomain. Upon comparing the X-ray crystal structures of **(*R*)11** bound to the CREBBP bromodomain (**Figure 3.1A**) and to BRD4(1) (**Figure 3.1B**), it was observed that **(*R*)11** adopts two distinct binding poses. When bound to the CREBBP bromodomain, it is observed that the THQ moiety forms a cation-π interaction with R1173 and is in close proximity to the THBD headgroup. In the BRD4(1) crystal structure, ligand **(*R*)11** sits in a linear conformation, with the THQ moiety orientated away from the THBD headgroup, forming hydrophobic interactions with the WPF shelf.

As the THQ and THBD groups are close in space when bound to the CREBBP bromodomain, it was rationalised that a macrocyclic design to link these groups together would promote the bioactive conformation of **(*R*)11** (**Figure 3.1A**). In contrast, ligand **(*R*)11** would be unable to adopt the conformation required to bind to BRD4(1), if constrained as a macrocycle (**Figure 3.1B**). These observations led to the prediction that a macrocyclic ligand for the CREBBP bromodomain would

provide high selectivity against the BET family of bromodomains. In addition, there is strong literature precedence for macrocyclic ligands to have high binding affinities, due to their ability to adopt a solution-state conformation that is closer to the protein-bound conformer.[46] The work in this chapter explores the use of a macrocyclic drug design approach, using molecular docking, to identify if a macrocyclic ligand that could be tolerated in the CREBBP bromodomain binding site.

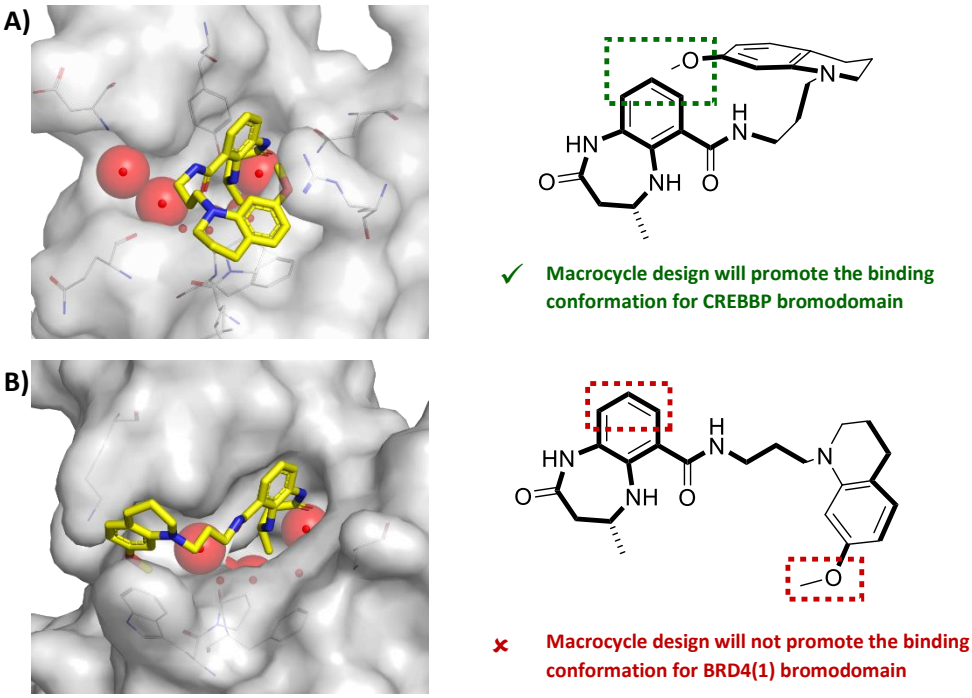


Figure 3.1 Co-crystal structures of **(*R*)11** (carbon:yellow) and (A) CREBBP bromodomain and (B) BRD4(1). Ligand **(*R*)11** adopts different conformations when binding to the two bromodomains. Based on these conformations, it is hypothesised that a macrocycle based on **(*R*)11** would be accommodated in the KAc binding site of CREBBP bromodomain but not that of BRD4(1).

3.2 Computational design

3.2.1 Macrocycle library design

The SAR data that was known at the start of this study is shown in **Figure 3.2**. Although ligand **(*R*)11** had lower affinity for the CREBBP bromodomain than **(*R*)10**, the benefits of using the more stable THBD headgroup was considered to be a more desirable starting point. Dr Michael Brand reported ligand **(*R*)55** to have higher selectivity against BRD4(1) when compared to **(*R*)10**, with the only difference being the removal of the THQ ring.[30] The use of weaker binding ligands to guide the design was not considered problematic, as there is potential for a significant improvement in affinity, if the macrocycle is able to bias the conformation closer to that of the binding pose.

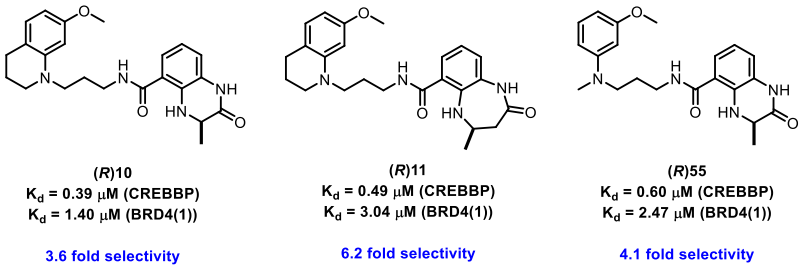


Figure 3.2 Previously reported SAR and selectivity data for the CREBBP bromodomain.[25,30]

Using **(*R*)11** as a template, the main consideration for the design of the macrocycle were; the position of linking to the THBD headgroup, removal of the THQ ring; the length of the linker chain and the consequent ring size. The linkers that would join the THQ and THBD groups together would initially be simple alkyl chains. The rationale was that, if a macrocycle bound to the CREBBP bromodomain, a structure-based drug design approach could then be used to explore more complex linkers. In this first instance, a small library of 30 macrocycles were designed around the considerations shown in **Figure 3.3**.

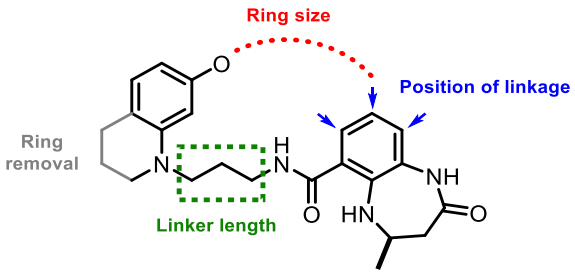
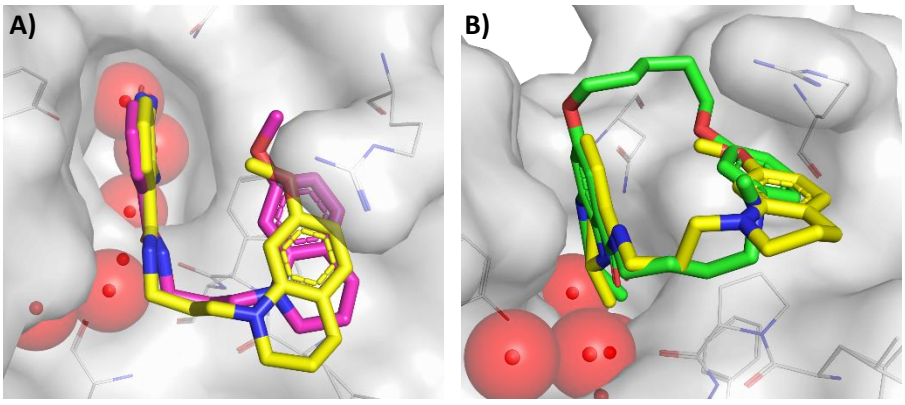


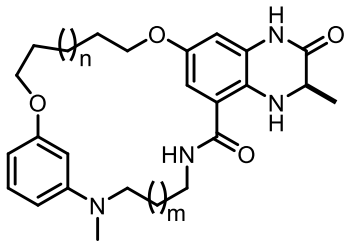
Figure 3.3 Macrocyclic library design considerations based on ligand **(*R*)11**.

3.2.2 Molecular docking of the macrocycle library

The computational study was performed using the molecular docking software CLC Drug Discovery Workbench 2.5. To validate the docking software's accuracy, the acyclic ligands **(*R*)10** and **(*R*)11** were docked with the CREBBP bromodomain and compared to the conformation observed in their respective X-ray crystal structures. The binding conformation was most accurately predicted for **(*R*)10**, with only a slight discrepancy observed for the THQ moiety (**Figure 3.4A**). This discrepancy is due to the software's inability to identify cation-π interactions, which are computationally demanding to predict. As this docking study matched well to the X-ray crystal structure of **(*R*)10**, the macrocycle library was modified to include the DHQ headgroup for the purpose of docking. The assumption was made that the DHQ and THBD headgroups adopt similar binding modes, therefore, any hits from the docking study would be prepared with the THBD headgroup for the reasons discussed in Section 3.2.1.



C)



	n, m values	Docking Score
(*R*)10	-	**−73.31**
(*R*)56	**n=1, m=2**	**−73.41**
(*R*)57	**n=1, m=1**	**−60.51**
(*R*)58	**n=2, m=1**	**−52.88**

Figure 3.4 Molecular docking study of macrocycle library with the CREBBP bromodomain. (A) Docked ligand **(*R*)10** (carbon:magenta) adopts a similar binding pose to the X-ray crystal structure (PDB:4NYX; carbon:yellow). (B) Docked macrocyclic ligand **(*R*)56** (carbon:green) adopts a similar binding pose to the X-ray crystal structure of acyclic ligand **(*R*)10** bound to the CREBBP bromodomain (PDB:4NYX; carbon:yellow) (C) Docking scores of the ranked macrocyclic hits compared against the acyclic ligand **(*R*)10**.

The library of macrocycles were screened and ranked on the basis of two criteria; their ability to adopt the desired binding conformation; and their relative docking scores. The docking scores that are generated by the CLC Drug Discovery Workbench 2.5 are calculated based on the sum of five contacts over a distance of 5.5 Å (Appendix B1).[80] This should not be over-interpreted and was only used as a guide for the ranking of the docked structures.

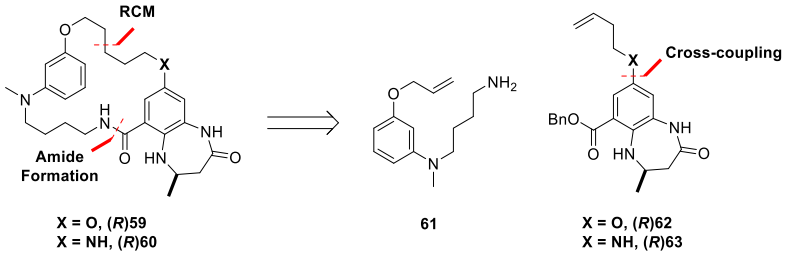
The computational study revealed **(*R*)57** as the only macrocycle predicted to adopt the desired binding pose. This hit enabled the prediction of the optimum position to attach the linker to the THBD headgroup, and also indicated that the removal of the THQ ring would lead to retained CREBBP bromodomain affinity. However, macrocycle **(*R*)57** gave a more unfavourable docking score compared to the acyclic ligand **(*R*)10** (**Figure 3.4C**). As the docking software allows the direct modification of docked structures in their binding sites, this feature was used to predict the optimum ring size for the macrocyclic ligand. Extending chain length between the aryl ethers gave **(*R*)58**, which had a worse docking score than the initial hit **(*R*)57**. However, extension of the chain length between the amide and tertiary amine gave **(*R*)56**, which had a similar docking score to the acyclic ligand **(*R*)10**, while retaining the desired binding pose (**Figure 3.4B**). Unfortunately, attempts to redock macrocycle **(*R*)56** were unsuccessful. Macrocycles are computationally challenging to model, as most docking software incorrectly treat them as rigid systems, ineffectively sampling the possible conformation they are able to adopt.[81] Nevertheless, the decision was made to pursue the synthesis of macrocyclic ligands based around the structure of macrocycle **(*R*)56**.

3.3 Synthesis of target macrocycles

3.3.1 Synthetic strategy: Ring closing metathesis macrocyclisation

3.3.1.1 Retrosynthetic Analysis

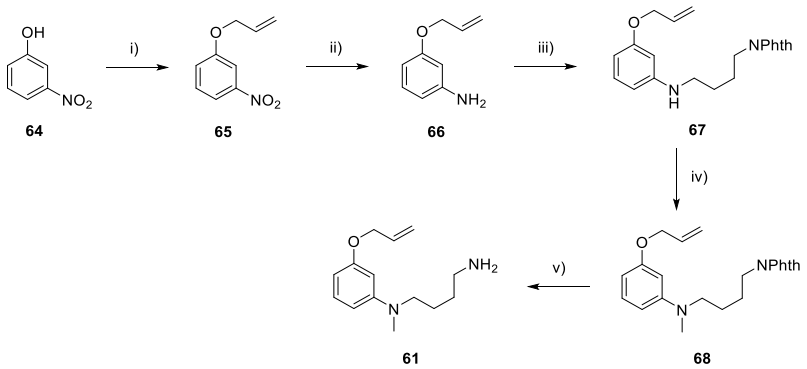
The computational study provided the key information with regards to the THBD headgroup point of attachment; linker length and macrocycle ring size; leading to the design of the target macrocycles **(*R*)59** and **(*R*)60**. The preparation of the macrocycles was envisaged to use a ring-closing metathesis (RCM) as the macrocyclisation step, and a disconnection at the amide bond to give the two fragments shown in **Scheme 3.1**. Macrocycles **(*R*)59** and **(*R*)60** differ by a single heteroatom which is due to the different cross-coupling reactions available to install the terminal alkene linkers onto the THBD headgroup.



Scheme 3.1 Retrosynthetic analysis of designed macrocycles ***(R)*59** and **(*R*)60** using RCM as the macrocyclisation step.

*3.3.1.2 Synthesis of fragment **61***

For the preparation of primary amine **61** (**Scheme 3.2**), 3-nitrophenol, **64**, was reacted in an allylation reaction, followed by reduction of the nitro- group using iron powder and ammonium chloride, to afford aniline **66**. A risk associated with heating allyloxy-aryl compounds is the possibility for a [3,3]-sigmatropic Claisen rearrangement,[82] however, this side-product was not observed. Aniline **66** was alkylated with *N*-(4-bromobutyl)phthalimide) and then iodomethane to afford the tertiary amine **68** in good yields. Initial attempts to methylate **67** were low yielding due to over alkylation. Lowering the number of equivalents of iodomethane led to improved yields. The final step used hydrazine to deprotect the phthalimide group to reveal primary amine **61**. Purification was achieved using an acid/base work-up, however, the amine intermediate was not stable for long periods and was used immediately after preparation. In addition, the reduction of the allyloxy- moiety was observed as a by-product of this reaction, due to the presence of diimide in hydrazine. However, this impurity was easy to remove in the subsequent steps of the synthetic route.



Scheme 3.2 Synthesis of primary amine fragment **61**. *Reagents and conditions*: (i) allyl bromide, K_2CO_3, Me_2CO, rt, 18 h, 98%; (ii) Fe, NH_4Cl, EtOH, H_2O, reflux, 24 h, 70%; (iii) *N*-(4-bromobutyl)phthalimide, K_2CO_3, DMF, 80 °C, 7 h, 67%; (iv) MeI, K_2CO_3, DMF, 85 °C, 5 h, 73%; (v) hydrazine monohydrate, CH_2Cl_2, MeOH, 70 °C, 2 h, 46%.

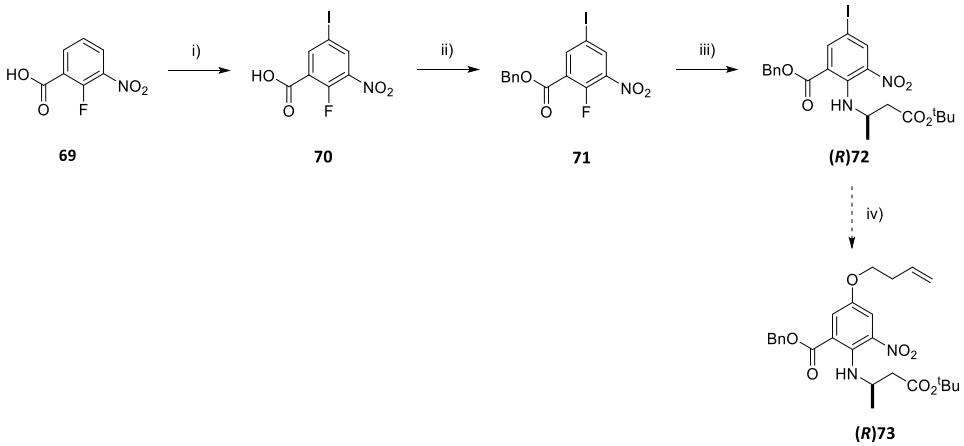
*3.3.1.3 Synthesis of THBD fragment **(R)62***

The first step to prepare the THBD headgroups involved the regioselective iodination of **69** at the 5-position, which occurs with no detectable side-products. This selectivity results from both carboxylic acid and nitro- groups being *meta*-directing, and the fluoro- substituent being *ortho*-/*para*-directing, resulting in the 5-position being the most electronically reactive towards iodination. Classical methods for benzene halogenation by electrophilic aromatic substitution (S_EAr) require the use of a Lewis acid, such as Fe^{III} or Al^{III}, which activates the halogen electrophile towards nucleophilic attack by the aromatic ring. However, S_EAr with iodine through this method produces HI as a by-product, which will act as a reductant to convert the aryl iodide back to iodine, resulting in an incomplete reaction. To overcome this issue, the reaction conditions make use of fuming sulfuric acid to oxidise iodine to iodonium ions (**Equation 3.1**). This removes the formation of the HI by-product and drives the reaction towards completion. Installation of this iodo- group proved to be a key step in the synthesis as it enables the cross-coupling reactions to occur at the desired 5-position.

$$I_2 + H_2SO_4 \longrightarrow 2I^+ + SO_3 + H_2O \qquad \textbf{(3.1)}$$

The decision was made to form the benzyl ester of intermediate **70**, as this protecting group is tolerant of mild base, acidic, and reducing conditions that are to be used in the synthesis of the THBD headgroup. Hydrogenolysis would not be considered for the removal of the benzyl group, as the terminal alkene handles introduced later in the synthesis are liable to be reduced under these

conditions. However, hydrolysis under basic conditions is suitable, as there is no racemisable center on the THBD headgroup.



Scheme 3.3 Synthesis of aniline **(*R*)72**. *Reagents and conditions*: (i) I_2, fuming H_2SO_4, 85°C, 17 h, 92%; (ii) BnBr, K_2CO_3, DMF, 60°C, 4 h, 91%; (iii) **(*R*)41**, Cs_2CO_3, Tol, 85 °C, 21 h, 98%; (iv) but-3-en-1-ol, CuI, 1,10-phen, Cs_2CO_3, Tol, 110 °C.

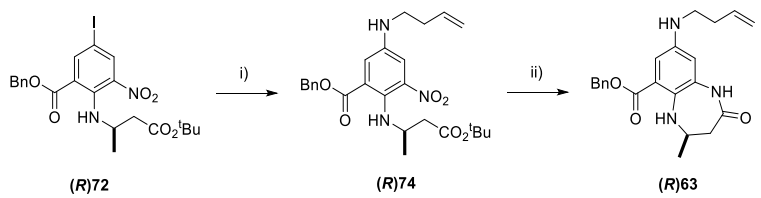
Intermediate **71** was used in an S_NAr reaction with *tert*-butyl (*R*)-3-aminobutanoate, **(*R*)41**, to give **(*R*)72** in high yields (**Scheme 3.3**). An excess of chiral amine **(*R*)41** (1.4 equivalents) was needed to drive the reaction to completion. This was important as both starting material **71** and product **(*R*)72** have very similar R_f values and would otherwise require a challenging purification. The next step explored the installation of the terminal alkene handle onto the THBD headgroup. Buchwald has published a series of papers based on Ullmann-type couplings, using ligand-assisted copper catalysis to perform *N*- and *O*- arylations.[83–87] *O*-Arylations typically require the use of phenanthroline-type bidentate ligands, mineral bases and high temperatures. The coupling of substrate **(*R*)72** to but-3-en-1-ol, using bidentate ligand 1,10-phenanthroline with caesium carbonate in toluene at 110 °C, did not afford the desired product. Attempts to use neat but-3-en-1-ol in a solvent-free reaction also failed. The decision was therefore made to investigate the *N*-arylation of **(*R*)72** instead.

*3.3.1.4 Synthesis of THBD fragment **(R)63***

N-Arylation of intermediate **(*R*)72** was explored using conditions described by Buchwald.[85,86] The difference between the conditions used for the *O*-arylation was the inclusion of the bidentate ligand 2-isobutyrylcyclohexanone; DMF as the solvent; and the use of lower temperatures. The terminal alkene **(*R*)74** was formed, however, this reaction only proceeded in a 60% yield. Approximately, a 10% side-product was isolated and confirmed by NMR and mass spectrometry to be the ethyl ester of **(*R*)74**. The consistent isolation of this side-product was surprising, as there was no evidence of ethanolic impurities in the DMF solvent, bidentate ligand or but-3-en-1-amine, to enable this transesterification

to occur. Nevertheless, sufficient amounts of **(*R*)74** could be prepared, and this side-product was still be amenable for the synthetic preparation of macrocycle **(*R*)60**, although was not used in its preparation.

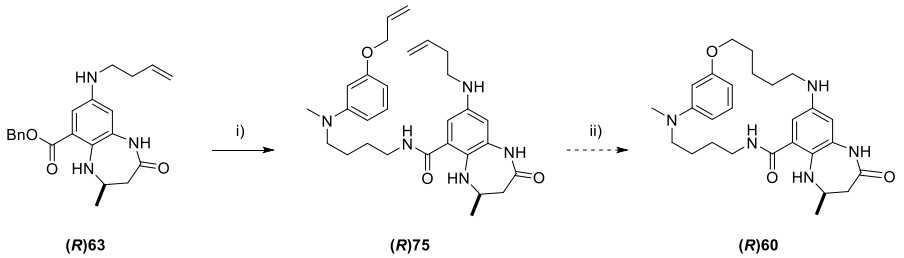
Preparation of THBD fragment **(*R*)63** followed a three-step, one pot reaction, using conditions previously described by Dr Michael Brand in the synthesis of ligand **(*R*)11**.[30] The first step in this sequence was a deprotection of the *tert*-butyl ester with trifluoroacetic acid, followed by a nitro- reduction with zinc and NH_4Cl. The aniline and carboxylic acid could then undergo an intramolecular amide coupling to form the lactam in an overall yield of 75% (**Scheme 3.4**). However, it was apparent that the THBD fragment **(*R*)63** may not be stable for long periods, as NMR samples would undergo a colour change from orange to black over the period of a month. The inherent instability of the THBD fragment was attributed to be an oxidation of the headgroup due to the 1,4-di-aniline motif and therefore is considered an undesirable feature to introduce to the macrocyclic ligands.



Scheme 3.4 Synthesis of THBD fragment **(*R*)63**. *Reagents and conditions*: (i) but-3-en-1-amine, CuI, 2-isobutyrylcyclohexan-1-one, Cs_2CO_3, DMF, rt, 17 h, 60%; (ii) TFA, CH_2Cl_2, rt, 2 h; then Zn, NH_4Cl, DMF, rt, 19 h; then PyBOP, DIPEA, DMF, rt, 24 h, 75% over 3 steps.

*3.3.1.5 Synthesis of macrocycle **(R)60***

Hydrolysis of **(*R*)63** using 1 M LiOH in THF/MeOH/H_2O (3:2:1) led to the deprotection of the benzyl group after a period of 5 h at room temperature. Mass spectrometry revealed that an initial transesterification to the methyl ester intermediate occurs, before hydrolysis with water to reveal the carboxylic acid group. Upon neutralisation of the basic reaction mixture and evaporation of the solvents, the carboxylic acid intermediate was reacted in an amide coupling with **61**, using PyBOP as the activating agent, to afford macrocycle precursor **(*R*)75** in a 64% yield over two steps (**Scheme 3.5**). In addition to fragment **(*R*)63**, the macrocycle precursor was observed to be unstable in solution for short periods, although isolation was possible. Unfortunately, the 1,4-di-aniline motif's susceptibility towards oxidation meant the macrocycle would likely be inherently air sensitive.



(*R*)63 (*R*)75 (*R*)60

Scheme 3.5 Synthesis of macrocycle precursor **(*R*)75**. *Reagents and conditions*: (i) 1 M LiOH, THF, MeOH, H_2O, rt, 5 h; then **61**, PyBOP, NEt_3, DMF, rt, 24 h, 64% over 2 steps; (ii) Hoveyda-Grubbs catalyst 2nd Generation, DCE, 65 °C; then H_2, Pd black, MeOH, rt.

Despite the evident instability issue, we were curious to see if a RCM, followed by hydrogenation, would lead to the desired macrocyclic structure **(*R*)60**. Initial conditions used Hoveyda-Grubbs catalyst™ 2nd generation, with a catalytic loading of 30 mol%, at 40 °C in anhydrous dichloromethane. The Hoveyda-Grubbs catalyst™ 2nd generation was chosen as it is reported to be very good for RCM due to its high reactivity at lower temperatures, compared to other Ru-based catalysts.[88] The reaction was stirred at a dilution of 0.001 M to avoid cross metathesis from occurring, however, starting material was still observed after 1 week. It was understood from the literature that RCM of large rings systems require elevated temperatures and high catalyst loadings. This is especially true for amine containing precursors, due to chelation to the ruthenium metal centres. This approach typically requires the use of Schrock's molybdenum alkylidene catalysts due to their higher functional group tolerance.[89]

Upon changing the solvent to anhydrous 1,2-dichloroethane, which allowed the reaction mixture to be heated to 65 °C, and increasing the concentration to 0.0015 M, full consumption of starting material was observed after 1.5 days. The RCM catalyst could not be removed using normal-phase chromatography, therefore, separation using reverse-phase chromatography gave macrocycle **(*R*)76** in a 1:3 diastereomer mixture. The ratio of *E/Z* isomers could not be determined due to NMR shift overlap, and the isolation of a single diastereomer proved challenging. The use of palladium black was required to hydrogenate the double bond to afford the desired macrocycle **(*R*)60**. The formation of macrocycle **(*R*)60** from the RCM precursor **(*R*)75** was easily monitored by ^{1}H NMR, observing the disappearance of the distinctive alkene chemical shifts between 5.0–6.5 ppm (**Figure 3.5**).

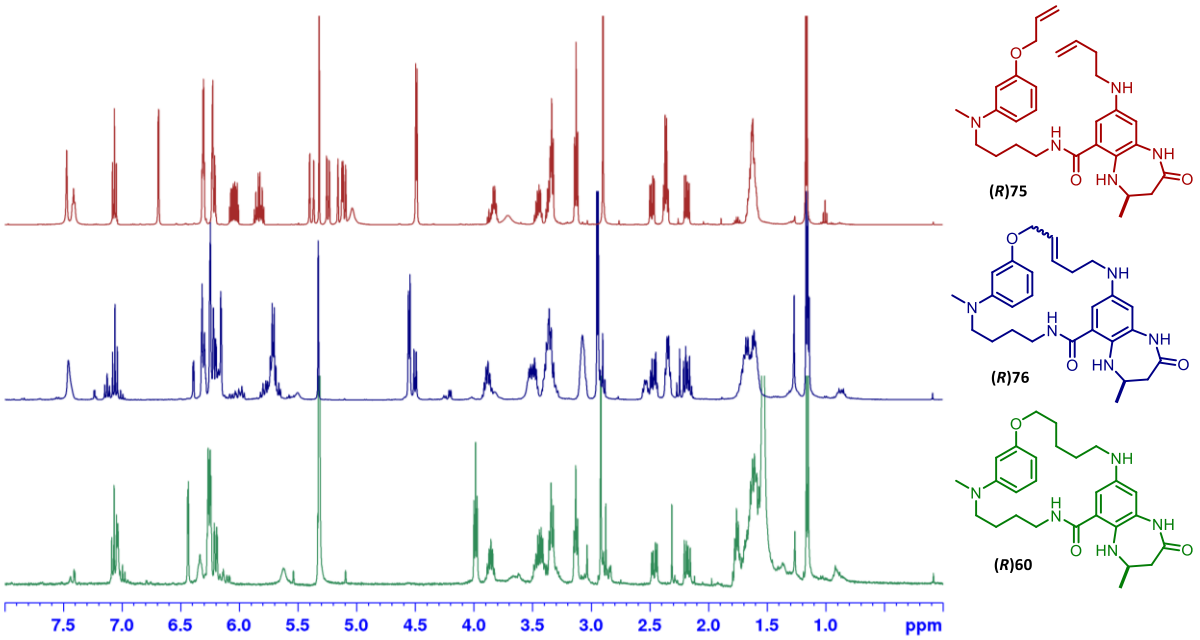


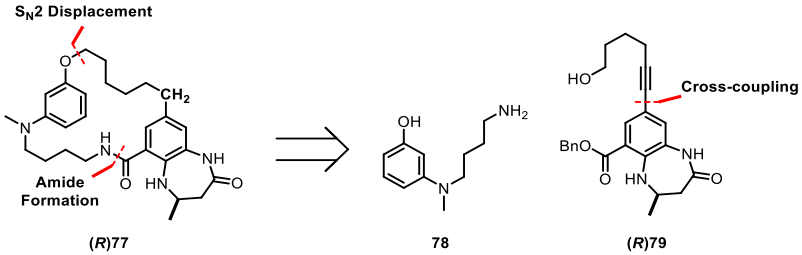
Figure 3.5 ^{1}H NMR (CD_2Cl_2) spectra showing the conversion from macrocycle precursor **(*R*)75** (red) to **(*R*)76** (blue) by RCM, followed by hydrogenation to **(*R*)60** (green).

After several purification attempts, target macrocycle **(*R*)60** was not obtained above 70% purity, determined by analytical HPLC. However, the remaining impurity was a macrocyclic side product, with a mass of 2 hydrogen atoms less than **(*R*)60**, determined by LRMS (Appendix F). As the double bond shifts are not observed by ^{1}H NMR analysis, it is hypothesised that this impurity is the oxidised macrocycle of **(*R*)60**, an expected side-product. Unfortunately, the instability of the 1,4-di-aniline motif present in macrocycle **(*R*)60** led to its preparation being abandoned. For future designs, it was decided that heteroatoms should not be used at the 5-position of the THBD to avoid this problem. Although the RCM was successful, giving a crude yield of 26% over 2 steps, a change in macrocyclisation strategy would also be explored.

3.3.2 Synthetic strategy: S_N2 macrocyclisation

3.3.2.1 Retrosynthetic Analysis

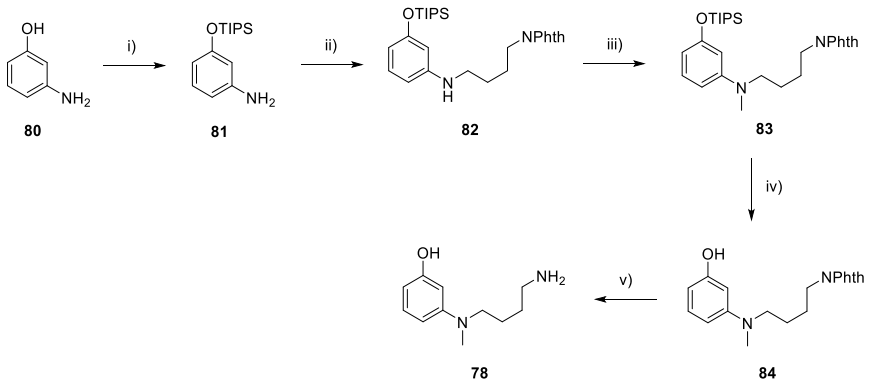
The instability of **(*R*)60** led to the design of macrocycle **(*R*)77**, in which the aniline is replaced by a methylene group. This unit would be installed using a Sonogashira cross-coupling hydrogenation sequence, as the Sonogashira cross-coupling is a reliable method to introduce carbon-aryl bonds. However, an alternative macrocyclisation strategy to RCM was needed, as the alkyne introduced at this step would be challenging to remove in the presence of a terminal alkene. Therefore, the disconnection at the aryl ether bond would explore an S_N2 displacement as the macrocyclisation step (**Scheme 3.6**). Compared to the RCM, this macrocyclisation strategy provides the advantage of a larger selection of ring sizes and linker types being explored for analogue generation.



Scheme 3.6 Retrosynthetic analysis of macrocycle ***(R)*77** using an S_N2 displacement as the macrocyclisation step.

*3.3.2.2 Synthesis of fragment **78***

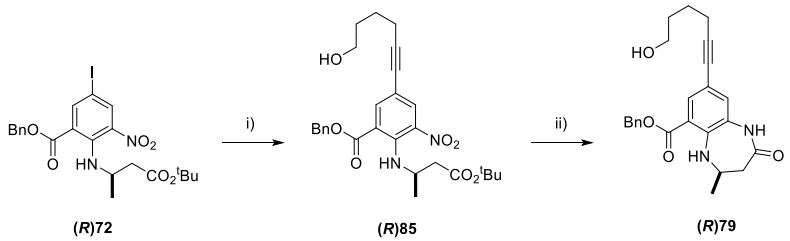
The synthesis of fragment **78** followed a similar route to the primary amine **61** (Section 3.3.1.2). Protection of 3-aminophenol with TIPS was necessary to avoid alkylation at the phenol, and would be tolerant to heat and basic conditions (**Scheme 3.7**). Complete regioselectivity of the phenol protection was observed, due to the oxyphilic nature of silyl groups, affording the TIPS-protected product **81** in a 99% yield. This intermediate was alkylated with *N*-(4-bromobutyl)phthalimide) and iodomethane, followed by the deprotection of the TIPS and phthalimide groups, to afford primary amine fragment **78**.



Scheme 3.7 Synthesis of primary **78**. *Reagents and conditions*: (i) TIPSCl, imidazole, THF, rt, 21 h, 99%; (ii) *N*-(4-bromobutyl)phthalimide, K_2CO_3, DMF, 80 °C, 24 h, 67%; (iii) MeI, K_2CO_3, DMF, 85 °C, 6 h, 60%; iv) 2 M HCl, CH_2Cl_2, EtOH, 80 °C, 17 h, 90% v) hydrazine monohydrate, CH_2Cl_2, MeOH, 70 °C, 5 h, 56%.

*3.3.2.3 Synthesis of THBD fragment **(R)79***

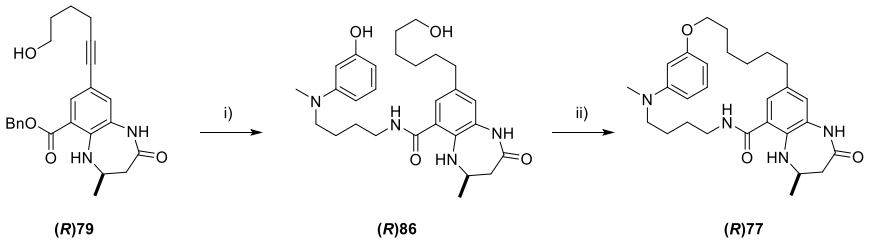
Intermediate **(*R*)72** was used in a Sonogashira cross-coupling with hex-5-yn-1-ol to afford **(*R*)85** (**Scheme 3.8**). Compared to the previously attempted Ullmann-type cross-couplings, this reaction gave excellent yields with no side-products, under mild conditions. Furthermore, no stability issues were seen for **(*R*)85**, as the carbon atom *para*- to the aniline prevents a quinone-type oxidation across the aromatic ring. Cyclisation to form THBD fragment **(*R*)79** used the same conditions as described in Section 3.3.1.4, however this resulted in a lower yield of 30% over 3-steps in this case.



Scheme 3.8 Synthesis of THBD fragment **(*R*)79**. *Reagents and conditions*: (i) hex-5-yn-1-ol, CuI, $Pd(PPh_3)_2Cl_2$, NEt_3, THF, rt, 5 h, 90%; (ii) TFA, CH_2Cl_2, rt, 2 h; then Zn, NH_4Cl, DMF, rt, 20 h; then PyBOP, DIPEA, DMF, rt, 24 h, 30% over 3 steps.

*3.3.2.4 Synthesis of macrocycle **(R)77***

Unlike fragment **(*R*)63**, which used a hydrolysis reaction to avoid hydrogenation of the terminal alkene handles, hydrogenolysis was used in the benzyl deprotection of **(*R*)79**. This approach was used because the hydrogenation of the internal alkyne bond could be achieved during the same reaction (**Scheme 3.9**). The carboxylic acid intermediate was reacted in an amide coupling with **78** to afford macrocycle precursor **(*R*)86** in 71% yield over 2-steps.



Scheme 3.9 Synthesis of macrocycle **(*R*)77**. *Reagents and conditions*: (i) H_2, 10% Pd/C, EtOAc, MeOH, rt, 20 h; then **78**, PyBOP, NEt_3, DMF, rt, 21 h, 71% over 2 steps; (ii) MsCl, NEt_3, THF, 0 °C to rt, 30 min; then DMF, Cs_2CO_3, 80 °C, 2 h, 6% over 2 steps.

Initial macrocyclisation attempts to form **(*R*)77** used the Mitsunobu reaction to activate the primary alcohol for displacement by the phenol. The Mitsunobu reaction is a suitable macrocyclisation strategy for this precursor,[90] as the phenol moiety can be deprotonated by the azo- intermediate which is a key step in the reaction mechanism. Four different Mitsunobu conditions were investigated in the optimisation of this transformation, however, none afforded **(*R*)77** in high purity (**Figure 3.6**). The activating agent DEAD gave over-reactivity, creating several by-products which were challenging to remove, whereas ADDP and CMBP gave no reaction. The Mitsunobu reagent DIAD did afford **(*R*)77** with few by-products, however, obtaining >95% purity by analytical HPLC could not be achieved. Triphenylphosphine oxide is a common impurity associated with this reaction, but was not the problem in this case, as it was easily removed using polymer-supported triphenylphosphine which was removed by filtration after the reaction. A review by Swamy *et al.*[91] highlighted that O-alkylation of amides can also occur under these conditions, and it was postulated that this might be a side-reaction in the Mitsunobu reaction of **(*R*)86**.

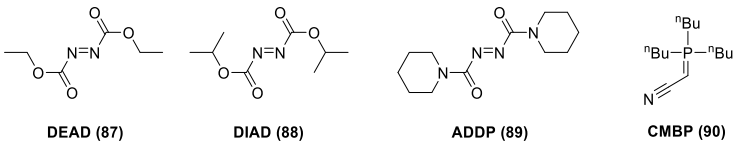


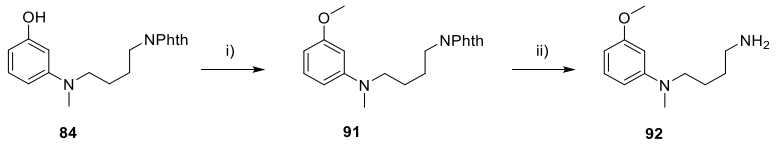
Figure 3.6 Mitsunobu activating reagents screened for the macrocyclisation of **(*R*)77**.

As the Mitsunobu reaction afforded the desired macrocycle, it indicated that an S_N2 displacement strategy was a suitable method for macrocyclisation. A stepwise approach was used to generate a primary alcohol leaving group, followed by its displacement under basic conditions. Precursor **(*R*)86** was treated with mesyl chloride, which reacted with the primary alcohol in the presence of the phenol. This activated intermediate was treated with cesium carbonate in DMF, at a dilution of 0.002 M. Heating to 80 °C was necessary for the macrocyclisation to occur, and unlike the RCM macrocyclisation, the reaction only took 2 hours to complete. Without the need of arduous purification, macrocycle **(*R*)77** isolated with a >99% purity by analytical HPLC, however, only in a yield of 6% over 2 steps (**Scheme 3.9**). Although macrocyclisations are often low yielding, typically ranging from 20–30% yields,

this poor yield was likely due to the inability to selectively mesylate the primary alcohol in the presence of the phenol. Optimisation of this reaction could explore the use of pyridine, which is known to have an alternative mechanism of mesyl chloride activation. This may result in the desired regioselectivity for the primary alcohol over the phenol moiety.

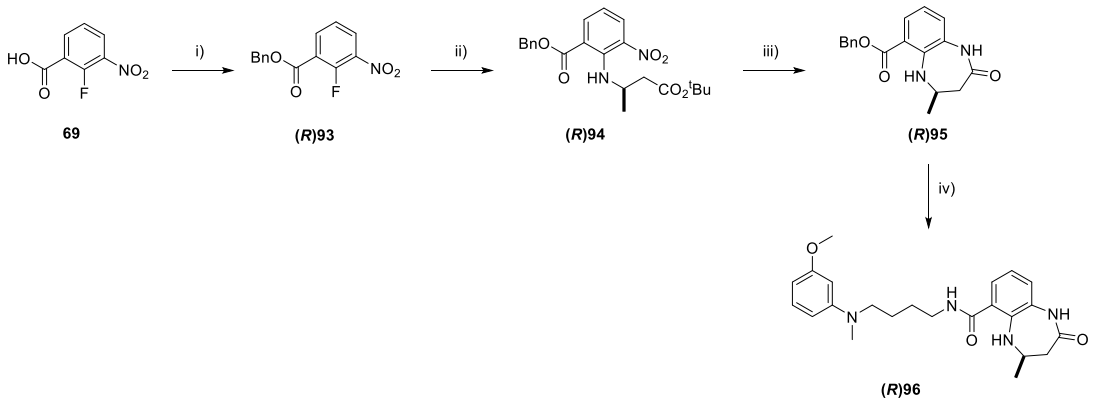
3.4 Synthesis of acyclic analogue of (*R*)96

As there was no SAR data known for extending the linker between the tertiary amine and amide, nor for the removal of the THQ ring in the presence of the THBD headgroup, the acyclic analogue **(*R*)96** was synthesised to compare its affinity with macrocycle **(*R*)77**. The primary amine fragment **92** was prepared by methylation of intermediate **84** with iodomethane, followed by deprotection of the phthalimide protecting group with hydrazine. (**Scheme 3.10**).



Scheme 3.10 Synthesis of primary **92**. *Reagents and conditions*: (i) MeI, K_2CO_3, DMF, 85 °C, 2 h, 53%; (ii) hydrazine monohydrate, CH_2Cl_2, MeOH, 70 °C, 5 h, 80%.

The preparation of **(*R*)95** was previously described by Dr Michael Brand and follows a similar route to the preparation of the THBD headgroups, already described in this chapter. However, the cyclisation of the THBD in this case was prepared using iron powder in acetic acid under reflux, without the need of an amide activating agent.[31] These conditions were previously described in Section 2.2 for the synthesis of **(*R*)48**. In addition to reducing the steps, the advantage of this route was its removal of zinc which can dehalogenate aryl halides through insertion into the aromatic systems.[92] This new method increases the number of viable routes available to prepare the macrocyclic ligands, as cross-couplings after the preparation of the THBD headgroup could be exploited. Fragment **(*R*)95** was then reacted in an hydrogenolysis, followed by an amide coupling with **92**, to afford the acyclic analogue **(*R*)96** in a 70% yield over 2 steps (**Scheme 3.11**).



Scheme 3.11 Synthesis of acyclic analoguet **(*R*)96**. *Reagents and conditions*: (i) BnBr, K_2CO_3, DMF, 60°C, 17 h, 89%; (ii) **(*R*)41**, Cs_2CO_3, Tol, 85 °C, 18 h, 99%; (iii) TFA, CH_2Cl_2, rt, 2 h, then Fe, AcOH, 100 °C, 4 h, 65% over 2 steps; (iv) H_2, 10% Pd/C, EtOAc, MeOH, rt, 20 h; then **92**, PyBOP, NEt_3, DMF, rt, 18 h, 70% over 2 steps.

3.5 Biophysical evaluation of CREBBP bromodomain binding affinity

ITC analysis determined macrocycle **(*R*)77** to have a K_d = 4.73 µM for the CREBBP bromodomain (**Figure 3.7**). This K_d is a considerable drop in affinity when compared to the previously reported ligands shown in (**Figure 3.2**). However, the acyclic analogue **(*R*)96** displayed a weaker binding affinity, which was not able to be determined by ITC analysis. This result means that there had been an improvement in affinity with respect to acyclic analogue **(*R*)96** and that a macrocyclic ligand can be tolerated in the CREBBP bromodomain binding site. It was decided that testing the selectivity against BRD4(1) would be undertaken once a higher affinity macrocyclic ligand was identified.

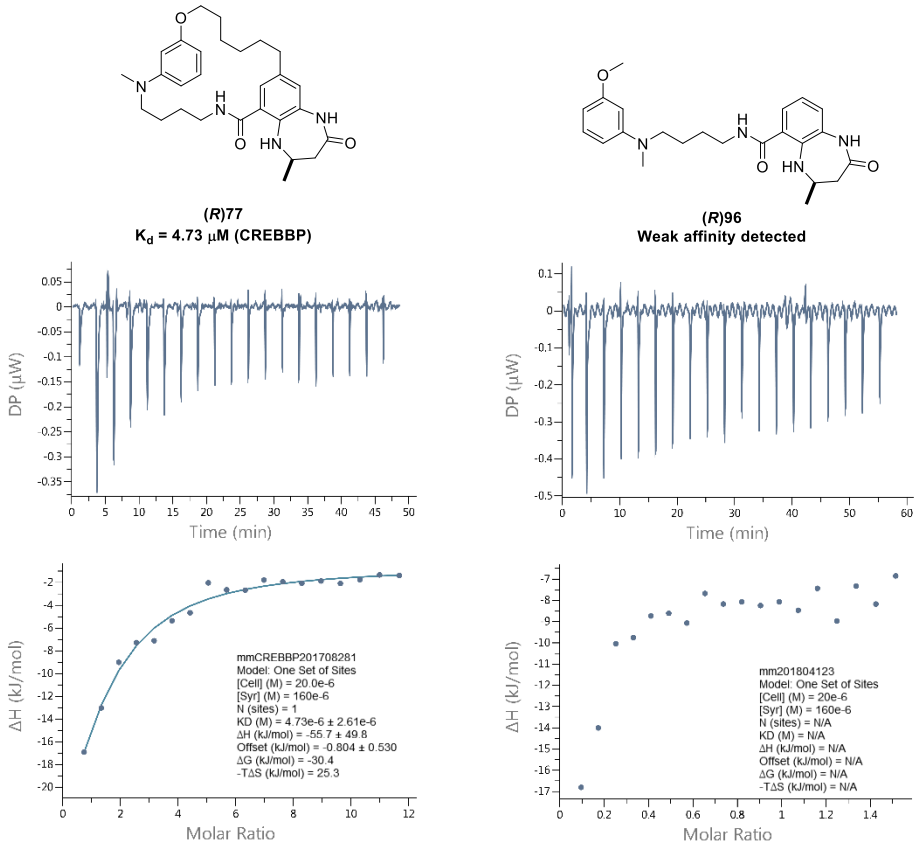


Figure 3.7 ITC data of macrocycle **(*R*)77** and acyclic analogue **(*R*)96** for the CREBBP bromodomain.

3.6 Conclusion

The analysis of the protein-ligand X-ray crystal structures shown in **Figure 3.1** led to the hypothesis that constraining ligand **(*R*)11** in a macrocycle would increase the selectivity for the CREBBP bromodomain over BRD4(1). The macrocycle library was designed based on previously known SAR data and were tested by computational docking. These studies identified a suitable point of attachment to the THBD headgroup; that the removal of the THQ ring could be tolerated; the linker length; and the consequent ring size of macrocyclic target. However, limitations in the software prevented the effective modelling of the macrocyclic ligands. The target macrocycle was initially prepared by RCM, however the macrocyclic ligand was unstable due to an oxidation of a 1,4-di-aniline motif present in the THBD headgroup. Heteroatoms *para*- to the THBD aniline were discounted for future designs, leading to an alternative macrocyclisation strategy. Macrocycle **(*R*)77** was prepared using an S_N2 macrocyclisation and was determined to have a K_d = 4.73 μM, which was a significant loss in affinity compared to the previously known CREBBP bromodomain ligand. However, there was no detectable binding for acyclic analogue **(*R*)96** and therefore macrocycle **(*R*)77** was shown to have an improved affinity for the CREBBP bromodomain.

This result confirmed that a macrocyclic ligand could be tolerated in the CREBBP bromodomain binding site and is a positive step toward the identification of a selective macrocyclic CREBBP bromodomain ligand.

Chapter 4

Macrocycles as CREBBP bromodomain ligands – second generation

4.1 Introduction and aims

In Section 3, the development of ligand **(*R*)77** showed that the CREBBP bromodomain could tolerate a macrocyclic binding motif, however, several issues were highlighted during its design and preparation. The design of the macrocycle library for computational studies was based on low affinity acyclic ligands, which ultimately led to the inherent weak binding of macrocycle **(*R*)77** to the CREBBP bromodomain. The *in silico* screening study failed to validate the docked macrocyclic poses to the CREBBP bromodomain, as the computational software could not effectively sample the conformations of the macrocycle library. The RCM macrocyclisation strategy used in the preparation of macrocycle **(*R*)60** was now considered to be an unfavourable route as (i) this method limits the number of ring sizes that can be explored for analogue generation and (ii) would require a non-selective cross-metathesis reaction to enable an alternative macrocyclisation strategy using the same fragments. The installation of a 1,4-dianiline motif on the THBD caused instability to the headgroup, due to a quinone-type oxidation across the aromatic ring, and therefore it was decided that no heteroatoms would be placed at the 5-position in future designs.

To identify a macrocycle with a higher affinity to the CREBBP bromodomain, all designs were based on ligand **(*R*)48**, the highest affinity ligand known in this series, with the only variation to be on the linker moiety that joins the THQ and the THBD together. Additionally, all routes will enable the possibility of three alternative macrocyclisation strategies, to avoid the problem of a failed macrocyclisation step, and would lead to three distinct fragments that comprise the macrocycle. These fragments would adhere to individual criteria; the THQ fragment should be used as a late-stage intermediate for all macrocycle routes; the THBD headgroup should have a modular synthesis and provide common intermediates in all macrocycle routes; and the linker moiety should be either commercially available or synthetically tractable with minimal route development (**Figure 4.1**).

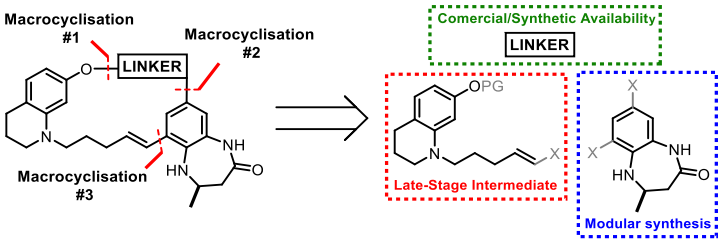


Figure 4.1 The design of macrocycles based on ligand **(*R*)48**, with the ability to have alternative macrocyclisation strategies within a chosen route. Disconnection of macrocycles will lead to three distinct fragments; THQ late-stage intermediate; THBD headgroup and the linker moiety.

To complement this synthetic approach, computational analysis will be used to screen large macrocycle libraries with software that can support macrocyclic docking. The docked structures will be ranked based on their propensity to adopt the desired binding pose in a conformational analysis study, and metadynamic simulations will be used to determine the relative stability energies of the docked macrocycles.

The rationale for using a synthesis-led drug design approach, with computational analysis, is that if a macrocycle with good affinity is identified for any given series, the developed route would allow quick analogue generation and the possibility of optimisation in a structure-based drug design approach.

4.2 Synthesis-led design of macrocycle series

With the synthesis criteria outlined in Section 4.1 (**Figure 4.1**) the macrocycles were split into three different series. Each series is based on their unique macrocyclisation and installation steps, with all routes using the Suzuki coupling and S_N2 displacement reactions, as they worked well in the preparation of **(*R*)48** and macrocycle **(*R*)77**, respectively. For Series 1, a Sonogashira coupling followed by hydrogenation sequence will be used to install the linker moiety. However, the Sonogashira coupling cannot be considered for a macrocyclisation method in this route, as it would not be possible to regioselectively hydrogenate the alkyne in the presence of the *E*-alkene. Series 2 will explore the 1,5-triazole formation for both the installation and macrocyclisation steps. Initial docking studies observed that the 1,4-triazole could not be tolerated in the binding site of the CREBBP bromodomain and was not considered for library design. Series 3 would use an amide coupling for both the linker installation and macrocyclisation steps (**Figure 4.2**).

The macrocycle libraries designed for each series were based on three general linker structures (**Figure 4.2**). A substructure search of the linkers for each series were performed on the online chemical database Reaxys®, with the criteria of being commercially available or easy to prepare. These results were enumerated into their respective series to generate a total of ~300 macrocycles for the computational study.

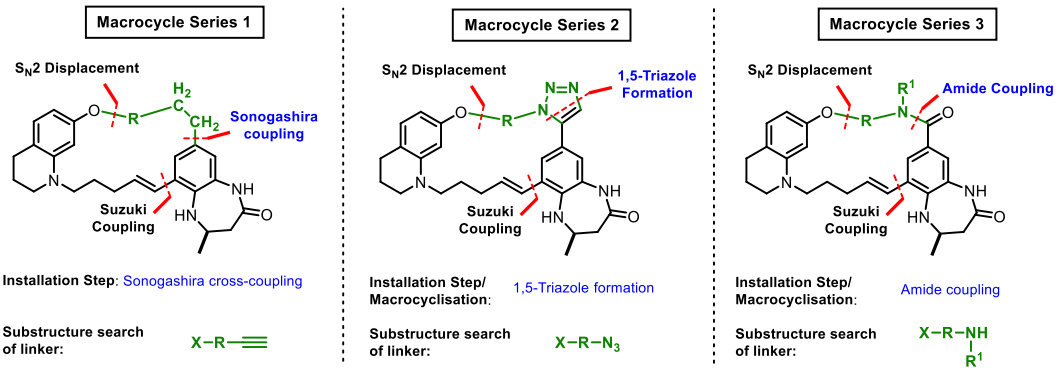


Figure 4.2 The design of the different macrocycle series for the computational screening, highlighting the key installation step of each series and the general structure of the linker moiety searched on Reaxys® to create the macrocycle libraries, where R = any group and X = OH, halide.

4.3 Computational analysis of the macrocycle series

The limitations observed in the computational analysis described in Section 3.2 represents the typical challenges faced by most computer-aided drug design software in macrocyclic drug design. When compared to acyclic molecules, macrocycles are often regarded as rigid systems due to having higher London dispersion forces and lower entropies, however, they can still be flexible in nature.[81] The algorithms used in conventional docking software identify the most energetically favourable conformations by sampling the rotatable bonds in the ligands. The sampling of the rotatable bonds in macrocycles are often impeded due to them having ring closure contraints.[93,94] Methods have been developed to improve macrocycle conformational sampling, however most are too computationally demanding and time consuming to screen large libraries in docking studies.[95,96]

The Schrödinger docking software 'Glide' (Grid-based Ligand Docking with Energetics) incorporated an algorithm known as Prime MCS (Prime Macrocycle Conformational Sampling) into their program which enables macrocyclic ligands to be screened at high speeds with better accuracies.[94] Prime MCS works by splitting the macrocycle into two "half-loops" which overcome the kinetic barriers to torsional rotation observed in macrocyclic structures. The loops are 'closed' back together if the conformations observe no violations or clashes when reforming the macrocycle backbone. This is repeated several times around the ring, before finally sampling the side chains around the macrocycle structure (**Figure 4.3**). Using this algorithm, Glide overcomes the limitations observed in conventional docking methods by using a two-step procedure; (i) sampling of all macrocycle conformations and (ii) docking the pre-sampled conformations. This method has been reported to predict known macrocyclic ligand binding poses with good levels of accuracy.[94]

Molecular docking will be able to identify macrocycles that can adopt the bioactive conformation, however, the improvement in affinity observed for macrocyclic ligands is driven by reducing the entropic penalty of binding. Therefore, the Prime MCS algorithm would also be used to observe what proportion of the low energy macrocycle conformations are predisposed towards the binding motif, by comparing their root-mean-square deviation (RMSD) against the acyclic ligand bioactive conformation.

To further strengthen the computational analysis, the macrocyclic docked structures that are ranked highest in their series will be used in a metadynamic simulation study to determine the relative stabilities of the docked poses.[97] This study will be able to assess the induced-fit interaction of residue

R1173 in the CREBBP bromodomain with the THQ moiety in the macrocyclic structures. This assessment cannot be done during molecular docking as the receptor is treated as a rigid system which is not allowed to move in the presence of the ligand, which can lead to the prediction of incorrect binding poses. For this reason, the results of the metadynamic simulation will have a greater influence in the decision of the macrocyclic structures chosen for synthetic preparation. This computational study was completed on an industrial placement at UCB under the supervision of Dr Matthew Selby, Dr James Reuberson and Dr William Pitt. Metadynamic simulation studies were performed in collaboration with Dr Rémi Cuchillo (UCB).

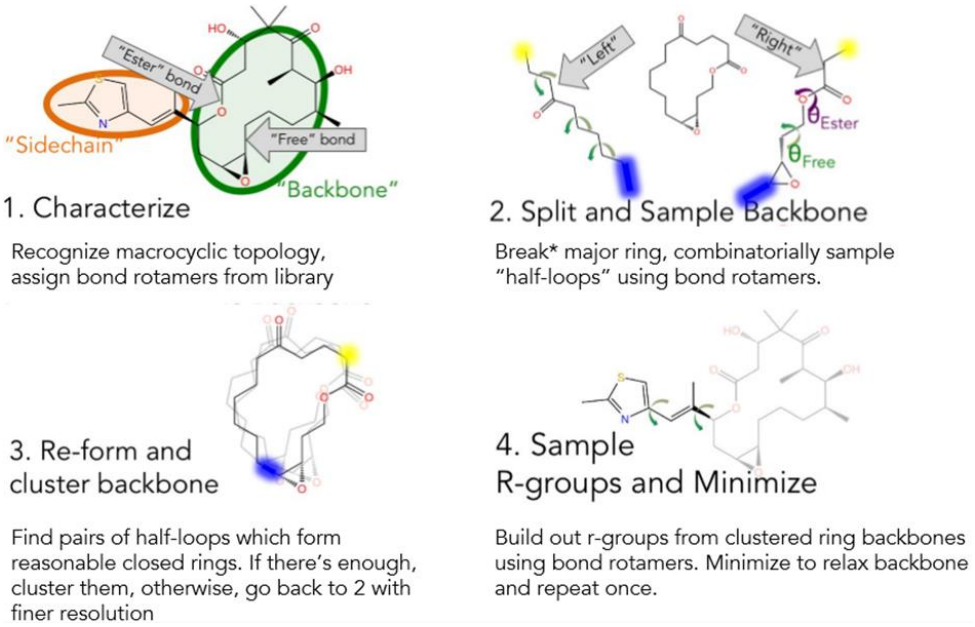
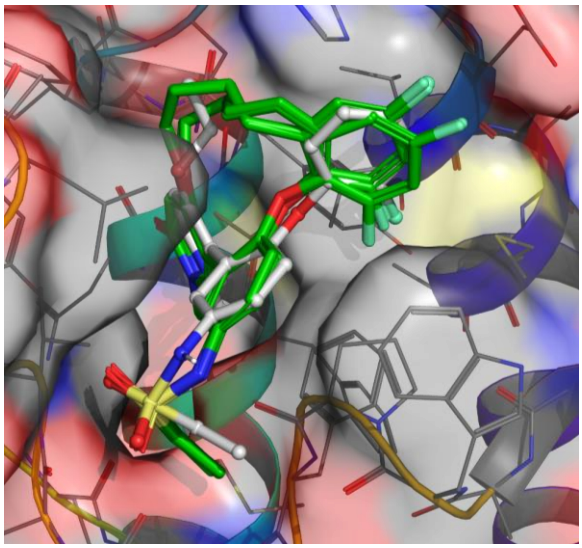
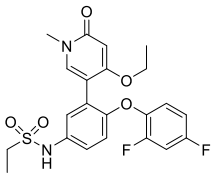


Figure 4.3 Prime MCS workflow summary diagram. Adapted with permission from D. Sindhikara *et al*.[94] Copyright 2017 American Chemical Society.

4.3.1 BRD4(1) macrocycle 22

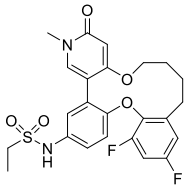
In 2017, the biopharmaceutical company AbbVie reported the BRD4(1) macrocyclic ligand **22**, as discussed in Section 1.4.1.1.[40] This ligand was chosen to validate the docking and conformational analysis procedure to be used for CREBBP bromodomain library, as the bioactive conformation of **22** is similar to the acyclic ligand **21**. In addition, macrocycle **22** was shown to have an improvement in EC_{50}, indicating a solution-based conformation predisposed towards the bioactive pose.





21

EC_{50} = 39 nM (BRD4(1))



22

EC_{50} = 6.5 nM (BRD4(1))

Molecular Docking			
	Glide Docking Score	Glide Emodel Score	Correct Binding Poses
21	−7.784	−83.447	5
22	−8.293	−83.750	5
22*	0.000	0.000	0

Favourable

Unfavourable

* without applying Prime MCS.

Figure 4.4 Docking study of **21** and **22** against BRD4(1) (PDB: 5UEY). Macrocycle **22** (carbon:green) shows all docked conformations to have high similarity to the X-ray crystal structure binding pose of ligand **21** (carbon:grey). Docking scores are in alignment with known efficacy of the reported BRD4(1) ligands.

Glide generates two scoring values; (i) Glide docking score (which approximates ligand binding free energy) and (ii) Glide Emodel score (which ranks the "best" poses against each other based on force-field parameters, including electrostatic and van der Waals interactions), with the more negative scores reflecting favourable binding. The calculation of these values is discussed in Appendix B2. Furthermore, the docking study generated five docked structures which were analysed to see what proportion adopt the desired binding pose, (defined as the docked conformation that is similar to the acyclic ligand's protein bound conformation).

In the case of the macrocycle **22**, all poses adopted the desired binding motif and gave an improved docking score with respect to the acyclic ligand **21** (**Figure 4.4**). Interestingly, if the Prime MCS algorithm was not used to sample the macrocycle conformations, the molecular docking program was not able to predict any desired binding poses. This supported the rationale that this computational method could predict desired binding poses for our macrocyclic library.

The macrocycle conformers of **22** that were generated from the Prime MCS algorithm were structurally aligned against the crystal structure bioactive conformation of ligand **21** bound to BRD4(1). The RMSD was calculated and plotted against the relative energies of the macrocyclic conformations (**Figure 4.5A**). The analysis determined that the low energy conformers which had a RMSD below 1.5 Å would allow the macrocyclic conformation to easily adopt the binding pose with minimal energy (**Figure 4.5B**). Macrocycle **22** had 40% of its low energy conformations below the RMSD threshold and this was considered the benchmark value for the study on the CREBBP bromodomain macrocycle library. As Prime MCS is designed to generate macrocycle structures only, this study would not be performed on the acyclic ligands.

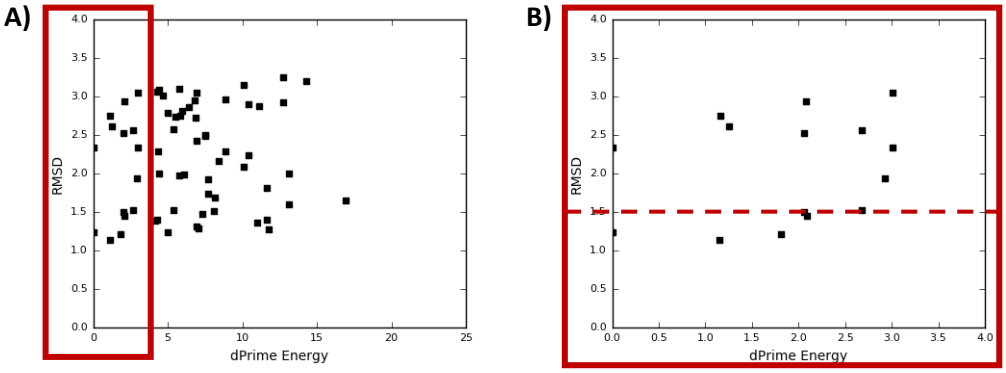


Figure 4.5 (A) Conformational analysis of **22** using Prime MCS to generate a series of possible conformations and their relative energies which are structural aligned against the acyclic bioactive conformation of **21**. (B) Focused area of the plot with the red dashed line indicating the RMSD cut off for conformations judged to be close to the bioactive conformation.

4.3.2 Acyclic CREBBP bromodomain ligands

The known CREBBP bromodomain ligands, shown in **Figure 4.6**, were used to determine whether the computational analysis could replicate known experimental ranking of affinities, as well as providing a comparison for the *in silico* screening of the macrocycle library. It was highlighted in preliminary docking studies that the Prime MCS software was not able to compute the THBD headgroup in the macrocyclic systems, therefore the library was modified to include the DHQ headgroup. As previously discussed in Section 3.2.2, the assumption was made that the DHQ and THBD headgroups adopt similar binding modes and that any hits from the docking study would be prepared with the THBD headgroup. For this reason, acyclic ligand **(*R*)97** was included in the study, even though there are no affinity data for this compound (**Figure 4.6**).

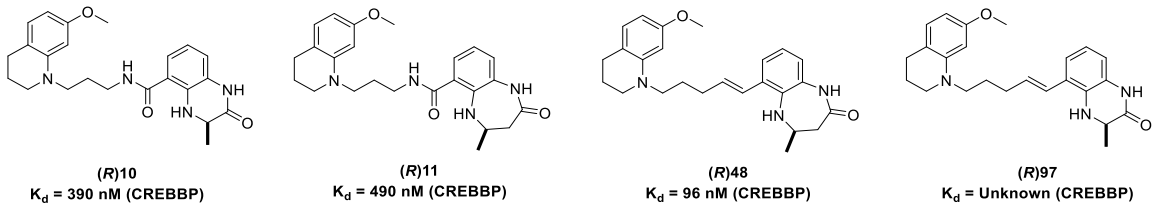


Figure 4.6 Acyclic CREBBP bromodomain ligands used to validate docking study by comparing known binding affinities.

The docking study correctly predicted the binding poses for the DHQ ligands **(*R*)10** and **(*R*)97**, however, struggled to replicate the correct poses for the THBD ligands **(*R*)11** and **(*R*)48** (**Table 4.1**). The CREBBP bromodomain forms an induced fit pocket with the THQ moiety of the ligands in with residue R1173, therefore, the inability to predict the correct binding poses could be due to the receptor being treated as a rigid system by the docking program.

Table 4.1 Molecular docking and metadynamic scores of acyclic ligands against the CREBBP bromodomain. Metadynamic simulation traces shown in Appendix B5.

	Molecular Docking			Metadynamic Simulation	
	Glide Docking Score	Glide Emodel Score	Correct Binding Poses	Stability Energy	Correct Binding Poses
(*R*)10	−8.483	−70.230	5	−2.821	7
(*R*)11	0.000	0.000	0	−3.155	4
(*R*)48	−7.989	−62.459	2	−3.239	10
(*R*)97	−7.505	−65.455	4	−3.186	5

Favourable

Unfavourable

The acyclic ligands were tested in the metadynamic simulations using the methodology described by Clark *et al*.[97] This simulation study would generate 10 poses of the ligands bound to the CREBBP bromodomain, with their associated stability energies. Ligands which had low stability energies and

high number of poses in the correct binding conformation are predicted to have high affinities for the CREBBP bromodomain. The simulation study correctly predicted ligand **(*R*)48** to have the highest affinity for the CREBBP bromodomain, observing the lowest stability energy, with all generated poses in the bioactive conformation. Ligand **(*R*)10** had a less favourable stability energy than **(*R*)11** but more correct binding poses, and was therefore considered to agree with the known experimental ranking. Although no binding data are known for ligand **(*R*)97**, the study predicted a favourable stability energy, with half the poses adopting the bioactive conformation, and therefore was a good acyclic comparison for the macrocycle computational analysis. These results demonstrated the importance of the metadynamic simulation to the computational analysis, as it was better able to predict the known experimental data of the acyclic ligands compared to the molecular docking study.

4.3.3 Macrocycle series 1 – Aliphatic linker

For series 1, 167 macrocycles were screened computationally against the CREBBP bromodomain, with the top 12 macrocycle results shown in Appendix B3. Macrocycle ligands **(*R*)98** (**Figure 4.7A**) and **(*R*)99** (**Figure 4.7B**) were chosen for the conformational analysis and metadynamic simulation studies as they had excellent docking scores with respect to acyclic ligand **(*R*)97**, and all docked structures adopted the desired binding pose (**Table 4.2**).

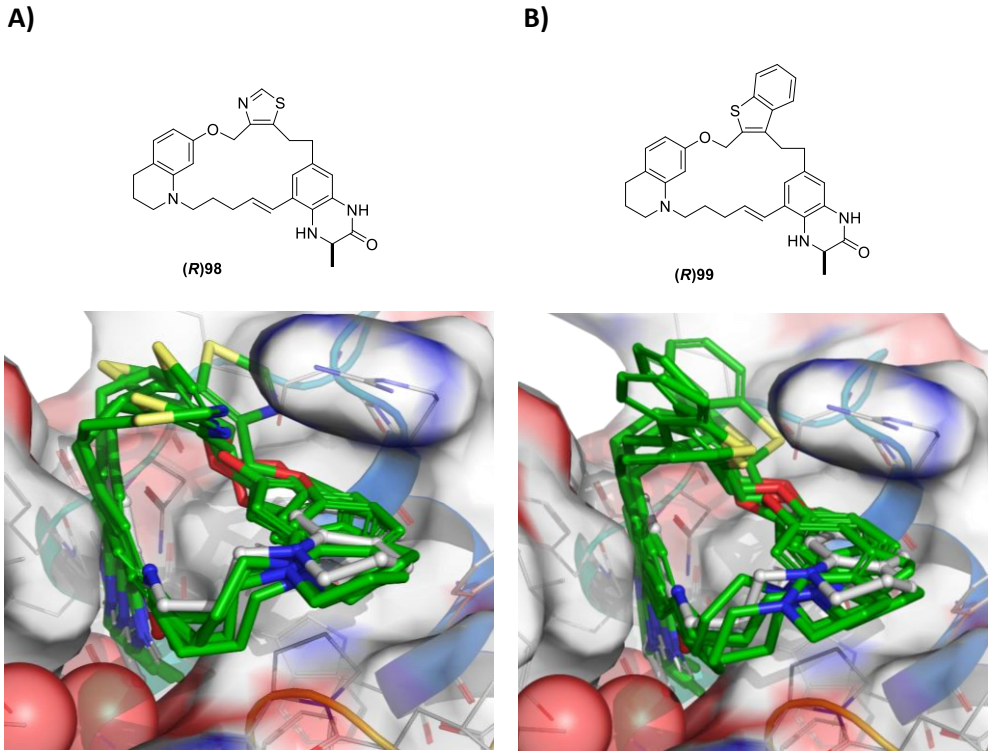


Figure 4.7 Docked conformations (carbon:green) of top hits (A) **(*R*)98** and (B) **(*R*)99** bound to the CREBBP bromodomain. Conformations are overlaid with the CREBBP bromodomain co-crystal structure of ligand **(*R*)10** (PDB:4NYX, carbon:grey) to indicate the desired binding pose. See Appendix B3 for top docked structures.

Conformational analysis did not differentiate between macrocycles **(*R*)98** and **(*R*)99**, which both showed similar percentage of low energy conformers below the RMSD threshold. However, the metadynamic simulation predicted **(*R*)98** to bind more preferentially than **(*R*)99**, with all 10 poses adopting the desired binding conformation. For macrocycle **(*R*)99**, the stability energy was heavily disfavoured, and therefore the THBD analogue of **(*R*)98** was chosen for synthetic preparation.

Table 4.2 Computational analysis the top hits from macrocycle series 1 compared against the acyclic ligand **(*R*)97**. The results from the molecular docking screening, conformation analysis and metadynamic simulation study can be found in Appendix B3−5.

	Molecular Docking			Conformational Analysis	Metadynamic Simulations	
	Glide Docking Score	Glide Emodel Score	Correct Binding Poses	Conformations below RMSD threshold	Stability Energy	Correct Binding Poses
(*R*)97	−7.505	65.455	4	n/a	−3.186	5
(*R*)98	−8.446	−74.297	5	43%	−3.162	10
(*R*)99	−8.359	−73.926	5	44%	+0.847	3

n/a: not applicable.

4.3.4 Macrocycle series 2 – Triazole linker

For series 2, 52 macrocycles were screened against the CREBBP bromodomain, with the top 6 macrocycle results shown in Appendix B3. Macrocycle **(*R*)100** (**Figure 4.8A**) gave the most favourable docking scores in the study, with most docked conformations adopting the correct binding pose. However, the remaining hits performed poorly in the docking study, with macrocycle **(*R*)101** (**Figure 4.8B**) chosen for further study due to its structural variation (**Table 4.3**).

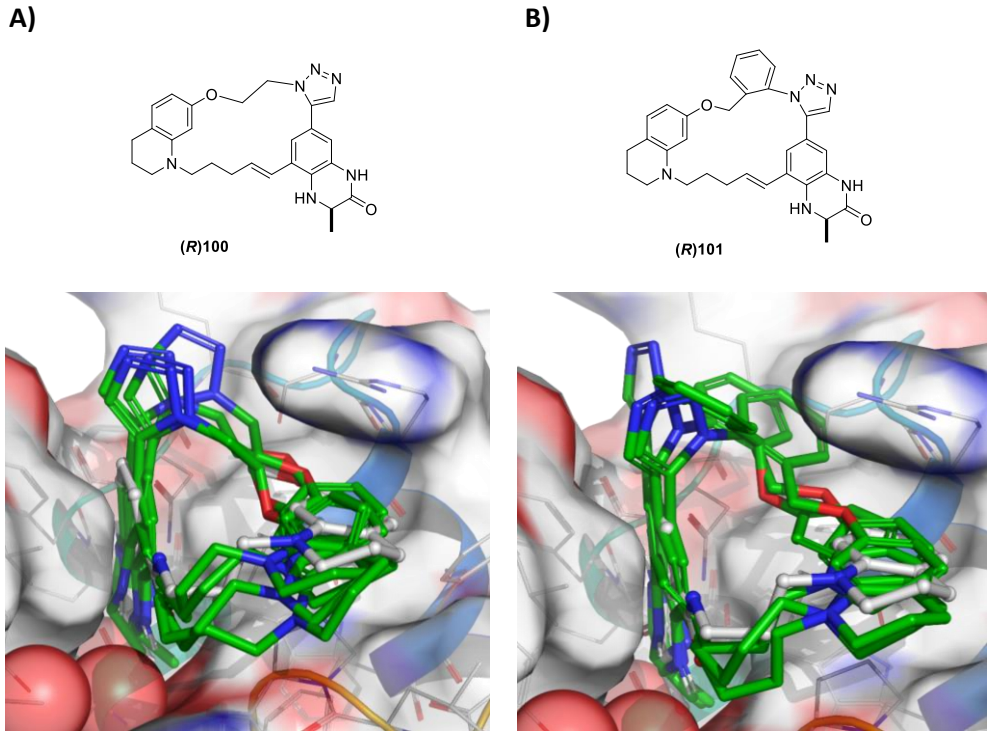


Figure 4.8 Docked conformations (carbon:green) of top hits (A) **(*R*)100** and (B) **(*R*)101** bound to the CREBBP bromodomain. Conformations are overlaid with the CREBBP bromodomain co-crystal structure of ligand **(*R*)10** (PDB:4NYX, carbon:grey) to indicate the desired binding pose. See Appendix B3 for top docked structures.

Macrocycle **(*R*)101** failed to give a low energy conformer below the RMSD threshold and no docked poses adopted the binding conformation in the metadynamic simulation study. As a result, the conformational analysis and metadynamic simulation both heavily favoured the THBD analogue of **(*R*)100** for synthetic preparation. However, the results for macrocycle **(*R*)100** were below the desired criteria, with the metadynamic simulation results indicating this series to have very weak or no affinity to the CREBBP bromodomain.

Table 4.3 Computational analysis the top hits from macrocycle series 2 compared against the acyclic ligand **(*R*)97**. The results from the molecular docking screening, conformation analysis and metadynamic simulation study can be found in Appendix B3−5.

	Molecular Docking			Conformational Analysis	Metadynamic Simulations	
	Glide Docking Score	Glide Emodel Score	Correct Binding Poses	Conformations below RMSD threshold	Stability Energy	Correct Binding Poses
(*R*)97	−7.505	−65.455	4	n/a	−3.186	5
(*R*)100	−8.870	−76.863	4	33%	−1.114	3
(*R*)101	−8.121	−71.202	3	0%	0	0

n/a: not applicable.

4.3.5 Macrocycle series 3 – Amide linker

Initial molecular docking studies of series 3 identified that all the macrocyclic poses had a *Z*-amide geometry, as seen for macrocycle **(*R*)102** (**Figure 4.9A**). Therefore, pyrrolidine moieties, which would preferentially favour the *Z*-amide conformation, were included in the design of the macrocycle library. This led to pyrrolidine macrocycle **(*R*)(*R*)103** (**Figure 4.9B**) and **(*S*)(*R*)103** (**Figure 4.9C**) to be the best ranked macrocycles in the docking studies (**Table 4.4**).

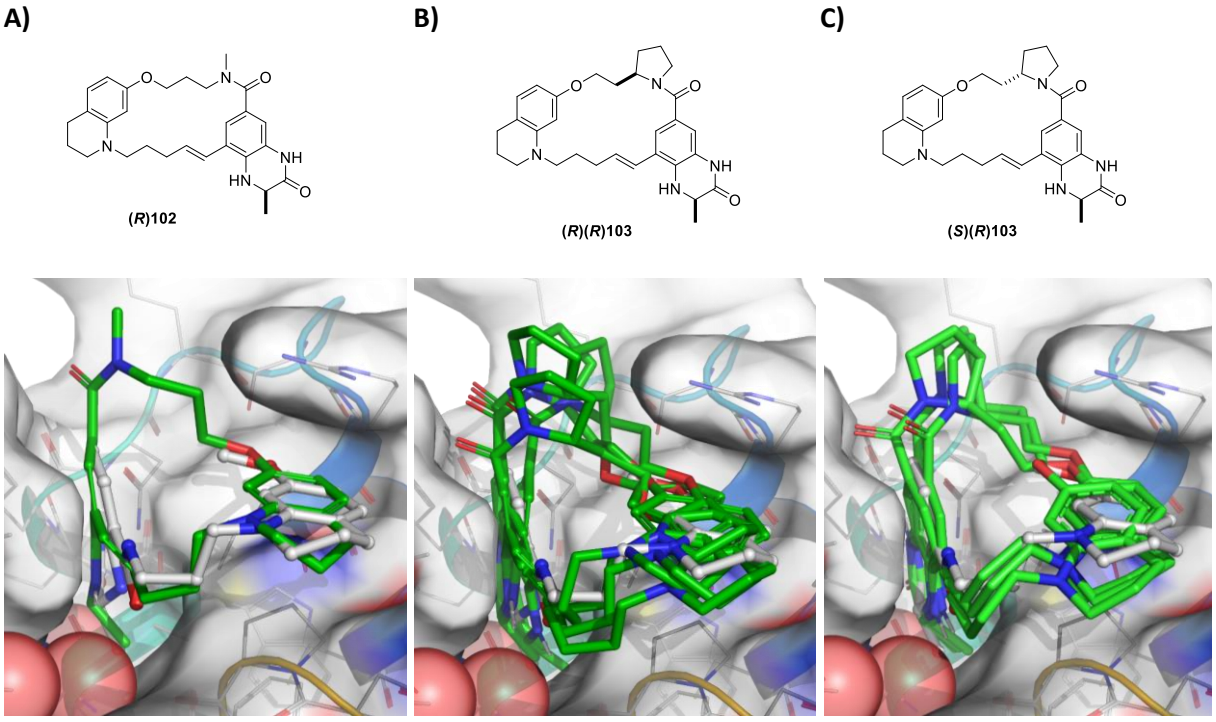


Figure 4.9 Docked conformation(s) (carbon:green) of initial hit (A) **(*R*)102** and top hits (B) **(*R*)(*R*)103** and (C) **(*S*)(*R*)103** bound to the CREBBP bromodomain. Conformations are overlaid with the CREBBP bromodomain co-crystal structure of ligand **(*R*)10** (PDB:4NYX, carbon:grey) to indicate the desired binding pose. See Appendix B3 for top docked structures.

The macrocycles shown in **Figure 4.9** were tested in the conformational analysis and it revealed that the macrocycle **(*R*)(*R*)103** preferentially adopts the desired binding pose, with 92% of the low energy conformers below the RMSD threshold. However, diastereomer **(*S*)(*R*)103** and macrocycle **(*R*)102** were shown to adopt the bioactive pose less favourably. The conformational analysis results were supported by the metadynamic simulations which showed **(*R*)(*R*)103** to have a favourable stability energy with the majority of poses in the desired conformation. Therefore, the decision was made to prepare the THBD analogue of **(*R*)(*R*)103**.

Table 4.4 Computational analysis the top hits from macrocycle series 3 compared against the acyclic ligand **(*R*)97**. The results from the molecular docking screening, conformation analysis and metadynamic simulation study can be found in Appendix B3−5.

	Molecular Docking			Conformational Analysis	Metadynamic Simulations	
	Glide Docking Score	Glide Emodel Score	Correct Binding Poses	Conformations below RMSD threshold	Stability Energy	Correct Binding Poses
(*R*)97	−7.505	−65.455	4	n/a	−3.186	5
(*R*)102	−8.092	−66.399	3	33%	n.t.	n.t.
(*R*)(*R*)103	−8.022	−70.943	5	92%	−3.028	9
(*S*)(*R*)103	−8.471	−76.865	3	24%	−1.947	5

n/a: not applicable; n.t.: not tested.

4.4 Synthesis of the macrocycle series

Macrocycles **(*R*)105**, **(*R*)106** and **(*R*)(*R*)110** were chosen for preparation based on the results from the computational analysis described in Section 4.3. Macrocycle **(*R*)104** would also be synthesised to validate the computational procedure, as the alkyl linker may not conformationally favour the bioactive pose. In addition, the 1,4-triazole regioisomer **(*R*)107** was predicted in the docking studies not to bind to the CREBBP bromodomain and therefore was synthesised as a negative control. Finally, macrocycles **(*R*)108** and **(*R*)109** were prepared to understand the effect that the different amide geometries have on the binding affinity. The macrocycle ligands in each series, shown in **Figure 4.10**, were prepared in the retrosynthetic analyses outlined in Section 4.2.

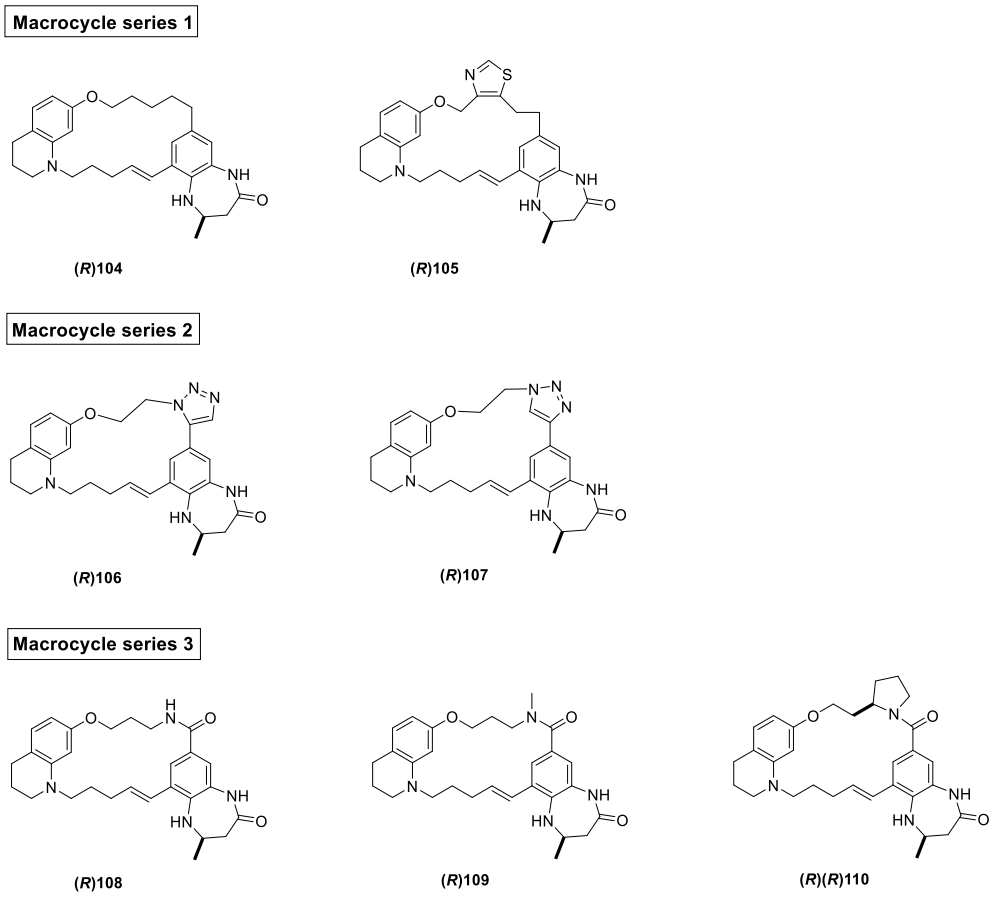
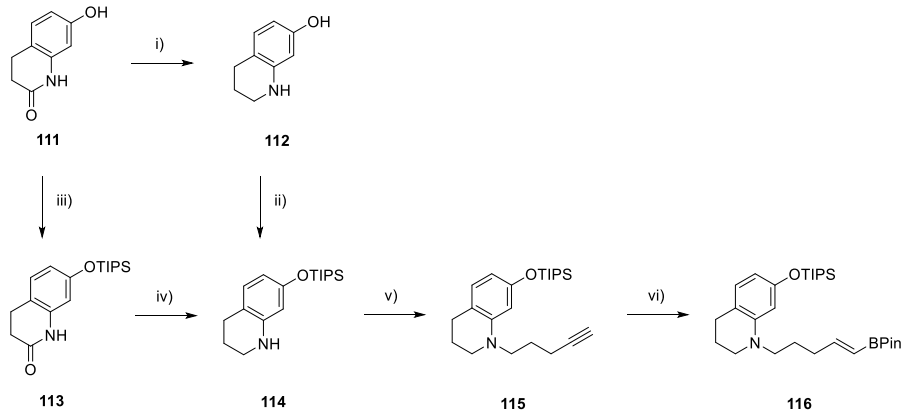


Figure 4.10 Target macrocycles for synthetic preparation in each macrocycle series.

4.4.1 Late-stage intermediate 116

The THQ fragment **116**, containing the pinacol borane ester and TIPS protected phenol, was designed to be used as a late-stage intermediate, as the synthetic routes for all macrocycle series use a Suzuki coupling and S_N2 displacement disconnection in their retrosyntheses. The preparation of this fragment is similar to the route outlined for intermediate **47** in Section 2.2.

Initial preparation of **114** used $LiAlH_4$ to reduce lactam **111** to the THQ fragment **112** in a 41% yield. This was followed by a TIPS protection of the phenol. The low yield observed for the reduction was attributed to the poor solubility of **111** in the THF solvent system. Therefore, the reaction steps were reversed to first TIPS protect **111**, increasing the solubility in ethereal solvents due to the addition of the lipophilic silyl group, which resulted in a 94% yield for the reduction of **113**. THQ intermediate **114** was alkylated with pent-4-yn-1-yl methanesulfonate under microwave conditions to give alkyne **115** in a 61% yield. Hydroboration of **115** was achieved in a solvent-free reaction, using Schwartz's reagent to catalyse the reaction and provide high *E*-selectivity in the preparation of late-stage intermediate **116** (**Scheme 4.1**).[73]

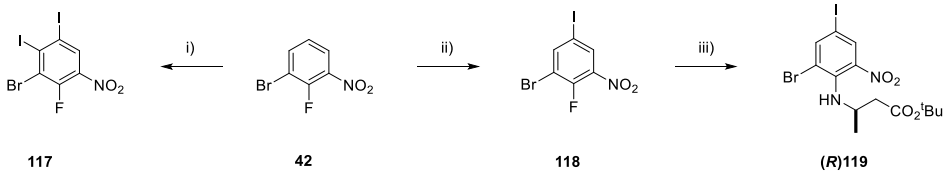


Scheme 4.1 Synthesis late-stage intermediate **116**. *Reagents and conditions*: (i) $LiAlH_4$, THF, 0 °C to rt, 20 h, 41%; (ii) TIPSCl, imidazole, THF, rt, 21 h, 94%; (iii) TIPSCl, imidazole, DMF, rt, 24 h, 96%; (iv) $LiAlH_4$, Et_2O, 0 °C to rt, 4 h, 91%; (v) pent-4-yn-1-yl methanesulfonate, KI, DIPEA, DMF, μλ, 100 °C, 1 h, 62%; (vi) HBPin, Cp_2ZrClH, 60 °C, 20 h, 79%.

4.4.2 Macrocycle series 1

*4.4.2.1 Macrocycle **(R)104** – S_N2 displacement macrocyclisation*

In Section 3.3.1.3, an important step for the synthesis of the macrocycle targets was the iodination of the 5-position of starting material **69**. This was achieved using iodine and fuming sulfuric acid, enabling subsequent attachment of linker chains to this position of the THBD headgroup. The iodination of **42** in the 5-position is also regarded as an important step, as intermediate **118** is needed for the preparation of the macrocycles from series 1 and 2. At the time of writing, there is only one commercial supplier for **118** (Alichem, $1579.40/g) but the cost of this material did not make it a viable option. In addition, there is a regioselectivity issue for the iodination of **42**, because although the fluoro- and nitro- moiety are electronically directing towards the 5-position, the bromo- substituent, is *ortho*-/*para*- directing to the 4- and 6-positions. Use of iodine and fuming sulfuric acid at 80 °C resulted in the doubly iodinated aromatic **117** as the only product in an 80% yield. Iodination occurred at the 4- and 5-positions (structure confirmed by X-ray crystallography, see Appendix E). It was proposed that a more controlled release of iodine at lower temperatures may lead to the desired product. Novel conditions were identified for the preparation of **118** using NIS and concentrated sulfuric acid at room temperature, to afford mono-iodination to the 5-position in a 95% yield. This functionalised aromatic compound was used in a regioselective S_NAr with **(*R*)41** to give aniline **(*R*)119** in excellent yields (**Scheme 4.2**).

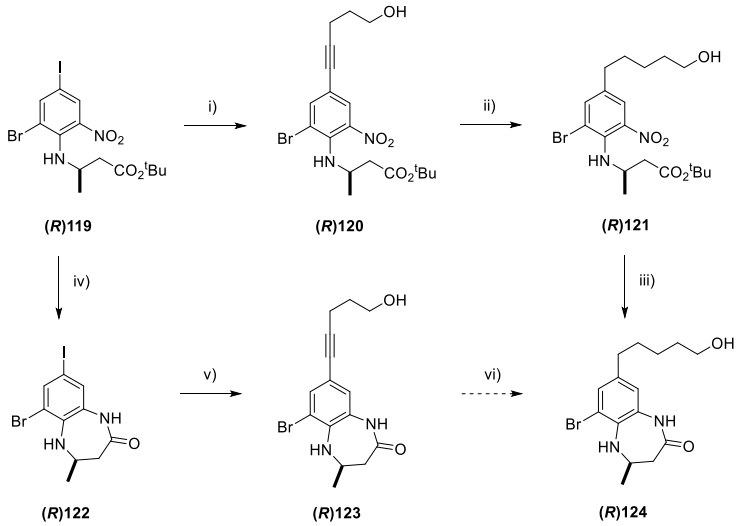


Scheme 4.2 Iodination of **42** and the preparation of intermediate **(*R*)119**. *Reagents and conditions*: (i) I_2, fuming H_2SO_4, 85 °C, 15 h, 80%; (ii) NIS, conc. H_2SO_4, rt, 19 h, 95%; (iii) **(*R*)41**, Cs_2CO_3, Tol, 85 °C, 18 h, 93%.

Iron powder and acetic acid was used in the preparation of the THBD headgroup without dehalogenation being observed. This allows for a modular synthesis of the THBD fragments in macrocycle series 1 and 2, as intermediate **(*R*)119** can be used in either a cross-coupling reaction or in the formation of THBD headgroup. However, cyclisation to afford **(*R*)122** was observed to be low yielding. A regioselective Sonogashira cross-coupling of **(*R*)119** was achieved at room temperature in excellent yields, as oxidative insertion into bromo-aryl bonds typically require elevated temperatures.

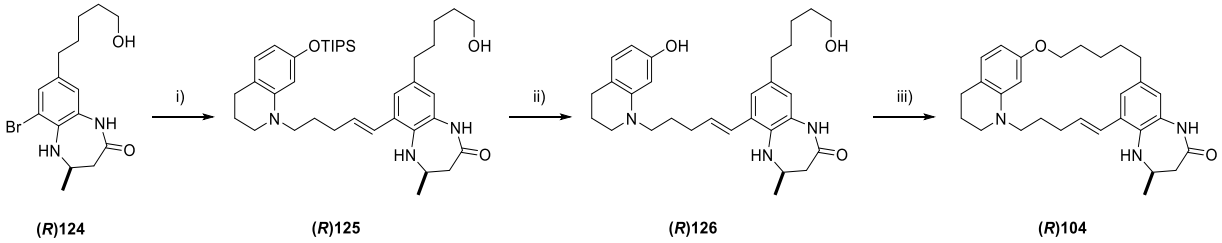
Conditions were also identified for the Sonogashira cross-coupling with intermediate **(*R*)122**, by changing the solvent to DMF to help solubilise the starting material, and raising the temperature to 40 °C. This reaction allows for the late-stage modification to the THBD headgroup with alternative linker chains, which will be beneficial for facile analogue generation.

The hydrogenation of the alkyne intermediate **(*R*)120** must be completed before the introduction of the *E*-alkene in the Suzuki coupling, as these functional groups will not be differentiated under hydrogenation conditions. In addition, these conditions must not reduce the nitro- substituent and cannot dehalogenate the bromo- substituent, which is the handle for the Suzuki coupling of late-stage intermediate **116**. Palladium catalysts are known to insert into aromatic halide therefore these conditions were avoided. There is precedent for Wilkinson's catalyst to reduce internal alkyne bonds in the presence of nitro- and halide moieties.[98] However, when using this catalyst, no reaction was observed at room temperature. The hydrogenation of the internal alkyne bonds adjacent to aryl groups using Wilkinson's catalyst often require elevated temperature and pressures, and therefore **(*R*)120** was heated to 60 °C to afford intermediate **(*R*)121** in a 90% yield. The R_f of starting material **(*R*)120** and hydrogenated product **(*R*)121** were identical, therefore the reaction was monitored using LRMS analysis and ^{1}H NMR to observe the formation of the alkyl chemical shifts. Cyclisation of this intermediate with iron and acetic acid afforded the THBD fragment **(*R*)124** in an 81% yield over two steps (**Scheme 4.3**). Hydrogenation of intermediate **(*R*)123** was attempted using Adam's catalyst, however, undesired debromination of the product was observed. As a viable route to prepare **(*R*)124** had been identified, optimisation of this step was abandoned.



Scheme 4.3 Viable synthetic routes for the preparation of THBD fragment **(*R*)124**. *Reagents and conditions*: (i) pent-4-yn-1-ol, CuI, $Pd(PPh_3)_2Cl_2$, NEt_3, THF, rt, 5 h, 96%; (ii) H_2, $Rh(PPh_3)_3Cl$, Tol, 60 °C, 5 h, 90%; (iii) TFA, CH_2Cl_2, rt, 2 h, then Fe, AcOH, 100 °C, 4 h, 81% over 2 steps; (iv) TFA, CH_2Cl_2, rt, 3 h, then Fe, AcOH, 100 °C, 4 h, 38% over 2 steps; (v) pent-4-yn-1-ol, CuI, $Pd(PPh_3)_2Cl_2$, NEt_3, DMF, 40 °C, 3 h, 81%; (vi) H_2, PtO_2, MeOH, rt.

The THBD fragment **(*R*)124** was used in a Suzuki coupling with late-stage intermediate **116**, followed by TIPS deprotection of **(*R*)125** to afford macrocycle precursor **(*R*)126** in excellent yields. The S_N2 displacement macrocyclisation method was developed in Section 3.3.2.4 for the preparation of macrocycle **(*R*)77**, however, a low yield of 6% over two steps was observed and was hypothesised to be due to non-selective mesylation of the phenol and primary alcohol moiety. Furthermore, it was rationalised that selective mesylation of the primary alcohol could be achieved by changing the base from triethylamine to pyridine, as they have an alternative mechanism of action. Pyridine was used in the preparation of **(*R*)104**, with exclusive mono-mesylation being observed by TLC, LRMS and ^{1}H NMR analysis, to afford the desired macrocycle product in a good yield of 26% (**Scheme 4.4**). The structure of the macrocycle was confirmed by small molecule X-ray crystallography (See Appendix E).

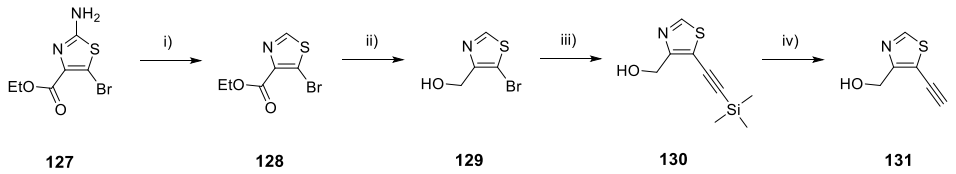


(*R*)124 (*R*)125 (*R*)126 (*R*)104

Scheme 4.4 Synthesis of macrocycle **(*R*)104**. *Reagents and conditions*: (i) **116**, $Pd(PPh_3)_2Cl_2$, K_2CO_3, 1,4-dioxane, H_2O, 100 °C, 24 h, 91%; (ii) 2 M HCl, CH_2Cl_2, EtOH, 80 °C, 21 h, 94%; (iii) MsCl, Py, THF, 0 °C to rt, 30 min; then DMF, Cs_2CO_3, 80 °C, 2 h, 22% over 2 steps.

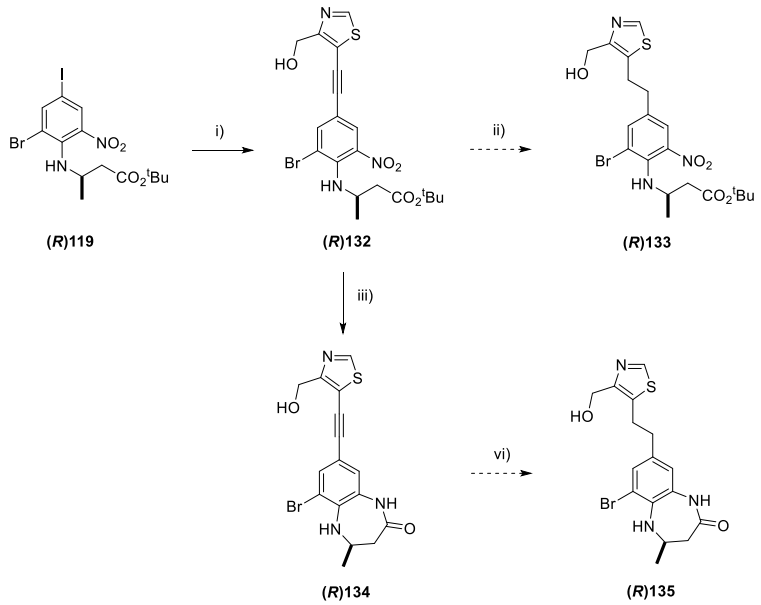
*4.4.2.2 Macrocycle **(R)105** – S_N2 displacement macrocyclisation*

Thiazole **131** was prepared following a literature procedure with the commercially available aminothiazole **127** (**Scheme 4.5**).[99,100] The first reaction uses sodium nitrite in the diazotisation of the amino moiety, which is then reduced in the presence of hypophosphorus acid to afford **128**. Reduction of ester **128** was achieved using $NaBH_4$, catalysed by $CaCl_2$ in moderate yields. Typically, $NaBH_4$ is not reactive towards esters, however, the reaction could occur due to the electron-withdrawing thiazole group. The final steps use a Sonogashira cross-coupling with trimethylsilylacetylene at 90 °C, followed by a TMS deprotection to afford the desired linker moiety **131**. Efforts to optimise the synthetic procedure were not attempted, as sufficient quantities of linker **131** were synthesised for the preparation of THBD fragment **(*R*)135**.



Scheme 4.5 Synthesis of linker **131**. *Reagents and conditions*: (i) $NaNO_2$, 50% aq. H_2SO_4, −5 °C, then 50% H_3PO_2, −5 °C, 2 h, 66% over 2 steps; (ii) $NaBH_4$, $CaCl_2$, THF, H_2O, 0 °C, 3 h, 54%; (iii) trimethylsilylacetylene, CuI, $Pd(PPh_3)_2Cl_2$, NEt_3, DMF, 90 °C, 2 h, 42%; (iv) K_2CO_3, MeOH, rt, 30 min, 88%.

Thiazole **131** was used in a Sonogashira coupling with common intermediate **(*R*)119** to afford **(*R*)132** in a 98% yield (**Scheme 4.6**). However, Wilkinson's catalyst failed to hydrogenate the alkyne in **(*R*)132**, returning only starting material. We hypothesised this was due the electron deficient internal alkyne being adjacent to aryl groups on either side. Intermediate **(*R*)132** was cyclised to THBD **(*R*)134**, however this reaction was poor yielding and the product was very insoluble. Hydrogenation of **(*R*)134** was attempted with Adam's catalyst but no reaction occurred. This was likely a result of the poor solubility of the starting material and poisoning of the platinum catalyst, known to be caused by sulfur substituents. The decision was made to focus on the route development for the other macrocycle series.

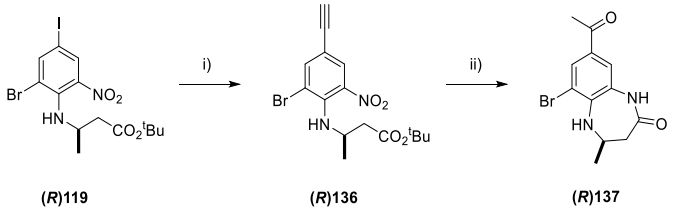


Scheme 4.6 Synthetic route towards the preparation of desired THBD fragment **(*R*)135**. *Reagents and conditions*: (i) **131**, CuI, $Pd(PPh_3)_2Cl_2$, NEt_3, THF, rt, 5 h, 98%; (ii) H_2, $Rh(PPh_3)_3Cl$, Tol, 60 °C; (iii) TFA, CH_2Cl_2, rt, 2 h, then Fe, AcOH, 100 °C, 4 h, 31% over 2 steps; (iv) H_2, PtO_2, MeOH, rt.

4.4.3 Macrocycle series 2

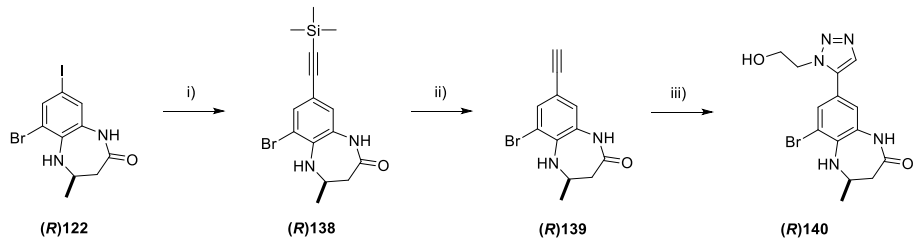
*4.4.3.1 Macrocycle **(R)106** – S_N2 displacement macrocyclisation*

We planned to synthesise macrocycle **(*R*)106** using the S_N2 displacement macrocyclisation method, as it has shown to work in the preparation of previous target macrocycles. Intermediate **(*R*)119** was reacted in a Sonogashira coupling with trimethylsilylacetylene, followed by a TMS deprotection to afford terminal alkyne **(*R*)136** (**Scheme 4.7**). However, cyclisation to the THBD led to the hydration of the alkyne bond to afford ketone **(*R*)137** in an 89% yield. The hydration of alkyne bonds to ketones had previous required the use of heavy and precious metals including; mercury, gold, palladium, platinum, ruthenium and rhodium, working with varying degrees of success. However, it was serendipitously identified by Damiano *et al.* in 1996 that this transformation can be achieved in high yields using stoichiometric iron(III) chloride.[101] A catalytic version of this reaction was later developed, and could be considered as a good method to protect aryl ketone functional groups.[102]



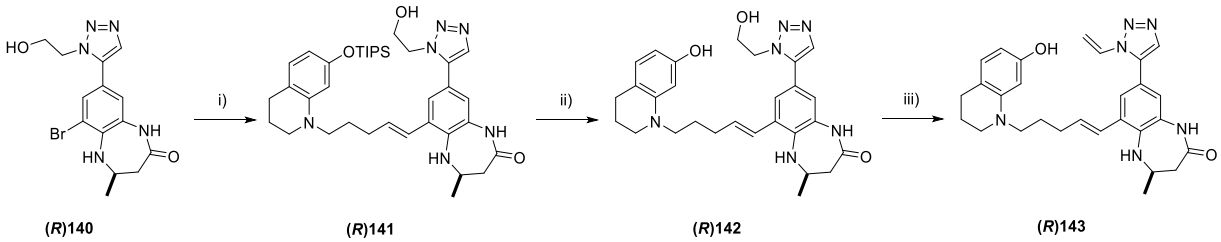
Scheme 4.7 Synthesis of by-product **(*R*)137**. *Reagents and conditions*: (i) trimethylsilylacetylene, CuI, $Pd(PPh_3)_2Cl_2$, NEt_3, THF, rt, 18 h; then K_2CO_3, MeOH, rt, 30 min, 67% over 2 steps; (ii) TFA, CH_2Cl_2, rt, 2 h, then Fe, AcOH, 100 °C, 4 h, 89% over 2 steps.

To avoid this side reaction, the Sonogashira coupling with trimethylsilylacetylene was performed on the THBD intermediate **(*R*)122**, followed by TMS deprotection to afford the intended THBD **(*R*)139**. This compound was reacted with 2-azidoethanol in a ruthenium-catalysed azide-alkyne cycloaddition (RuAAC) to afford the 1,5-triazole **(*R*)140**, with complete regioselectivity (**Scheme 4.8**).[103,104]



Scheme 4.8 Synthesis of THBD fragment **(*R*)140**. *Reagents and conditions*: (i) Trimethylsilylacetylene, CuI, $Pd(PPh_3)_2Cl_2$, NEt_3, DMF, rt, 18 h, 94% (ii) K_2CO_3, MeOH, rt, 30 min, 93% (iii) 2-Azidoethanol, $Cp^*RuCl(PPh_3)_2$, THF, 75 °C, 1 h, 52%.

The THBD fragment **(*R*)140** was reacted in a Suzuki coupling with late-stage intermediate **116**, followed by deprotection of the TIPS group to afford macrocycle precursor **(*R*)142** in a 76% yield. We initially used the same macrocyclisation conditions described in the preparation of **(*R*)104**. However, this led to the elimination of the mesylate intermediate to form a terminal alkene side-product **(*R*)143**. (**Scheme 4.9**). The temperature for the S_N2 displacement was lowered to try and avoid this side-reaction, but only starting material was observed at room temperature. The stepwise increase in temperature still resulted in the formation of the terminal alkene. This side-reaction was not observed in syntheses of the previously prepared macrocycles using this route, and was rationalised to be a result of the increased stabilisation of the terminal alkene bond by conjugation into the triazole ring.



Scheme 4.9 Synthesis of acyclic by-product **(*R*)143**. *Reagents and conditions*: (i) **116**, $Pd(PPh_3)_2Cl_2$, K_2CO_3, 1,4-dioxane, H_2O, 100 °C, 20 h, 92%; (ii) 2 M HCl, CH_2Cl_2, EtOH, 80 °C, 21 h, 83%; (iii) MsCl, Py, THF, 0 °C to rt; then DMF, Cs_2CO_3, rt to 45 °C.

The disadvantage of using the S_N2 displacement macrocyclisation was that both macrocycle product **(*R*)106** and elimination product **(*R*)143** have the same molecular weight, therefore LRMS analysis cannot be used to monitor the reaction. However, upon comparing the ^{1}H NMR spectra of macrocycle precursor **(*R*)142** and side-product **(*R*)143**, terminal alkene splitting patterns were observed in the aromatic region for **(*R*)143**, which confirmed the formation of the elimination product (**Figure 4.11**). The decision was made to try an alternative macrocyclisation method for the preparation of **(*R*)106**.

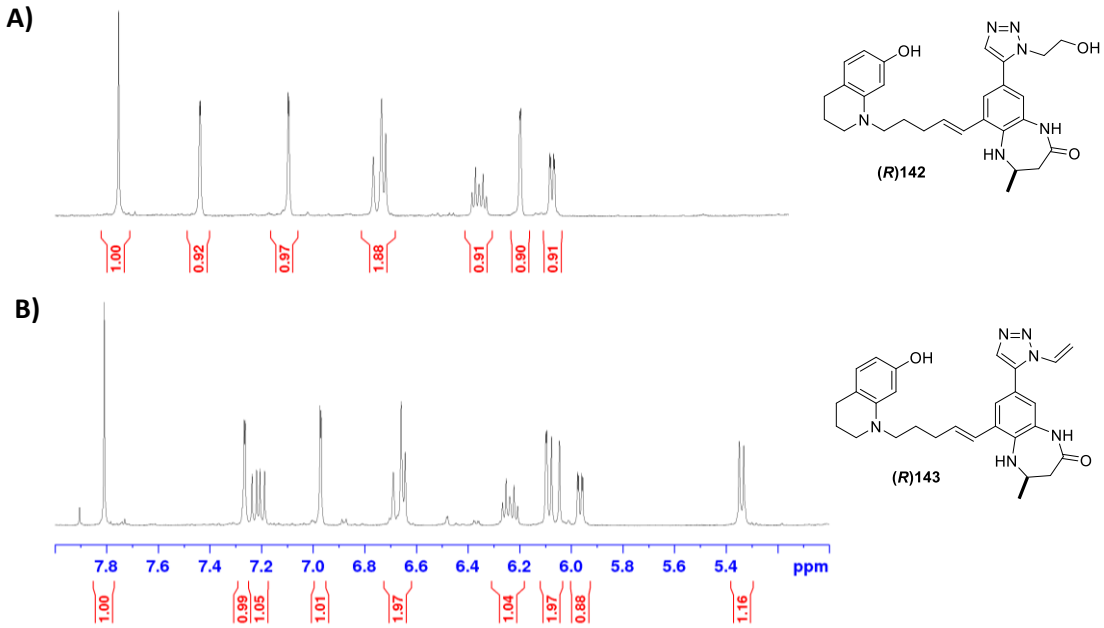
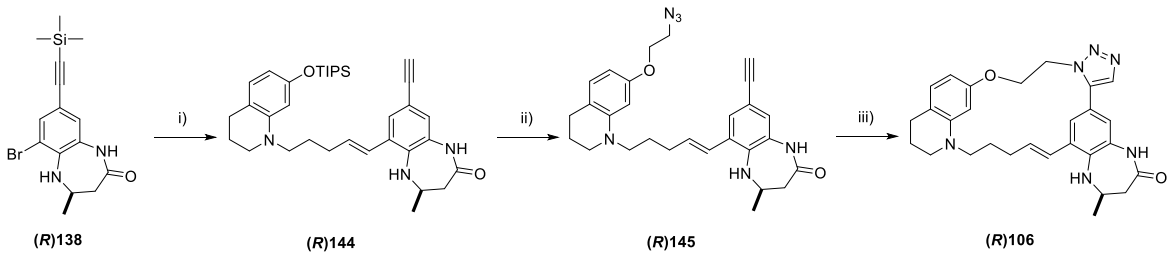


Figure 4.11 ^{1}H NMR (CD_3OD) spectra (between 5–8 ppm) of (A) macrocycle precursor **(*R*)142** and (B) terminal alkene side-product **(*R*)143**.

*4.4.3.2 Macrocycle **(R)106** – Ru-catalysed azide-alkyne cycloaddition macrocyclisation*

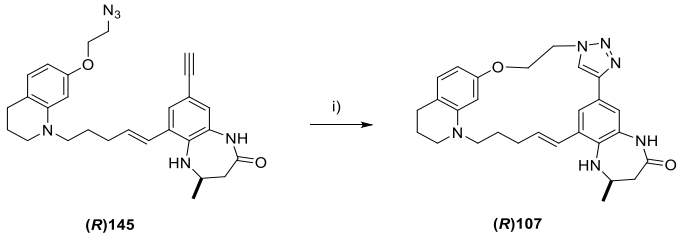
The RuAAC was already shown to work well in the preparation of **(*R*)140**, and therefore was considered for the macrocyclisation step of macrocycle **(*R*)106** (**Scheme 4.10**). Intermediate **(*R*)138** was reacted in a Suzuki coupling to late-stage intermediate **116**, followed by TMS deprotection to afford **(*R*)144**. The TIPS group was deprotected with 1 M TBAF, as these conditions could remove the protecting group in a shorter time and at room temperature. However, this unprotected phenol intermediate was unstable for long periods of time. To overcome this instability, the TIPS deprotected intermediate was reacted immediately after isolation with 2-azidoethyl methanesulfonate to afford **(*R*)145** in a 53% yield over two steps. Conditions identified in the preparation of 1,5-triazole **(*R*)140** were used in the preparation of **(*R*)106**, with the modification of diluting the concentration to 0.002 M, which gave the desired macrocycle in a 21% yield. Due to the entropic energy penalty to form the macrocycle, a 21% yield is typically considered good for a macrocyclisation step. However, this yield was curiously low, as full consumption of precursor **(*R*)145** was observed after 1 h with no other product being observed by TLC or isolated in column chromatography.



Scheme 4.10 Synthesis of macrocycle **(*R*)106**. *Reagents and conditions*: (i) **116**, $Pd(PPh_3)_2Cl_2$, K_2CO_3, 1,4-dioxane, H_2O, 100 °C, 18 h; then K_2CO_3, MeOH, rt, 30 min, 51% over 2 steps; (ii) 1 M TBAF, THF, rt, 1 h; then 2-azidoethyl methanesulfonate, K_2CO_3, DMF, 65 °C, 53%; (iii) $Cp^*RuCl(PPh_3)_2$, THF, 75 °C, 1 h, 21%.

*4.4.3.3 Macrocycle **(R)107** – Cu-catalysed azide-alkyne cycloaddition macrocyclisation*

The use of a cycloaddition as the macrocyclisation step for **(*R*)106** enabled the facile preparation of the 1,4-triazole macrocycle **(*R*)107** in a single step from the common intermediate **(*R*)145**. There is significant literature precedent for the regioselective 1,4-triazole formation using a copper-catalysed azide-alkyne cycloaddition (CuAAC).[105,106] However, this cycloaddition worked poorly, isolating the desired macrocycle **(*R*)107** in a 3% yield (**Scheme 4.11**). Optimisation of this macrocyclisation could explore the use of heat and use alternative solvents and copper catalysts, however, efforts to improve the yield were not attempted as enough material was isolated for characterisation and testing.



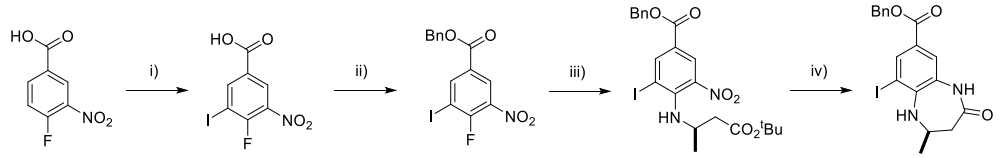
Scheme 4.11 Synthesis of macrocycle **(*R*)107**. *Reagents and conditions*: (i) $CuSO_4$, (+)-sodium L-ascorbate, THF, H_2O, rt, 20 h, 3%.

One disadvantage of using the triazole cycloaddition as the macrocyclisation step is that LRMS analysis could not be used to monitor the formation of the macrocycles, as the molecular weights of starting material **(*R*)145** and the corresponding macrocycles are identical. The regiochemistry of the triazoles in macrocycles **(*R*)106** and **(*R*)107** was determined by NOESY experiments.

4.4.4 Macrocycle series 3

*4.4.4.1 Macrocycle **(R)108** – Macrolactamisation*

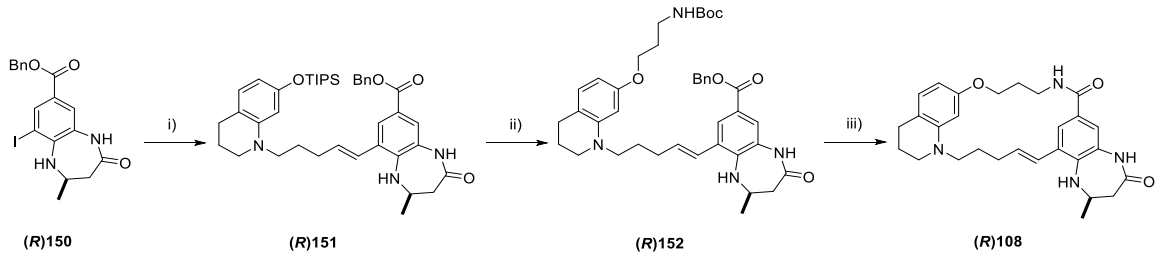
Macrocycle series 3 would use macrolactamisation for the ring closure, as there is literature precedent for its use as a macrocyclisation step.[107] The synthesis of THBD fragment **(*R*)150** is shown in **Scheme 4.12**. Interestingly, NIS and concentrated sulfuric acid conditions led to incomplete iodination of **146**, likely due to the electron-deficiency of the aromatic ring and therefore required more forcing conditions. The preparation of the aniline intermediate **(*R*)149** followed the same route described previously for its regioisomer **(*R*)72** in Section 3.3.1.3, differing only in the positions of the benzyl ester and iodo- substituents. Intermediate **(*R*)149** was cyclised using iron powder in acetic acid to form the THBD intermediate **(*R*)150** in a 94% yield over two steps.



146 **147** **148** **(*R*)149** **(*R*)150**

Scheme 4.12 Synthesis of THBD fragment **(*R*)150**. *Reagents and conditions*: (i) I_2, fuming H_2SO_4, 85°C, 20 h, 89%; (ii) BnBr, K_2CO_3, DMF, 60°C, 4 h, 64%; (iii) **(*R*)41**, Cs_2CO_3, Tol, 85 °C, 21 h, 97%; (iv) TFA, CH_2Cl_2, rt, 1 h, then Fe, AcOH, 100 °C, 4 h, 94% over 2 steps.

The THBD fragment **(*R*)150** was used in a Suzuki coupling with late-stage intermediate **116** to yield intermediate **(*R*)151** (**Scheme 4.13**). TIPS deprotection with 1 M TBAF revealed the free phenol intermediate which was observed to be unstable, therefore it was used immediately upon preparation in an alkylation reaction with *tert*-butyl (3-bromopropyl)carbamate to give macrocycle precursor **(*R*)152** in a 39% yield over two steps. This precursor was reacted in a three step macrocyclisation route to afford desired macrocycle **(*R*)108** in a 58% yield. First, the benzyl ester was hydrolysed with 1 M LiOH, followed by Boc deprotection with TFA, which also protonates the carboxylic acid. The reaction mixture was then diluted to 0.002 M in DMF, adjusted to pH 9 with DIPEA and PyBOP was used for the macrolactamisation. Unlike the S_N2 displacement and triazole cycloaddition macrocyclisations, LRMS analysis could be used to monitor the reaction as the reported mass would only correspond to the molecular weight of the macrocycle. The structure of macrocycle **(*R*)108** was confirmed by small molecule X-ray crystallography (see Appendix E) and gave confidence in preparation of the remaining macrocycles in this series using this macrocyclisation method.

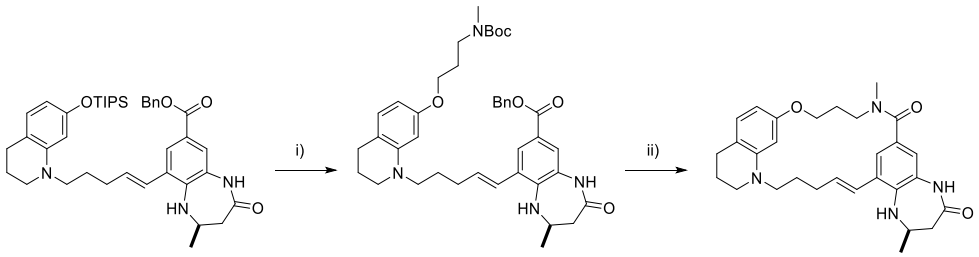


(*R*)150 (*R*)151 (*R*)152 (*R*)108

Scheme 4.13 Synthesis of macrocycle **(*R*)108**. *Reagents and conditions*: (i) **116**, $Pd(PPh_3)_2Cl_2$, K_2CO_3, 1,4-dioxane, H_2O, 100 °C, 18 h, 68%; (ii) 1 M TBAF, THF, rt, 1 h; then *tert*-butyl (3-bromopropyl)carbamate, K_2CO_3, DMF, 65 °C, 16 h, 39% over 2 steps; (iii) 1 M LiOH, THF, MeOH, H_2O, rt, 5 h; then TFA, CH_2Cl_2, rt, 2 h; then PyBOP, DIPEA, DMF, rt, 36 h, 58% over 3 steps.

*4.4.4.2 Macrocycle **(R)109** – Macrolactamisation*

Intermediate **(*R*)151** was TIPS deprotected and alkylated with 3-((*tert*-butoxycarbonyl)(methyl)amino)propyl methanesulfonate (**Scheme 4.14**). However, this reaction gave low yields due to the formation of a dialkylated side-product observed by LRMS analysis. This meant the reaction could not be pushed to completion by increasing the equivalence of 3-((*tert*-butoxycarbonyl)(methyl)amino)propyl methanesulfonate. Nevertheless, enough of **(*R*)153** was obtained for the macrolactamisation to be attempted. This reaction afforded the desired macrocycle **(*R*)109** in a 43% yield.

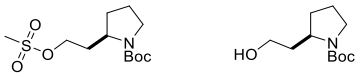


(*R*)151 (*R*)153 (*R*)109

Scheme 4.14 Synthesis of macrocycle **(*R*)109**. *Reagents and conditions*: (ii) 1 M TBAF, THF, rt, 1 h; then 3-((*tert*-butoxycarbonyl)(methyl)amino)propyl methanesulfonate, K_2CO_3, DMF, 65 °C, 22 h, 25% over 2 steps; (iii) 1 M LiOH, THF, MeOH, H_2O, rt, 5 h; then TFA, CH_2Cl_2, rt, 2 h; then PyBOP, DIPEA, DMF, rt, 36 h, 43% over 3 steps.

*4.4.4.3 Macrocycle **(R)(R)110** – Macrolactamisation*

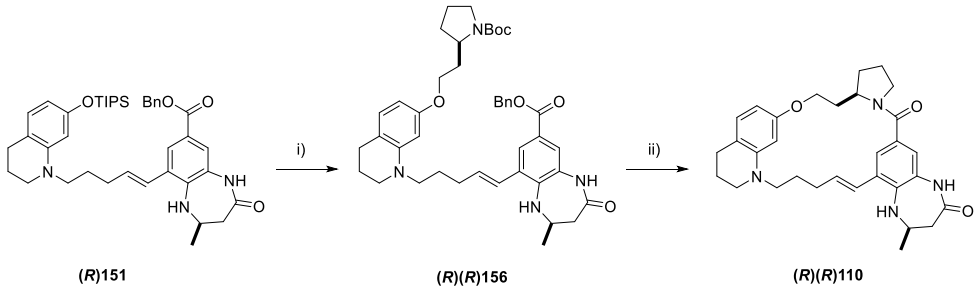
Attempts to alkylate the TIPS deprotected intermediate of **(*R*)151** with *tert*-butyl (*R*)-2-(2-((methylsulfonyl)oxy)ethyl)pyrrolidine-1-carboxylate **(*R*)154**, (**Figure 4.12**), using an S_N2 displacement were unsuccessful as only starting material remained. Recent literature has also identified reagent **(*R*)154** to be low yielding for S_N2 reactions, possibly due to instability at elevated temperatures.[108]



(*R*)154 (*R*)155

Figure 4.12 Reagents used to attach the linker to prepare macrocycle precursor **(*R*)(*R*)156**.

Mitsunobu conditions were instead investigated using DEAD and tributylphosphine with alcohol **(*R*)155**, to give macrocycle precursor **(*R*)(*R*)156** in a yield of 17%. A major impurity in this reaction was tributylphosphine oxide, which was easily removed by column chromatography using an Et_2O/pentane solvent system. Optimisation of the yield could not be performed due time constraints, but alternative Mitsunobu conditions could result in an improved yield. The macrocycle precursor was used in the three-step macrocyclisation route to give the computationally designed macrocycle **(*R*)(*R*)110** in a 12% yield (**Scheme 4.15**).

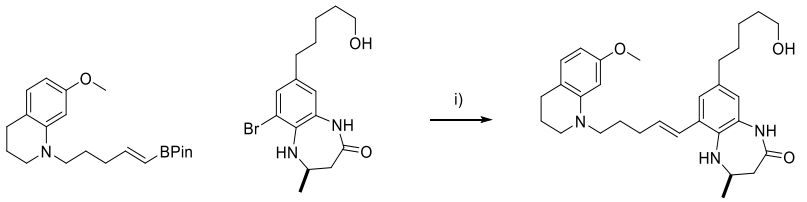


(*R*)151 (*R*)(*R*)156 (*R*)(*R*)110

Scheme 4.15 Synthesis of macrocycle **(*R*)(*R*)110**. *Reagents and conditions*: (ii) 1 M TBAF, THF, rt, 1 h; then *tert*-butyl (*R*)-2-(2-hydroxyethyl)pyrrolidine-1-carboxylate, DEAD, PBu_3, THF, rt, 12 h, 17% over 2 steps; (iii) 1 M LiOH, THF, MeOH, H_2O, rt, 5 h; then TFA, CH_2Cl_2, rt, 2 h; then PyBOP, DIPEA, DMF, rt, 36 h, 12% over 3 steps.

4.4.5 Acyclic analogues of macrocycle series

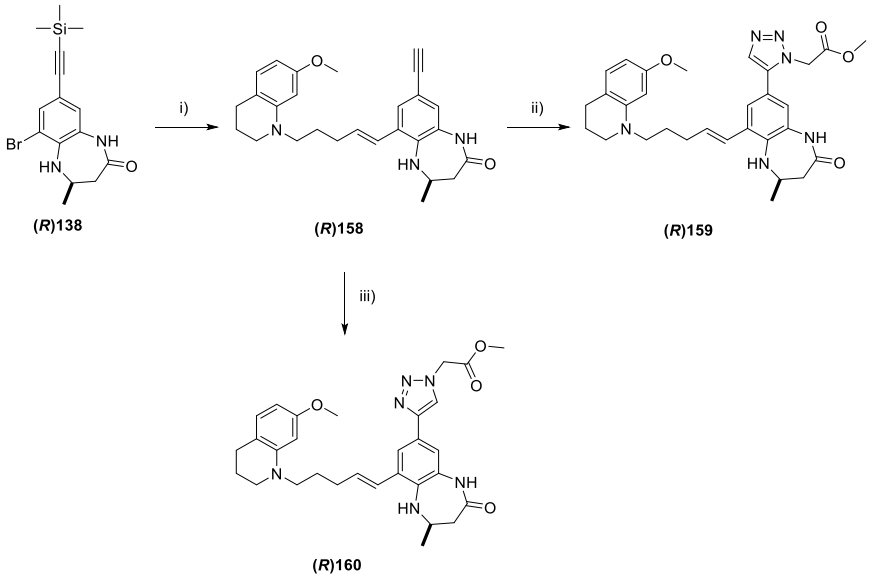
We have synthesised the corresponding acyclic analogue to determine whether there has been an improvement in the relative affinities of the designed macrocycles. For series 1, macrocycle **(*R*)104** was prepared with a flexible linker chain, therefore, the acyclic analogue **(*R*)157** was synthesised for comparison (**Scheme 4.16**). Analogue **(*R*)157** was prepared by a Suzuki coupling of intermediate **47** (synthetic route described in Section 2.2) and THBD fragment **(*R*)124** in a 33% yield. The synthesis shown in **Scheme 4.16** was performed by Katrina Andrews in the group of Prof. Stuart Conway (University of Oxford).



47 **(*R*)124** **(*R*)157**

Scheme 4.16 Synthesis of acyclic ligand **(*R*)157**. *Reagents and conditions*: (i) $Pd(PPh_3)_2Cl_2$, K_2CO_3, 1,4-dioxane, H_2O, 100 °C, 16 h, 33%.

For series 2, **(*R*)138** was used in a Suzuki coupling with **47**, followed by TMS deprotection to give intermediate **(*R*)158**. This intermediate was reacted in both a RuAAC and CuAAC to give 1,5-triazole **(*R*)159** and 1,4-triazole **(*R*)160** respectively (**Scheme 4.17**).

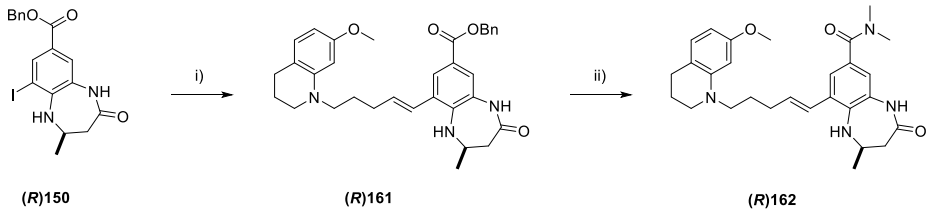


(*R*)138 **(*R*)158** **(*R*)159**

(*R*)160

Scheme 4.17 Synthesis of triazole ligands **(*R*)159** and **(*R*)160**. *Reagents and conditions*: (i) **47**, $Pd(PPh_3)_2Cl_2$, K_2CO_3, 1,4-dioxane, H_2O, 100 °C, 18 h, 45% then K_2CO_3, MeOH, rt, 2h, 45% over 2 steps; (ii) methyl 2-azidoacetate, $Cp^*RuCl(PPh_3)_2$, THF, 75 °C, 2 h, 46%; (iii) methyl 2-azidoacetate, $CuSO_4$, (+)-sodium L-ascorbate, THF, H_2O, rt, 2 h, 52%.

For series 3, the preparation of the dimethyl amide **(*R*)162** was considered to be a representative acyclic analogue for all the amide macrocycles to be compared against. Intermediate **(*R*)150** was reacted in a Suzuki coupling with **47**, followed by a benzyl deprotection of intermediate **(*R*)161** and amide coupling to afford **(*R*)162** (**Scheme 4.18**). The synthesis shown in **Scheme 4.18** was performed by Margarida Espadinha in the group of Prof. Stuart Conway (University of Oxford).



Scheme 4.18 Synthesis of amide ligand **(*R*)162**. *Reagents and conditions*: (i) **47**, $Pd(PPh_3)_2Cl_2$, K_2CO_3, 1,4-dioxane, H_2O, 100 °C, 18 h, 68%; (ii) 1 M LiOH, THF, MeOH, H_2O, rt, 5 h; then PyBOP, NEt_3, DMF, rt, 18 h, 51% over 2 steps.

4.5 Biophysical evaluation of the macrocycle series

4.5.1 CREBBP bromodomain binding affinity

The binding affinity for the CREBBP bromodomain was assessed using ITC. For the series 1, macrocycle **(*R*)104** which has an alkyl linker, showed no detectable binding towards the CREBBP bromodomain (**Figure 4.13**). However, its acyclic analogue, **(*R*)157**, retained good affinity with a K_d = 0.54 µM. The loss of binding for **(*R*)104** might be a result of the macrocycle not being able to favourably adopt the bioactive conformation. For series 2, both acyclic triazole analogues **(*R*)159** and **(*R*)160** showed affinity to the CREBBP bromodomain, with a K_d = 1.31 µM and K_d = 1.26 µM respectively. However, these K_d values are a >12-fold loss in affinity compared to acyclic ligand **(*R*)48** (**Figure 4.6**), which indicated that the triazole moiety was not tolerated well in the bromodomain binding pocket. Furthermore, both triazole macrocycles **(*R*)106** and **(*R*)107** gave no detectable binding (**Figure 4.14**). Although molecular docking studies predicted the 1,5-triazole macrocycle **(*R*)106** to adopt the bioactive pose, these results were in-line with the conformational analysis and metadynamic simulation studies shown in Section 4.3.4.

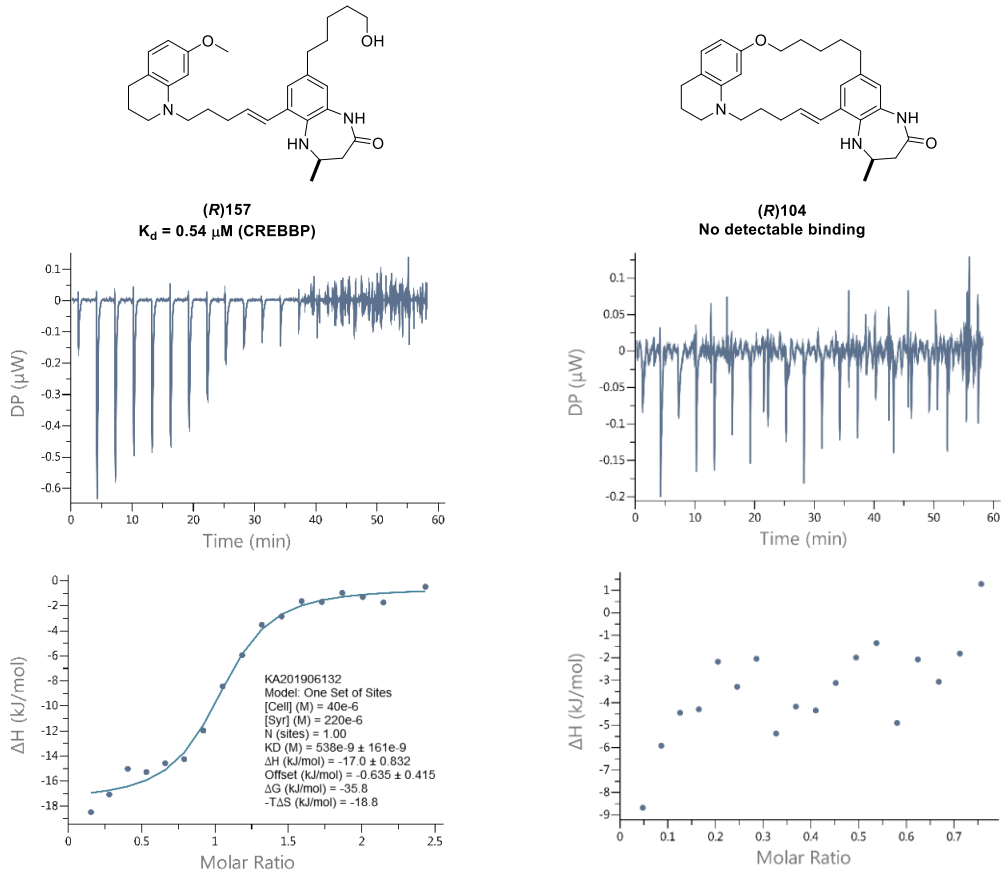


Figure 4.13 ITC binding data for series 1 against the CREBBP bromodomain.

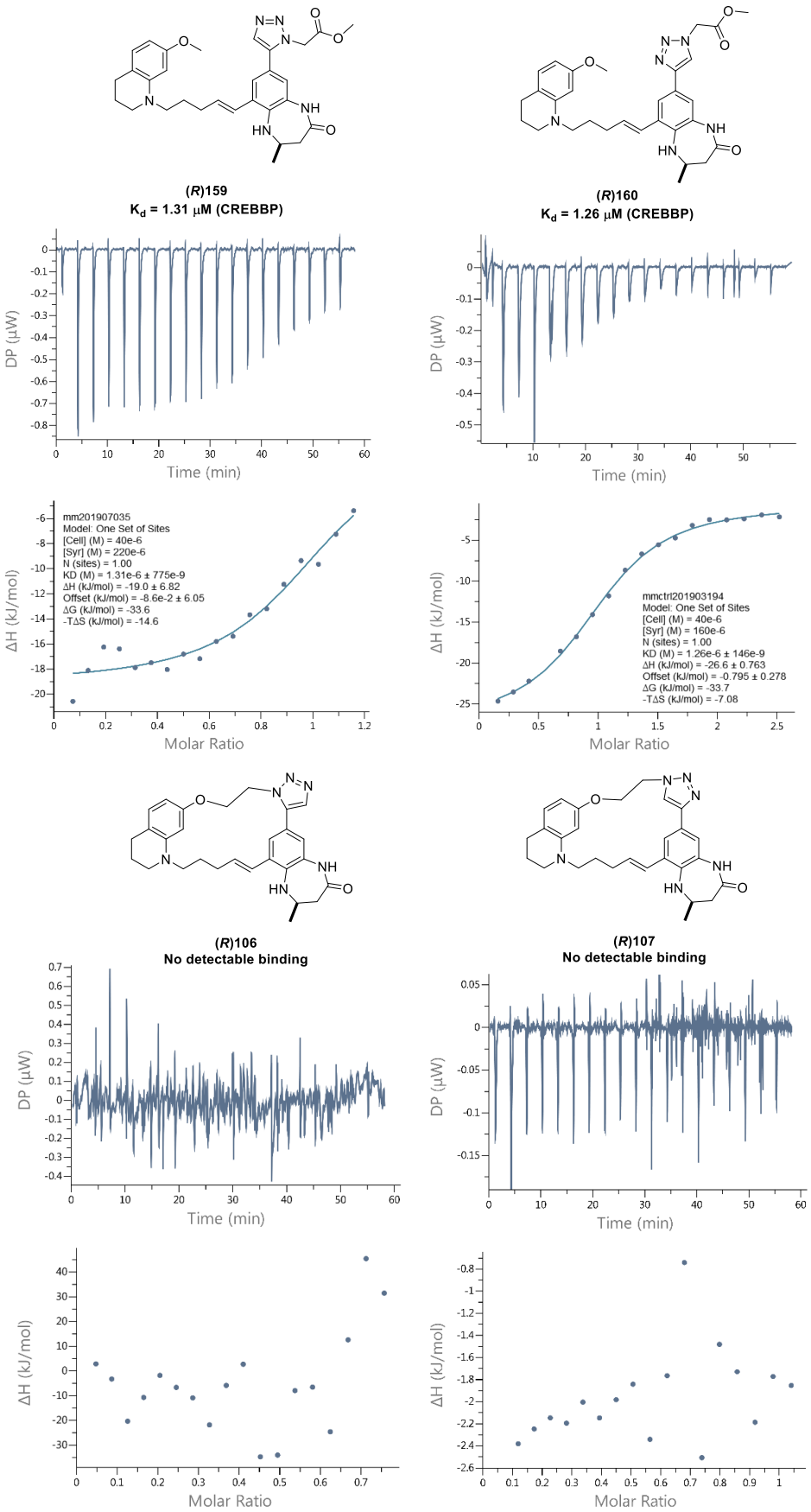


Figure 4.14 ITC binding data for series 2 against the CREBBP bromodomain.

For series 3, the acyclic analogue **(*R*)162** had a K_d = 1.30 µM for the CREBBP bromodomain, and similarly to the triazole acyclic analogues, it indicated that the amide moiety was also less tolerated in the KAc binding pocket. Despite this observed SAR, all amide macrocycles retained affinity for the CREBBP bromodomain (**Figure 4.15**). Macrocycle **(*R*)(*R*)110** had the highest affinity, with a K_d = 0.99 µM, and this result was in-line with the computational analysis shown in Section 4.3.5. Macrocycles **(*R*)108** and **(*R*)109** were predicted to have different amide geometries, *E*- and *Z*- respectively, and therefore it was thought that this may bias the *E*- amide **(*R*)108** to a non-bioactive conformation. Interestingly, macrocycle **(*R*)108** retained similar affinity to the acyclic analogue **(*R*)162**, with its methylated analogue **(*R*)109** displaying a weaker affinity.

Despite series 1 macrocycle **(*R*)104** having the same ring size as the series 3 amide macrocycles, **(*R*)104** shows no detectable binding to the CREBBP bromodomain. It can be interpreted that the amide moiety is able to conformationally bias the macrocycles into the bioactive poses, or alternatively, it has a favourable interaction in the bromodomain binding site. However, the >12-fold loss in affinity of analogue **(*R*)162** against ligand **(*R*)48** (**Figure 4.6**) would suggest that the amide is not contributing towards preferential binding interactions in the CREBBP bromodomain pocket.

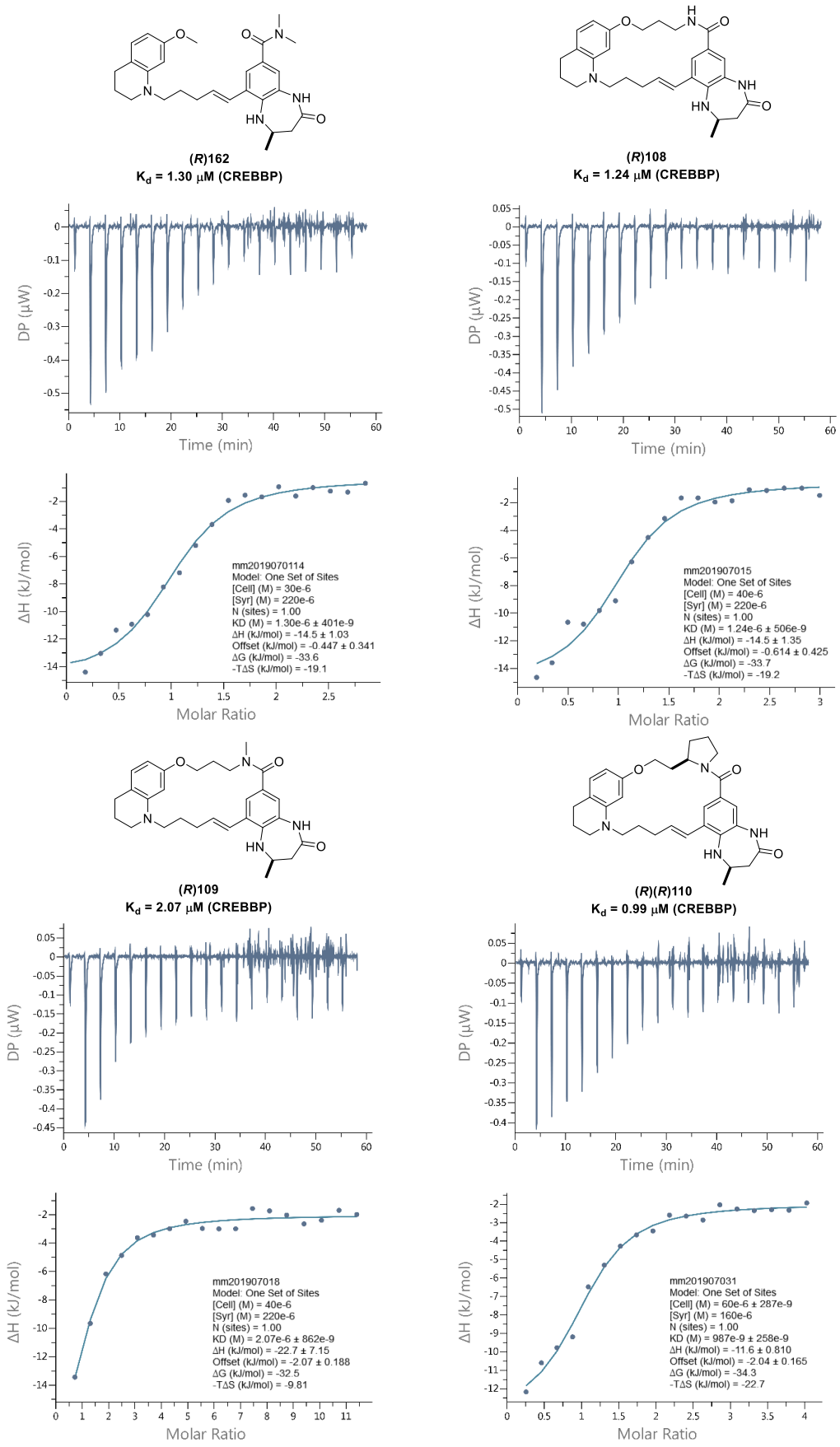


Figure 4.15 ITC binding data for series 3 against the CREBBP bromodomain.

4.5.2 BRD4(1) binding affinity

Series 3 included macrocycles with good affinity to the CREBBP bromodomain, therefore, we decided to assess the selectivity against BRD4(1). However, to prove the hypothesis that a macrocyclic conformation would disfavour binding to BRD4(1), as outlined in Section 3.1, their affinities would need to be compared against acyclic analogue **(*R*)162**. The affinity data of all the acyclic analogues to BRD4(1) is shown in **Figure 4.16**.

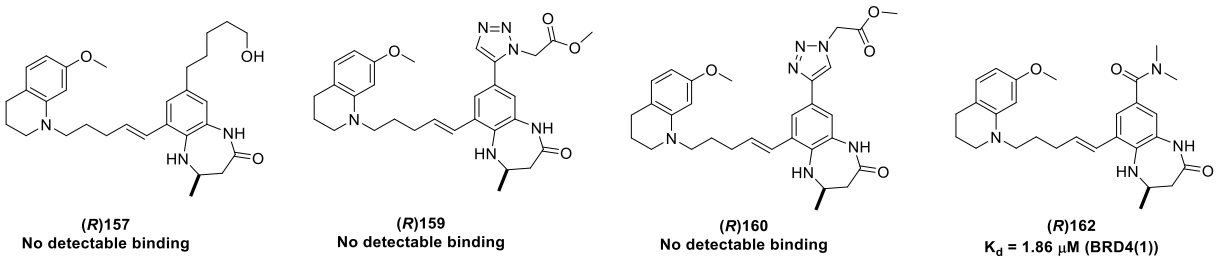


Figure 4.16 Acyclic ligands' observed affinity to BRD4(1) by ITC. ITC traces shown in Appendix C2.

Compounds **(*R*)157**, **(*R*)159** and **(*R*)160** showed no detectable binding to BRD4(1), corresponding to the SAR data identified for acyclic ligand **(*R*)48** in Section 2.3.3. Interestingly, analogue **(*R*)162** had a K_d = 1.86 μM to BRD4(1), which means that the amide moiety has a favourable interaction in the BRD4(1) binding site. Nevertheless, all series 3 macrocycles displayed no detectable binding to BRD4(1) and were selective for the CREBBP bromodomain (**Figure 4.17**). The macrocycles and acyclic analogue **(*R*)162** all having similar affinities for the CREBBP bromodomain, provides good evidence that a macrocyclic ligand can improve the selectivity against BRD4(1), and confirmed the macrocycle selectivity hypothesis.

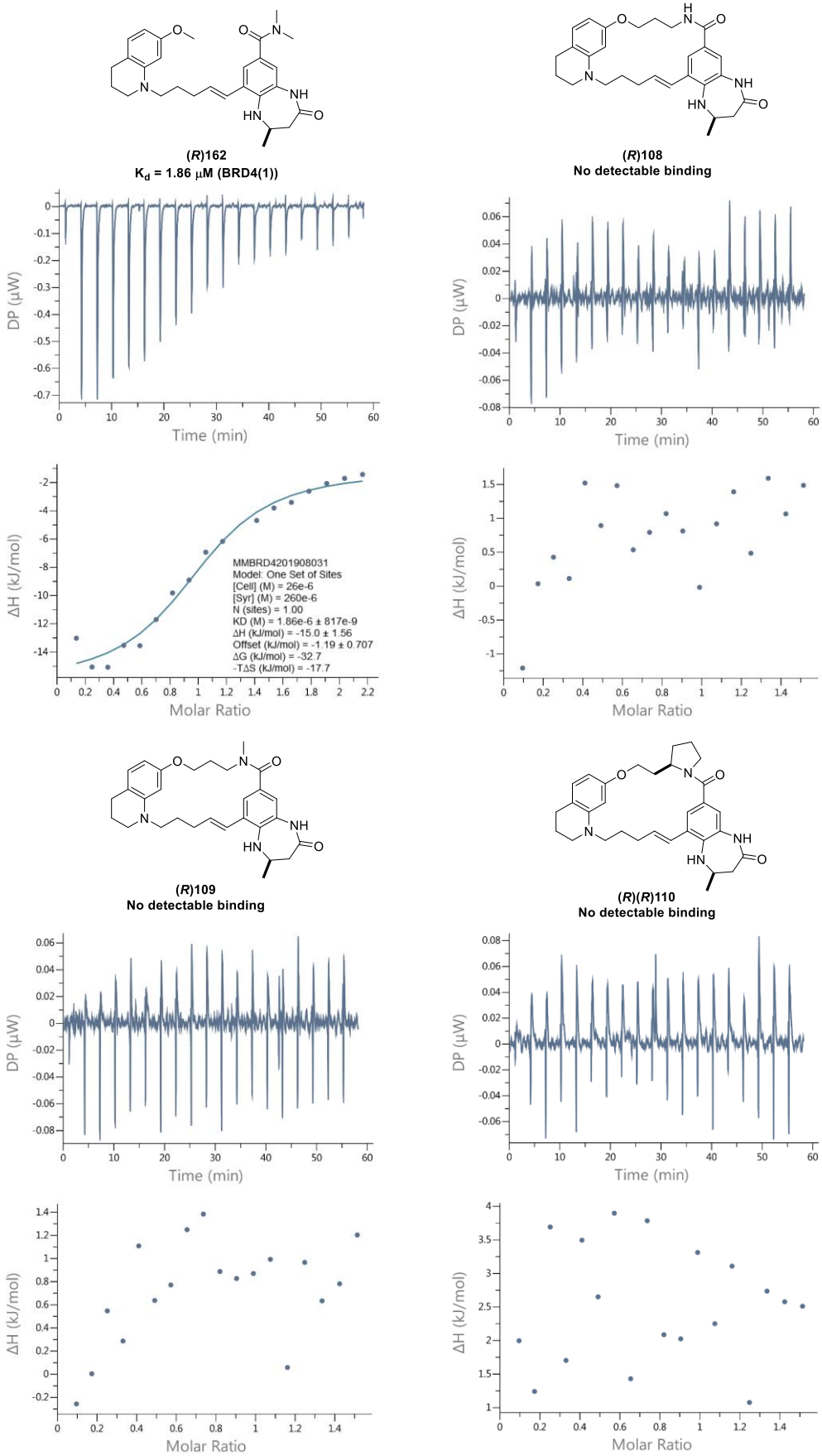


Figure 4.17 ITC binding data for series 3 against BRD4(1).

4.5.3 Conformational analysis

4.5.3.1 Small molecule X-ray crystal structures

The structure of macrocycles **(*R*)104** and **(*R*)108** were elucidated by small molecule X-ray crystallography. Interestingly, their solid-state conformations were almost identical, as both have two molecules in their unit cells (**Figure 4.18**). In addition, the crystal structure of **(*R*)108** shows the amide bond to adopt the *E*-geometry. However, only macrocycle **(*R*)108** has affinity to the CREBBP bromodomain, despite the macrocycles being the same ring size. Recent work published by Dr Elisabetta Chiarparin and co-workers showed that it was possible to use proposed conformations, from X-ray structures or docking models, to derive Quantum Mechanical (QM) calculations of the 1D NMR spectrum, including chemical shifts and *J*-couplings.[39] These values can be compared with experimental 1D NMR values to validate if this conformation is observed in solution.[39] Furthermore, knowledge of the free-ligand conformational preference in solution can aid structure-based drug design. A recent example of this was published by Johannes *et al.*[47] in their design of macrocyclic inhibitors of Mcl1. They observed anomalous proton NMR chemical shifts caused by anisotropic shielding for their most potent macrocycle, which contained a methylated amide. This was shown to have a conformational lock biased towards adopting the bioactive conformation in solution. However, the less potent desmethylated analogue did not display the same diagnostic chemical shift by ^{1}H NMR and was instead biased towards a non-bioactive conformation in solution.[109]

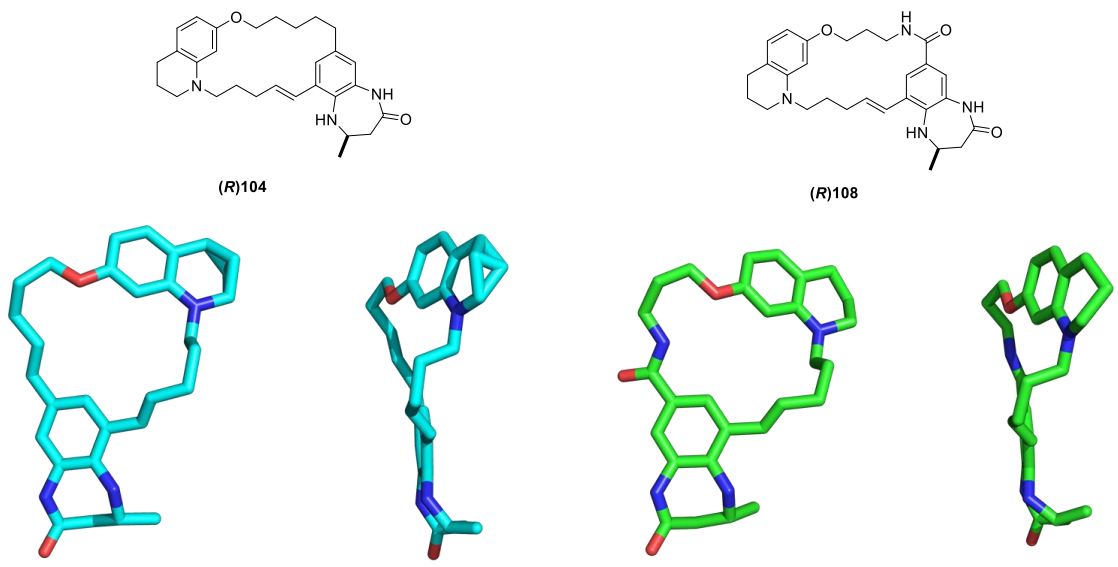


Figure 4.18 Small molecule crystal structure analysis of macrocycles **(*R*)104** (carbon:cyan) and **(*R*)108** (carbon:green).

The ^{1}H NMR spectra for **(*R*)104** and **(*R*)108** showed a difference in the chemical environments for the THBD headgroup, which may suggest that the solution conformations of the macrocycles are not as similar as the solid-state conformation (**Figure 4.19**). It is postulated that the loss of binding to the CREBBP bromodomain for macrocycle **(*R*)104** could be due to residual flexibility of the structure or a result of being energetically trapped in a non-bioactive conformation.

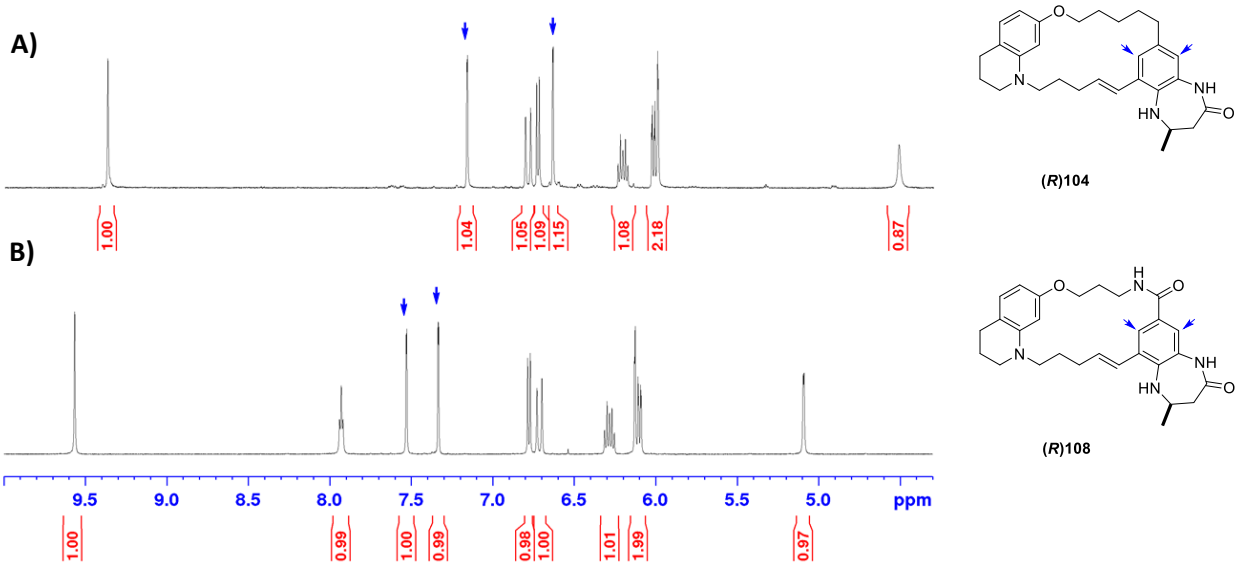


Figure 4.19 ^{1}H NMR (DMSO-d_6) spectra (between 4.3–10 ppm) highlighting the difference in chemical shift environments for (A) macrocycle **(*R*)104** and (B) macrocycle **(*R*)108**.

4.5.3.2 ^{1}H NMR of macrocycle series 3

A broadening of the chemical environments was observed in the ^{1}H NMR spectra for the macrocycles in series 3. This was hypothesised to be a result of the amide bond changing from the *E*- to *Z*- geometry in structures **(*R*)108** to **(*R*)(*R*)110**, with macrocycle **(*R*)109** in a median of the two geometries (**Figure 4.20**). Based on the chemical shift signatures of the aromatic region, it was rationalised that **(*R*)109** and **(*R*)(*R*)110** are pre-organised into a more similar dominant conformation than macrocycle **(*R*)108**. This supports the rationale of macrocycles having different amide orientations, with macrocycle **(*R*)109** biased towards a *Z*-amide conformation in solution. The broadening suggests rigidification of the macrocycles, as both macrocycles **(*R*)109** and **(*R*)(*R*)110** observed to be in slow exchange between two close conformations, with macrocycle **(*R*)(*R*)110** displaying more rigidity. Comparing this with the known binding affinities, it could suggest that macrocycle **(*R*)(*R*)110** has a stronger affinity to the CREBBP bromodomain than **(*R*)109** due to its ability to adopt the bioactive conformation more readily. Nevertheless, macrocycle **(*R*)108** also has good affinity to the CREBBP bromodomain but is thought to

take on an alternative conformation in solution to **(*R*)(*R*)110**. Variable temperature NMR was used to resolve the broadening observed for macrocycle **(*R*)(*R*)110** (see Appendix G).

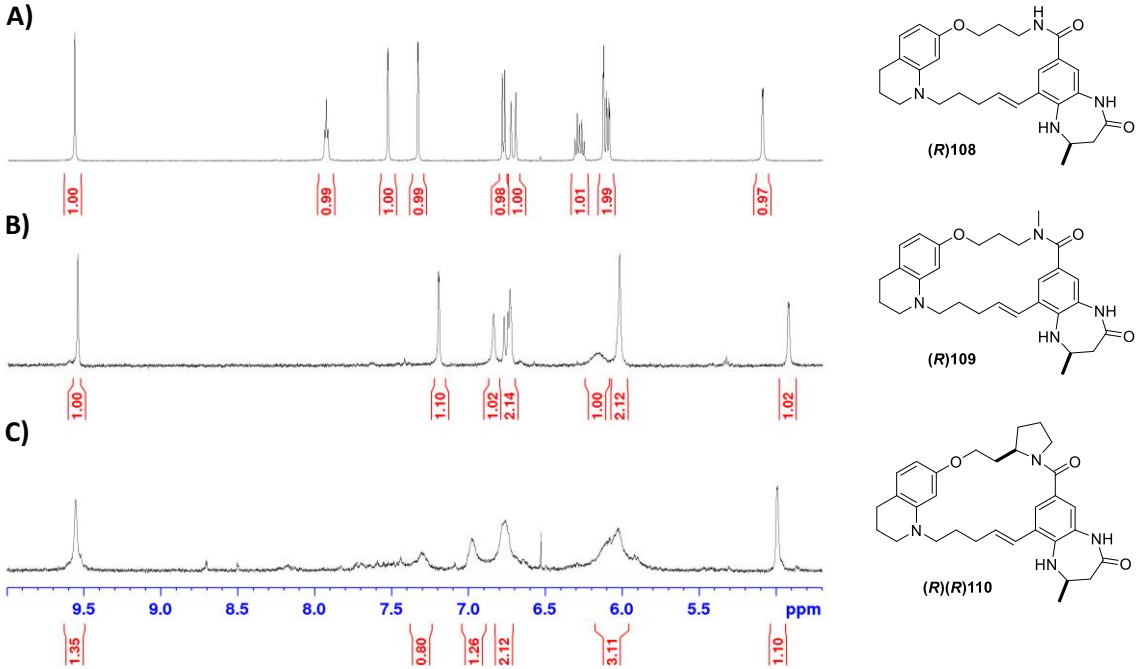


Figure 4.20 ^{1}H NMR (DMSO-d_6) spectra at 278 K (between 4.7–10 ppm). Analysis of macrocycle series 3 shows broadening in signals for macrocycles (A) **(*R*)108** (B) **(*R*)109** and (C) **(*R*)(*R*)110**, as amide geometry goes from an *E*- to *Z*-geometry.

4.6 Conclusion

A synthesis-led macrocyclic design approach, based on ligand **(*R*)48**, led to the development of three macrocycle series. Each series was tested in a three-step computational analysis that included molecular docking, conformational analysis and metadynamic simulations. This computational study identified macrocycles **(*R*)105**, **(*R*)106** and **(*R*)(*R*)110** for synthetic preparation. To validate the computational design, macrocycles **(*R*)104** and **(*R*)107** were also synthesised, as **(*R*)104** would have an alkyl linker which may not favourably adopt the bioactive conformation, and the 1,4-triazole macrocycle **(*R*)107** was shown not to adopt the bioactive pose by molecular docking. In addition, macrocycles **(*R*)108** and **(*R*)109** were prepared to explore the effects that the amide geometry has on the affinity to the CREBBP bromodomain. Macrocycle **(*R*)104** and triazole macrocycles **(*R*)106** and **(*R*)107** did not show affinity for the CREBBP bromodomain by ITC, however, their corresponding acyclic analogues were able to retain good affinity. The amide macrocycles gave similar affinity to the acyclic analogue **(*R*)162**, with macrocycle **(*R*)(*R*)110** displaying the tightest binding in the series. Furthermore, all macrocycle binding data were in-line with the predicted affinity from the computational study. The amide macrocycles showed selectivity against BRD4(1) when compared against the acyclic analogue **(*R*)162**. This supported the rationale that selectivity against BRD4(1) can be achieved by using a macrocyclic binding motif.

Future work for this project includes acquiring a protein-ligand crystal structure of macrocycles **(*R*)108** and **(*R*)(*R*)110** to the CREBBP bromodomain. This would enable a structure-based drug design approach to identify high affinity macrocyclic ligands. If the macrocyclic binding motif favours selective binding to the CREBBP bromodomain over other bromodomain families, this approach will identify probes that can elucidate the role of the CREBBP bromodomain without the phenotypic response being attributed to off-target proteins.

Chapter 5

Development of PROTACs for the degradation of CREBBP

5.1 Introduction and aims

Small molecule inhibitors are typically tested in cellular settings to determine the biological responses for their target proteins. The previous sections highlighted the importance of selective probes in the bromodomain field, as this allows the observed phenotypic response to be attributed to the protein of interest. The selective ligands **(*R*)48** and **(*R*)(*R*)110** (developed in Section 2 and Section 4, respectively) have good affinity for the CREBBP bromodomain, a single domain that is part of the multidomain protein. In the case of the multidomain protein TRIM24, the selective small molecule inhibition of its bromodomain did not give an overt anti-proliferative response in a pathological setting.[110,111] However, genetic knockdown studies of TRIM24 led to impaired cell growth and induction of apoptosis, validating TRIM24 as a good oncology target. This result, however, suggested that bromodomain inhibition alone may not always be a viable option for anti-cancer therapies targeting multidomain proteins.

PROTAC technology, introduced in Section 1.4.2, can have added advantages over small molecule inhibitors for elucidating the roles of intracellular targets. For example, for a biological response to be observed in cells, chemical probes require full target occupancy, typically dosed at high concentrations which need to be sustained for long periods. However, PROTACs operate catalytically, as several iterations of protein target degradation can be achieved with a single PROTAC.[112] In addition, the degradation of the whole multidomain protein, rather than the inhibition of a single domain, is likely to cause a significant effect on downfield signals that could show desired cellular responses for the treatment of a disease state.

Another advantage of PROTACs is the possibility to selectively degrade protein targets against their homologs using non-selective ligands. For example, Ciulli's group reported that the pan-selective BET bromodomain inhibitor (+)JQ1, when tethered to the E3 ubiquitin ligase VHL ligand, could selectively degrade BRD4 over its homologous proteins BRD2 and BRD3.[59] It is proposed that the formation of the ligase:PROTAC:target ternary complex can have an influence on the selectivity of target degradation.[60] Currently, all published CREBBP bromodomain ligands also have high affinity for the homologous EP300 bromodomain.[16] Using PROTAC technology, it could be possible to selectively degrade the CREBBP protein over EP300 using pan-selective bromodomain ligands. This chapter will discuss the development of PROTAC ligands based on ligand **(*R*)48** to provide validation of CREBBP protein degradation using this approach.

5.2 PROTAC drug-design

A PROTAC is a heterobifunctional compound that comprises of three components; a ligand for the target of interest; a ligand to recruit the ubiquitin E3 ubiquitin ligase; and a linker that connects the two ligands.[48] As the protein of interest is CREBBP, PROTACS will be based on the selective CREBBP bromodomain ligand **(*R*)48**, developed in Section 2. Using the CREBBP bromodomain X-ray crystal structure of ligand **(*R*)11**, which shares a similar binding pose to ligand **(*R*)48**, two attachment points for the linker component were identified (**Figure 5.1A**). The first point of attachment was located on the THBD headgroup, with the second point located at the methoxy group of the THQ moiety. These areas of the ligands were chosen as they are solvent exposed and are predicted to cause minimal disturbance to the binding pose. We believed that it was important to probe the SAR around the introduction of different linkers to these positions, to inform our PROTAC design strategy (**Figure 5.1B**). Surprisingly, affinity measurements upon attaching a linker to the target protein ligand are not always reported in PROTAC publications.

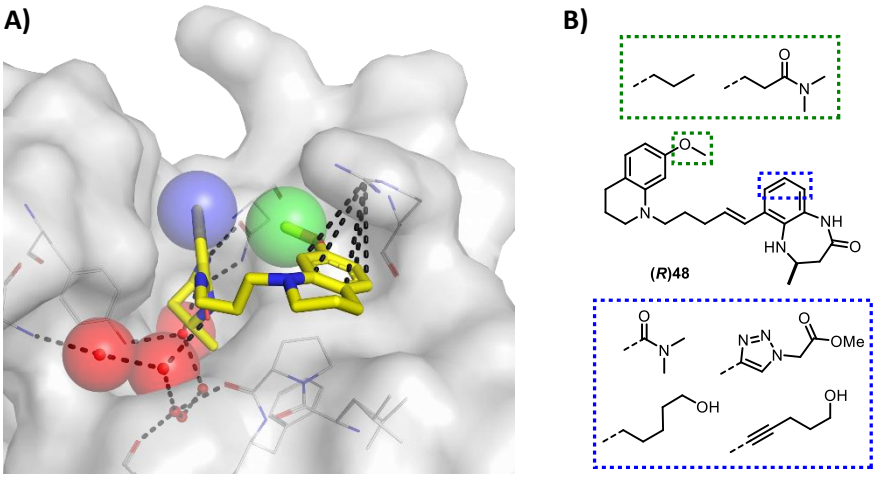


Figure 5.1 (A) The X-ray crystal structure of **(*R*)11** (carbon:yellow) bound to the CREBBP bromodomain highlighting the areas of space available for linker attachment on the ligand (Blue = 5-position of THBD headgroup; Green = THQ). (B) Planned modifications of ligand **(*R*)48** to explore SAR of linker attachment for the PROTAC approach.

Based on the acyclic ligands reported in Section 4.5.1, it was observed that the introduction of an amide, for ligand **(*R*)162**, and triazole, for ligand **(*R*)160**, to the THBD headgroup reduced the binding affinity >12-fold compared to the parent ligand **(*R*)48**. However, the saturated alkyl linker in ligand **(*R*)157** was better tolerated in the binding site, with only >5-fold reduction in affinity. It was rationalised that the alkyne geometry in ligand **(*R*)163** may improve binding by avoiding a steric clash with the ZA loop of the bromodomain. For the THQ region, substitution of the methoxy- moiety in ligand **(*R*)48** to a ^{n}propoxy- group in ligand **(*R*)164** would be prepared to understand if a longer alkyl

group is tolerated. In addition, amide ligand **(*R*)165** would also be prepared, providing a facile method for attaching the linker component. The CREBBP bromodomain ligands for preparation are shown in **Figure 5.2**.

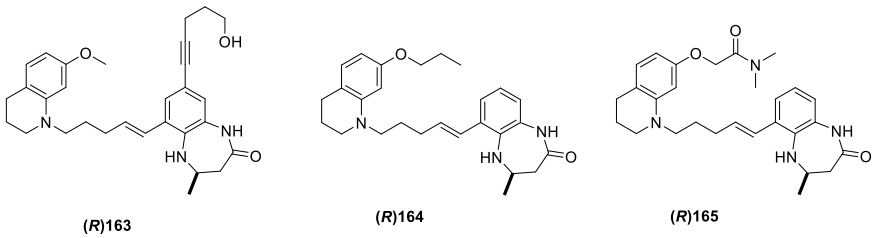


Figure 5.2 CREBBP bromodomains for synthetic preparation to probe the SAR of linker attachment.

The linker component plays an important role for the operation of the PROTAC with regard to effective target protein degradation and cell penetration. The target protein ligand and E3 ubiquitin ligase ligand should not interact with each other, as they must recruit the desired proteins. Therefore, the orientation of the ligase:PROTAC:target ternary complex is largely determined by the linker, forming surface complementarity and a local interaction minimum.[113] However, predicting the structure of the ternary complex is non-trivial, and therefore the current practice in PROTAC design is to use different chain lengths and linker types. For the initial study, the CREBBP bromodomain ligand will be connected to the E3 ubiquitin ligase ligand by commercially available PEG linkers of differing lengths.

For the E3 ubiquitin ligase component, the majority of PROTAC publications in recent years are based on selective VHL or cereblon ligands, shown in **Figure 5.3**.[48] The target protein's ternary complex complementarity may be different with alternative E3 ubiquitin ligase proteins, which provides another complication to the PROTAC design. Therefore, it is recognised that different E3 ubiquitin ligase ligands should be attached when identifying PROTACs for protein degradation.

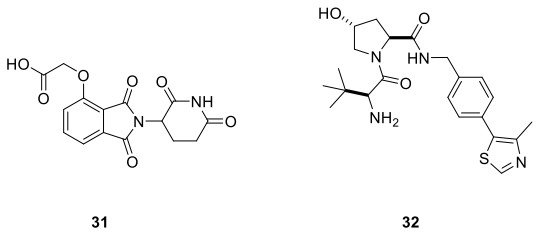
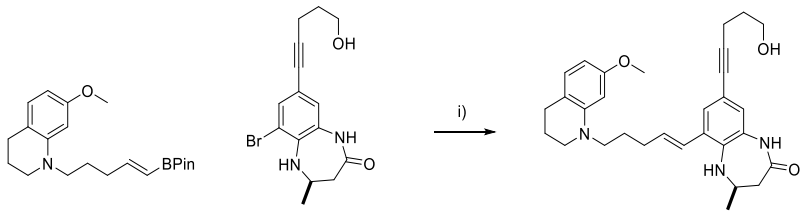


Figure 5.3 Chemical structure of cereblon ligand **31** and VHL ligand **32** used to recruit E3 ubiquitin ligases for the degradation of protein targets.[48]

5.3 CREBBP bromodomain SAR for linker attachment

5.3.1 Syntheses of CREBBP bromodomain ligands

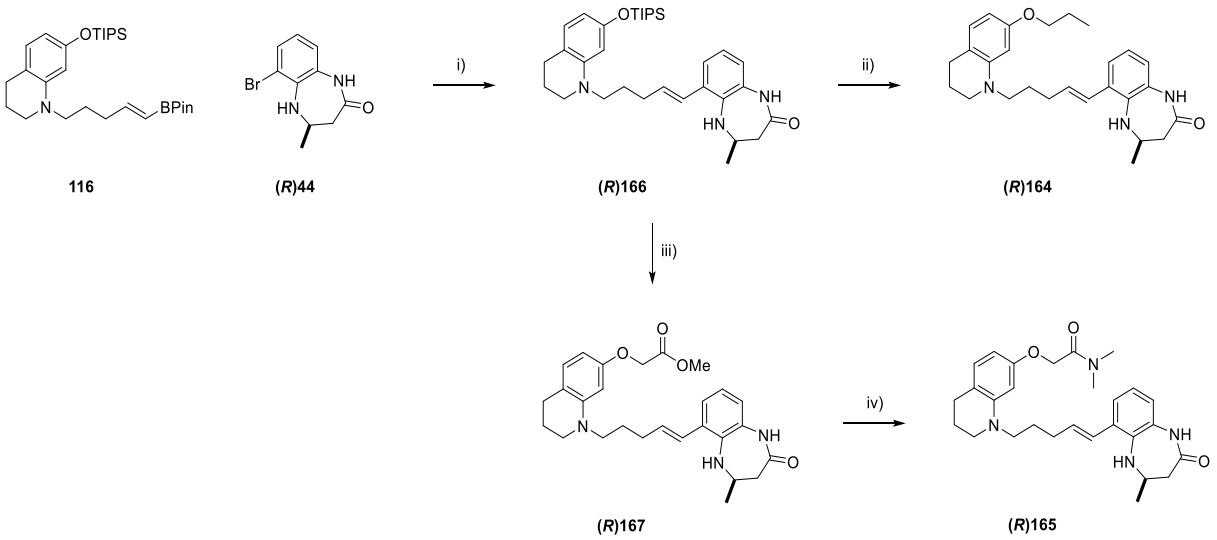
The synthetic routes that were developed for the macrocyclic CREBBP bromodomain ligands, described in Section 4.4, were utilised in the preparation of the ligands for the SAR study. Alkyne ligand **(*R*)163** was prepared using a Suzuki coupling of **47** and **(*R*)123** in a 14% yield (**Scheme 5.1**). The synthesis shown in **Scheme 5.1** was performed by Katrina Andrews in the group of Prof. Stuart Conway (University of Oxford).



47 (*R*)123 (*R*)163

Scheme 5.1 Synthesis of acyclic ligand **(*R*)163**. *Reagents and conditions*: (i) $Pd(PPh_3)_2Cl_2$, K_2CO_3, 1,4-dioxane, H_2O, 100 °C, 16 h, 14%.

The preparation of the THQ modified ligands used the common intermediate **(*R*)166**, synthesised in a Suzuki coupling with intermediates **116** and **(*R*)44** in a 99% yield. This intermediate was TIPS deprotected and alkylated with 1-bromopropane to afford the ^{n}propoxy THQ ligand **(*R*)164**, in a 46% yield over 2 steps. The TIPS deprotected intermediate was also alkylated with methyl bromoacetate to afford the ester **(*R*)167** in a 78% yield over 2 steps. The ester moiety enables the possibility for amide couplings of this late-stage intermediate, beneficial for creating libraries of PROTACs with different linkers and E3 ubiquitin ligase ligands. To explore the SAR, intermediate **(*R*)167** was hydrolysed and reacted with dimethylamine in an amide coupling to afford **(*R*)165** in a 39% yield over 2 steps (**Scheme 5.2**). The synthesis shown in **Scheme 5.2** was performed by Margarida Espadinha in the group of Prof. Stuart Conway (University of Oxford).

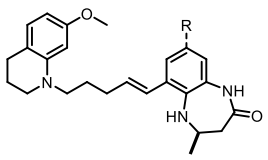


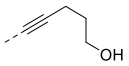
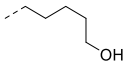
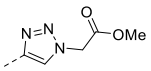
Scheme 5.2 Synthesis of acyclic ligands **(*R*)164** and **(*R*)165**. *Reagents and conditions*: (i) $Pd(PPh_3)_2Cl_2$, K_2CO_3, 1,4-dioxane, H_2O, 100 °C, 18 h, 99%; (ii) 1 M TBAF, THF, rt, 1 h; then 1-bromopropane, K_2CO_3, acetone, rt, 18 h, 46% over 2 steps; (iii) 1 M TBAF, THF, rt, 1 h; then methyl bromoacetate, KI, K_2CO_3, acetone, 60 °C, 24 h, 78% over 2 steps; (iv) 1 M LiOH, THF, MeOH, H_2O, rt, 1 h; then dimethylamine, PyBOP, NEt_3, THF, 70 °C, 18 h, 39% over 2 steps.

5.3.2 CREBBP bromodomain binding affinity

The K_d values for the SAR study were determined using ITC. For the THBD analogues, alkyne **(*R*)163** had a K_d = 1.13 μM, which is comparable to the affinities observed for to amide **(*R*)162** and triazole **(*R*)160**. However, the highest affinity was observed for the saturated alkyl ligand **(*R*)157**, which had a K_d = 0.54 μM (**Table 5.1**).

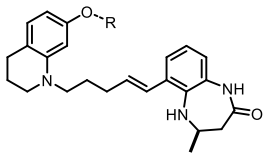
Table 5.1 Affinity data for THBD analogues against the CREBBP bromodomain. ITC traces are shown in Appendix C1.

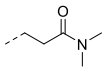


	Compounds (R groups)	ITC K_d/μM CREBBP
(*R*)163		1.13 ± 0.22
(*R*)157		0.538 ± 0.16
(*R*)160		1.26 ± 0.15
(*R*)162		1.30 ± 0.40

For the THQ region, the ^{n}propoxy- group for ligand **(*R*)164** gave a K_d = 1.81 μM which is a >18-fold decrease in affinity compared to the parent ligand **(*R*)48**. Furthermore, amide **(*R*)165** gave no detectable binding by ITC (**Table 5.2**). In conclusion, the ITC results indicated that the attachment of the linker component in the PROTACs should occur from the THBD headgroup.

Table 5.2 Affinity data for THQ analogues against the CREBBP bromodomain. ITC traces are shown in Appendix C1.



	Compounds (R groups)	ITC K_d/μM CREBBP
(*R*)164		1.81 ± 0.22
(*R*)165		n.b.

n.b.: no binding.

The results above indicate that ligand **(*R*)157** is an attractive starting point for PROTAC development. In addition to retaining nanomolar affinity to the CREBBP bromodomain, the alcohol handle provides great synthetic tractability for PROTAC design. For example, this group can be oxidised to a carboxylic acid for amide couplings, or displaced to afford an azido- moiety for triazole cycloaddition reactions. Nevertheless, PROTACs have been reported to degrade protein targets using weak affinity ligands.[114]

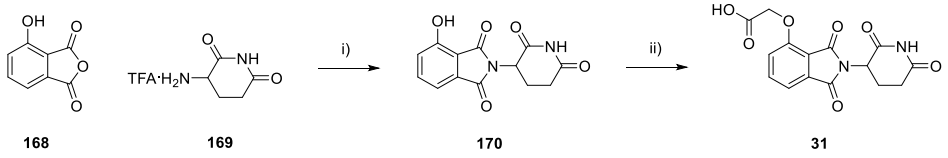
This is because PROTACs only need to bind for enough time to bring the target protein in close proximity to the E3 ubiquitin ligase. To validate our PROTAC approach, triazole **(*R*)160** was chosen for the ligand component of the PROTAC, as the ester moiety allows for quick installation of the linker component *via* an amide coupling. In addition, this ligand has low micromolar affinity to the CREBBP bromodomain and should enable target engagement in cells.

5.4 PROTAC approach using ligand (*R*)160

Three commercially available PEG-linkers of different sizes were chosen for the PROTAC synthesis based on triazole **(*R*)160**. For our initial study, the cereblon ligand **31** was chosen as the E3 ubiquitin ligase ligand. The affinity to the CREBBP bromodomain of the PROTAC scaffold will be tested by ITC, followed by *in vitro* testing. This procedure will help validate our design-synthesis-test approach for PROTAC development.

5.4.1 Synthetic preparation of CREBBP PROTACs

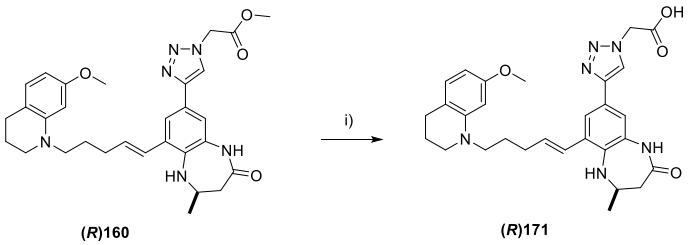
The cereblon ligand **31** was prepared following the procedure published by Lohbeck *et al*.,[115] shown in **Scheme 5.3**. Amine **169** was reacted in a condensation reaction with **168** to give thalidomide **170** in a 59% yield. Benzyl 2-glycolate was reacted with thalidomide intermediate **170** in a Mitsunobu reaction, followed by a hydrogenolysis of the benzyl group to afford carboxylic acid **31** in a 14% yield over 2 steps. The synthesis shown in **Scheme 5.3** was performed by Margarida Espadinha in the group of Prof. Stuart Conway (University of Oxford).



168 169 170 31

Scheme 5.3 Synthesis of CRBN ligand **31**. *Reagents and conditions*: (i) NEt_3, THF, 70 °C, 4 h; then DCC, DMAP, reflux, 19 h, 59% over 2 steps; (ii) benzyl 2-glycolate, DIAD, PPh_3, THF, rt, 18 h; then H_2, 10% Pd/C, EtOAc, CH_2Cl_2, rt, 3 h, 14% over 2 steps.

The CREBBP bromodomain ligand **(*R*)160** was hydrolysed to reveal carboxylic acid **(*R*)171** (**Scheme 5.4**), enabling the connection to the cereblon ligand **31** using a diamine linker.

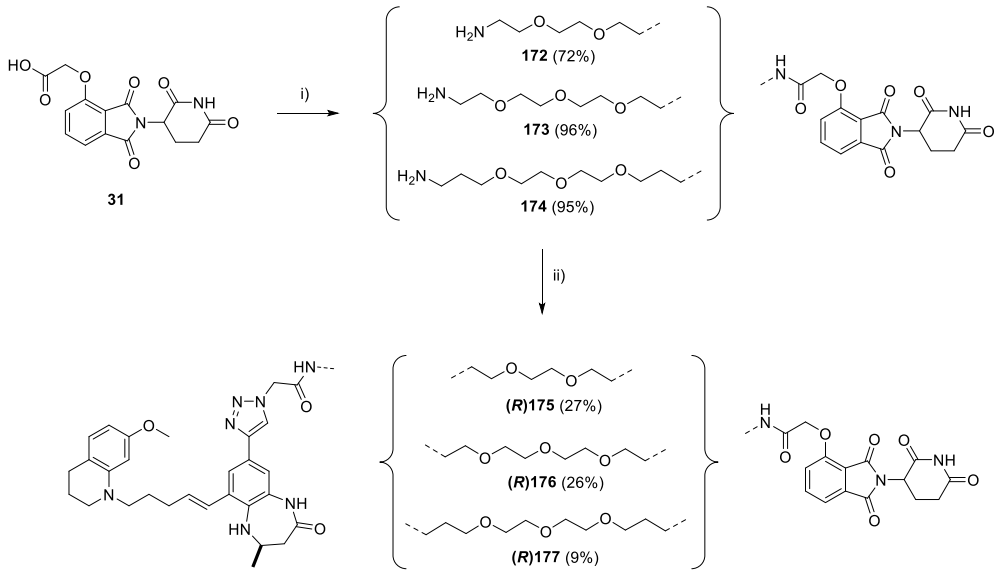


(*R*)160 (*R*)171

Scheme 5.4 Synthesis of carboxylic acid **(*R*)171**. *Reagents and conditions*: (i) LiOH, THF, MeOH, H_2O, rt, 30 min, 99%.

Three commercially available PEG linkers were reacted in an amide coupling with **31**, followed by Boc deprotection to afford the desired amine products in very high yields. The corresponding amine

intermediates were then coupled with **(*R*)171** to afford three PROTACs for *in vitro* testing (**Scheme 5.5**). The synthesis shown in **Scheme 5.5** was performed by Margarida Espadinha in the group of Prof. Stuart Conway (University of Oxford).



Scheme 5.5 Synthesis of PROTACs based on ligand **(*R*)160**. *Reagents and conditions*: (i) HATU, DIPEA, DMF, rt, 4 h; then TFA, CH_2Cl_2, rt, 1 h; (ii) **(*R*)A31A**, HATU, DIPEA, DMF, rt, 18 h.

5.4.2 CREBBP bromodomain binding affinity

The SAR study shown in Section 5.3.2 found that ligand **(*R*)160** had a K_d = 1.26 µM for the CREBBP bromodomain. PROTAC **(*R*)175** was chosen to validate if the affinity is retained to the CREBBP bromodomain by ITC experiments (**Figure 5.4**). Interestingly, **(*R*)175** observed an increased binding affinity of K_d = 0.43 µM. However, it has been reported that PEG chains in PROTACs can have favourable interactions with target proteins, through the observation of ligase:PROTAC:target X-ray crystal structures.[60] In addition, ITC experiments were performed on Boc protected thalidomide intermediate **178**, to rule out the interference of binding from the linker component attached to the **31** ligand, which resulted in no detectable binding. Therefore, the major contribution to the binding affinity is confirmed to be due to the CREBBP bromodomain ligand.

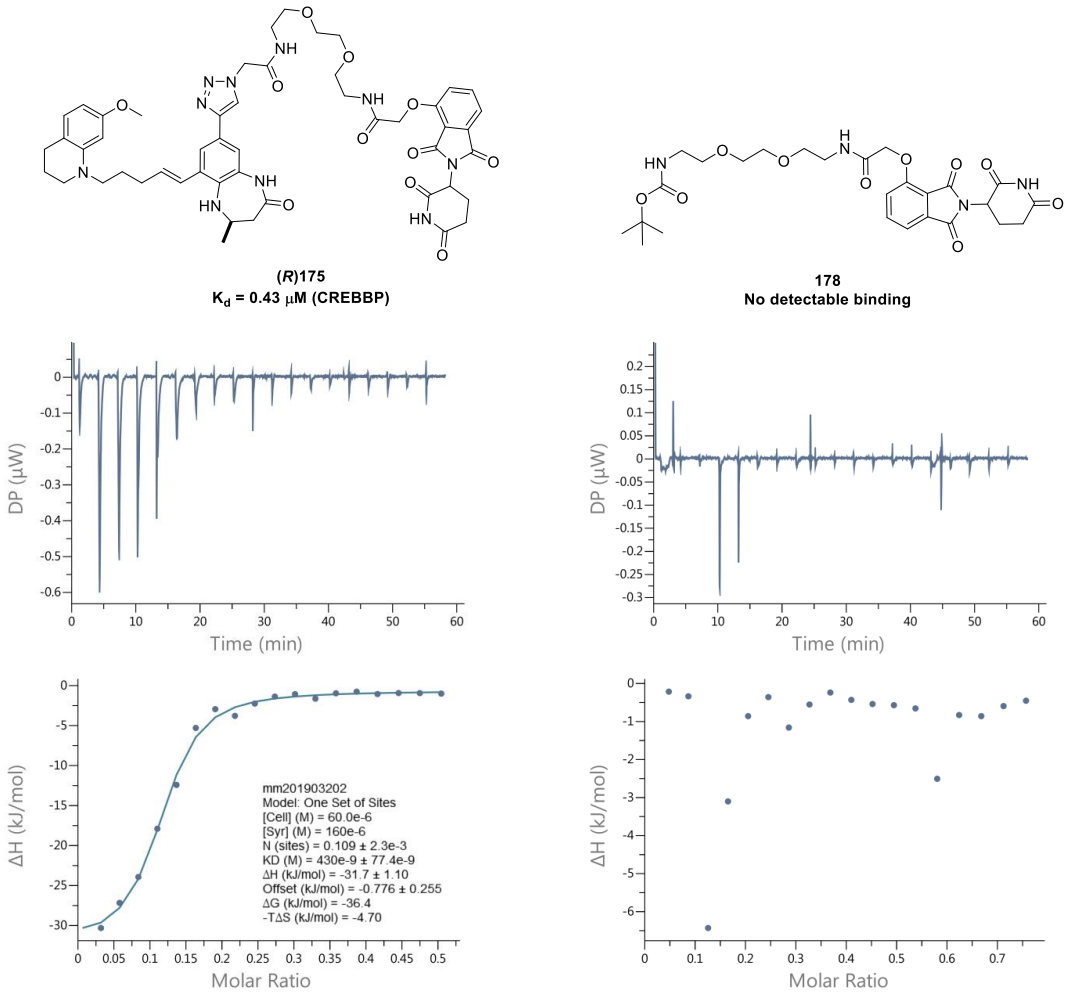


Figure 5.4 ITC binding data for PROTAC **(*R*)175** and CRBN ligand **(*R*)178** against the CREBBP bromodomain.

5.5 Conclusion

Work in this chapter explored the use of PROTAC technology, using selective CREBBP bromodomain ligands based on **(*R*)48**, to degrade the CREBBP protein. From X-ray crystal structure analysis, it was rationalised that the points of attachment should be from either the THBD headgroup or THQ moiety, as these groups are solvent exposed and were thought to cause minimal disturbance to the binding. However, an SAR study showed that the linker attachment was less tolerated on the THQ group, with the THBD modified ligands showing at least low micromolar affinity to the CREBBP bromodomain. The ligand with the highest affinity was **(*R*)157**, which has a pentanol chain attached to the THBD headgroup. This alcohol handle allows for alternative synthetic routes to be explored; examples include oxidation to the carboxylic acid for amide couplings; or installation of an azido- group for triazole formation.

To validate our procedure for CREBBP PROTAC development, three PROTACs were prepared based on the triazole ligand **(*R*)160**. The PROTACs comprised of alternative PEG linkers that were attached to the cereblon ligand **31**, used for the recruitment of the E3 ubiquitin ligase. PROTAC **(*R*)175** was observed to have an affinity (K_d = 0.43 μM) to the CREBBP bromodomain when compared against triazole **(*R*)160** (K_d = 1.26 μM). To rule out any interference of the linker and E3 ubiquitin ligase ligand, PROTAC precursor **178**, which is absent of the CREBBP bromodomain ligand, was tested by ITC and showed no detectable binding.

Degradation of target proteins using PROTAC technology currently appears to be case-dependent with no general rules.[116] Future work would require the preparation of several linker chains attached to different E3 ubiquitin ligase ligands to create a library for PROTAC testing. Upon the identification of a PROTAC for the degradation of CREBBP, selectivity against EP300 should also be tested. Consequently, this could lead to the first selective CREBBP PROTAC enabling the biological functions of this individual protein to be explored.

Chapter 6

Use of an ESAC library to identify novel CREBBP bromodomain ligands

6.1 Introduction and aims

The identification of high affinity probes for certain classes of proteins, including those involved in protein-protein interactions, can be a challenging task in drug discovery. In large pharmaceutical companies, HTS procedures are commonly used for hit identification, with chemical libraries often comprising >1 million compounds. However, they typically contain high molecular weight molecules, with complex structures that may not interact favourably with the target proteins. The assembly of such libraries have been estimated to cost between $0.4–2 billion.[62]

Fragment-based drug discovery is an alternative approach for the identification of lead compounds and chemical probes. This method uses low molecular weight compounds (typically ≤200 Da) that are more likely to bind to protein targets, due to them having fewer structural features to hinder binding.[117] The fragment hits are then connected *via* appropriate linking scaffolds in an effort to cumulatively improve the binding affinity. However, this requires the ability to acquire protein-ligand crystal structures upon fragment soaking. A major drawback with the fragment-based drug discovery approach is that the affinity determination of fragments is challenging, due to their weak binding interactions with the target proteins (K_d typically ranging from 100 µM to low mM).[117]

DNA-encoded chemical library technology, introduced in Section 1.4.3, has enabled the construction and screening of large sets of compounds for small molecule drug discovery. ESAC libraries facilitates the identification of synergistic fragments that can bind to adjacent pockets on target proteins, while individually coupled to DNA strands that serve as amplifiable identification barcodes.[70] Identified fragment pairs that bind in a complementary manner to the same protein are subsequently connected with suitable linkers. The binding affinities of the resulting compounds are determined in the absence of DNA.

The CREBBP bromodomain has two regions of the protein that are involved with compound interaction (Section 1.3.3); (i) the KAc binding pocket and (ii) the induced-fit pocket. It was hypothesised that the ESAC library technology could aid the identification of novel fragments that bind to the CREBBP bromodomain. To validate this screening method, fragments known to interact with the CREBBP bromodomain will be compared to the hits identified from the ESAC library. The identified fragments will subsequently be connected with suitable linkers to determine their binding affinities ‘off-DNA’.

6.2 Binding affinity of fragment pairs using known CREBBP bromodomain ligands

The hit fragments that are identified from the ESAC library screening will be tested in a fluorescence polarisation (FP) assay. To validate this binding assay, known CREBBP bromodomain ligands **(*R*)11** and **(*R*)12**[31] were converted into two fragment portions. The first fragments included the structural features that form interactions with residue R1173, responsible for the induced-fit pocket. The second fragment is the THBD headgroup which interacts with the KAc binding pocket. Ligands **(*R*)11** and **(*R*)12** were chosen as they share the THBD headgroup but have distinct binding affinities. This should enable the clear ranking of the fragments. In addition, the THBD (*S*)-enantiomer does not bind to the CREBBP bromodomain, providing a valuable negative control. The fragments will then be paired to fluorescently labelled complementary locked nucleic acid (LNA) strands by amide couplings for FP measurements (**Figure 6.1**). It was acknowledged that the THBD headgroup would make an intramolecular hydrogen bond with the amide linker, as discussed in Section 2, and this may have an unfavourable effect on the binding affinities.

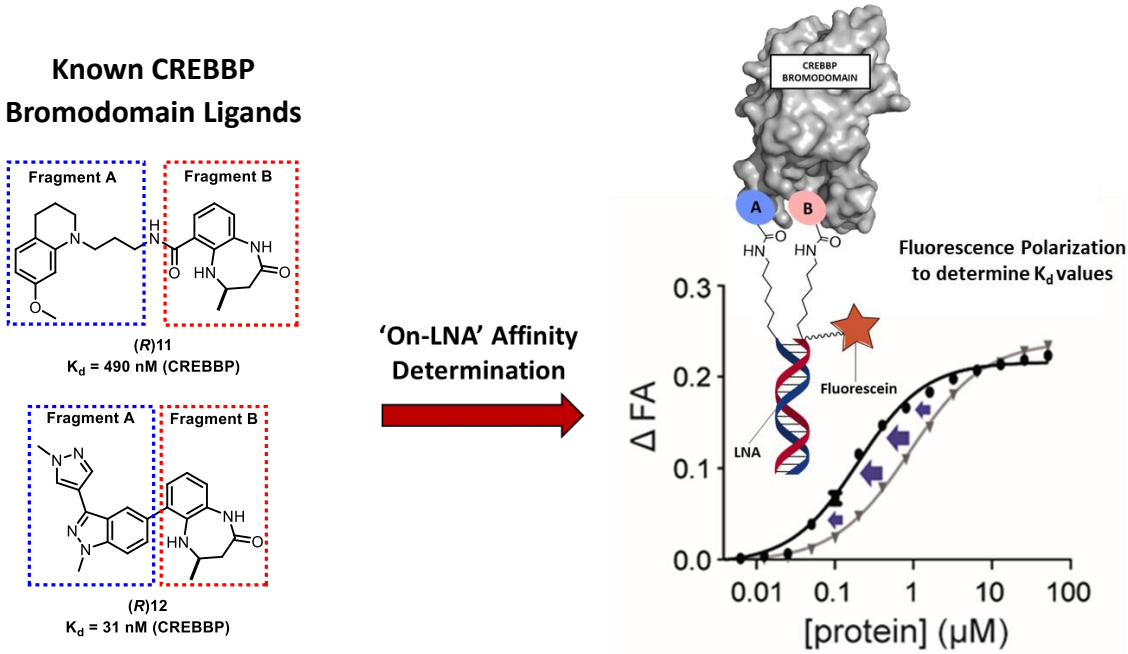
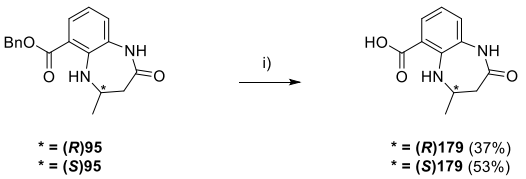


Figure 6.1 Known CREBBP bromodomain ligands **(*R*)11** and **(*R*)12**[31] used to validate 'on-LNA' binding affinity against the CREBBP bromodomain, determined by fluorescence polarisation.

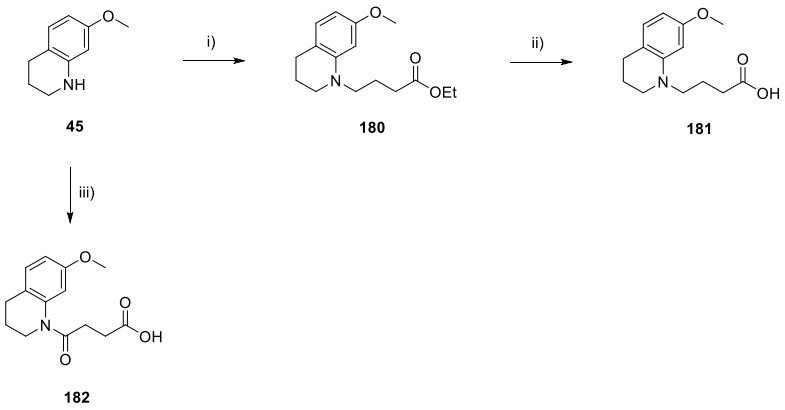
6.2.1 Syntheses of fragment pairs

The preparation of the THBD fragment **(*R*)95** was shown in Section 3.4. The benzyl group was removed in a hydrogenolysis reaction, affording the free acid fragments **(*R*)179** and **(*S*)179** (**Scheme 6.1**).



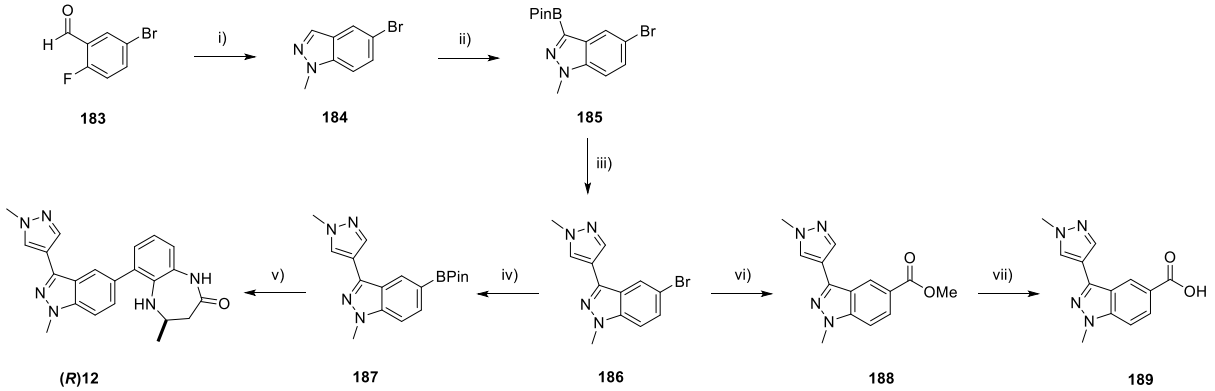
Scheme 6.1 Synthesis of THBD fragments **(*R*)179** and **(*S*)179**. *Reagents and conditions*: (i) H_2, 10% Pd/C, EtOAc, MeOH, rt, 20 h.

THQ intermediate **45** was alkylated with ethyl 4-bromobutanoate, followed by hydrolysis to afford the THQ fragment **181** (**Scheme 6.2**). The decision was made to react **45** with succinic anhydride to give modified THQ fragment **182**. Fragment **182** is not a known to interact with the CREBBP bromodomain but was prepared to provide some SAR comparison in the FP assay.



Scheme 6.2 Synthesis THQ fragments **181** and **182**. *Reagents and conditions*: (i) ethyl 4-bromobutanoate, KI, DIPEA, DMF, μλ, 100 °C, 1 h, 95%; (ii) 1 M LiOH, THF, MeOH, H_2O, rt, 16 h, 70%; (iii) succinic anhydride, THF, rt, 20 h, 91%.

The bromodomain ligand **(*R*)12**, outlined in **Scheme 6.3**, was synthesised by Dr James Clayton in the group of Prof. Stuart Conway (University of Oxford). In brief, aldehyde starting material **183** is reacted in a one-pot annulation to afford indazole **184** in a 66% yield. C-H borylation of the indazole enabled a Suzuki coupling with 4-iodo-1-methyl-1*H*-pyrazole to give pyrazole intermediate **186** in a 57% yield. Borylation of intermediate **186**, followed by the Suzuki coupling with THBD headgroup **(*R*)44** (preparation shown in Section 2.2) afforded ligand **(*R*)12** in good yields. (**Scheme 6.3**).[31]



Scheme 6.3 Synthesis of CREBBP bromodomain ligand **(*R*)12** and fragment **189**. *Reagents and conditions*: (i) methylhydrazine, DIPEA, NMP, 150 °C, 24 h, 66%; (ii) B_2Pin_2, $[Ir(OMe)COD]_2$, tmphen, MTBE, 60 °C, 3 h, 96%; (iii) 4-iodo-1-methyl-1*H*-pyrazole, $Pd(PPh_3)_4$, K_2CO_3, 1,4-dioxane, H_2O, 80 °C, 3 h, 66%; (iv) B_2Pin_2, $Pd(dppf)Cl_2$, KOAc, 1,4-dioxane, 100 °C, 4 h, 57%; (v) **(*R*)44**, $Pd(PPh_3)_2Cl_2$, K_2CO_3, 1,4-dioxane, H_2O, 100 °C, 2 h, 94%; (vi) CO, $Pd(dppf)Cl_2$, MeOH, NEt_3, 100 °C, 20 h, 46%; (vii) 1 M LiOH, THF, MeOH, H_2O, rt, 17 h, 98%.

Advanced intermediate **186** was used in the preparation of fragment **189**, as the material was available from the synthesis of **(*R*)12**. Indazole **186** was reacted in a carbonylation using $Pd(dppf)Cl_2$ in methanol to afford ester **188** in a 46% yield. Hydrolysis of the methyl ester with lithium hydroxide gave fragment **189** in excellent yields (**Scheme 6.3**). All synthesised fragments were attached to the LNA strands by amide couplings, performed by Marco Catalano in the group of Prof. Dario Neri (ETH Zurich).

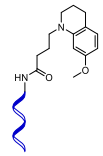
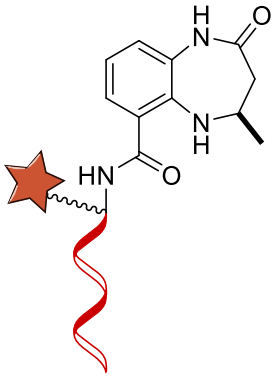
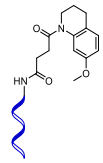
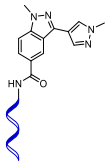
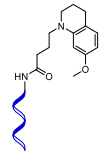
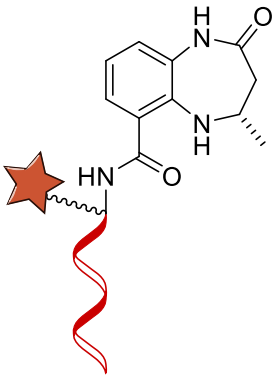
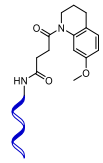
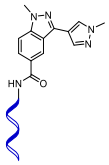
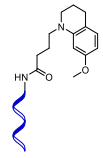
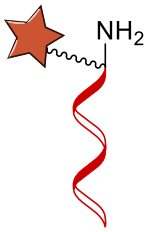
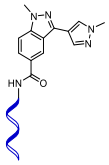
6.2.2 CREBBP bromodomain binding affinities

FP measurements can estimate the binding affinity for the combination of fragment A (which interacts with residue R1173 to form the induced-fit pocket) and fragment B (which interacts in the KAc pocket), when displayed on two complementary nucleic acid strands. The FP assay was performed with both enantiomers of the THBD headgroups, with the (*S*)-enantiomer acting as a negative control. In addition, LNA strands in the absence of either fragment A or fragment B were prepared as controls, as this is expected to have reduced affinities when compared against paired fragments.

The FP assay definitively showed that binding to the CREBBP bromodomain could only occur if the LNA strand contained the active (*R*)-enantiomer of the THBD fragment, as both the (*S*)-enantiomer and the LNA stands in the absence of fragment A showed no detectable binding (**Table 6.1**). This validated that the affinity observed by the FP measurements were due to favourable interactions with the protein and fragments, hence not due to an artefact of binding from the LNA strand. In addition, the FP assay allowed ranking of fragments binding affinities. LNA stand **(*R*)179-LNA-190** and modified THQ fragment **(*R*)179-LNA-182** both showed the expected weak affinities to the CREBBP bromodomain, with a K_d = 7.2 µM and K_d = 6.4 µM, respectively. The THQ fragment **(*R*)179-LNA-181**, with a K_d = 1.95 µM, and indazole fragment **(*R*)179-LNA-189**, with a K_d = 0.89 µM, both reflected the affinities observed in their parent ligands **(*R*)11** and **(*R*)12**. However, the 'on-LNA' affinities were considerably weaker than those observed for the 'off-LNA' ligands, which may be attributed to the presence of the LNA strand that holds the individual fragments. Furthermore, this difference in affinity highlights the importance of appropriate linker scaffolds. FP measurements were performed by Marco Catalano in the group of Prof. Dario Neri (ETH Zurich).

These results provided confidence that FP measurements would be suitable for affinity determination of hit fragments identified from the ESAC library screening against the CREBBP bromodomain. In addition, the affinity for the hit fragments will be compared against **(*R*)179-LNA-189**, identified as the best combination from the known CREBBP fragments. If an improvement in affinity is observed, the hit fragment pair will be synthesised 'off-LNA' and tested by ITC to determine K_d values.

Table 6.1 FP binding affinity data for 'on-LNA' fragments against CREBBP bromodomain. See Appendix D5 for FP data.

	Fragment A	Fragment B	FP K_d/μM CREBBP
(*R*)179-LNA-181			1.95
(*R*)179-LNA-182			6.4
(*R*)179-LNA-189			0.84
(*R*)179-LNA-190			7.2
(*S*)179-LNA-181			No detectable binding
(*S*)179-LNA-182			No detectable binding
(*S*)179-LNA-189			No detectable binding
NH_2-LNA-181			No detectable binding
NH_2-LNA-189			No detectable binding

6.3 ESAC library screening against the CREBBP bromodomain

6.3.1 Fragment hit identification using ESAC library

Initial ESAC library screening used a sub-library containing 788 fragment members individually paired with the THBD headgroup **(*R*)179-DNA**. The complementary DNA strands were incubated with biotinylated CREBBP bromodomain, immobilised onto streptavidin magnetic beads. Non-binders are washed away, while fragment pairs that show binding are enriched, amplified by PCR and identified based on the DNA coding information, as described in Section 1.4.3. The relative abundance of the fragment pairs are shown in HTDS plot (**Figure 6.2**), which identified **(*R*)179-DNA-192** as the most enriched fragment pair.

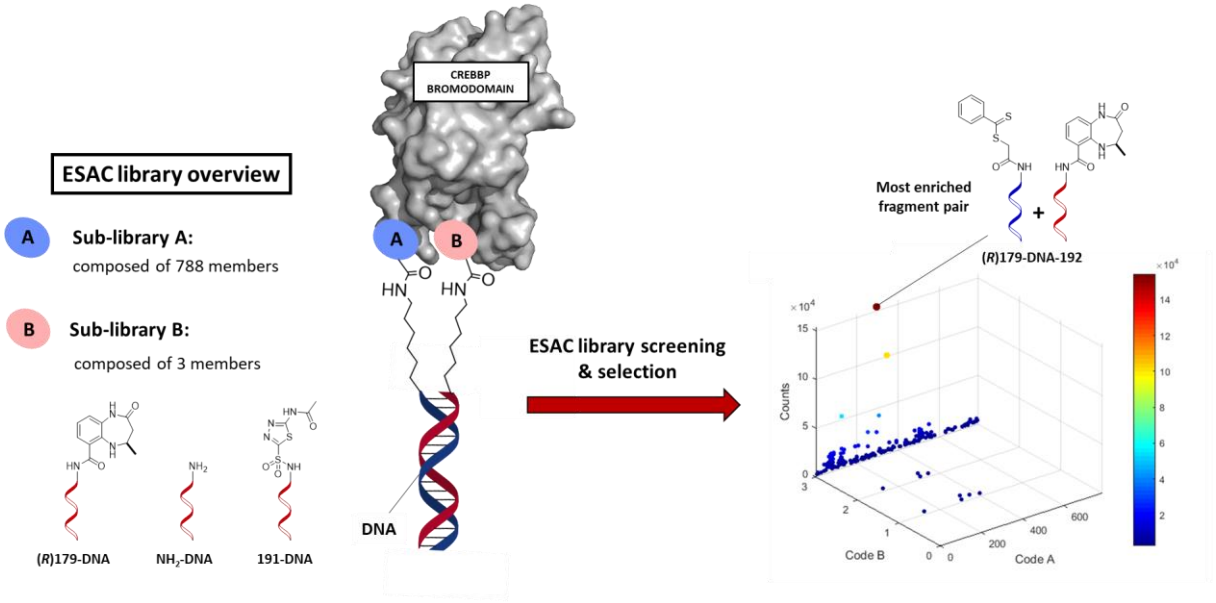


Figure 6.2 Selection results from the 788 *vs* 3-member dual-display library. High-throughput DNA sequencing (HTDS) plot selections against the CREBBP bromodomain.

A second screen was attempted which paired the sub-library containing 788 fragment members with a second sub-library containing 426 members. Fragment **DNA-192** was consistently enriched throughout the screening, dominating the selection procedure (**Figure 6.3**). This hit was also incorporated in the most enriched fragment pair from the first screening (**(*R*)179-DNA-192**), and is likely to have favourable interactions with the CREBBP bromodomain. To validate this hit, the fluorescent labelled fragment pair **(*R*)179-LNA-192** was prepared for FP measurements.

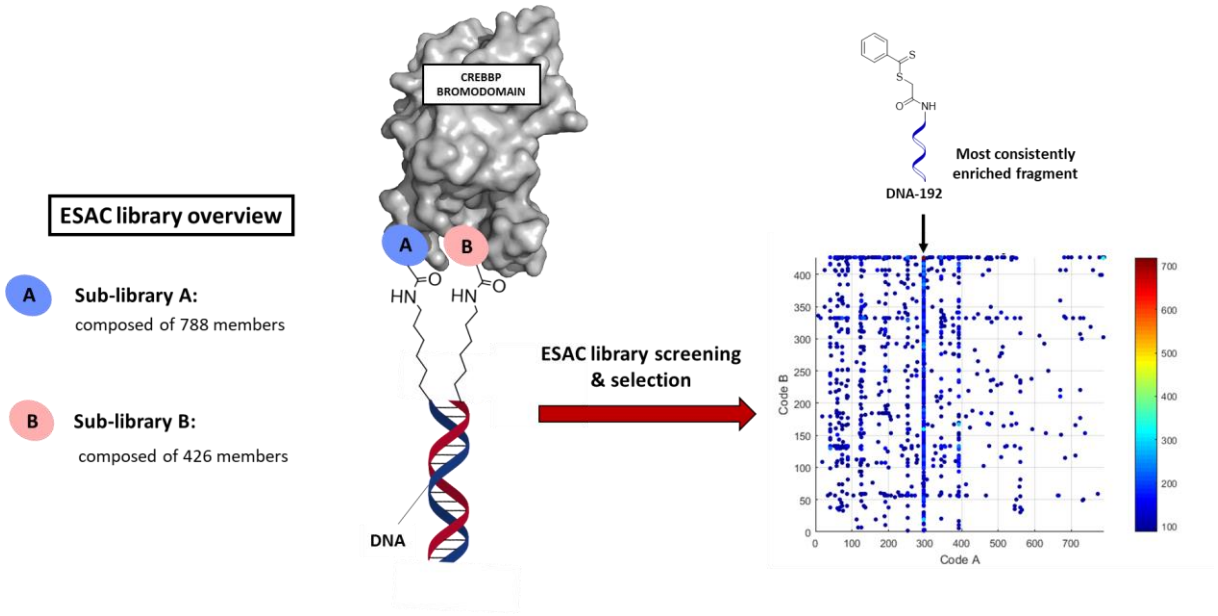


Figure 6.3 Selection results from the 788 *vs* 426-member dual-display library. High-throughput DNA sequencing (HTDS) plot selections against the CREBBP bromodomain.

However, it should be noted that hit fragment **192** contains a dithioester functionality, a motif that is not typically desirable from a medicinal chemistry perspective. Due to it susceptibility to react with radicals and undergo polymerisation reactions, this group is unlikely to be incorporated into a functional chemical probe.[118] Nevertheless, the aim of this project was to validate the DNA-encoded library technology in its ability to identify novel CREBBP bromodomain ligands, and not necessarily for the identification of a chemical probe. For this reason, the dithioester motif identified in fragment **192** was not a concern at this stage (**Figure 6.4**). The ESAC library screen was performed by Federica Mazzieri and Marco Catalano in the group of Prof. Dario Neri (ETH Zurich).

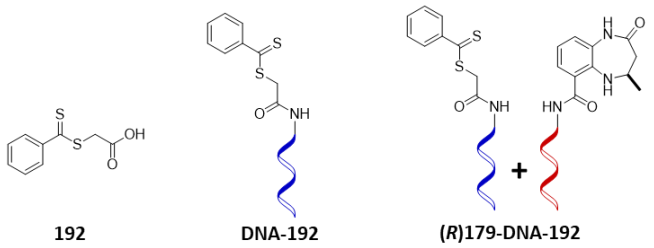


Figure 6.4 Dithioester fragment identified in the ESAC library screen.

6.3.2 CREBBP bromodomain binding affinity

The FP assay was used to validate the most enriched fragment pair **(*R*)179-DNA-192** from the ESAC library screen (**Figure 6.5**). This enriched fragment pair **(*R*)179-LNA-192** was compared against the previously tested CREBBP fragment pair **(*R*)179-LNA-189**, and control **(*R*)179-LNA-190**. The results showed that the dithioester fragment from **(*R*)179-LNA-192** (K_d = 0.46 µM) interacts more favourable with the CREBBP bromodomain than the indazole fragment in **(*R*)179-LNA-189** (K_d = 1.45 µM), previously the highest ranked CREBBP bromodomain fragment in Section 6.2.2. This result indicated that connecting the dithioester fragment **192** and THBD headgroup **(*R*)179** together with an appropriate linker could lead to a high affinity CREBBP bromodomain ligand. FP measurements were performed by Marco Catalano in the group of Prof. Dario Neri (ETH Zurich).

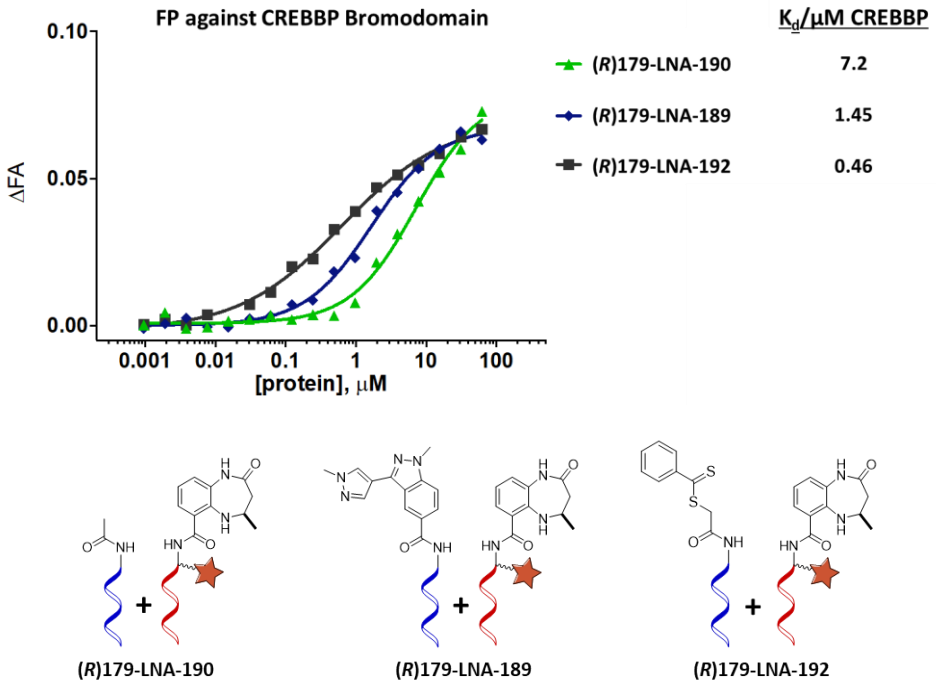


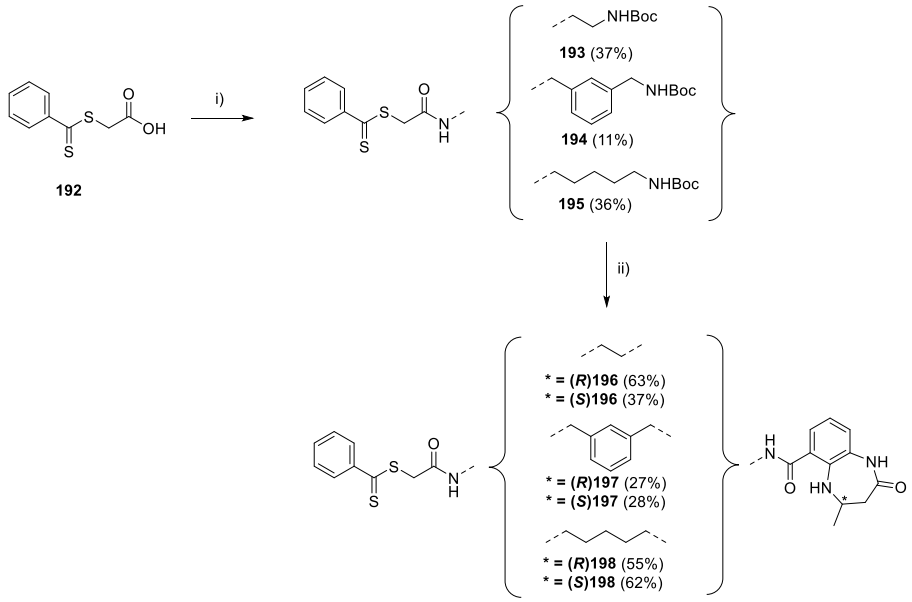
Figure 6.5 Raw FP data for enriched 'on-LNA' fragment **(*R*)179-LNA-192** against the CREBBP bromodomain.

6.4 Affinity determination of 'off-LNA' CREBBP bromodomain ligands

Upon identifying synergistic binding fragments with tight affinity to the CREBBP bromodomain, the next challenge was to identify a linker that would retain affinity in the absence of the LNA strand. Bigatti *et al.*[69] showed that fragments identified from their ESAC screen against the human AGP could be connected with diamine linkers using amide couplings, resulting in the identification of a ligand with a low nanomolar K_d value. The decision was made to use this same methodology to connect fragments **192** and **(*R*)179**, using ITC to determine their binding affinities.

6.4.1 Synthesis of 'off-LNA' CREBBP bromodomain ligands

Fragments **192** and **(*R*)179** would be connected using three alternative linkers, exploring different chain lengths and rotatable bonds. The first amide coupling was performed with acid **192** with a mono-Boc protected amines. This was followed by a one-pot Boc deprotection and amide coupling to fragment **(*R*)179** to afford the desired linked fragments (**Scheme 6.4**). In addition, enantiomer **(*S*)179** was also reacted in the amide coupling to provide a negative control for the ITC experiments. The amide couplings were low yielding in all cases due to the susceptibility of the dithioester moiety to react with the free amines. The ligands in **Scheme 6.4** were prepared by Marco Catalano in the group of Prof. Dario Neri (ETH Zurich).

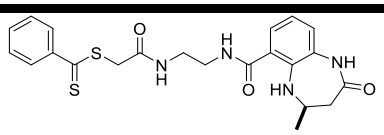
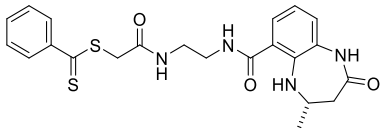
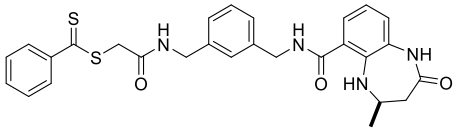
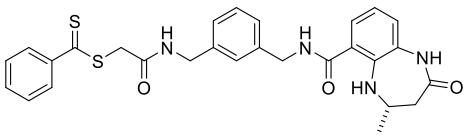
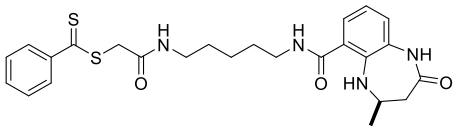
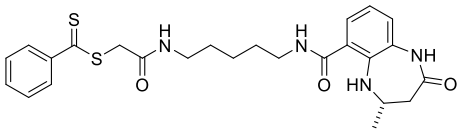


Scheme 6.4 Synthesis of 'off-LNA' CREBBP ligands based on fragment hit **192**. *Reagents and conditions*: (i) EDC, HOAt, DMF, rt, 16 h; (ii) TFA, CH_2Cl_2, rt, 2 h, then **(*R*)179**/**(*S*)179** HATU, NMP, DMSO, rt, 16 h.

6.4.2 CREBBP bromodomain binding affinity

The linked fragments prepared in Section 6.4.1 were tested, using ITC, for their affinity to the CREBBP bromodomain 'off-LNA'. Weak binding was observed for the (*R*)-enantiomers, with the inactive (*S*)-enantiomers displaying no detectable binding (**Table 6.2**). However, the K_d value could only be determined for **(*R*)196** (K_d = 17.8 μM) which was a considerable drop in affinity compared to the CREBBP bromodomain ligand starting points. In addition, ligand **(*R*)196** had the shortest linker, however, from our prior knowledge of the CREBBP bromodomain tertiary structure, the linker distance in **(*R*)196** remains too long for the fragments to have optimum interactions with the protein. Future work will involve directly connecting the fragments together, without the use of a diamine linker, to create a shorter distance between the fragments. We aim to have a more comparable structure to ligand **(*R*)11** which will allow for a more suitable comparison of the binding affinities. The ITC experiments were done in collaboration with Katrina Andrews in the group of Prof. Stuart Conway (University of Oxford).

Table 6.2 Affinity data for 'off-LNA' ligands against the CREBBP bromodomain. ITC traces are shown in Appendix C1.

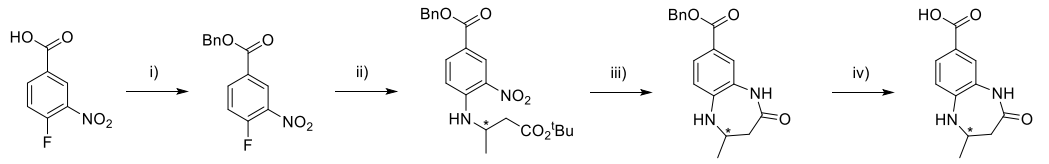
	Compounds	ITC K_d/μM CREBBP
(*R*)196		17.8 ± 32.2
(*S*)196		No detectable binding
(*R*)197		Weak binding detected
(*S*)197		No detectable binding
(*R*)198		Weak binding detected
(*S*)198		No detectable binding

6.5 Investigation of alternative THBD fragments

The intramolecular hydrogen bond present in solution for ligand **(*R*)11**, between the aniline N-H of the headgroup and the carbonyl oxygen of the linker amide, has an unfavourable contribution to the binding enthalpy (Δ*H*) (Section 2). This problem was solved by preparing the *E*-alkene ligand **(*R*)48** as a bioisostere, leading to a 5-fold increase in affinity. However, the THBD headgroup is connected to the LNA strand by an amide coupling, therefore the bioisosteric modification is not possible with this approach. A regioisomer of **(*R*)179**, whereby the acid moiety is *para*- to the aniline, would prevent the intramolecular hydrogen bond and was rationalised to improve the 'on-LNA' affinities of the fragment pairs to the CREBBP bromodomain.

6.5.1 Synthesis of THBD fragments (*R*)202 and (*S*)202

The preparation of the THBD enantiomers **(*R*)202** and **(*S*)202** used a similar route described for the synthesis of **(*R*)150** in Section 4.4.4.1. The acid starting material **146** was benzyl protected to afford **199** in excellent yields. This intermediate was reacted in an S_NAr with chiral amines **(*R*)41** and **(*S*)41** (synthesis outlined in Section 2.2) respectively, followed by cyclisation with iron powder in acetic acid to afford THBD intermediates **(*R*)201** and **(*S*)201** in good yields. The final step involved the hydrogenolysis of the benzyl ester to yield the desired acid fragments in high yields (**Scheme 4.12**). The synthesised THBD fragments were attached to the LNA strands by amide couplings, performed by Marco Catalano in the group of Prof. Dario Neri (ETH Zurich).



146 **199** * = (*R*)**200** (99%) * = (*S*)**200** (97%) * = (*R*)**201** (87%) * = (*S*)**201** (57%) * = (*R*)**202** (99%) * = (*S*)**202** (91%)

Scheme 6.5 Synthesis of THBD fragment **(*R*)202** and **(*S*)202**. *Reagents and conditions*: (i) BnBr, K_2CO_3, NMP, 60°C, 4 h, 94%; (ii) **(*R*)41**/**(*S*)41**, Cs_2CO_3, Tol, 85 °C, 18 h; (iii) TFA, CH_2Cl_2, rt, 1 h, then Fe, AcOH, 100 °C, 4 h; (iv) H_2, 10% Pd/C, EtOAc, MeOH, rt, 16 h.

6.5.2 CREBBP bromodomain binding affinity

The FP measurements were performed for the THBD fragments **(*R*)202** and **(*S*)202** paired with indazole **189** and dithioester fragment **192**. Fragments paired with the negative control **(*S*)202** displayed no binding (see Appendix D5). Interestingly, **(*R*)202** showed a marked improvement in affinity when compared against fragment pairs containing THBD fragment **(*R*)179** (**Figure 6.6**). This further validated the rationale that the intramolecular hydrogen bond of the amide carbonyl adjacent to the aniline N-H of the THBD headgroup causes significant hinderance to the binding affinity. However, there was no major difference in the affinities for the dithioester fragment **(*R*)192** paired with either of the THBD regioisomers. To investigate this result in more detail, 'off-LNA' ligands containing fragment **(*R*)202** will also be prepared, providing a comparison to ligands containing the regioisomer **(*R*)179**. Nevertheless, it was reported in the publication for ligand **(*R*)12** that substituents incorporated *para*- to the THBD aniline had reduced selectivity against BRD4(1).[31] This should be taken into consideration when using THBD **(*R*)90** for future ligand design.

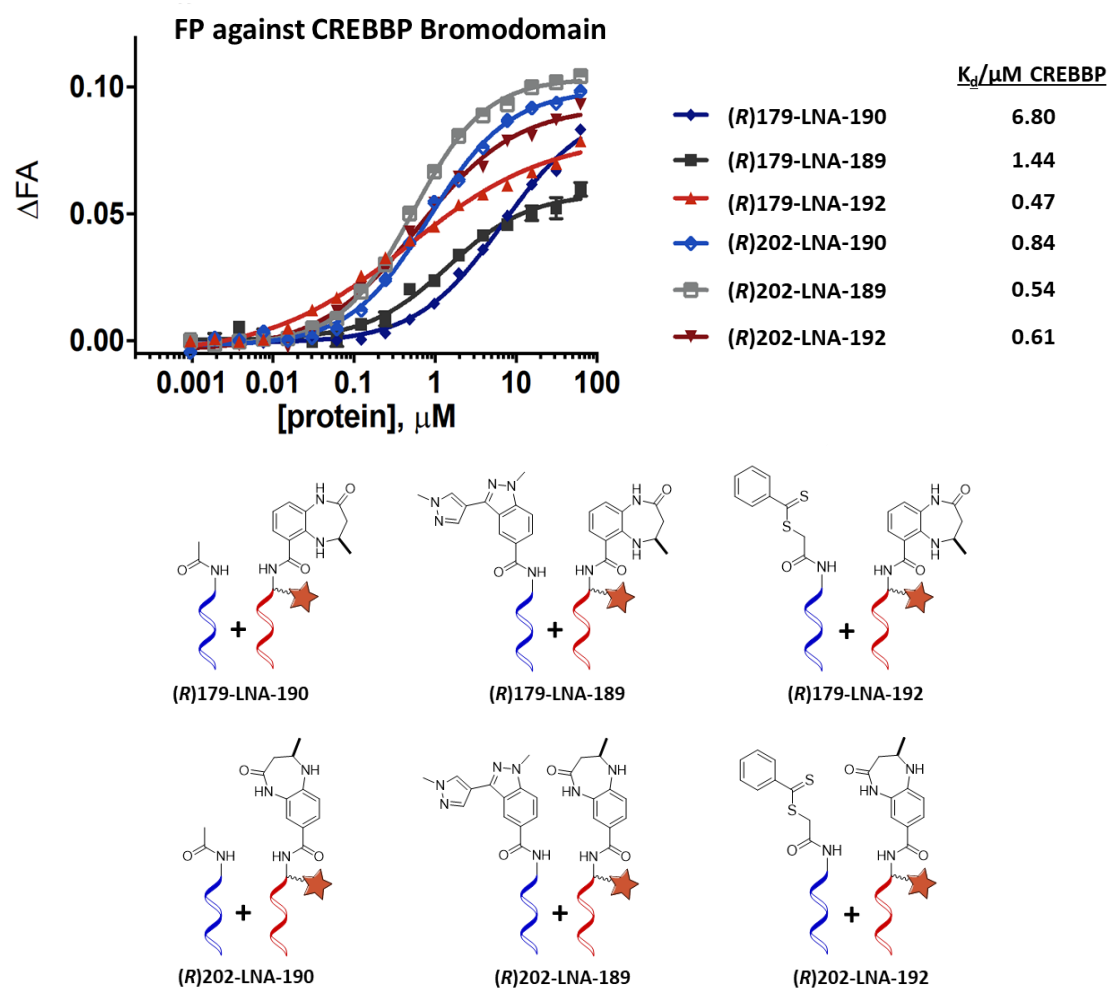


Figure 6.6 Raw FP data comparing 'on-LNA' THBD fragments **(*R*)179** and **(*R*)202** against the CREBBP bromodomain.

6.6 Conclusion

The pharmacophores identified in ligands **(*R*)11** and **(*R*)12**[31] were used as standards to validate the binding affinity of 'on-LNA' fragment pairs to the CREBBP bromodomain. This led to the ESAC library screening which identified dithioester **192** as a hit fragment, when paired to the THBD headgroup **(*R*)179**. Methodology described by Bigatti *et al*.[69] was used to connect fragments **(*R*)179** and **192** in the absence of LNA, however the linkers did not enable optimal interactions with the CREBBP bromodomain. This result highlighted the importance of linker selection, as both fragments must simultaneously interact with the respective regions on the CREBBP bromodomain to obtain high affinity. In addition to changing linker strategies, future ligand design could use THBD fragment **(*R*)202**, as this was shown to have a marked improvement in affinity for most of the fragments, when compared to LNA strands containing regioisomer **(*R*)179**. This was rationalised to be due to the absence of the intramolecular hydrogen bond that has been shown to have an unfavourable influence on the binding enthalpy, as discussed in Section 2.

The work in this chapter has shown that an ESAC library screen can identify new CREBBP bromodomain fragments, providing precedents for using this technology to identify novel hits for protein targets involved in protein-protein interactions. Future work will involve developing the linker strategy and testing the novel ligands by ITC to determine their affinity and selectivity for the CREBBP bromodomain.

Chapter 7

Conclusions and future work

7.1 Conclusions

The work in this thesis has focused on the application of medicinal chemistry-based approaches to improve the affinity and selectivity of the previously reported CREBBP bromodomain ligand **(*R*)11**.[30] In addition, this work has provided a solid foundation for future development of novel ligands and degraders using recent medicinal chemistry technology.

Chapter 2 reported an SAR study for the bioisosteric modifications of an amide moiety in ligand **(*R*)11**. We observed a 5-fold increase in affinity following the isosteric replacement of the amide with an *E*-alkene, in ligand **(*R*)48**. This increase in affinity was attributed to the removal of the enthalpic energy barrier for adopting the desired binding pose. Interestingly, ligand **(*R*)48** was observed to have a 100-fold selectivity against the BET family of bromodomains, however, its *Z*-alkene diastereomer, ligand **(*R*)50**, retained affinity to BRD4(1) with only 6-fold selectivity. This indicates that the geometry around this position plays a pivotal, yet subtle, role in dictating the selectivity over the BET family of bromodomain, which was not previously known.

The protein-ligand X-ray crystal structure of ligand **(*R*)11** bound to BRD4(1) enabled the identification of the off-target binding mode for this series of ligands. We rationalised that the constraint of the ligand as a macrocycle would only allow binding to the CREBBP bromodomain. This led to the hypothesis that a macrocyclic ligand would have an improved selectivity profile. Chapter 3 discussed the initial macrocycle drug design for this series of ligands, however, several limitations were observed for this approach. This included the inability of the computational software to correctly predict the conformations of the docked macrocycles; synthetic challenges caused by headgroup instability; and the inherent weak affinity of the acyclic starting scaffold which was carried into the macrocyclic ligand.

The above work guided the design of three new macrocycle series, described in Chapter 4, which were based on the high affinity ligand **(*R*)48**. A three-step computational analysis was used to screen the macrocycle series and identify targets for synthetic preparation. The acyclic counterparts were also synthesised to compare the affinity and selectivity profiles of the prepared macrocycles. Consistent with the computational study, only the amide macrocycle series retained affinity to the CREBBP bromodomain, displaying comparable binding affinities to the acyclic amide analogue **(*R*)162** (K_d = 1.30 μM). Furthermore, pyrrolidine macrocycle **(*R*)(*R*)110** gave a K_d = 0.99 μM and is the first sub-micromolar macrocyclic CREBBP bromodomain ligand to be reported. Upon the assessment of the selectivity profiles of these ligands, no amide macrocycles displayed any BRD4(1) affinity, however, the

acyclic analogue **(*R*)162** retained low micromolar affinity (K_d = 1.86 µM). This result confirmed the macrocycle selectivity hypothesis and uniquely exemplifies, through the use structure-guided X-ray crystal structure analysis, how macrocyclic drug design can improve the selectivity profiles of acyclic scaffolds. Furthermore, this result provides valuable information on desirable structural motifs for CREBBP bromodomain ligand design. This could lead to a major development in a field that has struggled to achieve high selectivity over the BET family of bromodomains.

Chapter 5 explored the application of PROTAC technology to develop small molecule degraders of the full-length CREBBP protein. This project was one of the few examples in the PROTAC field to explore the effect on the affinity when linker moieties were attached to the parent ligand scaffold. It was observed that linking from the THBD headgroup was most tolerated by the CREBBP bromodomain. Future work will involve testing the prepared triazole-based PROTACs in cells to observe if these molecules are able to induce the degradation of CREBBP. In addition, the use of different linkers and E3 ligase ligands will likely provide alternative surface complementarity with CREBBP that could promote its degradation. Nevertheless, this work has set the foundations for PROTAC development for CREBBP degradation, which there are currently no reports for in the field.

Chapter 6 describes a collaboration project with Prof. Dario Neri using ESAC library technology to identify novel CREBBP bromodomain ligands. This work was validated by the preparation of known CREBBP bromodomain fragments from ligands **(*R*)11** and **(*R*)12**. This led to the identification of fragment **192**, which was observed to make synergistic interactions, along with the THBD headgroup, to the CREBBP bromodomain in an FP assay. However, connecting these fragments with alternative linkers to prepare 'off-DNA' ligands resulted in significantly weaker affinity, when compared to ligands **(*R*)11** and **(*R*)12**. This was hypothesised to be due to suboptimal interaction of the fragments with their corresponding regions in the CREBBP bromodomain. Nevertheless, the ESAC library technology demonstrated its ability to identify novel scaffolds for the CREBBP bromodomain. This may provide a starting point for its use against less developed bromodomain targets for the identification of novel hit compounds.

7.2 Future work

The work in this thesis led to the discovery that macrocyclic ligands are selective scaffolds for the CREBBP bromodomain over the BET family of bromodomains. Pyrrolidine macrocycle **(*R*)(*R*)110** provides an excellent starting point for a structure-based drug design approach to improve its affinity to the CREBBP bromodomain. Future work could explore a step-wise SAR study which tests (i) alternative ring sizes; (ii) addition of structural features to the linker moiety (i.e. methyl, hydroxyl, fluoro) and (iii) addition of substituents to the *E*-alkene (i.e. methyl, fluoro, cyclopropyl) (**Figure 7.1**). These structural modifications could lead to improved affinities and enable the development of a valuable tool compound for the functional elucidation of the CREBBP bromodomain.

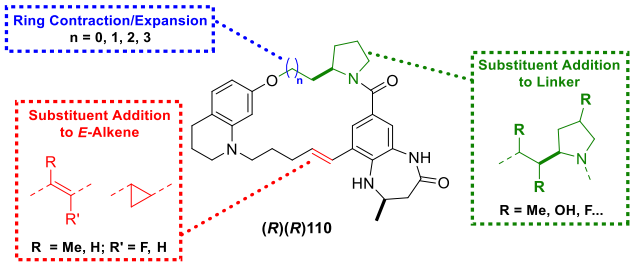


Figure 7.1 A proposed SAR study for the improving the affinity of macrocycle **(*R*)(*R*)110**.

The PROTAC project has identified ligand **(*R*)157** as a good starting point for PROTAC linker attachment. Most PROTAC endeavours reported in the literature rely on empirical data to guide the design, therefore, different linker types and lengths should be explored, alongside alternative E3 ligase ligands. Upon the identification of a CREBBP degrader, selective degradation should be tested against the paralogous protein EP300. The selective degradation could be rationalised through the tuning of surface complementarities between the paralogous CREBBP/EP300 proteins to the E3 ligase protein. However, these effects are currently very challenging to predict. Nevertheless, if such a selective PROTAC degrader is identified, this would be a major breakthrough in the elucidation of the biological functions for the individual CREBBP/EP300 proteins.

Finally, to improve the CREBBP bromodomain affinity of the 'off-DNA' ligands, which were identified by the ESAC library screen, shorter linker lengths should be explored. A comparable linker to ligand **(*R*)11** would be a suitable modification. However, as shown in Chapter 2, the amide moiety contributes toward unfavourable binding interactions, therefore, the substitution to the *E*-alkene should also be considered.

Chapter 8

Experimental Section

8.1 General Experimental

8.1.1 Computational methods

Molecular docking (by Joseph Bluck, Chapter 2). The protein model for CREBBP was extracted from the structure of **(*R*)48** bound to CREBBP, while a protein model for BRD4(1) was extracted from PDB:6CZV. All binding site H_2O molecules were retained in the protein model, which was protonated at pH 7.4 using the MOE (v. 2018.2) software package.

Macrocyclic computational studies were performed using CLC Drug Discovery Workbench 2.5 (Chapter 3), using default settings, or Schrödinger software Maestro 11 (Chapter 4), using GLIDE and Prime macrocycle conformational sampling (Prime-MCS). Ligands were docked using the PDB structure 4NYX, and the binding site setup included six conserved H_2O molecules identified for the CREBBP bromodomain. The binding site was centred around residues N1168 and R1173 in a docking sphere of 13 Å. Between three to five low energy conformations were generated for each ligand, with each conformation being docked against CREBBP bromodomain. Docking simulations were run with 300 iterations, with 5 repeated runs per docked ligand conformation.

8.1.2 Biochemical and biophysical methods

Protein expression and purification. The CREBBP bromodomain (Addgene plasmid # 38977) and BRD4(1) bromodomain (Addgene plasmid # 38942) constructs were transformed into *E. coli* BL21 (DE3) cells for expression. The proteins were purified using Immobilized Metal Affinity Chromatography (IMAC) with a HisTrap™ column (GE Healthcare) followed by gel filtration chromatography with Superdex 75 resin (GE Healthcare). The protein purity was assessed by Sodium dodecyl sulfate polyacrylamide gel electrophoresis (SDS-PAGE) (Appendix A2).

SDS-PAGE and Coomassie blue staining. Sodium dodecyl sulfate polyacrylamide gel was cast using Mini-PROTEAN® 3 Cell (Bio-Rad). SDS-PAGE was performed using Mini-PROTEAN® 3 Electrophoresis Module (Bio-Rad). The Tris-Glycine discontinuous buffer system was used in the SDS-PAGE experiments. Protein samples for SDS-PAGE was first prepared in 1× Laemmli sample buffer (diluted from 4× Laemmli sample buffer, Bio-Rad) containing 1.42 M β-mercaptoethanol (aliquoted from 14.2 M β-mercaptoethanol, Bio-Rad), and then denatured at 100 °C for 10 min. Chemicals for SDS-PAGE, Trizma® base, 30% acrylamide/bis-acrylamide solution, sodium dodecyl sulfate dust-free

pellets, *N*,*N*,*N*',*N*'-tetramethylethane-1,2-diamine (TEMED) and ammonium persulfate (APS), were purchased from Sigma Aldrich. Glycine was purchased from Fisher Scientific. After SDS-PAGE, the gels were stained with Staining Solution (0.5% Brilliant Blue G (Sigma Aldrich), 50% (*v/v*) MeOH (Sigma Aldrich), 10% (*v/v*) glacial acetic acid (Fisher Scientific), 40% (*v/v*) Milli-Q water) for 15 min. Destaining was performed with 40% (*v/v*) MeOH, 10% (*v/v*) glacial acetic acid, 50% (*v/v*) Milli-Q water until protein bands became visible.

Crystallisation (by Prof. Panagis Filippakopoulos and Dr Sarah Picaud). Aliquots of the complexes were set up for crystallisation using a mosquito® crystallisation robot (TTP Labtech, Royston UK). Coarse screens were setup in Greiner 3-well plates using three different drop ratios of precipitant to protein per condition (100+50 nL, 75+75 nL and 50+100 nL). Initial hits were optimized further scaling up the drop sizes. All crystallisations were carried out using the sitting drop vapor diffusion method at 4 °C. CREBBP crystals with **(*R*)48** were grown by mixing 150 nL of protein (6.45 mg/mL) with 150 nL of reservoir solution containing 20% ethylene glycol, 21 % PEG6K, 0.1 M TRIS pH 8.3 and 0.125 M LiCl. Diffraction quality crystals grew within two weeks. BRD4(1) crystals with **(*R*)11** were grown by mixing 150 nL of protein (9 mg/mL and 3 mM final ligand concentration) with an equal volume of reservoir solution containing 30% PEG1000 and 0.1 M MIB pH 7.0. Initial crystals were precipitated and used as seeds to obtain diffraction quality crystals which grew within a few days.

Data Collection and Structure Refinement (by Prof. Panagis Filippakopoulos and Dr Sarah Picaud). Crystals were cryo-protected using the well solution supplemented with additional ethylene glycol and were flash frozen in liquid nitrogen. Data were collected at Diamond beamline I03 on a Pilatus3 6M detector at a wavelength of 0.9763 Å. Indexing and integration was carried out using XDS[119] and scaling was performed with SCALA. Initial phases were calculated by molecular replacement with PHASER[120] using the previously determined model of CREBBP (PDB ID: 3DWY).[13] Initial models were built by ARP/wARP[121] followed by manual building in COOT.[122] Refinement was carried out in REFMAC5.[123] Thermal motions were analyzed using TLSMD[124] and hydrogen atoms were included in late refinement cycles.

SEC Dimerization Experiment. The dimeric state of the CREBBP bromodomain in solution was analyzed by gel filtration in a buffer containing 50 mM HEPES, pH 7.6, and 500 mM NaCl using a HiLoad® 16/600 Superdex® 75 column (GE Healthcare). Protein (50 µM) and ligand (50 µM) or DMSO were mixed and incubated at 20 °C for 30 min before injection. Eluting peaks were monitored using ultraviolet absorbance at 280 nm.

Ligand-Observed Proton NMR (in collaboration with Corentine Laurin). BRD4(1) bromodomain protein concentrations in the phosphate buffer were calculated by measuring the absorbance at 280 nm using a NanoDrop Lite spectrophotometer (Nanodrop® Technologies Inc.) and by using the predicted protein absorbance (ε_{280}: 28420 M^{-1} cm^{-1}). Samples were prepared to a total sample volume of 160 µL phosphate buffer, with 50 µM compound from 5 mM DMSO-d_6 stock solutions, 10% D_2O for signal locking and the appropriate amount of protein. After loading into 3 mm Hildenberg NMR tubes for Bruker Match™ system, samples were briefly centrifuged in a manual benchtop rotor. Spectra were recorded on a Bruker AVIII 700 MHz spectrometer with a TXI probe using a standard excitation-sculpting water suppression pulse sequence (256 or 512 scans each). For each compound, a compound only sample was recorded as a reference, followed by samples with protein. Each spectrum was processed with Bruker Topspin™ 3.2, the data was recorded on Microsoft Excel®, then the K_d was calculated with the "one site – specific binding; non-linear regression" function using Graphpad Prism®. In Topspin, spectra were phased corrected and calibrated to the residual DMSO peak, then local baseline corrections were performed ("absf n" function). The integral of the peaks of interests and the DMSO reference peaks were calculated in each spectrum for the determined chemical shift range (constant ranges were used for each compound studied). Using the ratio of integrals, the integral decrease of the peak of interest with increasing protein concentration was plotted for each compound.

Isothermal titration calorimetry. All calorimetric experiments were performed on a MicroCal iTC200 or MicroCal PEAQ-ITC Automated (Malvern) and analysed with the MicroCal PEAQ-ITC Analysis software (Malvern 1.1.0.1262) using a single binding site model. The first data point was excluded from the analysis. BRD4(1) and CREBBP bromodomains were dialysed at 4 °C overnight in a Slide-A-Lyzer® MINI Dialysis Device (2000 MWCO; Thermo Scientific Life Technologies) into 50 mM HEPES, 150 mM NaCl containing 0.2% DMSO at pH 7.4. Proteins were centrifuged to remove aggregates (3 min, 3,000 rpm, 25 °C). Protein concentrations were determined by measuring the absorbance at 280 nm using a NanoDrop Lite spectrophotometer (Nanodrop® Technologies Inc.) by using the predicted protein absorbance (ProtParam) (CREBBP: ε_{280}: 26930 M^{-1} cm^{-1} and BRD4(1): ε_{280}: 28420 M^{-1} cm^{-1}). Small molecule ligands were dissolved as 20 mM DMSO stock solution and diluted to the required concentration using dialysis buffer. The cell was stirred at 750 rpm, reference power set to 5 µcal/sec and temperature held at 25 ˚C. After an initial delay of 60 sec, 20 × 2 µL injections (first injection 0.4 µL) were performed with a spacing of 150 sec. Heat of dilutions were measured under the same conditions and subtracted for analysis. Small molecule solutions in the calorimetric cell (250 µL, (20 to 40 µM)) were titrated with the protein solutions in the syringe (60 µL, (160 to 250 µM)).

8.1.3 Synthetic methods

^{1}H NMR spectra were recorded on Bruker AVIIIHD 400 nanobay (400 MHz) spectrometer, Bruker AVII 500 (500 MHz) spectrometer with dual ^{13}C(^{1}H) cryoprobe, or Bruker AVIIIHD 500 (500 MHz) spectrometer in the stated solvents as a reference for the internal deuterium lock. The chemical shift data for each signal are given as δ_H in units of parts per million (ppm) relative to tetramethylsilane (TMS) where δ_H (TMS) = 0.00 ppm. The spectra were calibrated using the solvent peak with the data provided by Fulmer *et al*.[125] The multiplicity of each signal is indicated by s (singlet); br s (broad singlet); d (doublet); dd (doublet of doublets); t (triplet); q (quartet); or m (multiplet). The number of protons (n) for a given resonance signal is indicated by nH. Where appropriate, coupling constants (*J*) are quoted in Hz and are recorded to the nearest 0.1 Hz. Identical proton coupling constants (*J*) are averaged in each spectrum and reported to the nearest 0.1 Hz. The coupling constants were determined by analysis using MestReNova version 11.0 software. ^{1}H spectra were assigned using 2D NMR experiments including COSY, HMBC, HSQC and NOESY. Variable temperature (VT) ^{1}H NMR was performed in DMSO-d_6 at 65 °C.

^{13}C NMR spectra were recorded on a Bruker AVIIIHD 400 nanobay (101 MHz) spectrometer, or Bruker AVII 500 (126 MHz) spectrometer, with dual ^{13}C(^{1}H) cryoprobe, in the stated solvents, with broadband proton decoupling and an internal deuterium lock. The chemical shift data for each signal are given as δ_C in units of parts per million (ppm) relative to tetramethylsilane (TMS) where δ_C (TMS) = 0.00 ppm. The spectra were calibrated using the solvent peak with the data provided by *Fulmer et al*.[125] The chemical shift values of the resonances are quoted to 1 decimal place unless peaks have similar chemical shifts, in which case 2 decimal places are used. Coupling constants (*J*) are quoted in Hz and reported to the nearest 0.1 Hz. The coupling constants were determined by analysis using MestReNova version 11.0 software. ^{13}C spectra were assigned using 2D NMR experiments including HMBC and HSQC.

^{19}F NMR spectra were recorded on a Bruker AVIIIHD 400 nanobay (376 MHz) spectrometer using a deuterium internal lock. The chemical shift data for each signal are given as δ_F in units of parts per million (ppm). The multiplicity of each signal is indicated by: s (singlet); d (doublet); t (triplet); q (quartet) or m (multiplet). Coupling constants (*J*) are quoted in Hz and reported to the nearest 0.1 Hz. The coupling constants are determined by analysis using MestReNova version 11.0 software.

Low resolution electrospray ionisation (ESI) mass spectra were acquired on a Waters LCT Premier spectrometer or Agilent 6120 Quadrupole spectrometer.

High resolution mass spectra were recorded on a Bruker MicroTOF spectrometer, operating in positive or negative mode, as indicated, from solutions of MeOH, MeCN or H_2O. *m/z* values are reported in Daltons. Electron ionisation/field ionisation (EI/FI) was carried out on a Waters GCT with a temperature programmed solids probe inlet. MALDI was carried out on a Waters MALDI Micro MX. When a compound was not observed by LRMS, only HRMS is quoted.

Specific optical rotations were measured using either a Perkin Elmer Model 241 polarimeter or Schmidt + Haensch UniPol L2000 polarimeter, in cells with a path length of 1 dm, using a sodium lamp at 589 nm. The concentration (*c*) is expressed in g/100 mL (equivalent to g/0.1 dm^3). Specific rotations are denoted and are given in implied units of 10^{-1} deg cm^2 g^{-1} at the temperature stated.

Melting points were determined using a Leica Galen III hot stage microscope and are uncorrected. The solvents of crystallisation are shown in parentheses.

Infrared (IR) spectra were obtained from neat samples, either as liquids or solids using a diamond ATR module. The spectra were recorded on a Bruker Tensor 27 spectrometer. Absorption maxima are reported in wavenumbers (cm^{-1}) and reported as s (strong), m (medium), w (weak) or br (broad). Only the main, relevant peaks have been assigned.

Thin layer chromatography (TLC) was carried out on normal phase Merck silica gel 60 F_{254} aluminium-supported chromatography sheets. Visualisation was by absorption of UV light (λ_{max} 254 nm), exposure to iodine vapour or thermal development after dipping in either an ethanolic solution of ninhydrin or an aqueous solution of potassium permanganate.

Normal phase silica gel flash column chromatography was performed either manually using Geduran silica gel 60 (40–63 μM) or Sigma Aldrich silica gel 60 (40–63 μM) under a positive pressure of nitrogen; or on a Biotage SP1 automated column chromatography system using KP-Sil® SNAP Flash Silica Cartridges.

Analytical high-performance liquid chromatography (HPLC) was performed on a PerkinElmer Flexar system with a Binary LC Pump and UV/VIS LC Detector set at 254 nm. For determination of purity, a

Dionex Acclaim® 120 C18 column [5 µm, 12 Å, 150 mm × 4.6 mm] reverse phase column was used with a constant flow rate of 1.5 mL min^{-1} and gradient method of 10 min from (Method 1) 95:5 H_2O:MeCN to 5:95 H_2O:MeCN with a 5 min hold, or (Method 2) 95:5 in H_2O (0.1% TFA):MeCN (0.1% TFA) to 5:95 H_2O (0.1% TFA):MeCN (0.1% TFA) with a 5 min hold unless otherwise stated. Samples injected were prepared by dissolving in MeOH or MeCN and filtered.

In vacuo refers to the removal of solvents under reduced pressure using a Büchi™ rotary evaporator in a water bath at 40 °C, unless otherwise stated.

Lyophilisation refers to the removal of H_2O from aqueous solutions by freeze drying using a CHRIST Alpha 1-2 LD lyophiliser.

Celite® refers to Celite® 545 filter aid, treated with sodium carbonate, flux-calcined which was purchased from Sigma Aldrich.

Chemicals were purchased from Acros UK, Apollo Scientific, Enamine, Sigma Aldrich UK, Alfa Aesar UK, Fisher Scientific UK, Fluka UK, Fluorochem, Merck, Argo International Limited and TCI-Europe. All reagents were purified, when necessary, by standard techniques.[126] Zinc and iron metals were activated according to the Kishi's procedure.[127] Where appropriate and if not otherwise stated, all non-aqueous reactions were performed in a flame dried flask under an inert atmosphere.

Anhydrous solvents including, DMF, THF, Et_2O toluene, CH_2Cl_2 and NEt_3 were dried by passing through a column of activated basic alumina according to the Grubbs' procedure.[128] Anhydrous 1,2-dichloroethane, DMSO, MeOH and MeCN were purchased from Sigma Aldrich UK in SureSeal™ bottles and used without further purification. All other solvents were used as supplied (analytical or HPLC grade) without purification. Solvents used for cross coupling reactions were degassed with nitrogen for 30 min.

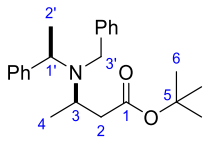
Brine refers to a saturated aqueous solution of sodium chloride.

Petroleum ether refers to the fraction of light petroleum ether boiling within the range of 40–60 °C.

8.2 Procedures

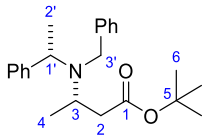
8.2.1 Chapter 2 - Amide bioisosteres

tert-Butyl (*R*)-3-(benzyl((*R*)-1'-phenylethyl)amino)butanoate ((*R*)(*R*)40)



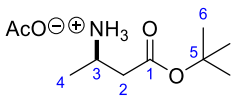
To a stirred colourless solution of (*R*)-*N*-benzyl-1-phenylethan-1-amine (**(*R*)39**) (4.04 g, 19.1 mmol, 1.5 eq.) in anhydrous THF (22 mL) at −78 °C was added *n*-BuLi in *n*-hexane (2.5 M, 8.16 mL, 20.1 mmol, 1.6 eq.), dropwise over a period of 15 min, and the pink reaction mixture was stirred at −78 °C for 30 min. *tert* Butyl crotonate (2.04 mL, 1.81 g, 12.8 mmol, 1.0 eq.) in THF (16 mL) was added dropwise over a period of 1 h and the reaction mixture was stirred at −78 °C for a further 4 h. The reaction mixture was quenched with sat. aq. NH_4Cl (20 mL) and was warmed to rt. The reaction mixture was evaporated *in vacuo*. 0.5 M aq. Citric acid (75 mL) was added to the residue and the resulting mixture was extracted with CH_2Cl_2 (3 × 100 ml). The combined organic components were washed with sat. aq. $NaHCO_3$ (150 mL), brine (150 mL) dried (Na_2SO_4), filtered, and evaporated *in vacuo* to afford a colourless oil. The crude oil was purified by silica gel chromatography (elution with 3% Et_2O in petroleum ether) to yield *tert*-butyl (*R*)-3-(benzyl((*R*)-1'-phenylethyl)amino)butanoate (**(*R*)(*R*)40**) as a colourless oil (3.75 g, 83%); R_f 0.52 (Et_2O/*n*-hexane 1:9); $[\alpha]_D^{25}$= −3.9 (*c* 1.0, $CHCl_3$); [Lit:[129] $[\alpha]_D^{25}$= −5.2 (c 1.1, $CHCl_3$)]; ^{1}H NMR (400 MHz; $CDCl_3$) δ_H 7.46–7.10 (10H, m, Ar-H), 3.89 (1H, q, *J* 6.9, H-1'), 3.76 (1H, d, *J* 15.0, H_AH_B-3'), 3.61 (1H, d, *J* 15.0, H_AH_B-3'), 3.42 (1H, dqd, *J* 9.1, 6.7, 4.7, H-3), 2.25 (1H, dd, *J* 14.1, 4.7, H_AH_B-2), 2.01 (1H, dd, *J* 14.1, 9.1, H_AH_B-2), 1.39 (9H, s, H-6), 1.33 (3H, d, *J* 6.9, H-2'), 1.11 (3H, d, *J* 6.7, H-4); LRMS *m/z* (ESI^+) 354 ($[M+H]^+$, 100%). These data are in accordance with the literature.[30,129]

tert-Butyl (_S_)-3-(benzyl((_S_)-1'-phenylethyl)amino)butanoate ((_S_)(_S_)40)



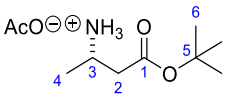
tert-Butyl (_S_)-3-(benzyl((_S_)-1'-phenylethyl)amino)butanoate (**(_S_)(_S_)40**) was synthesised using (_S_)-_N_-benzyl-1-phenylethan-1-amine (**(_S_)39**) following the same procedure to prepare _tert_-butyl (_R_)-3-(benzyl((_R_)-1'-phenylethyl)amino)butanoate (**(_R_)(_R_)40**) to yield a colourless oil (9.42 g, 56%); $[\alpha]_D^{25}$= +5.1 (_c_ 1.0, $CHCl_3$), [Lit:[129] $[\alpha]_D^{25}$= +5.1 (c 1.1, $CHCl_3$)]; other physical and spectroscopic properties are identical to those as _tert_-butyl (_R_)-3-(benzyl((_R_)-1'-phenylethyl)amino)butanoate (**(_R_)(_R_)40**). These data are in accordance with the literature.[30,129]

tert-Butyl (_R_)-3-aminobutanoate ((_R_)41)



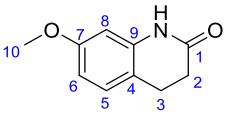
20 % $Pd(OH)_2/C$ (1.80 g, 2.57 mmol, 0.2 eq.) was added to a stirred solution of _tert_-butyl (_R_)-3-(benzyl((_R_)-1'-phenylethyl)amino)butanoate (**(_R_)(_R_)40**) (4.54 g, 12.8 mmol, 1.0 eq.) in H_2O (7.3 mL), glacial acetic acid (4.6 mL) and MeOH (182 mL), which was purged under a nitrogen atmosphere. The atmosphere was replaced with hydrogen gas and the suspension was stirred at rt for 20 h. The black suspension was filtered through Celite® (eluent MeOH) and evaporated _in vacuo_ to yield a yellow oil. The oil was azeotroped with toluene (3 × 50 mL) to yield _tert_-butyl (_R_)-3-aminobutanoate (**(_R_)41**) containing 1.24 eq. acetic acid as colourless solid (2.85 g, 95%); R_f 0.00 (EtOAc); $[\alpha]_D^{25}$= −17.3 (_c_ 0.5, $CHCl_3$), [Lit:[129] $[\alpha]_D^{25}$= −22.2 (_c_ 0.5, $CHCl_3$)]; ^{1}H NMR (400 MHz; $CDCl_3$) δ_H 3.57–3.47 (1H, m, H-3), 2.62–2.42 (2H, m, H-2), 2.09 (9H, s, H-6), 1.29 (3H, d, _J_ 6.6, H-4); LRMS _m/z_ (ESI^+) 160 ($[M+H]^+$, 81%). These data are in accordance with the literature.[30,129]

tert-Butyl (_S_)-3-aminobutanoate ((_S_)41)



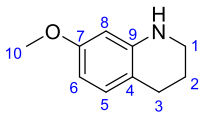
tert-Butyl (_S_)-3-aminobutanoate (**(_S_)41**) was synthesised using _tert_-butyl (_S_)-3-(benzyl((_S_)-1'-phenylethyl)amino)butanoate (**(_S_)(_S_)40**) following the same procedure to prepare _tert_-butyl (_R_)-3-aminobutanoate (**(_R_)41**) to yield a colourless oil (5.82 g, 87%); $[\alpha]_D^{25}$= +21.5 (_c_ 1.0, $CHCl_3$), [Lit:[129] $[\alpha]_D^{25}$= +21.2 (_c_ 0.6, $CHCl_3$)]; other physical and spectroscopic properties are identical to those as _tert_-butyl (_R_)-3-aminobutanoate (**(_R_)41**). These data are in accordance with the literature.[30,129]

7-Methoxy-3,4-dihydroquinolin-2(1_H_)-one (203)



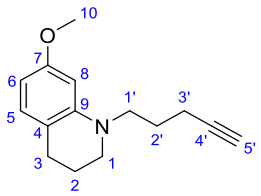
To a stirred suspension of 7-hydroxy-3,4-dihydroquinolin-2(1_H_)-one (**111**) (4.00 g, 24.5 mmol, 1.0 eq.) and K_2CO_3 (6.78 g, 49.0 mmol, 2.0 eq.) in DMF (40 mL) was added iodomethane (1.68 mL, 27.0 mmol, 1.1 eq.) at rt. The reaction mixture was stirred at 60 °C for 18 h. The cooled suspension was diluted with EtOAc (250 mL) and washed with 1 M aq. K_2CO_3 (3 × 100 mL). The organic component was further washed with 0.5 M aq. LiCl (3 × 100 mL), brine (200 mL), dried ($MgSO_4$), filtered, and evaporated _in vacuo_ to afford a colourless solid. The crude solid was crystallised from EtOH (50 mL) to yield 7-methoxy-3,4-dihydroquinolin-2(1_H_)-one (**203**) as a colourless solid (2.72 g, 63%); R_f 0.13 (EtOAc/petroleum ether 2:3); mp 130–132 °C (EtOH); ^{1}H NMR (400 MHz; $CDCl_3$) δ_H 8.00 (1H, s, NH-9), 7.05 (1H, d, _J_ 8.3, H-5), 6.53 (1H, dd, _J_ 8.3, 2.4, H-6), 6.32 (1H, d, _J_ 2.4, H-8), 3.78 (3H, s, H-10), 2.98–2.80 (2H, m, H-3), 2.66–2.56 (2H, m, H-2); LRMS _m/z_ (ESI$^+$) 178 ([M+H]$^+$, 100%). These data are in accordance with the literature.[30]

7-Methoxy-1,2,3,4-tetrahydroquinoline (45)



7-Methoxy-3,4-dihydroquinolin-2(1*H*)-one (**203**) (970 mg, 5.47 mmol, 1.0 eq.) was suspended in anhydrous THF (30 mL) and added portionwise to $LiAlH_4$ (312 mg, 8.21 mmol, 1.5 eq.) in anhydrous THF (25 mL) at 0 °C and the suspension was stirred at 0 °C for 10 min. The suspension was warmed to rt and was stirred for a further 5 h. The reaction was cooled to 0 °C and H_2O (0.4 mL), followed by 15% aq. NaOH (0.4 mL) and H_2O (1.2 mL) were added dropwise (Fieser work-up). $MgSO_4$ was added and the suspension was stirred at rt for 30 min. The reaction mixture was filtered and was washed with EtOAc (100 mL). The filtrate was evaporated *in vacuo* to afford 7-methoxy-1,2,3,4-tetrahydroquinoline (**45**) as a colourless oil (870 mg, 97%); R_f 0.60 (EtOAc/petroleum ether 2:3); ^{1}H NMR (400 MHz; $CDCl_3$) δ_H 6.84 (1H, d, *J* 8.2, H-5), 6.20 (1H, dd, *J* 8.2, 2.5, H-6), 6.04 (1H, d, *J* 2.5, H-8), 3.86 (1H, br s, NH-9), 3.73 (3H, s, H-10), 3.34–3.20 (2H, m, H-3), 2.74–2.64 (2H, m, H-1), 1.99–1.86 (2H, m, H-2); LRMS *m/z* (ESI$^+$) 164 ([M+H]$^+$, 100%). These data are in accordance with the literature.[30]

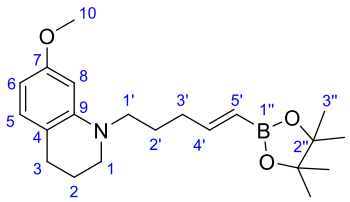
7-Methoxy-1-(pent-4-yn-1-yl)-1,2,3,4-tetrahydroquinoline (46)



Pent-4-yn-1-yl methanesulfonate (486 mg, 3.00 mmol, 1.5 eq.) was added to a solution of 7-methoxy-1,2,3,4-tetrahydroquinoline (**45**) (652 mg, 2.00 mmol, 1.0 eq.), potassium iodide (166 mg, 1.00 mmol, 0.5 eq.) and *N*,*N*-diisopropylethylamine (697 µL, 4.00 mmoL, 2.0 eq.) in DMF (10.5 mL). The reaction mixture was sealed and heated to 100 °C in a microwave for 1 h. The cooled orange solution was diluted with Et_2O (75 mL) and washed with H_2O (3 × 75 mL), brine (50 mL), dried ($MgSO_4$), filtered and evaporated *in vacuo* to afford an orange oil. The crude oil was purified by silica gel chromatography (elution with toluene) to afford 7-methoxy-1-(pent-4-yn-1-yl)-1,2,3,4-tetrahydroquinoline (**46**) as an orange oil (531 mg, 57%); R_f 0.38 (CH_2Cl_2); ^{1}H NMR (400 MHz; $CDCl_3$) δ_H 6.84 (1H, d, *J* 8.2, H-5), 6.20–6.10 (2H, m, H-6, H-8), 3.76 (3H, s, H-10), 3.39–3.31 (2H, m, H-1'), 3.31–3.24 (2H, m, H-1), 2.69 (2H, t,

J 8.2, H-3), 2.26 (2H, td, *J* 6.9, 2.6, H-3'), 2.00 (1H, t, *J* 2.6, H-5'), 1.97–1.87 (2H, m, H-2), 1.82 (2H, m, H-2'); LRMS *m/z* (ESI$^+$) 230 ([M+H]$^+$, 100%).

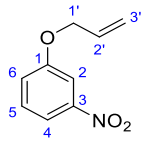
(*E*)-7-Methoxy-1-(5-(4,4,5,5-tetramethyl-1,3,2-dioxaborolan-2-yl)pent-4-en-1-yl)-1,2,3,4-tetrahydroquinoline (47)



7-Methoxy-1-(pent-4-yn-1-yl)-1,2,3,4-tetrahydroquinoline (**46**) (959 mg, 4.24 mmol, 1.0 eq.) and bis(cyclopentadienyl)zirconium(IV) chloride hydride (109 mg, 0.424 mmol, 0.1 eq.) were added to a tapered microwave vial and sealed under an argon atmosphere (evacuated and backfilled 3 × argon). Triethylamine (59.0 µL, 0.424 mmol, 0.1 eq.) and 4,4,5,5-tetramethyl-1,3,2-dioxaborolane (676 µL, 4.66 mmol, 1.1 eq.) were added and the reaction mixture was stirred at 60 °C under argon for 20 h in the absence of light. The reaction mixture was purified by silica gel chromatography (elution with 0% to 100% CH_2Cl_2 in petroleum ether) to yield (*E*)-7-methoxy-1-(5-(4,4,5,5-tetramethyl-1,3,2-dioxaborolan-2-yl)pent-4-en-1-yl)-1,2,3,4-tetrahydroquinoline (**47**) as an orange oil (875 mg, 58%); R_f 0.21 (CH_2Cl_2); ^{1}H NMR (400 MHz; $CDCl_3$) δ_H 6.82 (1H, d, *J* 8.7, H-5), 6.65 (1H, dt, *J* 18.0, 6.4, H-4'), 6.16–6.02 (2H, m, H-6, H-8), 5.47 (1H, dt, *J* 18.0, 1.6, H-5'), 3.28–3.18 (4H, m, H-1, H-1'), 2.67 (2H, t, *J* 6.3, H-3), 2.20 (2H, m, H-3'), 1.90 (2H, m, H-2), 1.78–1.69 (2H, m, H-2'), 1.26 (12H, s, H-3''); ^{11}B NMR (160 MHz; $CDCl_3$) δ_B 29.7 (B-1''); LRMS *m/z* (ESI$^+$) 358 ([M+H]$^+$, 100%).

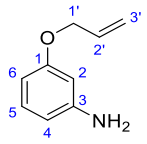
8.2.2 Chapter 3 - First Generation Macrocycles

1-(Allyloxy)-3-nitrobenzene (**65**)



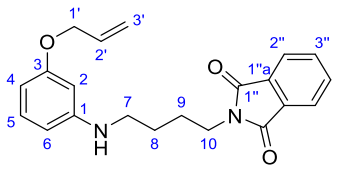
To a suspension of 3-nitrophenol (**64**) (2.54 g, 18.3 mmol, 1.0 eq.) and K_2CO_3 (5.04 g, 36.5 mmol, 2.0 eq.) in acetone (60 mL) was added allyl bromide (2.37 mL, 27.4 mmol, 1.5 eq.) and the suspension was stirred at rt for 18 h. The suspension was evaporated *in vacuo* to afford a yellow oil. The crude oil was purified by silica gel chromatography (elution with 10% EtOAc in petroleum ether) to yield 1-(allyloxy)-3-nitrobenzene (**65**) as a yellow oil (3.19 g, 98%); R_f 0.52 (EtOAc/petroleum ether 1:10); ^{1}H NMR (400 MHz; $CDCl_3$) δ_H 7.81 (1H, ddd, *J* 8.2, 2.3, 1.0, H-4), 7.73 (1H, dd, *J* 2.3, 2.3, H-2), 7.42 (1H, dd, *J* 8.2, 8.2, H-5), 7.24 (1H, ddd, *J* 8.2, 2.3, 1.0, H-6), 6.04 (1H, ddt, *J* 17.3, 10.6, 5.3, H-2'), 5.44 (1H, ddt, *J* 17.3, 1.4, 1.4, H_AH_B-3'), 5.34 (1H, ddt, *J* 10.6, 1.4, 1.4, H_AH_B-3'), 4.61 (2H, dt, *J* 5.3, 1.4, H-1'). These data are in accordance with the literature.[130]

3-(Allyloxy)aniline (66)



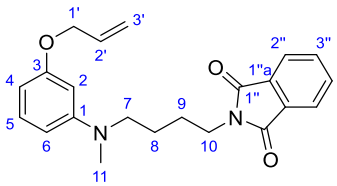
To a solution of 1-(allyloxy)-3-nitrobenzene (**65**) (2.90 g, 16.2 mmol, 1.0 eq.) in EtOH (72 mL) and H_2O (6 mL) was added iron powder (9.04 g, 55.9 mmol, 10.0 eq.) and NH_4Cl (8.67 g, 53.5 mmol, 10.0 eq.). The reaction mixture was stirred at 75 °C for 24 h. The suspension was filtered through Celite® and washed with EtOAc (250 mL). The filtrate was evaporated *in vacuo* to afford a brown oil. The crude oil was purified by silica gel chromatography (elution with 15% EtOAc in petroleum ether) to yield 3-(allyloxy)aniline (**66**) as an brown oil (1.68 g, 70%); R_f 0.33 (EtOAc/petroleum ether 1:4); ^{1}H NMR (400 MHz; $CDCl_3$) δ_H 7.08 (1H, dd, *J* 8.1, 8.1, H-5), 6.37 (1H, ddd, *J* 8.1, 2.2, 0.9, H-6), 6.32 (1H, ddd, *J* 7.9, 2.2, 0.9, H-4), 6.29 (1H, dd, *J* 2.2, 2.2, H-2), 6.07 (1H, ddt, *J* 17.3, 10.5, 5.3, H-2'), 5.43 (1H, ddt, *J* 17.3, 1.6, 1.6, H_AH_B-3'), 5.30 (1H, ddt, *J* 10.5, 1.6, 1.6, H_AH_B-3'), 4.52 (2H, dt, *J* 5.3, 1.6, H-1'), 3.68 (2H, s, NH-3); LRMS *m/z* (ESI$^+$) 150 ([M+H]$^+$, 15%). These data are in accordance with the literature.[131]

2-(4-((3-(Allyloxy)phenyl)amino)butyl)isoindoline-1,3-dione (67)



To a suspension of 3-(allyloxy)aniline (**66**) (352 mg, 2.36 mmol, 1.0 eq.) and K_2CO_3 (392 mg, 2.83 mmol, 1.2 eq.) in DMF (2 mL) was added *N*-(4-bromobutyl)phthalimide (799 mg, 2.83 mmol, 1.2 eq.) and the suspension was stirred at 80 °C for 7 h. The cooled suspension was diluted with EtOAc (70 mL) and washed with 2 M aq. K_2CO_3 (3 × 75 mL). The organic component was washed with brine (100 mL), dried (Na_2SO_4), filtered, and evaporated *in vacuo* to afford brown oil. The crude oil was purified by silica gel chromatography (elution with 30% EtOAc in petroleum ether) to yield 2-(4-((3-(allyloxy)phenyl)amino)butyl)isoindoline-1,3-dione (**67**) as a yellow solid (556 mg, 67%); R_f 0.41 (EtOAc/petroleum ether 1:2); mp 68–71 °C (EtOAc); $\bar{\nu}_{max}$ (neat)/cm^{-1} 3376 (N-H, m), 2997 (C-H, w), 1698 (C=C, s); ^{1}H NMR (500 MHz; $CDCl_3$) δ_H 7.84 (2H, dd, *J* 5.5, 3.0, H-3''), 7.71 (2H, dd, *J* 5.5, 3.0, H-2''), 7.04 (1H, dd, *J* 8.2, 8.2, H-5), 6.25 (1H, ddd, *J* 8.2, 2.3, 0.8, H-6), 6.21 (1H, ddd, *J* 8.2, 2.3, 0.8, H-4), 6.17 (1H, dd, *J* 2.3, 2.3, H-2), 6.05 (1H, ddt, *J* 17.3, 10.6, 5.3, H-2'), 5.40 (1H, ddt, *J* 17.3, 1.7, 1.7, H_AH_B-3'), 5.26 (1H, ddt, *J* 10.6, 1.7, 1.7, H_AH_B-3'), 4.49 (2H, ddd, *J* 5.3, 1.7, 1.7, H-1'), 3.74 (2H, t, *J* 7.1, H-10), 3.69 (1H, s, NH-1), 3.15 (2H, t, *J* 7.0, H-7), 1.84–1.76 (2H, m, H-9), 1.70–1.62 (2H, m, H-8); ^{13}C NMR (126 MHz; $CDCl_3$) δ_C 168.6 (C-1''), 160.0 (C-3), 149.7 (C-1), 134.1 (C-2''), 133.7 (C-2'), 132.2 (C-1''a), 130.0 (C-5), 123.4 (C-3''), 117.6 (C-3'), 106.2 (C-4), 103.3 (C-6), 99.5 (C-2), 68.8 (C-1'), 43.6 (C-7), 37.8 (C-10), 26.9 (C-8), 26.4 (C-9); HRMS *m/z* (ESI$^+$) [Found: 351.1700, $C_{21}H_{23}N_2O_3$ requires M$^+$ 351.1703]; LRMS *m/z* (ESI$^+$) 351 ([M+H]$^+$, 100%); HPLC Method 1: Retention time 11.1 min, purity 98.0%.

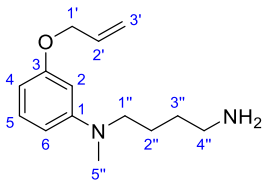
2-(4-((3-(Allyloxy)phenyl)(methyl)amino)butyl)isoindoline-1,3-dione (68)



To a stirred suspension of 2-(4-((3-(allyloxy)phenyl)amino)butyl)isoindoline-1,3-dione (**67**) (500 mg, 1.43 mmol, 1.0 eq.) and K_2CO_3 (236 mg, 1.71 mmol, 1.2 eq.) in DMF (5 mL) was added iodomethane (100 µL, 1.61 mmol, 1.1 eq.) at rt. The reaction mixture was stirred at 85 °C for 5 h. To the cooled

suspension was added 1 M aq. K_2CO_3 (100 mL) and the resulting mixture was extracted with CH_2Cl_2 (3 × 70 mL). The combined organic components were washed with 0.5 M aq. LiCl (3 × 100 mL), brine (100 mL), dried ($MgSO_4$), filtered, and evaporated *in vacuo* to afford a yellow oil. The crude oil was purified by silica gel chromatography (elution with 0% to 20% EtOAc in petroleum ether) to yield 2-(4-((3-(allyloxy)phenyl)(methyl)amino)butyl)isoindoline-1,3-dione (**68**) as a red solid (379 mg, 73%); R_f 0.15 (EtOAc/petroleum ether 1:10); mp 48–50 °C (EtOAc); $\bar{\nu}_{max}$ (neat)/cm^{-1} 2932 (C-H, w), 1612 (C=C, s); ^{1}H NMR (500 MHz; $CDCl_3$) δ_H 7.84 (2H, dd, *J* 5.4, 3.0, H-2''), 7.71 (2H, dd, *J* 5.4, 3.0, H-3''), 7.09 (1H, dd, *J* 8.4, 8.4, H-5), 6.31 (1H, ddd, *J* 8.4, 2.3, 1.0, H-4), 6.26–6.22 (2H, m, H-2, H-6), 6.06 (1H, ddt, *J* 17.3, 10.6, 5.4, H-2'), 5.41 (1H, ddt, *J* 17.3, 1.5, 1.5, H_AH_B-3'), 5.27 (1H, ddt, *J* 10.6, 1.5, 1.5, H_AH_B-3'), 4.51 (2H, ddd, *J* 5.4, 1.5, 1.5, H-1'), 3.71 (2H, t, *J* 7.1, H-10), 3.33 (2H, t, *J* 7.3, H-7), 2.90 (3H, s, H-11), 1.76–1.67 (2H, m, H-9), 1.67–1.59 (2H, m, H-8); ^{13}C NMR (126 MHz; $CDCl_3$) δ_C 168.5 (C-1''), 159.9 (C-3), 150.7 (C-1), 134.0 (C-3''), 133.8 (C-2'), 132.2 (C-1''a), 129.9 (C-5), 123.4 (C-2''), 117.6 (C-3'), 105.6 (C-4), 101.8 (C-6), 99.6 (C-2), 68.9 (C-1'), 52.4 (C-7), 38.6 (C-11), 37.9 (C-10), 26.4 (C-9), 24.3 (C-8); HRMS *m/z* (ESI$^+$) [Found: 365.1862, $C_{22}H_{25}N_2O_3$ requires M^+ 365.1860]; LRMS *m/z* (ESI$^+$) 365 ([M+H]$^+$, 100%); HPLC Method 1: Retention time 11.8 min, purity 96.7%.

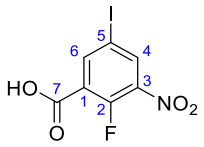
N^1-(3-(Allyloxy)phenyl)- N^1-methylbutane-1,4-diamine (61)



Hydrazine monohydrate (65%, 100 µL, 2.06 mmol, 4.0 eq.) was added to a stirred solution of 2-(4-((3-(allyloxy)phenyl)(methyl)amino)butyl)isoindoline-1,3-dione (**68**) (184 mg, 0.505 mmol, 1.0 eq.) in CH_2Cl_2 (1.3 mL) and MeOH (1.3 mL). The reaction mixture was stirred at 70 °C for 2 h. The cooled reaction mixture was diluted in CH_2Cl_2 (15 mL), filtered through Celite® (eluent MeOH) and evaporated *in vacuo* to yield a colourless solid. Purification *via* acid base extraction was performed as follows: The crude solid was dissolved in EtOAc (25 mL) and washed with 20% aq. NH_4Cl (3 × 20 mL). The combined aqueous components were basified with 2 M aq. NaOH and extracted with CH_2Cl_2 (3 × 25 mL). The combined organic components were washed with brine (20 mL), dried (Na_2SO_4), filtered, and evaporated *in vacuo* to yield N^1-(3-(allyloxy)phenyl)- N^1-methylbutane-1,4-diamine (**61**) as a yellow oil (58 mg, 46%) and was used without further purification; R_f 0.0 (EtOAc); ^{1}H NMR (400 MHz; $CDCl_3$) δ_H 7.13 (1H, dd, *J* 8.5, 8.5, H-2), 6.36–6.31 (1H, m, H-4), 6.30–6.23 (2H, m, H-5, H-6), 6.09 (1H, ddt, *J* 17.3, 10.5, 5.4, H-2'), 5.43 (1H, ddt, *J* 17.3, 1.5, 1.5, H_AH_B-3'), 5.29 (1H, ddt, *J* 10.5, 1.5, 1.5, H_AH_B-3'), 4.54 (2H,

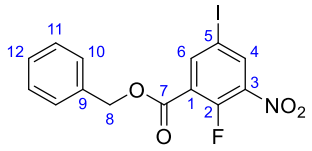
ddd, *J* 5.4, 1.5, 1.5, H-1'), 3.32 (2H, t, *J* 7.4, H-1''), 2.93 (3H, s, H-5''), 2.75 (2H, t, *J* 7.0, H-4''), 1.83 (2H, br s, NH-4''), 1.68–1.56 (2H, m, H-2''), 1.54–1.41 (2H, m, H-3''); ^{13}C NMR (126 MHz; $CDCl_3$) δ_C 160.0 (C-3), 150.7 (C-1), 133.8 (C-2'), 129.9 (C-5), 117.6 (C-3'), 105.6 (C-6), 101.6 (C-4), 99.7 (C-2), 68.9 (C-1'), 52.8 (C-1''), 42.1 (C-4''), 38.6 (C-5''), 31.0 (C-2''), 24.3 (C-3''); HRMS *m/z* (ESI^+) [Found: 235.1806, $C_{14}H_{23}N_2O$ requires M^+ 235.1805]; LRMS *m/z* (ESI^+) 235 ($[M+H]^+$, 100%).

2-Fluoro-5-iodo-3-nitrobenzoic acid (70)



2-Fluoro-5-nitro-benzoic acid (**69**) (1.00 g, 5.40 mmol, 1.0 eq.) was added to a solution of iodine (1.92 g, 7.56 mmol, 1.4 eq.) in fuming sulfuric acid (10 mL) and the reaction mixture was stirred at 85 °C for 17 h. The cooled reaction mixture was slowly added portionwise to ice (100 g) and the resulting precipitate was extracted with CH_2Cl_2 (3 × 75 mL). The combined organic components were washed with 10% aq. $Na_2S_2O_3$ (100 mL), brine (100 mL), dried (Na_2SO_4), filtered, and evaporated *in vacuo* to yield 2-fluoro-5-iodo-3-nitrobenzoic acid (**70**) as a pale yellow solid (1.54 g, 92%); R_f 0.30 (MeOH/CH_2Cl_2 1:19); mp 168–171 °C (CH_2Cl_2); $\bar{\nu}_{max}$ (neat)/cm^{-1} 3073 (C-H, w), 2852 (COO-H, br w), 1695 (C=O, s), 1530 (N-O, s); ^{1}H NMR (500 MHz; DMSO-d_6) δ_H 14.07 (1H, br s, OH-7), 8.60 (1H, dd, *J* 6.3, 2.4, H-4), 8.42 (1H, dd, *J* 5.8, 2.4, H-6); ^{13}C NMR (126 MHz; DMSO-d_6) δ_C 162.4 (d, *J* 2.3, C-7), 153.7 (d, *J* 273.4, C-2), 144.8 (C-6), 139.0 (d, *J* 9.3, C-1), 137.4 (C-4), 123.9 (d, *J* 10.8, C-3), 87.6 (d, *J* 5.4, C-5); ^{19}F NMR (376 MHz; DMSO-d_6) δ_F −120.8 (dd, *J* 6.3, 6.3); HRMS *m/z* (ESI^-) [Found: 309.9016, $C_7H_2O_4NF^{127}I$ requires M^- 309.9018]; LRMS *m/z* (ESI^-) 310 ($[M-H]^-$, 100%). HPLC Method 2: Retention time 7.6 min, purity 99.5%.

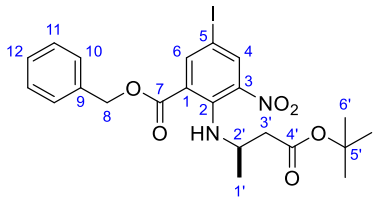
Benzyl 2-fluoro-5-iodo-3-nitrobenzoate (71)



To a solution of 2-fluoro-5-iodo-3-nitrobenzoic acid (**70**) (1.50 g, 4.82 mmol, 1.0 eq.) in DMF (11 mL) was added K_2CO_3 (1.00 g, 7.24 mmol, 1.5 eq.) and the reaction mixture was stirred at rt for 5 min. Benzyl bromide (860 µL, 7.24 mmol, 1.5 eq.) was added and the reaction mixture was stirred at 60 °C

for 4 h. The cooled reaction mixture was diluted with EtOAc (100 mL) and was washed with 2 M aq. K_2CO_3 (3 × 100 mL). The organic component was washed with 0.5 M aq. LiCl (3 × 100 mL), brine (100 mL), dried ($MgSO_4$), filtered, and evaporated *in vacuo* to afford an orange solid. The crude solid was purified by silica gel chromatography (elution with 0% to 20% EtOAc in petroleum ether) to yield benzyl 2-fluoro-5-iodo-3-nitrobenzoate (**71**) as a yellow solid (1.76 g, 91%); R_f 0.50 (EtOAc/petroleum ether 1:10); mp 86–89 °C (EtOAc); $\bar{\nu}_{max}$ (neat)/cm^{-1} 3091 (C-H, w), 1719 (C=O, s), 1534 (N-O, s); ^{1}H NMR (500 MHz; $CDCl_3$) δ_H 8.49 (1H, dd, *J* 5.7, 2.4, H-6), 8.44 (1H, dd, *J* 6.1, 2.4, H-4), 7.50–7.34 (5H, m, H-10, H-11, H-12), 5.41 (2H, s, H-8); ^{13}C NMR (126 MHz; $CDCl_3$) δ_C 161.4 (d, *J* 3.5, C-7), 154.8 (d, *J* 279.1, C-2), 145.8 (C-6), 139.3 (d, *J* 9.4, C-3), 138.3 (d, *J* 2.1, C-4), 134.8 (C-9), 128.9 (C-11, C-12), 128.6 (C-10), 123.4 (d, *J* 10.7, C-1), 85.5 (d, *J* 5.8, C-5), 68.4 (C-8); ^{19}F NMR (377 MHz; $CDCl_3$) δ_F −117.1 (dd, *J* 6.1, 6.1); HPLC Method 1: Retention time 11.5 min, purity 100.0 %.

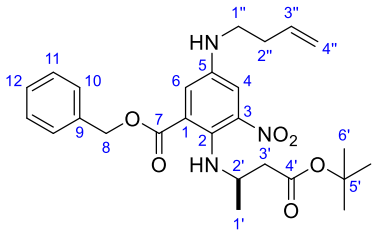
Benzyl (*R*)-2-((4'-(*tert*-butoxy)-4'-oxobutan-2'-yl)amino)-5-iodo-3-nitrobenzoate ((*R*)72)



To a stirred suspension of benzyl 2-fluoro-5-iodo-3-nitrobenzoate (**71**) (2.90 g, 7.23 mmol, 1.0 eq.) and Cs_2CO_3 (9.42 g, 28.9 mmol, 4.0 eq.) in toluene (115 mL) at rt was added *tert*-butyl (*R*)-3-aminobutanoate (**(*R*)41**) containing 2.65 eq. acetic acid (1.35 g, 8.48 mmol, 1.2 eq.) and the suspension was stirred at 85 °C for 21 h. To the cooled suspension was added 1 M aq. K_2CO_3 (200 mL) and the resulting mixture was extracted with EtOAc (3 × 250 mL). The combined organic components were washed with brine (200 mL), dried ($MgSO_4$), filtered, and evaporated *in vacuo* to afford a dark orange oil. The crude oil was purified by silica gel chromatography (elution with 5% to 10% Et_2O in *n*-hexane) to yield benzyl (*R*)-2-((4'-(*tert*-butoxy)-4'-oxobutan-2'-yl)amino)-5-iodo-3-nitrobenzoate (**(*R*)72**) as a dark orange oil (3.82 g, 98%); R_f 0.34 (Et_2O/ *n*-hexane 1:5); $[\alpha]_D^{25}$= +45.8 (*c* 1.0, $CHCl_3$); $\bar{\nu}_{max}$ (neat)/cm^{-1} 3307 (N-H, w), 2978 (C-H, w), 1729 (C=O, m), 1694 (C=O, m), 1526 (N-O, s), 1241 (C-O, s); ^{1}H NMR (500 MHz; $CDCl_3$) δ_H 8.26–8.21 (2H, m, NH-2, H-6), 8.18 (1H, d, *J* 2.3, H-4), 7.50–7.31 (5H, m, H-10, H-11, H-12), 5.34 (2H, s, H-8), 3.58 (1H, dqt, *J* 9.7, 6.4, 6.2, H-2'), 2.37 (2H, d, *J* 6.2, H-3'), 1.35 (9H, s, H-6'), 1.23 (3H, d, *J* 6.4, H-1'); ^{13}C NMR (126 MHz; $CDCl_3$) δ_C 169.9 (C-4'), 166.0 (C-7), 144.7 (C-6), 144.1 (C-2), 139.1 (C-3), 139.0 (C-4), 135.2 (C-9), 128.90 (C-11), 128.86 (C-12), 128.7 (C-10), 120.1 (C-1), 81.2 (C-5'), 73.9 (C-5), 67.7 (C-8), 50.0 (C-2'), 43.5 (C-3'), 28.0 (C-6'), 20.9 (C-1'); HRMS *m/z* (ESI$^-$) [Found: 539.0684,

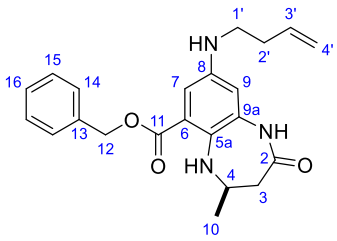
$C_{22}H_{24}{}^{127}IN_2O_6$ requires M^- 539.0685]; LRMS *m/z* (ESI^-) 539 ($[M-H]^-$, 100%); HPLC Method 1: Retention time 13.6 min, purity 100.0%.

Benzyl (*R*)-5-(but-3''-en-1''-ylamino)-2-((4'-(tert-butoxy)-4'-oxobutan-2'-yl)amino)-3-nitrobenzoate ((*R*)74)



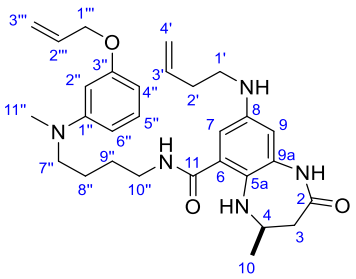
A solution of benzyl (*R*)-2-((4'-(*tert*-butoxy)-4'-oxobutan-2'-yl)amino)-5-iodo-3-nitrobenzoate (**(*R*)72**) (1.05 g, 1.94 mmol, 1.0 eq.) in DMF (5.3 mL) was added to copper(I) iodide (37.0 mg, 0.194 mmol, 0.1 eq.) and Cs_2CO_3 (1.26 g, 3.87 mmol, 2.0 eq.) at rt under a nitrogen atmosphere (evacuated and backfilled 3 × nitrogen). 2-Isobutyrylcyclohexan-1-one (131 µL, 0.776 mmol, 0.4 eq.) was added, followed by but-3-en-1-amine (530 µL, 5.83 mmol, 3.0 eq.) and the suspension was stirred at rt under a nitrogen atmosphere for 17 h. To the suspension was added 1 M aq. K_2CO_3 (250 mL) and the resulting mixture was extracted with EtOAc (3 × 150 mL). The combined organic components were washed with 0.5 M aq. LiCl (3 × 100 mL), brine (200 mL), dried ($MgSO_4$), filtered, and evaporated *in vacuo* to afford a red oil. The crude oil was purified by silica gel chromatography (elution with 5% to 15% EtOAc in petroleum ether) to afford a red oil. The red oil was further purified by silica gel chromatography (elution with 2% Et_2O in toluene) to yield benzyl (*R*)-5-(but-3''-en-1''-ylamino)-2-((4'-(*tert*-butoxy)-4'-oxobutan-2'-yl)amino)-3-nitrobenzoate (**(*R*)74**) as a red oil (565 mg, 60%); R_f 0.60 (Et_2O/toluene 1:19); $\bar{\nu}_{max}$ (neat)/cm^{-1} 3397 (N-H, w), 2977 (C-H, w), 1722 (C=O, s), 1532 (N-O, s), 1230 (C-O, s); ^1H NMR (500 MHz; CD_3CN) δ_H 7.50–7.34 (5H, m, H-10, H-11, H-12), 7.37 (1H, d, *J* 3.0, H-6), 7.21 (1H, d, *J* 3.0, H-4), 6.79 (1H, d, *J* 10.3, NH-2), 5.85 (1H, ddt, *J* 17.2, 10.3, 6.8, H-3''), 5.33 (1H, s, H_AH_B-8), 5.32 (1H, s, H_AH_B-8), 5.10 (1H, ddt, *J* 17.2, 1.7, 1.7, H_AH_B-4''), 5.05 (1H, ddt, *J* 10.3, 2.2, 1.2, H_AH_B-4''), 4.43 (1H, t, *J* 5.6, NH-5), 3.45–3.35 (1H, m, H-2'), 3.10 (2H, td, *J* 6.8, 5.6, H-1''), 2.33–2.27 (2H, m, H-2''), 2.25 (2H, dd, *J* 6.2, 5.0, H-3'), 1.30 (9H, s, H-6'), 1.09 (3H, d, *J* 6.5, H-1'); ^{13}C NMR (126 MHz; CD_3CN) δ_C 171.3 (C-4'), 167.9 (C-7), 142.0 (C-3), 141.6 (C-1), 136.89 (C-3''), 136.87 (C-9), 136.1 (C-2), 129.6 (C-11), 129.3 (C-12), 129.2 (C-10), 123.5 (C-5), 122.7 (C-6), 117.1 (C-4''), 112.7 (C-4), 81.1 (C-5'), 68.0 (C-8), 52.2 (C-2'), 44.4 (C-3'), 44.0 (C-1''), 33.9 (C-2''), 28.1 (C-6'), 21.2 (C-1'); HRMS *m/z* (ESI^+) [Found: 484.2440, $C_{26}H_{34}N_3O_6$ requires M^+ 484.2442]; LRMS *m/z* (ESI^+) 484 ($[M+H]^+$, 38%); HPLC Method 1: Retention time 12.9 min, purity 98.0%.

Benzyl (*R*)-8-(but-3'-en-1'-ylamino)-4-methyl-2-oxo-2,3,4,5-tetrahydro-1*H*-benzo[*b*][1,4]diazepine-6-carboxylate ((*R*)63)



To a solution of benzyl (*R*)-5-(but-3''-en-1''-ylamino)-2-((4'-(*tert*-butoxy)-4'-oxobutan-2'-yl)amino)-3-nitrobenzoate (**(*R*)74**) (491 mg, 1.02 mmol, 1.0 eq.) in CH_2Cl_2 (5 mL) was added trifluoroacetic acid (5 mL) and the red solution was stirred at rt for 2 h. The reaction mixture was evaporated *in vacuo* and the resulting residue was dissolved in DMF (12 mL). Zinc dust (1.64 g, 25.5 mmol, 25.0 eq.) and NH_4Cl (1.36 g, 25.5 mmol 25.0 eq.) were added and the brown suspension was stirred at rt for 19 h. The suspension was filtered through Celite® and washed with DMF (5 mL). The filtrate was adjusted to pH 9 with *N*,*N*-diisopropylethylamine (5.5 mL). Benzotriazol-1-yl-oxytripyrrolidinophosphonium hexafluorophosphate (530 mg, 1.02 mmol, 1.0 eq.) was added to the filtrate and the brown suspension was stirred at rt for 24 h. To the suspension was added 1 M aq. K_2CO_3 (300 mL) and the resulting mixture was extracted with EtOAc (3 × 100 mL). The combined organic components were washed with 0.5 M aq. LiCl (3 × 100 mL), brine (150 mL), dried ($MgSO_4$), filtered, and evaporated *in vacuo* to afford a brown oil. The crude oil was purified by silica gel chromatography (elution with 40% to 70% EtOAc in petroleum ether) to afford benzyl (*R*)-8-(but-3'-en-1'-ylamino)-4-methyl-2-oxo-2,3,4,5-tetrahydro-1*H*-benzo[*b*][1,4]diazepine-6-carboxylate (**(*R*)63**) as an orange solid (289 mg, 75%); R_f 0.15 (EtOAc/petroleum ether 2:3); $[\alpha]_D^{25}$= −23.6 (*c* 1.3, MeOH); mp 104–106 °C (EtOAc); $\bar{\nu}_{max}$ (neat)/cm^{-1} 3323 (N-H, w), 2921 (C-H, w), 1661 (C=O, s), 1221 (C-O, s); ^{1}H NMR (500 MHz; CD_3CN) δ_H 7.77 (1H, br s, NH-9a), 7.50–7.30 (5H, m, H-14, H-15, H-16), 7.04 (1H, d, *J* 2.8, H-7), 6.49 (1H, d, *J* 2.8, H-9), 6.23 (1H, br s, NH-5a), 5.86 (1H, ddt, *J* 17.1, 10.2, 6.9, H-3'), 5.31 (1H, s, H_AH_B-12), 5.30 (1H, s, H_AH_B-12), 5.10 (1H, ddt, *J* 17.1, 1.7, 1.7, H_AH_B-4'), 5.04 (1H, ddt, *J* 10.2, 2.1, 1.1, H_AH_B-4'), 4.23 (1H, br s, NH-8), 3.95–3.86 (1H, m, H-4), 3.07 (2H, t, *J* 6.9, H-1'), 2.45 (1H, dd, *J* 13.2, 5.2, H_AH_B-3), 2.31 (2H, dddt, *J* 6.9, 6.9, 1.4, 1.4, H-2'), 2.18 (1H, dd, *J* 13.2, 7.1, H_AH_B-3), 1.15 (3H, d, *J* 6.3, H-10); ^{13}C NMR (126 MHz; CD_3CN) δ_C 173.1 (C-2), 168.9 (C-11), 143.4 (C-8), 137.4 (C-13), 137.1 (C-3'), 134.4 (C-5a), 133.8 (C-9a), 129.5 (C-15), 129.1 (C-16), 128.9 (C-14), 120.9 (C-6), 116.9 (C-4'), 112.6 (C-9), 111.7 (C-7), 67.3 (C-12), 56.3 (C-4), 44.1 (C-1'), 41.2 (C-3), 34.1 (C-2'), 23.5 (C-10); HRMS *m/z* (ESI$^+$) [Found: 380.1964, $C_{22}H_{26}N_3O_3$ requires M^+ 380.1969]; LRMS *m/z* (ESI$^+$) 380 ([M+H]$^+$, 100%); HPLC Method 1: Retention time 10.1 min, purity 100.0%.

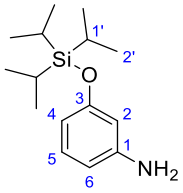
(*R*)-*N*-(4-((3-(Allyloxy)phenyl)(methyl)amino)butyl)-8-(but-3-en-1-ylamino)-4-methyl-2-oxo-2,3,4,5-tetrahydro-1*H*-benzo[*b*][1,4]diazepine-6-carboxamide ((*R*)75)



To a stirred solution of benzyl (*R*)-8-(but-3'-en-1'-ylamino)-4-methyl-2-oxo-2,3,4,5-tetrahydro-1*H*-benzo[*b*][1,4]diazepine-6-carboxylate (**(*R*)63**) (0.096 g, 0.25 mmol, 1.0 eq.) in THF/MeOH/H_2O (3:2:1, 2.5 mL) was added LiOH (0.061 g, 2.5 mmol, 10.0 eq.) and the reaction mixture was stirred at rt for 5 h. The reaction mixture was neutralised to pH 7 with 1 M aq. HCl (2.5 mL) and evaporated *in vacuo* and the resulting residue was lyophilised to afford a red solid. The red solid was dissolved in DMF (2 mL) and triethylamine (0.71 ml, 0.51 mmol, 2.0 eq.). Benzotriazol-1-yl-oxytripyrrolidinophosphonium hexafluorophosphate (0.13 g, 0.25 mmol, 1.0 eq.) was added to the solution and the reaction mixture was stirred at rt for 15 min. N^1-(3-(Allyloxy)phenyl)-N^1-methylbutane-1,4-diamine (**61**) (0.075 g, 0.32 mmol, 1.3 eq.) in DMF (1.9 mL) was added and the reaction mixture was stirred at rt for 24 h. The reaction mixture was diluted with EtOAc (30 mL) and washed with 1 M aq. K_2CO_3 (3 × 15 mL). The organic component was washed with 0.5 M aq. LiCl (3 × 10 mL), brine (10 mL), dried ($MgSO_4$), filtered, and evaporated *in vacuo* to afford a brown oil. The crude oil was purified by silica gel chromatography (elution with 80% to 100% EtOAc in petroleum ether) to yield (*R*)-*N*-(4-((3-(allyloxy)phenyl)(methyl)amino)butyl)-8-(but-3-en-1-ylamino)-4-methyl-2-oxo-2,3,4,5-tetrahydro-1*H*-benzo[*b*][1,4]diazepine-6-carboxamide (**(*R*)75**) as a yellow oil (82 mg, 64%); R_f 0.20 (EtOAc); $[\alpha]_D^{25}$= −8.2 (*c* 1.0, CH_2Cl_2); $\bar{\nu}_{max}$ (neat)/cm^{-1} 3323 (N-H, w), 2977 (C-H, w), 1668 (C=O, m), 1607 (C=C, s); ^{1}H NMR (500 MHz; CD_2Cl_2) δ_H 7.51 (1H, s, NH-9a), 7.45 (1H, t, *J* 6.2, NH-11), 7.11 (1H, dd, *J* 8.1, 8.1, H-5''), 6.73 (1H, d, *J* 2.7, H-7), 6.37–6.32 (2H, m, H-9, H-6''), 6.28–6.23 (2H, m, H-2'', H-4''), 6.09 (1H, ddt, *J* 17.3, 10.5, 5.3, H-2'''), 5.87 (1H, ddt, *J* 17.3, 10.2, 6.8, H-3'), 5.43 (1H, ddt, *J* 17.3, 3.2, 1.7, H_AH_B-3'''), 5.29 (1H, ddt, *J* 10.5, 3.2, 1.7, H_AH_B-3'''), 5.19 (1H, ddt, *J* 17.3, 3.6, 1.4, H_AH_B-4'), 5.15 (1H, ddt, *J* 10.2, 2.2, 1.4, H_AH_B-4'), 5.08 (1H, s, NH-5a), 4.53 (2H, dt, *J* 5.3, 1.5, H-1'''), 3.91–3.83 (1H, m, H-4), 3.75 (1H, s, NH-8), 3.51–3.30 (4H, m, H-7'', H-10''), 3.17 (2H, t, *J* 6.8, H-1'), 2.94 (3H, s, H-11''), 2.52 (1H, dd, *J* 13.0, 5.7, H_AH_B-3), 2.40 (2H, ddt, *J* 13.6, 6.8, 1.4, H-2'), 2.23 (1H, dd, *J* 13.0, 7.0, H_AH_B-3), 1.72–1.59 (4H, m, H-8'', H-9''), 1.21 (3H, d, *J* 6.3, H-10); ^{13}C NMR (126 MHz; CD_2Cl_2) δ_C 173.0 (C-2), 168.6 (C-11), 160.2 (C-3''), 151.1 (C-1''), 144.4 (C-5a), 136.1 (C-3'), 135.3 (C-8), 134.3 (C-2'''), 130.1 (C-5''), 129.5

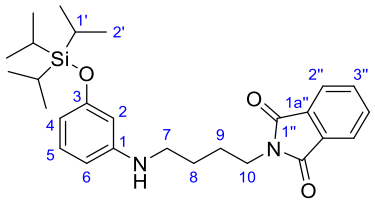
(C-6), 129.4 (C-9a), 117.32 (C-4'), 117.27 (C-3'''), 109.6 (C-7), 108.9 (C-9), 105.8 (C-2''), 101.9 (C-4''), 99.7 (C-6''), 69.0 (C-1'''), 56.2 (C-4), 52.7 (C-7''), 43.5 (C-1'), 41.0 (C-3), 39.9 (C-10''), 38.7 (C-11''), 33.9 (C-2'), 27.7 (C-9''), 24.7 (C-8''), 22.7 (C-10); HRMS *m/z* (ESI$^+$) [Found: 506.3124, $C_{29}H_{40}N_5O_3$ requires M^+ 506.3126]; LRMS *m/z* (ESI$^+$) 506 ([M+H]$^+$, 100%); HPLC Method 1: Retention time 10.2 min, purity 95.6%.

3-((Triisopropylsilyl)oxy)aniline (81)



Triisopropylsilyl chloride (2.60 mL, 11.9 mmol, 1.3 eq.) was added to a solution of 3-aminophenol (**80**) (1.00 g, 9.16 mmol, 1.0 eq.) and imidazole (1.25 g, 18.3 mmol, 2.0 eq.) in THF (8 mL) and the reaction mixture was stirred at rt for 21 h. The reaction mixture was evaporated *in vacuo* and the resulting colourless solid was dissolved in Et_2O (100 mL) and washed with H_2O (3 × 150 mL). The organic component was washed with brine (100 mL), dried ($MgSO_4$), filtered, and evaporated *in vacuo* to afford a brown oil. The crude oil was purified by silica gel chromatography (elution with 0% to 10% EtOAc in petroleum ether) to afford 3-((triisopropylsilyl)oxy)aniline (**81**) as an orange oil (2.40 g, 99%); R_f 0.19 (EtOAc/petroleum ether 1:4); ^{1}H NMR (400 MHz; $CDCl_3$) δ_H 6.98 (1H, dd, *J* 7.9, 7.9, H-5), 6.32–6.26 (2H, m, H-4, H-6), 6.24 (1H, dd, *J* 2.2, 2.2, H-2), 3.57 (2H, br s, NH-1), 1.33–1.19 (3H, m, H-1'), 1.10 (18H, d, *J* 7.3, H-2'); LRMS *m/z* (ESI$^+$) 266 ([M+H]$^+$, 100%). These data are in accordance with the literature.[82]

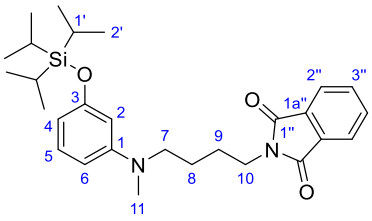
2-(4-((3-((Triisopropylsilyl)oxy)phenyl)amino)butyl)isoindoline-1,3-dione (82)



N-(4-Bromobutyl)phthalimide (2.16 g, 7.64 mmol, 1.2 eq.) was added to a suspension of 3-((triisopropylsilyl)oxy)aniline (**81**) (1.69 g, 6.37 mmol, 1.0 eq.) and K_2CO_3 (1.06 g, 7.64 mmol, 1.2 eq.)

in DMF (2 mL) and the reaction mixture was stirred at 80 °C for 24 h. The cooled suspension was diluted with EtOAc (250 mL) and washed with 1 M aq. K_2CO_3 (3 × 150 mL). The organic component was washed with 0.5 M aq. LiCl (3 × 100 mL), brine (100 mL), dried (Na_2SO_4), filtered, and evaporated *in vacuo* to afford brown oil. The crude oil was purified by silica gel chromatography (elution with 20% EtOAc in petroleum ether) to yield 2-(4-((3-((triisopropylsilyl)oxy) phenyl)amino)butyl)isoindoline-1,3-dione (**82**) as a yellow solid (1.98 g, 67%); R_f 0.28 (EtOAc/petroleum ether 1:4); $\bar{\nu}_{max}$ (neat)/cm^{-1} 3400 (N-H, w), 2943 (C-H, w), 1708 (C=O, s); ^{1}H NMR (500 MHz; $CDCl_3$) δ_H 7.84 (2H, dd, *J* 5.5, 3.0, H-2''), 7.71 (2H, dd, *J* 5.5, 3.0, H-3''), 6.97 (1H, dd, *J* 8.0, 8.0, H-5), 6.22 (1H, ddd, *J* 8.0, 2.3, 0.9, H-4), 6.19 (1H, ddd, *J* 8.0, 2.3, 0.9, H-6), 6.14 (1H, dd, *J* 2.3, 2.3, H-2), 3.73 (2H, t, *J* 7.1, H-10), 3.64 (1H, br s, NH-1), 3.12 (2H, t, *J* 7.0, H-7), 1.86–1.76 (2H, m, H-9), 1.69–1.62 (2H, m, H-8), 1.29–1.18 (3H, m, H-1'), 1.09 (18H, d, *J* 7.4, H-2'); ^{13}C NMR (126 MHz; $CDCl_3$) δ_C 168.6 (C-1''), 157.2 (C-3), 149.7 (C-1), 134.1 (C-3''), 132.2 (C-1a''), 129.8 (C-5), 123.4 (C-2''), 109.2 (C-4), 106.2 (C-6), 104.6 (C-2), 43.7 (C-7), 37.9 (C-10), 26.9 (C-8), 26.5 (C-9), 18.1 (C-2'), 12.8 (C-1'); HRMS *m/z* (ESI^+) [Found: 467.2721, $C_{27}H_{39}N_2O_3{}^{28}Si$ requires M^+ 467.2725]; LRMS *m/z* (ESI^+) 467 ($[M+H]^+$, 100%); HPLC Method 1: Retention time 15.8 min, purity 96.8%. (Gradient method of 10 min from 95:5 H_2O:MeCN to 5:95 H_2O:MeCN with a 10 min hold).

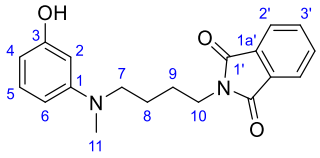
2-(4-(Methyl(3-((triisopropylsilyl)oxy)phenyl)amino)butyl)isoindoline-1,3-dione (83)



To a suspension of 2-(4-((3-((triisopropylsilyl)oxy)phenyl)amino)butyl)isoindoline-1,3-dione (**82**) (1.90 g, 4.07 mmol, 1.0 eq.) and K_2CO_3 (675 mg, 4.88 mmol, 1.2 eq.) in DMF (14 mL) was added iodomethane (279 µL, 4.48 mmol, 1.1 eq.). The reaction mixture was stirred at 85 °C for 6 h. To the cooled suspension was added 1 M aq. K_2CO_3 (3 × 150 mL) and the resulting mixture was extracted with EtOAc (250 mL). The organic component was washed with 0.5 M aq. LiCl (3 × 100 mL), brine (150 mL), dried ($MgSO_4$), filtered, and evaporated *in vacuo* to afford a yellow oil. The crude oil was purified by silica gel chromatography (elution with 10% EtOAc in petroleum ether) to yield 2-(4-(methyl(3-((triisopropylsilyl)oxy)phenyl)amino)butyl)isoindoline-1,3-dione (**83**) as a yellow oil (1.17 g, 60%); R_f 0.20 (EtOAc/petroleum ether 1:9); $\bar{\nu}_{max}$ (neat)/cm^{-1} 2943 (C-H, w), 1705 (C=O, s); ^{1}H NMR (500 MHz; $CDCl_3$) δ_H 7.84 (2H, dd, *J* 5.4, 3.0, H-2''), 7.71 (2H, dd, *J* 5.4, 3.0, H-3''), 7.02 (1H, dd, *J* 8.2, 8.2, H-5), 6.27 (1H, d, *J* 8.2 H-6), 6.23–6.20 (2H, m, H-2, H-4), 3.70 (2H, t, *J* 7.1. H-10), 3.31 (2H, t, *J* 7.2, H-7), 2.88 (3H,

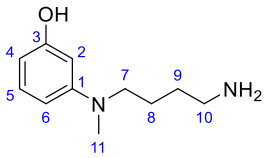
s, H-11), 1.70 (2H, m, H-9), 1.62 (2H, m, H-8), 1.32–1.19 (3H, m, H-1'), 1.09 (18H, d, *J* 7.3, H-2'); ^{13}C NMR (126 MHz; $CDCl_3$) δ_C 168.5 (C-1''), 157.2 (C-3), 150.7 (C-1), 134.1 (C-3''), 132.3 (C-1a''), 129.7 (C-5), 123.4 (C-2''), 108.1 (C-4), 105.6 (C-6), 104.3 (C-2), 52.5 (C-7), 38.5 (C-11), 37.9 (C-10), 26.4 (C-9), 24.3 (C-8), 18.1 (C-2'), 12.9 (C-1'); HRMS *m/z* (ESI$^+$) [Found: 481.2878, $C_{28}H_{41}N_2O_3{}^{28}Si$ requires M^+ 481.2881]; LRMS *m/z* (ESI$^+$) 481 ([M+H]$^+$, 100%).

2-(4-((3-Hydroxyphenyl)(methyl)amino)butyl)isoindoline-1,3-dione (84)



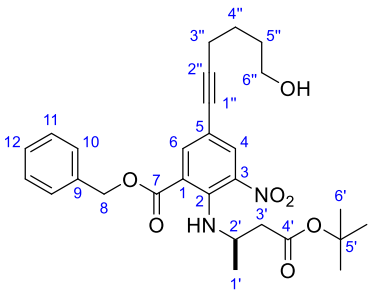
To a solution of 2-(4-(methyl(3-((triisopropylsilyl)oxy)phenyl)amino) butyl)isoindoline-1,3-dione (**83**) (460 mg, 0.957 mmol, 1.0 eq.) in EtOH (2 mL) and CH_2Cl_2 (1 mL) was added 2 M aq. HCl (3.5 mL) and the reaction mixture was stirred at 80 °C for 17 h. The cooled reaction mixture was evaporated *in vacuo* to afford a yellow residue. Sat. aq. $NaHCO_3$ (150 mL) was added to the residue and the resulting mixture extracted with EtOAc (3 × 100 mL). The combined organic components were washed with brine (100 mL), dried ($MgSO_4$), filtered, and evaporated *in vacuo* to afford a dark yellow oil. The crude oil was triturated with *n*-hexane (50 mL) to yield 2-(4-((3-hydroxyphenyl)(methyl)amino)butyl)isoindoline-1,3-dione (**84**) as an orange solid (280 mg, 90%); R_f 0.75 (EtOAc); mp 113–116 °C (EtOAc); $\bar{\nu}_{max}$ (neat)/cm^{-1} 3220 (O-H, w), 2940 (C-H, w), 1689 (C=O, s); ^{1}H NMR (500 MHz; $CDCl_3$) δ_H 7.86–7.81 (2H, m, H-2'), 7.75–7.67 (2H, m, H-3'), 7.05 (1H, dd, *J* 7.9, 7.9 H-5), 6.26–6.22 (2H, m, H-2, H-6), 6.17 (1H, dd, *J* 7.9, 2.2, H-4), 5.18 (1H, br s, OH-3), 3.74 (2H, t, *J* 7.1, H-10), 3.33 (2H, t, *J* 7.4, H-7), 2.89 (3H, s, H-11), 1.79–1.70 (2H, m, H-9), 1.67–1.56 (2H, m, H-8); ^{13}C NMR (126 MHz; $CDCl_3$) δ_C 168.8 (C-1'), 157.0 (C-3), 150.8 (C-1), 134.2 (C-3'), 132.1 (C-1a'), 130.2 (C-5), 123.4 (C-2'), 104.9 (C-2), 103.3 (C-4), 99.3 (C-6), 52.2 (C-7), 38.4 (C-11), 37.7 (C-10), 26.0 (C-9), 23.8 (C-8); HRMS *m/z* (ESI$^+$) [Found: 325.1454, $C_{19}H_{21}N_2O_3$ requires M^+ 325.1457]; LRMS *m/z* (ESI$^+$) 323 ([M+H]$^+$, 100%); HPLC Method 1: Retention time 9.6 min, purity 98.4%.

3-((4-Aminobutyl)(methyl)amino)phenol (78)



Hydrazine monohydrate (65%, 161 µL, 2.32 mmol, 4.0 eq.) was added to a stirred solution of 2-(4-((3-hydroxyphenyl)(methyl)amino)butyl)isoindoline-1,3-dione (**84**) (269 mg, 0.829 mmol, 1.0 eq.) in CH_2Cl_2 (1.3 mL) and MeOH (1.3 mL) and the reaction mixture was stirred at 70 °C for 4.5 h. The cooled reaction mixture was diluted in CH_2Cl_2 (15 mL), filtered through Celite® (eluent MeOH) and evaporated *in vacuo* to yield a colourless solid. The solid was dissolved in $CHCl_3$/IPA (9:1, 30 mL) and washed with H_2O (3 × 20 mL). The organic component was washed with brine, dried (Na_2SO_4), filtered, and evaporated *in vacuo* to yield 3-((4-aminobutyl)(methyl)amino)phenol (**78**) as a brown oil (90 mg, 56%) and was used without further purification; R_f 0.00 (EtOAc); ^{1}H NMR (500 MHz; CD_3OD) δ_H 7.05–6.87 (1H, m, H-5), 6.23 (1H, ddd, *J* 8.3, 2.1, 2.1, H-6), 6.19–6.17 (1H, m, H-2), 6.11 (1H, ddd, *J* 7.7, 2.1, 2.1, H-4), 3.31 (2H, t, *J* 7.5, H-7), 2.88 (3H, s, H-11), 2.66 (2H, t, *J* 7.2, H-10), 1.65–1.56 (2H, m, H-8), 1.54–1.44 (2H, m, H-9); ^{13}C NMR (126 MHz; CD_3OD) δ_C 159.3 (C-3), 152.3 (C-1), 130.7 (C-5), 105.6 (C-6), 104.6 (C-4), 100.8 (C-2), 53.6 (C-7), 42.4 (C-10), 38.7 (C-11), 31.1 (C-9), 25.2 (C-8); LRMS *m/z* (ESI$^+$) 195 ([M+H]$^+$, 100%).

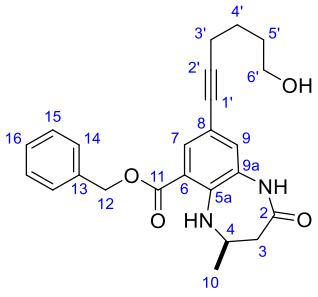
Benzyl (*R*)-2-((4-(*tert*-butoxy)-4-oxobutan-2-yl)amino)-5-(6-hydroxyhex-1-yn-1-yl)-3-nitrobenzoate ((*R*)85)



A solution of benzyl (*R*)-2-((4'-(*tert*-butoxy)-4'-oxobutan-2'-yl)amino)-5-iodo-3-nitrobenzoate (**(*R*)72**) (1.00 g, 1.85 mmol, 1.0 eq.) in THF (5 mL) was added to bis(triphenylphosphine)palladium(II) dichloride (26 mg, 0.037 mmol, 0.02 eq.) and copper(I) iodide (11 mg, 0.056 mmol, 0.03 eq.) at rt under an argon

atmosphere (evacuated and backfilled 3 × argon). Triethylamine (3 mL) was added, followed by 5-hexyn-1-ol (245 µL, 2.22 mmol, 1.2 eq.) and the suspension was stirred at rt under an argon atmosphere for 5 h. The reaction mixture was evaporated *in vacuo* to afford an orange oil. The oil was diluted with EtOAc (250 mL) and washed with sat. aq. $NaHCO_3$ (3 × 100 mL). The organic component was washed with brine (200 mL), dried ($MgSO_4$), filtered, and evaporated *in vacuo* to afford an orange oil. The crude oil was purified by silica gel chromatography (elution with 0% to 50% EtOAc in petroleum ether) to yield benzyl (*R*)-2-((4-(*tert*-butoxy)-4-oxobutan-2-yl)amino)-5-(6-hydroxyhex-1-yn-1-yl)-3-nitrobenzoate (**(*R*)85**) as an orange oil (931 mg, 90%); R_f 0.40 (EtOAc/petroleum ether 1:1); $[\alpha]_D^{25}$= +74.2 (*c* 1.0, MeOH); $\bar{\nu}_{max}$ (neat)/cm^{-1} 3310 (N-H, w), 2940 (C-H, w), 1703 (C=O, s), 1530 (N-O, s), 1229 (C-O, s); ^{1}H NMR (500 MHz; $CDCl_3$) δ_H 8.31 (1H, d, *J* 9.7, NH-2), 8.02 (1H, d, *J* 2.2, H-6), 7.94 (1H, d, *J* 2.2, H-4), 7.50–7.33 (5H, m, H-10, H-11, H-12), 5.34 (2H, s, H-8), 3.70 (2H, t, *J* 6.1, H-6''), 3.61 (1H, m, H-2'), 2.41 (2H, t, *J* 6.7, H-3''), 2.38 (2H, d, *J* 6.1, H-3'), 1.76–1.62 (4H, m, H-4'', H-5''), 1.58 (1H, s, OH-6''), 1.34 (9H, s, H-6'), 1.24 (3H, d, *J* 6.4, H-1'); ^{13}C NMR (126 MHz; $CDCl_3$) δ_C 170.0 (C-7), 166.7 (C-4'), 143.6 (C-2), 139.5 (C-6), 138.0 (C-3), 135.3 (C-9), 133.9 (C-4), 128.9 (C-12), 128.8 (C-11), 128.7 (C-10), 118.1 (C-1), 111.4 (C-5), 90.1 (C-2''), 81.2 (C-5'), 78.4 (C-1''), 67.5 (C-8), 62.6 (C-6''), 50.0 (C-2'), 43.6 (C-3'), 32.0 (C-5''), 28.0 (C-6'), 25.0 (C-4''), 21.0 (C-1'), 19.3 (C-3''); HRMS *m/z* (ESI$^+$) [Found: 511.2446, $C_{27}H_{33}N_2O_7$ requires M^+ 511.2444]; LRMS *m/z* (ESI$^+$) 455 ([M-^{t}Bu]$^+$, 100%); HPLC Method 1: Retention time 12.4 min, purity 100.0%.

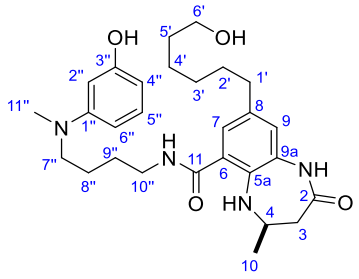
Benzyl (*R*)-8-(6-hydroxyhex-1-yn-1-yl)-4-methyl-2-oxo-2,3,4,5-tetrahydro-1*H*-benzo[*b*][1,4]diazepine-6-carboxylate ((*R*)79)



To a solution of benzyl (*R*)-2-((4-(*tert*-butoxy)-4-oxobutan-2-yl)amino)-5-(6-hydroxyhex-1-yn-1-yl)-3-nitrobenzoate (**(*R*)85**) (860 mg, 1.68 mmol 1.0 eq.) in CH_2Cl_2 (8 mL) was added trifluoroacetic acid (8 mL) and the orange solution was stirred at rt for 2 h. The reaction mixture was evaporated *in vacuo* and the resulting residue was dissolved in DMF (20 mL). Zinc dust (2.75 g, 42.0 mmol, 25.0 eq.) and NH_4Cl (2.25 g, 42.0 mmol, 25.0 eq.) were added and the resulting yellow suspension was stirred at rt for 20 h. The suspension was filtered through Celite® and washed with DMF (10 mL). The filtrate was

adjusted to pH 9 with *N*,*N*-diisopropylethylamine (14 mL). Benzotriazol-1-yl-oxytripyrrolidinophosphonium hexafluorophosphate (875 mg, 1.68 mmol, 1.0 eq.) was added to the filtrate and the brown suspension was stirred at rt for 24 h. To the suspension was added 1 M aq. K_2CO_3 (600 mL) and the resulting mixture was extracted with EtOAc (3 × 250 mL). The combined organic components were washed with 0.5 M aq. LiCl (3 × 150 mL), brine (300 mL), dried ($MgSO_4$), filtered, and evaporated *in vacuo* to afford a brown oil. The crude oil was purified by silica gel chromatography (elution with 50% to 100% EtOAc in petroleum ether) to afford benzyl (*R*)-8-(6-hydroxyhex-1-yn-1-yl)-4-methyl-2-oxo-2,3,4,5-tetrahydro-1*H*-benzo[*b*][1,4]diazepine-6-carboxylate (**(*R*)79**) as an off-white solid (205 mg, 30%); R_f 0.29 (EtOAc); $[\alpha]_D^{25}$ = −15.3 (*c* 1.0, MeOH); mp 119–122 °C (EtOAc); $\bar{\nu}_{max}$ (neat)/cm^{-1} 3309 (N-H, w), 2930 (C-H, w), 1662 (C=O, s), 1215 (C-O, s); ^{1}H NMR (500 MHz; $CDCl_3$) δ_H 8.21 (1H, d, *J* 2.6, NH-5a), 7.86 (1H, d, *J* 2.0, H-7), 7.74 (1H, s, NH-9a), 7.48–7.31 (5H, m, H-14, H-15, H-16), 7.00 (1H, d, *J* 2.0, H-9), 5.31 (2H, s, H-12), 4.10–3.98 (1H, m, H-4), 3.76–3.65 (2H, m, H-6'), 2.66 (1H, d, *J* 14.0, H_AH_B-3), 2.59 (1H, dd, *J* 14.0, 8.4, H_AH_B-3), 2.41 (2H, t, *J* 6.8, H-3'), 1.77–1.58 (4H, m, H-4', H-5'), 1.42 (1H, s, OH-6'), 1.39 (3H, d, *J* 6.4, H-10); ^{13}C NMR (126 MHz; $CDCl_3$) δ_C 172.6 (C-2), 168.0 (C-11), 142.5 (C-5a), 135.8 (C-13), 132.0 (C-7), 129.8 (C-9), 128.8 (C-16), 128.6 (C-15), 128.4 (C-14), 125.4 (C-9a), 114.3 (C-6), 112.0 (C-8), 88.9 (C-2'), 79.6 (C-1'), 66.9 (C-12), 62.6 (C-6'), 51.0 (C-4), 42.6 (C-3), 32.1 (C-5'), 25.1 (C-4'), 24.0 (C-10), 19.3 (C-3'); HRMS *m/z* (ESI$^+$) [Found: 407.1970, $C_{24}H_{27}N_2O_4$ requires M^+ 407.1965]; LRMS *m/z* (ESI$^+$) 407 ([M+H]$^+$, 100%); HPLC Method 1: Retention time 9.8 min, purity 97.8%.

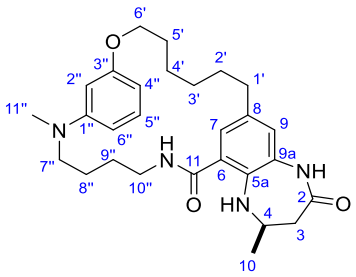
(*R*)-8-(6-Hydroxyhexyl)-*N*-(4-((3-hydroxyphenyl)(methyl)amino)butyl)-4-methyl-2-oxo-2,3,4,5-tetrahydro-1*H*-benzo[*b*][1,4]diazepine-6-carboxamide ((*R*)86)



10% Pd/C (52 mg, 0.049 mmol, 0.1 eq.) was added to a stirred solution of benzyl (*R*)-8-(6-hydroxyhex-1-yn-1-yl)-4-methyl-2-oxo-2,3,4,5-tetrahydro-1*H*-benzo[*b*][1,4]diazepine-6-carboxylate (**(*R*)79**) (200 mg, 0.492 mmol, 1.0 eq.) in EtOAc (3 mL) and MeOH (3 mL), which was purged under a nitrogen atmosphere. The atmosphere was replaced with hydrogen gas and the suspension was stirred at rt for 20 h. The black suspension was filtered through Celite® (eluent MeOH) and evaporated *in vacuo* to

afford a green oil. The oil was dissolved in DMF (4 mL) and triethylamine (137 µl, 0.984 mmol, 2.0 eq.). Benzotriazol-1-yl-oxytripyrrolidinophosphonium hexafluorophosphate (256 mg, 0.491 mmol, 1.0 eq.) was added to the solution and the reaction mixture was stirred at rt for 15 min. 3-((4-Aminobutyl)(methyl)amino)phenol (**78**) (124 mg, 0.640 mmol, 1.3 eq.) in DMF (5.5 mL) was added and the reaction mixture was stirred at rt for 21 h. The reaction mixture was diluted with EtOAc (30 mL) and washed with H_2O (3 × 15 mL). The organic component was washed with 0.5 M aq. LiCl (3 × 15 mL), brine (20 mL), dried ($MgSO_4$), filtered, and evaporated *in vacuo* to afford a brown oil. The crude oil was purified by silica gel chromatography (elution with 80% to 100% EtOAc in petroleum ether) to afford (*R*)-8-(6-hydroxyhexyl)-*N*-(4-((3-hydroxyphenyl)(methyl)amino)butyl)-4-methyl-2-oxo-2,3,4,5-tetrahydro-1*H*-benzo[*b*][1,4]diazepine-6-carboxamide (**(*R*)86**) as an green oil (174 mg, 71%); R_f 0.11 (EtOAc); $[\alpha]_D^{25}$= −10.3 (*c* 1.0, MeOH); $\bar{\nu}_{max}$ (thin film)/cm^{-1} 3306 (O-H, br s), 2926 (C-H, w), 1662 (C=O, s); ^{1}H NMR (500 MHz; CD_3OD) δ_H 7.13 (1H, d, *J* 2.0, H-7), 6.95 (1H, dd, *J* 8.2, 8.2, H-5''), 6.92 (1H, d, *J* 2.0, H-9), 6.24 (1H, dd, *J* 8.2, 2.3, H-6''), 6.18 (1H, dd, *J* 2.3, 2.3, H-2''), 6.10 (1H, dd, *J* 8.0, 2.3, H-4''), 3.97–3.89 (1H, m, H-4), 3.54 (2H, t, *J* 6.5, H-10''), 3.40–3.30 (4H, m, H-6', H-7''), 2.89 (3H, s, H-11''), 2.56 (2H, t, *J* 7.7, H-1'), 2.48 (1H, dd, *J* 13.3, 4.9, H_AH_B-3), 2.23 (1H, dd, *J* 13.3, 7.5, H_AH_B-3), 1.69–1.57 (6H, m, H-2', H-3', H-5'), 1.57–1.49 (2H, m, H-9''), 1.44–1.32 (4H, m, H-4', H-8''), 1.20 (3H, d, *J* 6.3, H-10); ^{13}C NMR (126 MHz; CD_3OD) δ_C 175.4 (C-2), 171.8 (C-11), 159.2 (C-1''), 152.2 (C-3''), 138.4 (C-5a), 136.6 (C-9a), 132.4 (C-6), 130.8 (C-5''), 127.2 (C-8), 125.8 (C-7), 125.6 (C-9), 105.6 (C-6''), 104.5 (C-4''), 100.7 (C-2''), 62.9 (C-10''), 57.1 (C-4), 53.5 (C-6'), 41.4 (C-3), 40.6 (C-7''), 38.8 (C-11''), 35.9 (C-1'), 32.5 (9''), 30.8 (C-5'), 30.1 (C-2'), 28.1 (C-3'), 26.8 (C-8''), 25.1 (C-4'), 23.7 (C-10); HRMS *m/z* (ESI$^+$) [Found: 497.3120, $C_{28}H_{41}N_4O_4$ requires M^+ 497.3122]; LRMS *m/z* (ESI$^+$) 497 ([M+H]$^+$, 100%); HPLC Method 1: Retention time 8.1 min, purity 99.2%.

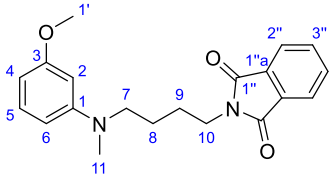
(*R*)-1^4,8-Dimethyl-1^2,1^3,1^4,1^5-tetrahydro-1^1*H*-10-oxa-3,8-diaza-1(6,8)-benzo[*b*][1,4]diazepina-9(1,3)-benzenacyclohexadecaphane-1^2,2-dione ((*R*)77)



To a stirred solution of (*R*)-8-(6-hydroxyhexyl)-*N*-(4-((3-hydroxyphenyl)(methyl)amino)butyl)-4-methyl-2-oxo-2,3,4,5-tetrahydro-1*H*-benzo[*b*][1,4]diazepine-6-carboxamide (**(*R*)86**) (36 mg,

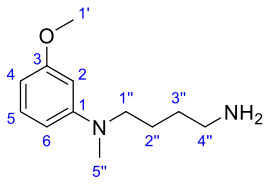
0.073 mmol, 1.00 eq.) in anhydrous THF (0.7 ml) and anhydrous triethylamine (30 µl, 0.22 mmol, 3.00 eq.) at 0 °C was added methanesulfonyl chloride (7.0 µl, 0.097 mmol, 1.25 eq.). The reaction mixture was warmed to rt and stirred for 30 min. The reaction mixture was evaporated *in vacuo* to afford a pale orange oil. The crude oil was purified by silica gel chromatography (elution with 80% to 100% EtOAc in petroleum ether) to afford a colourless oil (20 mg). The oil was dissolved in DMF (17 mL). Cs_2CO_3 (34 mg, 0.10 mmol, 1.4 eq.) was added and the reaction mixture was stirred at 80 °C for 2 h. The reaction mixture was concentrated under a constant stream of nitrogen to afford a pale yellow solid. H_2O (30 mL) was added to the crude solid and the resulting mixture was extracted with $CHCl_3$/IPA (9:1, 3 × 20 mL). The combined organic components were washed with brine (10 mL), dried ($MgSO_4$), filtered, and evaporated *in vacuo* to afford a pale yellow oil. The crude oil was purified by silica gel chromatography (elution with 0% to 5% MeOH in CH_2Cl_2) and re-purified by silica gel chromatography (elution with 50% to 100% EtOAc in petroleum ether) to yield (*R*)-1^4,8-dimethyl-1^2,1^3,1^4,1^5-tetrahydro-1^1*H*-10-oxa-3,8-diaza-1(6,8)-benzo[*b*][1,4]diazepina-9(1,3)-benzenacyclohexadecaphane-1^2,2-dione (**(*R*)77**) as a colourless solid (2 mg, 6%); R_f 0.34 (EtOAc); mp 236–238 °C (EtOAc); $[\alpha]_D^{25}$= +3.8 (*c* 0.2, DMSO); $\bar{\nu}_{max}$ (thin film)/cm^{-1} 3334 (N-H, w), 2921 (C-H, s), 1674 (C=O, s), 1295 (C-O, m); ^{1}H NMR (400 MHz; CD_3OD) δ_H 7.10 (1H, d, *J* 2.0, H-7), 7.03 (1H, dd, *J* 8.1, 8.1, H-5''), 6.92 (1H, d, *J* 2.0, H-9), 6.27 (1H, dd, *J* 8.1, 2.3, H-4''), 6.24 (1H, dd, *J* 2.3, 2.3, H-2''), 6.19 (1H, dd, *J* 8.1, 2.3, H-6''), 3.95–3.83 (3H, m, H-4, H-10''), 3.52–3.31 (4H, m, H-6', H-7''), 2.94 (3H, s, H-11''), 2.58 (2H, t, *J* 6.8, H-1'), 2.42 (1H, dd, *J* 13.3, 4.9, H_AH_B-3), 2.17 (1H, dd, *J* 13.3, 7.4, H_AH_B-3), 1.76–1.60 (8H, m, H-2', H-3', H-4', H-5'), 1.54–1.41 (2H, m, H-9''), 1.40–1.26 (2H, m, H-8''), 1.18 (3H, d, *J* 6.3, H-10); ^{13}C NMR (126 MHz; CD_3OD) δ_C 175.4 (C-2), 171.8 (C-11), 161.3 (C-3''), 151.9 (C-1''), 138.9 (C-5a), 136.2 (C-8), 132.5 (C-6), 130.8 (C-5''), 126.5 (C-9a), 126.0 (C-7), 125.9 (C-9), 106.4 (C-4''), 103.1 (C-6''), 100.4 (C-2''), 67.9 (C-6'), 57.1 (C-4), 54.0 (C-7''), 41.3 (C-3), 40.2 (C-10''), 39.2 (C-11''), 35.0 (C-1'), 31.1 (C-3'), 29.5 (C-5'), 28.4 (C-4'), 27.9 (C-8''), 26.5 (C-9''), 24.8 (C-2'), 23.7 (C-10); HRMS *m/z* (ESI$^+$) [Found: 479.3012, $C_{28}H_{39}N_4O_3$ requires M^+ 479.3016]; LRMS *m/z* (ESI$^+$) 479 ([M+H]$^+$, 100%); HPLC Method 1: Retention time 10.4 min, purity 99.5%.

2-(4-((3-Methoxyphenyl)(methyl)amino)butyl)isoindoline-1,3-dione (91)



To a stirred suspension of 2-(4-((3-hydroxyphenyl)(methyl)amino)butyl)isoindoline-1,3-dione (**84**) (203 mg, 0.623 mmol, 1.0 eq.) and K_2CO_3 (103 mg, 0.748 mmol, 1.2 eq.) in DMF (5 mL) was added iodomethane (43.0 µL, 0.748 mmol, 1.1 eq.) at rt. The reaction mixture was stirred at 80 °C for 2 h. The cooled suspension was diluted with EtOAc (50 mL) and washed with 1 M aq. K_2CO_3 (3 × 20 mL). The organic component was further washed with 0.5 M aq. LiCl (3 × 100 mL), brine (25 mL), dried ($MgSO_4$), filtered, and evaporated *in vacuo* to afford an orange oil. The crude oil was purified by silica gel chromatography (elution with 20% to 40% EtOAc in petroleum ether) to yield 2-(4-((3-methoxyphenyl)(methyl)amino)butyl)isoindoline-1,3-dione (**91**) as a yellow oil (111 mg, 53%); R_f 0.21 (EtOAc/petroleum ether 1:9); $\bar{\nu}_{max}$ (neat)/cm^{-1} 2939 (C-H, w), 1705 (C=O, s); ^{1}H NMR (500 MHz; $CDCl_3$) δ_H 7.84 (2H, dd, *J* 5.5, 3.0, H-2''), 7.71 (2H, dd, *J* 5.5, 3.0, H-3''), 7.11 (1H, d, *J* 8.3, 8.3, H-5), 6.31 (1H, ddd, *J* 8.3, 2.5, 0.8, H-6), 6.24 (1H, ddd, *J* 8.3, 2.5, 0.8, H-4), 6.22 (1H, dd, *J* 2.5, 2.5, H-2), 3.78 (3H, s, H-1'), 3.71 (2H, t, *J* 7.1, H-10), 3.34 (2H, t, *J* 8.0, H-7), 2.91 (3H, s, H-11), 1.76–1.66 (2H, m, H-9), 1.66–1.60 (2H, m, H-8); ^{13}C NMR (126 MHz; $CDCl_3$) δ_C 168.6 (C-1''), 160.9 (C-3), 150.7 (C-1), 134.1 (C-3''), 132.2 (C-1''a), 130.0 (C-5), 123.4 (C-2''), 105.5 (C-6), 100.9 (C-4), 98.8 (C-2), 55.2 (C-10), 52.4 (C-7), 38.6 (C-11), 37.9 (C-1'), 26.4 (C-9), 24.3 (C-8); HRMS *m/z* (ESI^+) [Found: 339.1700, $C_{20}H_{23}N_2O_3$ requires M^+ 339.1703]; LRMS *m/z* (ESI^+) 339 ($[M+H]^+$, 100%).

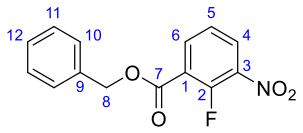
N^1-(3-Methoxyphenyl)-N^1-methylbutane-1,4-diamine (92)



Hydrazine monohydrate (65%, 58.0 µL, 1.19 mmol, 4.0 eq.) was added to a stirred solution of 2-(4-((3-methoxyphenyl)(methyl)amino)butyl)isoindoline-1,3-dione (**91**) (101 mg, 0.298 mmol, 1.0 eq.) in CH_2Cl_2 (1.3 mL) and MeOH (1.3 mL). The reaction mixture was stirred at 70 °C for 5 h. The cooled reaction mixture was diluted in CH_2Cl_2 (15 mL), filtered through Celite® (eluent MeOH) and evaporated *in vacuo* to yield an orange residue. The residue was dissolved in EtOAc (30 mL) and washed with H_2O (3 × 15 mL). The organic component was washed with brine (15 mL), dried (Na_2SO_4), filtered, and evaporated *in vacuo* to yield N^1-(3-methoxyphenyl)-N^1-methylbutane-1,4-diamine (**92**) as an orange oil (50 mg, 80%) and was used without further purification; R_f 0.00 (EtOAc); ^{1}H NMR (500 MHz; CD_3OD) δ_H 7.09–7.02 (1H, m, H-2), 6.37–6.31 (1H, m, H-4), 6.26–6.20 (2H, m, H-5, H-6), 3.75 (3H, s, H-5''), 3.34 (2H, dd, *J* 7.2, 3.2, H-1''), 2.69 (2H, t, *J* 7.2, H-4''), 1.67–1.56 (2H, m, H-2''), 1.56–1.45 (2H, m, H-3'');

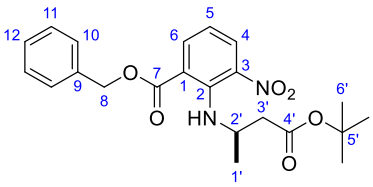
HRMS *m/z* (ESI$^+$) [Found: 209.1648, $C_{12}H_{21}N_2O$ requires M^+ 209,1648]; LRMS *m/z* (ESI$^+$) 209 ([M+H]$^+$, 100%).

Benzyl 2-fluoro-3-nitrobenzoate (93)



To a solution of 2-fluoro-3-nitrobenzoic acid (**69**) (1.00 g, 5.40 mmol, 1.0 eq.) in DMF (12.5 mL) was added K_2CO_3 (1.12 g, 8.10 mmol, 1.5 eq.) and the reaction mixture was stirred at rt for 5 min. Benzyl bromide (964 µL, 8.10 mmol, 1.5 eq.) was added and the reaction mixture was stirred at 60 °C for 17 h. The cooled reaction mixture was diluted with EtOAc (150 mL) and was washed with 1 M aq. K_2CO_3 (3 × 100 mL). The organic component was washed with 0.5 M aq. LiCl (3 × 100 mL), brine (100 mL), dried ($MgSO_4$), filtered, and evaporated *in vacuo* to afford an orange solid. The crude solid was purified by silica gel chromatography (elution with 10% to 20% EtOAc in petroleum ether) to yield benzyl 2-fluoro-3-nitrobenzoate (**93**) as a pale yellow oil (1.33 g, 89%); R_f 0.19 (EtOAc/petroleum ether 1:9); ^{1}H NMR (400 MHz; $CDCl_3$) δ_H 8.28–8.15 (2H, m, H-4, H-6), 7.49–7.33 (6H, m, H-5, H-10, H-11, H-12), 5.42 (2H, s, H-8); ^{19}F NMR (376 MHz; $CDCl_3$) δ_F −116.1 (dd, *J* 6.4, 6.4); LRMS *m/z* (ESI$^+$) 298 ([M+Na]$^+$, 100%). These data are in accordance with the literature.[30]

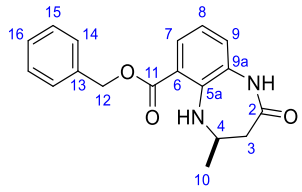
Benzyl (*R*)-2-((4-(*tert*-butoxy)-4-oxobutan-2-yl)amino)-3-nitrobenzoate ((*R*)94)



To a stirred suspension of benzyl 2-fluoro-3-nitrobenzoate (**93**) (939 mg, 3.41 mmol, 1.0 eq.) and Cs_2CO_3 (3.34 g, 10.2 mmol, 4.0 eq.) in toluene (54 mL) at rt was added *tert*-butyl (*R*)-3-aminobutanoate (**(*R*)41**) containing 1.63 eq. acetic acid (1.23 g, 4.78 mmol, 1.2 eq.) and the suspension was stirred at 85 °C for 18 h. To the cooled suspension was added 1 M aq. K_2CO_3 (150 mL) and the resulting mixture was extracted with EtOAc (3 × 150 mL). The combined organic components were washed with brine (100 mL), dried ($MgSO_4$), filtered, and evaporated *in vacuo* to afford an orange oil. The crude oil was purified by silica gel chromatography (elution with 10% to 20% EtOAc in petroleum ether) to yield

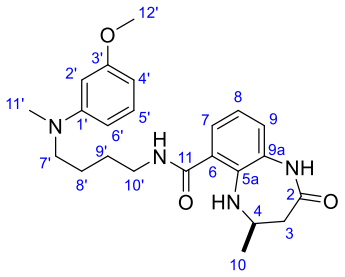
benzyl (*R*)-2-((4-(*tert*-butoxy)-4-oxobutan-2-yl)amino)-3-nitrobenzoate (**(*R*)94**) as an orange oil (1.40 g, 99%); R_f 0.33 (EtOAc/petroleum ether 1:4); $[\alpha]_D^{25}$= +69.6 (*c* 1.0, $CHCl_3$); ^{1}H NMR (400 MHz; $CDCl_3$) δ_H 8.20 (1H, d, *J* 9.8, NH-2), 8.04 (1H, dd, *J* 8.0, 1.7, H-6), 7.94 (1H, dd, *J* 8.0, 1.7, H-4), 7.47–7.33 (5H, m, H-10, H-11, H-12), 6.70 (1H, dd, *J* 7.8, 7.8, H-5), 5.35 (2H, s, H-8), 3.63 (1H, m, H-2'), 2.39 (2H, dd, *J* 6.4, 1.8, H-3'), 1.33 (9H, s, H-6'), 1.25 (3H, d, *J* 6.4, H-1'); LRMS *m/z* (ESI$^+$) 437 ([M+Na]$^+$, 100%). These data are in accordance with the literature.[30]

Benzyl (*R*)-4-methyl-2-oxo-2,3,4,5-tetrahydro-1*H*-benzo[*b*][1,4]diazepine-6-carboxylate ((*R*)95)



To a solution of benzyl (*R*)-2-((4-(*tert*-butoxy)-4-oxobutan-2-yl)amino)-3-nitrobenzoate (**(*R*)94**) (1.29 g, 3.11 mmol 1.0 eq.) in CH_2Cl_2 (10 mL) was added trifluoroacetic acid (10 mL) and the orange solution was stirred at rt for 2 h. The reaction mixture was evaporated *in vacuo* and the resulting residue was dissolved in glacial acetic acid (30 mL). Iron powder (868 mg, 15.6 mmol, 5.0 eq.) was added and the brown suspension was stirred under reflux for 4 h. 1 M aq. K_2CO_3 (300 mL) was added to the cooled suspension and the resulting mixture was extracted with EtOAc (3 × 200 mL). The combined organic components were washed with 0.5 M aq. LiCl (3 × 100 mL), brine (150 mL), dried ($MgSO_4$), filtered, and evaporated *in vacuo* to afford a brown oil. The crude oil was purified by silica gel chromatography (elution with 0% to 50% EtOAc in petroleum ether) to afford benzyl (*R*)-4-methyl-2-oxo-2,3,4,5-tetrahydro-1*H*-benzo[*b*][1,4]diazepine-6-carboxylate (**(*R*)95**) as a pale yellow solid (632 mg, 65%); R_f 0.14 (EtOAc/petroleum ether 2:3); $[\alpha]_D^{25}$= −49.1 (*c* 1.0, $CHCl_3$); mp 105–107 °C (EtOAc); ^{1}H NMR (400 MHz; $CDCl_3$) δ_H 8.00 (1H, br s, NH-9a), 7.87 (1H, br s, NH-5a), 7.84 (1H, dd, *J* 7.9, 1.6, H-9), 7.47–7.31 (5H, m, H-14, H-15, H-16), 6.99 (1H, dd, *J* 7.9, 1.6, H-7), 6.67 (1H, dd, *J* 7.9, 7.9 H-8), 5.32 (2H, s, H-12), 4.12–4.02 (1H, m, H-4), 2.68 (1H, d, *J* 14.2, H_AH_B-3), 2.58 (1H, dd, *J* 14.2, 8.3, H_AH_B-3), 1.39 (3H, d, *J* 6.5, H-10); LRMS *m/z* (ESI$^+$) 311 ([M+H]$^+$, 100%). These data are in accordance with the literature.[30]

(*R*)-*N*-(4-((3-Methoxyphenyl)(methyl)amino)butyl)-4-methyl-2-oxo-2,3,4,5-tetrahydro-1*H*-benzo[*b*][1,4]diazepine-6-carboxamide ((*R*)96)

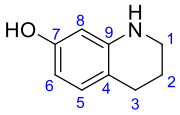


10% Pd/C (16 mg, 0.015 mmol, 0.1 eq.) was added to a stirred solution of benzyl (*R*)-4-methyl-2-oxo-2,3,4,5-tetrahydro-1*H*-benzo[*b*][1,4]diazepine-6-carboxylate (**(*R*)95**) (47 mg, 0.15 mmol, 1.0 eq.) in EtOAc (2 mL), which was purged under a nitrogen atmosphere. The atmosphere was replaced with hydrogen gas and the suspension was stirred at rt for 20 h. The black suspension was filtered through Celite® (eluent EtOAc) and evaporated *in vacuo* to afford a yellow oil. The oil was dissolved in DMF (1.9 mL) and triethylamine (42 µl, 0.30 mmol, 2.0 eq.). Benzotriazol-1-yl-oxytripyrrolidinophosphonium hexafluorophosphate (78 mg, 0.15 mmol, 1.0 eq.) was added to the solution and the reaction mixture was stirred at rt for 15 min. N^1-(3-Methoxyphenyl)-N^1-methylbutane-1,4-diamine (**92**) (40 mg, 0.19 mmol, 1.3 eq.) in DMF (1 mL) was added and the reaction mixture was stirred at rt for 18 h. The reaction mixture was diluted with EtOAc (30 mL) and washed with H_2O (3 × 15 mL). The organic component was washed with 0.5 M aq. LiCl (3 × 10 mL), brine (10 mL), dried ($MgSO_4$), filtered, and evaporated *in vacuo* to afford a brown oil. The crude oil was purified by silica gel chromatography (elution with 0% to 50% EtOAc in petroleum ether) to afford (*R*)-*N*-(4-((3-methoxyphenyl)(methyl)amino)butyl)-4-methyl-2-oxo-2,3,4,5-tetrahydro-1*H*-benzo[*b*][1,4]diazepine-6-carboxamide (**(*R*)96**) as a colourless solid (43 mg, 70%); R_f 0.36 (MeOH/CH_2Cl_2 1:9); $[\alpha]_D^{25}$= −11.1 (*c* 1.0, MeOH); mp 49–52 °C (EtOAc); $\bar{\nu}_{max}$ (neat)/cm^{-1} 3296 (N-H, br s), 2931 (C-H, w), 1667 (C=O, s); ^{1}H NMR (500 MHz; CD_3OD) δ_H 7.27 (1H, dd, *J* 7.8, 1.6, H-7), 7.08–7.02 (2H, m, H-5', H-9), 6.89 (1H, dd, *J* 7.8, 7.8, H-8), 6.36–6.32 (1H, m, H-6'), 6.26–6.20 (2H, m, H-2', H-4'), 4.02–3.03 (1H, m, H-4), 3.73 (3H, s, H-12'), 3.42–3.34 (4H, m, H-7', H-10'), 2.92 (3H, s, H-11'), 2.50 (1H, dd, *J* 13.4, 4.6, H_AH_B-3), 2.29 (1H, dd, *J* 13.4, 7.7, H_AH_B-3), 1.70–1.58 (4H, m, H-8', H-9'), 1.22 (3H, d, *J* 6.3, H-10); ^{13}C NMR (126 MHz; CD_3OD) δ_C 175.3 (C-2), 171.8 (C-11), 162.3 (C-3'), 152.1 (C-1'), 140.9 (C-5a), 131.8 (C-9a), 130.7 (C-5'), 126.8 (C-6), 126.0 (C-7), 125.8 (C-9), 121.1 (C-8), 106.8 (C-6'), 102.3

(C-4'), 100.0 (C-2'), 56.7 (C-4), 55.4 (C-12'), 53.4 (C-7'), 41.5 (C-3), 40.5 (C-10'), 38.8 (C-11'), 28.1 (C-9'), 25.1 (C-8'), 23.9 (C-10); HRMS *m/z* (ESI^+) [Found: 411.2380, $C_{23}H_{31}N_4O_3$ requires M^+ 411.2391]; LRMS *m/z* (ESI^+) 411 ($[M+H]^+$, 100%); HPLC Method 1: Retention time 8.9 min, purity 99.9%.

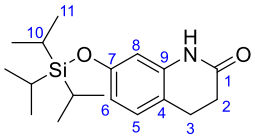
8.2.3 Chapter 4 - Second Generation Macrocycles

1,2,3,4-Tetrahydroquinolin-7-ol (112)



7-Hydroxy-3,4-dihydroquinolin-2(1*H*)-one (**111**) (2.00 g, 12.3 mmol, 1.0 eq.) was suspended in anhydrous THF (30 mL) and added portionwise to $LiAlH_4$ (698 mg, 18.4 mmol, 1.5 eq.) in anhydrous THF (21 mL) at 0 °C and the suspension was stirred at 0 °C for 10 min. The suspension was warmed to rt and was stirred for a further 20 h. The reaction was cooled to 0 °C and H_2O (0.7 mL), followed by 15% aq. NaOH (0.7 mL) and H_2O (2.1 mL) were added dropwise (Fieser work-up). $MgSO_4$ was added and the suspension was stirred at rt for 30 min. The reaction mixture was filtered and was washed with EtOAc (100 mL). The filtrate was evaporated *in vacuo* to afford a yellow oil. The crude oil was purified by silica gel chromatography (elution with 0% to 50% EtOAc in petroleum ether) to yield 7-((triisopropylsilyl)oxy)-3,4-dihydroquinolin-2(1*H*)-one (**112**) as a yellow oil (752 mg, 41%); R_f 0.60 (EtOAc/petroleum ether 1:1); ^{1}H NMR (400 MHz; $CDCl_3$) δ_H 6.79 (1H, d, *J* 8.1, H-5), 6.09 (1H, dd, *J* 8.1, 2.5, H-6), 5.97 (1H, d, *J* 2.5, H-8), 3.32–3.21 (2H, m, H-1), 2.68 (2H, t, *J* 6.2, H-3), 1.98–1.86 (2H, m, H-2); LRMS *m/z* (ESI^-) 148 ($[M-H]^-$, 100%). These data are in accordance with the literature.[132]

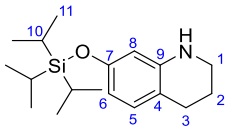
7-((Triisopropylsilyl)oxy)-3,4-dihydroquinolin-2(1*H*)-one (113)



Triisopropylsilyl chloride (3.41 mL, 15.9 mmol, 1.3 eq.) was added to a solution of 7-hydroxy-3,4-dihydroquinolin-2(1*H*)-one (**111**) (2.00 g, 12.3 mmol, 1.0 eq.) and imidazole (1.67 g, 24.6 mmol, 2.0 eq.) in DMF (14 mL) and the reaction mixture was stirred at rt for 24 h. The reaction mixture was dissolved in Et_2O (75 mL) and washed with H_2O (3 × 50 mL). The organic component was washed with brine (50 mL), dried ($MgSO_4$), filtered and evaporated *in vacuo* to afford a colourless oil. The crude oil was purified by silica gel chromatography (elution with 0% to 50% EtOAc in petroleum ether) to yield 7-((triisopropylsilyl)oxy)-3,4-dihydroquinolin-2(1*H*)-one (**113**) as a colourless solid (3.77 g, 96%); R_f 0.53 (EtOAc/petroleum ether 1:1); mp 72–75 °C (EtOAc); $\bar{\nu}_{max}$ (neat)/cm^{-1} 3918 (N-H, w), 2960 (C-H, w), 1673

(C=O, s), 1174 (C-O, s); ^{1}H NMR (500 MHz; $CDCl_3$) δ_H 7.80 (1H, s, NH-9), 6.97 (1H, d, *J* 8.2, H-5), 6.49 (1H, dd, *J* 8.2, 2.4, H-6), 6.29 (1H, d, *J* 2.4, H-8), 2.88 (2H, dd, *J* 8.4, 6.6, H-3), 2.61 (2H, dd, *J* 8.4, 6.6, H-2), 1.30–1.20 (3H, m, H-10), 1.10 (18H, d, *J* 7.4, H-11); ^{13}C NMR (126 MHz; $CDCl_3$) δ_C 171.6 (C-1), 155.7 (C-7), 138.1 (C-9), 128.7 (C-5), 116.2 (C-4), 114.3 (C-6), 107.2 (C-8), 31.2 (C-2), 24.8 (C-3), 18.1 (C-10), 12.8 (C-11); HRMS *m/z* (ESI$^+$) [Found: 320.2040, $C_{18}H_{30}N_2O^{28}Si$ requires M^+ 320.2040]; LRMS *m/z* (ESI$^+$) 320 ([M+H]$^+$, 100%); HPLC Method 1: Retention time 13.4 min, purity 99.3 %.

7-((Triisopropylsilyl)oxy)-1,2,3,4-tetrahydroquinoline (114)



Method 1:

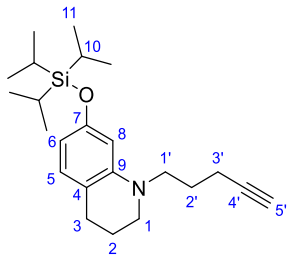
Triisopropylsilyl chloride (1.33 mL, 6.23 mmol, 1.3 eq.) was added to a solution of 1,2,3,4-tetrahydroquinolin-7-ol (**112**) (715 mg, 4.79 mmol, 1.0 eq.) and imidazole (652 mg, 9.58 mmol, 2.0 eq.) in THF (5.5 mL) and the reaction mixture was stirred at rt for 21 h. The reaction mixture was evaporated *in vacuo* and the resulting colourless solid was dissolved in Et_2O (100 mL) and washed with H_2O (3 × 150 mL). The organic component was washed with brine (100 mL), dried ($MgSO_4$), filtered and evaporated *in vacuo* to afford a brown oil. The crude oil was purified by silica gel chromatography (elution with 0% to 10% EtOAc in petroleum ether) to yield 7-((triisopropylsilyl)oxy)-1,2,3,4-tetrahydroquinoline **(114)** as a colourless oil (1.38 g, 94%).

Method 2:

7-((Triisopropylsilyl)oxy)-3,4-dihydroquinolin-2(1*H*)-one (**113**) (3.60 g, 11.3 mmol, 1.0 eq.) was dissolved in anhydrous Et_2O (17 mL) and added portionwise to $LiAlH_4$ (641 mg, 16.9 mmol, 1.5 eq.) in anhydrous Et_2O (20 mL) at 0 °C and the suspension was stirred at 0 °C for 10 min. The suspension was warmed to rt and was stirred for a further 4 h. The reaction was cooled to 0 °C and H_2O (0.7 mL), followed by 15% aq. NaOH (0.7 mL) and H_2O (2.1 mL) were added dropwise (Fieser work-up). $MgSO_4$ was added and the suspension was stirred at rt for 30 min. The reaction mixture was filtered and was washed with EtOAc (100 mL). The filtrate was evaporated *in vacuo* to afford a colourless oil. The crude oil was purified by silica gel chromatography (elution with 0% to 10% EtOAc in petroleum ether) to yield 7-((triisopropylsilyl)oxy)-1,2,3,4-tetrahydroquinoline (**114**) as a colourless oil (3.22 g, 93%).

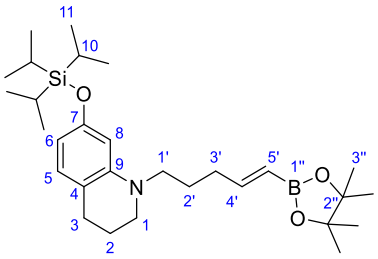
R_f 0.43 (EtOAc/petroleum ether 1:9); $\bar{\nu}_{max}$ (neat)/cm^{-1} 3410 (N-H, w), 2943 (C-H, w), 1183 (C-O, s); ^1H NMR (500 MHz; $CDCl_3$) δ_H 6.75 (1H, d, *J* 8.2, H-5), 6.16 (1H, dd, *J* 8.2, 2.4, H-6), 6.03 (1H, d, *J* 2.4, H-8), 3.69 (1H, br s, NH-9), 3.32–3.18 (2H, m, H-3), 2.68 (2H, t, *J* 6.3, H-1), 1.95–1.87 (2H, m, H-2), 1.29–1.17 (3H, m, H-10), 1.10 (18H, d, *J* 7.4, H-11); ^{13}C NMR (126 MHz; $CDCl_3$) δ_C 155.0 (C-7), 145.5 (C-9), 130.0 (C-5), 114.5 (C-4), 109.0 (C-6), 105.5 (C-8), 42.0 (C-1), 26.4 (C-3), 22.6 (C-2), 18.1 (C-11), 12.8 (C-10); HRMS *m/z* (ESI^+) [Found: 306.2245, $C_{18}H_{32}NO^{28}Si$ requires M^+ 306.2248]; LRMS *m/z* (ESI^+) 306 ($[M+H]^+$, 100%).

1-(Pent-4-yn-1-yl)-7-((triisopropylsilyl)oxy)-1,2,3,4-tetrahydroquinoline (115)



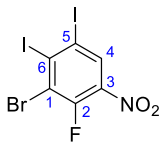
Pent-4-yn-1-yl methanesulfonate (448 mg, 2.95 mmol, 1.5 eq.) was added to a solution of 7-((triisopropylsilyl)oxy)-1,2,3,4-tetrahydroquinoline (**114**) (600 mg, 1.96 mmol, 1.0 eq.), potassium iodide (137 mg, 0.820 mmol, 0.5 eq.) and *N*,*N*-diisopropylethylamine (685 µL, 3.93 mmoL, 2.0 eq.) in DMF (11 mL). The reaction mixture was sealed and heated to 100 °C in a microwave for 1 h. The cooled orange solution was diluted with Et_2O (75 mL) and washed with H_2O (3 × 75 mL), brine (50 mL), dried ($MgSO_4$), filtered and evaporated *in vacuo* to afford an orange oil. The crude oil was purified by silica gel chromatography (elution with toluene) to yield 1-(pent-4-yn-1-yl)-7-((triisopropylsilyl)oxy)-1,2,3,4-tetrahydroquinoline (**115**) as a yellow oil (438 mg, 60%); R_f 0.67 (toluene); $\bar{\nu}_{max}$ (neat)/cm^{-1} 2943 (C-H, w); ^1H NMR (500 MHz; $CDCl_3$) δ_H 6.74 (1H, d, *J* 8.0, H-5), 6.15 (1H, d, *J* 2.3, H-8), 6.10 (1H, dd, *J* 8.0, 2.3, H-6), 3.33–3.27 (2H, m, H-1), 3.27–3.19 (2H, m, H-1'), 2.66 (2H, t, *J* 6.4, H-3'), 2.25 (2H, td, *J* 6.9, 2.7, H-3), 1.98 (1H, t, *J* 2.7, H-5'), 1.93–1.85 (2H, m, H-2'), 1.79 (2H, t, *J* 7.0, H-2), 1.30–1.17 (3H, m, H-10), 1.10 (18H, d, *J* 7.4, H-11); ^{13}C NMR (126 MHz; $CDCl_3$) δ_C 155.4 (C-7), 146.0 (C-9), 129.5 (C-5), 115.2 (C-4), 107.1 (C-6), 102.7 (C-8), 83.9 (C-4'), 68.9 (C-5'), 50.5 (C-1), 49.7 (C-1'), 27.5 (C-3'), 25.1 (C-2), 22.7 (C-2'), 18.2 (C-11), 16.2 (C-3), 12.9 (C-10); HRMS *m/z* (ESI^+) [Found: 372.2712, $C_{23}H_{38}N_2O^{28}Si$ requires M^+ 372.2712]; LRMS *m/z* (ESI^+) 372 ($[M+H]^+$, 100%).

(*E*)-1-(5-(4,4,5,5-Tetramethyl-1,3,2-dioxaborolan-2-yl)pent-4-en-1-yl)-7-((triisopropylsilyl)oxy)-1,2,3,4-tetrahydroquinoline (116)



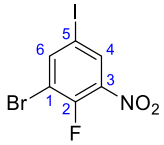
1-(Pent-4-yn-1-yl)-7-((triisopropylsilyl)oxy)-1,2,3,4-tetrahydroquinoline (**115**) (310 mg, 0.834 mmol, 1.0 eq.) and bis(cyclopentadienyl)zirconium(IV) chloride hydride (22.0 mg, 0.0834 mmol, 0.1 eq.) were added to a tapered microwave vial and sealed under an argon atmosphere (evacuated and backfilled 3 × argon). Triethylamine (12.0 µL, 0.0834 mmol, 0.1 eq.) and 4,4,5,5-tetramethyl-1,3,2-dioxaborolane (134 µL, 0.918 mmol, 1.1 eq.) were added and the reaction mixture was stirred at 60 °C under argon for 20 h in the absence of light. The reaction mixture was purified by silica gel chromatography (elution with 0% to 100% CH_2Cl_2 in petroleum ether) to yield (*E*)-1-(5-(4,4,5,5-tetramethyl-1,3,2-dioxaborolan-2-yl)pent-4-en-1-yl)-7-((triisopropylsilyl)oxy)-1,2,3,4-tetrahydroquinoline (**116**) as an orange oil (330 mg, 79%) and was used without further purification; R_f 0.44 (EtOAc/petroleum ether 1:9); $\bar{\nu}_{max}$ (neat)/cm^{-1} 2942 (C-H, w); ^{1}H NMR (500 MHz; $CDCl_3$) δ_H 6.73 (1H, d, *J* 8.2, H-5), 6.64 (1H, dt, *J* 17.9, 6.4, H-4'), 6.09 (2H, m, H-6, H-8), 5.46 (1H, dt, *J* 17.9, 1.6, H-5'), 3.27–3.13 (4H, m, H-1, H-1'), 2.65 (2H, t, *J* 6.3, H-3), 2.24–2.15 (2H, m, H-3'), 1.92–1.85 (2H, m, H-2), 1.74–1.65 (2H, m, H-2'), 1.26 (15H, m, H-10, H-3''), 1.10 (18H, d, *J* 7.3, H-11); ^{11}B NMR (160 MHz; $CDCl_3$) δ_B 29.1 (B-1''); ^{13}C NMR (126 MHz; $CDCl_3$) δ_C 155.4 (C-7), 153.7 (C-4'), 146.0 (C-9), 129.5 (C-5), 119.2 (C-5'), 115.2 (C-4), 107.0 (C-6), 102.6 (C-8), 83.2 (C-2''), 51.4 (C-1'), 49.5 (C-1), 33.6 (C-3'), 27.6 (C-3), 24.94 (C-2'), 24.92 (C-3''), 22.7 (C-2), 18.2 (C-11), 12.9 (C-10); HRMS *m/z* (ESI$^+$) [Found: 500.3751, $C_{29}H_{51}{}^{11}BNO_3{}^{28}Si$ requires M^+ 500.3731]; LRMS *m/z* (ESI$^+$) 500 ([M+H]$^+$, 100%).

3-Bromo-2-fluoro-4,5-diiodo-1-nitrobenzene (117)



1-Bromo-2-fluoro-3-nitrobenzoic (**42**) (200 mg, 0.910 mmol, 1.0 eq.) was added to a solution of iodine (324 mg, 1.27 mmol, 1.4 eq.) in fuming sulfuric acid (1.5 mL) and the reaction mixture was stirred at 85 °C for 15 h. The cooled reaction mixture was slowly added portionwise to ice (30 g) and the resulting precipitate was extracted with CH_2Cl_2 (3 × 40 mL). The combined organic components were washed with 10% aq. $Na_2S_2O_3$ (30 mL), brine (20 mL), dried (Na_2SO_4), filtered, and evaporated *in vacuo* to yield 3-bromo-2-fluoro-4,5-diiodo-1-nitrobenzene (**117**) as a pale yellow solid (340 mg, 80%); R_f 0.53 (EtOAc/petroleum ether 1:9); mp 155–158 °C (CH_2Cl_2); $\bar{\nu}_{max}$ (neat)/cm^{-1} 3063 (C-H, w), 1574 (N-O, s); ^{1}H NMR (400 MHz; $CDCl_3$) δ_H 8.54 (1H, dd, *J* 7.1, H-4); ^{13}C NMR (126 MHz; $CDCl_3$) δ_C 150.8 (d, *J* 267.6, C-2), 137.7 (C-3), 133.6 (d, *J* 3.0, C-4), 125.4 (d, *J* 1.7, C-6), 121.0 (d, *J* 21.5, C-1), 101.7 (d, *J* 5.3, C-5); ^{19}F NMR (376 MHz; $CDCl_3$) δ_F −97.56 (d, *J* 7.1); HRMS *m/z* (EI^+) [Found: 470.7264, $C_6H^{79}BrF^{127}INO_2$ requires M^+ 470.7259]; HPLC Method 1: Retention time 11.0 min, purity 98.4%. Structure confirmed by X-ray crystallography (See Appendix E).

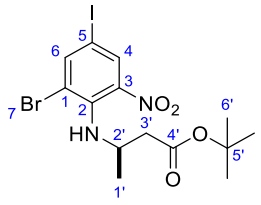
1-Bromo-2-fluoro-5-iodo-3-nitrobenzene (118)



N-Iodosuccinimide (2.88 g, 12.8 mmol, 1.4 eq.) was added to a solution of 1-bromo-2-fluoro-3-nitrobenzoic acid (**42**) (2.00 g, 9.13 mmol, 1.0 eq.) in concentrated sulfuric acid (10 mL) and the reaction mixture was stirred at rt for 19 h. The cooled reaction mixture was slowly added portionwise to ice (100 g) and the resulting precipitate was extracted with CH_2Cl_2 (3 × 70 mL). The combined organic components were washed with 10% aq. $Na_2S_2O_3$ (100 mL), brine (100 mL), dried (Na_2SO_4), filtered, and evaporated *in vacuo* to yield 1-bromo-2-fluoro-5-iodo-3-nitrobenzene (**118**) as a pale yellow solid (2.98 g, 95%); R_f 0.69 (EtOAc/petroleum ether 1:9); mp 33–36 °C (CH_2Cl_2); $\bar{\nu}_{max}$ (neat)/cm^{-1} 3072 (C-H, w), 1527 (N-O, s); ^{1}H NMR (500 MHz; $CDCl_3$) δ_H 8.27 (1H, dd, *J* 6.2, 2.2, H-4), 8.16 (1H, dd, *J* 5.5, 2.2, H-6); ^{13}C NMR (126 MHz; $CDCl_3$) δ_C 152.7 (d, *J* 265.7, C-2), 146.7 (C-6), 138.7 (C-3), 133.8 (d, *J*

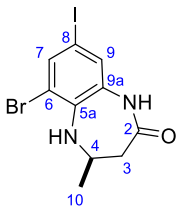
3.2, C-4), 113.4 (d, *J* 21.7, C-1), 86.1 (d, *J* 5.9, C-5); ^{19}F NMR (376 MHz; $CDCl_3$) δ_F −110.8 (dd, *J* 5.8, 5.8); HRMS *m/z* (ESI^+) [Found: 334.8290, $C_6H_2{}^{79}BrF^{127}INO_2$ requires M^+ 334.8292]; HPLC Method 1: Retention time 11.0 min, purity 93.1%.

tert-Butyl (*R*)-3-((2-bromo-4-iodo-6-nitrophenyl)amino)butanoate ((*R*)119)



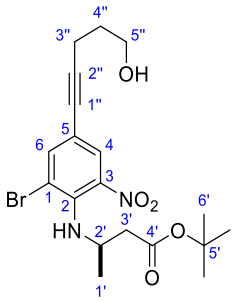
To a stirred suspension of 1-bromo-2-fluoro-5-iodo-3-nitrobenzene (**118**) (2.10 g, 6.11 mmol, 1.0 eq.) and Cs_2CO_3 (5.98 g, 18.3 mmol, 3.0 eq.) in toluene (97 mL) at rt was added *tert*-butyl (*R*)-3-aminobutanoate (**(*R*)41**) containing 1.63 eq. acetic acid (2.20 g, 8.56 mmol, 1.4 eq.) and the suspension was stirred at 85 °C for 18 h. To the cooled suspension was added 1 M aq. K_2CO_3 (200 mL) and the resulting mixture was extracted with EtOAc (3 × 200 mL). The combined organic components were washed with brine (100 mL), dried ($MgSO_4$), filtered, and evaporated *in vacuo* to afford an orange oil. The crude oil was purified by silica gel chromatography (elution with 0% to 10% EtOAc in petroleum ether) to yield *tert*-butyl (*R*)-3-((2-bromo-4-iodo-6-nitrophenyl)amino)butanoate (**(*R*)119**) as an orange solid (2.76 g, 93%); R_f 0.32 (EtOAc/petroleum ether 1:9); $[\alpha]_D^{25}$= −78.4 (*c* 1.0, $CHCl_3$); mp 43–46 °C (EtOAc); $\bar{\nu}_{max}$ (neat)/cm^{-1} 3348 (N-H, w), 2977 (C-H, w), 1720 (C=O, s), 1523 (N-O, s); ^{1}H NMR (500 MHz; $CDCl_3$) δ_H 8.20 (1H, d, *J* 2.1, H-4), 7.98 (1H, d, *J* 2.1, H-6), 6.40 (1H, d, *J* 10.2, NH-2), 4.25–4.15 (1H, m, H-2'), 2.51–2.38 (2H, m, H-3'), 1.39 (9H, s, H-6'), 1.27 (3H, d, *J* 6.4, H-1'); ^{13}C NMR (126 MHz; $CDCl_3$) δ_C 170.3 (C-4'), 147.0 (C-6), 142.4 (C-2), 141.0 (C-3), 134.1 (C-4), 116.9 (C-1), 81.4 (C-5'), 78.9 (C-5), 50.1 (C-2'), 43.5 (C-3'), 28.1 (C-6'), 21.4 (C-1'); HRMS *m/z* (ESI^+) [Found: 484.9568, $C_{14}H_{19}{}^{79}Br^{127}IN_2O_4$ requires M^+ 484.9567]; LRMS *m/z* (ESI^-) 483 ($[M-H]^-$, 50%); 485 ($[M-H]^-$, 50%); HPLC Method 1: Retention time 13.3 min, purity 100.0%.

(*R*)-6-Bromo-8-iodo-4-methyl-1,3,4,5-tetrahydro-2*H*-benzo[*b*][1,4]diazepin-2-one ((*R*)122)



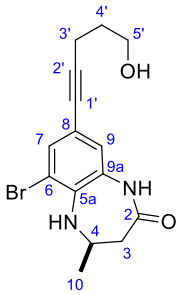
To a solution of *tert*-butyl (*R*)-3-((2-bromo-4-iodo-6-nitrophenyl)amino)butanoate (**(*R*)119**) (860 mg, 1.77 mmol 1.0 eq.) in CH_2Cl_2 (8 mL) was added trifluoroacetic acid (8 mL) and the orange solution was stirred at rt for 3 h. The reaction mixture was evaporated *in vacuo* and the resulting residue was dissolved in glacial acetic acid (17 mL). Iron powder (495 mg, 8.86 mmol, 5.0 eq.) was added and the brown suspension was stirred under reflux for 4 h. 1 M aq. K_2CO_3 (300 mL) was added to the cooled suspension and the resulting mixture was extracted with EtOAc (3 × 150 mL). The combined organic components were washed with brine (150 mL), dried ($MgSO_4$), filtered, and evaporated *in vacuo* to afford a brown oil. The crude oil was purified by silica gel chromatography (elution with 20% to 80% EtOAc in petroleum ether) to afford an orange solid. The orange solid was triturated with CH_2Cl_2 (3 × 10 mL) to yield (*R*)-6-bromo-8-iodo-4-methyl-1,3,4,5-tetrahydro-2*H*-benzo[*b*][1,4]diazepin-2-one (**(*R*)122**) as a colourless solid (259 mg, 38%); R_f 0.45 (EtOAc/petroleum ether 4:1); $[\alpha]_D^{25}$= +27.4 (*c* 1.0, DMSO); mp 157–160 °C (CH_2Cl_2); $\bar{\nu}_{max}$ (neat)/cm^{-1} 3349 (N-H, w), 3326 (N-H, w), 3076 (C-H, w), 1676 (C=O, s); ^{1}H NMR (500 MHz; DMSO-d_6) δ_H 9.68 (1H, s, NH-9a), 7.58 (1H, d, *J* 2.0, H-7), 7.21 (1H, d, *J* 2.0, H-9), 4.82 (1H, d, *J* 2.7, NH-5a), 4.08–3.88 (1H, m, H-4), 2.46 (1H, dd, *J* 13.5, 4.1, H_AH_B-3), 2.27 (1H, dd, *J* 13.5, 8.1, H_AH_B-3), 1.23 (3H, d, *J* 6.2, H-10); ^{13}C NMR (126 MHz; DMSO-d_6) δ_C 171.2 (C-2), 136.6 (C-9a), 134.9 (C-7), 131.5 (C-5a), 129.3 (C-9), 115.7 (C-6), 81.1 (C-8), 53.8 (C-4), 40.8 (C-3), 23.5 (C-10); HRMS *m/z* (ESI^+) [Found: 380.9094, $C_{10}H_{11}{}^{79}Br^{127}IN_2O$ requires M^+ 380.9094]; LRMS *m/z* (ESI^-) 379 ($[M-H]^-$, 44%); 381 ($[M-H]^-$, 56%). HPLC Method 1: Retention time 8.4 min, purity 94.7%.

tert-Butyl (_R_)-3-((2-bromo-4-(5-hydroxypent-1-yn-1-yl)-6-nitrophenyl)amino)butanoate ((_R_)120)



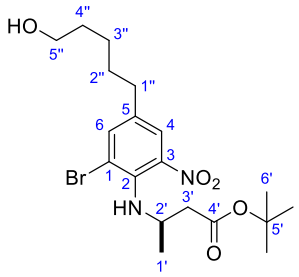
A solution of *tert*-butyl (*R*)-3-((2-bromo-4-iodo-6-nitrophenyl)amino)butanoate (**(*R*)119**) (300 mg, 0.620 mmol, 1.0 eq.) in THF (1.7 mL) was added to bis(triphenylphosphine)palladium(II) dichloride (9.00 mg, 0.0124 mmol, 0.02 eq.) and copper(I) iodide (4.00 mg, 0.0186 mmol, 0.03 eq.) at rt under an argon atmosphere (evacuated and backfilled 3 × argon). Triethylamine (1.0 mL) was added, followed by 4-pentyn-1-ol (70.0 µL, 0.744 mmol, 1.2 eq.) and the suspension was stirred at rt under an argon atmosphere for 5 h. The reaction mixture was evaporated *in vacuo* to afford an orange oil. The oil was diluted with EtOAc (150 mL) and washed with sat. aq. $NaHCO_3$ (3 × 75 mL). The organic component was washed with brine (20 mL), dried ($MgSO_4$), filtered, and evaporated *in vacuo* to afford an orange oil. The crude oil was purified by silica gel chromatography (elution with 0% to 50% EtOAc in petroleum ether) to yield *tert*-butyl (*R*)-3-((2-bromo-4-(5-hydroxypent-1-yn-1-yl)-6-nitrophenyl)amino)butanoate (**(*R*)120**) as an orange oil (263 mg, 96%); R_f 0.45 (EtOAc/petroleum ether 1:1); $[\alpha]_D^{25}$= −79.3 (*c* 1.0, $CHCl_3$); $\bar{\nu}_{max}$ (neat)/cm^{-1} 3354 (N-H, w), 2977 (C-H, w), 2228 (C≡C, w), 1724 (C=O, s), 1528 (N-O, s); ^{1}H NMR (500 MHz; $CDCl_3$) δ_H 7.95 (1H, d, *J* 2.0, H-4), 7.73 (1H, d, *J* 2.0, H-6), 6.47 (1H, d, *J* 10.1, NH-2), 4.34–4.16 (1H, m, H-2'), 3.88–3.72 (2H, m, H-5''), 2.52 (2H, t, *J* 7.0, H-3''), 2.45 (1H, d, *J* 1.3, H_AH_B-3'), 2.45 (1H, d, *J* 1.3, H_AH_B-3'), 1.88–1.79 (2H, m, H-4''), 1.39 (9H, s, H-6'), 1.27 (3H, d, *J* 6.6, H-1'); ^{13}C NMR (126 MHz; $CDCl_3$) δ_C 170.4 (C-4'), 142.0 (C-6), 141.9 (C-2), 139.9 (C-3), 128.8 (C-4), 115.9 (C-1), 115.4 (C-5), 91.1 (C-2''), 81.3 (C-5'), 77.9 (C-1''), 61.8 (C-5''), 50.1 (C-2'), 43.6 (C-3'), 31.3 (C-4''), 28.1 (C-6'), 21.5 (C-1'), 16.0 (C-3''); HRMS *m/z* (ESI^+) [Found: 463.0839, $C_{19}H_{25}{}^{79}BrN_2{}^{23}NaO_5$ requires M^+ 463.0839]; LRMS *m/z* (ESI^+) 463 ($[M+Na]^+$, 50%), 465 ($[M+Na]^+$, 50%); HPLC Method 1: Retention time 7.8 min, purity 98.5%.

(*R*)-6-Bromo-8-(6-hydroxyhex-1-yn-1-yl)-4-methyl-1,3,4,5-tetrahydro-2*H*-benzo[*b*][1,4]diazepin-2-one ((*R*)123)



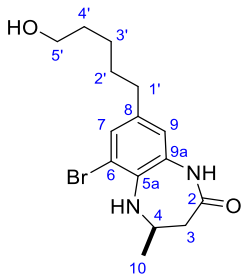
A solution of (*R*)-6-bromo-8-iodo-4-methyl-1,3,4,5-tetrahydro-2*H*-benzo[*b*][1,4]diazepin-2-one (**(*R*)122**) (50 mg, 0.13 mmol, 1.0 eq.) in DMF (0.35 mL) was added to bis(triphenylphosphine)palladium(II) dichloride (2.0 mg, 0.0028 mmol, 0.02 eq.) and copper(I) iodide (1.0 mg, 0.0053 mmol, 0.04 eq.) at rt under an argon atmosphere (evacuated and backfilled 3 × argon). Triethylamine (0.2 mL) was added, followed by 4-pentyn-1-ol (15 µL, 0.16 mmol, 1.2 eq.) and the suspension was stirred at 40 °C under an argon atmosphere for 3 h. The reaction mixture was diluted with EtOAc (30 mL) and washed with sat. aq. $NaHCO_3$ (3 × 20 mL). The organic component was washed with 0.5 M aq. LiCl (3 × 10 mL), brine (20 mL), dried ($MgSO_4$), filtered, and evaporated *in vacuo* to afford an orange oil. The crude oil was purified by silica gel chromatography (elution with 50% to 100% EtOAc in petroleum ether) to yield (*R*)-6-bromo-8-(6-hydroxyhex-1-yn-1-yl)-4-methyl-1,3,4,5-tetrahydro-2*H*-benzo[*b*][1,4]diazepin-2-one (**(*R*)123**) as a colourless oil (36 mg, 81%); R_f 0.10 (EtOAc/petroleum ether 4:1); $[\alpha]_D^{25}$= −20.4 (*c* 1.0, MeOH); $\bar{\nu}_{max}$ (neat)/cm^{-1} 3351 (N-H, w), 2956 (C-H, w), 2360 (C≡C, w) 1670 (C=O, s); ^{1}H NMR (500 MHz; CD_3OD) δ_H 7.35 (1H, d, *J* 1.9, H-7), 6.94 (1H, d, *J* 1.9, H-9), 4.12 (1H, m, H-4), 3.69 (2H, t, *J* 6.3, H-5'), 2.56 (1H, dd, *J* 13.5, 4.3, H_AH_B-3), 2.48 (2H, t, *J* 7.1, H-3'), 2.37 (1H, dd, *J* 13.5, 8.0, H_AH_B-3), 1.83–1.73 (2H, m, H-4'), 1.35 (3H, d, *J* 6.3, H-10); ^{13}C NMR (126 MHz; CD_3OD) δ_C 173.5 (C-2), 136.9 (C-5a), 131.5 (C-7), 129.1 (C-9a), 124.3 (C-9), 116.7 (C-8), 114.7 (C-6), 88.9 (C-2'), 78.4 (C-1'), 60.2 (C-5'), 55.1 (C-4), 40.3 (C-3), 31.3 (C-3'), 22.7 (C-10), 15.1 (C-4'); HRMS *m/z* (ESI$^+$) [Found: 337.0546, $C_{15}H_{18}{}^{79}BrN_2O_2$ requires M^+ 337.0546]; LRMS *m/z* (ESI$^+$) 359 ([M+Na]$^+$, 49%), 361 ([M+Na]$^+$, 51%); HPLC Method 1: Retention time 11.7 min, purity 99.8%.

tert-Butyl (_R_)-3-((2-bromo-4-(5-hydroxypentyl)-6-nitrophenyl)amino)butanoate ((_R_)121)



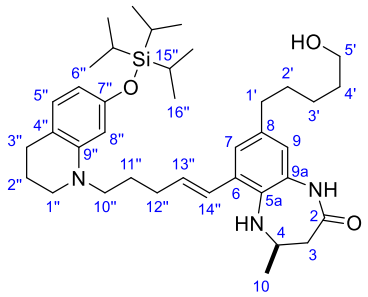
Tris(triphenylphosphine)rhodium(I) chloride (2.0 mg, 0.0022 mmol, 0.05 eq.) was added to a solution of *tert*-butyl (*R*)-3-((2-bromo-4-(5-hydroxypent-1-yn-1-yl)-6-nitrophenyl)amino)butanoate (**(*R*)120**) (20 mg, 0.045 mmol, 1.0 eq.) in toluene (0.6 mL). The atmosphere was replaced with hydrogen gas and the orange solution was stirred at 60 °C for 5 h. The reaction mixture was evaporated *in vacuo* to afford a dark orange oil. The crude oil was purified by silica gel chromatography (elution with 0% to 50% EtOAc in petroleum ether) to yield *tert*-butyl (*R*)-3-((2-bromo-4-(5-hydroxypentyl)-6-nitrophenyl)amino)butanoate (**(*R*)121**) as an orange oil (18 mg, 90%); R_f 0.45 (EtOAc/petroleum ether 1:1); $[\alpha]_D^{25}$= −63.8 (*c* 1.0, $CHCl_3$); $\bar{\nu}_{max}$ (thin film)/cm^{-1} 3355 (N-H, w), 2933 (C-H, w), 1726 (C=O, s), 1531 (N-O, s); ^{1}H NMR (500 MHz; $CDCl_3$) δ_H 7.74 (1H, d, *J* 2.1, H-6), 7.57 (1H, d, *J* 2.1, H-4), 6.19 (1H, d, *J* 10.4, NH-2), 4.23–4.13 (1H, m, H-2'), 3.65 (2H, t, *J* 6.7, H-5''), 2.60–2.51 (2H, t, *J* 7.8, H-1''), 2.47–2.37 (2H, m, H-3'), 1.66–1.56 (4H, m, H-2'', H-4''), 1.45–1.40 (2H, m, H-3''), 1.39 (9H, s, H-6'), 1.25 (3H, d, *J* 6.5, H-1'); ^{13}C NMR (126 MHz; $CDCl_3$) δ_C 170.6 (C-6'), 141.3 (C-2), 140.6 (C-3), 139.9 (C-6), 135.6 (C-5), 125.1 (C-4), 117.1 (C-1), 81.1 (C-5'), 62.9 (C-5''), 50.4 (C-2'), 43.8 (C-3'), 34.5 (C-1''), 32.6 (C-2''), 30.9 (C-3''), 28.1 (C-6'), 25.4 (C-4''), 21.4 (C-1'); HRMS *m/z* (ESI^+) [Found: 445.1334, $C_{19}H_{30}{}^{79}BrN_2O_5$ requires M^+ 445.1332]; LRMS *m/z* (ESI^+) 445 ($[M+H]^+$, 66%), 447 ($[M+H]^+$, 34%); HPLC Method 1: Retention time 11.8 min, purity 100.0%.

(*R*)-6-Bromo-8-(5-hydroxypentyl)-4-methyl-1,3,4,5-tetrahydro-2*H*-benzo[*b*][1,4]diazepin-2-one ((*R*)124)



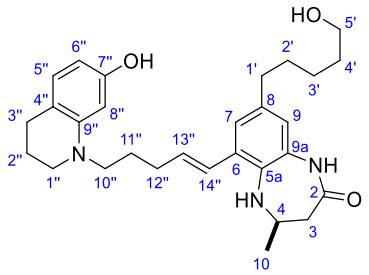
To a solution of *tert*-butyl (*R*)-3-((2-bromo-4-(5-hydroxypentyl)-6-nitrophenyl)amino)butanoate (**(*R*)121**) (565 mg, 1.27 mmol 1.0 eq.) in CH_2Cl_2 (4.7 mL) was added trifluoroacetic acid (4.7 mL) and the orange solution was stirred at rt for 2 h. The reaction mixture was evaporated *in vacuo* and the resulting residue was dissolved in glacial acetic acid (11 mL). Iron powder (354 mg, 6.34 mmol, 5.0 eq.) was added and the brown suspension was stirred under reflux for 4 h. 1 M aq. K_2CO_3 (100 mL) was added to the cooled suspension and the resulting mixture was extracted with EtOAc (3 × 70 mL). The combined organic components were washed with brine (100 mL), dried ($MgSO_4$), filtered, and evaporated *in vacuo* to afford a yellow oil. The crude yellow oil was dissolved in THF/MeOH/H_2O (3:2:1, 12 mL) and LiOH (304 mg, 12.7 mmol, 10.0 eq.) was added. The reaction mixture was stirred at rt for 2 h. The mixture was evaporated *in vacuo* and the resulting residue was diluted with H_2O (50 mL) and was extracted with EtOAc (3 × 50 mL). The combined organic components were washed with brine (50 mL), dried ($MgSO_4$), filtered, and evaporated *in vacuo* to afford a yellow oil. The crude oil was purified by silica gel chromatography (elution with 50% to 100% EtOAc in petroleum ether) to yield (*R*)-6-bromo-8-(5-hydroxypentyl)-4-methyl-1,3,4,5-tetrahydro-2*H*-benzo[*b*][1,4]diazepin-2-one (**(*R*)124**) as a colourless solid (350 mg, 81%); R_f 0.12 (EtOAc); $[\alpha]_D^{25}$= +12.6 (*c* 0.8, MeOH); $\bar{\nu}_{max}$ (neat)/cm^{-1} 3375 (N-H, w), 2935 (C-H, w), 1667 (C=O, s); ^{1}H NMR (500 MHz; CD_3OD) δ_H 7.21 (1H, d, *J* 1.9, H-7), 6.80 (1H, d, *J* 1.9, H-9), 4.16–3.99 (1H, m, H-4), 3.55 (2H, t, *J* 6.6, H-5'), 2.59–2.44 (3H, m, H-1', H_AH_B-3), 2.29 (1H, dd, *J* 13.2, 7.8, H_AH_B-3), 1.68–1.48 (4H, m, H-2', H-4'), 1.43–1.36 (2H, m, H-3'), 1.33 (3H, d, *J* 6.2, H-10); ^{13}C NMR (126 MHz; CD_3OD) δ_C 175.3 (C-2), 138.4 (C-5a), 136.2 (C-8), 132.2 (C-9a), 130.1 (C-7), 122.8 (C-9), 117.5 (C-6), 62.8 (C-5'), 57.6 (C-4), 41.5 (C-3), 35.6 (C-1'), 33.4 (C-4'), 32.3 (C-2'), 26.5 (C-3'), 23.9 (C-10); HRMS *m/z* (ESI$^+$) [Found: 341.0863, $C_{15}H_{22}{}^{79}BrN_2O_2$ requires M^+ 341.0865]; LRMS *m/z* (ESI$^+$) 341 ([M+H]$^+$, 51%), 343 ([M+H]$^+$, 49%); HPLC Method 1: Retention time 8.0 min, purity 92.0%.

(*R,E*)-8-(5-Hydroxypentyl)-4-methyl-6-(5-(7-((triisopropylsilyl)oxy)-3,4-dihydroquinolin-1(2*H*)-yl)pent-1-en-1-yl)-1,3,4,5-tetrahydro-2*H*-benzo[*b*][1,4]diazepin-2-one ((*R*)125)



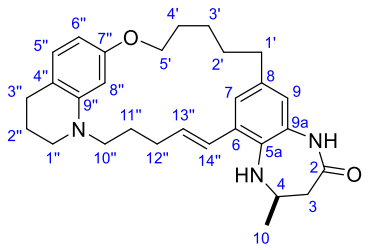
(*R*)-6-Bromo-8-(5-hydroxypentyl)-4-methyl-1,3,4,5-tetrahydro-2*H*-benzo[*b*][1,4]diazepin-2-one (**(*R*)124**) (349 mg, 1.02 mmol, 1.0 eq.), bis(triphenylphosphine)palladium(II) dichloride (36.0 mg, 0.0512 mmol, 0.05 eq.) and K_2CO_3 (425 mg, 3.07 mmol, 3.0 eq.) were added to a Schlenk flask under a nitrogen atmosphere (evacuated and backfilled 3 × nitrogen). (*E*)-1-(5-(4,4,5,5-Tetramethyl-1,3,2-dioxaborolan-2-yl)pent-4-en-1-yl)-7-((triisopropylsilyl)oxy)-1,2,3,4-tetrahydroquinoline (**116**) (767 mg, 1.53 mmol, 1.5 eq.) in 1,4-dioxane (7 mL) was added, followed by H_2O (1.75 mL) and the reaction mixture was stirred at 100 °C for 24 h. The reaction mixture was evaporated *in vacuo* and diluted with EtOAc (150 mL). The organic component was washed with brine (3 × 50 mL), dried ($MgSO_4$), filtered, and evaporated *in vacuo* to afford a brown oil. The crude oil was purified by silica gel chromatography (elution with 50% to 100% EtOAc in petroleum ether) to yield (*R,E*)-8-(5-hydroxypentyl)-4-methyl-6-(5-(7-((triisopropylsilyl)oxy)-3,4-dihydroquinolin-1(2*H*)-yl)pent-1-en-1-yl)-1,3,4,5-tetrahydro-2*H*-benzo[*b*][1,4]diazepin-2-one (**(*R*)125**) as a yellow oil (593 mg, 91%); R_f 0.13 (EtOAc); $[\alpha]_D^{25}$= +8.7 (*c* 1.0, MeOH); $\bar{\nu}_{max}$ (thin film)/cm^{-1} 3362 (O-H, br s), 2964 (C-H, s), 1668 (C=O, s); ^{1}H NMR (500 MHz; CD_3OD) δ_H 7.04 (1H, d, *J* 2.0, H-7), 6.76–6.70 (2H, m, H-9, H-5''), 6.70–6.62 (1H, dt, *J* 15.5, 1.5, H-14''), 6.18–6.08 (2H, m, H-8'', H-13'',), 6.05 (1H, dd, *J* 8.0, 2.3, H-6''), 4.08–3.98 (1H, m, H-4), 3.55 (2H, t, *J* 6.6, H-5'), 3.29–3.26 (4H, m, H-1'', H-10''), 2.66 (2H, t, *J* 6.3, H-3''), 2.55 (2H, t, *J* 7.7, H-1'), 2.50 (1H, dd, *J* 12.9, 5.5, H_AH_B-3), 2.38–2.30 (2H, m, H-12''), 2.22 (1H, dd, *J* 12.9, 7.0, H_AH_B-3), 1.96–1.87 (2H, m, H-2''), 1.80 (2H, m, H-11''), 1.63 (2H, m, H-2'), 1.59–1.52 (2H, m, H-4'), 1.45–1.38 (2H, m, H-3'), 1.29 (3H, d, *J* 6.2, H-10), 1.28–1.17 (3H, m, H-15''), 1.09 (18H, d, *J* 7.2, H-16''); ^{13}C NMR (126 MHz; CD_3OD) δ_C 175.8 (C-2), 156.4 (C-7''), 147.2 (C-9''), 137.8 (C-5a), 135.3 (C-8), 134.4 (C-9a), 133.1 (C-13''), 132.7 (C-6), 130.5 (C-9), 127.2 (C-4''), 124.8 (C-8''), 122.0 (C-7), 116.8 (C-5''), 108.2 (C-6''), 103.8 (C-14''), 62.9 (C-5'), 58.3 (C-4), 52.2 (C-10''), 50.4 (C-1''), 41.2 (C-3), 36.2 (C-1'), 33.5 (C-4'), 32.6 (C-2'), 32.1 (C-12''), 28.5 (C-3''), 26.8 (C-11''), 26.6 (C-3'), 23.72 (C-2''), 23.67 (C-10), 18.5 (C-16''), 14.0 (C-15''); HRMS *m/z* (ESI$^+$) [Found: 634.4395, $C_{38}H_{60}N_3O_3{}^{28}Si$ requires M^+ 634.4399]; LRMS *m/z* (ESI$^+$) 634 ([M+H]$^+$, 100%).

(*R,E*)-6-(5-(7-Hydroxy-3,4-dihydroquinolin-1(2*H*)-yl)pent-1-en-1-yl)-8-(5-hydroxypentyl)-4-methyl-1,3,4,5-tetrahydro-2*H*-benzo[*b*][1,4]diazepin-2-one ((*R*)126)



To a solution of (*R,E*)-8-(5-hydroxypentyl)-4-methyl-6-(5-(7-((triisopropylsilyl)oxy)-3,4-dihydroquinolin-1(2*H*)-yl)pent-1-en-1-yl)-1,3,4,5-tetrahydro-2*H*-benzo[*b*][1,4]diazepin-2-one (**(*R*)125**) (100 mg, 0.158 mmol, 1.0 eq.) in EtOH (1.3 mL) and CH_2Cl_2 (0.5 mL) was added 2 M aq. HCl (2 mL) and the reaction mixture was stirred at 80 °C for 21 h. The reaction mixture was evaporated *in vacuo* to afford an orange residue. Sat. aq. $NaHCO_3$ (50 mL) was added to the residue and the resulting mixture extracted with $CHCl_3$/IPA (9:1, 3 × 30 mL). The combined organic components were washed with brine (50 mL), dried ($MgSO_4$), filtered, and evaporated *in vacuo* to afford a dark orange oil. The crude oil was purified by silica gel chromatography (elution with 0% to 5% EtOH in EtOAc) to yield (*R,E*)-6-(5-(7-hydroxy-3,4-dihydroquinolin-1(2*H*)-yl)pent-1-en-1-yl)-8-(5-hydroxypentyl)-4-methyl-1,3,4,5-tetrahydro-2*H*-benzo[*b*][1,4]diazepin-2-one (**(*R*)126**) as a colourless oil (71 mg, 94%); R_f 0.44 (EtOH/EtOAc 1:9); $[\alpha]_D^{25}$= +6.7 (*c* 0.9, MeOH); $\bar{\nu}_{max}$ (thin film)/cm^{-1} 3259 (O-H, br s), 2928 (C-H, w), 1661 (C=O, s); ^{1}H NMR (500 MHz; CD_3OD) δ_H 7.07 (1H, d, *J* 2.0, H-7), 6.72 (1H, d, *J* 2.0, H-9), 6.69–6.62 (2H, m, H-5'', H-14''), 6.17 (1H, dt, *J* 15.5, 6.9, H-13''), 6.11 (1H, d, *J* 2.3, H-8''), 6.01–5.94 (1H, m, H-6''), 4.08–4.00 (1H, m, H-4), 3.55 (2H, t, *J* 6.6, H-5'), 3.30–3.21 (4H, m, H-10'', H-1''), 2.62 (2H, t, *J* 6.3, H-3''), 2.55 (2H, t, *J* 7.6, H-1'), 2.49 (1H, dd, *J* 12.9, 5.5, H_AH_B-3), 2.36–2.30 (2H, m, H-12''), 2.21 (1H, dd, *J* 12.9, 7.0, H_AH_B-3), 1.95–1.84 (2H, m, H-2''), 1.83–1.76 (2H, m, H-11''), 1.66–1.59 (2H, m, H-2'), 1.59–1.51 (2H, m, H-4'), 1.45–1.37 (2H, m, 3'), 1.28 (3H, d, *J* 6.2, H-10); ^{13}C NMR (126 MHz; CD_3OD) δ_C 175.9 (C-2), 157.4 (C-7''), 147.5 (C-9''), 137.9 (C-9a), 135.2 (C-6), 134.7 (C-13''), 133.1 (C-8), 132.7 (C-5a), 130.6 (C-8''), 127.1 (C-6''), 124.8 (C-7), 121.9 (C-9), 115.2 (C-4''), 103.6 (C-5''), 99.2 (C-14''), 62.9 (C-5'), 58.3 (C-4), 52.0 (C-10''), 50.4 (C-1''), 41.2 (C-3), 36.2 (C-1'), 33.5 (C-4'), 32.5 (C-2'), 32.0 (C-12''), 28.5 (C-3''), 27.0 (C-11''), 26.6 (C-3'), 23.8 (C-2''), 23.6 (C-10); HRMS *m/z* (ESI$^+$) [Found: 478.3060, $C_{29}H_{40}N_3O_3$ requires M^+ 478.3064]; LRMS *m/z* (ESI$^+$) 478 ([M+H]$^+$, 100%); HPLC Method 1: Retention time 9.6 min, purity 97.0%.

(2*R*,24*Z*)-2-Methyl-1,2,3,9,10,11,12,18,19,21,22,23-dodecahydro-8*H*,17*H*-14,16-etheno-26,7-(metheno)[1,4]diazepino[2,3-*l*]pyrido[2,1-*d*][1,5]oxazacycloicosin-4(5*H*)-one ((*R*)104)

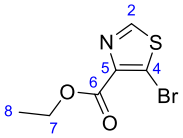


To a stirred solution of (*R,E*)-6-(5-(7-hydroxy-3,4-dihydroquinolin-1(2*H*)-yl)pent-1-en-1-yl)-8-(5-hydroxypentyl)-4-methyl-1,3,4,5-tetrahydro-2*H*-benzo[*b*][1,4]diazepin-2-one (**(*R*)126**) (71 mg, 0.15 mmol, 1.0 eq.) in anhydrous THF (1.4 ml) and anhydrous pyridine (36 µl, 0.45 mmol, 3.0 eq.) at 0 °C was added methanesulfonyl chloride (15 µl, 0.19 mmol, 1.25 eq.). The reaction mixture was warmed to rt and stirred for 30 min. The suspension was evaporated *in vacuo* to afford a brown oil. The crude oil was purified by silica gel chromatography (elution with EtOAc) to afford a colourless oil (77 mg). The oil was dissolved in DMF (69 mL, 0.002 M). Cs_2CO_3 (145 mg, 0.45 mmol, 3.0 eq.) was added and the reaction mixture was stirred at 80 °C for 2 h. The reaction mixture was concentrated under a constant stream of nitrogen to afford a brown oil. Brine (30 mL) was added to the crude solid and the resulting mixture was extracted with $CHCl_3$/IPA (9:1, 3 × 20 mL). The combined organic components were dried ($MgSO_4$), filtered, and evaporated *in vacuo* to afford a brown oil. The crude oil was purified by silica gel chromatography (elution with 50% to 100% EtOAc in petroleum ether) to yield (2*R*,24*Z*)-2-methyl-1,2,3,9,10,11,12,18,19,21,22,23-dodecahydro-8*H*,17*H*-14,16-etheno-26,7-(metheno)[1,4]diazepino[2,3-*l*]pyrido[2,1-*d*][1,5]oxazacycloicosin-4(5*H*)-one (**(*R*)104**)

as a colourless solid (15 mg, 22%); R_f 0.37 (EtOAc); $[\alpha]_D^{25}$= +8.5 (*c* 0.8, DMSO); mp 203–206 °C (MeOH); $\bar{\nu}_{max}$ (thin film)/cm^{-1} 2925 (C-H, s), 1656 (C=O, s); ^{1}H NMR (500 MHz; DMSO-d_6) δ_H 9.37 (1H, s, NH-9a), 7.16 (1H, d, *J* 2.0, H-9), 6.79 (1H, d, *J* 14.9, H-14''), 6.73 (1H, d, *J* 8.0, H-5''), 6.64 (1H, d, *J* 2.0, H-7), 6.21 (1H, dt, *J* 14.9, 7.1, H-13''), 6.02 (1H, dd, *J* 8.0, 2.3, H-6''), 5.99 (1H, d, *J* 2.3, H-8''), 4.51 (1H, s, NH-5a), 4.00–3.90 (1H, m, H-4), 3.83 (2H, t, *J* 5.6, H-5'), 3.26–3.13 (4H, m, H-1'', H-10''), 2.58 (2H, t, *J* 6.3, H-3''), 2.56–2.52 (2H, m, H-1'), 2.37 (1H, dd, *J* 12.7, 5.4, H_AH_B-3), 2.29–2.21 (2H, m, H-12''), 2.06 (1H, dd, *J* 12.7, 7.0, H_AH_B-3), 1.85–1.77 (2H, m, H-2''), 1.76–1.61 (6H, m, H-11'', H-2', H-4'), 1.46–1.37 (2H, m, H-3'), 1.20 (3H, d, *J* 6.1. H-10); ^{13}C NMR (126 MHz; DMSO-d_6) δ_C 171.8 (C-2), 158.3 (C-7''), 145.4 (C-9''), 134.4 (C-5a), 134.0 (C-8), 132.6 (C-9a), 131.0 (C-13''), 129.5 (C-6), 129.2 (C-5''), 127.3 (C-14''), 121.8 (C-9), 120.9 (C-7), 114.5 (C-4''), 99.4 (C-6''), 97.7 (C-8''), 67.4 (C-5'), 55.7 (C-4), 48.6 (C-10''), 48.0 (C-1''), 40.4 (C-3), 33.0 (C-1'), 29.4 (C-2'), 29.2 (C-12''), 27.7 (C-4'), 26.8 (C-3''), 24.0 (C-3'), 23.4 (C-11''), 23.1

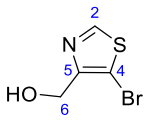
(C-10), 22.0 (C-2''); HRMS *m/z* (ESI$^+$) [Found: 460.2952, $C_{29}H_{38}N_3O_2$ requires M^+ 460.2959]; LRMS *m/z* (ESI$^+$) 460 ([M+H]$^+$, 100%); HPLC Method 1: Retention time 13.5 min, purity 95.4%. (Gradient method of 10 min from 95:5 H_2O:MeCN to 5:95 H_2O:MeCN with a 10 min hold). Structure confirmed by X-ray crystallography (See Appendix E).

Ethyl 5-bromothiazole-4-carboxylate (128)



A solution of $NaNO_2$ (332 mg) in H_2O (2 mL) was added dropwise to a suspension of ethyl 2-amino-5-bromothiazole-4-carboxylate (**127**) (1.00 g, 3.98 mmol, 1.0 eq.) in 50% aq. H_2SO_4 (31 mL) at −5 °C. The resulting diazonium solution was added dropwise to 50% aq. H_3PO_2 (6 mL) at −5 °C (CARE: The reaction temperature was not allowed to exceed 5 °C). The solution was stirred at −5 °C for 2 h. The reaction mixture was diluted with H_2O (50 mL) and extracted with EtOAc (3 × 50 mL). The combined organic components were washed with brine (50 mL), dried ($MgSO_4$), filtered and evaporated *in vacuo* to yield ethyl 5-bromothiazole-4-carboxylate (**128**) as a brown solid (620 mg, 66%); R_f 0.40 (EtOAc/petroleum ether 1:1); mp 68–70 °C (EtOAc); ^{1}H NMR (400 MHz; $CDCl_3$) δ_H 8.79 (1H, s, H-2), 4.45 (2H, q, *J* 7.1, H-7), 1.44 (3H, t, *J* 7.1, H-8); LRMS *m/z* (ESI$^+$) 257 ([M+Na]$^+$, 49%), 259 ([M+Na]$^+$, 51%). These data are in accordance with the literature.[99]

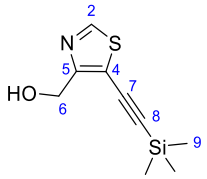
(5-Bromothiazol-4-yl)methanol (129)



$NaBH_4$ (195 mg, 5.14 mmol, 2.0 eq.) was added portionwise to a solution of ethyl 5-bromothiazole-4-carboxylate (**128**) (607 mg, 2.57 mmol, 1.0 eq.) and $CaCl_2$ (1.14 g, 10.3 mmol, 4.0 eq.) in THF (2 mL) and H_2O (4 mL) at 0 °C and reaction mixture was stirred at 0 °C for 3 h. Acetone (1 mL) and 6 M aq. HCl (1 mL) was added and the reaction mixture was stirred for 30 min. The reaction mixture was extracted with EtOAc (3 × 20 mL). The combined organic components were washed with brine (50 mL), dried ($MgSO_4$), filtered and evaporated *in vacuo* to to afford a brown oil. The crude oil was purified by silica gel chromatography (elution with 0% to 75% EtOAc in petroleum ether) to yield (5-bromothiazol-4-

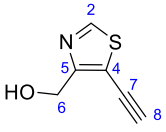
yl)methanol (**129**) as a pale yellow solid (268 mg, 54%); R_f 0.25 (EtOAc/petroleum ether 1:1); mp 53–55 °C (EtOAc); ^{1}H NMR (400 MHz; $CDCl_3$) δ_H 8.78 (1H, s, H-2), 4.76 (2H, s, H-6), 2.38 (1H, s, OH-6); LRMS *m/z* (ESI$^+$) 193 ([M+H]$^+$, 50%), 195 ([M+H]$^+$, 50%). These data are in accordance with the literature.[100]

(5-((Trimethylsilyl)ethynyl)thiazol-4-yl)methanol (130)



A solution of (5-bromothiazol-4-yl)methanol (**129**) (260 mg, 1.34 mmol, 1.0 eq.) in DMF (1 mL) was added to bis(triphenylphosphine)palladium(II) dichloride (19.0 mg, 0.0268 mmol, 0.02 eq.) and copper(I) iodide (8.00 mg, 0.0536 mmol, 0.04 eq.) in a Schlenk flask at rt under a nitrogen atmosphere (evacuated and backfilled 3 × nitrogen). Triethylamine (0.4 mL) was added, followed by trimethylsilylacetylene (229 µL, 1.61 mmol, 1.2 eq.) and the suspension was stirred at 90 °C under a nitrogen atmosphere for 2 h. The suspension was evaporated *in vacuo* and the residue was suspended in sat. aq. H_2O (50 mL). The suspension was extracted with EtOAc (3 × 30 mL). The combined organic components were washed with brine (20 mL), dried ($MgSO_4$), filtered, and evaporated *in vacuo* to afford a brown oil. The crude oil was purified by silica gel chromatography (elution with 0% to 75% EtOAc in petroleum ether) to yield (5-((trimethylsilyl)ethynyl)thiazol-4-yl)methanol (**130**) as a yellow oil (120 mg, 42%); R_f 0.30 (EtOAc/petroleum ether 1:1); ^{1}H NMR (400 MHz; $CDCl_3$) δ_H 8.64 (1H, s, H-2), 4.84 (2H, d, *J* 4.5, H-6), 2.47 (1H, s, OH-6), 0.26 (9H, s, H-9); LRMS *m/z* (ESI$^+$) 212 ([M+H]$^+$, 100%). These data are in accordance with the literature.[100]

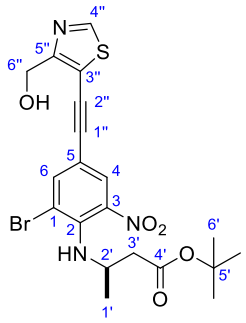
(5-Ethynylthiazol-4-yl)methanol (131)



K_2CO_3 (19.0 mg, 0.133 mmol, 0.1 eq.) was added to a solution of (5-((trimethylsilyl)ethynyl)thiazol-4-yl)methanol (**130**) (282 mg, 1.33 mmol, 1.0 eq.) in MeOH (0.5 mL) and the reaction mixture was stirred at rt for 5 min. 10% aq. Citric acid (5 mL) was added to the reaction mixture and stirred at rt for 30 min. The reaction mixture was extracted with EtOAc (3 × 20 mL). The combined organic components were

washed with brine (30 mL), dried ($MgSO_4$), filtered, and evaporated *in vacuo* to yield (5-ethynylthiazol-4-yl)methanol (**131**) as a brown solid (162 mg, 88%); R_f 0.25 (EtOAc/petroleum ether 3:2); mp 53–55 °C (EtOAc); ^{1}H NMR (400 MHz; $CDCl_3$) δ_H 8.68 (1H, s, H-2), 4.86 (2H, d, *J* 6.2, H-6), 3.60 (1H, s, H-8), 2.41 (1H, t, *J* 6.2, OH-6); LRMS *m/z* (ESI$^+$) 140 ([M+H]$^+$, 100%). These data are in accordance with the literature.[99]

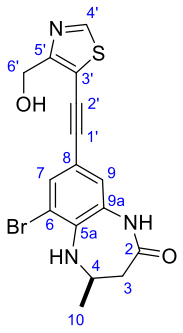
tert-Butyl (*R*)-3-((2-bromo-4-((4-(hydroxymethyl)thiazol-5-yl)ethynyl)-6-nitrophenyl)amino)butanoate (132)



A solution of *tert*-butyl (*R*)-3-((2-bromo-4-iodo-6-nitrophenyl)amino)butanoate (**(*R*)119**) (634 mg, 1.31 mmol, 1.0 eq.) in THF (3.6 mL) was added to (5-ethynylthiazol-4-yl)methanol (220 mg, 1.58 mmol, 1.2 eq.), bis(triphenylphosphine)palladium(II) dichloride (18.0 mg, 0.0262 mmol, 0.02 eq.) and copper(I) iodide (7.00 mg, 0.0393 mmol, 0.03 eq.) at rt under an argon atmosphere (evacuated and backfilled 3 × argon). Triethylamine (2.1 mL) was added and the suspension was stirred at rt under an argon atmosphere for 19 h. The reaction mixture was evaporated *in vacuo* to afford an orange oil. The oil was diluted with EtOAc (100 mL) and washed with sat. aq. $NaHCO_3$ (3 × 70 mL). The organic component was washed with brine (50 mL), dried ($MgSO_4$), filtered, and evaporated *in vacuo* to afford an orange oil. The crude oil was purified by silica gel chromatography (elution with 0% to 60% EtOAc in petroleum ether) to yield *tert*-butyl (*R*)-3-((2-bromo-4-((4-(hydroxymethyl)thiazol-5-yl)ethynyl)-6-nitrophenyl)amino)butanoate (**(*R*)132**) as an orange oil (633 mg, 98%); R_f 0.27 (EtOAc/petroleum ether 2:3); $[\alpha]_D^{25}$= −82.0 (*c* 1.0, $CHCl_3$); $\bar{\nu}_{max}$ (neat)/cm^{-1} 3349 (N-H, w), 2977 (C-H, w), 2361 (C≡C, w), 1723 (C=O, s), 1533 (N-O, s); ^{1}H NMR (500 MHz; $CDCl_3$) δ_H 8.72 (1H, s, H-4''), 8.08 (1H, d, *J* 2.0, H-6), 7.84 (1H, d, *J* 2.0, H-4), 6.70 (1H, d, *J* 9.9, NH-2), 4.88 (2H, d, *J* 6.2, H-6''), 4.32 (1H, m, H-2'), 2.53–2.42 (3H, m, H-3', OH-6''), 1.40 (9H, s, H-6'), 1.32 (3H, d, *J* 6.5, H-1'); ^{13}C NMR (126 MHz; $CDCl_3$) δ_C 170.3 (C-4'), 159.7 (C-5''), 153.3 (C-4''), 142.9 (C-2), 141.6 (C-6), 139.3 (C-3), 129.0 (C-4), 114.9 (C-1), 114.5 (C-3''), 113.3 (C-5), 95.4 (C-1''), 81.5 (C-5'), 79.2 (C-2''), 59.5 (C-6''), 50.0 (C-2'), 43.5 (C-3'), 28.1 (C-6'), 21.5 (C-1');

HRMS *m/z* (ESI$^+$) [Found: 496.0536, $C_{20}H_{23}{}^{79}BrN_3O_5{}^{32}S$ requires M^+ 496.0536]; LRMS *m/z* (ESI$^-$) 494 ([M-H]$^-$, 50%), 496 ([M-H]$^-$, 50%); HPLC Method 1: Retention time 11.5 min, purity 98.7%.

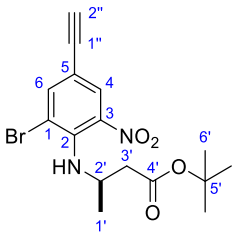
(*R*)-6-Bromo-8-((4-(hydroxymethyl)thiazol-5-yl)ethynyl)-4-methyl-1,3,4,5-tetrahydro-2*H*-benzo[*b*][1,4]diazepin-2-one ((*R*)134)



To a solution of *tert*-butyl (*R*)-3-((2-bromo-4-((4-(hydroxymethyl)thiazol-5-yl)ethynyl)-6-nitrophenyl)amino)butanoate (**(*R*)132**) (280 mg, 0.569 mmol 1.0 eq.) in CH_2Cl_2 (2 mL) was added trifluoroacetic acid (2 mL) and the orange solution was stirred at rt for 2 h. The reaction mixture was evaporated *in vacuo* and the resulting residue was dissolved in glacial acetic acid (5 mL). Iron powder (159 mg, 2.84 mmol, 5.0 eq.) was added and the brown suspension was stirred under reflux for 4 h. 1 M aq. K_2CO_3 (50 mL) was added to the cooled suspension and the resulting mixture was extracted with $CHCl_3$/IPA (9:1, 3 × 30 mL). The combined organic components were washed with brine (50 mL), dried ($MgSO_4$), filtered, and evaporated *in vacuo* to afford a brown oil. The crude oil was dissolved in THF/MeOH/H_2O (3:2:1, 5.4 mL) and LiOH (137 mg) was added. The reaction mixture was stirred at rt for 6 h. The mixture was evaporated *in vacuo* and the resulting residue was diluted with H_2O (25 mL) and was extracted with $CHCl_3$/IPA (9:1, 3 × 15 mL). The combined organic components were washed with brine (25 mL), dried ($MgSO_4$), filtered, and evaporated *in vacuo* to afford a yellow oil. The crude oil was purified by silica gel chromatography (elution with 0% to 5% EtOH in EtOAc) to yield (*R*)-6-bromo-8-((4-(hydroxymethyl)thiazol-5-yl)ethynyl)-4-methyl-1,3,4,5-tetrahydro-2*H*-benzo[*b*][1,4]diazepin-2-one (**(*R*)134**) as a colourless solid (70 mg, 31%); R_f 0.30 (EtOAc); $[\alpha]_D^{25}$= +14.6 (*c* 1.0, MeOH); mp 198–201 °C (EtOAc); $\bar{\nu}_{max}$ (neat)/cm^{-1} 3399 (N-H, w), 3052 (C-H, w), 1636 (C=O, s); ^{1}H NMR (500 MHz; CD_3OD) δ_H 8.94 (1H, s, H-4'), 7.57 (1H, d, *J* 1.9, H-7), 7.13 (1H, d, *J* 1.9, H-9), 4.82 (2H, s, H-6'), 4.21–4.11 (1H, m, H-4), 2.65 (1H, dd, *J* 13.7, 3.8, H_AH_B-3), 2.48 (1H, dd, *J* 13.7, 8.0, H_AH_B-3), 1.41 (3H, d, *J* 6.3, H-10); ^{13}C NMR (126 MHz; CD_3OD) δ_C 174.7 (C-2), 160.3 (C-5'), 155.0 (C-4'), 139.5 (C-5a), 132.9 (C-7), 129.5 (C-9a), 125.8 (C-9), 117.2 (C-3'), 115.6 (C-6), 115.1 (C-8), 97.8 (C-1'), 78.6 (C-2'), 59.0 (C-6'), 55.6 (C-4), 42.0 (C-3), 24.1 (C-10); HRMS *m/z* (ESI$^+$) [Found: 413.9884,

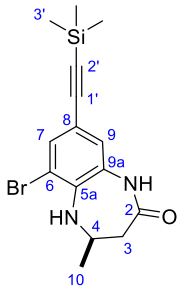
$C_{16}H_{14}{}^{79}BrN_3{}^{23}NaO_2$ requires M^+ 413.9882]; LRMS *m/z* (ESI^+) 392 ($[M+H]^+$, 51%), 394 ($[M+H]^+$, 49%); HPLC Method 1: Retention time 7.9 min, 97.9%.

tert-Butyl (*R*)-3-((2-bromo-4-ethynyl-6-nitrophenyl)amino)butanoate ((*R*)136)



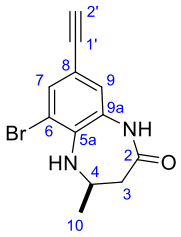
A solution of *tert*-butyl (*R*)-3-((2-bromo-4-iodo-6-nitrophenyl)amino)butanoate (**(*R*)119**) (427 mg, 0.882 mmol, 1.0 eq.) in THF (2.4 mL) was added to bis(triphenylphosphine)palladium(II) dichloride (13.0 mg, 0.0176 mmol, 0.02 eq.) and copper(I) iodide (5.00 mg, 0.0265 mmol, 0.03 eq.) at rt under an argon atmosphere (evacuated and backfilled 3 × argon). Triethylamine (1.5 mL) followed by ethynyltrimethylsilane (150 µL, 1.06 mmol, 1.2 eq.) were added and the suspension was stirred at rt under an argon atmosphere for 18 h. The reaction mixture was evaporated *in vacuo* to afford an orange oil. The oil was diluted with EtOAc (100 mL) and washed with sat. aq. $NaHCO_3$ (3 × 70 mL). The organic component was washed with brine (50 mL), dried ($MgSO_4$), filtered, and evaporated *in vacuo* to afford an orange oil. The crude oil was purified by silica gel chromatography (elution with 0% to 50% EtOAc in petroleum ether) to yield an orange oil (359 mg). The orange oil was dissolved in MeOH (0.5 mL) and K_2CO_3 (11 mg) was added and the reaction mixture was stirred at rt for 30 min. 1 M aq. K_2CO_3 (20 mL) was added and the mixture was extracted with EtOAc (3 × 20mL). The combined organic components were washed with brine (20 mL), dried ($MgSO_4$), filtered and evaporated *in vacuo* to afford an orange oil. The crude oil was purified by silica gel chromatography (elution with 0% to 10% EtOAc in petroleum ether) to yield *tert*-butyl (*R*)-3-((2-bromo-4-ethynyl-6-nitrophenyl)amino)butanoate (**(*R*)136**) as an orange oil (227 mg, 67%); R_f 0.40 (EtOAc/petroleum ether 1:9); $[\alpha]_D^{25}$= −98.4 (*c* 1.0, $CHCl_3$); $\bar{\nu}_{max}$ (thin film)/cm^{-1} 3290 (N-H, w), 2976 (C-H, w), 2109 (C≡C, w), 1724 (C=O, s), 1529 (N-O, s); ^1H NMR (500 MHz; $CDCl_3$) δ_H 8.05 (1H, d, *J* 2.0, H-6), 7.80 (1H, d, *J* 2.0, H-4), 6.60 (1H, d, *J* 10.0, NH-2), 4.29 (1H, m, H-2'), 3.08 (1H, s, H-2''), 2.51–2.40 (2H, m, H-3'), 1.39 (9H, s, H-6'), 1.30 (3H, d, *J* 6.6, H-1'); ^{13}C NMR (126 MHz; $CDCl_3$) δ_C 170.3 (C-4'), 142.8 (C-2), 142.3 (C-4), 139.4 (C-3), 129.6 (C-6), 115.0 (C-5), 113.6 (C-1), 81.4 (C-1''), 80.4 (C-2''), 78.6 (C-5'), 50.0 (C-2'), 43.5 (C-3'), 28.1 (C-6'), 21.5 (C-1'); HRMS *m/z* (ESI^+) [Found: 405.0421, $C_{16}H_{20}{}^{79}BrN_2O_4$ requires M^+ 405.0421]; LRMS *m/z* (ESI^+) 405 ($[M+Na]^+$, 50%), 407 ($[M+Na]^+$, 50%); HPLC Method 1: Retention time 12.4 min. purity 98.7%.

(*R*)-6-Bromo-4-methyl-8-((trimethylsilyl)ethynyl)-1,3,4,5-tetrahydro-2*H*-benzo[*b*][1,4]diazepin-2-one ((*R*)138)



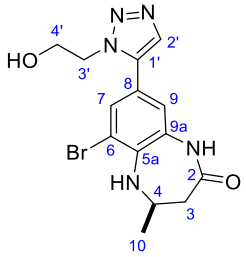
A solution of (*R*)-6-bromo-8-iodo-4-methyl-1,3,4,5-tetrahydro-2*H*-benzo[*b*][1,4]diazepin-2-one (**(*R*)122**) (136 mg, 0.357 mmol, 1.0 eq.) in DMF (1 mL) was added to bis(triphenylphosphine)palladium(II) dichloride (5.00 mg, 0.00714 mmol, 0.02 eq.) and copper(I) iodide (2.00 mg, 0.0107 mmol, 0.03 eq.) at rt under an argon atmosphere (evacuated and backfilled 3 × argon). Triethylamine (0.5 mL) was added, followed by ethynyltrimethylsilane (61.0 µL, 0.428 mmol, 1.2 eq.) and the suspension was stirred at rt under an argon atmosphere for 4 h. The reaction mixture was diluted with EtOAc (75 mL) and washed with sat. aq. $NaHCO_3$ (3 × 30 mL). The organic component was washed with 0.5 M aq. LiCl (3 × 20 mL), brine (30 mL), dried ($MgSO_4$), filtered, and evaporated *in vacuo* to afford a yellow solid. The crude oil was purified by silica gel chromatography (elution with 40% to 80% EtOAc in petroleum ether) to yield (*R*)-6-bromo-4-methyl-8-((trimethylsilyl)ethynyl)-1,3,4,5-tetrahydro-2*H*-benzo[*b*][1,4]diazepin-2-one (**(*R*)138**) as a colourless solid (117 mg, 94%); R_f 0.57 (EtOAc/petroleum ether 1:1); $[\alpha]_D^{25}$= +21.7 (*c* 1.0, MeOH); mp 188–191 °C (EtOAc); $\bar{\nu}_{max}$ (neat)/cm^{-1} 3209 (N-H, w), 2961 (C-H, w), 2150 (C≡C, w), 1676 (C=O, s); ^{1}H NMR (500 MHz; $CDCl_3$) δ_H 7.45 (1H, d, *J* 1.8, H-9), 7.37 (1H, s, NH-9a), 6.91 (1H, d, *J* 1.8, H-7), 4.37 (1H, d, *J* 2.3, NH-5a), 4.15–4.04 (1H, m, H-4), 2.63 (1H, dd, *J* 13.8, 3.5, H_AH_B-3), 2.48 (1H, dd, *J* 13.8, 8.3, H_AH_B-3), 1.39 (3H, d, *J* 6.3, H-10), 0.23 (9H, s, H-3'); ^{13}C NMR (126 MHz; $CDCl_3$) δ_C 172.0 (C-2), 137.0 (C-5a), 132.7 (C-9), 126.8 (C-9a), 125.0 (C-7), 115.4 (C-8), 114.7 (C-6), 102.9 (C-1'), 94.7 (C-2'), 53.6 (C-4), 41.6 (C-3), 24.2 (C-10), 0.1 (C-3'); HRMS *m/z* (ESI$^+$) [Found: 351.0524, $C_{15}H_{20}{}^{79}BrN_2O^{28}Si$ requires M^+ 351.0523]; LRMS *m/z* (ESI$^+$) 351 ([M+H]$^+$, 50%), 353 ([M+H]$^+$, 50%); HPLC Method 1: Retention time 11.7 min, purity 96.0%.

(*R*)-6-Bromo-8-ethynyl-4-methyl-1,3,4,5-tetrahydro-2*H*-benzo[*b*][1,4]diazepin-2-one ((*R*)139)



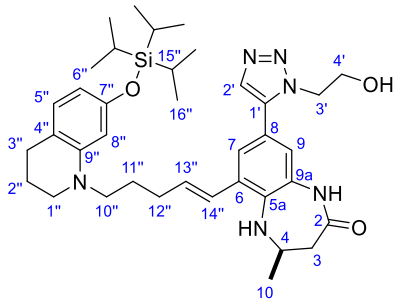
K_2CO_3 (5.00 mg, 0.0332 mmol, 0.1 eq.) was added to (*R*)-6-bromo-4-methyl-8-((trimethylsilyl)ethynyl)-1,3,4,5-tetrahydro-2*H*-benzo[*b*][1,4]diazepin-2-one (**(*R*)138**) (113 mg, 0.332 mmol, 1.0 eq.) in MeOH (1 mL) and the reaction mixture was stirred at rt for 30 min. The reaction mixture was evaporated *in vacuo* to afford a colourless oil. 1 M aq. K_2CO_3 (30 mL) was added to the oil and the resulting mixture was extracted with EtOAc (3 × 20 mL). The combined organic components were washed with brine (30 mL), dried ($MgSO_4$), filtered, and evaporated *in vacuo* to afford a brown oil. The crude oil was purified by silica gel chromatography (elution with 50% to 100% EtOAc in petroleum ether) to yield (*R*)-6-bromo-8-ethynyl-4-methyl-1,3,4,5-tetrahydro-2*H*-benzo[*b*][1,4]diazepin-2-one (**(*R*)139**) as a colourless solid (86 mg, 93%); R_f 0.43 (EtOAc/petroleum ether 4:1); $[\alpha]_D^{25}$= +21.1 (*c* 0.5, MeOH); mp 190–193 °C (EtOAc); $\bar{\nu}_{max}$ (neat)/cm^{-1} 3290 (N-H, w), 2969 (C-H, w), 2361 (C≡C, w), 1673 (C=O, s); ^{1}H NMR (500 MHz; CD_3OD) δ_H 7.44 (1H, d, *J* 1.8, H-9), 7.04 (1H, d, *J* 1.8, H-7), 4.21–4.00 (1H, m, H-4), 3.45 (1H, s, H-2'), 2.58 (1H, dd, *J* 13.6, 4.0, H_AH_B-3), 2.41 (1H, dd, *J* 13.6, 8.0, H_AH_B-3), 1.36 (3H, d, *J* 6.3, H-10); ^{13}C NMR (126 MHz; CD_3OD) δ_C 174.8 (C-2), 139.2 (C-5a), 133.4 (C-9), 129.9 (C-9a), 126.3 (C-7), 115.9 (C-6), 115.7 (C-8), 82.6 (C-1'), 78.5 (C-2'), 56.0 (C-4), 41.8 (C-3), 24.1 (C-10); HRMS *m/z* (ESI^+) [Found: 279.0129, $C_{12}H_{12}{}^{79}BrN_2O$ requires M^+ 279.0128]; LRMS *m/z* (ESI^+) 301 ([M+Na]$^+$, 50%), 303 ([M+Na]$^+$, 50%); HPLC Method 1: Retention time 8.6 min, purity 96.0%.

(*R*)-6-Bromo-8-(1-(2-hydroxyethyl)-1*H*-1,2,3-triazol-5-yl)-4-methyl-1,3,4,5-tetrahydro-2*H*-benzo[*b*][1,4]diazepin-2-one ((*R*)140)



A solution of 2-azidoethanol (37 mg, 0.43 mmol, 1.1 eq.) in THF (2.5 mL) was added to (*R*)-6-bromo-8-ethynyl-4-methyl-1,3,4,5-tetrahydro-2*H*-benzo[*b*][1,4]diazepin-2-one (**(*R*)139**) (79 mg, 0.39 mmol, 1.0 eq.) and pentamethylcyclopentadienylbis(triphenylphosphine)ruthenium(II) chloride (16 mg, 0.019 mmol, 0.05 eq.) at rt under a nitrogen atmosphere (evacuated and backfilled 3 × nitrogen). The reaction mixture was stirred at 75 °C under nitrogen for 1 h. The reaction mixture was purified by silica gel chromatography (elution with 0% to 10% EtOH in EtOAc) to yield (*R*)-6-bromo-8-(1-(2-hydroxyethyl)-1*H*-1,2,3-triazol-5-yl)-4-methyl-1,3,4,5-tetrahydro-2*H*-benzo[*b*][1,4]diazepin-2-one (**(*R*)140**) as a pale yellow solid (74 mg, 52%); R_f 0.07 (EtOAc); $[\alpha]_D^{25}$= −16.4 (*c* 0.5, $CHCl_3$); mp 218–222 °C (CH_2Cl_2); $\bar{\nu}_{max}$ (neat)/cm^{-1} 3263 (N-H, w), 2922 (C-H, w), 1680 (C=O, s); ^{1}H NMR (500 MHz; $CDCl_3$) δ_H 8.29 (1H, s, NH-9a), 7.69 (1H, s, H-2'), 7.42 (1H, d, *J* 2.0, H-9), 7.05 (1H, d, *J* 2.0, H-7), 4.54 (1H, d, *J* 2.2, NH-5a), 4.45–4.36 (2H, m, H-3'), 4.20 (2H, t, *J* 5.4, H-4'), 4.07–4.08 (1H, m, H-4), 3.13 (1H, s, OH-4'), 2.72 (1H, dd, *J* 14.2, 3.2, H_AH_B-3), 2.59 (1H, dd, *J* 14.2, 8.4, H_AH_B-3), 1.44 (3H, d, *J* 6.4, H-10); ^{13}C NMR (126 MHz; $CDCl_3$) δ_C 172.8 (C-2), 137.3 (C-5a), 137.0 (C-1'), 132.9 (C-2'), 129.6 (C-9), 126.8 (C-9a), 122.1 (C-7), 118.5 (C-8), 115.2 (C-6), 61.4 (C-4'), 52.8 (C-4), 50.4 (C-3'), 42.2 (C-3), 24.2 (C-10); HRMS *m/z* (ESI^+) [Found: 366.0562, $C_{14}H_{17}{}^{79}BrN_5O_2$ requires M^+ 366.0562]; LRMS *m/z* (ESI^+) 366 ([M+Na]$^+$, 50%), 368 ([M+Na]$^+$, 50%); HPLC Method 1: Retention time 6.4 min, purity 93.6%.

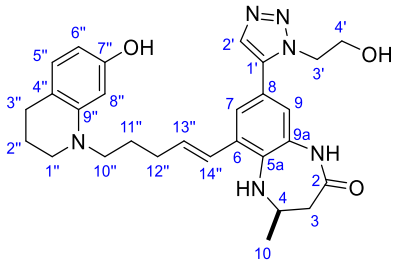
(*R,E*)-8-(1-(2-Hydroxyethyl)-1*H*-1,2,3-triazol-5-yl)-4-methyl-6-(5-(7-((triisopropylsilyl)oxy)-3,4-dihydroquinolin-1(2*H*)-yl)pent-1-en-1-yl)-1,3,4,5-tetrahydro-2*H*-benzo[*b*][1,4]diazepin-2-one ((*R*)141)



(*R*)-6-Bromo-8-(1-(2-hydroxyethyl)-1*H*-1,2,3-triazol-5-yl)-4-methyl-1,3,4,5-tetrahydro-2*H*-benzo[*b*][1,4]diazepin-2-one (**(*R*)140**) (54.0 mg, 0.147 mmol, 1.0 eq.), bis(triphenylphosphine)palladium(II) dichloride (5.00 mg, 0.00735 mmol, 0.05 eq.) and K_2CO_3 (61.0 mg, 0.441 mmol, 3.0 eq.) were added to a Schlenk flask under a nitrogen atmosphere (evacuated and backfilled 3 × nitrogen). (*E*)-1-(5-(4,4,5,5-Tetramethyl-1,3,2-dioxaborolan-2-yl)pent-4-en-1-yl)-7-((triisopropylsilyl)oxy)-1,2,3,4-tetrahydroquinoline (**116**) (111 mg, 0.221 mmol, 1.5 eq.) in 1,4-dioxane (1 mL) was added, followed by H_2O (0.25 mL) and the reaction mixture was stirred at 100 °C for 20 h. The reaction mixture was evaporated *in vacuo* and diluted with EtOAc (50 mL). The organic component was washed with brine (3 × 20 mL), dried ($MgSO_4$), filtered, and evaporated *in vacuo* to afford a orange oil. The crude oil was purified by silica gel chromatography (elution with 0% to 10% EtOH in EtOAc) to yield (*R,E*)-8-(1-(2-hydroxyethyl)-1*H*-1,2,3-triazol-5-yl)-4-methyl-6-(5-(7-((triisopropylsilyl)oxy)-3,4-dihydroquinolin-1(2*H*)-yl)pent-1-en-1-yl)-1,3,4,5-tetrahydro-2*H*-benzo[*b*][1,4]diazepin-2-one (**(*R*)140**) as a yellow oil (89 mg, 92%); R_f 0.60 (EtOH/EtOAc 1:9); $[\alpha]_D^{25}$= −1.16 (*c* 1.0, $CHCl_3$); $\bar{\nu}_{max}$ (thin film)/cm^{-1} 3350 (O-H, br s), 2942 (C-H, w), 1670 (C=O, s); ^{1}H NMR (500 MHz; $CDCl_3$) δ_H 8.19 (1H, s, NH-9a), 7.69 (1H, s, H-2'), 7.12 (1H, d, *J* 2.0, H-7), 6.98 (1H, d, *J* 2.0, H-9), 6.75 (1H, d, *J* 7.8, H-5''), 6.42 (1H, d, *J* 15.5, H-14''), 6.17–6.05 (3H, m, H-6'', H-8'', H-13''), 4.41 (2H, t, *J* 5.8, H-3'), 4.20–4.14 (2H, m, H-4'), 4.14–4.05 (1H, m, H-4), 3.78 (1H, s, NH-5a), 3.30–3.21 (4H, m, H-1'',H-10''), 2.72–2.64 (3H, m, H_AH_B-3, H-3''), 2.52 (1H, dd, *J* 13.8, 8.0, H_AH_B-3), 2.33–2.27 (2H, m, H-12''), 1.94–1.86 (2H, m, H-2''), 1.82–1.75 (2H, m, H-11''), 1.39 (3H, d, *J* 6.3, H-10), 1.24–1.18 (3H, m, H-15''), 1.08 (18H, d, *J* 7.3, H-16''); ^{13}C NMR (126 MHz; $CDCl_3$) δ_C 173.1 (C-2), 155.4 (C-7''), 146.0 (C-9''), 138.2 (C-1'), 136.8 (C-5a), 136.7 (C-13''), 132.7 (C-2'), 130.8 (C-6), 129.6 (C-5''), 128.2 (C-9a), 125.2 (C-7), 124.7 (C-14''), 121.3 (C-9), 118.7 (C-4''), 115.4 (C-8), 107.2 (C-6''), 102.6 (C-8''), 61.5 (C-4'), 54.0 (C-4), 51.4 (C-10''), 50.4 (C-3'), 49.7 (C-1''), 41.5 (C-3), 31.3 (C-12''), 27.5 (C-3''), 26.0 (C-11''), 24.4 (C-10), 22.6 (C-2''), 18.2 (C-16''), 12.9 (C-15''); HRMS

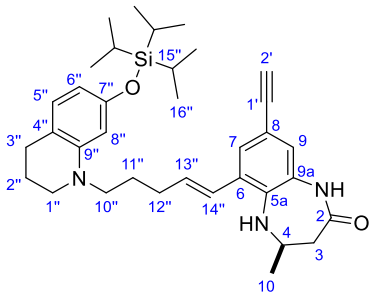
m/z (ESI$^+$) [Found: 659.4096, $C_{37}H_{55}N_6O_3{}^{28}Si$ requires M^+ 659.4099]; LRMS *m/z* (ESI$^+$) 659 ([M+H]$^+$, 100%); HPLC Method 1: Retention time 8.4 min, purity 94.7 %.

(*R,E*)-6-(5-(7-Hydroxy-3,4-dihydroquinolin-1(2*H*)-yl)pent-1-en-1-yl)-8-(1-(2-hydroxyethyl)-1*H*-1,2,3-triazol-5-yl)-4-methyl-1,3,4,5-tetrahydro-2*H*-benzo[*b*][1,4]diazepin-2-one ((*R*)142)



To a solution of (*R,E*)-8-(1-(2-hydroxyethyl)-1*H*-1,2,3-triazol-5-yl)-4-methyl-6-(5-(7-((triisopropylsilyl)oxy)-3,4-dihydroquinolin-1(2*H*)-yl)pent-1-en-1-yl)-1,3,4,5-tetrahydro-2*H*-benzo[*b*][1,4]diazepin-2-one (**(*R*)141**) (102 mg, 0.155 mmol, 1.0 eq.) in EtOH (1.3 mL) and CH_2Cl_2 (0.5 mL) was added 2 M aq. HCl (2 mL) and the reaction mixture was stirred at 80 °C for 16 h. The reaction mixture was evaporated *in vacuo* to afford an orange residue. Sat. aq. $NaHCO_3$ (50 mL) was added to the residue and the resulting mixture extracted with $CHCl_3$/IPA (9:1, 3 × 30 mL). The combined organic components were washed with brine (50 mL), dried ($MgSO_4$), filtered, and evaporated *in vacuo* to afford a dark orange oil. The crude oil was purified by silica gel chromatography (elution with 0% to 10% EtOH in EtOAc) to yield (*R,E*)-6-(5-(7-hydroxy-3,4-dihydroquinolin-1(2*H*)-yl)pent-1-en-1-yl)-8-(1-(2-hydroxyethyl)-1*H*-1,2,3-triazol-5-yl)-4-methyl-1,3,4,5-tetrahydro-2*H*-benzo[*b*][1,4]diazepin-2-one (**(*R*)142**) as a pale brown oil (65 mg, 83%); R_f 0.26 (EtOH/EtOAc 1:9); $[\alpha]_D^{25}$= +11.2 (*c* 1.0, MeOH); $\bar{\nu}_{max}$ (thin film)/cm^{-1} 3320 (O-H, br s), 2927 (C-H, w), 1664 (C=O, s); ^{1}H NMR (500 MHz; CD_3OD) δ_H 7.74 (1H, s, H-2'), 7.41 (1H, d, *J* 2.1, H-7), 7.05 (1H, d, *J* 2.1, H-9), 6.75–6.59 (2H, m, H-5'', H-14''), 6.27 (1H, dt, *J* 14.7, 7.7, H-13''), 6.10 (1H, d, *J* 2.3, H-8''), 5.97 (1H, dd, *J* 7.9, 2.3, H-6''), 4.48 (2H, t, *J* 5.5, H-3'), 4.13 (1H, m, H-4), 3.99 (2H, t, *J* 5.5, H-4'), 3.32–3.24 (4H, m, H-1'', H-10''), 2.67–2.54 (3H, m, H_AH_B-3, H-3''), 2.43–2.32 (3H, m, H_AH_B-3, H-12''), 1.94–1.86 (2H, m, H-2''), 1.85–1.76 (2H, m, H-11''), 1.34 (3H, d, *J* 6.2, H-10); ^{13}C NMR (126 MHz; CD_3OD) δ_C 175.4 (C-2), 157.4 (C-7''), 147.4 (C-9''), 140.3 (C-1'), 138.9 (C-5a), 136.2 (C-13''), 133.2 (C-2'), 132.6 (C-8), 131.8 (C-9a), 130.5 (C-6), 126.4 (C-5''), 125.6 (C-14''), 122.5 (C-7), 120.2 (C-9), 115.2 (C-4''), 103.5 (C-6''), 99.2 (C-8''), 61.6 (C-4'), 57.1 (C-4), 52.0 (C-10''), 51.6 (C-3'), 50.4 (C-1''), 41.4 (C-3), 32.0 (C-12''), 28.5 (C-3''), 26.9 (C-11''), 24.0 (C-10), 23.8 (C-2''); HRMS *m/z* (ESI$^+$) [Found: 503.2763, $C_{28}H_{35}N_6O_3$ requires M^+ 503.2765]; LRMS *m/z* (ESI$^+$) 503 ([M+H]$^+$, 100%); HPLC Method 1: Retention time 8.3 min, purity 95.8%.

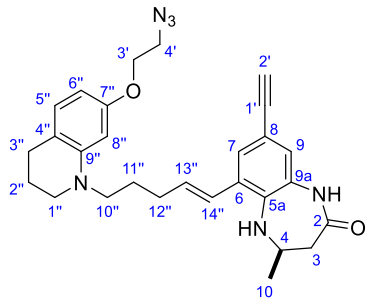
(*R,E*)-8-Ethynyl-4-methyl-6-(5-(7-((triisopropylsilyl)oxy)-3,4-dihydroquinolin-1(2*H*)-yl)pent-1-en-1-yl)-1,3,4,5-tetrahydro-2*H*-benzo[*b*][1,4]diazepin-2-one ((*R*)144)



(*R*)-6-Bromo-4-methyl-8-((trimethylsilyl)ethynyl)-1,3,4,5-tetrahydro-2*H*-benzo[*b*][1,4]diazepin-2-one (**(*R*)138**) (200 mg, 0.568 mmol, 1.0 eq.), bis(triphenylphosphine)palladium(II) dichloride (20.0 mg, 0.0269 mmol, 0.05 eq.) and K_2CO_3 (236 mg, 1.71 mmol, 3.0 eq.) were added to a Schlenk flask under a nitrogen atmosphere (evacuated and backfilled 3 × nitrogen). (*E*)-1-(5-(4,4,5,5-Tetramethyl-1,3,2-dioxaborolan-2-yl)pent-4-en-1-yl)-7-((triisopropylsilyl)oxy)-1,2,3,4-tetrahydroquinoline (**116**) (426 mg, 0.853 mmol, 1.5 eq.) in 1,4-dioxane (3.6 mL) was added, followed by H_2O (0.9 mL) and the reaction mixture was stirred at 100 °C for 18 h. The reaction mixture was evaporated *in vacuo* and diluted with EtOAc (50 mL). The organic component was washed with brine (3 × 20 mL), dried ($MgSO_4$), filtered, and evaporated *in vacuo* to afford an orange oil. The crude oil was dissolved in MeOH (3 mL) and K_2CO_3 (10 mg) was added. The reaction mixture was stirred at rt for 30 mins. The reaction mixture was evaporated *in vacuo* to afford an orange oil. The crude oil was dissolved in 1 M aq. K_2CO_3 (30 mL) and extracted with EtOAc (3 × 20 mL). The combined organic components were washed with brine (20 mL), dried ($MgSO_4$), filtered, and evaporated *in vacuo* to afford an orange oil. The crude oil was purified by silica gel chromatography (elution with 0% to 50% EtOAc in petroleum ether) to yield (*R,E*)-8-ethynyl-4-methyl-6-(5-(7-((triisopropylsilyl)oxy)-3,4-dihydroquinolin-1(2*H*)-yl)pent-1-en-1-yl)-1,3,4,5-tetrahydro-2*H*-benzo[*b*][1,4]diazepin-2-one (**(*R*)144**) as a yellow oil (167 mg, 51%); R_f 0.21 (EtOAc/petroleum ether 2:3); $[\alpha]_D^{25}$= +5.92 (*c* 1.0, $CHCl_3$); $\bar{\nu}_{max}$ (thin film)/cm^{-1} 3309 (N-H, br s), 2942 (C-H, s), 1672 (C=O, s); ^{1}H NMR (500 MHz; $CDCl_3$) δ_H 7.36 (1H, s, NH-9a), 7.22 (1H, d, *J* 1.9, H-9), 6.91 (1H, d, *J* 1.9, H-7), 6.75 (1H, d, *J* 7.8, H-5''), 6.36 (1H, d, *J* 15.2, H-14''), 6.15–6.04 (3H, m, H-6'', H-8'', H-13''), 4.14–4.05 (1H, m, H-4), 3.67 (1H, br s, NH-5a), 3.32–3.19 (4H, m, H-1'', H-10''), 3.00 (1H, s, H-2'), 2.72–2.57 (3H, m, H-3'', H_AH_B-3), 2.47–2.39 (1H, m, H_AH_B-3), 2.32–2.21 (2H, m, H-12''), 1.96–1.87 (2H, m, H-2''), 1.81–1.73 (2H, m, H-11''), 1.35 (3H, d, *J* 6.3, H-10), 1.27–1.17 (3H, m, H-15''), 1.09 (18H, d, *J* 7.2, H-16''); ^{13}C NMR (126 MHz; $CDCl_3$) δ_C 172.4 (C-2), 155.4 (C-7''), 146.0 (C-9''), 136.7 (C-5a), 136.3 (C-14''), 130.4 (C-9a), 129.6 (C-5''), 128.5 (C-9), 128.2 (C-6), 124.7 (C-13''), 124.5 (C-7), 115.3 (C-4''), 114.1 (C-8), 107.2 (C-6''), 102.6 (C-8''), 83.2 (C-1'), 76.5 (C-2'), 54.4 (C-4), 51.3 (C-1''), 49.6 (C-10''), 41.0

(C-3), 31.3 (C-12''), 27.5 (C-3''), 26.0 (C-11''), 24.3 (C-10), 22.7 (C-2''), 18.2 (C-16''), 12.9 (C-15''); HRMS *m/z* (ESI$^+$) [Found: 572.3665, $C_{35}H_{50}N_3O_2{}^{28}Si$ requires M^+ 572.3667]; LRMS *m/z* (ESI$^+$) 572 ($[M+H]^+$, 100%); HPLC Method 1: Retention time 17.3 min, purity 91.3 %. (Gradient method of 10 min from 95:5 H_2O:MeCN to 5:95 H_2O:MeCN with a 10 min hold).

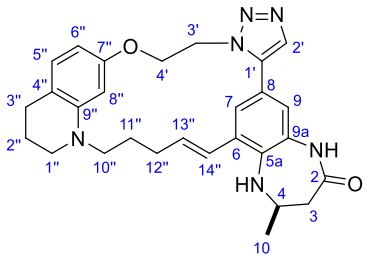
(*R,E*)-6-(5-(7-(2-Azidoethoxy)-3,4-dihydroquinolin-1(2*H*)-yl)pent-1-en-1-yl)-8-ethynyl-4-methyl-1,3,4,5-tetrahydro-2H-benzo[*b*][1,4]diazepin-2-one ((*R*)145)



To a solution of (*R,E*)-8-ethynyl-4-methyl-6-(5-(7-((triisopropylsilyl)oxy)-3,4-dihydroquinolin-1(2*H*)-yl)pent-1-en-1-yl)-1,3,4,5-tetrahydro-2*H*-benzo[*b*][1,4]diazepin-2-one (**(*R*)144**) (130 mg, 0.227 mmol, 1.0 eq.) in THF (4.4 mL) was added 1 M TBAF in THF (455 µL, 0.455 mmol, 2.0 eq.) and the reaction mixture was stirred at rt for 1 h. The reaction mixture was evaporated *in vacuo* to afford an orange residue. H_2O (30 mL) was added to the residue and the resulting mixture extracted with $CHCl_3$/IPA (9:1, 3 × 20 mL). The combined organic components were washed with brine (30 mL), dried (Na_2SO_4), filtered, and evaporated *in vacuo* to afford a dark orange oil. The crude oil was purified by silica gel chromatography (elution with 50% to 70% EtOAc in petroleum ether) to yield a brown oil. The brown oil was dissolved in anhydrous DMF (1 mL). K_2CO_3 (51 mg, 0.368 mmol, 1.6 eq.) and 2-azidoethyl methanesulfonate (61 mg, 0.368 mmol, 1.6 eq.) were added to the solution and the reaction mixture was stirred at 65 °C for 16 h. The reaction mixture was diluted with $CHCl_3$/IPA (9:1, 50 mL) and was washed with 0.5 M aq. LiCl (3 × 20 mL), brine (30 mL), dried (Na_2SO_4), filtered and evaporated *in vacuo* to afford a brown oil. The crude oil was purified by silica gel chromatography (elution with 30% to 100% EtOAc in petroleum ether) to yield (*R,E*)-6-(5-(7-(2-azidoethoxy)-3,4-dihydroquinolin-1(2*H*)-yl)pent-1-en-1-yl)-8-ethynyl-4-methyl-1,3,4,5-tetrahydro-2H-benzo[*b*][1,4]diazepin-2-one (**(*R*)145**) as a yellow oil (58 mg, 53%); R_f 0.40 (EtOAc/petroleum ether 7:3); $[\alpha]_D^{25}$= +10.95 (*c* 1.0, $CHCl_3$); $\bar{\nu}_{max}$ (thin film)/cm^{-1} 3287 (N-H, br s), 2361 (C-H, w), 2104 (N=N$^-$=N$^+$, w), 1672 (C=O, s); ^{1}H NMR (500 MHz; $CDCl_3$) δ_H 7.76 (1H, s, NH-9a), 7.23 (1H, d, *J* 1.8, H-9), 6.94 (1H, d, *J* 1.8, H-7), 6.85 (1H, d, *J* 8.0, H-5''), 6.37 (1H, dt, *J* 15.6, 1.6, H-14''), 6.17 (1H, d, *J* 2.5, H-8''), 6.14–6.05 (2H, m, H-6'', H-13''), 4.16–4.00 (3H, m, H-4,

H-3'), 3.68 (1H, s, NH-5a), 3.53 (2H, t, *J* 5.0, H-4'), 3.33–3.14 (4H, m, H-1'', H-10''), 3.01 (1H, s, H-2'), 2.69 (2H, t, *J* 6.3, H-3''), 2.62 (1H, dd, *J* 13.5, 4.1, H_AH_B-3), 2.43 (1H, dd, *J* 13.5, 7.8, H_AH_B-3), 2.35–2.23 (2H, m, H-12''), 1.98–1.86 (2H, m, H-2''), 1.83–1.73 (2H, m, H-11''), 1.35 (3H, d, *J* 6.3, H-10); ^{13}C NMR (126 MHz; $CDCl_3$) δ_C 172.7 (C-2), 158.0 (C-7''), 146.3 (C-9''), 136.7 (C-5a), 136.0 (C-14''), 130.4 (C-9a), 129.7 (C-5''), 128.4 (C-6), 128.3 (C-9), 124.9 (C-13''), 124.5 (C-7), 116.1 (C-4''), 114.1 (C-8), 100.3 (C-6''), 98.4 (C-8''), 83.3 (C-1'), 76.5 (C-2'), 67.1 (C-3'), 54.6 (C-4), 51.0 (C-10''), 50.3 (C-4'), 49.5 (C-1''), 41.0 (C-3), 31.1 (C-12''), 27.5 (C-3''), 25.9 (C-11''), 24.3 (C-10), 22.5 (C-2''); HRMS *m/z* (ESI$^+$) [Found: 485.2659, $C_{28}H_{33}N_6O_2$ requires M^+ 485.2660]; LRMS *m/z* (ESI$^+$) 485 ($[M+H]^+$, 100%).

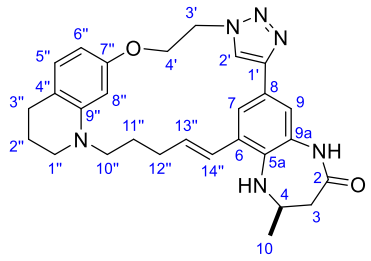
(*R,E*)-1^4-Methyl-1^2,1^3,1^4,1^5,6^1,6^2,6^3,6^4-octahydro-1^1*H*,2^1*H*-5-oxa-1(8,6)-benzo[*b*][1,4]diazepina-6(7,1)-quinolina-2(5,1)-triazolacycloundecaphan-10-en-1^2-one ((*R*)106)



To a solution of (*R,E*)-6-(5-(7-(2-azidoethoxy)-3,4-dihydroquinolin-1(2*H*)-yl)pent-1-en-1-yl)-8-ethynyl-4-methyl-1,3,4,5-tetrahydro-2H-benzo[*b*][1,4]diazepin-2-one (**(*R*)145**) (27 mg, 0.060 mmol, 1.0 eq.) in THF (30 mL) was added to pentamethylcyclopentadienylbis(triphenylphosphine)ruthenium(II) chloride (5.0 mg, 0.0060 mmol, 0.1 eq.) at rt under a nitrogen atmosphere (evacuated and backfilled 3 × nitrogen) and the reaction mixture was stirred at 75 °C under nitrogen for 1 h. The reaction mixture was evaporated *in vacuo* to yield a brown solid. The crude solid was purified by silica gel chromatography (elution with 80% to 100% EtOAc in petroleum ether, followed by 0% to 10% EtOH in EtOAc) to yield (*R,E*)-1^4-methyl-1^2,1^3,1^4,1^5,6^1,6^2,6^3,6^4-octahydro-1^1*H*,2^1*H*-5-oxa-1(8,6)-benzo[*b*][1,4]diazepina-6(7,1)-quinolina-2(5,1)-triazolacycloundecaphan-10-en-1^2-one (**(*R*)106**) as a pale yellow solid (6 mg, 21%); R_f 0.41 (EtOH/EtOAc 1:9); $[\alpha]_D^{25}$= +37.4 (*c* 0.1, DMSO); mp 299–301 °C (MeCN); $\bar{\nu}_{max}$ (thin film)/cm^{-1} 2926 (C-H, w), 2031 (s), 1672 (C=O, s); ^{1}H NMR (500 MHz; DMSO-d_6) δ_H 9.58 (1H, s, NH-9a), 7.70 (1H, s, H-2'), 7.59 (1H, d, *J* 2.0, H-7), 6.85 (1H, d, *J* 2.0, H-9), 6.82–6.74 (2H, m, H-5'', H-14''), 6.30 (1H, dt, *J* 15.1, 7.4, H-13''), 6.08 (1H, dd, *J* 8.1, 2.3, H-6''), 6.04 (1H, d, *J* 2.3, H-8''), 5.01 (1H, d, *J* 2.9, NH-5a), 4.53–4.42 (2H, m, H-3'), 4.34–4.28 (2H, m, H-4'), 4.04 (1H, m, H-4), 3.22 (4H, m, H-1'', H-10''), 2.58 (2H, t, *J* 6.4, H-3''), 2.56–2.51 (1H, m, H_AH_B-3), 2.23 (3H, m, H_AH_B-3, H-12''), 1.88–1.73 (2H, m, H-2''), 1.62 (2H, m, H-11''), 1.27 (3H, d, *J* 6.2, H-10); ^{13}C NMR (126 MHz; DMSO-d_6) δ_C 171.5

(C-2), 157.3 (C-7''), 145.1 (C-9''), 138.9 (C-1'), 137.4 (C-5a), 133.6 (C-13''), 132.5 (C-2'), 129.6 (C-9a, C-6), 129.1 (C-5''), 127.4 (C-14''), 125.1 (C-7), 121.9 (C-9), 117.5 (C-8), 115.4 (C-4''), 98.5 (C-8''), 98.0 (C-6''), 66.7 (C-4'), 54.1 (C-4), 48.0 (C-10''), 47.8 (C-1''), 47.4 (C-3'), 40.8 (C-3), 29.2 (C-12''), 26.6 (C-3''), 23.9 (C-11''), 23.5 (C-10), 22.0 (C-2''); HRMS *m/z* (ESI^+) [Found: 485.2661, $C_{28}H_{33}N_6O_2$ requires M^+ 485.2660]; LRMS *m/z* (ESI^+) 485 ($[M+H]^+$, 100%); HPLC Method 1: Retention time 10.1 min, purity 96.3%.

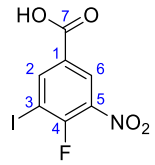
(15*R*,19*Z*)-15-Methyl-2-oxa-5,6,7,12,16,24-hexaazahexacyclo[22.6.2.1^{5,8}.1^{9,18}.0^{11,17}.0^{28,32}] tetratriaconta-1(30),6,8(34),9(33),10,17,19,28,31-nonaen-13-one ((*R*)107)



To a solution of (*R,E*)-6-(5-(7-(2-azidoethoxy)-3,4-dihydroquinolin-1(2*H*)-yl)pent-1-en-1-yl)-8-ethynyl-4-methyl-1,3,4,5-tetrahydro-2H-benzo[*b*][1,4]diazepin-2-one (**(*R*)145**) (30 mg, 0.062 mmol, 1.0 eq.) in THF (15 mL) and H_2O (15 mL) was added copper (II) sulfate (2.0 mg, 0.010 mmol, 0.15 eq.) and (+)-sodium L-ascorbate (2.0 mg, 0.011 mmol, 0.15 eq.) and the blue solution was stirred at rt for 20 h. Copper (II) sulfate (2.0 mg, 0.0101 mmol, 0.15 eq.) and (+)-sodium L-ascorbate (2.0 mg, 0.011 mmol, 0.15 eq.) were added and the reaction mixture was stirred for a further 16 h. Copper (II) sulfate (2.0 mg, 0.010 mmol, 0.15 eq.) and (+)-sodium L-ascorbate (2.0 mg, 0.011 mmol, 0.15 eq.) were added and the reaction mixture was stirred for a further 24 h. Copper (II) sulfate (2.0 mg, 0.010 mmol, 0.15 eq.) and (+)-sodium L-ascorbate (2.0 mg, 0.011 mmol, 0.15 eq.) were added and the reaction mixture was stirred for a further 24 h. The reaction mixture was evaporated *in vacuo* to yield a red solid. The crude solid was purified by silica gel chromatography (elution with 90% to 100% EtOAc in petroleum ether, followed by 0% to 15% EtOH in EtOAc) to yield (15*R*,19*Z*)-15-methyl-2-oxa-5,6,7,12,16,24-hexaazahexacyclo[22.6.2.1^{5,8}.1^{9,18}.0^{11,17}.0^{28,32}]tetratriaconta-1(30),6,8(34),9(33),10,17,19,28,31-nonaen-13-one (**(*R*)107**) as a pale yellow oil (1 mg, 3%); R_f 0.41 (EtOH/EtOAc 1:9); $[\alpha]_D^{25}$= +33.1 (*c* 0.1, DMSO); $\bar{\nu}_{max}$ (thin film)/cm^{-1} 2927 (C-H, w), 1666 (C=O, s); ^{1}H NMR (500 MHz; DMSO-d_6) δ_H 9.56 (1H, s, NH-9a), 8.75 (1H, s, H-2'), 7.37 (1H, d, *J* 2.0, H-7), 7.27 (1H, d, *J* 2.0, H-9), 6.77 (1H, d, *J* 8.1, H-5''), 6.71 (1H, d, *J* 15.1, H-14''), 6.54 (1H, d, *J* 2.3, H-8''), 6.43 (1H, dt, *J* 15.1, 7.3, H-13''), 6.13 (1H, dd, *J* 8.1, 2.3, H-6''), 4.81–4.73 (3H, m, H-3', NH-5a), 4.12 (2H, t, *J* 5.0,

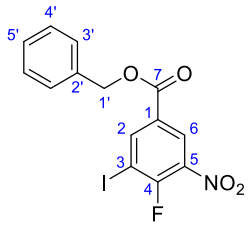
H-4'), 4.02–3.90 (1H, m, H-4), 3.25–3.18 (2H, m, H-1''), 3.16 (2H, t, *J* 5.6, H-10''), 2.58 (2H, t, *J* 6.3, H-3''), 2.44 (1H, dd, *J* 13.1, 4.7, H_AH_B-3), 2.34–2.28 (2H, m, H-12''), 2.17 (1H, dd, *J* 13.1, 7.2, H_AH_B-3), 1.82–1.72 (4H, m, H-2'', H-11''), 1.23 (3H, d, *J* 7.4, H-10); ^{13}C NMR (126 MHz; DMSO-d_6) δ_C 171.6 (C-2), 157.7 (C-7''), 147.1 (C-1'), 146.9 (C-9''), 135.8 (C-5a), 134.2 (C-13''), 130.9 (C-9a), 130.7 (C-6), 129.2 (C-5''), 126.6 (C-14''), 124.5 (C-7), 123.5 (C-2'), 122.7 (C-8), 116.5 (C-4''), 116.4 (C-9), 99.4 (C-6''), 99.3 (C-8''), 67.4 (C-4'), 54.9 (C-4), 49.5 (C-3'), 48.9 (C-1''), 46.9 (C-10''), 40.6 (C-3), 29.0 (C-12''), 27.1 (C-3''), 26.7 (C-11''), 23.5 (C-10), 21.8 (C-2''); HRMS *m/z* (ESI$^+$) [Found: 485.2660, $C_{28}H_{33}N_6O_2$ requires M^+ 485.2660]; LRMS *m/z* (ESI$^+$) 485 ([M+H]$^+$, 100%); HPLC Method 1: Retention time 5.5 min, purity 95.6%.

4-Fluoro-3-iodo-5-nitrobenzoic acid (147)



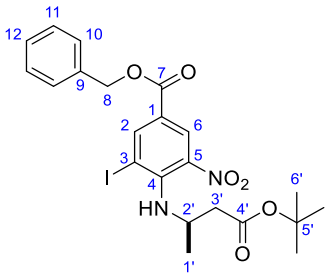
4-Fluoro-3-nitro-benzoic acid (**146**) (200 mg, 1.08 mmol, 1.0 eq.) was added to a solution of iodine (548 mg, 2.16 mmol, 2.0 eq.) in fuming sulfuric acid (2 mL) and the reaction mixture was stirred at 85 °C for 20 h. The cooled reaction mixture was slowly added portionwise to ice (50 g) and the resulting precipitate was extracted with CH_2Cl_2 (3 × 20 mL). The combined organic components were washed with 10% aq. $Na_2S_2O_3$ (20 mL), brine (20 mL), dried (Na_2SO_4), filtered, and evaporated *in vacuo* to yield 4-fluoro-3-iodo-5-nitrobenzoic acid (**147**) as a colourless solid (300 mg, 89%); R_f 0.40 (MeOH/CH_2Cl_2 1:9); mp 155–159 °C (CH_2Cl_2); $\bar{\nu}_{max}$ (neat)/cm^{-1} 3084 (C-H, w), 2822 (COO-H, br w), 1698 (C=O, s), 1535 (N-O, s); ^{1}H NMR (500 MHz; DMSO-d_6) δ_H 13.90 (1H, br s, CO_2H-7), 8.61 (1H, dd, *J* 5.2, 2.1, H-2), 8.49 (1H, dd, *J* 6.5, 2.1, H-6); ^{13}C NMR (126 MHz; DMSO-d_6) δ_C 163.9 (C-7), 156.4 (d, *J* 261.9, C-4), 144.8 (d, *J* 4.2, C-2), 136.8 (d, *J* 11.0, C-5), 129.0 (d, *J* 4.2, C-6), 127.1 (C-1), 86.6 (d, *J* 27.4, C-3); ^{19}F NMR (377 MHz; $CDCl_3$) δ_F −92.8 (dd, *J* 6.5, 5.2); HRMS *m/z* (ESI$^-$) [Found: 309.9017, $C_7H_2O_4NF^{127}I$ requires M^- 309.9018]; LRMS *m/z* (ESI$^-$) 310 ([M-H]$^-$, 100%); HPLC Method 2: Retention time 8.7 min, purity 96.7%.

Benzyl 4-fluoro-3-iodo-5-nitrobenzoate (148)



To a solution of 4-fluoro-3-iodo-5-nitrobenzoic acid (**147**) (1.00 g, 3.21 mmol, 1.0 eq.) in DMF (7 mL) was added K_2CO_3 (668 mg, 4.83 mmol, 1.5 eq.) and the reaction mixture was stirred at rt for 5 mins. Benzyl bromide (574 µL, 4.83 mmol, 1.5 eq.) was added and the reaction mixture was stirred at 60 °C for 4 h. The cooled reaction mixture was diluted with EtOAc (100 mL) and was washed with 1 M aq. K_2CO_3 (3 × 100 mL). The separated organic component was washed with 0.5 M aq. LiCl (3 × 100 mL), brine (100 mL), dried ($MgSO_4$), filtered and evaporated *in vacuo* to afford an orange oil. The crude solid was purified by silica gel chromatography (elution with 0% to 20% EtOAc in petroleum ether) to yield benzyl 4-fluoro-3-iodo-5-nitrobenzoate (**148**) as a yellow oil (833 mg, 64%); R_f 0.39 (EtOAc/petroleum ether 1:4); $\bar{\nu}_{max}$ (neat)/cm^{-1} 3089 (C-H, w), 1726 (C=O, s), 1539 (N-O, s); ^{1}H NMR (500 MHz; $CDCl_3$) δ_H 8.69 (1H, dd, *J* 5.0, 2.1, H-2), 8.66 (1H, dd, *J* 6.6, 2.1, H-6), 7.50–7.33 (5H, m, H-3', H-4', H-5'), 5.40 (2H, s, H-1'); ^{13}C NMR (126 MHz; $CDCl_3$) δ_C 162.6 (C-7), 157.3 (d, *J* 267.6, C-4), 145.6 (d, *J* 3.7, C-2), 137.3 (d, *J* 10.5, C-5), 135.0 (C-2'), 129.02 (C-5'), 128.97 (C-4'), 128.8 (C-3'), 128.4 (d, *J* 4.7, C-1), 127.8 (d, *J* 1.8, C-6), 84.4 (d, *J* 26.7, C-3), 68.3 (C-1'); ^{19}F NMR (377 MHz; $CDCl_3$) δ_F −89.3 (dd, *J* 6.6, 5.0); HPLC Method 1: Retention time 11.7 min, purity 91.9 %.

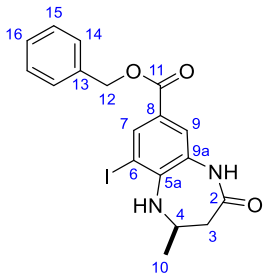
Benzyl (*R*)-4-((4-(tert-butoxy)-4-oxobutan-2-yl)amino)-3-iodo-5-nitrobenzoate ((*R*)149)



To a stirred suspension of 4-fluoro-3-iodo-5-nitrobenzoate (**148**) (816 mg, 2.03 mmol, 1.0 eq.) and Cs_2CO_3 (1.99 g, 6.10 mmol, 3.0 eq.) in toluene (32 mL) at rt was added *tert*-butyl (*R*)-3-aminobutanoate (**(*R*)41**) containing 1.63 eq. acetic acid (733 mg, 2.85 mmol, 1.4 eq.) and the suspension was stirred at

85 °C for 21 h. To the cooled suspension was added 1 M aq. K_2CO_3 (150 mL) and the resulting mixture was extracted with EtOAc (3 × 150 mL). The combined organic components were washed with brine (100 mL), dried ($MgSO_4$), filtered, and evaporated *in vacuo* to afford an orange oil. The crude oil was purified by silica gel chromatography (elution with 10% Et_2O in *n*-hexane) to yield benzyl (*R*)-4-((4-(*tert*-butoxy)-4-oxobutan-2-yl)amino)-3-iodo-5-nitrobenzoate (**(*R*)149**) as a dark orange oil (1.06 g, 97%); R_f 0.21 (Et_2O/hexane 1:4); $[\alpha]_D^{25}$= −35.1 (*c* 1.0, $CHCl_3$); $\bar{\nu}_{max}$ (thin film)/cm^{-1} 3339 (N-H, w), 2978 (C-H, w), 1717 (C=O, m), 1532 (N-O, s), 1251 (C-O, s); ^{1}H NMR (500 MHz; $CDCl_3$) δ_H 8.59 (1H, d, *J* 2.0, H-6), 8.55 (1H, d, *J* 2.0, H-2), 7.45–7.32 (5H, m, H-10, H-11, H-12), 6.39 (1H, d, *J* 10.1, NH-4), 5.34 (2H, s, H-8), 4.20–4.11 (1H, m, H-2'), 2.58–2.39 (2H, m, H-3'), 1.39 (9H, s, H-6'), 1.31 (3H, d, *J* 6.5, H-1'); ^{13}C NMR (126 MHz, $CDCl_3$) δ_C 170.2 (C-4'), 163.6 (C-7), 146.8 (C-4), 146.3 (C-6), 137.9 (C-5), 135.6 (C-9), 128.83 (C-11), 128.75 (C-12), 128.7 (C-2), 128.6 (C-10), 121.8 (C-1), 88.9 (C-3), 81.5 (C-5'), 67.4 (C-8), 50.4 (C-2'), 43.2 (C-3'), 28.1 (C-6'), 21.2 (C-1'); HRMS *m/z* (ESI^+) [Found: 541.0831, $C_{22}H_{26}{}^{127}IN_2O_6$ requires M^+ 541.0830]; LRMS *m/z* (ESI^+) 507 ([(M−^{t}Bu)+Na]$^+$, 100%); HPLC Method 1: Retention time 13.1 min, purity 97.1%.

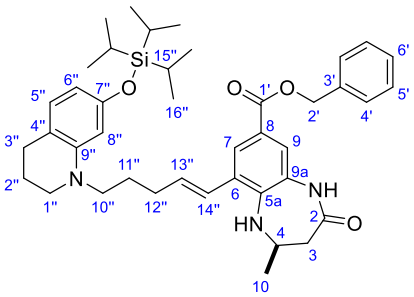
Benzyl (*R*)-9-iodo-2-methyl-4-oxo-2,3,4,5-tetrahydro-1*H*-benzo[*b*][1,4]diazepine-7-carboxylate ((*R*)150)



To a solution of benzyl (*R*)-4-((4-(*tert*-butoxy)-4-oxobutan-2-yl)amino)-3-iodo-5-nitrobenzoate (**(*R*)149**) (842 mg, 1.56 mmol 1.0 eq.) in CH_2Cl_2 (6 mL) was added trifluoroacetic acid (6 mL) and the orange solution was stirred at rt for 1 h. The reaction mixture was evaporated *in vacuo* and the resulting residue was dissolved in glacial acetic acid (14 mL). Iron powder (435 mg, 7.79 mmol, 5.0 eq.) was added and the brown suspension was stirred under reflux for 4 h. 1 M aq. K_2CO_3 (300 mL) was added to the cooled suspension and the resulting mixture was extracted with EtOAc (3 × 100 mL). The combined organic components were washed with brine (150 mL), dried ($MgSO_4$), filtered, and evaporated *in vacuo* to yield benzyl (*R*)-9-iodo-2-methyl-4-oxo-2,3,4,5-tetrahydro-1*H*-benzo[*b*][1,4]diazepine-7-carboxylate (**(*R*)150**) as a colourless solid (642 mg, 94%); R_f 0.55 (EtOAc); $[\alpha]_D^{25}$= −24.8 (*c* 1.0, $CHCl_3$); mp 154–156 °C (EtOAc); $\bar{\nu}_{max}$ (neat)/cm^{-1} 3370 (N-H, w), 3311 (N-H, w),

2921 (C-H, w), 1698 (C=O, s), 1668 (C=O, s); ^{1}H NMR (500 MHz; DMSO-d_6) δ_H 9.74 (1H, s, NH-9a), 8.04 (1H, d, *J* 2.0, H-7), 7.58 (1H, d, *J* 2.0, H-9), 7.47–7.32 (5H, m, H-14, H-15, H-16), 5.29 (2H, s, H-12), 5.17 (1H, d, *J* 3.1, NH-5a), 4.13–4.05 (1H, m, H-4), 2.56–2.49 (1H, dd, H-3, *J* 13.9, 3.1, H_AH_B-3), 2.40 (1 H, dd, *J* 13.9, 8.2, H_AH_B-3), 1.29 (3H, d, *J* 6.3, H-10); ^{13}C NMR (126 MHz; DMSO-d_6) δ_C 171.1 (C-2), 164.0 (C-11), 143.0 (C-9a), 136.2 (C-13), 135.8 (C-9), 128.5 (C-15), 128.1 (C-16), 127.9 (C-14), 125.6 (C-5a), 123.7 (C-7), 120.5 (C-8), 90.1 (C-6), 65.9 (C-12), 52.6 (C-4), 41.2 (C-3), 23.7 (C-10); HRMS *m/z* (ESI$^+$) [Found: 437.0355, $C_{18}H_{18}{}^{127}IN_2O_3$ requires M^+ 437.0357]; LRMS *m/z* (ESI$^+$) 437 ([M+H]$^+$, 100%); HPLC Method 1: Retention time 10.5 min, purity 99.0%.

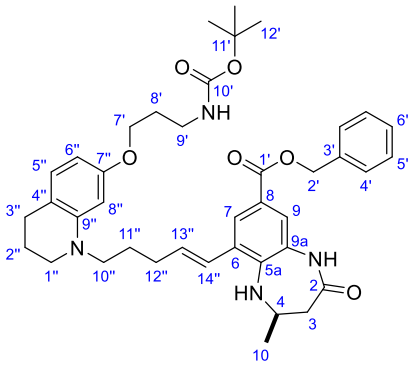
Benzyl (*R*,*E*)-2-methyl-4-oxo-9-(5-(7-((triisopropylsilyl)oxy)-3,4-dihydroquinolin-1(2*H*)-yl)pent-1-en-1-yl)-2,3,4,5-tetrahydro-1*H*-benzo[*b*][1,4]diazepine-7-carboxylate ((*R*)151)



Benzyl (*R*)-9-iodo-2-methyl-4-oxo-2,3,4,5-tetrahydro-1*H*-benzo[*b*][1,4]diazepine-7-carboxylate (**(*R*)150**) (248 mg, 0.535 mmol, 1.0 eq.), bis(triphenylphosphine)palladium(II) dichloride (19.0 mg, 0.0803 mmol, 0.05 eq.) and K_2CO_3 (222 mg, 1.61 mmol, 3.0 eq.) were added to a Schlenk flask under a nitrogen atmosphere (evacuated and backfilled 3 × nitrogen). (*E*)-1-(5-(4,4,5,5-Tetramethyl-1,3,2-dioxaborolan-2-yl)pent-4-en-1-yl)-7-((triisopropylsilyl)oxy)-1,2,3,4-tetrahydroquinoline (**116**) (401 mg, 0.803 mmol, 1.5 eq.) in 1,4-dioxane (3.4 mL) was added, followed by H_2O (0.8 mL) and the reaction mixture was stirred at 100 °C for 18 h. The reaction mixture was evaporated *in vacuo* and diluted with EtOAc (50 mL). The organic component was washed with brine (3 × 20 mL), dried ($MgSO_4$), filtered, and evaporated *in vacuo* to afford an orange oil. The crude oil was purified by silica gel chromatography (elution with 20% to 60% EtOAc in petroleum ether) to yield benzyl (*R*,*E*)-2-methyl-4-oxo-9-(5-(7-((triisopropylsilyl)oxy)-3,4-dihydroquinolin-1(2*H*)-yl)pent-1-en-1-yl)-2,3,4,5-tetrahydro-1*H*-benzo[*b*][1,4]diazepine-7-carboxylate (**(*R*)151**) as a yellow oil (248 mg, 68%) and was used without further purification; R_f 0.48 (EtOAc/petroleum ether 1:1); $[\alpha]_D^{25}$= +20.48 (*c* 1.0, $CHCl_3$); $\bar{\nu}_{max}$ (thin film)/cm^{-1} 2942 (C-H, s), 1708 (C=O, s), 1673 (C=O, s); ^{1}H NMR (500 MHz; $CDCl_3$) δ_H 7.74 (1H, d, *J* 1.9, H-9), 7.56 (1H, s, NH-9a), 7.49 (1H, d, *J* 1.9, H-7), 7.45–7.30 (5H, m, H-4', H-5', H-6'), 6.75 (1H, d, *J* 7.7, H-5''), 6.34 (1H, d, *J* 15.6, H-14''), 6.16–6.00 (3H, m, H-6'', H-8'', H-13''), 5.33 (2H, s, H-2'), 4.14–4.05

(1H, m, H-4), 4.00 (1H, d, *J* 1.9, NH-5a), 3.32–3.18 (4H, m, H-1'', H-10''), 2.70–2.59 (3H, m, H_AH_B-3, H-3''), 2.51 (1H, dd, *J* 13.9, 8.2, H_AH_B-3), 2.34–2.24 (2H, m, H-12''), 1.94–1.88 (2H, m, H-2''), 1.82–1.74 (2H, m, H-11''), 1.37 (3H, d, *J* 6.4, H-10), 1.25–1.18 (3H, m, H-15''), 1.08 (18H, d, *J* 7.4, H-16''); ^{13}C NMR (126 MHz; $CDCl_3$) δ_C 172.2 (C-2), 166.0 (C-1'), 155.3 (C-7''), 145.9 (C-9''), 139.9 (C-5a), 136.7 (C-13''), 136.3 (C-3'), 129.6 (C-5''), 129.0 (C-6), 128.7 (C-5'), 128.33 (C-6'), 128.30 (C-4'), 126.3 (C-9), 125.9 (C-9a), 124.7 (C-14''), 122.8 (C-7), 121.1 (C-8), 115.2 (C-4''), 107.1 (C-6''), 102.5 (C-8''), 66.6 (C-2'), 53.1 (C-4), 51.3 (C-10''), 49.6 (C-1''), 41.6 (C-3), 31.3 (C-12''), 27.5 (C-3''), 25.8 (C-11''), 24.5 (C-10), 22.6 (C-2''), 18.1 (C-16''), 12.8 (C-15''); HRMS *m/z* (ESI$^+$) [Found: 682.4030, $C_{41}H_{56}N_3O_4{}^{28}Si$ requires M^+ 682.4035]; LRMS *m/z* (ESI$^+$) 682 ($[M+H]^+$, 100%).

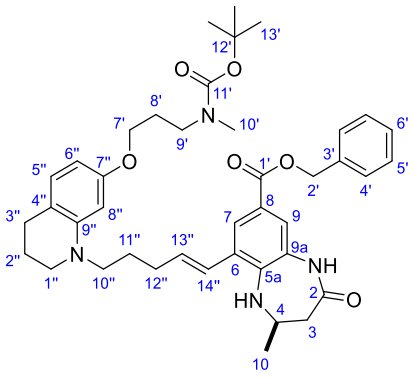
Benzyl (*R*,*E*)-9-(5-(7-(3-((*tert*-butoxycarbonyl)amino)propoxy)-3,4-dihydroquinolin-1(2*H*)-yl)pent-1-en-1-yl)-2-methyl-4-oxo-2,3,4,5-tetrahydro-1*H*-benzo[*b*][1,4]diazepine-7-carboxylate ((*R*)152)



To a solution of benzyl (*R*,*E*)-2-methyl-4-oxo-9-(5-(7-((triisopropylsilyl)oxy)-3,4-dihydroquinolin-1(2*H*)-yl)pent-1-en-1-yl)-2,3,4,5-tetrahydro-1*H*-benzo[*b*][1,4]diazepine-7-carboxylate (**(*R*)151**) (53.0 mg, 0.0780 mmol, 1.0 eq.) in THF (1.6 mL) was added 1 M TBAF in THF (156 µL, 0.156 mmol, 2.0 eq.) and the reaction mixture was stirred at rt for 1 h. The reaction mixture was evaporated *in vacuo* to afford an orange residue. The crude oil was purified by silica gel chromatography (elution with 50% to 100% EtOAc in petroleum ether) to yield a brown solid. The brown solid was dissolved in anhydrous DMF (0.4 mL). K_2CO_3 (16.0 mg, 0.262 mmol, 1.5 eq.) and *tert*-butyl (3-bromopropyl)carbamate (23.0 mg, 0.0936 mmol, 1.5 eq.) were added to the solution and the reaction mixture was stirred at 65 °C for 16 h. The reaction mixture was diluted with 1 M aq. K_2CO_3 (20 mL) and was extracted with EtOAc (3 × 10 mL). The combined organic components were washed with 0.5 M LiCl (3 × 20 mL), brine (20 mL), dried (Na_2SO_4), filtered and evaporated *in vacuo* to afford a brown oil. The crude oil was purified by silica gel chromatography (elution with 10% to 20% acetone in toluene) to yield benzyl (*R*,*E*)-9-(5-(7-(3-((*tert*-butoxycarbonyl)amino)propoxy)-3,4-dihydroquinolin-1(2*H*)-yl)pent-1-en-1-yl)-

2-methyl-4-oxo-2,3,4,5-tetrahydro-1*H*-benzo[*b*][1,4]diazepine-7-carboxylate (**(*R*)152**) as a yellow oil (21 mg, 39%); R_f 0.30 (acetone/ toluene 1:4); $[\alpha]_D^{25}$= −8.14 (*c* 0.5, $CHCl_3$); $\bar{\nu}_{max}$ (thin film)/cm^{-1} 3371 (N-H, br w), 2931 (C-H, w), 1692 (C=O, s), 1674 (C=O, s); ^{1}H NMR (500 MHz; $CDCl_3$) δ_H 7.75 (1H, d, *J* 1.9, H-9), 7.53 (1H, s, NH-9a), 7.48 (1H, d, *J* 1.9, H-7), 7.45–7.30 (5H, m, H-4', H-5', H-6'), 6.83 (1H, d, *J* 7.8, H-5''), 6.36 (1H, d, *J* 15.4, H-14''), 6.19–6.06 (3H, m, H-6'', H-8'', H-13''), 5.33 (2H, s, H-2'), 4.78 (1H, s, NH-10'), 4.12–4.05 (1H, m, H-4), 3.99 (1 H, d, *J* 2.4, NH-5a), 3.93 (2H, t, *J* 6.0, H-7'), 3.31–3.20 (6H, m, H-9', H-1'', H-10''), 2.69 (2H, t, *J* 6.4, H-3''), 2.63 (1H, dd, *J* 13.8, 3.3, H_AH_B-3), 2.50 (1H, dd, *J* 13.8, 8.3, H_AH_B-3), 2.34–2.26 (2H, m, H-12''), 1.95–1.86 (4H, m, H-8', H-2''), 1.83–1.76 (2H, m, H-11''), 1.43 (9H, s, H-12'), 1.35 (3H, d, *J* 6.4, H-10); ^{13}C NMR (126 MHz; $CDCl_3$) δ_C 172.1 (C-2), 166.0 (C-1'), 158.5 (C-7''), 156.2 (C-10'), 146.3 (C-9''), 140.0 (C-5a), 136.6 (C-13''), 136.3 (C-3'), 129.7 (C-5''), 129.1 (C-6), 128.7 (C-5'), 128.33 (C-6'), 128.30 (C-4'), 126.3 (C-9), 126.2 (C-9a), 125.0 (C-14''), 122.8 (C-7), 121.2 (C-8), 115.6 (C-4''), 100.4 (C-6''), 98.0 (C-8''), 79.3 (C-11'), 66.6 (C-2'), 65.7 (C-7'), 53.2 (C-4), 50.8 (C-10''), 49.4 (C-1''), 41.5 (C-3), 38.3 (C-9'), 31.0 (C-12''), 29.7 (C-12'), 28.6 (C-8'), 27.6 (C-3''), 26.0 (C-11''), 24.5 (C-10), 22.6 (C-2''); HRMS *m/z* (ESI$^+$) [Found: 683.3796, $C_{40}H_{51}N_6O_4$ requires M^+ 683.3803]; LRMS *m/z* (ESI$^+$) 583 ([M−Boc]$^+$, 100%); HPLC Method 1: Retention time 12.7 min, purity 98.3%.

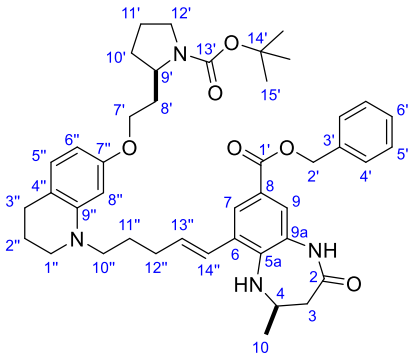
Benzyl (*R,E*)-9-(5-(7-(3-((*tert*-butoxycarbonyl)(methyl)amino)propoxy)-3,4-dihydroquinolin-1(2*H*)-yl)pent-1-en-1-yl)-2-methyl-4-oxo-2,3,4,5-tetrahydro-1*H*-benzo[*b*][1,4]diazepine-7-carboxylate ((*R*)153**)**



To a solution of benzyl (*R*,*E*)-2-methyl-4-oxo-9-(5-(7-((triisopropylsilyl)oxy)-3,4-dihydroquinolin-1(2*H*)-yl)pent-1-en-1-yl)-2,3,4,5-tetrahydro-1*H*-benzo[*b*][1,4]diazepine-7-carboxylate (**(*R*)151**) (120 mg, 0.176 mmol, 1.0 eq.) in THF (3.4 mL) was added 1 M TBAF in THF (352 µL, 0.352 mmol, 2.0 eq.) and the reaction mixture was stirred at rt for 1 h. The reaction mixture was evaporated *in vacuo* to afford an orange residue. The crude oil was purified by silica gel chromatography (elution with 50% to 100% EtOAc in petroleum ether) to yield a brown solid. The brown solid was dissolved in anhydrous DMF

(0.7 mL). K_2CO_3 (37.0 mg, 0.262 mmol, 1.5 eq.) and 3-((*tert*-butoxycarbonyl)(methyl)amino)propyl methanesulfonate (71.0 mg, 0.262 mmol, 1.5 eq.) were added to the solution and the reaction mixture was stirred at 65 °C for 16 h. K_2CO_3 (37.0 mg, 0.262 mmol, 1.5 eq.) and 3-((*tert*-butoxycarbonyl)(methyl)amino)propyl methanesulfonate (71.0 mg, 0.262 mmol, 1.5 eq.) were added to the solution and the reaction mixture was stirred at 65 °C for a further 6 h. The reaction mixture was diluted with $CHCl_3$/IPA (9:1, 50 mL) and was washed with 0.5 M LiCl (3 × 20 mL), brine (30 mL), dried (Na_2SO_4), filtered and evaporated *in vacuo* to afford a brown oil. The crude oil was purified by silica gel chromatography (elution with 10% to 20% acetone in toluene) to yield benzyl (*R,E*)-9-(5-(7-(3-((*tert*-butoxycarbonyl)(methyl)amino)propoxy)-3,4-dihydroquinolin-1(2*H*)-yl)pent-1-en-1-yl)-2-methyl-4-oxo-2,3,4,5-tetrahydro-1*H*-benzo[*b*][1,4]diazepine-7-carboxylate (**(*R*)153**) as a yellow oil (31 mg, 25%) and was used without further purification; R_f 0.41 (acetone/toluene 3:7); $[\alpha]_D^{25}$= +13.41 (*c* 1.0, MeOH); $\bar{\nu}_{max}$ (thin film)/cm^{-1} 3359 (N-H, br w), 2931 (C-H, w), 1678 (C=O, s); ^{1}H NMR (500 MHz; $CDCl_3$) δ_H 7.75 (1H, d, *J* 1.9, H-9), 7.48 (1H, d, *J* 1.9, H-7), 7.44–7.30 (5H, m, H-4', H-5', H-6'), 6.83 (1H, d, *J* 8.0, H-5''), 6.36 (1H, d, *J* 15.4, H-14''), 6.18–6.08 (3H, m, H-6'', H-8'', H-13''), 5.33 (2H, s, H-2'), 4.13–4.06 (1H, m, H-4), 3.94–3.85 (2H, m, H-7'), 3.35 (2H, t, *J* 7.1, H-9'), 3.31–3.20 (4H, m, H-1'', H-10''), 2.85 (3H, s, H-10'), 2.71–2.59 (3H, m, H_AH_B-3, H-3''), 2.50 (1H, dd, *J* 13.8, 8.2, H_AH_B-3), 2.33–2.27 (2H, m, H-12''), 1.96–1.88 (4H, m, H-8', H-2''), 1.84–1.76 (2H, m, H-11''), 1.44 (9H, s, H-13'), 1.36 (3H, d, *J* 6.4, H-10); ^{13}C NMR (126 MHz; $CDCl_3$) δ_C 172.1 (C-2), 166.0 (C-1'), 158.6 (C-7''), 155.9 (C-11'), 146.2 (C-9''), 140.0 (C-5a), 136.6 (C-13''), 136.3 (C-3'), 129.7 (C-5''), 129.0 (C-6), 128.7 (C-5'), 128.33 (C-6'), 128.30 (C-4'), 126.3 (C-9), 125.4 (C-9a), 124.9 (C-14''), 122.8 (C-7), 121.2 (C-8), 115.4 (C-4''), 100.3 (C-6''), 98.0 (C-8''), 79.5 (C-12'), 66.6 (C-2'), 65.3 (C-7'), 53.1 (C-4), 51.0 (C-10''), 49.6 (C-1''), 46.1 (C-9'), 41.6 (C-3), 34.7 (C-10'), 31.1 (C-12''), 28.6 (C-13'), 28.3 (C-8'), 27.6 (C-3''), 26.1 (C-11''), 24.4 (C-10), 22.6 (C-2''); HRMS *m/z* (ESI^+) [Found: 697.3955, $C_{41}H_{53}N_4O_6$ requires M^+ 697.3960]; LRMS *m/z* (ESI^+) 597 ($[M-Boc]^+$, 100%).

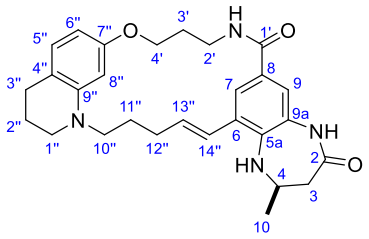
Benzyl (*R*)-9-((*E*)-5-(7-(2-((*R*)-1-(*tert*-butoxycarbonyl)pyrrolidin-2-yl)ethoxy)-3,4-dihydroquinolin-1(2*H*)-yl)pent-1-en-1-yl)-2-methyl-4-oxo-2,3,4,5-tetrahydro-1*H*-benzo[*b*][1,4]diazepine-7-carboxylate ((*R*)(*R*)156)



To a solution of benzyl (*R*,*E*)-2-methyl-4-oxo-9-(5-(7-((triisopropylsilyl)oxy)-3,4-dihydroquinolin-1(2*H*)-yl)pent-1-en-1-yl)-2,3,4,5-tetrahydro-1*H*-benzo[*b*][1,4]diazepine-7-carboxylate (**(*R*)151**) (110 mg, 0.162 mmol, 1.0 eq.) in THF (3.1 mL) was added 1 M TBAF in THF (324 µL, 0.324 mmol, 2.0 eq.) and the reaction mixture was stirred at rt for 1 h. The reaction mixture was evaporated *in vacuo* to afford an orange residue. The crude oil was purified by silica gel chromatography (elution with 50% to 100% EtOAc in petroleum ether) to yield a brown solid. The brown solid was dissolved in anhydrous THF (0.3 mL) and anhydrous DMF (0.7 mL). *tert*-Butyl (*R*)-2-(2-hydroxyethyl)pyrrolidine-1-carboxylate (44.0 mg, 0.202 mmol, 1.25 eq.), tributylphosphine (80.0 mg, 0.324 mmol, 2.0 eq.) and diethyl azodicarboxylate (50.0 mg, 0.324 mmol, 2.0 eq.) in anhydrous THF (0.4 mL) were added to the solution and the reaction mixture was stirred at rt for 6 h. *tert*-Butyl (*R*)-2-(2-hydroxyethyl)pyrrolidine-1-carboxylate (44.0 mg, 0.202 mmol, 1.25 eq.), tributylphosphine (40.0 mg, 0.162 mmol, 1.0 eq.) and diethyl azodicarboxylate (25.0 mg, 0.162 mmol, 1.0 eq.) in anhydrous THF (0.4 mL) were added to the solution and the reaction mixture was stirred at rt for a further 6 h. The reaction mixture was evaporated *in vacuo* to afford a brown oil. The crude oil was purified by silica gel chromatography (elution with 20% acetone in toluene) to afford a colourless solid. The crude solid was further purified by silica gel chromatography (elution with 50% to 100% Et_2O in pentane) to yield benzyl (*R*)-9-((*E*)-5-(7-(2-((*R*)-1-(*tert*-butoxycarbonyl)pyrrolidin-2-yl)ethoxy)-3,4-dihydroquinolin-1(2*H*)-yl)pent-1-en-1-yl)-2-methyl-4-oxo-2,3,4,5-tetrahydro-1*H*-benzo[*b*][1,4]diazepine-7-carboxylate (**(*R*)(*R*)156**) as a brown oil (20 mg, 17%) and was used without further purification; R_f 0.24 (Et_2O); $[\alpha]_D^{25}$= −3.58 (*c* 0.5, $CHCl_3$); $\bar{\nu}_{max}$ (thin film)/cm^{-1} 2930 (C-H, w), 1707 (C=O, m), 1674 (C=O, s); ^{1}H NMR (500 MHz; $CDCl_3$) δ_H 7.75 (1H, d, *J* 2.0, H-9), 7.46 (1H, d, *J* 2.0, H-7), 7.45–7.31 (5H, m, H-4', H-5', H-6'), 7.22 (1H, s, NH-9a), 6.83 (1H, d, *J* 8.1, H-5''), 6.35 (1H, d, *J* 15.5, H-14''), 6.28 (1H, dd, *J* 8.1, 2.3, H-6''), 6.24 (1H, d, *J* 2.3,

H-8''), 6.18–6.08 (1H, m, H-13''), 5.33 (2H, s, H-2'), 4.13–4.07 (1H, m, H-4), 4.04–3.99 (2H, m, H-12'), 3.95–3.85 (3H, m, H-7', H-9'), 3.34–3.20 (4H, m, H-1'', H-10''), 2.71–2.61 (3H, m, H_AH_B-3, H-3''), 2.50 (1H, dt, *J* 14.4, 7.3, H_AH_B-3), 2.34–2.28 (2H, m, H-12''), 2.15–2.02 (2H, m, H-8'), 1.95–1.86 (2H, m, H-2''), 1.83–1.75 (2H, m, H-11''), 1.44 (9H, s, H-15''), 1.37 (3H, d, *J* 7.3, H-10), 1.31–1.19 (4H, m, H-10', H-11'); ^{13}C NMR (126 MHz; $CDCl_3$) δ_C 172.0 (C-2), 166.0 (C-1'), 156.8 (C-7''), 146.2 (C-9''), 140.0 (C-5a), 136.8 (C-13''), 136.3 (C-3'), 135.9 (C-13'), 129.7 (C-5''), 129.1 (C-6), 128.7 (C-5'), 128.4 (C-6'), 128.3 (C-4'), 126.4 (C-9), 125.9 (C-9a), 124.8 (C-14''), 122.6 (C-7), 121.2 (C-8), 116.1 (C-4''), 103.1 (C-8''), 99.7 (C-6''), 68.0 (C-7', C-12'), 66.7 (C-2'), 55.2, (C-9'),* 53.0 (C-4), 51.1 (C-10''), 49.6 (C-1''), 41.6 (C-3), 32.8 (C-8'), 31.2 (C-12''), 29.9 (C-10'), 28.7 (C-15'), 27.6 (C-3''), 26.1 (C-11''), 24.4 (C-10), 22.6 (C-2''), 14.8 (C-11'); HRMS *m/z* (ESI^+) [Found: 723.4113, $C_{43}H_{55}N_6O_4$ requires M^+ 723.4116]; LRMS *m/z* (ESI^+) 623 ([M−Boc]$^+$, 100%). *Observed by ^{1}H-^{13}C-HSQC correlation.

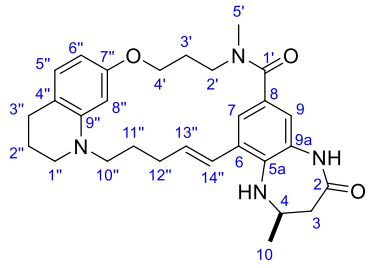
(2*R*,24*Z*)-2-Methyl-1,2,3,9,10,11,12,18,19,21,22,23-dodecahydro-8*H*,17*H*-14,16-etheno-26,7-(metheno)[1,4]diazepino[2,3-*l*]pyrido[2,1-*d*][1,5,17]oxadiazacycloicosine-4,8(5*H*)-dione ((*R*)108)



To a stirred solution of benzyl (*R*,*E*)-9-(5-(7-(3-((*tert*-butoxycarbonyl)amino)propoxy)-3,4-dihydroquinolin-1(2*H*)-yl)pent-1-en-1-yl)-2-methyl-4-oxo-2,3,4,5-tetrahydro-1*H*-benzo[*b*][1,4]diazepine-7-carboxylate (**(*R*)152**) (20 mg, 0.029 mmol, 1.0 eq.) in THF/MeOH/H_2O (3:2:1, 0.42 mL) was added LiOH (10 mg, 0.418 mmol, 14.0 eq.) and the reaction mixture was stirred at rt for 5 h. The reaction mixture was evaporated *in vacuo* to afford a yellow residue. To the residue dissolved in CH_2Cl_2 (0.2 mL) was added trifluoroacetic acid (0.2 mL) and the brown solution was stirred at rt for 2 h. The reaction mixture was evaporated *in vacuo* to afford a brown residue. The residue was dissolved in DMF (14.5 mL) and was adjusted to pH 9 with *N*,*N*-diisopropylethylamine (1.0 mL). Benzotriazol-1-yl-oxytripyrrolidinophosphonium hexafluorophosphate (17 g, 0.032 mmol, 1.1 eq.) was added to the solution and the reaction mixture was stirred at rt for 36 h. The reaction mixture was concentrated under a constant stream of nitrogen to afford a brown oil. The crude oil was diluted with 1 M aq. K_2CO_3 (20 mL) and extracted with $CHCl_3$/IPA (9:1, 3 × 10 mL). The combined organic components were washed with 0.5 M aq. LiCl (3 × 10 mL), brine (10 mL), dried ($MgSO_4$), filtered, and evaporated *in vacuo* to afford a brown oil. The crude oil was purified by silica gel chromatography

(elution with 20% to 100% acetone in Et_2O) to yield (2*R*,24*Z*)-2,9-dimethyl-1,2,3,9,10,11,12,18,19,21,22,23-dodecahydro-8*H*,17*H*-14,16-etheno-26,7-(metheno)[1,4]diazepino[2,3-*l*]pyrido[2,1-*d*][1,5,17]oxadiazacycloicosine-4,8(5*H*)-dione (**(*R*)108**) as a colourless solid (8 mg, 58%); R_f 0.52 (acetone/Et_2O 9:1); $[\alpha]_D^{25}$ = −51.1 (*c* 0.4, DMSO); mp 290 °C decomposed (acetone); $\bar{\nu}_{max}$ (thin film)/cm^{-1} 3448 (N-H, br w), 3248 (N-H, br w), 2928 (C-H, w), 1671 (C=O, s); ^{1}H NMR (500 MHz; DMSO-d_6) δ_H 9.57 (1H, s, NH-9a), 7.93 (1H, t, *J* 5.5, NH-1'), 7.53 (1H, d, *J* 2.0, H-9), 7.33 (1H, d, *J* 2.0, H-7), 6.78 (1H, d, *J* 8.1, H-5''), 6.71 (1H, d, *J* 15.1, H-14''), 6.28 (1H, dt, *J* 15.1, 7.3, H-13''), 6.13 (1H, d, *J* 2.3, H-8''), 6.10 (1H, dd, *J* 8.1, 2.3, H-6''), 5.09 (1H, d, *J* 3.0, NH-5a), 4.07–3.96 (3H, m, H-4, H-4'), 3.53–3.43 (2H, m, H-2'), 3.26–3.15 (4H, m, H-1'', H-10''), 2.61 (2H, t, *J* 6.3, H-3''), 2.48 (1H, dd, *J* 13.3, 4.1, H_AH_B-3), 2.32–2.26 (2H, m, H-12''), 2.21 (1H, dd, *J* 13.3, 7.2, H_AH_B-3), 1.96–1.89 (2H, m, H-3'), 1.86–1.77 (2H, m, H-2''), 1.72–1.63 (2H, m, H-11''), 1.25 (3H, d, *J* 6.2, H-10); ^{13}C NMR (126 MHz; DMSO-d_6) δ_C 171.3 (C-2), 165.1 (C-1'), 158.3 (C-7''), 145.4 (C-9''), 138.7 (C-5a), 133.3 (C-13''), 129.3 (C-5''), 129.2 (C-9a), 128.3 (C-6), 127.7 (C-14''), 125.5 (C-8), 121.1 (C-9), 120.7 (C-7), 114.9 (C-4''), 98.5 (C-6''), 97.8 (C-8''), 68.4 (C-4'), 53.9 (C-4), 48.7 (C-10''), 48.1 (C-1''), 40.7 (C-3), 39.1 (C-2'),* 29.5 (C-12''), 28.5 (C-3'), 27.0 (C-3''), 23.5 (C-11''), 23.3 (C-10), 21.9 (C-2''); HRMS *m/z* (ESI$^+$) [Found: 475.2702, $C_{28}H_{35}N_4O_3$ requires M^+ 475.2704]; LRMS *m/z* (ESI$^+$) 475 ([M+H]$^+$, 100%); HPLC Method 1: Retention time 9.4 min, purity 98.2%. *Observed by ^{1}H-^{13}C-HSQC correlation. Structure confirmed by X-ray crystallography (See Appendix E).

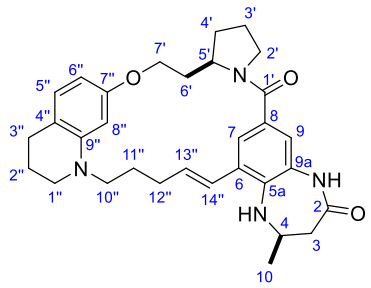
(2*R*,24*Z*)-2,9-Dimethyl-1,2,3,9,10,11,12,18,19,21,22,23-dodecahydro-8*H*,17*H*-14,16-etheno-26,7-(metheno)[1,4]diazepino[2,3-*l*]pyrido[2,1-*d*][1,5,17]oxadiazacycloicosine-4,8(5*H*)-dione ((*R*)109)



To a stirred solution of benzyl (*R,E*)-9-(5-(7-(3-((*tert*-butoxycarbonyl)(methyl)amino)propoxy)-3,4-dihydroquinolin-1(2*H*)-yl)pent-1-en-1-yl)-2-methyl-4-oxo-2,3,4,5-tetrahydro-1*H*-benzo[*b*][1,4]diazepine-7-carboxylate (**(*R*)153**) (23 mg, 0.033 mmol, 1.0 eq.) in THF/MeOH/H_2O (3:2:1, 0.42 mL) was added LiOH (10 mg, 0.418 mmol, 10.0 eq.) and the reaction mixture was stirred at rt for 5 h. The reaction mixture was evaporated *in vacuo* to afford a yellow residue. To the residue dissolved in CH_2Cl_2 (0.5 mL) was added trifluoroacetic acid (0.5 mL) and the brown solution was stirred at rt for

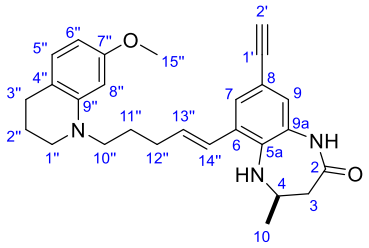
2 h. The reaction mixture was evaporated *in vacuo* to afford a brown residue. The residue was dissolved in DMF (16.5 mL) and was adjusted to pH 9 with *N*,*N*-diisopropylethylamine (1.0 mL). Benzotriazol-1-yl-oxytripyrrolidinophosphonium hexafluorophosphate (19 mg, 0.036 mmol, 1.1 eq.) was added to the solution and the reaction mixture was stirred at rt for 36 h. The reaction mixture was concentrated under a constant stream of nitrogen to afford a brown oil. The crude oil was diluted with 1 M aq. K_2CO_3 (20 mL) and extracted with $CHCl_3$/IPA (9:1, 3 × 10 mL). The combined organic components were washed with 0.5 M aq. LiCl (3 × 10 mL), brine (10 mL), dried ($MgSO_4$), filtered, and evaporated *in vacuo* to afford a brown oil. The crude oil was purified by silica gel chromatography (elution with 80% to 100% acetone in Et_2O) to yield (2*R*,24*Z*)-2,9-dimethyl-1,2,3,9,10,11,12,18,19,21,22,23-dodecahydro-8*H*,17*H*-14,16-etheno-26,7-(metheno)[1,4]diazepino[2,3-*l*]pyrido[2,1-*d*][1,5,17]oxadiazacycloicosine-4,8(5*H*)-dione (**(*R*)109**) as a yellow oil (7 mg, 43%); R_f 0.42 (acetone/Et_2O 4:1); $[\alpha]_D^{25}$ = +16.1 (*c* 0.6, DMSO); $\bar{\nu}_{max}$ (thin film)/cm^{-1} 3353 (N-H, br w), 2928 (C-H, w), 1699 (C=O, s), 1671 (C=O, s); ^{1}H NMR (400 MHz; DMSO-d_6) δ_H 9.55 (1H, s, NH-9a), 7.20 (1H, d, *J* 1.9, H-9), 6.85 (1H, br s, H-5''), 6.78–6.70 (2H, m, H-7, H-14''), 6.23–6.11 (1H, m, H-13''), 6.06–5.98 (2H, m, H-6'', H-8''), 4.92 (1H, d, *J* 2.9, NH-5a), 4.07–3.95 (1H, m, H-4), 3.95–3.85 (2H, m, H-4'), 3.26–3.19 (4H, m, H-1'', H-10''), 2.96 (3H, s, H-5'), 2.59 (2H, t, *J* 6.3, H-3''), 2.50–2.48 (2H, m, H-2'), 2.30–2.22 (3H, m, H-12'', H_AH_B-3), 2.19 (1H, dd, *J* 13.1, 7.2, H_AH_B-3), 2.00–1.90 (2H, m, H-3'), 1.86–1.77 (2H, m, H-2''), 1.74–1.62 (2H, m, H-11''), 1.24 (3H, d, *J* 6.2, H-10); ^{13}C NMR (126 MHz; DMSO-d_6) δ_C 171.5 (C-2), 169.9 (C-1'), 158.2 (C-7''), 145.5 (C-9''), 137.0 (C-5a), 133.0 (C-13''), 130.5 (C-14''), 129.3 (C-9a), 128.3 (C-6), 127.4 (C-9), 120.8 (C-7),* 119.8 (C-5''), 114.3 (C-4''), 96.9 (C-6'', C-8''), 65.8 (C-4'), 55.8 (C-2'), 54.4 (C-4), 48.4 (C-10''), 48.0 (C-1''), 47.5 (C-5'), 40.6 (C-3), 29.3 (C-12''), 27.3 (C-3'), 26.9 (C-3''), 23.43 (C-11''), 23.40 (C-10), 21.9 (C-2''); HRMS *m/z* (ESI^+) [Found: 489.2853, $C_{29}H_{37}N_4O_3$ requires M^+ 489.2860]; LRMS *m/z* (ESI^+) 489 ($[M+H]^+$, 100%); HPLC Method 1: Retention time 9.7 min, purity 97.3%. *Observed by ^{1}H-^{13}C-HSQC correlation.

(2*R*,12a*R*,26*Z*)-2-Methyl-1,2,3,10,11,12,12a,13,14,20,21,23,24,25-tetradecahydro-8*H*,19*H*-16,18-etheno-28,7-(metheno)[1,4]diazepino[2,3-*i*]pyrido[1,2-*q*]pyrrolo[2,1-*d*][1,5,17]oxadiazacycloicosine-4,8(5*H*)-dione ((*R*)(*R*)110)



To a stirred solution of benzyl (*R*)-9-((*E*)-5-(7-(2-((*R*)-1-(*tert*-butoxycarbonyl)pyrrolidin-2-yl)ethoxy)-3,4-dihydroquinolin-1(2*H*)-yl)pent-1-en-1-yl)-2-methyl-4-oxo-2,3,4,5-tetrahydro-1*H*-benzo[*b*][1,4]diazepine-7-carboxylate (**(*R*)(*R*)156**) (34 mg, 0.047 mmol, 1.0 eq.) in THF/MeOH/H_2O (3:2:1, 0.42 mL) was added LiOH (11 mg, 0.47 mmol, 10.0 eq.) and the reaction mixture was stirred at rt for 5 h. The reaction mixture was evaporated *in vacuo* to afford a yellow residue. To the residue dissolved in CH_2Cl_2 (0.2 mL) was added trifluoroacetic acid (0.2 mL) and the brown solution was stirred at rt for 2 h. The reaction mixture was evaporated *in vacuo* to afford a brown residue. The residue was dissolved in DMF (23.5 mL) and was adjusted to pH 9 with *N*,*N*-diisopropylethylamine (1.5 mL). Benzotriazol-1-yl-oxytripyrrolidinophosphonium hexafluorophosphate (27 mg, 0.052 mmol, 1.1 eq.) was added to the solution and the reaction mixture was stirred at rt for 36 h. The reaction mixture was concentrated under a constant stream of nitrogen to afford a brown oil. The crude oil was diluted with 1 M aq. K_2CO_3 (20 mL) and extracted with $CHCl_3$/IPA (9:1, 3 × 10 mL). The combined organic components were washed with 0.5 M aq. LiCl (3 × 10 mL), brine (10 mL), dried ($MgSO_4$), filtered, and evaporated *in vacuo* to afford a brown oil. The crude oil was purified by silica gel chromatography (elution with 20% to 100% acetone in Et_2O) to yield (2*R*,12a*R*,26*Z*)-2-methyl-1,2,3,10,11,12,12a,13,14,20,21,23,24,25-tetradecahydro-8*H*,19*H*-16,18-etheno-28,7-(metheno)[1,4]diazepino[2,3-*i*]pyrido[1,2-*q*]pyrrolo[2,1-*d*][1,5,17]oxadiazacycloicosine-4,8(5*H*)-dione (**(*R*)(*R*)110**) as a yellow oil (3 mg, 12%); R_f 0.37 (acetone); $[\alpha]_D^{25}$= +11.8 (*c* 0.2, DMSO); $\bar{\nu}_{max}$ (thin film)/cm^{-1} 2927 (C-H, w), 1673 (C=O, s); VT ^{1}H NMR (500 MHz; DMSO-d_6) δ_H 9.53 (1H, s, NH-9a), 7.72 (1H, d, *J* 2.0, H-7 or H-9), 7.47–7.33 (1H, m, H-7 or H-9), 7.21–7.05 (2H, m, H-5'', H-14''), 6.59–6.50 (1H, m, H-13''), 6.50–6.42 (2H, m, H-6'', H-8''), 5.04 (1H, s, NH-5a);* HRMS *m/z* (ESI$^+$) [Found: 515.3012, $C_{31}H_{39}N_4O_3$ requires M^+ 515.3017]; LRMS *m/z* (ESI$^+$) 515 ([M+H]$^+$, 100%); HPLC Method 1: Retention time 9.4 min, purity 95.0%. *Assignment of aromatic peaks only due to weak signal intensity. See Appendix for ^{1}H NMR spectrum.

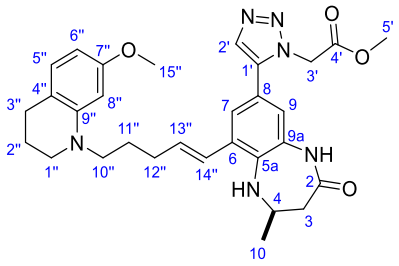
(*R,E*)-8-Ethynyl-6-(5-(7-methoxy-3,4-dihydroquinolin-1(2*H*)-yl)pent-1-en-1-yl)-4-methyl-1,3,4,5-tetrahydro-2*H*-benzo[*b*][1,4]diazepin-2-one ((*R*)158)



(*R*)-6-Bromo-4-methyl-8-((trimethylsilyl)ethynyl)-1,3,4,5-tetrahydro-2*H*-benzo[*b*][1,4]diazepin-2-one (**(*R*)138**) (440 mg, 1.25 mmol, 1.0 eq.), bis(triphenylphosphine)palladium(II) dichloride (44.0 mg, 0.0626 mmol, 0.05 eq.) and K_2CO_3 (520 mg, 3.75 mmol, 3.0 eq.) were added to a Schlenk flask under a nitrogen atmosphere (evacuated and backfilled 3 × nitrogen). (7-Methoxy-1-(5-(4,4,5,5-tetramethyl-1,3,2-dioxaborolan-2-yl)pent-4-en-1-yl)-1,2,3,4-tetrahydroquinoline (**47**) (671 mg, 1.88 mmol, 1.5 eq.) in 1,4-dioxane (8 mL) was added, followed by H_2O (1.9 mL) and the reaction mixture was stirred at 100 °C for 18 h. The reaction mixture was evaporated *in vacuo* and diluted with EtOAc (100 mL). The organic component was washed with brine (3 × 50 mL), dried ($MgSO_4$), filtered, and evaporated *in vacuo* to afford an orange oil. The crude oil was dissolved in MeOH (13 mL) and K_2CO_3 (200 mg) was added. The reaction mixture was stirred at rt for 2 h. The reaction mixture was evaporated *in vacuo* to afford an orange oil. The crude oil was dissolved in 1 M aq. K_2CO_3 (100 mL) and extracted with EtOAc ((3 × 50 mL). The combined organic components were washed with brine (20 mL), dried ($MgSO_4$), filtered, and evaporated *in vacuo* to afford an orange oil. The crude oil was purified by silica gel chromatography (elution with 50% to 100% EtOAc in petroleum ether) to yield (*R,E*)-8-ethynyl-6-(5-(7-methoxy-3,4-dihydroquinolin-1(2*H*)-yl)pent-1-en-1-yl)-4-methyl-1,3,4,5-tetrahydro-2*H*-benzo[*b*][1,4]diazepin-2-one (**(*R*)158**) as a yellow oil (240 mg, 45%) and was used without further purification; R_f 0.38 (EtOAc/petroleum ether 4:1); $[\alpha]_D^{25}$ = +2.49 (*c* 1.0, $CHCl_3$); $\bar{\nu}_{max}$ (thin film)/cm^{-1} 3306 (N-H, br s), 2934 (C-H, s), 1670 (C=O, s); ^{1}H NMR (500 MHz; $CDCl_3$) δ_H 7.24–7.20 (2H, m, H-9, NH-9a), 6.90 (1H, d, *J* 1.9, H-7), 6.85 (1H, d, *J* 7.3, H-5''), 6.37 (1H, d, *J* 15.4, H-14''), 6.17–6.04 (3H, m, H-6'', H-8'', H-13''), 4.04–3.98 (1H, m, H-4), 3.75 (3H, s, H-15''), 3.74 (1H, d, *J* 2.0, NH-5a), 3.32–3.17 (4H, m, H-1'', H-10''), 3.01 (1H, s, H-2'), 2.69 (2H, t, *J* 6.8, H-3''), 2.62 (1H, ddd, *J* 13.6, 4.0, 1.0, H_AH_B-3), 2.43 (1H, dd, *J* 13.6, 7.8, H_AH_B-3), 2.33–2.25 (2H, m, H-12''), 1.97–1.87 (2H, m, H-2''), 1.84–1.74 (2H, m, H-11''), 1.35 (3H, d, *J* 6.3, H-10); ^{13}C NMR (126 MHz; $CDCl_3$) δ_C 172.3 (C-2), 159.3 (C-7''), 146.2 (C-9''), 136.7 (C-5a), 136.2 (C-13''), 130.4 (C-9a), 129.7 (C-5''), 128.5 (C-9), 128.3 (C-6), 124.8 (C-14''), 124.5 (C-7), 115.5 (C-4''), 114.1 (C-8), 99.5 (C-6''), 97.7 (C-8''), 83.2 (C-1'), 76.5 (C-2'), 55.3 (C-15''), 54.4 (C-4),

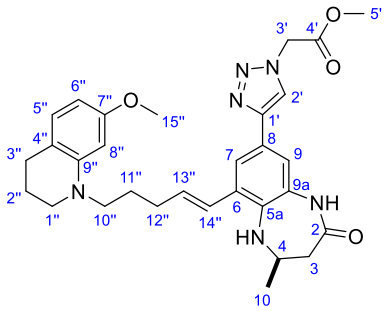
51.1 (C-1''), 49.6 (C-10''), 41.0 (C-3), 31.1 (C-12''), 27.6 (C-3''), 26.0 (C-11''), 24.3 (C-10), 22.6 (C-2''); HRMS *m/z* (ESI$^+$) [Found: 430.2485, $C_{27}H_{32}N_3O_2$ requires M^+ 430.2489]; LRMS *m/z* (ESI$^+$) 430 ([M+H]$^+$, 100%).

Methyl (*R,E*)-2-(5-(9-(5-(7-methoxy-3,4-dihydroquinolin-1(2*H*)-yl)pent-1-en-1-yl)-2-methyl-4-oxo-2,3,4,5-tetrahydro-1*H*-benzo[*b*][1,4]diazepin-7-yl)-1*H*-1,2,3-triazol-1-yl)acetate ((*R*)159)



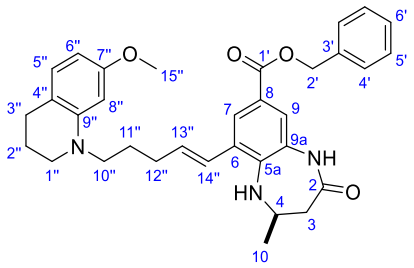
A solution of methyl 2-azidoacetate (11 µL, 0.12 mmol, 1.2 eq.) in THF (0.8 mL) was added to (*R,E*)-8-ethynyl-6-(5-(7-methoxy-3,4-dihydroquinolin-1(2*H*)-yl)pent-1-en-1-yl)-4-methyl-1,3,4,5-tetrahydro-2*H*-benzo[*b*][1,4]diazepin-2-one (**(*R*)158**) (41 mg, 0.095 mmol, 1.0 eq.) and pentamethylcyclopentadienylbis(triphenylphosphine)ruthenium(II) chloride (4.0 mg, 0.0047 mmol, 0.05 eq.) at rt under a nitrogen atmosphere (evacuated and backfilled 3 × nitrogen). The reaction mixture was stirred at 75 °C under nitrogen for 2 h. The reaction mixture was evaporated *in vacuo* to afford a red oil. The crude oil was purified by silica gel chromatography (elution with 80% to 100% EtOAc in petroleum ether) to yield methyl (*R*)-2-(5-(9-bromo-2-methyl-4-oxo-2,3,4,5-tetrahydro-1*H*-benzo[*b*][1,4]diazepin-7-yl)-1*H*-1,2,3-triazol-1-yl)acetate (**(*R*)159**) as a pale yellow oil (24 mg, 46%); R_f 0.19 (EtOAc); $[\alpha]_D^{25}$= −1.93 (*c* 1.0, $CHCl_3$); $\bar{\nu}_{max}$ (thin film)/cm^{-1} 3352 (N-H, w), 2934 (C-H, w), 1754 (C=O, s), 1673 (C=O, s); ^{1}H NMR (500 MHz; $CDCl_3$) δ_H 7.70 (1H, s, H-2'), 7.06 (1H, d, *J* 1.9, H-7), 6.85 (1H, d, *J* 8.5, H-5''), 6.78 (1H, d, *J* 1.9, H-9), 6.42 (1H, d, *J* 15.5, H-14''), 6.17–5.98 (3H, m, H-6'', H-8'', H-13''), 5.11 (2H, s, H-3'), 4.13 (1H, m, H-4), 3.77 (3H, s, H-5'), 3.73 (3H, s, H-15''), 3.31–3.24 (4H, m, H-1'', H-10''), 2.73–2.63 (3H, m, H-3'', H_AH_B-3), 2.50 (1H, dd, *J* 13.7, 7.9, H_AH_B-3), 2.34–2.28 (2H, m, H-12''), 1.95–1.87 (2H, m, H-2''), 1.79 (2H, tt, *J* 7.4, 7.4 H-11''), 1.39 (3H, d, *J* 6.3, H-10); ^{13}C NMR (126 MHz; $CDCl_3$) δ_C 172.2 (C-2), 167.3 (C-4'), 159.3 (C-7''), 146.2 (C-9''), 138.3 (C-1'), 137.1 (C-5a), 136.7 (C-13''), 133.0 (C-2'), 130.9 (C-9a), 129.7 (C-5''), 128.6 (C-6), 124.9 (C-14''), 124.8 (C-7), 120.9 (C-9), 118.4 (C-4''), 115.6 (C-8), 99.3 (C-6''), 97.8 (C-8''), 55.3 (C-15''), 54.1 (C-4), 53.2 (C-5'), 51.1 (C-1''), 49.6 (C-10''), 49.2 (C-3'), 41.2 (C-3), 31.2 (C-12''), 27.5 (C-3''), 26.0 (C-11''), 24.4 (C-10), 22.6 (C-2''); HRMS *m/z* (ESI$^+$) [Found: 545.2860, $C_{30}H_{37}N_6O_4$ requires M^+ 545.2871]; LRMS *m/z* (ESI$^+$) 545 ([M+H]$^+$, 100%); HPLC Method 1: Retention time 6.1 min, purity 97.5%.

Methyl (*R,E*)-2-(4-(9-(5-(7-methoxy-3,4-dihydroquinolin-1(2*H*)-yl)pent-1-en-1-yl)-2-methyl-4-oxo-2,3,4,5-tetrahydro-1*H*-benzo[*b*][1,4]diazepin-7-yl)-1*H*-1,2,3-triazol-1-yl)acetate ((*R*)160)



Methyl 2-azidoacetate (12 µL, 0.13 mmol, 1.1 eq.) was added to a solution of (*R,E*)-8-ethynyl-6-(5-(7-methoxy-3,4-dihydroquinolin-1(2*H*)-yl)pent-1-en-1-yl)-4-methyl-1,3,4,5-tetrahydro-2*H*-benzo[*b*][1,4]diazepin-2-one (**(*R*)158**) (51 mg, 0.12 mmol, 1.0 eq.), copper (II) sulfate (3.0 mg, 0.012 mmol, 0.1 eq.) and (+)-sodium L-ascorbate (3.0 mg, 0.012 mmol, 0.1 eq.) in THF (0.4 mL) and H_2O (0.4 mL) and the reaction mixture was stirred at rt for 2 h. The reaction mixture was purified by silica gel chromatography (elution with 80% to 100% EtOAc in petroleum ether) to yield methyl (*R,E*)-2-(4-(9-(5-(7-methoxy-3,4-dihydroquinolin-1(2*H*)-yl)pent-1-en-1-yl)-2-methyl-4-oxo-2,3,4,5-tetrahydro-1*H*-benzo[*b*][1,4]diazepin-7-yl)-1*H*-1,2,3-triazol-1-yl)acetate (**(*R*)160**) as a dark yellow oil (34 mg, 52%); R_f 0.22 (EtOAc); $[\alpha]_D^{25}$= +8.57 (*c* 1.0, $CHCl_3$); $\bar{\nu}_{max}$ (neat)/cm^{-1} 3364 (N-H, w), 2934 (C-H, w), 1754 (C=O, s), 1670 (C=O, s); ^{1}H NMR (500 MHz; $CDCl_3$) δ_H 7.84 (1H, s, H-2'), 7.56 (1H, d, *J* 2.0, H-7), 7.31 (1H, d, *J* 2.0, H-9), 7.19 (1H, s, NH-9a), 6.86 (1H, d, *J* 8.1, H-5''), 6.47 (1H, d, *J* 15.5, H-14''), 6.22–6.10 (3H, m, H-6'', H-8'', H-13''), 5.22 (2H, s, H-3'), 4.12 (1H, m, H-4), 3.83 (3H, s, H-5'), 3.74 (3H, s, H-15''), 3.62 (1H, s, NH-5a), 3.33–3.23 (4H, m, H-1'', H-10''), 2.71–2.67 (2H, m, H-3''), 2.65 (1H, dd, *J* 13.5, 4.5, H_AH_B-3), 2.44 (1H, dd, *J* 13.5, 7.6, H_AH_B-3), 2.36–2.28 (2H, m, H-12''), 1.96–1.88 (2H, m, H-2''), 1.84–1.76 (2H, m, H-11''), 1.37 (3H, d, *J* 6.2, H-10); ^{13}C NMR (126 MHz; $CDCl_3$) δ_C 172.4 (C-2), 166.8 (C-4'), 159.4 (C-7''), 147.7 (C-1'), 146.3 (C-9''), 136.1 (C-5a), 135.8 (C-13''), 131.3 (C-9a), 129.73 (C-6), 129.66 (C-5''), 125.3 (C-14''), 123.6 (C-4''), 122.0 (C-7), 120.5 (C-2'), 118.3 (C-9), 115.5 (C-8), 99.5 (C-6''), 97.7 (C-8''), 55.3 (C-15''), 55.1 (C-4), 53.3 (C-5'), 51.2 (C-1''), 51.0 (C-3'), 49.6 (C-10''), 40.9 (C-3), 31.2 (C-12''), 27.6 (C-3''), 26.1 (C-11''), 24.3 (C-10), 22.6 (C-2''); HRMS *m/z* (ESI$^+$) [Found: 545.2860, $C_{30}H_{37}N_6O_4$ requires M^+ 545.2871]; LRMS *m/z* (ESI$^+$) 545 ([M+H]$^+$, 100%); HPLC Method 1: Retention time 6.2 min, purity 97.2%.

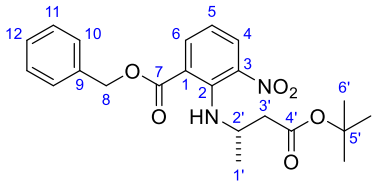
Benzyl (*R*,*E*)-9-(5-(7-methoxy-3,4-dihydroquinolin-1(2*H*)-yl)pent-1-en-1-yl)-2-methyl-4-oxo-2,3,4,5-tetrahydro-1*H*-benzo[*b*][1,4]diazepine-7-carboxylate ((*R*)161)



Benzyl (*R*)-9-iodo-2-methyl-4-oxo-2,3,4,5-tetrahydro-1*H*-benzo[*b*][1,4]diazepine-7-carboxylate (**(*R*)150**) (57 mg, 0.13 mmol, 1.0 eq.), bis(triphenylphosphine)palladium(II) dichloride (5.0 mg, 0.0055 mmol, 0.05 eq.) and K_2CO_3 (54 mg, 0.39 mmol, 3.0 eq.) were added to a Schlenk flask under a nitrogen atmosphere (evacuated and backfilled 3 × nitrogen). (7-Methoxy-1-(5-(4,4,5,5-tetramethyl-1,3,2-dioxaborolan-2-yl)pent-4-en-1-yl)-1,2,3,4-tetrahydroquinoline (**47**) (70 mg, 0.39 mmol, 1.5 eq.) in 1,4-dioxane (0.85 mL) was added, followed by H_2O (0.1 mL) and the reaction mixture was stirred at 100 °C for 18 h. The reaction mixture was evaporated *in vacuo* and diluted with EtOAc (20 mL). The organic component was washed with brine (3 × 10 mL), dried ($MgSO_4$), filtered, and evaporated *in vacuo* to afford an orange oil. The crude oil was purified by silica gel chromatography (elution with 50% to 80% EtOAc in petroleum ether) to yield benzyl (*R*,*E*)-2-methyl-4-oxo-9-(5-(7-((triisopropylsilyl)oxy)-3,4-dihydroquinolin-1(2*H*)-yl)pent-1-en-1-yl)-2,3,4,5-tetrahydro-1*H*-benzo[*b*][1,4]diazepine-7-carboxylate (**(*R*)161**) as an orange oil (34 mg, 48%) and was used without further purification; R_f 0.40 (EtOAc/petroleum ether 1:1); $[\alpha]_D^{25}$= −40.9 (*c* 1.0, $CHCl_3$); $\bar{\nu}_{max}$ (thin film)/cm^{-1} 2935 (C-H, s), 1705 (C=O, m), 1671 (C=O, s); ^{1}H NMR (500 MHz; $CDCl_3$) δ_H 7.74 (1H, d, *J* 2.0, H-9), 7.48–7.31 (7H, m, H-7, NH-9a, H-4', H-5', H-6'), 6.85 (1H, d, *J* 7.8, H-5''), 6.35 (1H, d, *J* 15.5, H-14''), 6.17–6.08 (3H, m, H-6'', H-8'', H-13''), 5.33 (2H, s, H-2'), 4.16–4.05 (1H, m, H-4), 4.02 (1H, s, NH-5a), 3.74 (3H, s, H-15''), 3.33–3.23 (4H, m, H-1'', H-10''), 2.72–2.64 (3H, m, H_AH_B-3, H-3''), 2.51 (1H, dd, *J* 13.9, 8.2, H_AH_B-3), 2.34–2.25 (2H, m, H-12''), 1.95–1.89 (2H, m, H-2''), 1.80 (2H, tt, *J* 7.5, H-11''), 1.37 (3H, d, *J* 6.3, H-10); ^{13}C NMR (126 MHz; $CDCl_3$) δ_C 172.0 (C-2), 166.0 (C-1'), 159.3 (C-7''), 146.2 (C-9''), 140.0 (C-5a), 136.7 (C-13''), 136.3 (C-3'), 129.7 (C-5''), 129.1 (C-6), 128.7 (C-5'), 128.4 (C-6'), 128.3 (C-4'), 126.4 (C-9), 125.9 (C-9a), 124.8 (C-14''), 122.7 (C-7), 121.2 (C-8), 115.5 (C-4''), 99.5 (C-6''), 97.7 (C-8''), 66.7 (C-2'), 55.3 (C-15''), 53.0 (C-4), 51.2 (C-10''), 49.6 (C-1''), 41.6 (C-3), 31.1 (C-12''), 27.6 (C-3''), 26.0 (C-11''), 24.4 (C-10), 22.6 (C-2''); HRMS *m/z* (ESI$^+$) [Found: 540.2860, $C_{33}H_{38}N_3O_4$ requires M^+ 540.2857]; LRMS *m/z* (ESI$^+$) 540 ([M+H]$^+$, 100%); HPLC Method 1: Retention time 10.5 min, purity 83.7%.

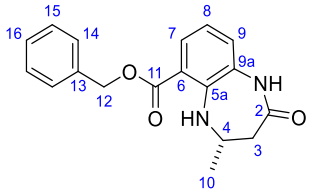
8.2.4 Chapter 6 - ESAC Library

Benzyl (*S*)-2-((4-(*tert*-butoxy)-4-oxobutan-2-yl)amino)-3-nitrobenzoate ((*S*)94)



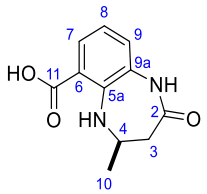
Benzyl (*S*)-2-((4-(*tert*-butoxy)-4-oxobutan-2-yl)amino)-3-nitrobenzoate (**(*S*)94**) was synthesised using benzyl 2-fluoro-3-nitrobenzoate (**93**) following the same procedure to prepare benzyl (*R*)-2-((4-(*tert*-butoxy)-4-oxobutan-2-yl)amino)-3-nitrobenzoate (**(*R*)94**) to yield an orange oil (523 mg, 98%); $[\alpha]_D^{25}$= −66.5 (*c* 1.0, $CHCl_3$), other physical and spectroscopic properties are identical to those as benzyl (*R*)-2-((4-(*tert*-butoxy)-4-oxobutan-2-yl)amino)-3-nitrobenzoate (**(*R*)94**). These data are in accordance with the literature.[30]

Benzyl (*S*)-4-methyl-2-oxo-2,3,4,5-tetrahydro-1*H*-benzo[*b*][1,4]diazepine-6-carboxylate ((*S*)95)



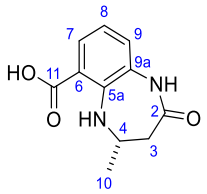
Benzyl (*S*)-4-methyl-2-oxo-2,3,4,5-tetrahydro-1*H*-benzo[*b*][1,4]diazepine-6-carboxylate (**(*S*)95**) was synthesised using benzyl (*S*)-2-((4-(*tert*-butoxy)-4-oxobutan-2-yl)amino)-3-nitrobenzoate (**(*S*)94**) following the same procedure to prepare benzyl (*R*)-4-methyl-2-oxo-2,3,4,5-tetrahydro-1*H*-benzo[*b*][1,4]diazepine-6-carboxylate (**(*R*)95**) to yield a pale yellow solid (327 mg, 89%); $[\alpha]_D^{25}$= +51.4 (*c* 1.0, $CHCl_3$), other physical and spectroscopic properties are identical to those as benzyl (*R*)-4-methyl-2-oxo-2,3,4,5-tetrahydro-1*H*-benzo[*b*][1,4]diazepine-6-carboxylate (**(*R*)95**). These data are in accordance with the literature.[30]

(*R*)-4-Methyl-2-oxo-2,3,4,5-tetrahydro-1*H*-benzo[*b*][1,4]diazepine-6-carboxylic acid ((*R*)179)



10% Pd/C (33 mg, 0.030 mmol, 0.1 eq.) was added to a stirred solution of benzyl (*R*)-4-methyl-2-oxo-2,3,4,5-tetrahydro-1*H*-benzo[*b*][1,4]diazepine-6-carboxylate (**(*R*)95**) (94 mg, 0.30 mmol, 1.0 eq.) in EtOAc (2 mL) and MeOH (2 mL), which was purged under a nitrogen atmosphere. The atmosphere was replaced with hydrogen gas and the suspension was stirred at rt for 6 h. The black suspension was filtered through Celite® and washed with MeOH (50 mL). The filtrate was evaporated *in vacuo* to yield (*R*)-4-methyl-2-oxo-2,3,4,5-tetrahydro-1*H*-benzo[*b*][1,4]diazepine-6-carboxylic acid (**(*R*)179**) as a yellow solid (24 mg, 37%); R_f 0.11 (AcOH/EtOAc 1:99); $[\alpha]_D^{25}$= −34.8 (*c* 0.5, MeOH); mp 254–257 °C (EtOAc); $\bar{\nu}_{max}$ (thin film)/cm^{-1} 3030 (C-H, w), 1655 (C=O, s); ^{1}H NMR (500 MHz; DMSO-d_6) δ_H 9.55 (1H, br s, OH-11), 7.63 (1H, dd, *J* 7.8, 1.6, H-7), 7.07 (1H, dd, *J* 7.8, 1.6, H-9), 6.68 (1H, dd, *J* 7.8, 7.8, H-8), 3.95 (1H, m, H-4), 2.50 (1H, m, H_AH_B-3), 2.37 (1H, dd, *J* 13.8, 8.2, H_AH_B-3), 1.24 (3H, d, *J* 6.3, H-10); ^{13}C NMR (126 MHz; DMSO-d_6) δ_C 171.3 (C-2), 170.3 (C-11), 142.6 (C-5a), 127.9 (C-9a), 127.6 (C-7), 126.4 (C-9), 116.8 (C-8), 51.9 (C-4), 41.8 (C-3), 23.8 (C-10), C-6 could not be observed with ^{1}H-^{13}C correlations; HRMS *m/z* (ESI$^+$) [Found: 221.0921, $C_7H_{13}O_3N_2$ requires M^+ 221.0921]; LRMS *m/z* (ESI$^-$) 219 ([M-H]$^-$, 100%); HPLC Method 2: Retention time 5.2 min, purity 99.1%.

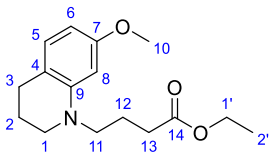
(*S*)-4-Methyl-2-oxo-2,3,4,5-tetrahydro-1*H*-benzo[*b*][1,4]diazepine-6-carboxylic acid ((*S*)179)



(*S*)-4-Methyl-2-oxo-2,3,4,5-tetrahydro-1*H*-benzo[*b*][1,4]diazepine-6-carboxylic acid (**(*S*)179**) was synthesised using benzyl (*S*)-4-methyl-2-oxo-2,3,4,5-tetrahydro-1*H*-benzo[*b*][1,4]diazepine-6-carboxylate (**(*S*)95**) following the same procedure to prepare (*R*)-4-methyl-2-oxo-2,3,4,5-tetrahydro-1*H*-benzo[*b*][1,4]diazepine-6-carboxylic acid (**(*R*)179**) to yield a yellow solid (55 mg, 53%); $[\alpha]_D^{25}$= +44.3 (*c* 0.5, MeOH), other physical and spectroscopic properties are identical to those as (*R*)-

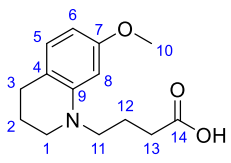
4-methyl-2-oxo-2,3,4,5-tetrahydro-1*H*-benzo[*b*][1,4]diazepine-6-carboxylic acid (**(*R*)179**). HPLC Method 2: Retention time 5.0 min, purity 98.2%.

Ethyl 4-(7-methoxy-3,4-dihydroquinolin-1(2*H*)-yl)butanoate (180)



Ethyl 4-bromobutanoate (172 µL, 1.20 mmol, 1.5 eq.) was added to a solution of 7-methoxy-1,2,3,4-tetrahydroquinoline (**45**) (131 mg, 0.800 mmol, 1.0 eq.), potassium iodide (78.0 mg, 0.400 mmol, 0.5 eq.) and *N*,*N*-diisopropylethylamine (279 µL, 1.60 mmoL, 2.0 eq.) in DMF (4 mL). The reaction mixture was sealed and heated to 100 °C in a microwave for 1 h. The cooled orange solution was diluted with EtOAc (70 mL) and washed with H_2O (3 × 50 mL). The organic component was further washed with 0.5 M aq. LiCl (3 × 30 mL), brine (50 mL), dried ($MgSO_4$), filtered and evaporated *in vacuo* to afford a brown oil. The crude oil as purified by silica gel chromatography (elution with toluene) to yield ethyl 4-(7-methoxy-3,4-dihydroquinolin-1(2*H*)-yl)butanoate (**181**) as a pale brown oil (323 mg, 95%); R_f 0.23 (EtOAc/petroleum ether 1:9); $\bar{\nu}_{max}$ (thin film)/cm^{-1} 2935 (C-H, w), 1730 (C=O, s); ^{1}H NMR (500 MHz; $CDCl_3$) δ_H 6.83 (1H, d, *J* 8.1, H-5), 6.18 (1H, d, *J* 2.4, H-8), 6.13 (1H, dd, *J* 8.1, 2.4, H-6), 4.13 (2H, q, *J* 7.2, H-1'), 3.76 (3H, s, H-10), 3.30–3.19 (4H, m, H-1, H-11), 2.68 (2H, t, *J* 6.4, H-3), 2.35 (2H, t, *J* 7.2, H-13), 1.98–1.85 (4H, m, H-2, H-12), 1.25 (3H, t, *J* 7.2, H-2'); ^{13}C NMR (126 MHz; $CDCl_3$) δ_C 173.5 (C-14), 159.4 (C-7), 146.1 (C-9), 129.6 (C-5), 115.3 (C-4), 100.0 (C-6), 97.6 (C-8), 60.6 (C-1'), 55.3 (C-10), 50.9 (C-11), 49.6 (C-1), 31.8 (C-13), 27.5 (C-3), 22.6 (C-12), 21.8 (C-2), 14.4 (C-2'); HRMS *m/z* (ESI^+) [Found: 278.1750, $C_{16}H_{24}NO_3$ requires M^+ 278.1751]; LRMS *m/z* (ESI^+) 278 ($[M+H]^+$, 100%); HPLC Method 1: Retention time 11.3 min, purity 99.6%.

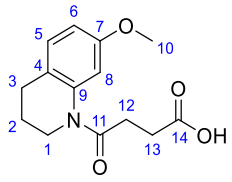
4-(7-Methoxy-3,4-dihydroquinolin-1(2*H*)-yl)butanoic acid (181)



To a stirred solution of ethyl 4-(7-methoxy-3,4-dihydroquinolin-1(2*H*)-yl)butanoate (**180**) (277 mg, 1.00 mmol, 1.0 eq.) in THF/MeOH/H_2O (3:2:1, 10 mL) was added LiOH (240 mg, 10.0 mmol, 10.0 eq.)

and the reaction mixture was stirred for 16 h. The reaction mixture was evaporated *in vacuo*. The resulting residue was diluted with 2 M aq. NaOH (30 mL). and was washed with CH_2Cl_2 (3 × 30 mL). The aqueous component was acidified with concentrated HCl to pH 1 and extracted with EtOAc (3 × 50 mL). The combined organic components were washed with brine (50 mL), dried ($MgSO_4$), filtered, and evaporated *in vacuo* to yield 4-(7-methoxy-3,4-dihydroquinolin-1(2*H*)-yl)butanoic acid (**181**) as a green solid (174 mg, 70%); R_f 0.48 (AcOH/EtOAc/petroleum ether 1:10:39); mp 47–49 °C (EtOAc); $\bar{\nu}_{max}$ (thin film)/cm^{-1} 2996 (C-H, w), 1697 (C=O, s); ^{1}H NMR (500 MHz; DMSO-d_6) δ_H 12.12 (1H, s, OH-14), 6.74 (1H, d, *J* 8.1, H-5), 6.17 (1H, d, *J* 2.4, H-8), 6.04 (1H, dd, *J* 8.1, 2.4, H-6), 3.66 (3H, s, H-10), 3.23–3.14 (4H, m, H-1, H-11), 2.59 (2H, t, *J* 6.3, H-3), 2.27 (2H, t, *J* 7.2, H-13), 1.85–1.75 (2H, m, H-2), 1.72 (2H, tt, *J* 7.2, 7.2, H-12); ^{13}C NMR (126 MHz; DMSO-d_6) δ_C 174.4 (C-14), 158.8 (C-7), 145.7 (C-9), 129.2 (C-5), 114.2 (C-4), 100.1 (C-6), 96.6 (C-8), 54.7 (C-10), 49.9 (C-11), 48.5 (C-1), 30.8 (C-13), 26.9 (C-3), 22.0 (C-2), 20.7 (C-12); HRMS *m/z* (ESI^+) [Found: 250.1440, $C_{14}H_{20}NO_3$ requires M^+ 250.1440]; LRMS *m/z* (ESI^+) 250 ($[M+H]^+$, 100%); HPLC Method 2: Retention time 5.5 min, purity 97.0%.

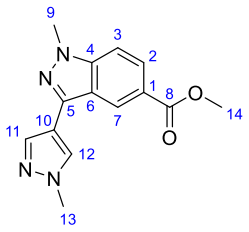
4-(7-Methoxy-3,4-dihydroquinolin-1(2*H*)-yl)-4-oxobutanoic acid (182)



Succinic anhydride (134 mg, 1.35 mmol, 1.1 eq.) was added to 7-methoxy-1,2,3,4-tetrahydroquinoline (**45**) (277 mg, 1.23 mmol, 1.0 eq.) dissolved in THF (2.8 mL) and the reaction mixture was stirred at rt for 20 h. The reaction mixture was evaporated *in vacuo* to afford a yellow oil. The resulting oil was diluted with 2 M aq. NaOH (20 mL) and was washed with CH_2Cl_2 (3 × 30 mL). The aqueous component was acidified with concentrated HCl to pH 1 and extracted with EtOAc (3 × 30 mL). The combined organic components were washed with brine (20 mL), dried ($MgSO_4$), filtered, and evaporated *in vacuo* to yield 4-(7-methoxy-3,4-dihydroquinolin-1(2*H*)-yl)-4-oxobutanoic acid (**182**) as a pale yellow solid (296 mg, 91%); R_f 0.34 (AcOH/EtOAc/petroleum ether 1:10:39); mp 90–92 °C (EtOAc); $\bar{\nu}_{max}$ (thin film)/cm^{-1} 2938 (C-H, s), 1726 (C=O, s), 1607 (C=O, s); ^{1}H NMR (500 MHz; DMSO-d_6) δ_H 11.26 (1H, br s, OH-14), 6.28 (1H, br s, H-8), 6.25 (1H, d, *J* 8.4, H-5), 5.87 (1H, dd, *J* 8.4, 2.6, H-6), 2.88 (3H, s, H-10), 2.83 (2H, t, *J* 6.3, H-1), 1.90–1.84 (2H, m, H-12), 1.80 (2H, t, *J* 6.6, H-3), 1.67–1.65 (2H, m, H-13), 1.01 (2H, m, H-2); ^{13}C NMR (126 MHz; DMSO-d_6) δ_C 173.9 (C-14), 171.1 (C-11), 157.1 (C-7), 139.4 (C-9), 129.0 (C-5), 110.5 (C-8), 110.4 (C-6), 79.2 (C-4),* 55.2 (C-10), 43.2 (C-1), 29.4 (C-13), 29.2 (C-12), 25.5 (C-3), 23.5 (C-2); HRMS *m/z* (ESI^+) [Found: 264.1231, $C_{14}H_{18}NO_4$ requires M^+ 264.1230]; LRMS *m/z* (ESI^-) 262

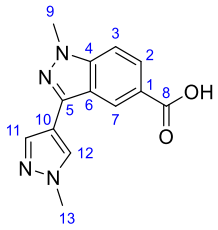
([M-H]$^-$, 100%); HPLC Method 2: Retention time 7.4 min, purity 99.3%. *Observed by ^{1}H-^{13}C-HMBC correlation.

Methyl 1-methyl-3-(1-methyl-1*H*-pyrazol-4-yl)-1*H*-indazole-5-carboxylate (188)



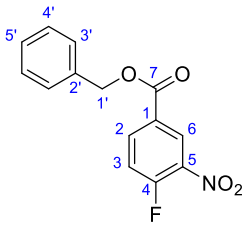
5-Bromo-1-methyl-3-(1-methyl-1*H*-pyrazol-4-yl)-1*H*-indazole (**186**) (0.10 g, 0.35 mmol, 1.0 eq.) and [1,1'-Bis(diphenylphosphino)ferrocene]dichloropalladium(II), complex with CH_2Cl_2 (0.015 g, 0.018 mmol, 0.05 eq.) were added to a Schlenk flask under a nitrogen atmosphere (evacuated and backfilled 3 × nitrogen). NEt_3 (98 µL, 0.70 mmol, 2.0 eq.) and MeOH (1 mL) were added and the atmosphere was replaced with carbon monoxide gas (CARE: Toxic Gas). The brown suspension was stirred at 100 °C for 20 h. The Schlenk flask was replaced with a nitrogen atmosphere (evacuated and backfilled 3 × nitrogen). The reaction was evaporated *in vacuo* and was purified by silica gel chromatography (elution with 0% to 10% EtOH in EtOAc) to yield methyl 1-methyl-3-(1-methyl-1*H*-pyrazol-4-yl)-1*H*-indazole-5-carboxylate (**188**) as a pale brown oil (44 mg, 46%); R_f 0.35 (EtOAc); $\bar{\nu}_{max}$ (thin film)/cm^{-1} 2948 (C-H, w), 1707 (C=O, s); ^{1}H NMR (500 MHz; $CDCl_3$) δ_H 8.61 (1H, dd, *J* 1.5, 0.8, H-7), 8.08 (1H, dd, *J* 8.9, 1.5, H-2), 8.06 (1H, d, *J* 0.8, H-11), 7.95 (1H, s, H-12), 7.38 (1H, dd, *J* 8.8, 0.8, H-3), 4.09 (3H, s, H-9), 4.02 (3H, s, H-13), 3.97 (3H, s, H-14); ^{13}C NMR (126 MHz; $CDCl_3$) δ_C 167.5 (C-8), 142.8 (C-4), 139.3 (C-5), 137.8 (C-11), 128.2 (C-12), 127.4 (C-2), 124.5 (C-7), 122.9 (C-6), 121.5 (C-1), 114.9 (C-10), 109.0 (C-3), 52.3 (C-14), 39.3 (C-13), 35.7 (C-9); HRMS *m/z* (ESI$^+$) [Found: 271.1190, $C_{14}H_{15}N_4O_2$ requires M$^+$ 271.1190]; LRMS *m/z* (ESI$^+$) 271 ([M+H]$^+$, 100%); HPLC Method 1: Retention time 7.9 min, purity 98.1%.

1-Methyl-3-(1-methyl-1*H*-pyrazol-4-yl)-1*H*-indazole-5-carboxylic acid (189)



To a stirred solution of methyl 1-methyl-3-(1-methyl-1*H*-pyrazol-4-yl)-1*H*-indazole-5-carboxylate (**188**) (40 mg, 0.15 mmol, 1.0 eq.) in THF/MeOH/H_2O (3:2:1, 1.5 mL) was added LiOH (36 mg, 1.5 mmol, 10.0 eq.) and the reaction mixture was stirred for 17 h. The reaction mixture was evaporated *in vacuo*. The resulting residue was diluted with 2 M aq. NaOH (20 mL). and was washed with CH_2Cl_2 (3 × 20 mL). The aqueous component was acidified with concentrated HCl to pH 1 and extracted with EtOAc (3 × 20 mL). The combined organic components were washed with brine (20 mL), dried ($MgSO_4$), filtered, and evaporated *in vacuo* to yield 1-methyl-3-(1-methyl-1*H*-pyrazol-4-yl)-1*H*-indazole-5-carboxylic acid (**189**) as a colourless solid (37 mg, 98%); R_f 0.44 (AcOH/EtOH/EtOAc 1:9:90); mp 243–245 °C (EtOAc); $\bar{\nu}_{max}$ (thin film)/cm^{-1} 2850 (C-H, s), 2537 (COO-H, s), 1675 (C=O, w); ^{1}H NMR (500 MHz; DMSO-d_6) δ_H 12.87 (1H, s, OH-8), 8.56 (1H, s, H-7), 8.43 (1H, s, H-12), 7.98 (1H, dd, *J* 8.9, 1.5, H-2), 7.95 (1H, s, H-11), 7.71 (1H, d, *J* 8.9, H-3), 4.08 (3H, s, H-9), 3.96 (3H, s, H-13); ^{13}C NMR (126 MHz; DMSO-d_6) δ_C 167.6 (C-8), 142.2 (C-5), 138.2 (C-4), 136.5 (C-11), 128.7 (C-12), 126.8 (C-2), 123.3 (C-7), 120.3 (C-6), 113.8 (C-10), 109.8 (C-3), 38.6 (C-13), 35.5 (C-9) C-1 could not be observed with ^{1}H-^{13}C correlations; HRMS *m/z* (ESI$^+$) [Found: 257.1034, $C_{13}H_{13}N_4O_2$ requires M^+ 257.1033]; LRMS *m/z* (ESI$^+$) 257 ([M+H]$^+$, 100%); HPLC Method 2: Retention time 6.4 min, purity 99.1%.

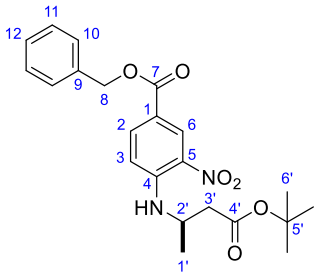
Benzyl 4-fluoro-3-nitrobenzoate (199)



To a solution of 4-fluoro-3-nitrobenzoic acid (**146**) (1.00 g, 5.41 mmol, 1.0 eq.) in NMP (12 mL) was added K_2CO_3 (1.12 g, 8.10 mmol, 1.5 eq.) and the reaction mixture was stirred at rt for 5 mins. Benzyl bromide (964 µL, 8.10 mmol, 1.5 eq) was added and the reaction mixture was stirred at 60 °C for 4 h.

The cooled reaction mixture was diluted with EtOAc (100 mL) and was washed with 1 M aq. K_2CO_3 (3 × 100 mL). The separated organic component was washed with 0.5 M aq. LiCl (3 × 100 mL), brine (100 mL), dried ($MgSO_4$), filtered and evaporated *in vacuo* to afford an orange oil. The crude solid was purified by silica gel chromatography (elution with 0% to 10% EtOAc in petroleum ether) to yield benzyl 4-fluoro-3-nitrobenzoate (**199**) as a pale yellow solid (1.40 g, 94%); R_f 0.51 (EtOAc/petroleum ether 1:4); mp 50–52 °C (EtOAc); ^{1}H NMR (500 MHz; $CDCl_3$) δ_H 8.75 (1H, dd, *J* 7.1, 2.2, H-6), 8.34 (1H, ddd, *J* 8.7, 4.3, 2.2, H-2), 7.49–7.32 (6H, m, H-3, H-3', H-4', H-5'), 5.40 (2H, s, H-1'); ^{13}C NMR (126 MHz; $CDCl_3$) δ_C 163.6 (C-7), 158.2 (d, *J* 271.8, C-4), 137.5 (d, *J* 8.0, C-5), 136.8 (d, *J* 10.0, C-2), 135.2 (C-2'), 128.92 (C-4'), 128.89 (C-5'), 128.7 (C-3'), 128.1 (d, *J* 2.1, C-6), 127.4 (d, *J* 3.9, C-1), 118.9 (d, *J* 21.4, C-3), 67.9 (C-1'); ^{19}F NMR (377 MHz; $CDCl_3$) δ_F −110.3 (ddd, *J* 10.1, 7.1, 4.3); HRMS *m/z* (ESI^+) [Found: 298.0488, $C_{14}H_{10}F^{23}NaNO_4$ requires M^+ 298.0486]; HPLC Method 1: Retention time 9.1 min, purity 99.0%.

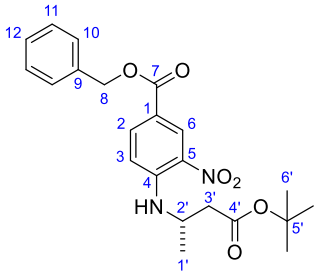
Benzyl (*R*)-4-((4-(*tert*-butoxy)-4-oxobutan-2-yl)amino)-3-nitrobenzoate ((*R*)200)



To a stirred suspension of benzyl 4-fluoro-3-nitrobenzoate (**199**) (300 mg, 1.08 mmol, 1.0 eq.) and Cs_2CO_3 (1.07 g, 3.27 mmol, 3.0 eq.) in toluene (17 mL) at rt was added *tert*-butyl (*R*)-3-aminobutanoate containing 1.63 eq. acetic acid (358 mg, 1.53 mmol, 1.4 eq.) and the suspension was stirred at 85 °C for 18 h. To the cooled suspension was added 1 M aq. K_2CO_3 and the resulting mixture was extracted with EtOAc (3 × 50 mL). The combined organic components were washed with brine (100 mL), dried ($MgSO_4$), filtered, and evaporated *in vacuo* to afford an orange oil. The crude oil was purified by silica gel chromatography (elution with 0% to 20% EtOAc in petroleum ether) to yield benzyl (*R*)-4-((4-(*tert*-butoxy)-4-oxobutan-2-yl)amino)-3-nitrobenzoate (**(*R*)200**) as an orange oil (450 mg, 99%); R_f 0.40 (EtOAc/petroleum ether 1:4); $[\alpha]_D^{25}$= −97.2 (*c* 1.0, $CHCl_3$); $\bar{\nu}_{max}$ (thin film)/cm^{-1} 3355 (N-H, w), 2978 (C-H, w), 1716 (C=O, m), 1530 (N-O, s), 1285 (C-O, s); ^{1}H NMR (500 MHz; $CDCl_3$) δ_H 8.91 (1H, d, *J* 2.1, H-6), 8.50 (1H, d, *J* 8.0, NH-4), 8.08 (1H, dd, *J* 9.1, 2.1, H-2), 7.46–7.31 (5H, m, H-10, H-11, H-12), 6.93 (1H, d, *J* 9.1, H-3), 5.35 (2H, s, H-8), 4.17 (1H, m, H-2'), 2.60 (1H, dd, *J* 15.1, 5.8, H_AH_B-3'), 2.51 (1H, dd, *J* 15.1, 6.6, H_AH_B-3'), 1.44 (9H, s, H-6'), 1.39 (3H, d, *J* 6.6, H-1'); ^{13}C NMR (126 MHz, $CDCl_3$) δ_C 170.0 (C-4'), 165.0 (C-7), 146.7 (C-4), 136.7 (C-2), 136.1 (C-9), 131.5 (C-5), 130.0 (C-6), 128.8 (C-11), 128.5 (C-12),

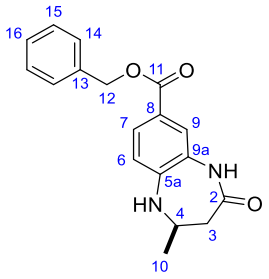
128.4 (C-10), 117.4 (C-1), 113.7 (C-3), 81.8 (C-5'), 66.9 (C-8), 46.1 (C-2'), 42.3 (C-3'), 28.2 (C-6'), 20.5 (C-1'); HRMS *m/z* (ESI$^+$) [Found: 415.1863, $C_{22}H_{27}N_2O_6$ requires M^+ 415.1864]; LRMS *m/z* (ESI$^-$) 413 ([M-H]$^-$, 100%); HPLC Method 1: Retention time 11.9 min, purity 99.9%.

Benzyl (*S*)-4-((4-(*tert*-butoxy)-4-oxobutan-2-yl)amino)-3-nitrobenzoate ((*S*)200)



Benzyl (*S*)-4-((4-(*tert*-butoxy)-4-oxobutan-2-yl)amino)-3-nitrobenzoate nitrobenzoate (**(*S*)200**) was synthesised using benzyl 4-fluoro-3-nitrobenzoate (**199**) following the same procedure to prepare benzyl (*R*)-4-((4-(*tert*-butoxy)-4-oxobutan-2-yl)amino)-3-nitrobenzoate nitrobenzoate (**(*R*)200**) to yield an orange oil (436 mg, 97%); $[\alpha]_D^{25}$= +100.6 (*c* 1.0, $CHCl_3$), other physical and spectroscopic properties are identical to those as benzyl (*R*)-4-((4-(*tert*-butoxy)-4-oxobutan-2-yl)amino)-3-nitrobenzoate nitrobenzoate (**(*R*)200**). HPLC Method 1: Retention time 11.8 min, purity 99.7%.

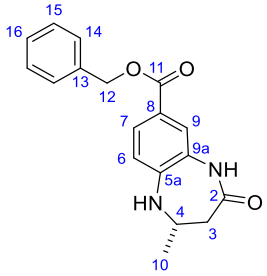
Benzyl (*R*)-2-methyl-4-oxo-2,3,4,5-tetrahydro-1*H*-benzo[*b*][1,4]diazepine-7-carboxylate ((*R*)201)



To a solution of benzyl (*R*)-4-((4-(*tert*-butoxy)-4-oxobutan-2-yl)amino)-3-nitrobenzoate (**(*R*)200**) (404 mg, 0.975 mmol 1.0 eq.) in CH_2Cl_2 (4.4 mL) was added trifluoroacetic acid (4.4 mL) and the orange solution was stirred at rt for 2 h. The reaction mixture was evaporated *in vacuo* and the resulting residue was dissolved in glacial acetic acid (9 mL). Iron powder (272 mg, 4.48 mmol, 5.0 eq.) was added and the brown suspension was stirred under reflux for 4 h. 1 M aq. K_2CO_3 (100 mL) was added to the cooled suspension and the resulting mixture was extracted with EtOAc (3 × 75 mL). The combined

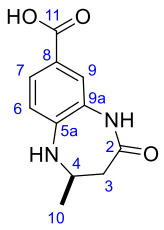
organic components were washed brine (50 mL), dried ($MgSO_4$), filtered, and evaporated *in vacuo* to a brown oil. The crude oil was purified by silica gel chromatography (elution with 50% to 80% EtOAc in petroleum ether) to yield benzyl (*R*)-2-methyl-4-oxo-2,3,4,5-tetrahydro-1*H*-benzo[*b*][1,4]diazepine-7-carboxylate (**(*R*)201**) as a pale yellow solid (263 mg, 87%); R_f 0.35 (EtOAc/petroleum ether 4:1); $[\alpha]_D^{25}$= −3.95 (*c* 1.0, $CHCl_3$); mp 140–142 °C (EtOAc); $\bar{\nu}_{max}$ (neat)/cm^{-1} 3324 (N-H, w), 2969 (C-H, w), 1667 (C=O, s), 1608 (C=O, s); ^{1}H NMR (500 MHz; $CDCl_3$) δ_H 7.67 (1H, dd, *J* 8.4, 1.9, H-7), 7.53 (1H, d, *J* 1.9, H-9), 7.45–7.30 (5H, m, H-14, H-15, H-16), 7.25 (1H, s, NH-9a), 6.67 (1H, d, *J* 8.4, H-6), 5.32 (2H, s, H-12), 4.10–3.97 (2H, m, H-4, NH-5a), 2.69 (1H, ddd, *J* 14.1, 2.7, 1.3, H_AH_B-3), 2.57 (1H, dd, *J* 14.1, 8.3, H_AH_B-3), 1.37 (3H, d, *J* 6.4, H-10); ^{13}C NMR (126 MHz, $CDCl_3$) δ_C 171.8 (C-2), 165.8 (C-11), 142.3 (C-5a), 136.3 (C-13), 128.7 (C-15), 128.4 (C-16), 128.3 (C-14), 127.5 (C-7), 124.2 (C-9), 124.0 (C-8), 121.3 (C-9a), 119.2 (C-6), 66.6 (C-12), 51.5 (C-4), 42.5 (C-3), 24.1 (C-10); HRMS *m/z* (ESI^+) [Found: 311.1391, $C_{18}H_{19}N_2O_3$ requires M^+ 311.1390]; LRMS *m/z* (ESI^+) 311 ($[M+H]^+$, 100%); HPLC Method 1: Retention time 7.3 min, purity 99.1%.

Benzyl (*S*)-2-methyl-4-oxo-2,3,4,5-tetrahydro-1*H*-benzo[*b*][1,4]diazepine-7-carboxylate ((*S*)201)



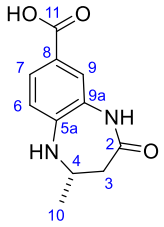
Benzyl (*S*)-2-methyl-4-oxo-2,3,4,5-tetrahydro-1*H*-benzo[*b*][1,4]diazepine-7-carboxylate (**(*S*)201**) was synthesised using benzyl (*S*)-4-((4-(*tert*-butoxy)-4-oxobutan-2-yl)amino)-3-nitrobenzoate (**(*S*)200**) following the same procedure to prepare benzyl (*R*)-2-methyl-4-oxo-2,3,4,5-tetrahydro-1*H*-benzo[*b*][1,4]diazepine-7-carboxylate (**(*R*)201**) to yield a pale brown solid (173 mg, 57%); $[\alpha]_D^{25}$= +9.4 (*c* 1.0, $CHCl_3$), other physical and spectroscopic properties are identical to those as benzyl (*S*)-2-methyl-4-oxo-2,3,4,5-tetrahydro-1*H*-benzo[*b*][1,4]diazepine-7-carboxylate (**(*R*)201**). HPLC Method 1: Retention time 7.1 min, purity 99.2%.

(*R*)-2-Methyl-4-oxo-2,3,4,5-tetrahydro-1*H*-benzo[*b*][1,4]diazepine-7-carboxylic acid ((*R*)202)



10% Pd/C (39.0 mg, 0.0367 mmol, 0.1 eq.) was added to a stirred solution benzyl (*R*)-2-methyl-4-oxo-2,3,4,5-tetrahydro-1*H*-benzo[*b*][1,4]diazepine-7-carboxylate (**(*R*)201**) (114 mg, 0.367 mmol, 1.0 eq.) in MeOH (5 mL), which was purged under a nitrogen atmosphere. The atmosphere was replaced with hydrogen gas and the suspension was stirred at rt for 16 h. The black suspension was filtered through Celite® and washed with MeOH (50 mL). The filtrate was evaporated *in vacuo* to yield (*R*)-2-methyl-4-oxo-2,3,4,5-tetrahydro-1*H*-benzo[*b*][1,4]diazepine-7-carboxylic acid (**(*R*)202**) as a colourless solid (80 mg, 99%); R_f 0.21 (AcOH/EtOAc 1:99); $[\alpha]_D^{25}$= +34.7 (*c* 1.0, MeOH); mp 240–243 °C (EtOAc); $\bar{\nu}_{max}$ (thin film)/cm^{-1} 3338 (O-H, w), 2972 (C-H, w), 1662 (C=O, s), 1609 (C=O, s); ^{1}H NMR (500 MHz; DMSO-d_6) δ_H 12.29 (1H, br s, OH-11), 9.56 (1H, s, NH-9a), 7.47 (1H, d, *J* 2.0, H-9), 7.40 (1H, dd, *J* 8.4, 2.0, H-7), 6.77 (1H, d, *J* 8.4, H-6), 6.24 (1H, s, NH-5a), 3.84 (1H, m, H-4), 2.53–2.45 (1H, m, H_AH_B-3), 2.41–2.28 (1H, m, H_AH_B-3), 1.22 (3H, d, *J* 6.4, H-10); ^{13}C NMR (126 MHz; DMSO-d_6) δ_C 171.1 (C-2), 167.1 (C-11), 143.0 (C-5a), 125.8 (C-7), 124.1 (C-9a), 123.8 (C-9), 118.1 (C-6), 50.5 (C-4), 42.6 (C-3), 23.4 (C-10), C-8 could not be observed with ^{1}H-^{13}C correlations; HRMS *m/z* (ESI$^+$) [Found: 221.0920, $C_{11}H_{13}N_2O_3$ requires M^+ 221.0921]; LRMS *m/z* (ESI$^+$) 221 ([M+H]$^+$, 100%); HPLC Method 2: Retention time 4.9 min, purity 99.6%.

(*S*)-2-Methyl-4-oxo-2,3,4,5-tetrahydro-1*H*-benzo[*b*][1,4]diazepine-7-carboxylic acid ((*S*)202)



(*S*)-2-Methyl-4-oxo-2,3,4,5-tetrahydro-1*H*-benzo[*b*][1,4]diazepine-7-carboxylic acid (**(*S*)202**) was synthesised using benzyl (*S*)-2-methyl-4-oxo-2,3,4,5-tetrahydro-1*H*-benzo[*b*][1,4]diazepine-7-carboxylate (**(*S*)201**) following the same procedure to prepare (*R*)-2-methyl-4-oxo-2,3,4,5-tetrahydro-

1*H*-benzo[*b*][1,4]diazepine-7-carboxylic acid (**(*R*)202**) to yield a colourless solid (79 mg, 91%); $[\alpha]_D^{25}$= −31.5 (*c* 1.0, $CHCl_3$); other physical and spectroscopic properties are identical to those as benzyl (*R*)-2-methyl-4-oxo-2,3,4,5-tetrahydro-1*H*-benzo[*b*][1,4]diazepine-7-carboxylic acid (**(*R*)202**). HPLC Method 2: Retention time 5.2 min, purity 99.4%.

References

1 C. H. Waddington, *Endeavour*, 1942, **1**, 18–20.

2 S. L. Berger, T. Kouzarides, R. Shiekhattar and A. Shilatifard, *Genes Dev.*, 2009, **23**, 781–783.

3 A. Portela and M. Esteller, *Nat. Biotechnol.*, 2010, **28**, 1057–1068.

4 K. A. Janssen, S. Sidoli and B. A. Garcia, *Methods Enzymol.*, 2017, **586**, 359–378.

5 E. Ferri, C. Petosa and C. E. McKenna, *Biochem. Pharmacol.*, 2016, **106**, 1–18.

6 Z. Chen, S. Li, S. Subramaniam, J. Y.-J. Shyy and S. Chien, *Annu. Rev. Biomed. Eng.*, 2017, **19**, 195–219.

7 G. Zhang and S. Pradhan, *IUBMB Life*, 2014, **66**, 240–256.

8 T. Jenuwein and C. D. Allis, *Science*, 2001, **293**, 1074–1081.

9 V. A. DeWoskin and R. P. Million, *Nat. Rev. Drug Discov.*, 2013, **12**, 661–662.

10 P. Hunter, *EMBO Rep.*, 2015, **16**, 276–279.

11 R. Deuring, M. P. Scott, M. Kissinger, A. M. Pattatucci, T. C. Kaufman and J. A. Kennison, *Cell*, 1992, **68**, 561–572.

12 T. Fujisawa and P. Filippakopoulos, *Nat. Rev. Mol. Cell Biol.*, 2017, **18**, 246–262.

13 P. Filippakopoulos, S. Picaud, M. Mangos, T. Keates, J. P. Lambert, D. Barsyte-Lovejoy, I. Felletar, R. Volkmer, S. Müller, T. Pawson, A. C. Gingras, C. H. Arrowsmith and S. Knapp, *Cell*, 2012, **149**, 214–231.

14 P. Filippakopoulos, J. Qi, S. Picaud, Y. Shen, W. B. Smith, O. Fedorov, E. M. Morse, T. Keates, T. T. Hickman, I. Felletar, M. Philpott, S. Munro, M. R. Mckeown, Y. Wang, A. L. Christie, N. West, M. J. Cameron, B. Schwartz, T. D. Heightman, N. La Thangue, C. A. French, O. Wiest, A. L. Kung, S. Knapp and J. E. Bradner, *Nature*, 2010, **468**, 1067–1073.

15 O. Mirguet, R. Gosmini, J. Toum, C. A. Clement, J. Brusq, J. E. Mordaunt, R. M. Grimes, M. Crowe, O. Pineau, M. Ajakane, A. Daugan, P. Je, L. Cutler, A. C. Haynes, N. N. Smithers, C. Chung, P. Bamborough, I. J. Uings, A. Lewis, J. Witherington, N. Parr, R. K. Prinjha and E. Nicodeme, *J. Med. Chem.*, 2013, **56**, 7501–7515.

16 A. G. Cochran, A. R. Conery and R. J. Sims, *Nat. Rev. Drug Discov.*, 2019, **18**, 609–628.

17 N. G. Iyer, H. Özdag and C. Caldas, *Oncogene*, 2004, **23**, 4225–4231.

18 B. M. Dancy and P. A. Cole, *Chem. Rev.*, 2015, **115**, 2419–2452.

19 S. N. Meyer, C. Scuoppo, S. Vlasevska, E. Bal, A. B. Holmes, M. Holloman, L. Garcia-Ibanez, S. Nataraj, R. Duval, T. Vantrimpont, K. Basso, N. Brooks, R. Dalla-Faver and Laura Pasqualucci, *Immunity*, 2019, **51**, 1–13.

20 V. Garcia-Carpizo, S. Ruiz-Llorente, J. Sarmentero, A. Gonzalez-Corpas and M. J. Barrero, *Mol. Cancer Res.*, 2019, **17**, 720–731.

21 H. Yang, C. E. Pinello, J. Luo, D. Li, Y. Wang, Y. Lisa, S. C. Jahn, S. A. Saldanha, J. Planck, K. R. Geary, H. Ma, B. K. Law, W. R. Roush, P. Hodder and D. Liao, *Mol. Cancer Ther.*, 2014, **12**, 610–620.

22 L. M. Lasko, C. G. Jakob, R. P. Edalji, W. Qiu, D. Montgomery, E. L. Digiammarino, T. M. Hansen, R. M. Risi, R. Frey, B. Shaw, M. Algire, P. Hessler, L. T. Lam, T. Uziel, D. Ferguson, F. G. Buchanan, R. L. Martin, M. Torrent, G. Gary, K. Karukurichi, J. W. Langston, B. T. Weinert, P. De Vries, J. H. Van Drie, D. Mcelligott, E. Kesicki, R. Marmorstein, C. Sun, P. A. Cole, S. H. Rosenberg, M. R. Michaelides, A. Lai and K. D. Bromberg, *Nature*, 2017, **550**, 128–132.

23 A. R. Henderson, M. J. Henley, N. J. Foster, A. L. Peiffer, M. S. Beyersdorf, K. D. Stanford, S. M. Sturlis, B. M. Linhares, Z. B. Hill, J. A. Wells, T. Cierpicki, C. L. B. III, C. A. Fierke and A. K. Mapp, *Proc. Natl. Acad. Sci.*, 2018, **115**, 8960–8965.

24 S. Kushal, B. Bullock, L. K. Henchey, R. Dubey, H. Mesallati, N. J. Traaseth, B. Z. Olenyuk and P. S. Arora, *Proc. Natl. Acad. Sci.*, 2013, **110**, 15602–15607.

25 T. P. C. Rooney, P. Filippakopoulos, O. Fedorov, S. Picaud, W. A. Cortopassi, D. A. Hay, S. Martin, A. Tumber, C. M. Rogers, M. Philpott, M. Wang, A. L. Thompson, T. D. Heightman, D. C. Pryde, A. Cook, R. S. Paton, S. Müller, S. Knapp, P. E. Brennan and S. J. Conway, *Angew. Chemie Int. Ed.*, 2014, **53**, 6126–6130.

26 L. R. Vidler, N. Brown, S. Knapp and S. Hoelder, *J. Med. Chem.*, 2012, **55**, 7346–7359.

27 Sachchidanand, L. Resnick-Silverman, S. Yan, S. Mutjaba, W.-J. J. Liu, L. Zeng, J. J. Manfredi and M.-M. M. Zhou, *Chem. Biol.*, 2006, **13**, 81–90.

28 J. C. Borah, S. Mujtaba, I. Karakikes, L. Zeng, M. Muller, J. Patel, N. Moshkina, K. Morohashi, W. Zhang, G. Gerona-Navarro, R. J. Hajjar and M. M. Zhou, *Chem. Biol.*, 2011, **18**, 531–541.

29 G. Gerona-Navarro, Yoel-Rodríguez, S. Mujtaba, A. Frasca, J. Patel, L. Zeng, A. N. Plotnikov, R. Osman and M. M. Zhou, *J. Am. Chem. Soc.*, 2011, **133**, 2040–2043.

30 M. Brand, Thesis "Developing small molecule ligands for the study of bromodomain-histone interactions", University of Oxford, 2017.

31 A. M. Taylor, A. Côté, M. C. Hewitt, R. Pastor, Y. Leblanc, C. G. Nasveschuk, F. A. Romero, T. D. Crawford, N. Cantone, H. Jayaram, J. Setser, J. Murray, M. H. Beresini, G. De Leon Boenig, Z. Chen, A. R. Conery, R. T. Cummings, L. A. Dakin, E. M. Flynn, O. W. Huang, S. Kaufman, P. J. Keller, J. R. Kiefer, T. Lai, Y. Li, J. Liao, W. Liu, H. Lu, E. Pardo, V. Tsui, J. Wang, Y. Wang, Z. Xu, F. Yan, D. Yu, L. Zawadzke, X. Zhu, X. Zhu, R. J. Sims, A. G. Cochran, S. Bellon, J. E. Audia, S. Magnuson and B. K. Albrecht, *ACS Med. Chem. Lett.*, 2016, **7**, 531–536.

32 T. D. Crawford, F. A. Romero, K. W. Lai, V. Tsui, A. M. Taylor, G. de Leon Boenig, C. L. Noland, J. Murray, J. Ly, E. F. Choo, T. L. Hunsaker, E. W. Chan, M. Merchant, S. Kharbanda, K. E. Gascoigne, S. Kaufman, M. H. Beresini, J. Liao, W. Liu, K. X. Chen, Z. Chen, A. R. Conery, A. Côté, H. Jayaram, Y. Jiang, J. R. Kiefer, T. Kleinheinz, Y. Li, J. Maher, E. Pardo, F. Poy, K. L. Spillane, F. Wang, J. Wang, X. Wei, Z. Z. Xu, I. Yen, L. E. Zawadzke, X. Zhu, S. F. Bellon, R. T. Cummings, A. G. Cochran, B. K. Albrecht and S. Magnuson, *J. Med. Chem.*, 2016, **59**, 10549–10563.

33 L. Jin, J. Garcia, E. Chan, C. De Cruz, E. Segal, M. Merchant, S. Kharbanda, R. Raisner, P. M. Haverty, Z. Modrusan, J. Ly, E. Choo, S. Kaufman, M. H. Beresini, F. A. Romero, S. Magnuson and K. E. Gascoigne, *Cancer Res.*, 2017, **77**, 5564–5576.

34 N. Pegg, N. Brooks, J. Worthington, B. Young, A. Prosser, J. Lane, D. Taddei, R. Brown, G. Harbottle, J. Shannon, S. Paoletta and K. E. Knudsen, *J. Clin. Oncol.*, 2017, **35**, 11590.

35 I. B. Campbell, S. J. F. Macdonald and P. A. Procopiou, *Drug Discov. Today*, 2018, **23**, 219–234.

36 E. M. Driggers, S. P. Hale, J. Lee and N. K. Terrett, *Nat. Rev. Drug Discov.*, 2008, **7**, 608–624.

37 E. Marsault and M. L. Peterson, *J. Med. Chem.*, 2011, **54**, 1961–2004.

38 J. Mallinson and I. Collins, *Future Med. Chem.*, 2012, **4**, 1409–1438.

39 A. Y. S. Balazs, R. J. Carbajo, N. L. Davies, Y. Dong, A. W. Hird, W. Johannes, M. L. Lamb, W. Mccoull, P. Raubo, G. R. Robb, M. J. Packer and E. Chiarparin, *Free Ligand 1D NMR Conformational Signatures To Enhance Structure Based Drug Design of a Mcl -1 Inhibitor (AZD5991) and Other Synthetic Macrocycles*, 2019.

40 L. Wang, J. K. Pratt, T. Soltwedel, G. S. Sheppard, S. D. Fidanze, D. Liu, L. A. Hasvold, R. A. Mantei, J. H. Holms, W. J. Mcclellan, M. D. Wendt, C. Wada, R. Frey, T. M. Hansen, R. Hubbard, C. H. Park, L. Li, T. J. Magoc, D. H. Albert, X. Lin, S. E. Warder, P. Kovar, X. Huang, D. Wilcox, R. Wang, G. Rajaraman, A. M. Petros, C. W. Hutchins, S. C. Panchal, C. Sun, S. W. Elmore, Y. Shen, W. M. Kati and K. F. Mcdaniel, *J. Med. Chem.*, 2017, **60**, 3828–3850.

41 H. J. Breslin, B. M. Lane, G. R. Ott, A. K. Ghose, T. S. Angeles, M. S. Albom, M. Cheng, W. Wan, R. C. Haltiwanger, K. J. Wells-Knecht and B. D. Dorsey, *J. Med. Chem.*, 2012, **55**, 449–464.

42 C. A. Lipinski, *J. Pharmacol. Toxicol. Methods*, 2000, **44**, 235–249.

43 D. F. Veber, S. R. Johnson, H. Cheng, B. R. Smith, K. W. Ward and K. D. Kopple, *J. Med. Chem.*, 2002, **45**, 2615–2623.

44 A. Whitty, M. Zhong, L. Viarengo, D. Beglov, D. R. Hall and S. Vajda, *Drug Discov. Today*, 2016, **21**, 712–717.

45 M. R. Sebastiano, B. C. Doak, M. Backlund, V. Poongavanam, B. Over, G. Ermondi, G. Caron, P. Matsson and J. Kihlberg, *J. Med. Chem.*, 2018, **61**, 4189–4202.

46 W. Mccoull, R. D. Abrams, E. Anderson, K. Blades, P. Barton, M. Box, J. Burgess, K. Byth, Q. Cao, C. Chuaqui, R. J. Carbajo, T. Cheung, E. Code, A. D. Ferguson, S. Fillery, N. O. Fuller, E. Gangl, N. Gao, M. Grist, D. Hargreaves, M. R. Howard, J. Hu, P. D. Kemmitt, J. E. Nelson, N. O. Connell, D. B. Prince, P. Raubo, P. B. Rawlins, G. R. Robb, J. Shi, M. J. Waring, D. Whittaker, M. Wylot and X. Zhu, *J. Med. Chem.*, 2017, **60**, 4386–4402.

47 W. Johannes, S. Bates, C. Beigie, M. A. Belmonte, J. Breen, S. Cao, P. A. Centrella, M. A. Clark, J. W. Cuozzo, C. E. Dumelin, A. D. Ferguson, S. Habeshian, D. Hargreaves, C. Joubran, S. Kazmirski, A. D. Keefe, M. L. Lamb, H. Lan, Y. Li, H. Ma, S. Mlynarski, M. J. Packer, P. B. Rawlins, D. W. Robbins, H. Shen, E. A. Sigel, H. H. Soutter, N. Su, D. M. Troast, H. Wang, K. F. Wickson, C. Wu, Y. Zhang, Q. Zhao, X. Zheng and A. W. Hird, *ACS Med. Chem. Lett.*, 2017, **8**, 239–244.

48 H. Pei, Y. Peng, Q. Zhao and Y. Chen, *RSC Adv.*, 2019, **9**, 16967–16976.

49 J. Salami and C. M. Crews, *Science*, 2017, **355**, 1163–1167.

50 Arvinas; A Phase 1 Clinical Trial of ARV-110 in Patients With Metastatic Castration-resistant Prostate Cancer. (mCRPC); 25th March 2019. [Accessed 3rd September 2019]; Available from https://clinicaltrials.gov/ct2/show/NCT03888612.

51 Arvinas; Clinical Trial of ARV-471 in Patients With ER+/HER2- Locally Advanced or Metastatic Breast Cancer (mBC); 5th August 2019 [Accessed 3rd September 2019]; Available from https://clinicaltrials.gov/ct2/show/NCT04072952.

52 A. R. Smith, M. Pucheault, H. S. Tae and C. M. Crews, *Bioorg. Med. Chem. Lett.*, 2008, **18**, 5904–5908.

53 K. M. Sakamoto, K. B. Kim, A. Kumagai, F. Mercurio, C. M. Crews and R. J. Deshaies, *Proc. Natl. Acad. Sci.*, 2001, **98**, 8554–8559.

54 J. S. Schneekloth, F. N. Fonseca, M. Koldobskiy, A. Mandal, R. Deshaies, K. Sakamoto and C. M. Crews, *J. Am. Chem. Soc.*, 2004, **126**, 3748–3754.

55 Y. Itoh, M. Ishikawa, M. Naito and Y. Hashimoto, *J. Am. Chem. Soc.*, 2010, **132**, 5820–5826.

56 G. E. Winter, D. L. Buckley, J. Paulk, J. M. Roberts, A. Souza, S. Dhe-Paganon and J. E. Bradner, *Science*, 2015, **348**, 1376–1382.

57 R. P. Nowak, S. L. Deangelo, D. Buckley, Z. He, K. A. Donovan, J. An, N. Safaee, M. P. Jedrychowski, C. M. Ponthier, M. Ishoey, T. Zhang, J. D. Mancias, N. S. Gray, J. E. Bradner and E. S. Fischer, *Nat. Chem. Biol.*, 2018, **14**, 706–714.

58 K. Raina, J. Lu, Y. Qian, M. Altieri, D. Gordon, A. M. K. Rossi, J. Wang, X. Chen, H. Dong, K. Siu, J. D. Winkler, A. P. Crew, C. M. Crews and K. G. Coleman, *Proc. Natl. Acad. Sci.*, 2016, **113**, 7124–7129.

59 M. Zengerle, K.-H. Chan and A. Ciulli, *ACS Chem. Biol.*, 2015, **10**, 1770–1777.

60 M. S. Gadd, A. Testa, X. Lucas, K. Chan, W. Chen, D. J. Lamont, M. Zengerle and A. Ciulli, *Nat. Chem. Biol.*, 2017, **13**, 514–521.

61 L. Bai, B. Zhou, C.-Y. Yang, J. Ji, D. Mceachern, S. Przybranowski, H. Jiang, J. Hu, F. Xu, Y. Zhao, L. Liu, E. Fernandez-Salas, J. Xu, Y. Dou, B. Wen, D. Sun, J. Meagher, J. Stuckey, D. F. Hayes, S. Li, M. J. Ellis and S. Wang, *Cancer Res.*, 2017, **77**, 2476–2487.

62 D. Neri and R. A. Lerner, *Annu. Rev. Biochem.*, 2017, **87**, 5.1-5.24.

63 N. Favalli, G. Bassi, J. Scheuermann and D. Neri, *FEBS Lett.*, 2018, **592**, 2168–2180.

64 L. S. Jespers, A. Roberts, S. M. Mahler, G. Winter and H. R. Hoogenboom, *Nat. Biotechnol.*, 1994, **12**, 899–903.

65 S. Brenner and R. A. Lerner, *Proc. Natl. Acad. Sci.*, 1992, **89**, 5381–5383.

66 Z. Wu, T. L. Graybill, X. Zeng, M. Platchek, J. Zhang, V. Q. Bodmer, D. D. Wisnoski, J. Deng, F. T. Coppo, G. Yao, A. Tamburino, G. Scavello, G. J. Franklin, S. Mataruse, K. L. Bedard, Y. Ding, J. Chai, J. Summer, P. A. Centrella, A. J. Messer, A. J. Pope and D. I. Israel, *ACS Comb. Sci.*, 2015, **17**, 722–731.

67 A. Litovchick, C. E. Dumelin, S. Habeshian, D. Gikunju, M.-A. Guié, P. Centrella, Y. Zhang, E. A. Sigel, J. W. Cuozzo, A. D. Keefe and M. A. Clark, *Sci. Rep.*, 2015, **5:10916**, 1–8.

68 M. Wichert, N. Krall, W. Decurtins, R. M. Franzini, F. Pretto, P. Schneider, D. Neri and J. Scheuermann, *Nat. Chem.*, 2015, **7**, 241–249.

69 M. Bigatti, D. Corso, S. Vanetti, S. Cazzamalli, U. Rieder, J. Scheuermann, D. Neri and F. Sladojevich, *ChemMedChem*, 2017, **12**, 1748–1752.

70 G. Zimmermann, U. Rieder, D. Bajic, S. Vanetti, A. Chaikuad, S. Knapp, J. Scheuermann, M. Mattarella and D. Neri, *Chem. - A Eur. J.*, 2017, **23**, 1–5.

71 A. Choudhary and R. T. Raines, *ChemBioChem*, 2011, **12**, 1801–1807.

72 S. G. Davies, A. M. Fletcher, P. M. Roberts and J. E. Thomson, *Tetrahedron: Asymmetry*, 2012, **23**, 1111–1153.

73 S. Pereira and M. Srebnik, *Organometallics*, 1995, **14**, 3127–3128.

74 C. S. Aricó and L. R. Cox, *Org. Biomol. Chem.*, 2004, **2**, 2558–2562.

75 Q. Wu, D. Heidenreich, S. Zhou, S. Ackloo, A. Krämer, K. Nakka, E. Lima-fernandes, G. Deblois, S. Duan, R. N. Vellanki, F. Li, M. Vedadi, J. Dilworth, M. Lupien, P. E. Brennan, C. H. Arrowsmith, S. Müller, O. Fedorov, P. Filippakopoulos and S. Knapp, *Nat. Commun.*, 2019, **10**, 1–14.

76 M. Tanaka, J. M. Roberts, H. S. Seo, A. Souza, J. Paulk, T. G. Scott, S. L. Deangelo, S. Dhe-Paganon and J. E. Bradner, *Nat. Chem. Biol.*, 2016, **12**, 1089–1096.

77 A. E. Fernández-Montalván, M. Berger, B. Kuropka, S. J. Koo, V. Badock, J. Weiske, V. Puetter, S. J. Holton, D. Stöckigt, A. Ter Laak, P. A. Centrella, M. A. Clark, C. E. Dumelin, E. A. Sigel, H. H. Soutter, D. M. Troast, Y. Zhang, J. W. Cuozzo, A. D. Keefe, D. Roche, V. Rodeschini, A. Chaikuad, L. Díaz-Sáez, J. M. Bennett, O. Fedorov, K. V. M. Huber, J. Hübner, H. Weinmann, I. V. Hartung and M. Gorjánácz, *ACS Chem. Biol.*, 2017, **12**, 2730–2736.

78 C. H. Arrowsmith, J. E. Audia, C. Austin, J. Baell, J. Bennett, J. Blagg, C. Bountra, P. E. Brennan, P. J. Brown, M. E. Bunnage, C. Buser-Doepner, R. M. Campbell, A. J. Carter, P. Cohen, R. A. Copeland, B. Cravatt, J. L. Dahlin, D. Dhanak, A. M. Edwards, M. Frederiksen, S. V Frye, N. Gray, C. E. Grimshaw, D. Hepworth, T. Howe, K. V. M. Huber, J. Jin, S. Knapp, J. D. Kotz, R. G. Kruger, D. Lowe, M. M. Mader, B. Marsden, A. Mueller-Fahrnow, S. Müller, R. C. O'Hagan, J. P. Overington, D. R. Owen, S. H. Rosenberg, R. Ross, B. Roth, M. Schapira, S. L. Schreiber, B. Shoichet, M. Sundström, G. Superti-Furga, J. Taunton, L. Toledo-Sherman, C. Walpole, M. A. Walters, T. M. Willson, P. Workman, R. N. Young and W. J. Zuercher, *Nat. Chem. Biol.*, 2015, **11**, 536–541.

79 C. Galdeano and A. Ciulli, *Future Med. Chem.*, 2016, **8**, 1655–1680.

80 O. Korb, T. Stu and T. E. Exner, *J. Chem. Inf. Model.*, 2009, **49**, 84–96.

81 P. Bonnet, D. K. Agrafiotis, F. Zhu and E. Martin, *J. Chem. Inf. Model.*, 2009, **49**, 2242–2259.

82 R. Hesse, M. P. Krahl, A. Jäger, O. Kataeva, A. W. Schmidt and H.-J. Knölker, *European J. Org. Chem.*, 2014, **19**, 4014–4028.

83 G. E. Job and S. L. Buchwald, *Org. Lett.*, 2002, **4**, 3703–3706.

84 F. Y. Kwong and S. L. Buchwald, *Org. Lett.*, 2003, **5**, 793–796.

85 A. Shafir and S. L. Buchwald, *J. Am. Chem. Soc.*, 2006, **2**, 8742–8743.

86 A. Shafir, P. A. Lichtor and S. L. Buchwald, *J. Am. Chem. Soc.*, 2007, **129**, 3490–3491.

87 R. A. Altman, A. Shafir, A. Choi, P. A. Lichtor and S. L. Buchwald, *J. Org. Chem.*, 2008, **73**, 284–286.

88 S. B. Garber, J. S. Kingsbury, B. L. Gray and A. H. Hoveyda, *J. Am. Chem. Soc.*, 2000, **122**, 8168–8179.

89 P. Compain, *Adv. Synth. Catal.*, 2007, **349**, 1829–1846.

90 K. X. Chen, F. G. Njoroge, B. Vibulbhan, A. Buevich, T. Chan and V. Girijavallabhan, *J. Org. Chem.*, 2002, 2730–2733.

91 K. C. K. Swamy, N. N. B. Kumar, E. Balaraman and K. V. P. P. Kumar, *Chem. Rev.*, 2009, **109**, 2551–2651.

92 A. Krasovskiy, V. Malakhov, A. Gavryushin and P. Knochel, *Angew. Chemie Int. Ed.*, 2006, **45**, 6040–6044.

93 I. Ugur, M. Schroft, A. Marion, M. Glaser and I. Antes, *J. Mol. Model.*, 2019, **25**, 1–13.

94 D. Sindhikara, S. A. Spronk, T. Day, K. Borrelli, D. L. Cheney and S. L. Posy, *J. Chem. Inf. M*, 2017, **57**, 1881–1894.

95 K. S. Watts, P. Dalal, A. J. Tebben, D. L. Cheney and J. C. Shelley, *J. Chem. Inf. Model.*, 2014, **54**, 2680–2696.

96 P. Labute, *J. Chem. Inf. Model.*, 2010, **50**, 792–800.

97 A. J. Clark, P. Tiwary, K. Borrelli, S. Feng, E. B. Miller, R. Abel, R. A. Friesner and B. J. Berne, *J. Chem. Theory Comput.*, 2016, **12**, 2990–2998.

98 A. Jourdant, E. González-Zamora and J. Zhu, *J. Org. Chem.*, 2002, **67**, 3163–3164.

99 B. Blank, N. W. Ditullio, F. F. Owings, L. Deviney, C. K. Miao and H. L. Saunders, *J. Med. Chem.*, 1977, **20**, 572–576.

100 Patent, 2-Thioethenyl substituted carbapenem derivatives, WO2006JP307698 20060412, 2006.

101 J. P. Damiano and M. Postel, *J. Organomet. Chem.*, 1996, **522**, 303–305.

102 J. Park, J. Yeon, P. H. Lee and K. Lee, *Tetrahedron Lett.*, 2013, **54**, 4414–4417.

103 L. Zhang, X. Chen, P. Xue, H. H. Y. Sun, I. D. Williams, K. B. Sharpless, V. V Fokin and G. Jia, *J. Am. Chem. Soc.*, 2005, **127**, 15998–15999.

104 B. C. Boren, S. Narayan, L. K. Rasmussen, L. Zhang, H. Zhao, Z. Lin, G. Jia and V. V Fokin, *J. Am. Chem. Soc.*, 2008, **130**, 8923–8930.

105 V. V Rostovtsev, L. G. Green, V. V Fokin and K. B. Sharpless, *Angew. Chemie Int. Ed.*, 2002, **41**, 2596–2599.

106 B. T. Worrell, J. A. Malik and V. V Fokin, *Science*, 2013, **340**, 457–460.

107 X. Yu and D. Sun, *Molecules*, 2013, **18**, 6230–6268.

108 E. T. L. Estrade, F. G. Edgar, M. Xiong, V. Shalgunov, S. L. Baerentzen, M. Erlandsson, T. G. Ohlsson, M. Palner, G. M. Knudsen and M. M. Herth, *ACS Omega*, 2019, **4**, 7344–7353.

109 E. Chiarparin, M. J. Packer and D. M. Wilson, *Future Med. Chem.*, 2019, **11**, 79–82.

110 Y. Zhan, M. K. Alimova, X. Shi, E. Leo, J. P. Bardenhagen, H. E. Shepard, S. Appikonda, B. Vangamudi, S. Zhao, T. N. Tieu, S. Jiang, T. P. Heffernan, J. R. Marszalek, C. Toniatti, G. Draetta, J. Tyler, M. Barton, P. Jones, W. S. Palmer, M. K. G. Do and J. N. Andersen, *Epigenetics Chromatin*, 2015, **8**, 1–19.

111 L. N. Gechijian, D. L. Buckley, M. A. Lawlor, J. M. Reyes, J. Paulk, C. J. Ott, G. E. Winter, M. A. Erb, T. G. Scott, M. Xu, H. Seo, S. Dhe-paganon, N. P. Kwiatkowski, J. A. Perry, J. Qi, N. S. Gray and J. E. Bradner, *Nat. Chem. Biol.*, 2018, **14**, 405–412.

112 S. An and L. Fu, *EBioMedicine*, 2018, **36**, 553–562.

113 M. Scheepstra, K. F. W. Hekking, L. Van Hijfte and R. H. A. Folmer, *Comput. Struct. Biotechnol. J.*, 2019, **17**, 160–176.

114 D. P. Bondeson, B. E. Smith, G. M. Burslem, A. D. Buhimschi, J. Hines, S. Jaime-Figueroa, J. Wang, B. D. Hamman, A. Ishchenko and C. M. Crews, *Cell Chem. Biol.*, 2019, **25**, 78–87.

115 J. Lohbeck and A. K. Miller, *Bioorg. Med. Chem. Lett.*, 2016, **26**, 5260–5262.

116 M. Toure and C. M. Crews, *Angew. Chemie Int. Ed.*, 2016, **55**, 1966–1973.

117 B. Lamoree and R. E. Hubbard, *Essays Biochem.*, 2017, **61**, 453–464.

118 M. M. Cerda, T. D. Newton, Y. Zhao, B. K. Collins, C. H. Hendon and M. D. Pluth, *Chem. Sci.*, 2019, **10**, 1773–1779.

119 W. Kabsch, *Acta Crystallogr. Sect. D Biol. Crystallogr.*, 2010, **66**, 125–132.

120 A. J. McCoy, R. W. Grosse-Kunstleve, L. C. Storoni and R. J. Read, *Acta Crystallogr. Sect. D Biol. Crystallogr.*, 2005, **61**, 458–464.

121 A. Perrakis, R. Morris and V. S. Lamzin, *Nat. Struct. Biol.*, 1999, **6**, 458–463.

122 P. Emsley and K. Cowtan, *Acta Crystallogr. Sect. D Biol. Crystallogr.*, 2004, **60**, 2126–2132.

123 G. N. Murshudov, A. A. Vagin and E. J. Dodson, *Acta Crystallogr. Sect. D Biol. Crystallogr.*, 1997, **53**, 240–255.

124 J. Painter and E. A. Merritt, *Acta Crystallogr. Sect. D Biol. Crystallogr.*, 2006, **62**, 439–450.

125 G. R. Fulmer, A. J. M. Miller, N. H. Sherden, H. E. Gottlieb, A. Nudelman, B. M. Stoltz, J. E. Bercaw and K. I. Goldberg, *Organometallics*, 2010, **29**, 2176–2179.

126 W. L. F. Armarego and C. L. L. Chai, *Purification of Laboratory Chemicals*, Butterworth-Heinemann, Oxford, Waltham, 2013.

127 S. M. Hannick and Y. Kishi, *J. Org. Chem.*, 1983, **2**, 3833–3835.

128 A. B. Pangborn, M. A. Giardello, R. H. Grubbs, R. K. Rosen and F. J. Timmers, *Organometallics*, 1996, **15**, 1518–1520.

129 S. G. Davies, A. W. Mulvaney, A. J. Russell and A. D. Smith, *Tetrahedron: Asymmetry*, 2007, **18**, 1554–1566.

130 F. C. Gozzo, S. A. Fernandes, D. C. Rodrigues, M. N. Eberlin and A. J. Marsaioli, *J. Org. Chem.*, 2003, **68**, 5493–5499.

131 A. D. William, A. C.-H. Lee, S. Blanchard, A. Poulsen, E. L. Teo, H. Nagaraj, E. Tan, D. Chen, M. Williams, E. T. Sun, K. C. Goh, W. C. Ong, S. K. Goh, S. Hart, R. Jayaraman, M. K. Pasha, K. Ethirajulu, J. M. Wood and B. W. Dymock, *J. Med. Chem.*, 2011, **54**, 4638–4658.

132 S. M. Pauff and S. C. Miller, *Org. Lett.*, 2011, **13**, 6196–6199.

Appendices

A1 Protein sequence data of CREBBP bromodomain & BRD4(1)

Molecular weights for proteins in Daltons (Da) were predicted using the ProtParama tool.

(Available at: https://web.expasy.org/protparam/).

Protein: His_6-CREBBP

Addgene: #38977

Protein Sequence:
```
MHHHHHHSSG VDLGTENLYF QSMRKKIFKP EELRQALMPT
LEALYRQDPE SLPFRQPVDP QLLGIPDYFD IVKNPMDLST
IKRKLDTGQY QEPWQYVDDV WLMFNNAWLY NRKTSRVYKF
CSKLAEVFEQ EIDPVMQSLG
```

Molecular Weight: 16673.04 Daltons

Extinction coefficient: 26930 M^{-1} cm^{-1}

Protein: His_6-BRD4(1)

Addgene: #38942

Protein Sequence:
```
MHHHHHHSSG VDLGTENLYF QSMNPPPPET SNPNKPKRQT
NQLQYLLRVV LKTLWKHQFA WPFQQPVDAV KLNLPDYYKI
IKTPMDMGTI KKRLENNYYW NAQECIQDFN TMFTNCYIYN
KPGDDIVLMA EALEKLFLQK INELPTEE
```

Molecular Weight: 17549.07 Daltons

Extinction coefficient: 28420 M^{-1} cm^{-1}

A2 Protein expression & purification of CREBBP bromodomain & BRD4(1)

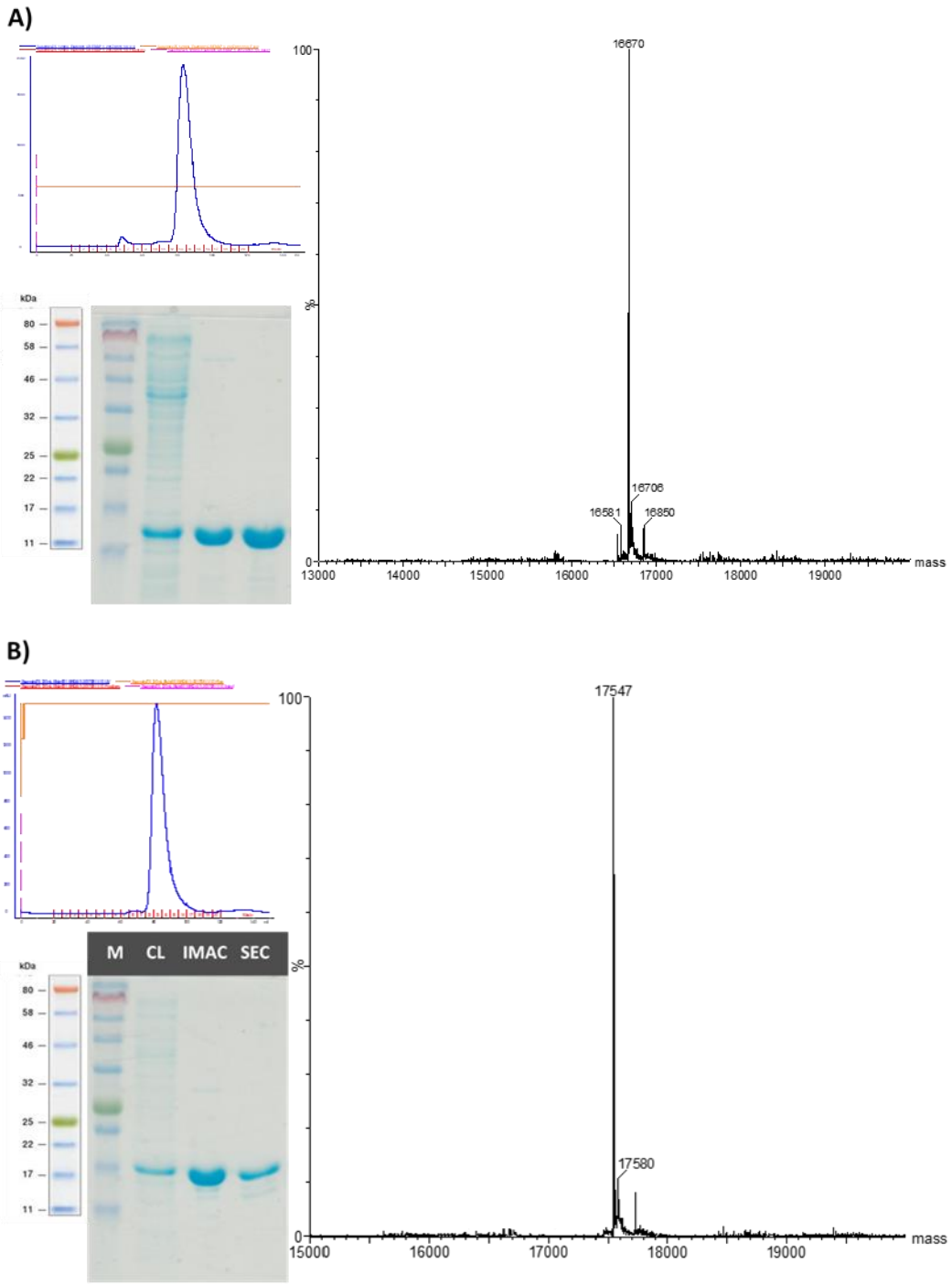


Figure A2.1 Recombinant protein purification of (A) CREBBP and (B) BRD4(1). SDS-PAGE analyses, gel filtration profiles, and LC-MS detection of purified proteins. M: colour Prestained Protein Standard, Broad Range (11-245 kDa) (New England Biolabs). The band sizes of the protein marker are shown on the left-hand side of the SDS-PAGs. CL: Unpurified cell lysate. IMAC: IMAC-purified fraction. SEC: SEC (size exclusion chromatography)-purified fraction. LC-MS analysis of both SEC-purified proteins are shown on right-hand side of the SDS-PAGs, and their expected monomeric sizes are indicated, Inspection and deconvolution of the mass spectra were performed using MassLynx 4.1 (Waters Corp.).

B Computational data

B1 CLC Drug Discovery Workbench 2.5

The docking score used in the Drug Discovery Workbench is the $PLANTS_{PLP}$ score. The score mimics the potential energy change, when the protein and ligand come together. This means that a very negative score corresponds to a strong binding and a less negative or even positive score corresponds to a weak or non-existing binding.

$$Score = S_{target-ligand} + S_{ligand}$$

This term is a sum over contributions from all heavy atom contacts between the ligand and the molecules included in the binding site setup. It scores the complementarity between binding site and ligand by rewarding and punishing different types of heavy atom contacts (inter atom distance below ~5.5 Å).

Five different types of contacts are defined:

Rewarded contacts

1. Hydrogen bond interactions
2. Lone-pair - metal ion interactions
3. Non-polar interactions

Punished contacts

4. Non-polar - polar contacts
5. Repulsive contacts:
    - Hydrogen bond donor-donor contacts
    - Hydrogen bond donor-metal contacts
    - Hydrogen bond acceptor-acceptor contacts

These contact types are associated with a pairwise linear potential (PLP), which determines the distance-dependence of the contribution to the score.

For more complete descriptions, please see the following paper:

- O. Korb, T. Stu and T. E. Exner, *J. Chem. Inf. Model.*, 2009, **49**, 84–96.

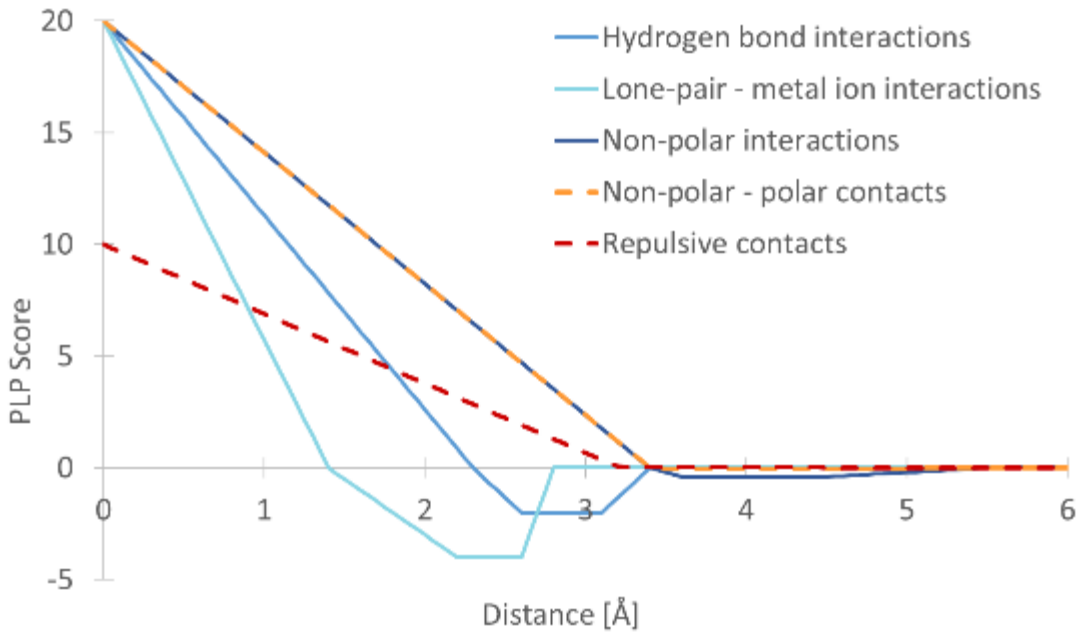


Figure B1.1. The pairwise linear potentials defining the score contributions for different types of heavy atom contacts.

B2 Schrödinger Glide docking score

Glide Docking Score is an empirical scoring function that approximates the ligand binding free energy. It has many terms, including force field (electrostatic, van der Waals) contributions and terms rewarding or penalizing interactions known to influence ligand binding. It has been optimized for docking accuracy, database enrichment, and binding affinity prediction. As it simulates a binding free energy, more negative values represent tighter binders.

Glide Emodel Score has a more significant weighting of the force field components (electrostatic and van der Waals energies), which makes it well-suited for comparing conformers, but much less so for comparing chemically-distinct species. Therefore, Glide uses Emodel Score to pick the "best" pose of a ligand (pose selection), and then ranks these best poses against one another with Glide Docking Score.

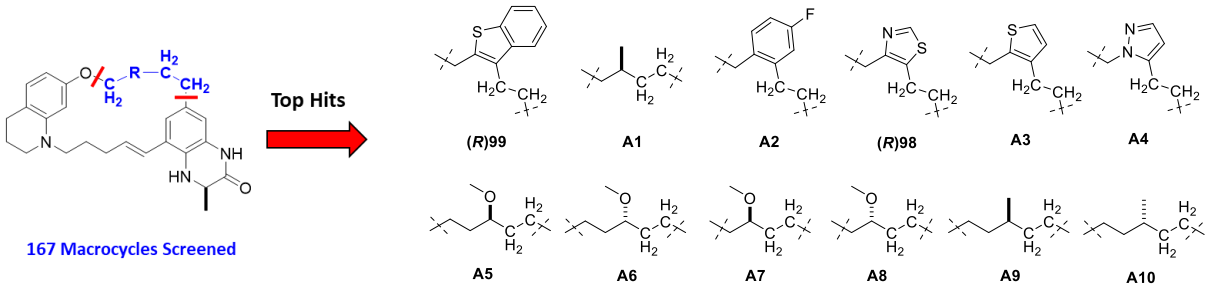
For more complete descriptions, please see the following papers:

- Glide 6.7 User Manual, Schrödinger press, May 2015.
- "Glide: A New Approach for Rapid, Accurate Docking and Scoring. 1. Method and Assessment of Docking Accuracy", *J. Med. Chem.* **2004**, *47*, 1739-1749.
- "Extra Precision Glide: Docking and Scoring Incorporating a Model of Hydrophobic Enclosure for Protein-Ligand Complexes", *J. Med. Chem.* **2006**, *49*, 6177-6196.

The exact formula for Emodel Score is proprietary.

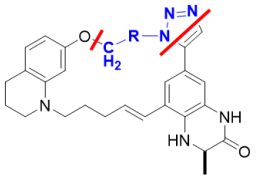
B3 Molecular Docking – Top docked macrocycles

Table B3.1 Top docked poses for macrocycle series 1.

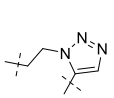


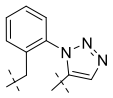
	Glide Docking Score	Glide Emodel Score	Correct Binding Poses
DHQ-James	−7.505	−65.455	4
(*R*)99	−8.359	−73.926	5
(*R*)98	−8.446	−74.297	5
A3	−7.794	−69.778	3
A4	−8.191	−71.069	4
A5	−8.102	−68.701	5
A6	−8.638	−68.684	5
A7	−8.102	−65.252	1
A8	−8.171	−66.785	5
A9	−8.351	−71.867	5
A10	−8.451	−72.806	3

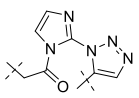
Table B3.2 Top docked poses for macrocycle series 2.

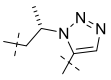


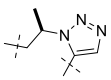
Top Hits

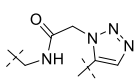

(*R*)100


(*R*)101


A11

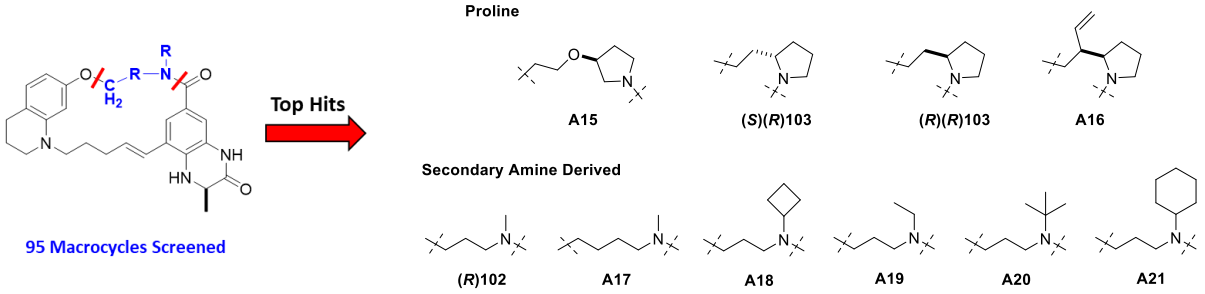

A12


A13


A14

	Glide Docking Score	Glide Emodel Score	Correct Binding Poses
DHQ-James	−7.505	−65.455	4
(*R*)100	−8.870	−76.863	4
(*R*)101	−8.121	−71.202	3
A11	−8.022	−83.561	3
A12	−8.488	−72.519	3
A13	−8.098	−70.326	2
A14	−7.984	−74.498	4

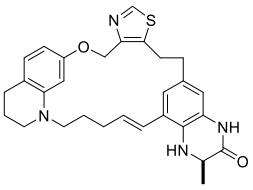
Table B3.3 Top docked poses for macrocycle series 3.

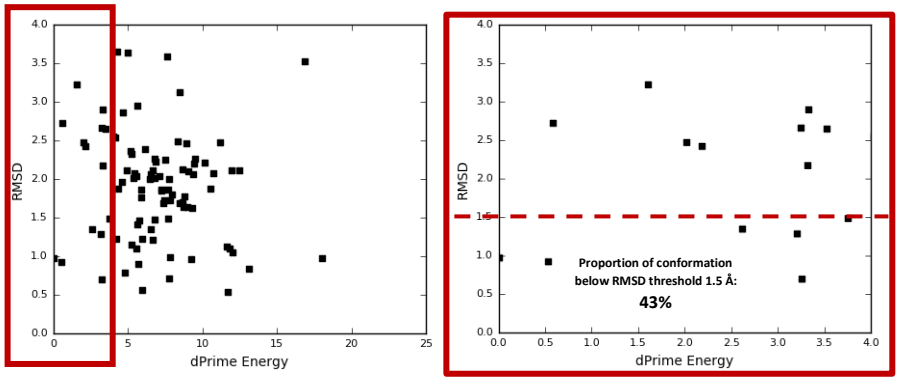


Compound	Glide Docking Score	Glide emodel Score	Correct Binding Poses
DHQ-James	−7.505	−65.455	4
A15	−8.241	−76.690	1
(*S*)(*R*)103	−8.471	−76.865	3
(*R*)(*R*)103	−8.022	−70.943	5
A16	−8.224	−70.738	5
(*R*)102	−8.092	−66.399	3
A17	−8.013	−67.543	5
A18	−7.326	−72.117	5
A19	−8.224	−69.485	3
A20	−7.448	−65.477	5
A21	−8.364	−76.117	5

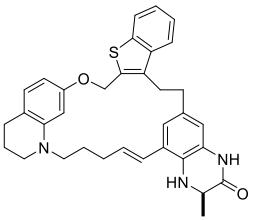
B4 Conformational analysis traces

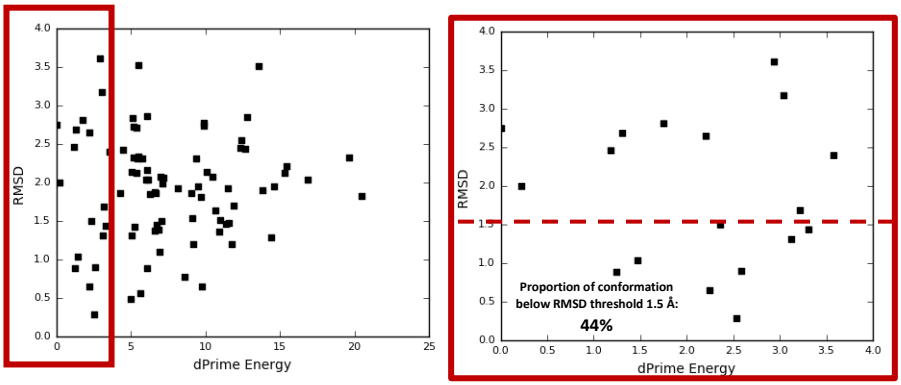
*Macrocycle **(R)98***



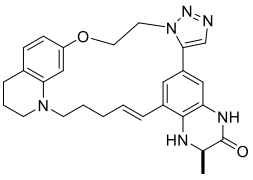


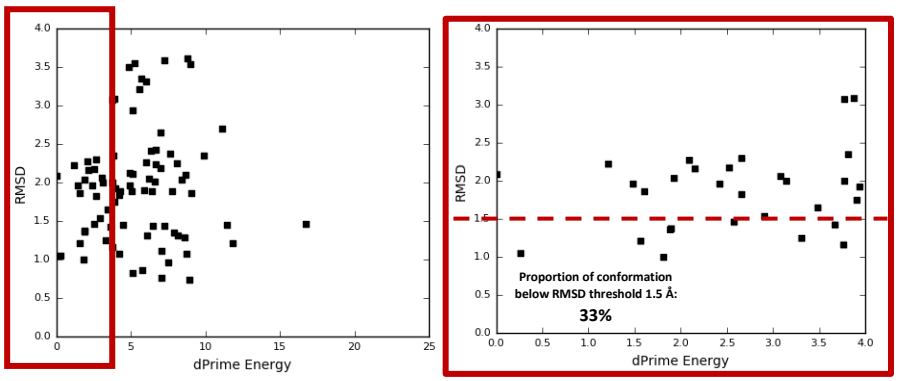
*Macrocycle **(R)99***



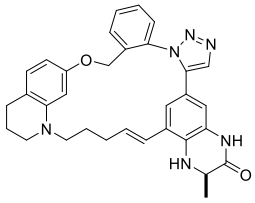


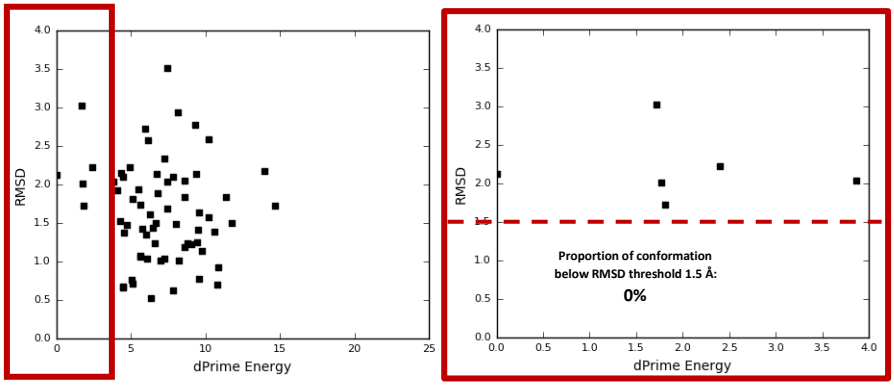
*Macrocycle **(R)100***



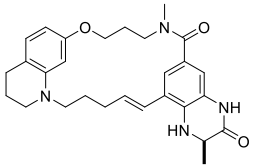


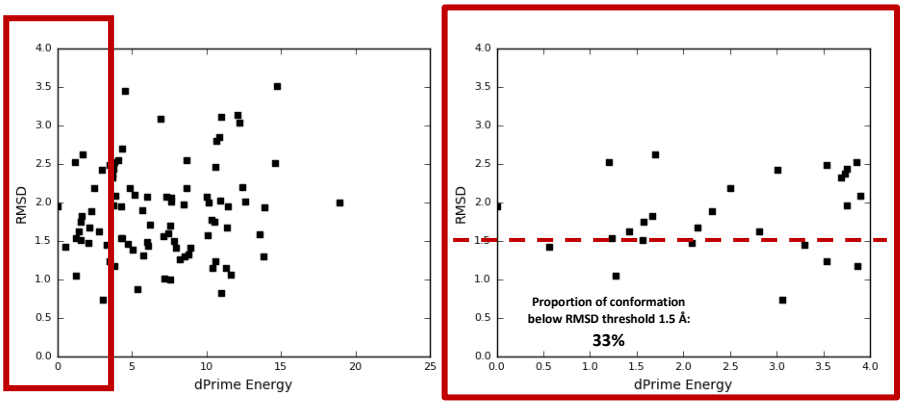
*Macrocycle **(R)101***



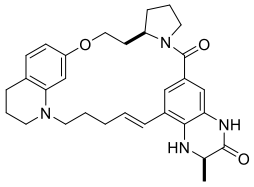


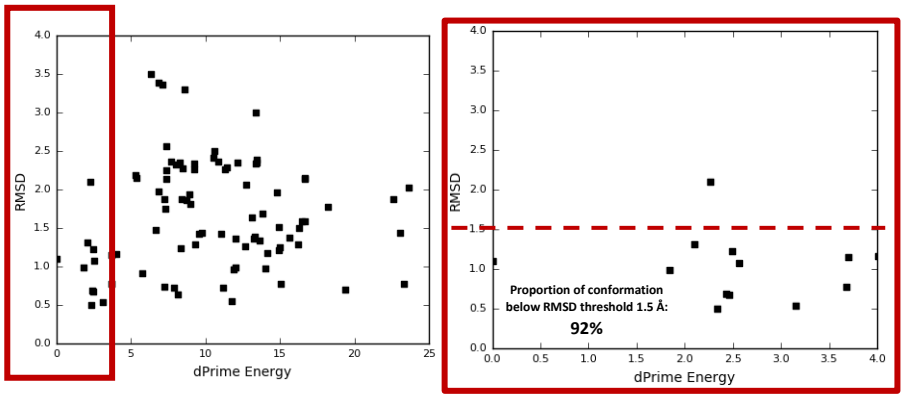
*Macrocycle **(R)102***



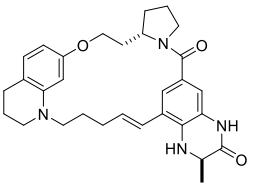


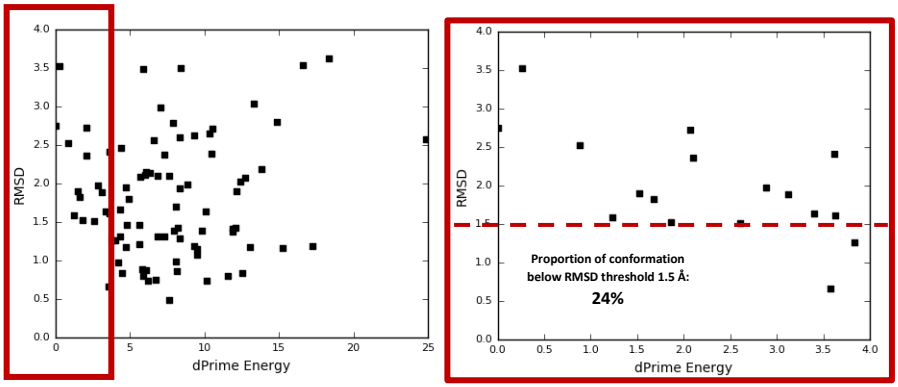
*Macrocycle **(R)(R)103***





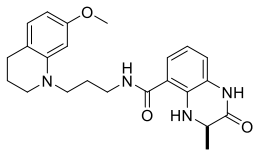
*Macrocycle **(S)(R)103***

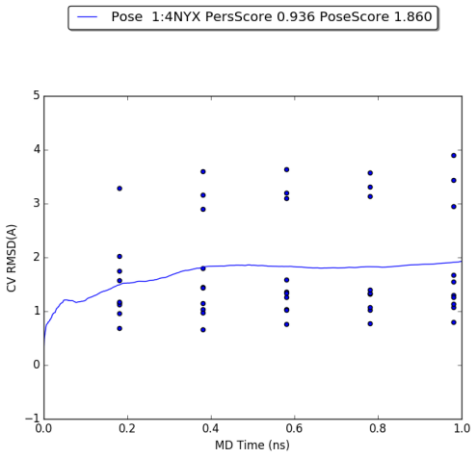




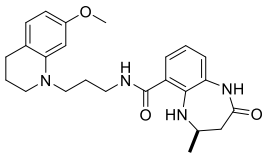
B5 Metadynamic simulation traces

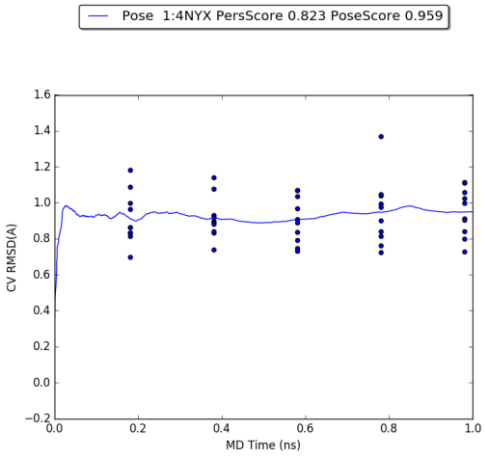
*Compound **(R)10***



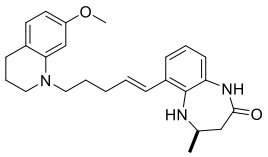


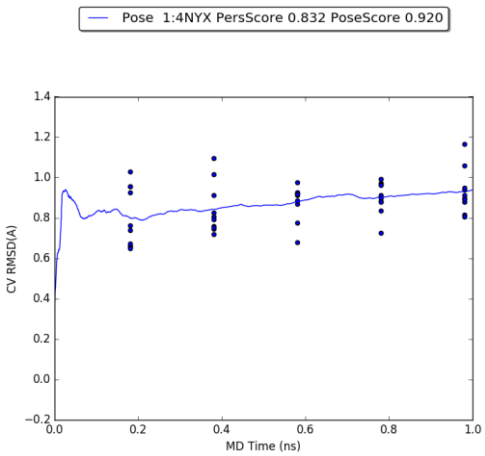
*Compound **(R)11***



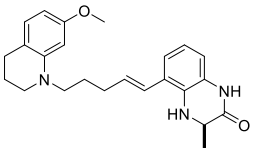


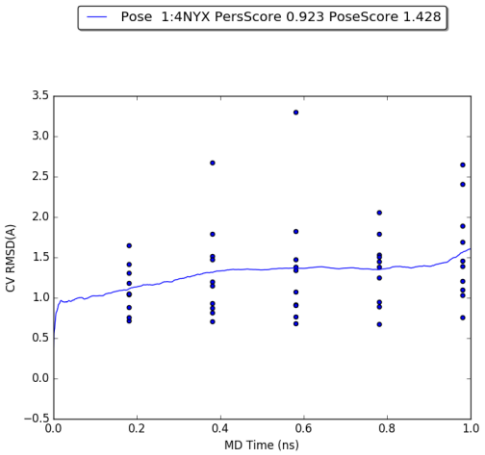
*Compound **(R)48***



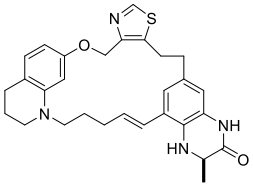


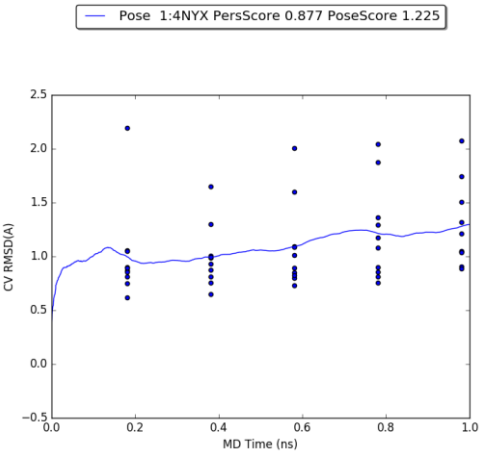
*Compound **(R)97***



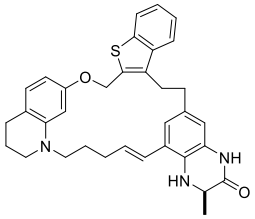


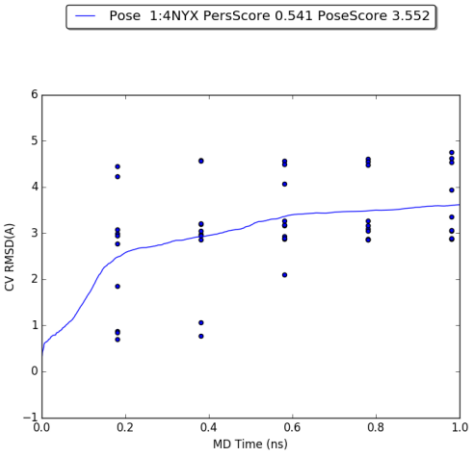
*Macrocycle **(R)98***



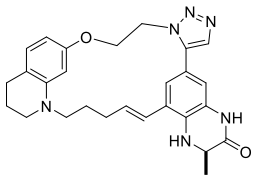


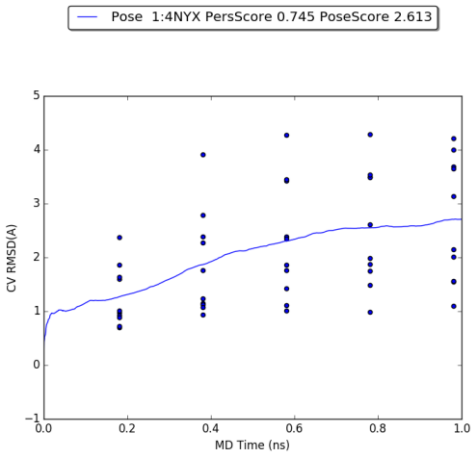
*Macrocycle **(R)99***



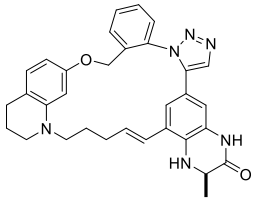


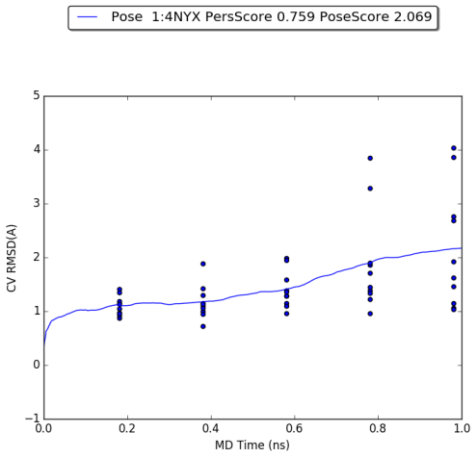
*Macrocycle **(R)100***



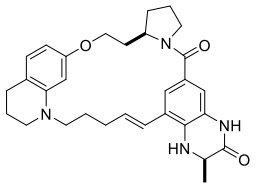


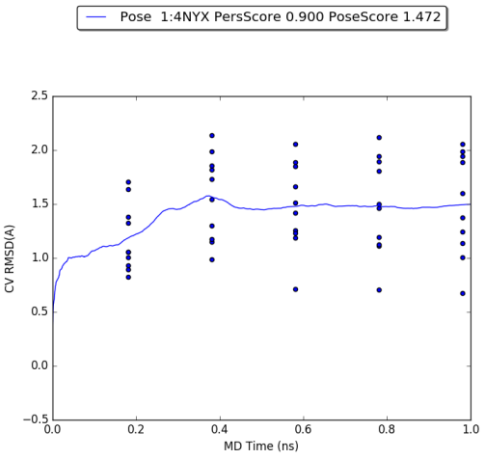
*Macrocycle **(R)101***



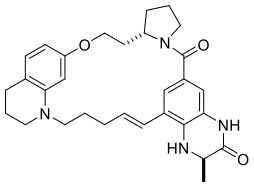


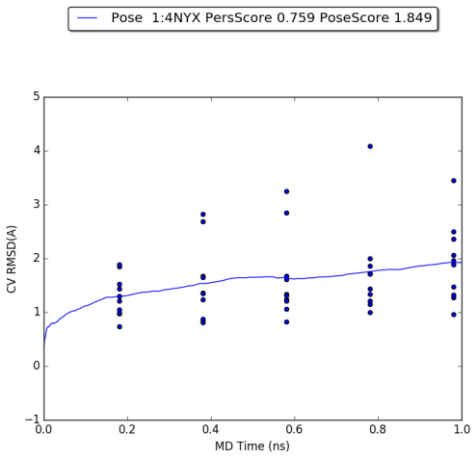
*Macrocycle **(R)(R)103***



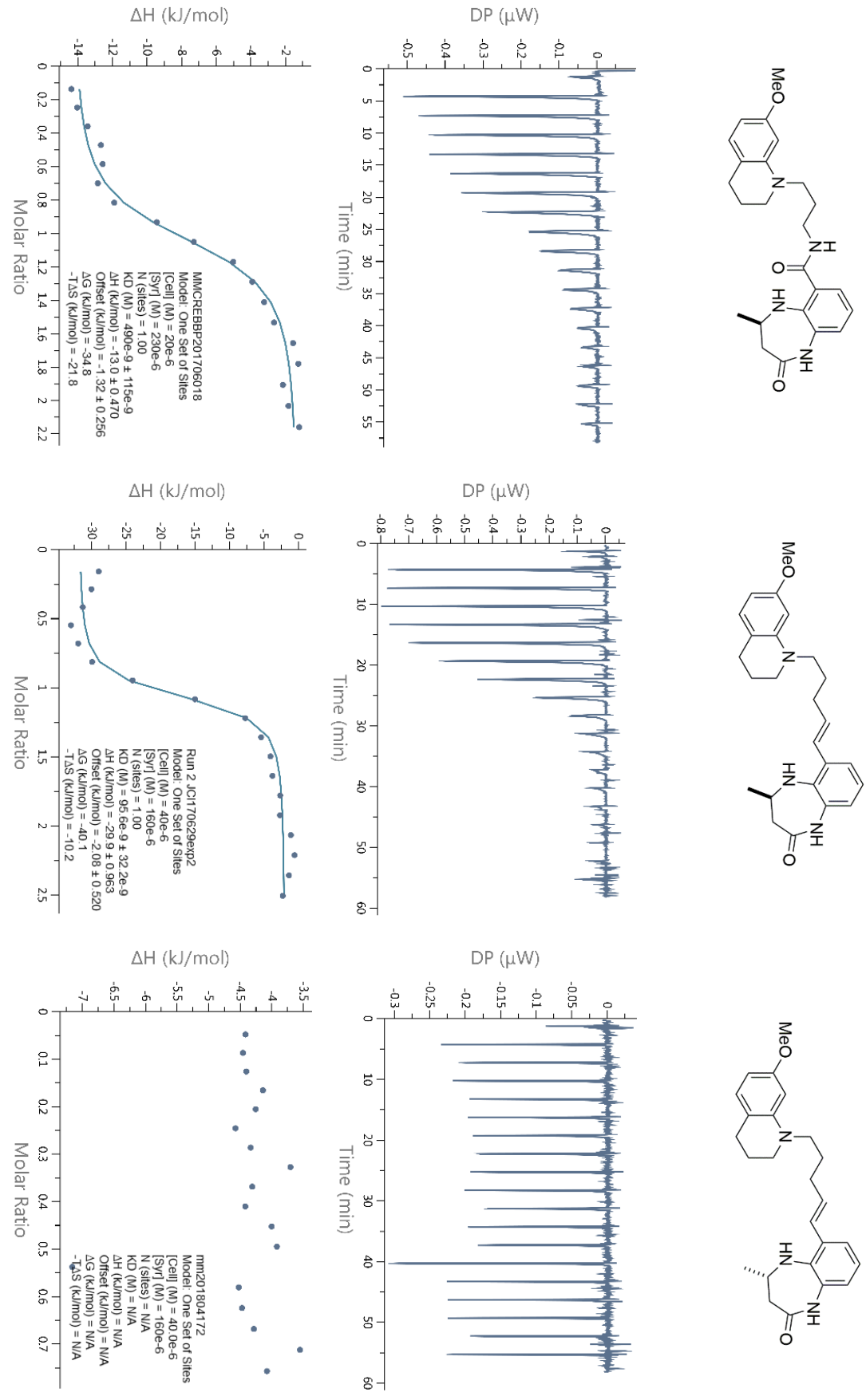


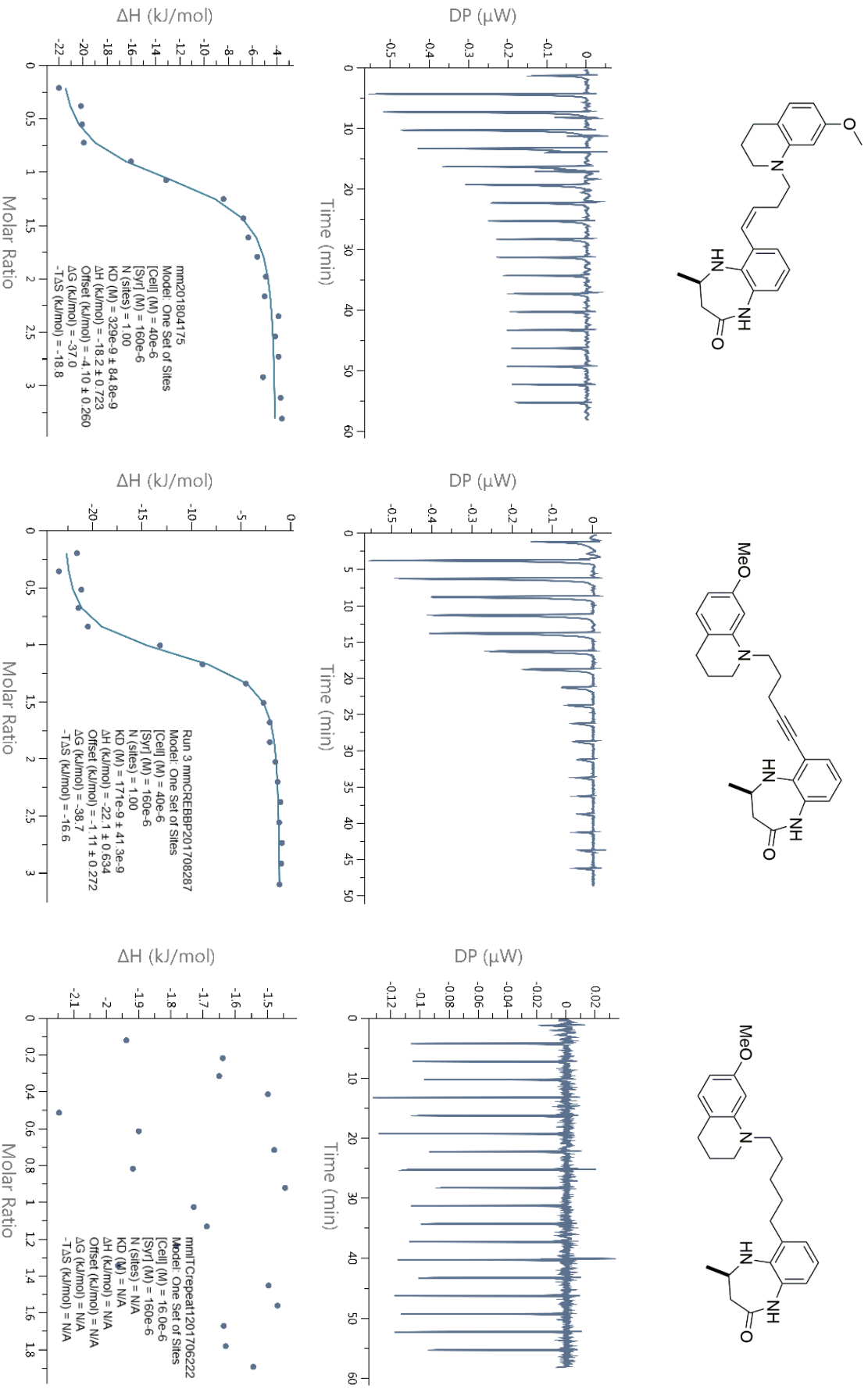
Macrocycle ***(S)(R)103***

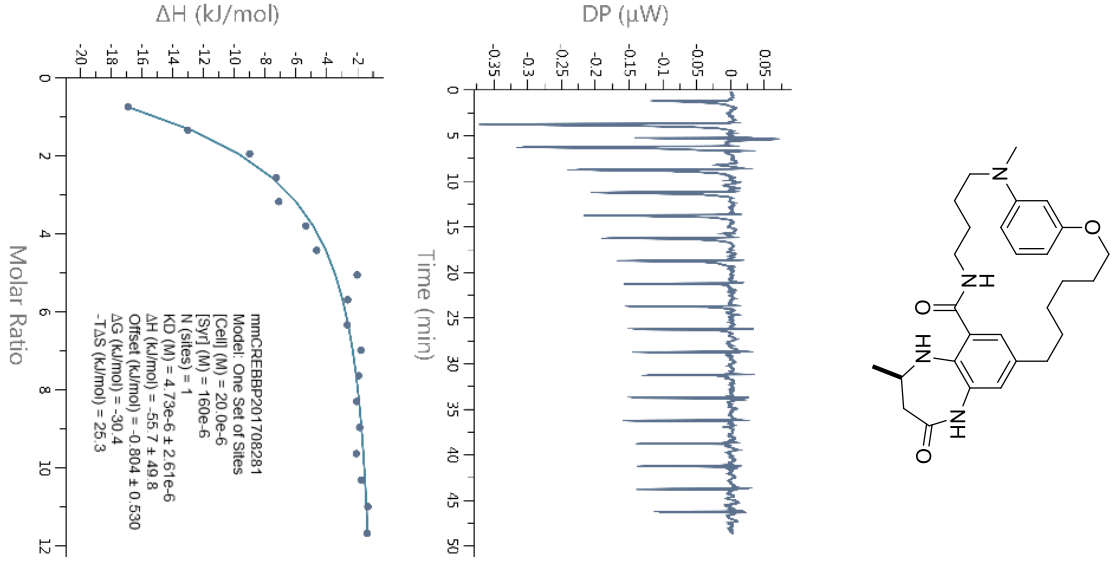


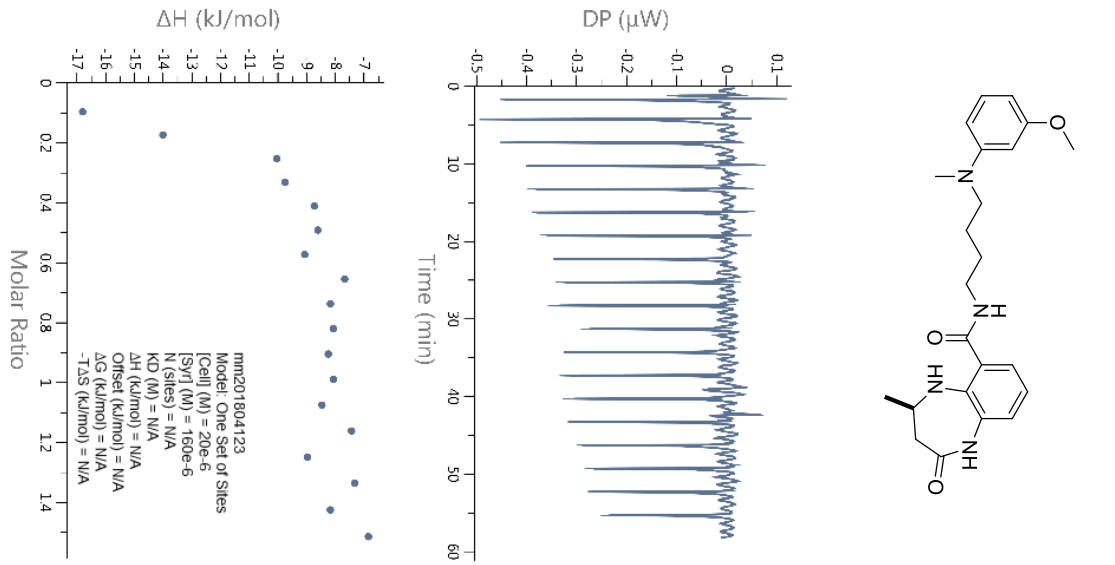


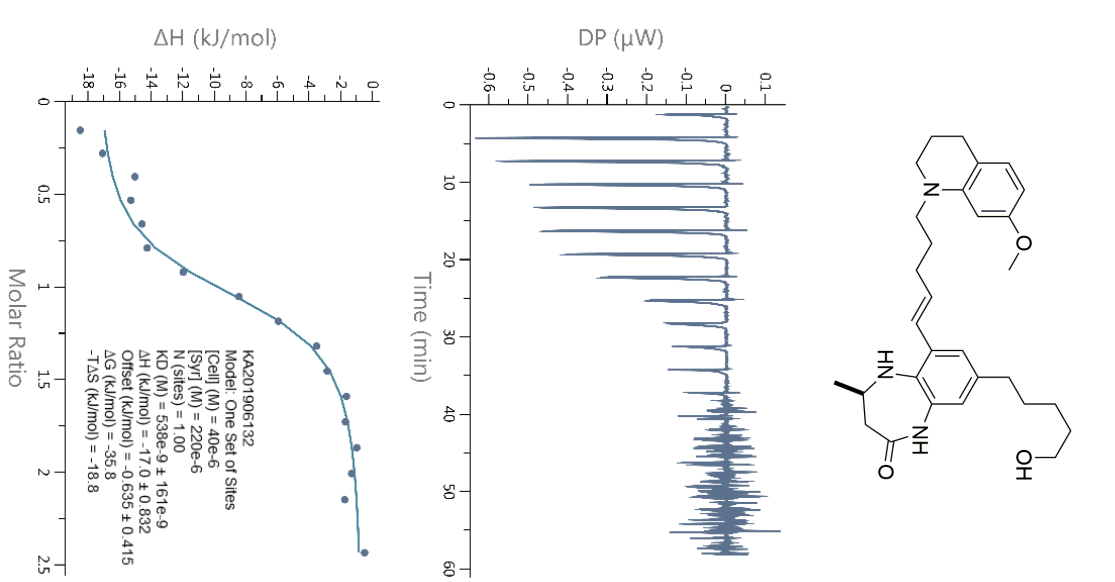
C1 ITC raw data for CREBBP bromodomain

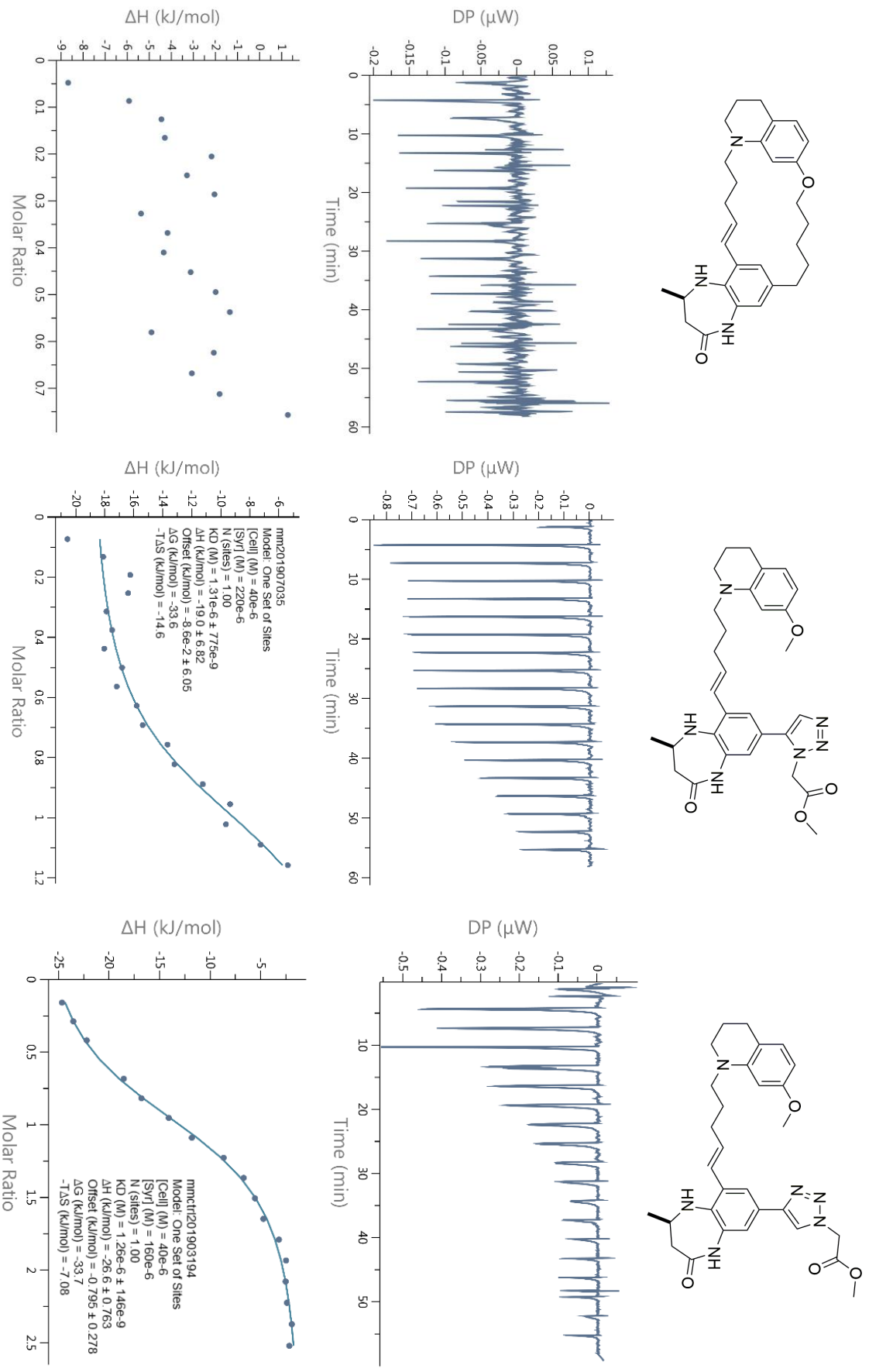


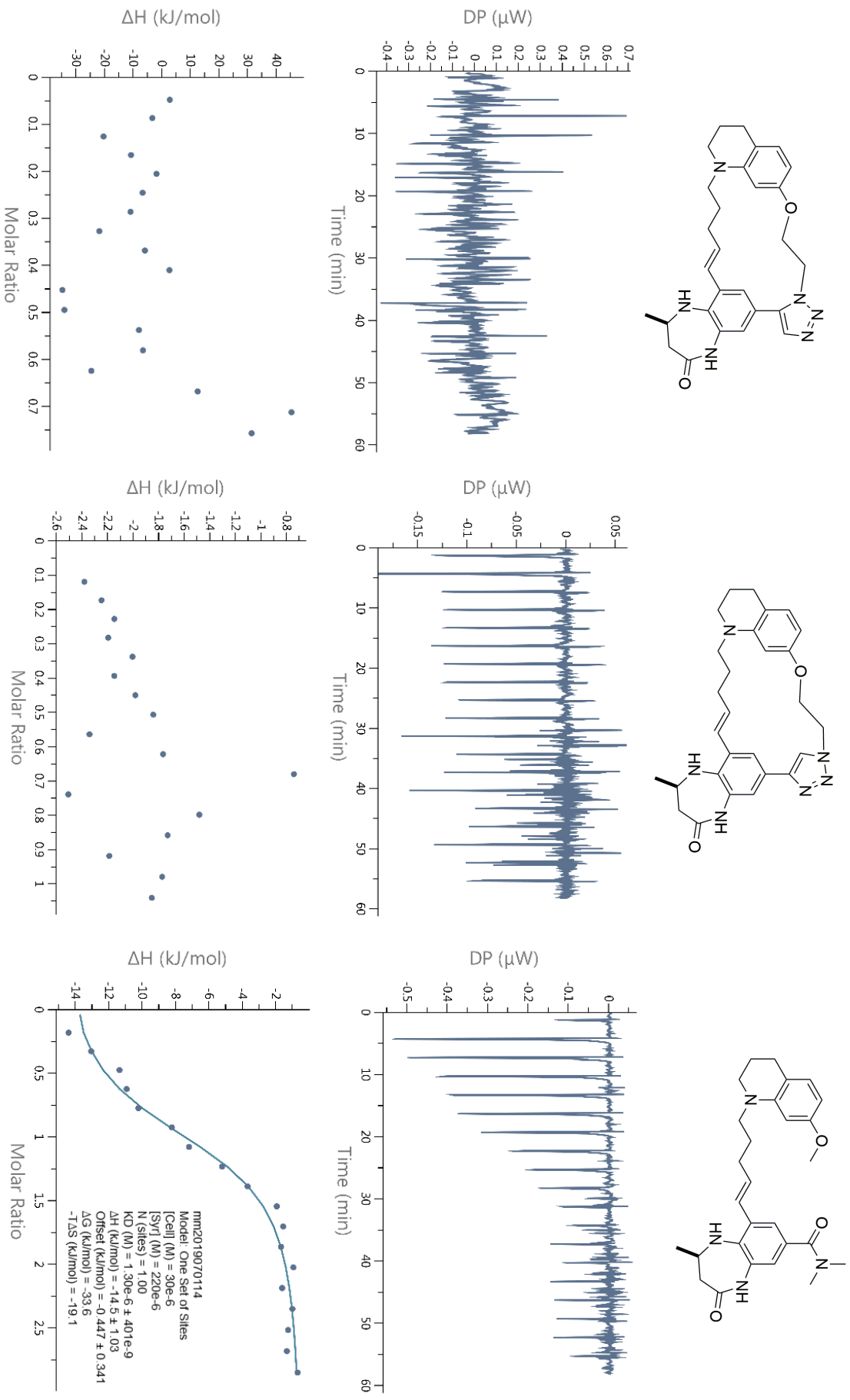

DP (µW)
Time (min)
ΔH (kJ/mol)
Molar Ratio
mm20180417S
Model: One Set of Sites
[Cell] (M) = 40e-6
[Syr] (M) = 160e-6
N (sites) = 1.00
KD (M) = 329e-9 ± 84.8e-9
ΔH (kJ/mol) = -18.2 ± 0.723
Offset (kJ/mol) = -4.10 ± 0.260
ΔG (kJ/mol) = -37.0
-TΔS (kJ/mol) = -18.8
MeO
HN
NH
O
Run 3 mmCREBBP20170828
Model: One Set of Sites
[Cell] (M) = 40e-6
[Syr] (M) = 160e-6
N (sites) = 1.00
KD (M) = 171e-9 ± 41.3e-9
ΔH (kJ/mol) = -22.1 ± 0.634
Offset (kJ/mol) = -1.11 ± 0.272
ΔG (kJ/mol) = -38.7
-TΔS (kJ/mol) = -16.6
mmITCrepeat120170622
Model: One Set of Sites
[Cell] (M) = 16.0e-6
[Syr] (M) = 160e-6
N (sites) = N/A
KD (M) = N/A
ΔH (kJ/mol) = N/A
Offset (kJ/mol) = N/A
ΔG (kJ/mol) = N/A
-TΔS (kJ/mol) = N/A

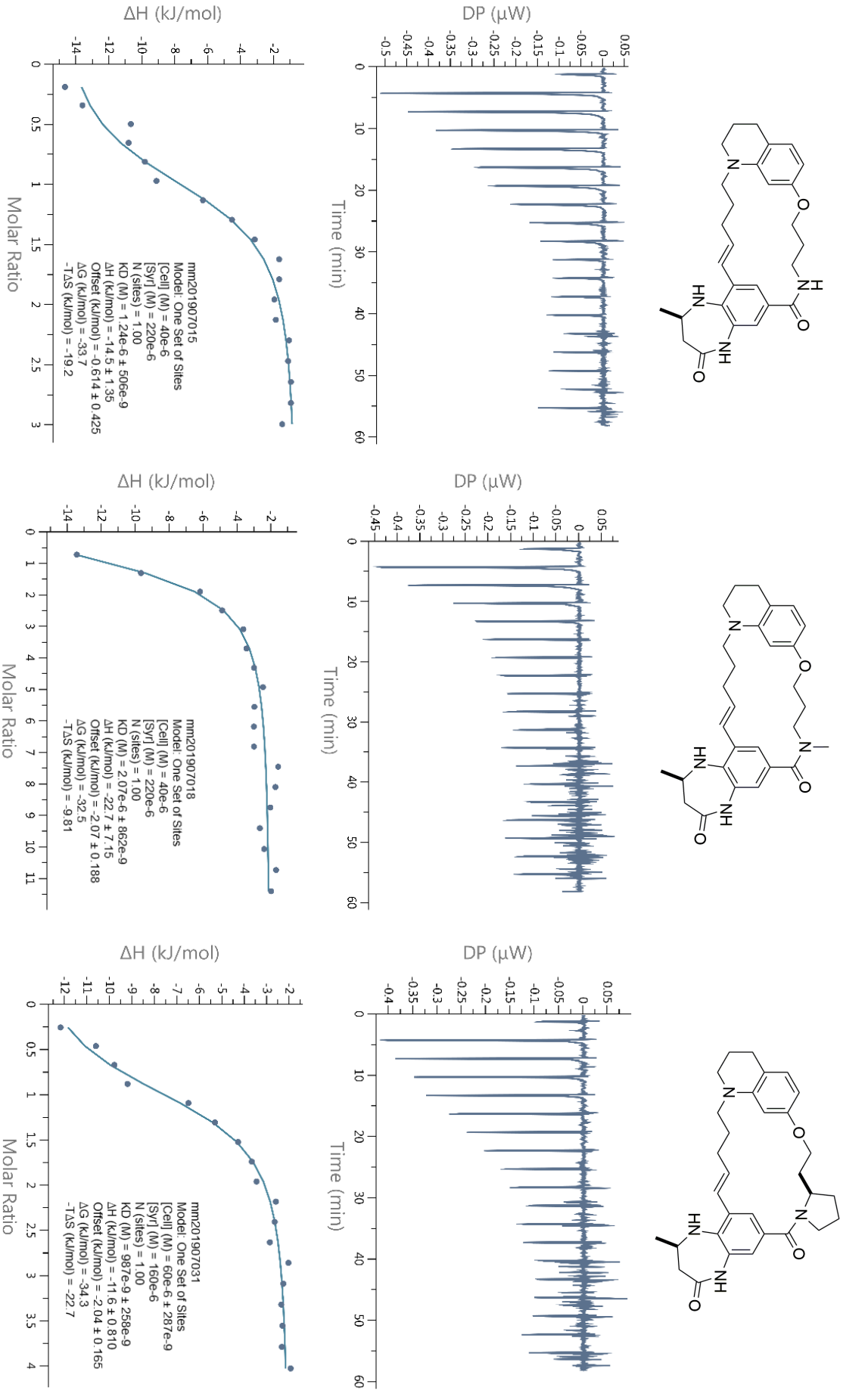

DP (µW)
Time (min)
ΔH (kJ/mol)
Molar Ratio
mmCREBBP20170281
Model: One Set of Sites
[Cell] (M) = 20.0e-6
[Syr] (M) = 160e-6
N (sites) = 1
KD (M) = 4.73e-6 ± 2.61e-6
ΔH (kJ/mol) = -55.7 ± 49.8
Offset (kJ/mol) = -0.804 ± 0.530
ΔG (kJ/mol) = -30.4
-TΔS (kJ/mol) = 25.3

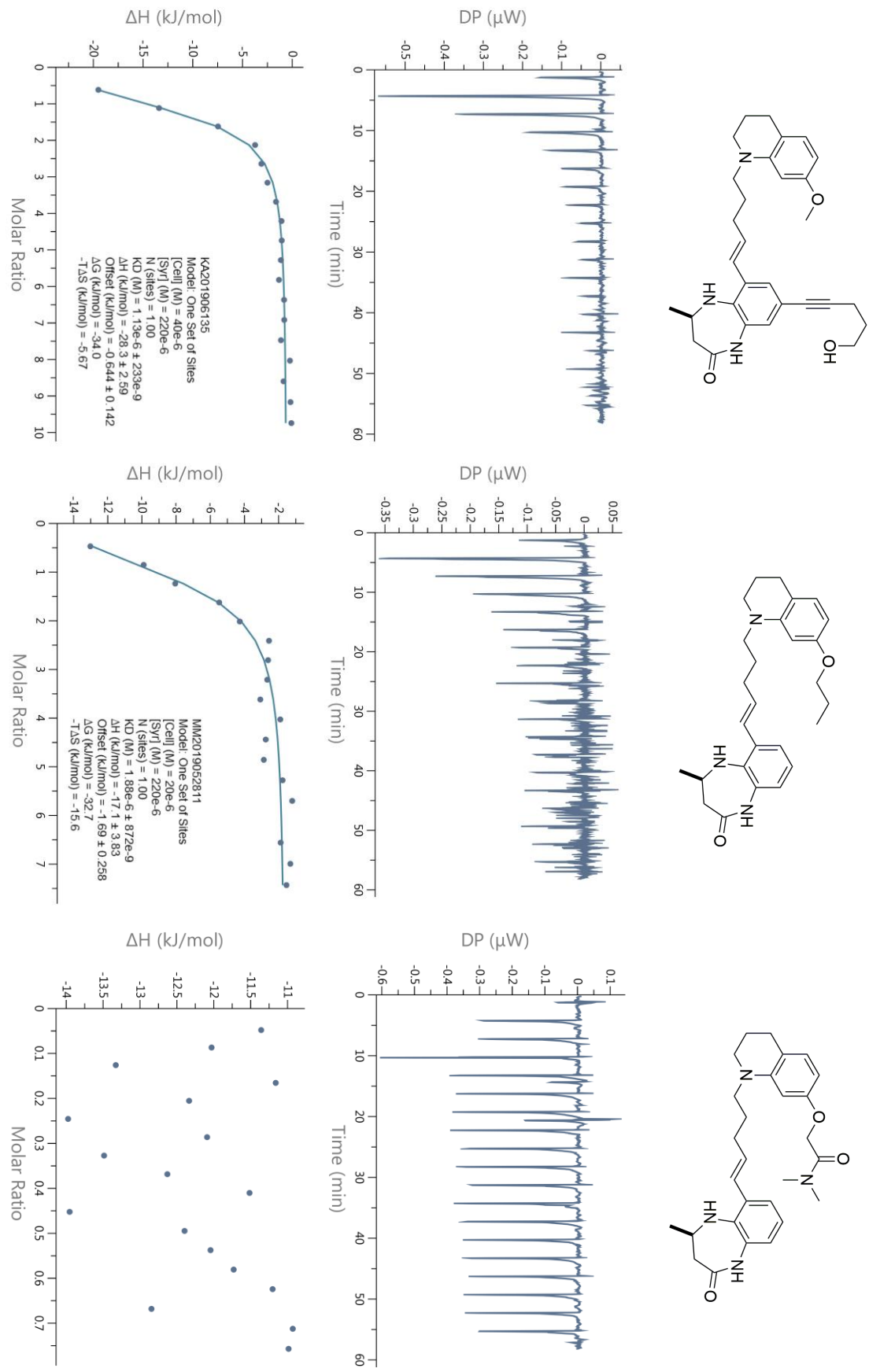

DP (µW)
Time (min)
ΔH (kJ/mol)
Molar Ratio
mm20180423
Model: One Set of Sites
[Cell] (M) = 20e-6
[Syr] (M) = 160e-6
N (sites) = N/A
KD (M) = N/A
ΔH (kJ/mol) = N/A
Offset (kJ/mol) = N/A
ΔG (kJ/mol) = N/A
-TΔS (kJ/mol) = N/A

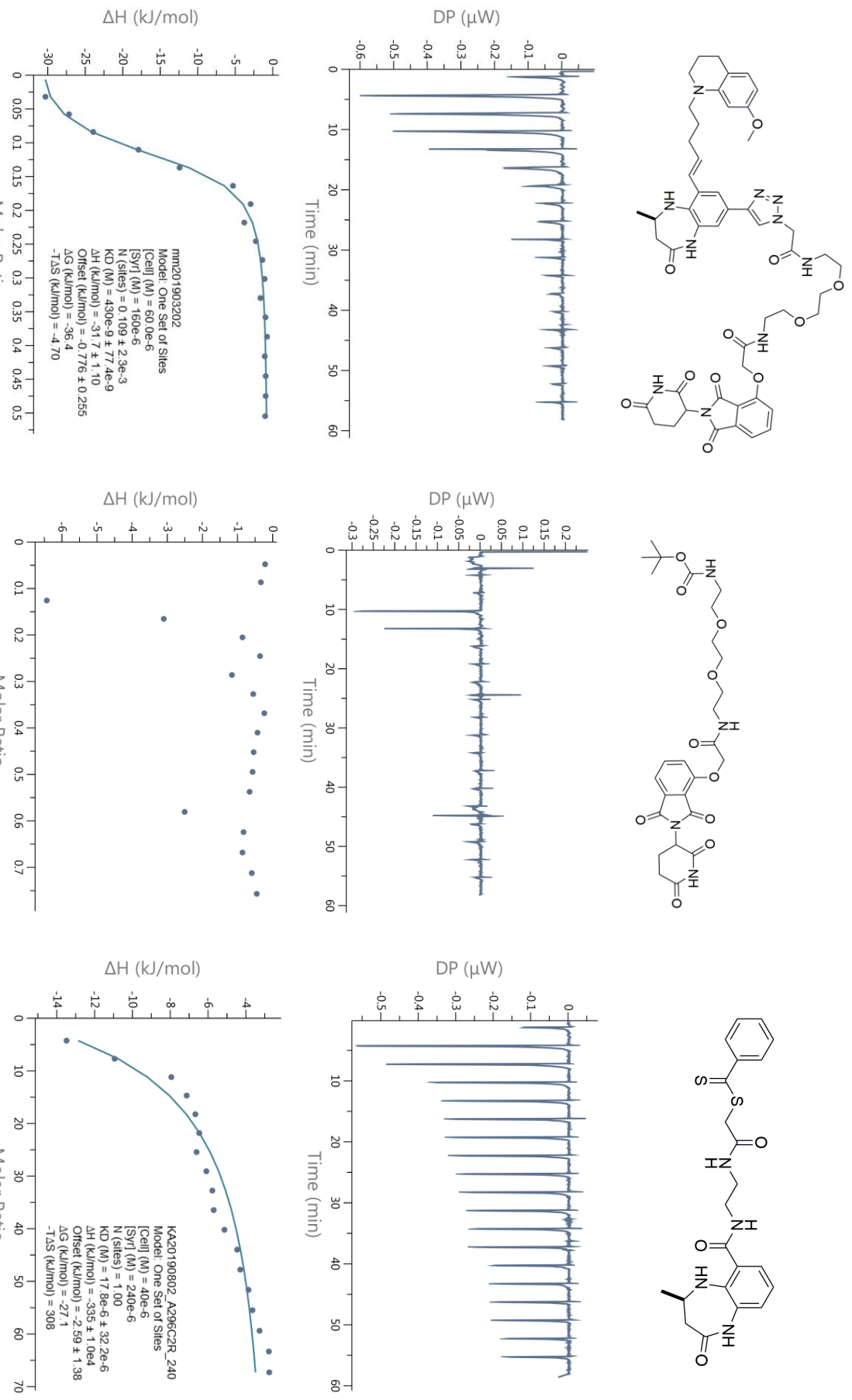

DP (µW)
Time (min)
ΔH (kJ/mol)
Molar Ratio
KA201906132
Model: One Set of Sites
[Cell] (M) = 40e-6
[Syr] (M) = 220e-6
N (sites) = 1.00
KD (M) = 538e-9 ± 161e-9
ΔH (kJ/mol) = -17.0 ± 0.832
Offset (kJ/mol) = -0.635 ± 0.415
ΔG (kJ/mol) = -35.8
-TΔS (kJ/mol) = -18.8

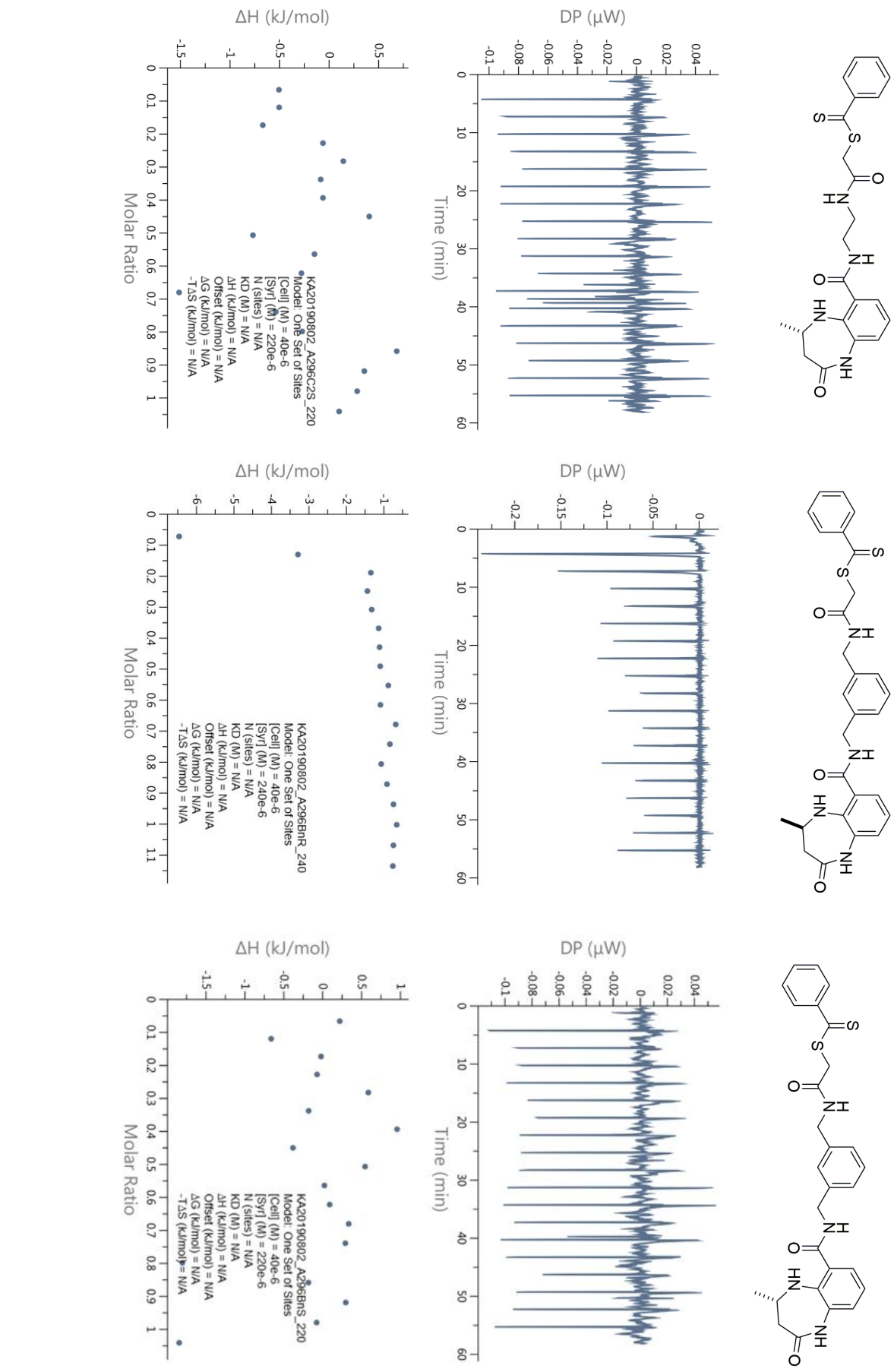

DP (µW)
Time (min)
ΔH (kJ/mol)
Molar Ratio
mm20190703
Model: One Set of Sites
[Cell] (M) = 40e-6
[Syr] (M) = 220e-6
N (sites) = 1.00
KD (M) = 1.31e-6 ± 775e-9
ΔH (kJ/mol) = -19.0 ± 6.82
Offset (kJ/mol) = -8.6e-2 ± 6.05
ΔG (kJ/mol) = -33.6
-TΔS (kJ/mol) = -14.6
mmctrl201903194
Model: One Set of Sites
[Cell] (M) = 40e-6
[Syr] (M) = 160e-6
N (sites) = 1.00
KD (M) = 1.26e-6 ± 146e-9
ΔH (kJ/mol) = -26.6 ± 0.763
Offset (kJ/mol) = -0.795 ± 0.278
ΔG (kJ/mol) = -33.7
-TΔS (kJ/mol) = -7.08

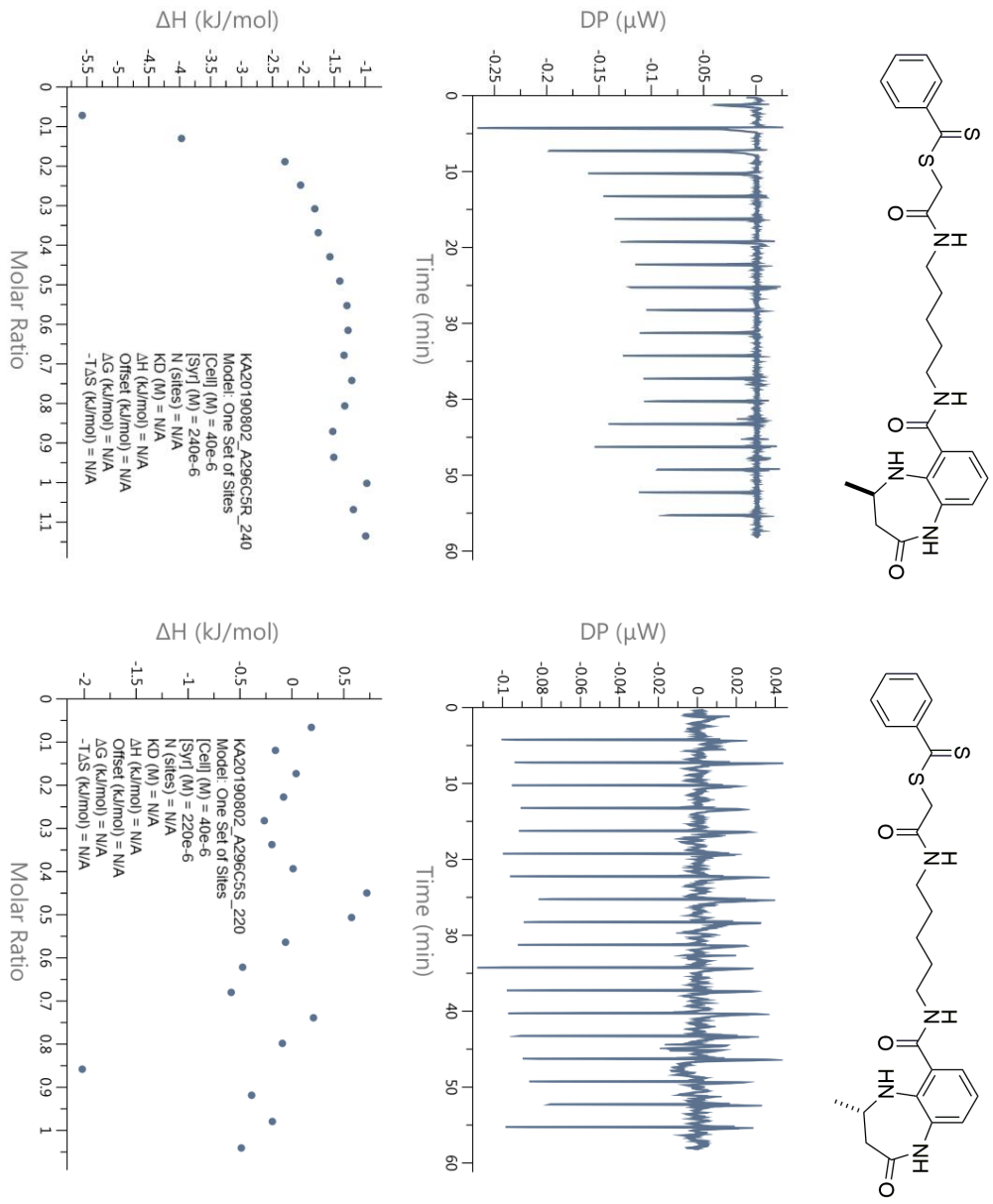

DP (µW)
Time (min)
ΔH (kJ/mol)
Molar Ratio
mm20190701 14
Model: One Set of Sites
[Cell] (M) = 30e-6
[Syr] (M) = 220e-6
N (sites) = 1.00
KD (M) = 1.30e-6 ± 401e-9
ΔH (kJ/mol) = -14.5 ± 1.03
Offset (kJ/mol) = -0.447 ± 0.341
ΔG (kJ/mol) = -33.6
-TΔS (kJ/mol) = -19.1


DP (µW)
Time (min)
ΔH (kJ/mol)
Molar Ratio
mm20190701
Model: One Set of Sites
[Cell] (M) = 40e-6
[Syr] (M) = 220e-6
N (sites) = 1.00
KD (M) = 1.24e-6 ± 506e-9
ΔH (kJ/mol) = -14.5 ± 1.35
Offset (kJ/mol) = -0.614 ± 0.425
ΔG (kJ/mol) = -33.7
-TΔS (kJ/mol) = -19.2
mm20190702
Model: One Set of Sites
[Cell] (M) = 40e-6
[Syr] (M) = 220e-6
N (sites) = 1.00
KD (M) = 2.07e-6 ± 862e-9
ΔH (kJ/mol) = -22.7 ± 7.15
Offset (kJ/mol) = -2.07 ± 0.188
ΔG (kJ/mol) = -32.5
-TΔS (kJ/mol) = -9.81
mm20190703
Model: One Set of Sites
[Cell] (M) = 60e-6 ± 287e-9
[Syr] (M) = 160e-6
N (sites) = 1.00
KD (M) = 987e-9 ± 258e-9
ΔH (kJ/mol) = -11.6 ± 0.810
Offset (kJ/mol) = 2.04 ± 0.165
ΔG (kJ/mol) = -34.3
-TΔS (kJ/mol) = -22.7

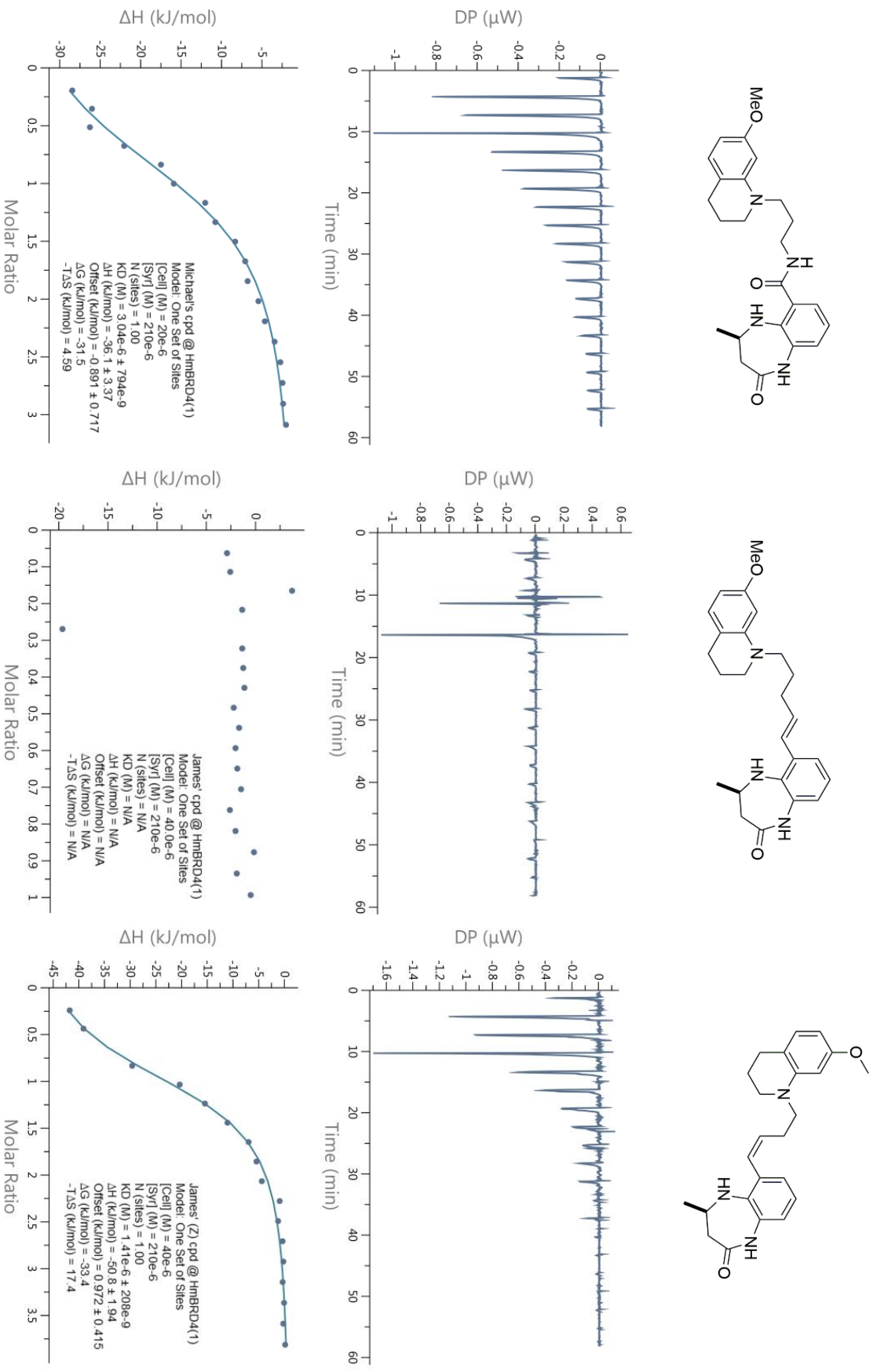

DP (µW)
Time (min)
ΔH (kJ/mol)
Molar Ratio
KA201906135
Model: One Set of Sites
[Cell] (M) = 40e-6
[Syr] (M) = 220e-6
N (sites) = 1.00
KD (M) = 1.13e-6 ± 233e-9
ΔH (kJ/mol) = -28.3 ± 2.59
Offset (kJ/mol) = -0.644 ± 0.142
ΔG (kJ/mol) = -34.0
-TΔS (kJ/mol) = -5.67
MM201905281 1
Model: One Set of Sites
[Cell] (M) = 20e-6
[Syr] (M) = 220e-6
N (sites) = 1.00
KD (M) = 1.88e-6 ± 872e-9
ΔH (kJ/mol) = -17.1 ± 3.83
Offset (kJ/mol) = -1.69 ± 0.258
ΔG (kJ/mol) = -32.7
-TΔS (kJ/mol) = -15.6

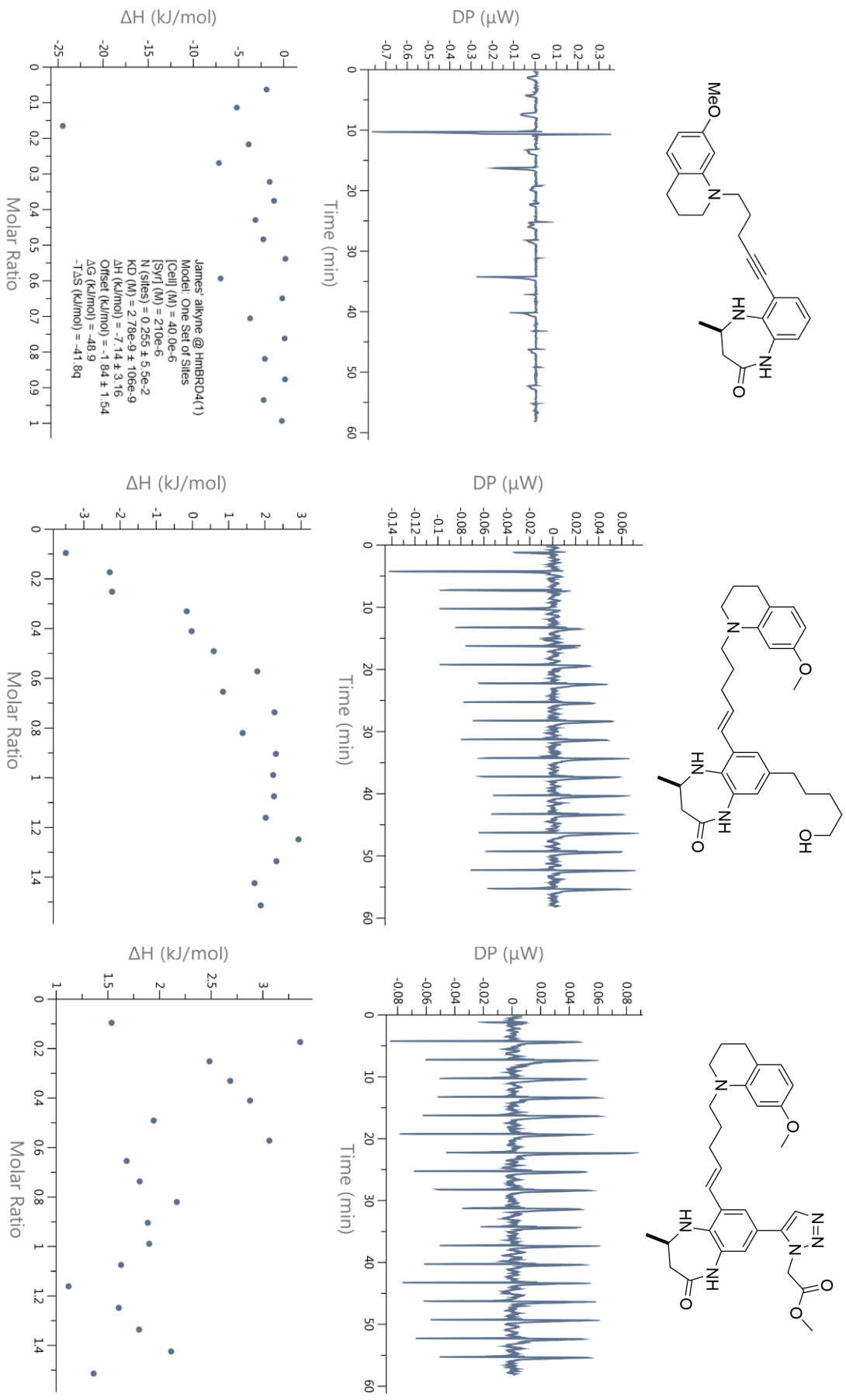

DP (μW)
Time (min)
ΔH (kJ/mol)
Molar Ratio
mm20190320
Model: One Set of Sites
[Cell] (M) = 60.0e-6
[Syr] (M) = 160e-6
N (sites) = 0.109 ± 2.3e-3
KD (M) = 430e-9 ± 77.4e-9
ΔH (kJ/mol) = -31.7 ± 1.10
Offset (kJ/mol) = -0.776 ± 0.255
ΔG (kJ/mol) = -36.4
-TΔS (kJ/mol) = -4.70
KA20190802_A296C2R_240
Model: One Set of Sites
[Cell] (M) = 40e-6
[Syr] (M) = 240e-6
N (sites) = 1.00
KD (M) = 17.8e-6 ± 32.2e-6
ΔH (kJ/mol) = -335 ± 1.0e4
Offset (kJ/mol) = -2.59 ± 1.38
ΔG (kJ/mol) = -27.1
-TΔS (kJ/mol) = 308

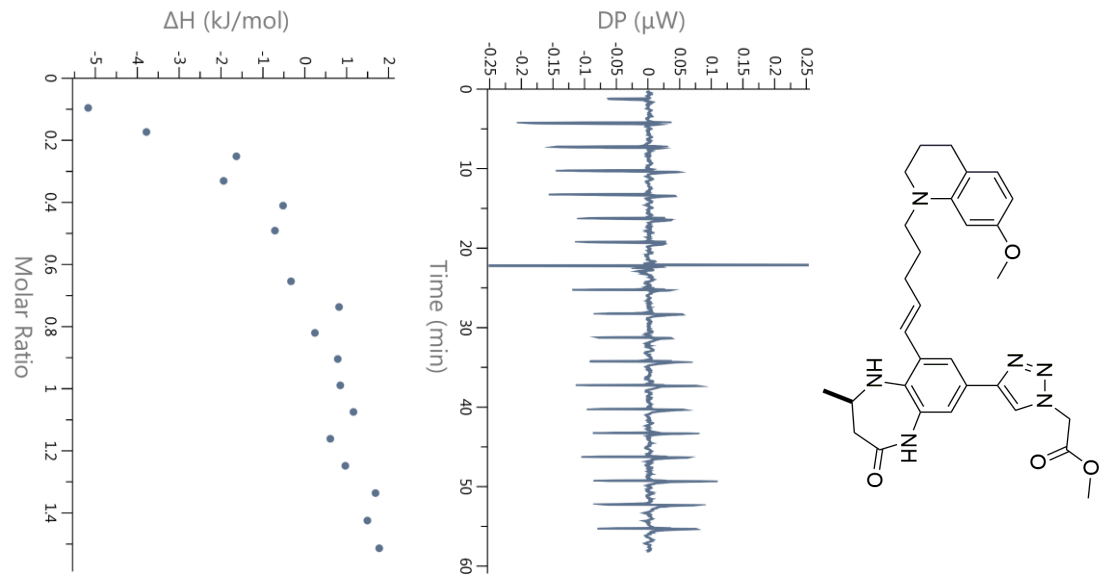

DP (µW)
Time (min)
ΔH (kJ/mol)
Molar Ratio
KA20190802_A296C2S_220
Model: One Set of Sites
[Cell] (M) = 40e-6
[Syr] (M) = 220e-6
N (sites) = N/A
KD (M) = N/A
ΔH (kJ/mol) = N/A
Offset (kJ/mol) = N/A
ΔG (kJ/mol) = N/A
-TΔS (kJ/mol) = N/A
KA20190802_A296BnR_240
Model: One Set of Sites
[Cell] (M) = 40e-6
[Syr] (M) = 240e-6
N (sites) = N/A
KD (M) = N/A
ΔH (kJ/mol) = N/A
Offset (kJ/mol) = N/A
ΔG (kJ/mol) = N/A
-TΔS (kJ/mol) = N/A
KA20190802_A296BnS_220
Model: One Set of Sites
[Cell] (M) = 40e-6
[Syr] (M) = 220e-6
N (sites) = N/A
KD (M) = N/A
ΔH (kJ/mol) = N/A
Offset (kJ/mol) = N/A
ΔG (kJ/mol) = N/A
-TΔS (kJ/mol) = N/A

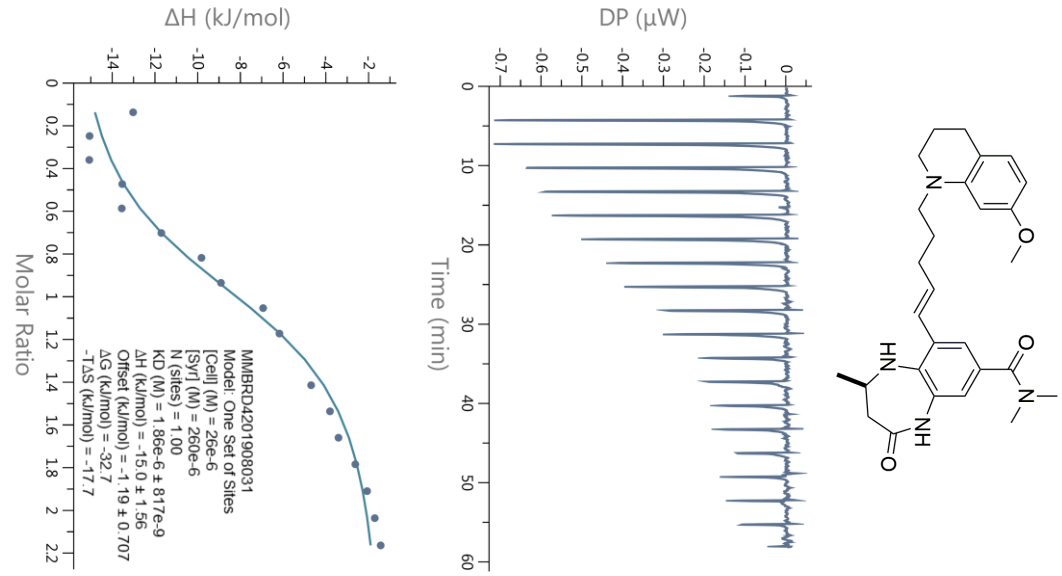

ΔH (kJ/mol)
DP (μW)
Time (min)
Molar Ratio
KA20190802_A296C5R_240
Model: One Set of Sites
[Cell] (M) = 40e-6
[Syr] (M) = 240e-6
N (sites) = N/A
KD (M) = N/A
ΔH (kJ/mol) = N/A
Offset (kJ/mol) = N/A
ΔG (kJ/mol) = N/A
-TΔS (kJ/mol) = N/A
ΔH (kJ/mol)
DP (μW)
Time (min)
Molar Ratio
KA20190802_A296C5S_220
Model: One Set of Sites
[Cell] (M) = 40e-6
[Syr] (M) = 220e-6
N (sites) = N/A
KD (M) = N/A
ΔH (kJ/mol) = N/A
Offset (kJ/mol) = N/A
ΔG (kJ/mol) = N/A
-TΔS (kJ/mol) = N/A

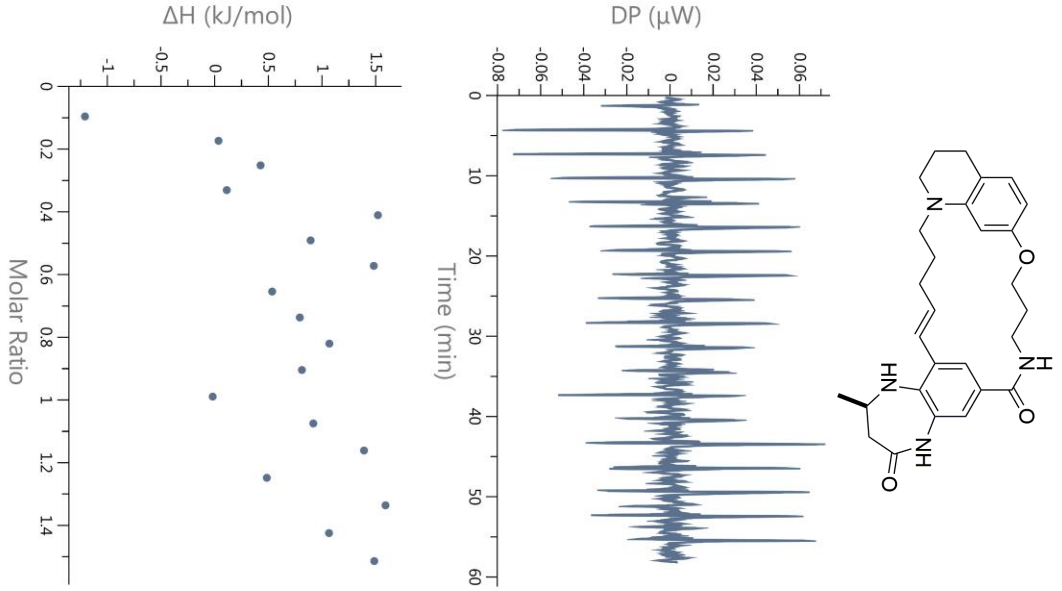
C2 ITC raw data for BRD4(1) bromodomain

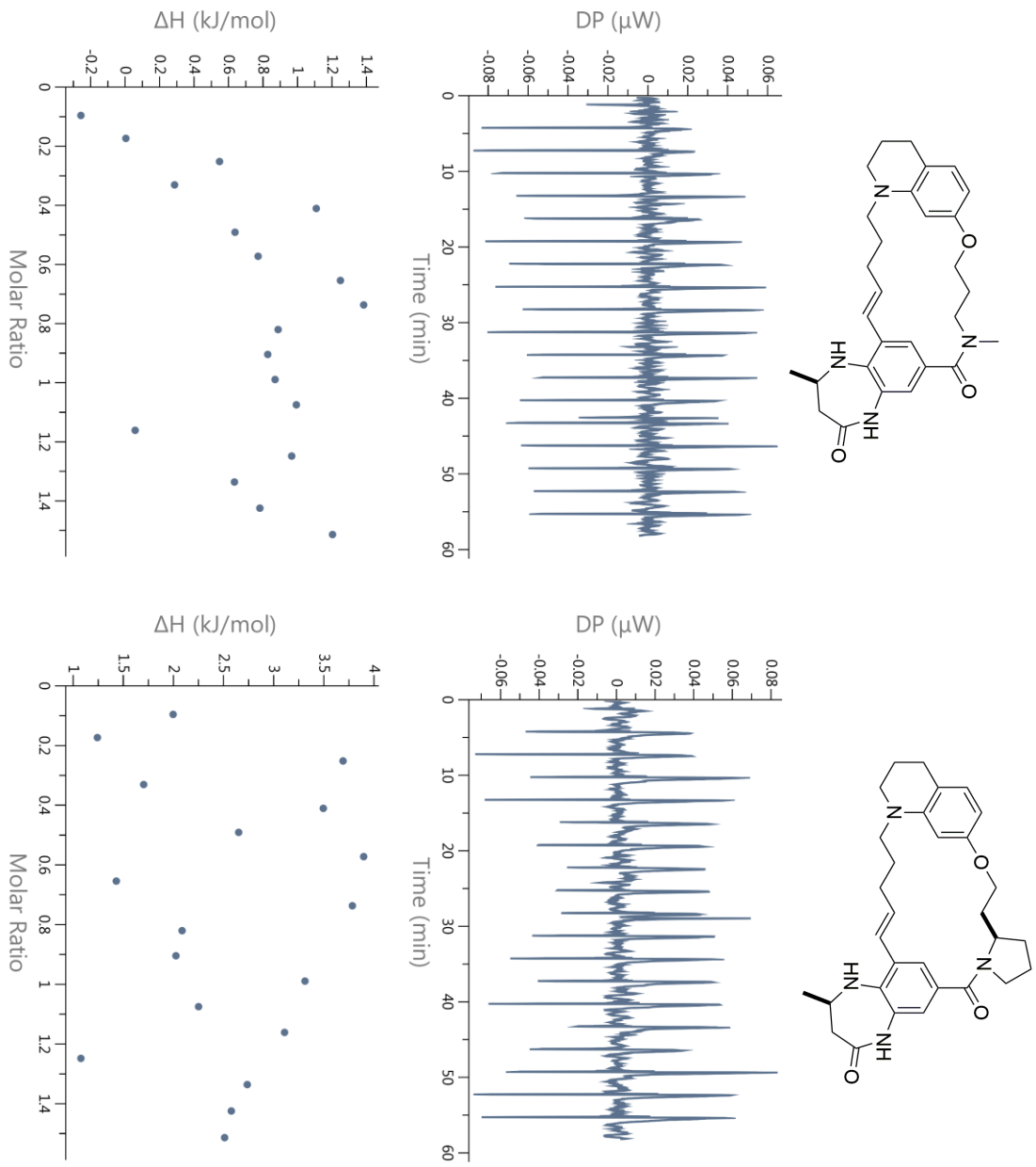



DP (µW)
Time (min)
ΔH (kJ/mol)
Molar Ratio
James' alkyne @ HmBRD4(1)
Model: One Set of Sites
[Cell] (M) = 40.0e-6
[Syr] (M) = 210e-6
N (sites) = 0.255 ± 5.5e-2
KD (M) = 2.78e-9 ± 106e-9
ΔH (kJ/mol) = -7.14 ± 3.16
Offset (kJ/mol) = -1.84 ± 1.54
ΔG (kJ/mol) = -48.9
-TΔS (kJ/mol) = -41.8q
MeO
HN
NH
O
N
OH
N=N


DP (µW)
Time (min)
ΔH (kJ/mol)
Molar Ratio


DP (µW)
Time (min)
ΔH (kJ/mol)
Molar Ratio
MMBRD4201908031
Model: One Set of Sites
[Cell] (M) = 26e-6
[Syr] (M) = 260e-6
N (sites) = 1.00
KD (M) = 1.86e-6 ± 817e-9
ΔH (kJ/mol) = -15.0 ± 1.56
Offset (kJ/mol) = -1.19 ± 0.707
ΔG (kJ/mol) = -32.7
-TΔS (kJ/mol) = -17.7


DP (µW)
Time (min)
ΔH (kJ/mol)
Molar Ratio


ΔH (kJ/mol)
DP (μW)
Time (min)
Molar Ratio
ΔH (kJ/mol)
DP (μW)
Time (min)
Molar Ratio

D Biophysical data and results

D1 BromoScan data for CREBBP bromodomain

SDL002-01-s-00001 Study Results

Table 1 - Matrix of Kds for SDL002-01-s-00001.

Compound	CREBBP
Compound Name	Kd (nM)
(*R*)48	180
(*R*)11	330

Kd Legend

x<100nM	100nM≤x<1uM	x≥1uM	No Binding	Not Requested

SDL002-01-s-00001 Curve Images

Table 2 - Curve Images for SDL002-01-s-00001. The amount of bromodomain measured by qPCR (Signal; y-axis) is plotted against the corresponding compound concentration in nM in log10 scale (x-axis). Data points marked with an "x" were not used for Kd determination.

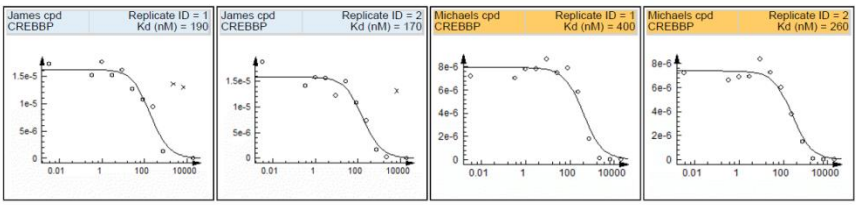


Figure D1.1 BromoScan binding data for the CREBBP bromodomain for ligands **(*R*)48** and **(*R*)11**.

D2 BromoScan data for BRD4(1) bromodomain

BVZ003-01-s-00001 Study Results

Table 1 - Matrix of Kds for BVZ003-01-s-00001.

Target	(*S*)48	(*R*)48
Gene Symbol	Kd (nM)	Kd (nM)
ATAD2B	>1000	>1000
BRD2(1)	>1000	>1000
BRD4(1)	>1000	>1000
BRD7	>1000	>1000
BRD9	>1000	>1000
BRPF1	>1000	>1000
CREBBP	>1000	200
EP300	>1000	230
PCAF	>1000	>1000
SMARCA4	>1000	>1000
TAF1(2)	>1000	>1000
TRIM24(PHD,Bromo.)	>1000	>1000

Kd Legend

x<100nM	100nM≤x<1uM	x≥1uM	No Binding	Not Requested

Figure D2.1 BromoScan selectivity data for ligands **(*S*)48** and **(*R*)48**.

D3 Ligand observed ^{1}H NMR study with BRD4(1)

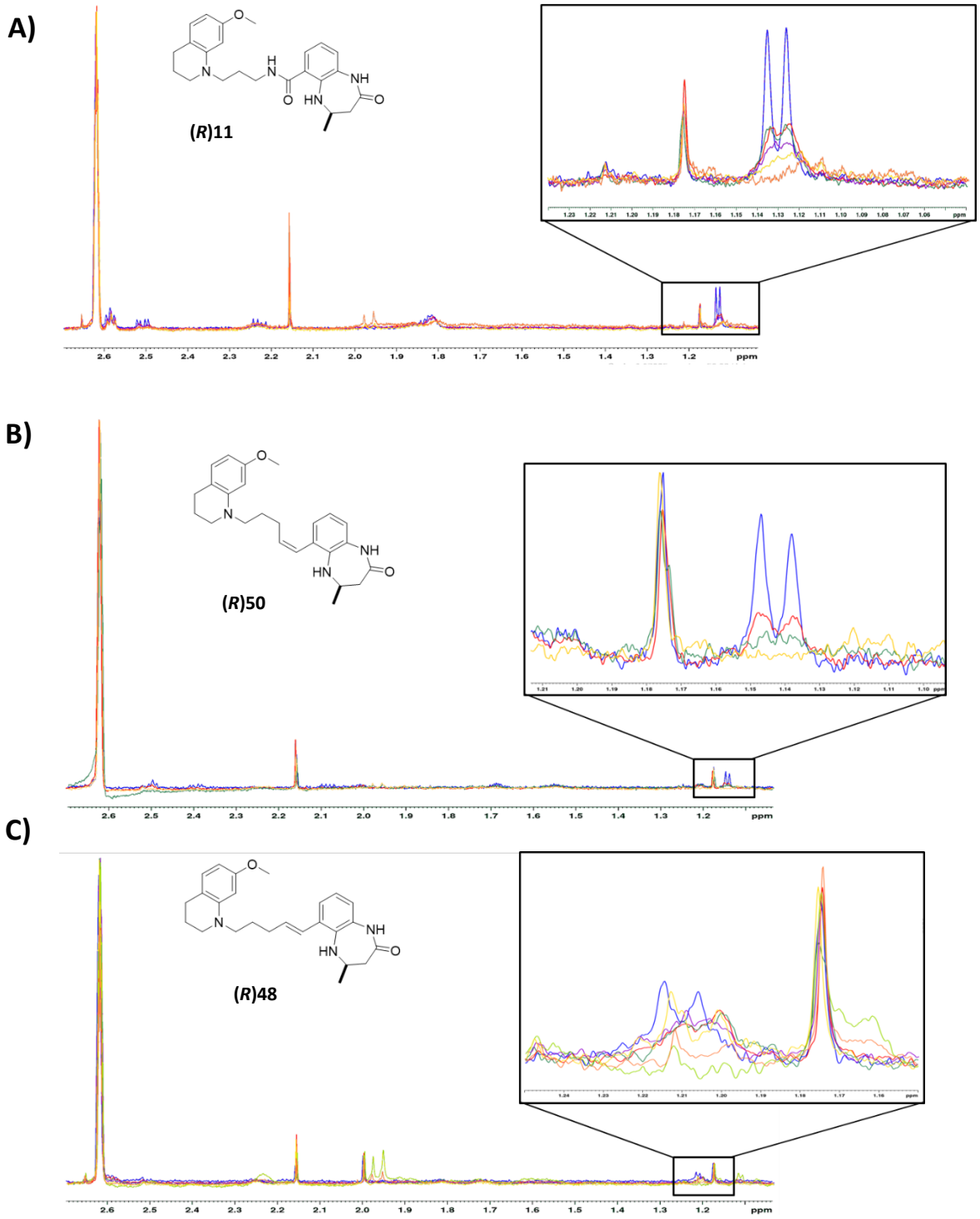


Figure D3.1 (A) Overlay of spectra of the free ligand **(*R*)11** (blue), and the ligand in the presence of BRD4(1) at 1 uM (red), 2 µM (green), 3 µM (purple), 5 µM (yellow) and 10 µM (orange). (B) Overlay of spectra of the free ligand **(*R*)50** (blue), and the ligand in the presence of BRD4(1) at 1 uM (red), 2 µM (green), 2.5 µM (purple), 5 µM (yellow), 10 µM (orange) and 25 µM (light green). (C) Overlay of spectra of the free ligand **(*R*)48** (blue), and the ligand in the presence of BRD4(1) at 1 uM (red), 2 µM (green) and 5 µM (yellow).

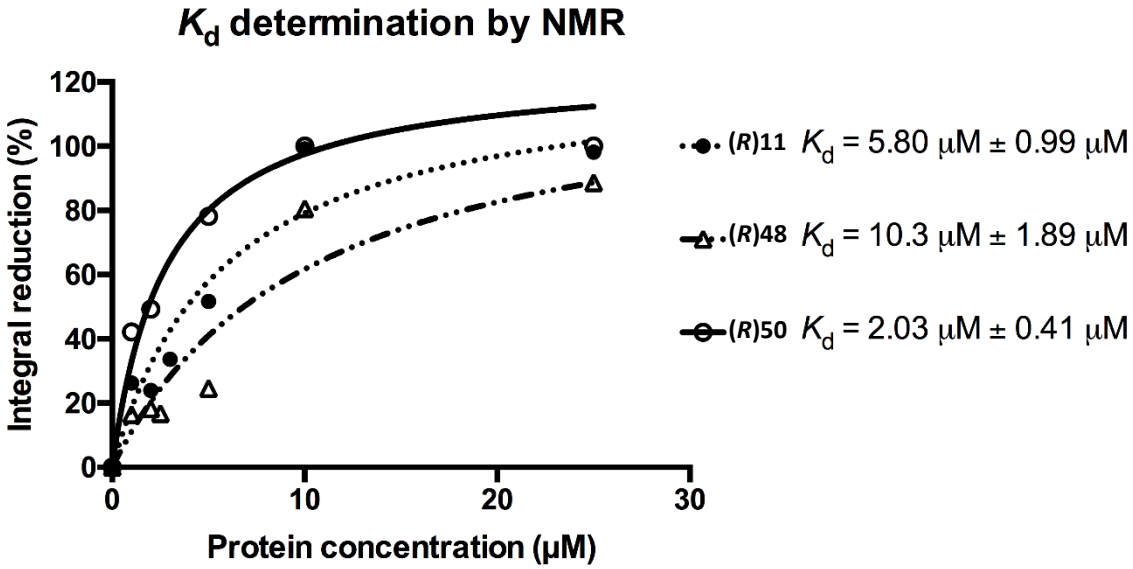


Figure D3.2 Ligand-observed ^{1}H NMR of BRD4(1) against **(*R*)11**, **(*R*)48** and **(*R*)50**.

D4 Size Exclusion Chromatography – CREBBP bromodomain dimerization experiment

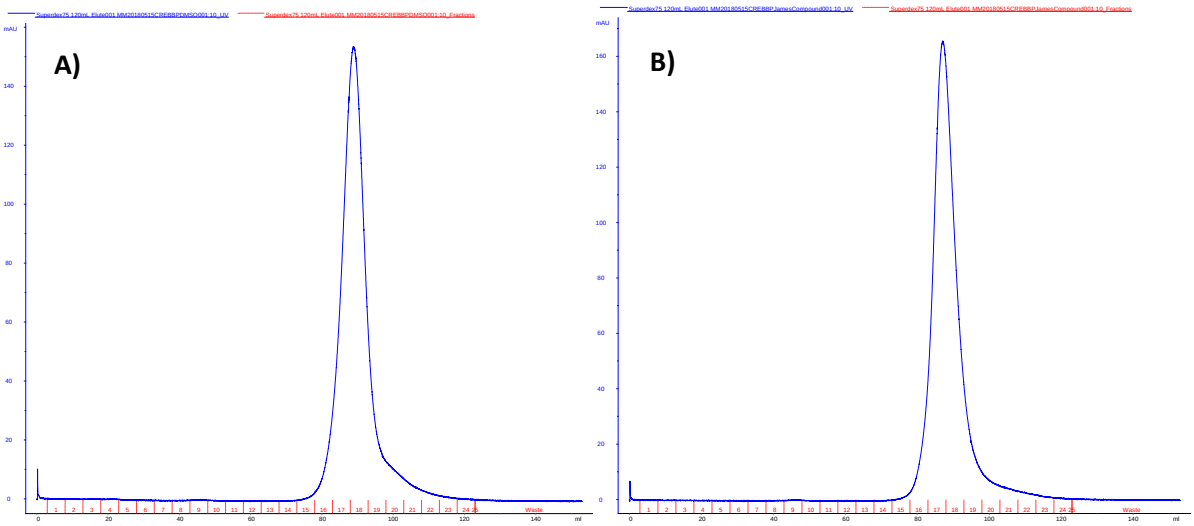


Figure D4.1 Size Exclusion Chromatography (SEC) to study dimerization in solution between CREBBP bromodomain and (A) DMSO and (B) **(*R*)48**. No change in SEC profile meant no protein dimer between ligand and protein could be observed.

D5 Fluorescence Polarization affinity data for the CREBBP Bromodomain

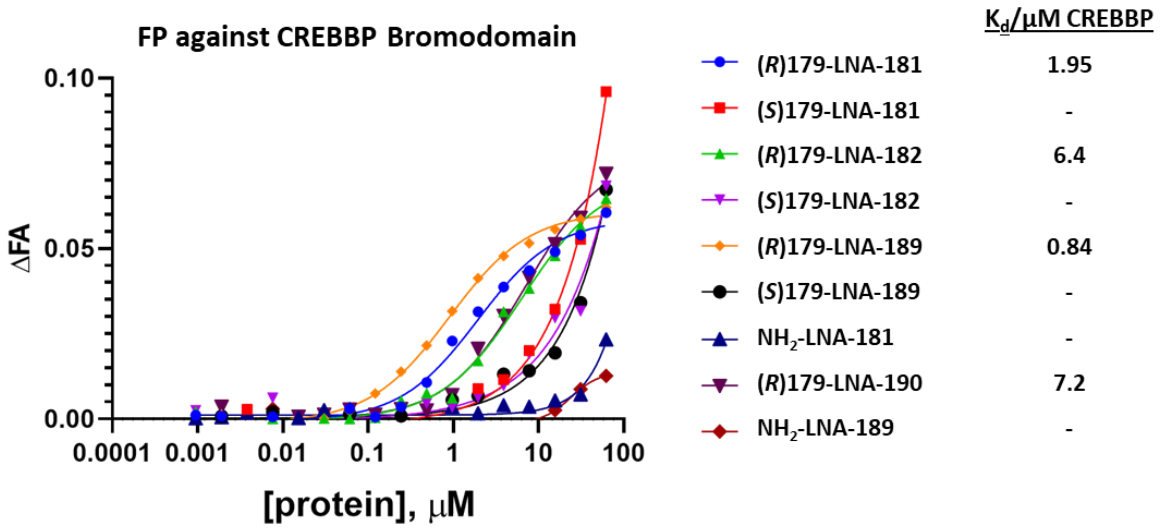


Figure D5.1 Raw FP data for 'on-LNA' fragments of known ligands **(*R*)11** and **(*R*)12** against the CREBBP bromodomain.

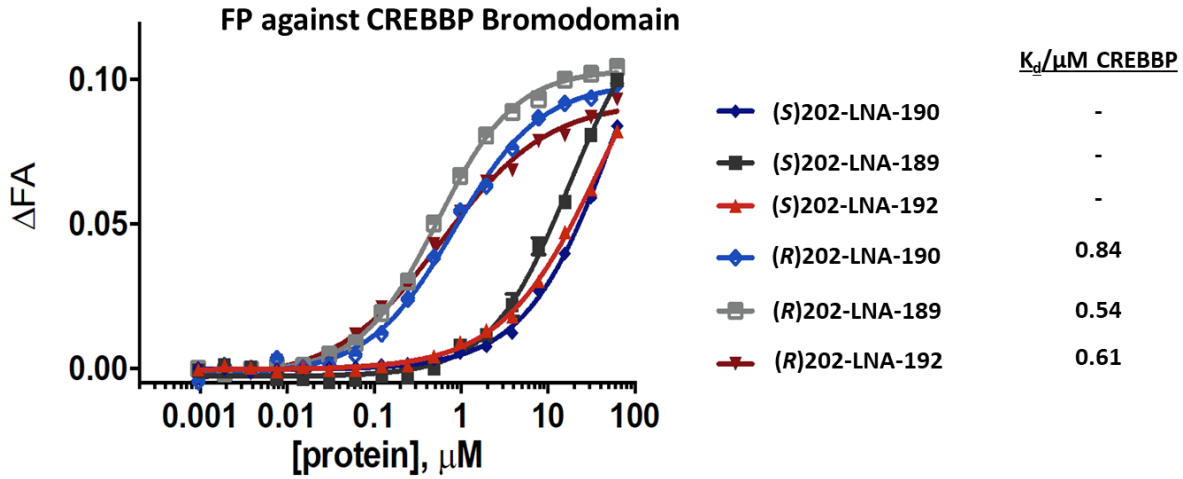


Figure D5.2 Raw FP data for 'on-LNA' fragments of alternative THBD headgroups **(*R*)202** and **(*S*)202** against the CREBBP bromodomain.

E Small molecule X-ray crystal structures

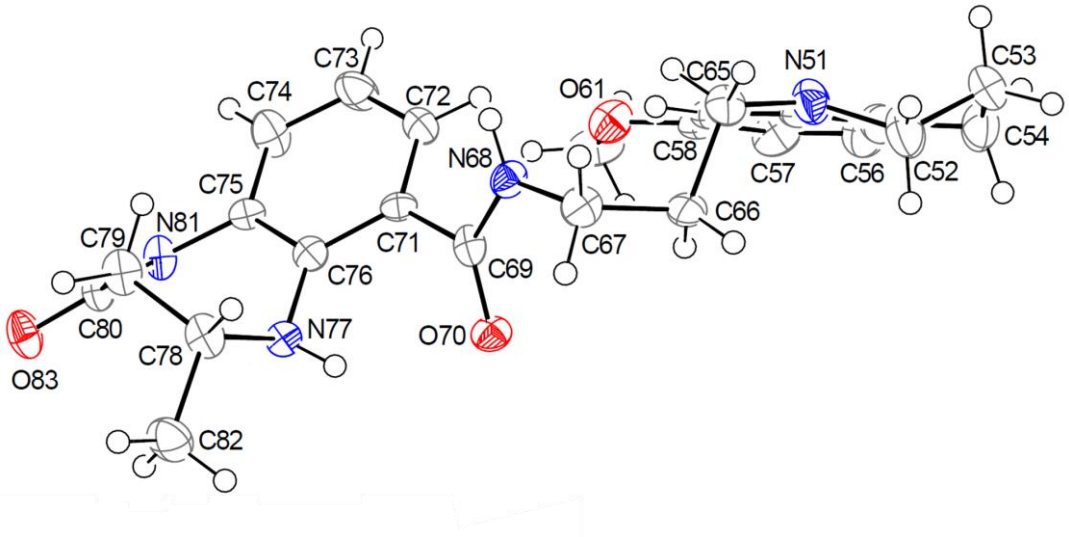


Figure E.1 Small molecule X-ray structure of **(*R*)11**. Intramolecular H-bond is observed between atoms N77-H and O70.

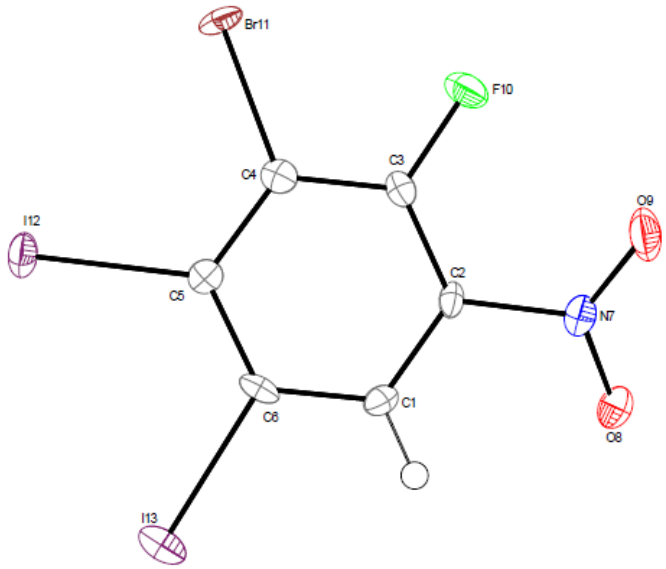


Figure E.2 Small molecule X-ray structure of **117**.

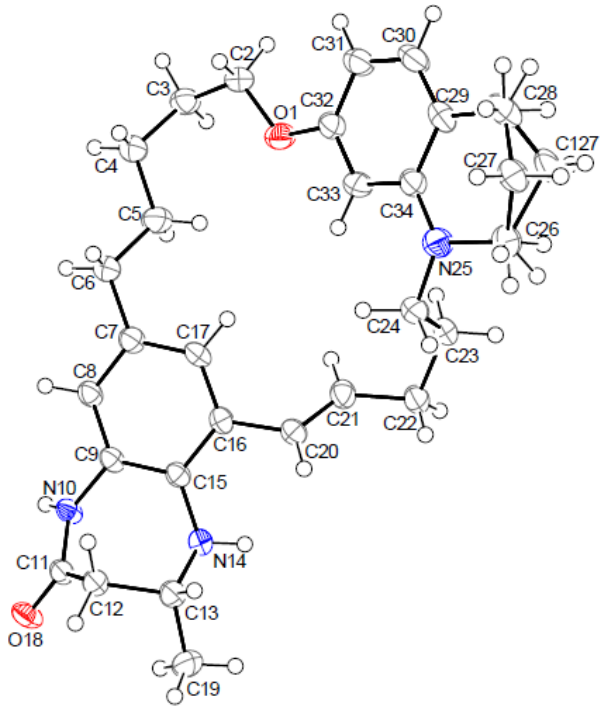


Figure E.3 Small molecule X-ray structure of **(*R*)104**.

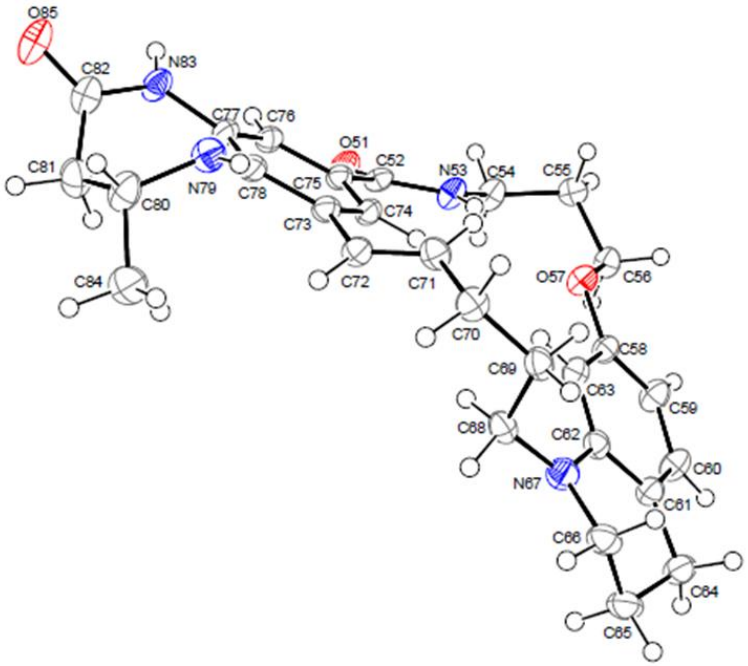


Figure E.4 Small molecule X-ray structure of **(*R*)108**.

F Oxidation of macrocycle (*R*)60

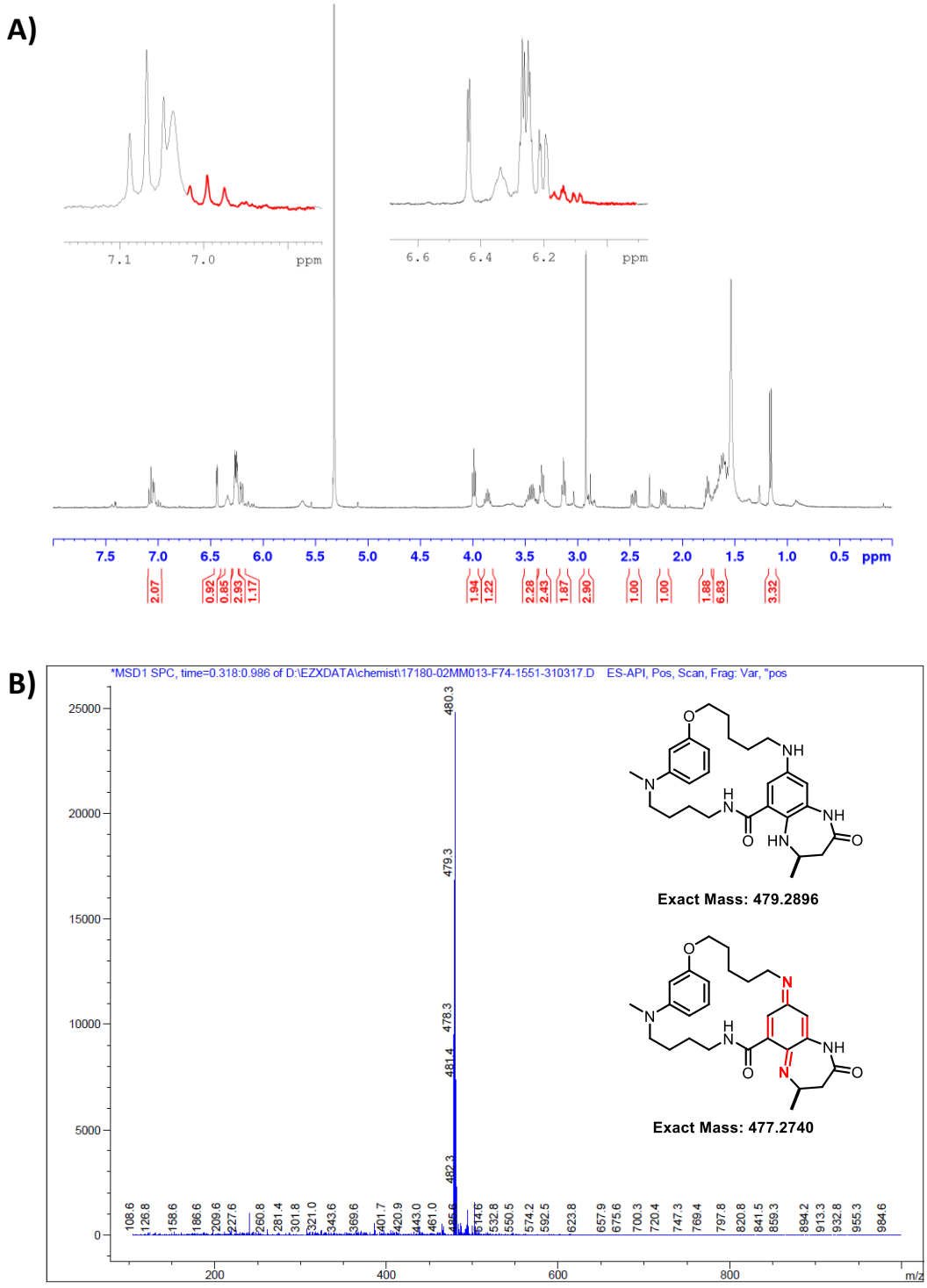
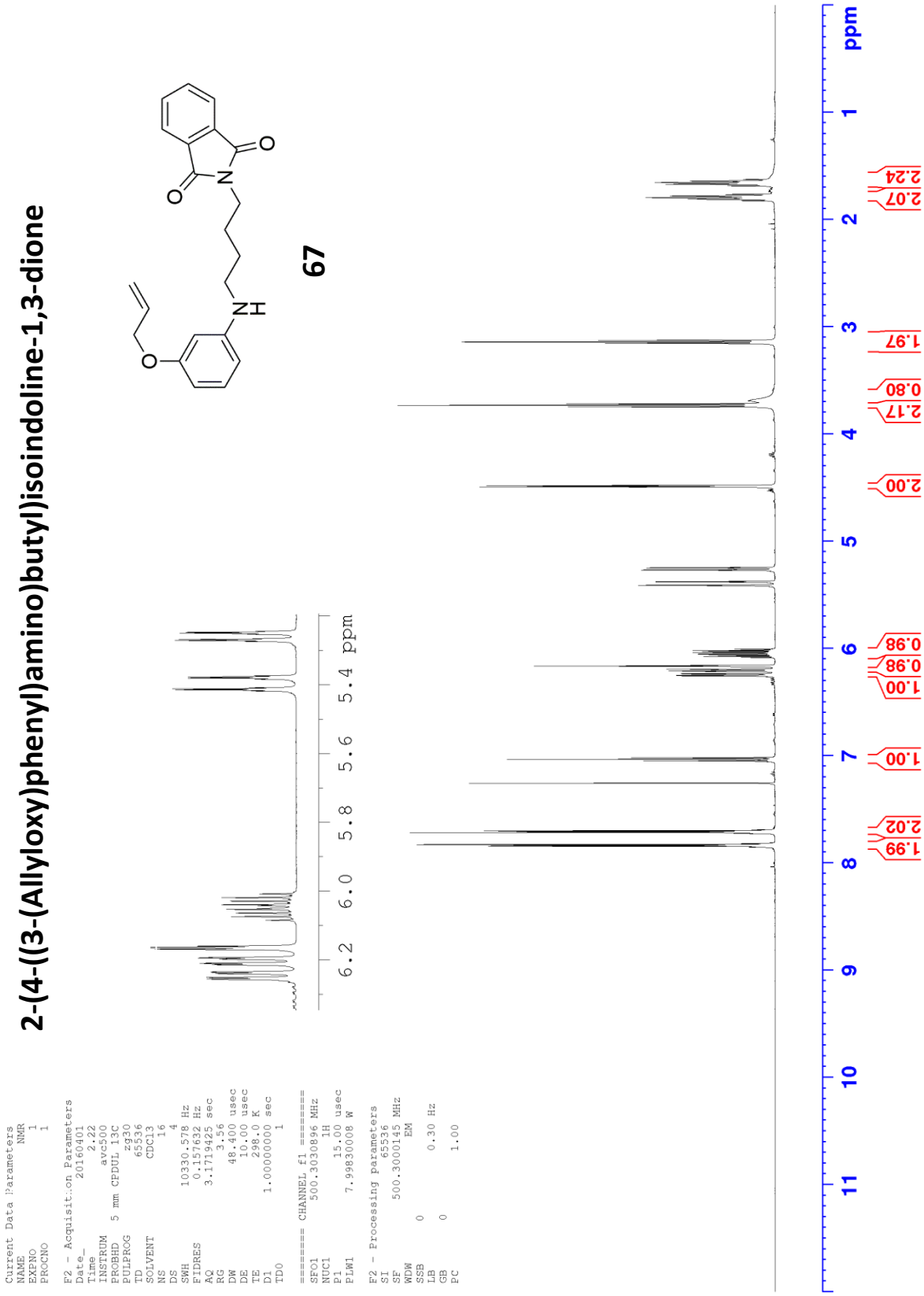
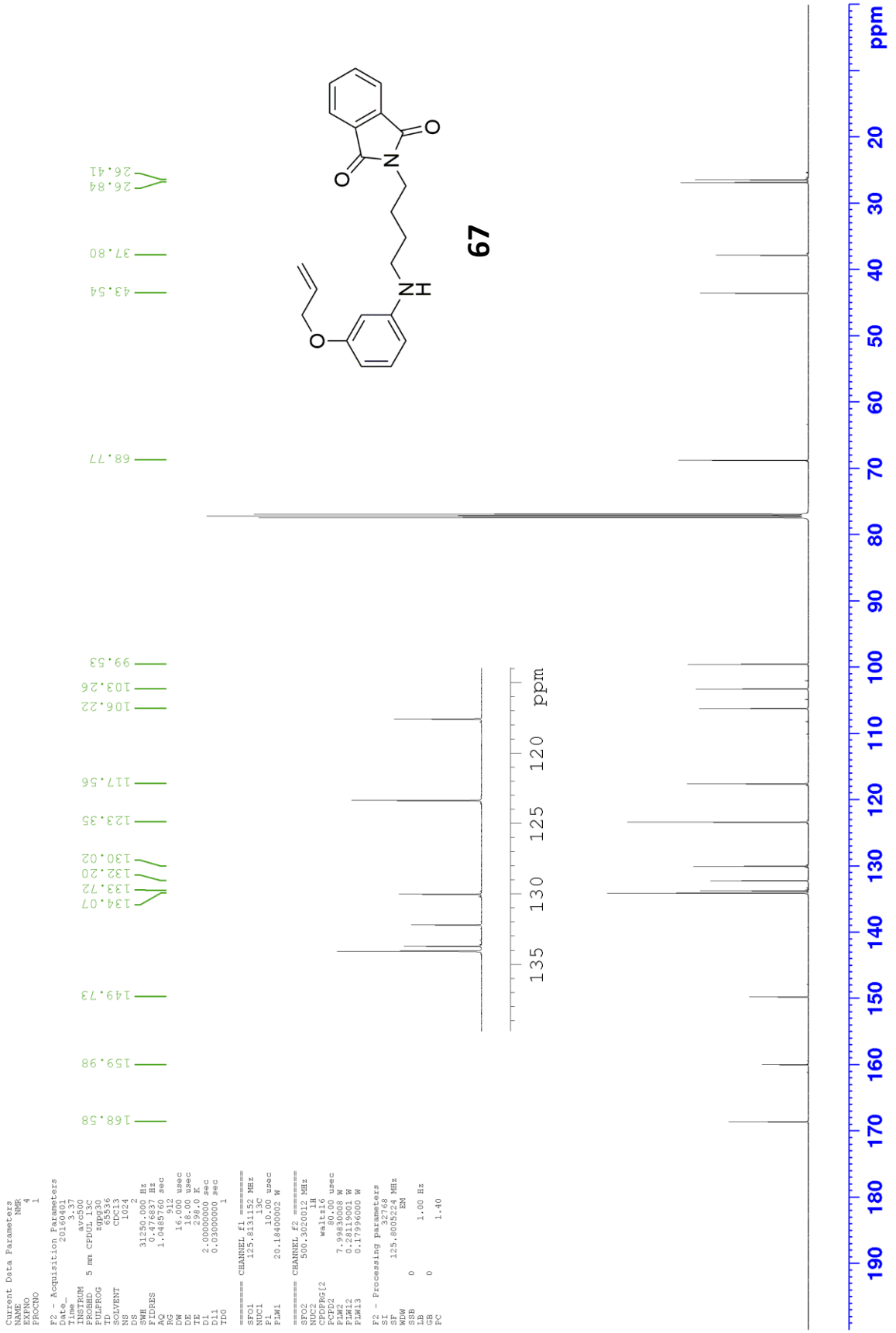


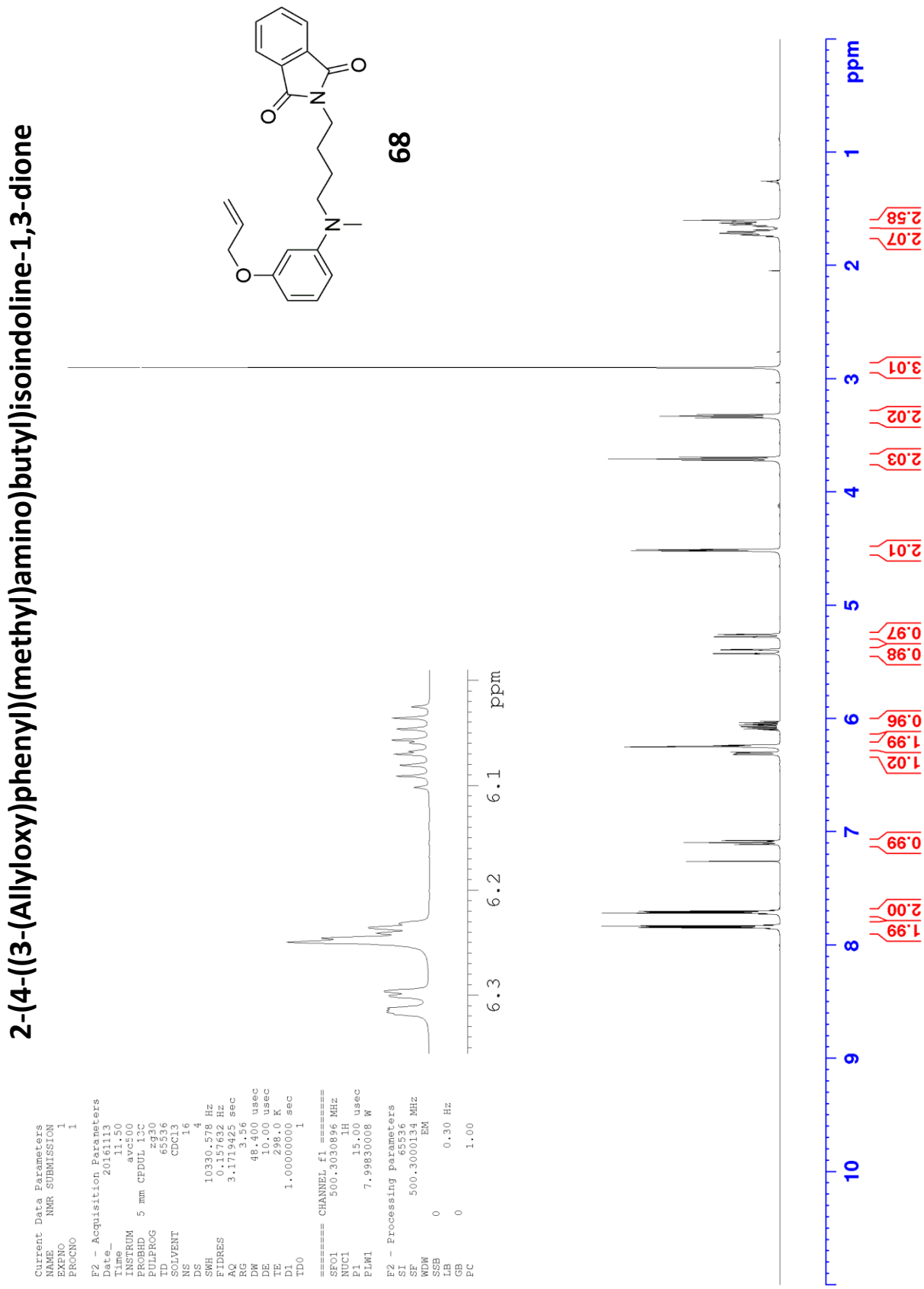
Figure F.1 (A) ^{1}H NMR (CD_2Cl_2) spectrum and (B) LRMS data highlighting the presence of oxidised by-product for macrocycle **(*R*)A11A**.

G NMR spectra of novel compounds

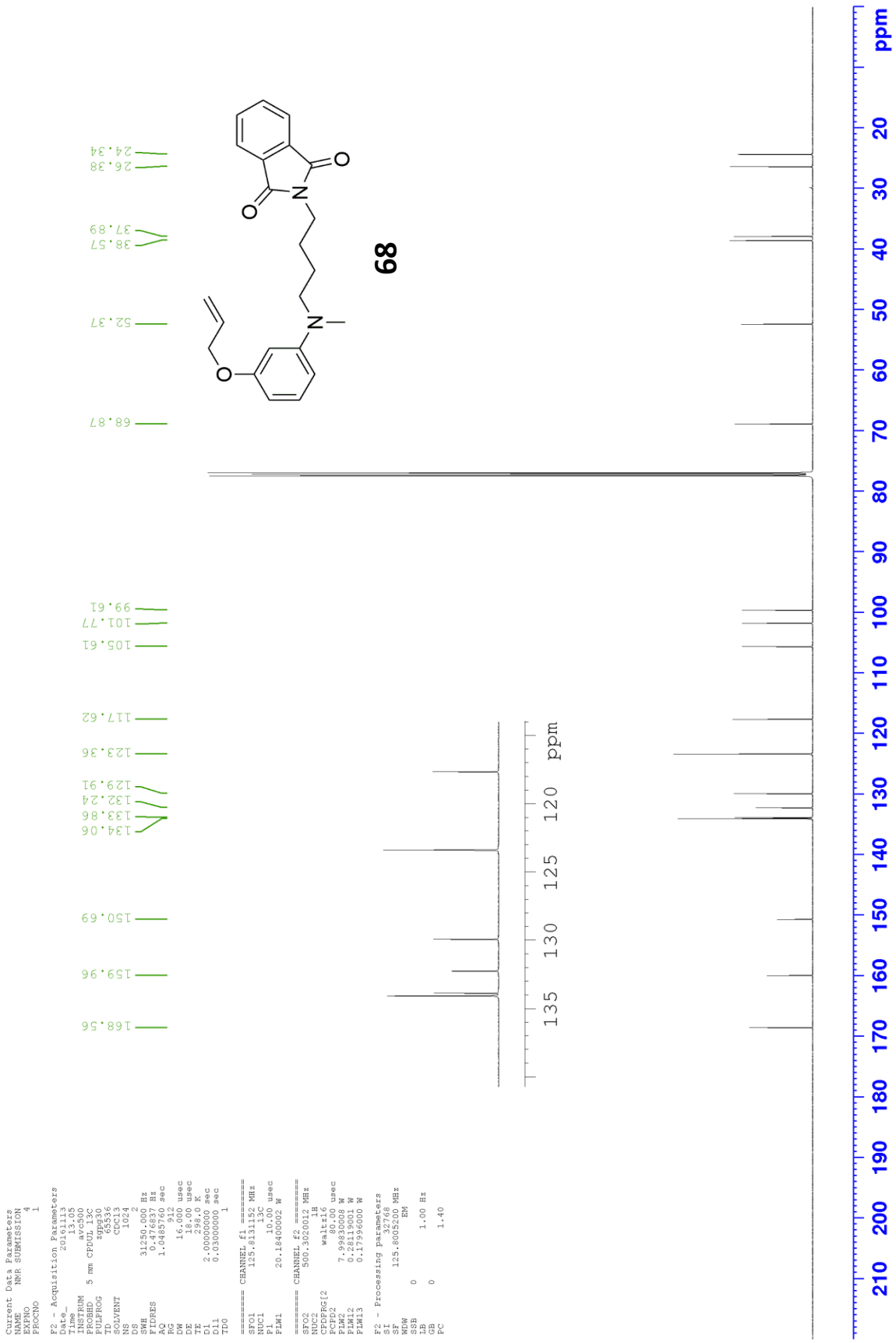


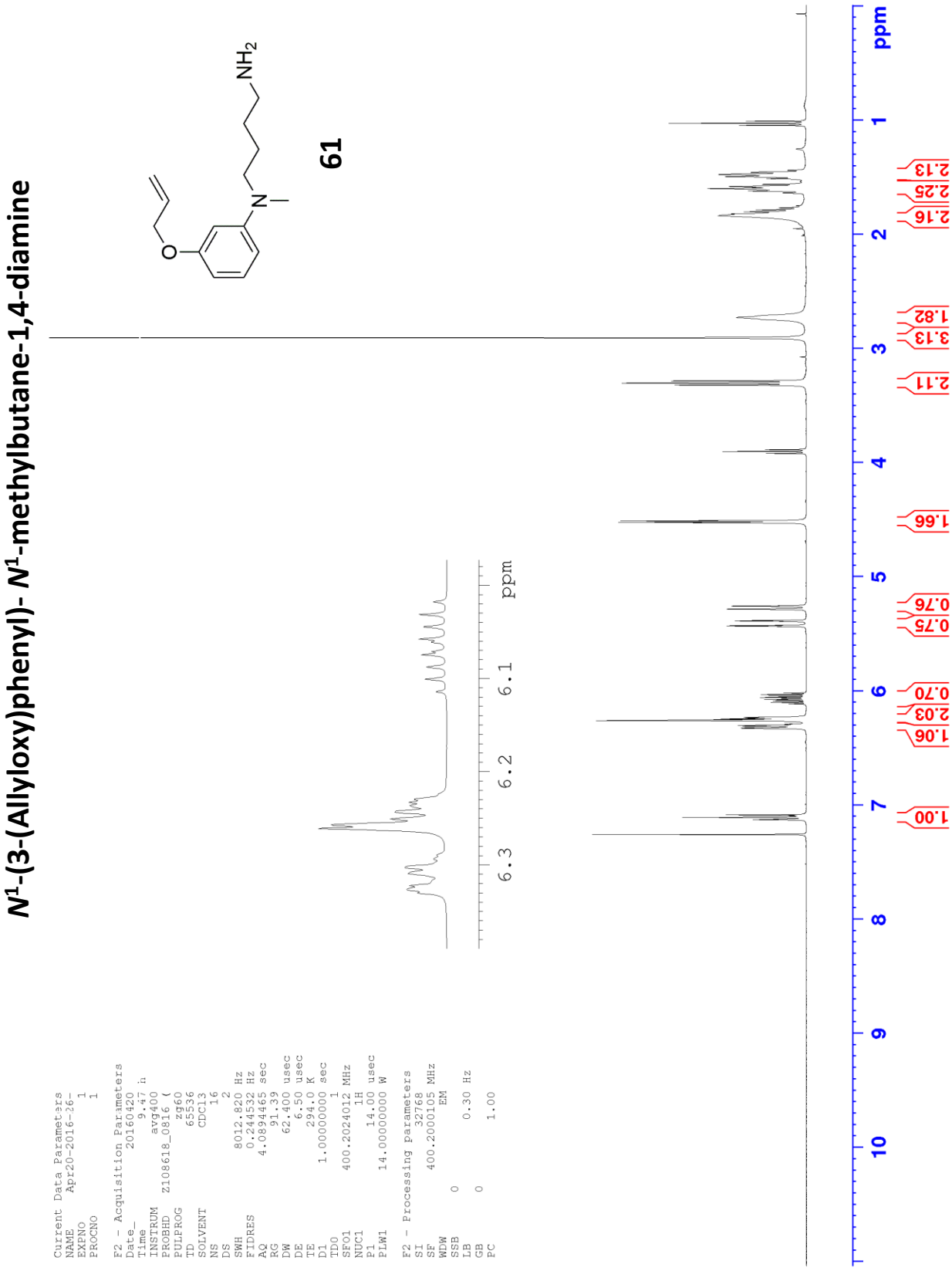
2-(4-((3-(Allyloxy)phenyl)amino)butyl)isoindoline-1,3-dione

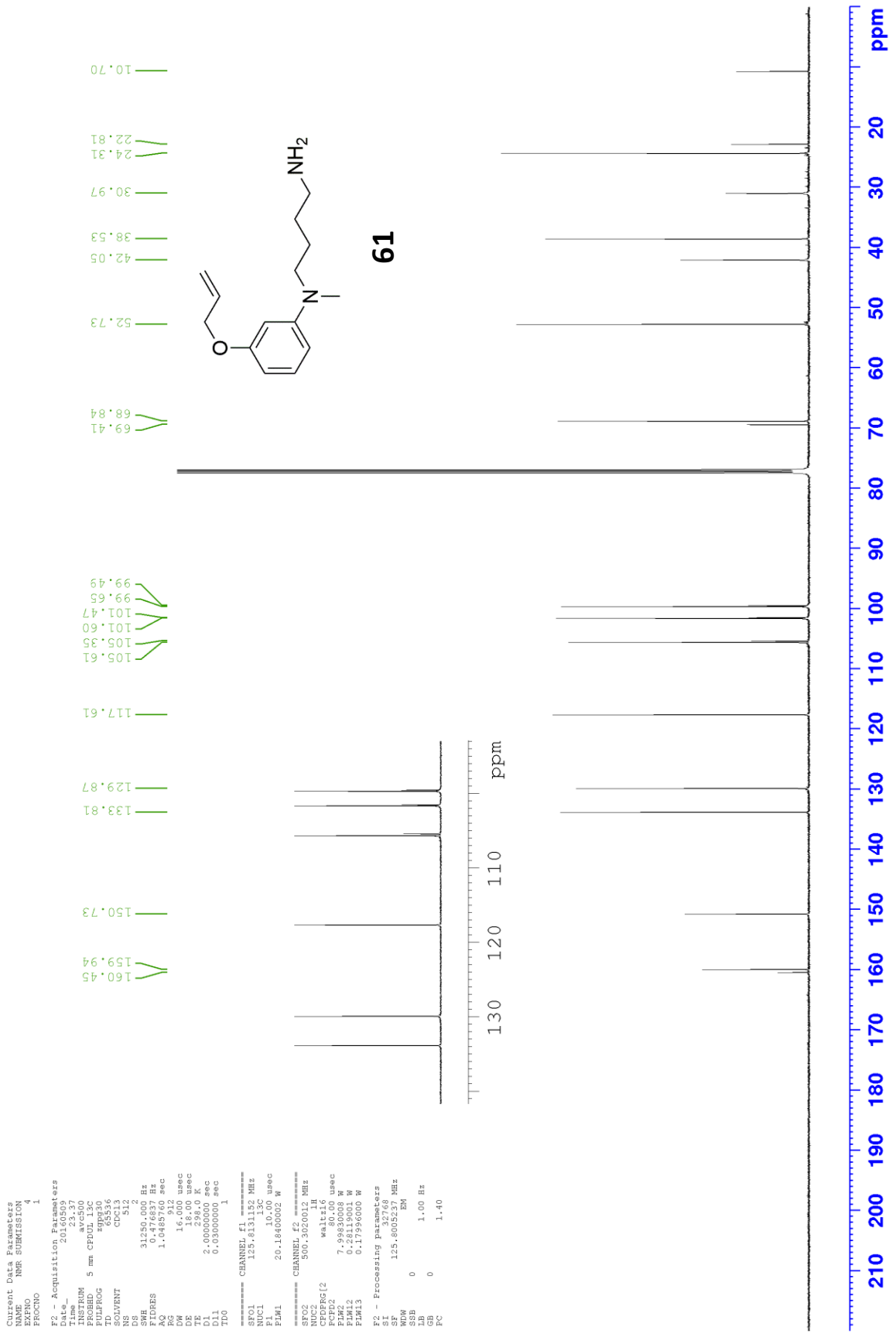



2-(4-((3-(Allyloxy)phenyl)(methyl)amino)butyl)isoindoline-1,3-dione
68
Current Data Parameters
NAME NMR SUBMISSION
EXPNO 1
PROCNO 1
F2 - Acquisition Parameters
Date_ 20161113
Time 11.50
INSTRUM avc500
PROBHD 5 mm CPDUL 13C
PULPROG zg30
TD 65536
SOLVENT CDCl3
NS 16
DS 4
SWH 10330.578 Hz
FIDRES 0.157632 Hz
AQ 3.1719425 sec
RG 3.56
DW 48.400 usec
DE 10.00 usec
TE 298.0 K
D1 1.00000000 sec
TD0 1
======== CHANNEL f1 ========
SFO1 500.3030896 MHz
NUC1 1H
P1 15.00 usec
PLW1 7.99830008 W
F2 - Processing parameters
SI 65536
SF 500.3000134 MHz
WDW EM
SSB 0
LB 0.30 Hz
GB 0
PC 1.00
6.3
6.2
6.1
ppm
10
9
8
7
6
5
4
3
2
1
ppm
1.99
2.00
0.99
1.02
1.99
0.96
0.98
0.97
2.01
2.03
2.02
3.01
2.07
2.58

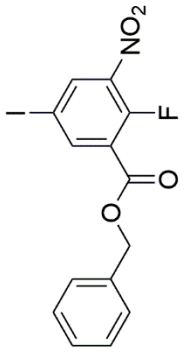
2-(4-((3-(Allyloxy)phenyl)(methyl)amino)butyl)isoindoline-1,3-dione



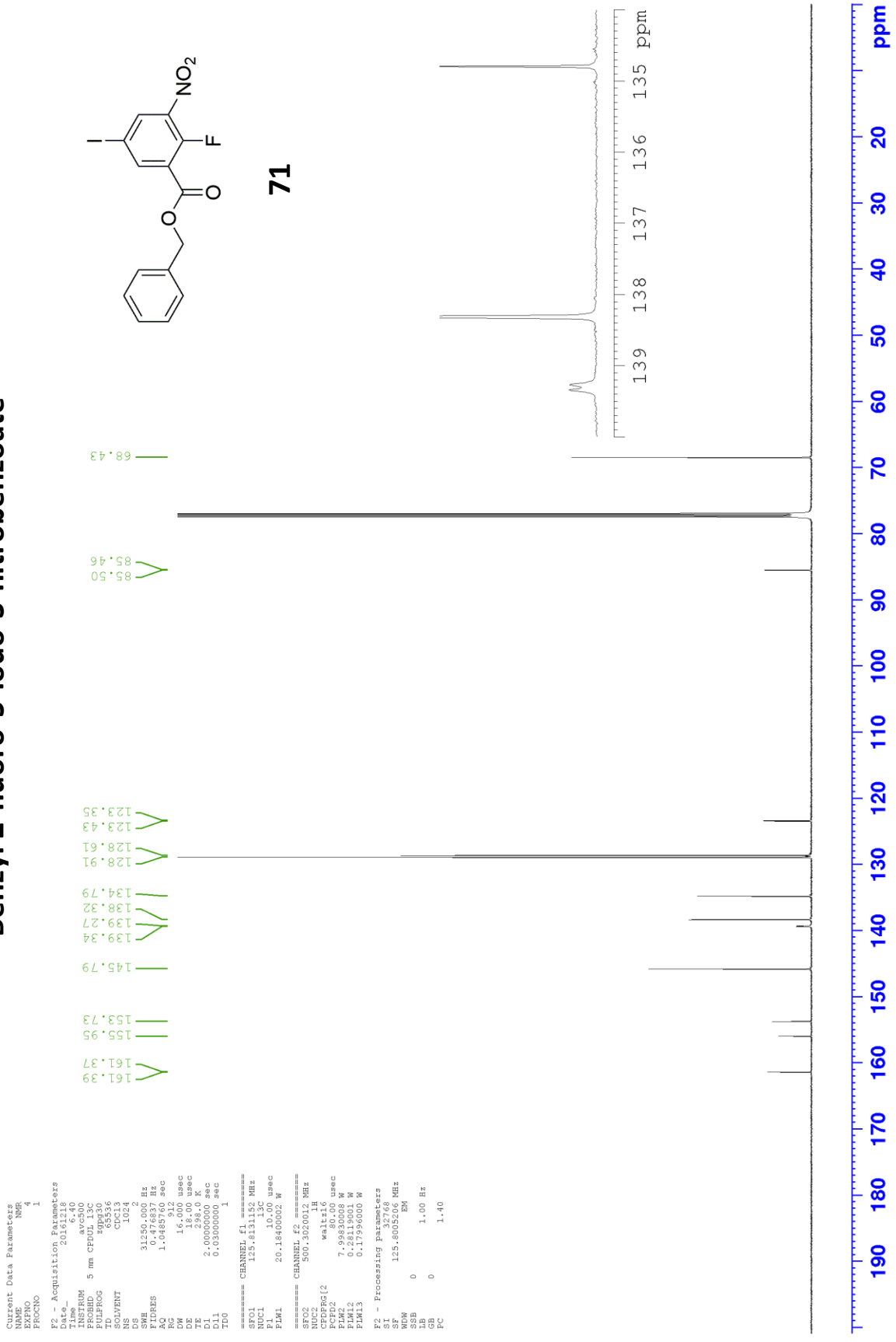

N^1-(3-(Allyloxy)phenyl)- N^1-methylbutane-1,4-diamine
61
NH2
N
O
Current Data Parameters
NAME Apr20-2016-26-
EXPNO 1
PROCNO 1
F2 - Acquisition Parameters
Date_ 20160420
Time_ 9.47 h
INSTRUM avg400
PROBHD Z108618_0816 (
PULPROG zg60
TD 65536
SOLVENT CDCl3
NS 16
DS 2
SWH 8012.820 Hz
FIDRES 0.244532 Hz
AQ 4.0894465 sec
RG 91.39
DW 62.400 usec
DE 6.50 usec
TE 294.0 K
D1 1.00000000 sec
TD0 1
SFO1 400.2024012 MHz
NUC1 1H
P1 14.00 usec
PLW1 14.00000000 W
F2 - Processing parameters
SI 32768
SF 400.2000105 MHz
WDW EM
SSB 0
LB 0.30 Hz
GB 0
PC 1.00
6.3
6.2
6.1
ppm
10
9
8
7
6
5
4
3
2
1
ppm
1.00
1.06
2.03
0.70
0.75
0.76
1.66
2.11
3.13
1.82
2.16
2.25
2.13

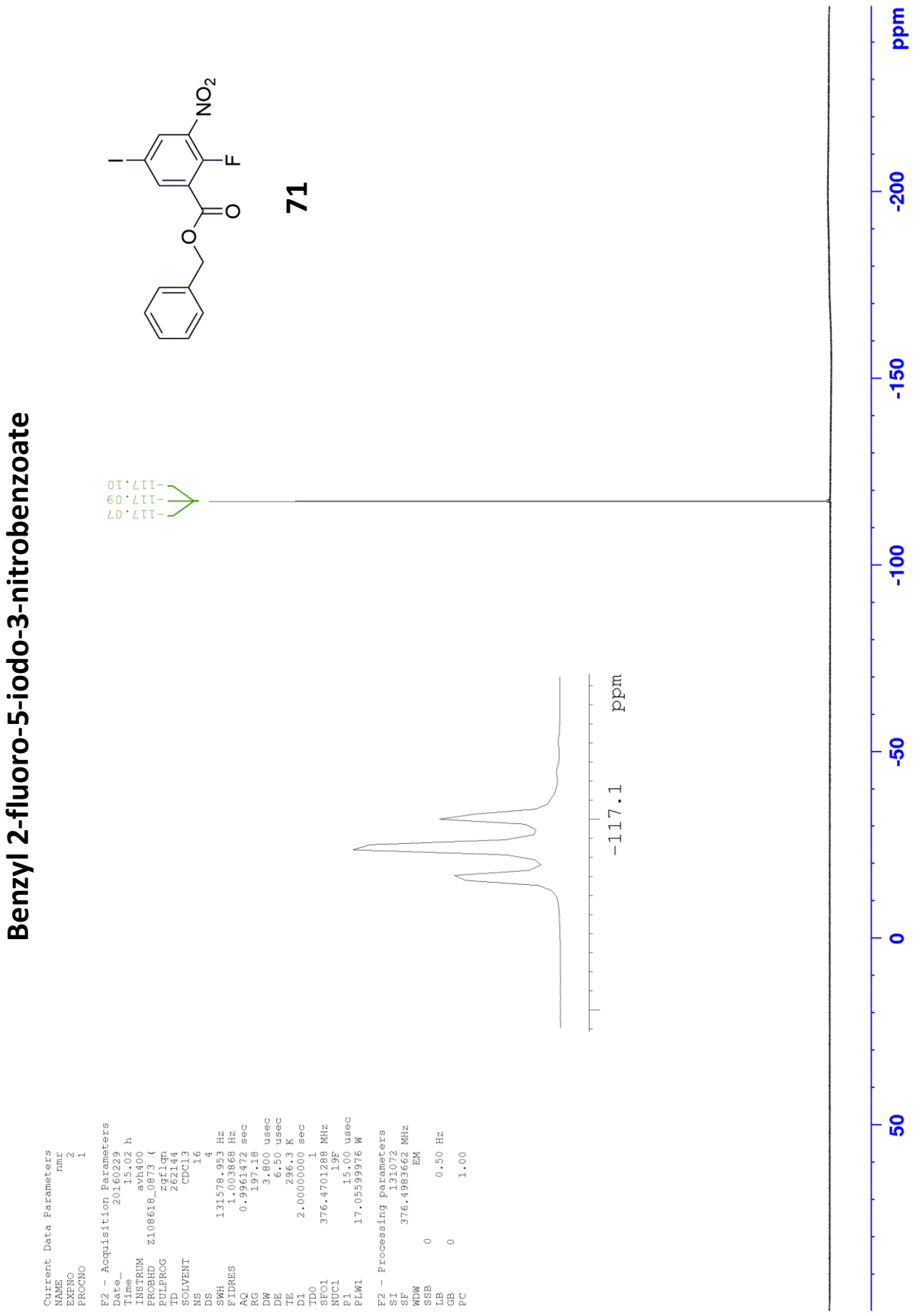

N^1-(3-(Allyloxy)phenyl)- N^1-methylbutane-1,4-diamine
61
Current Data Parameters
NAME NMR SUBMISSION
EXPNO 4
PROCNO 1
F2 - Acquisition Parameters
Date_ 20160509
Time 23.37
INSTRUM av500
PROBHD 5 mm CPDUL 13C
PULPROG zgpg30
TD 65536
SOLVENT CDCl3
NS 512
DS 2
SWH 31250.000 Hz
FIDRES 0.476837 Hz
AQ 1.0485760 sec
RG 203
DW 16.000 usec
DE 18.00 usec
TE 298.0 K
D1 2.00000000 sec
D11 0.03000000 sec
TD0 1
======== CHANNEL f1 ========
SFO1 125.8131152 MHz
NUC1 13C
P1 10.00 usec
PLW1 20.18400002 W
======== CHANNEL f2 ========
SFO2 500.3020012 MHz
NUC2 1H
CPDPRG[2 waltz16
PCPD2 80.00 usec
PLW2 7.99830008 W
PLW12 0.28119901 W
PLW13 0.17996000 W
F2 - Processing parameters
SI 32768
SF 125.8005237 MHz
WDW EM
SSB 0
LB 1.00 Hz
GB 0
PC 1.40
160.45
159.94
150.73
133.81
129.87
117.61
105.61
105.35
101.60
101.47
99.65
99.49
69.41
68.84
52.73
42.05
38.53
30.97
24.31
22.81
10.70
NH2
N
O
130
120
110
ppm
210
200
190
180
170
160
150
140
130
120
110
100
90
80
70
60
50
40
30
20
ppm

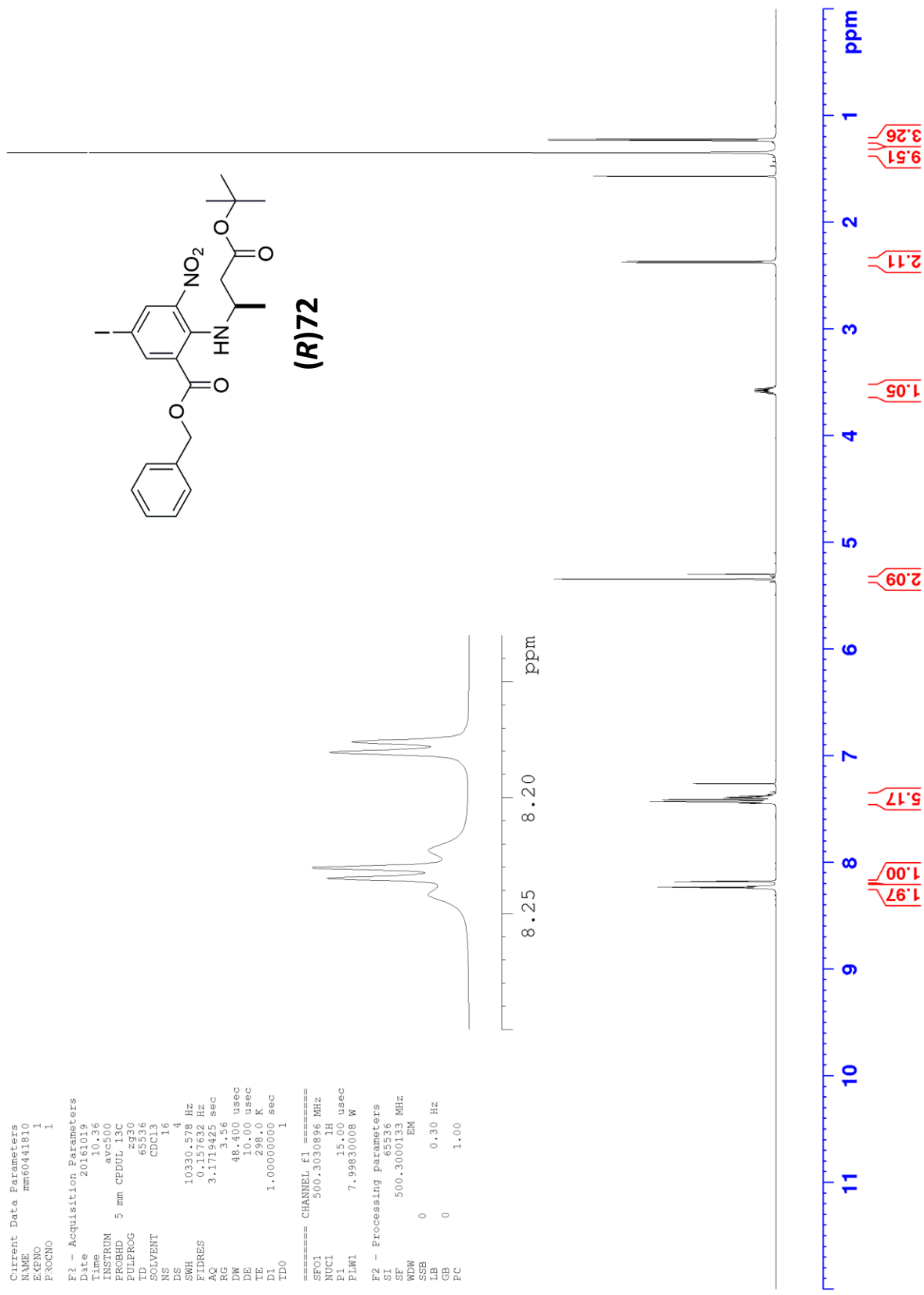
Benzyl 2-fluoro-5-iodo-3-nitrobenzoate



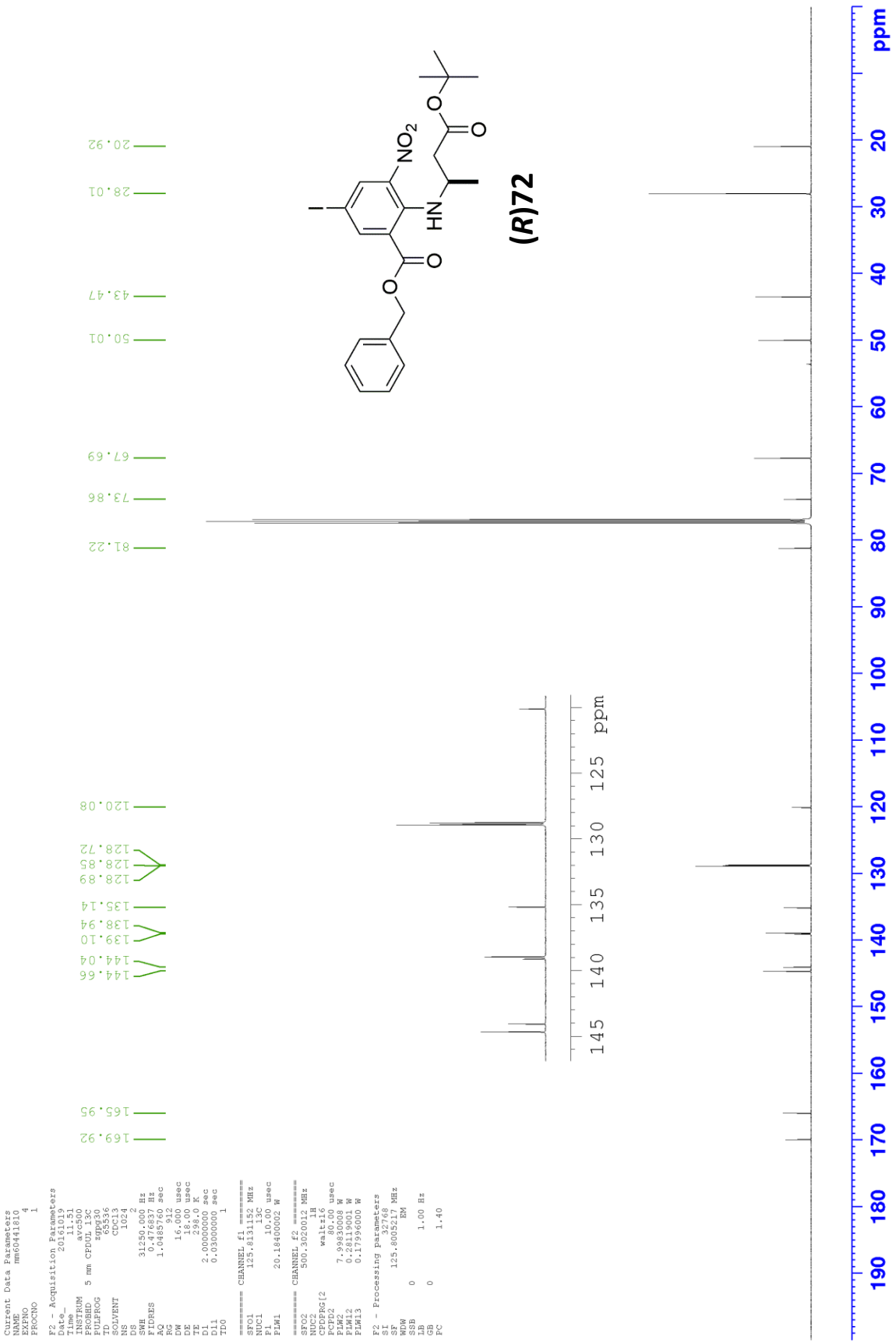
71

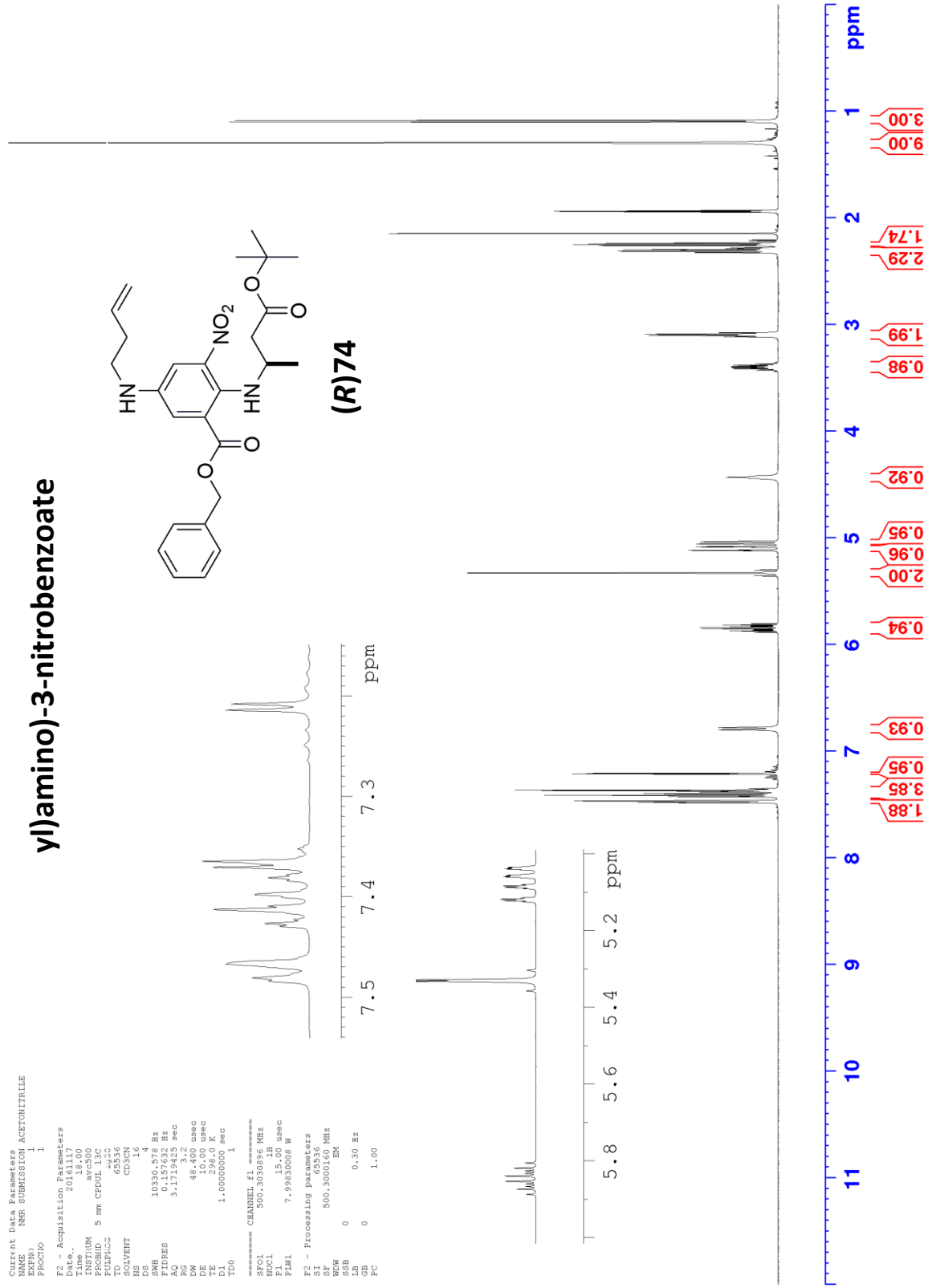

Benzyl 2-fluoro-5-iodo-3-nitrobenzoate
71
68.43
85.50
85.46
123.35
123.43
128.61
128.91
134.79
138.32
139.27
139.34
145.79
153.73
155.95
161.37
161.39
139 138 137 136 135 ppm
190 180 170 160 150 140 130 120 110 100 90 80 70 60 50 40 30 20 ppm

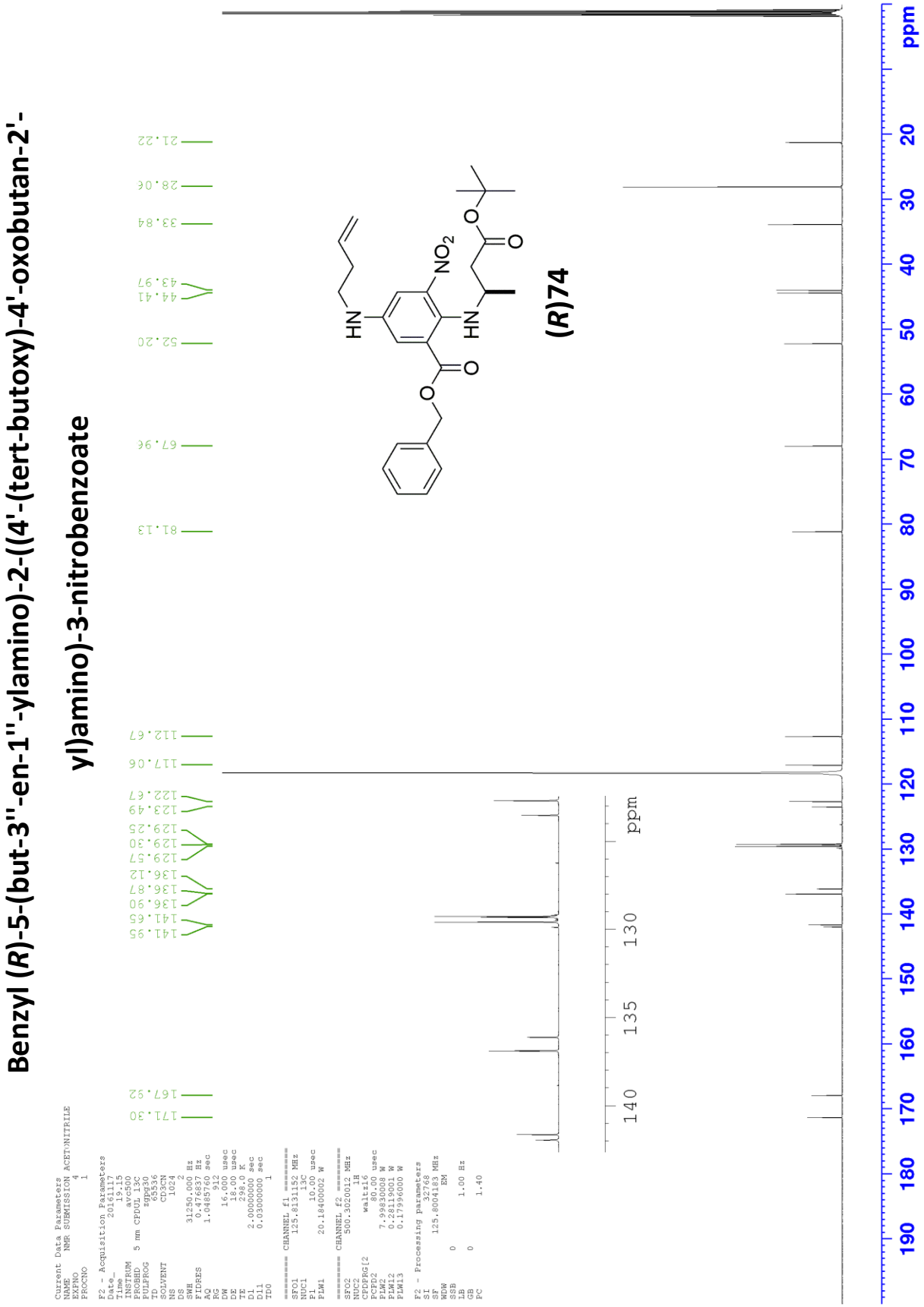

Benzyl 2-fluoro-5-iodo-3-nitrobenzoate
71
Current Data Parameters
NAME nmr
EXPNO 2
PROCNO 1
F2 - Acquisition Parameters
Date_ 20160229
Time_ 15.02 h
INSTRUM avh400
PROBHD Z108618_0873 (
PULPROG zgflqn
TD 262144
SOLVENT CDCl3
NS 16
DS 4
SWH 131578.953 Hz
FIDRES 1.003868 Hz
AQ 0.9961472 sec
RG 197.18
DW 3.800 usec
DE 6.50 usec
TE 296.3 K
D1 2.00000000 sec
TD0 1
SFO1 376.4701288 MHz
NUC1 19F
P1 15.00 usec
PLW1 17.05599976 W
F2 - Processing parameters
SI 131072
SF 376.4983662 MHz
WDW EM
SSB 0
LB 0.50 Hz
GB 0
PC 1.00
-117.07
-117.09
-117.10
-117.1 ppm
50
0
-50
-100
-150
-200
ppm

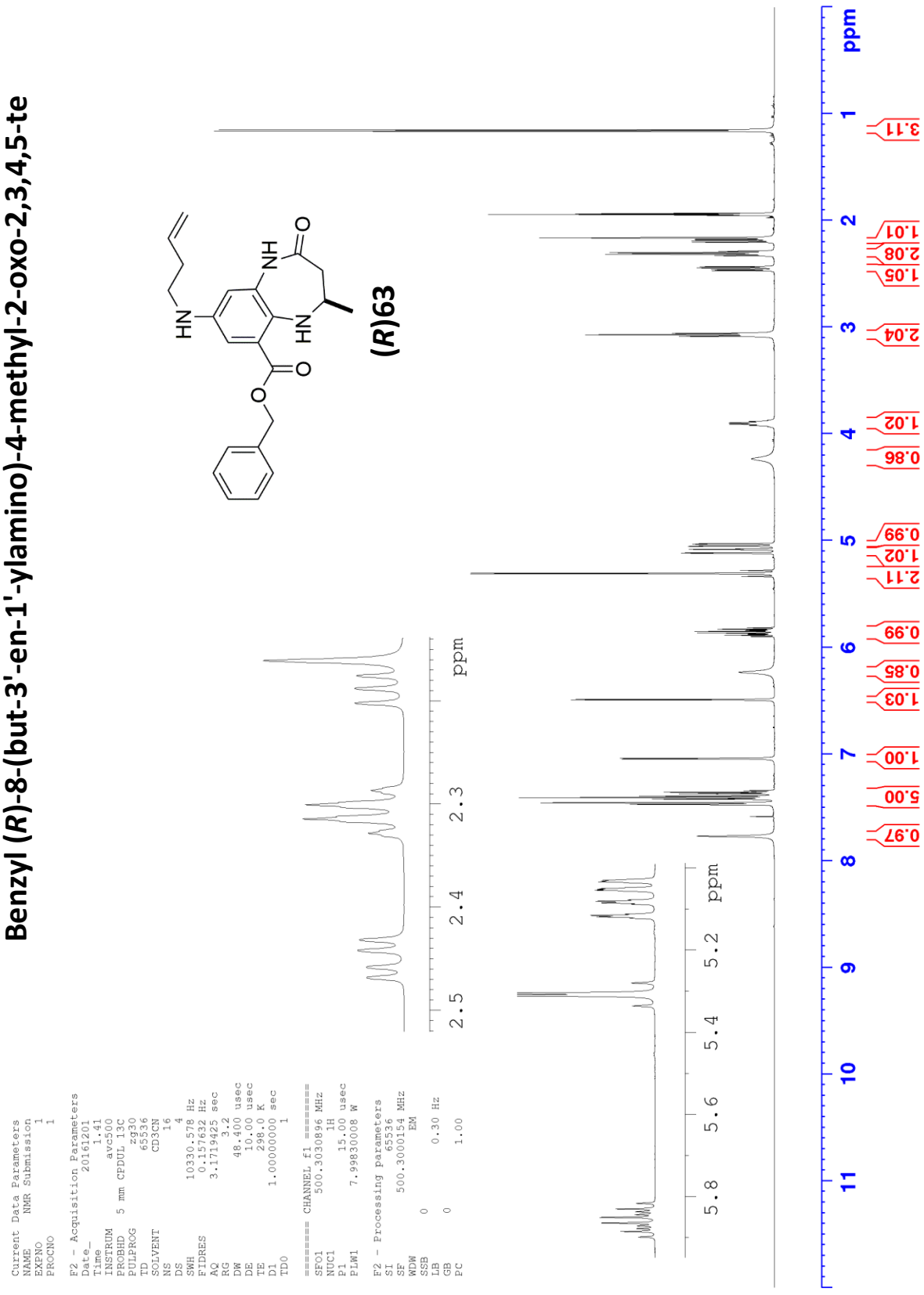

Benzyl (R)-2-((4'-(tert-butoxy)-4'-oxobutan-2'-yl)amino)-5-iodo-3-nitrobenzoate
(R)72
Current Data Parameters
NAME mm60441810
EXPNO 1
PROCNO 1
F2 - Acquisition Parameters
Date 20161019
Time 10.36
INSTRUM avc500
PROBHD 5 mm CPDUL 13C
PULPROG zg30
TD 65536
SOLVENT CDCl3
NS 16
DS 4
SWH 10330.578 Hz
FIDRES 0.157632 Hz
AQ 3.1719425 sec
RG 3.56
DW 48.400 usec
DE 10.00 usec
TE 298.0 K
D1 1.00000000 sec
TD0 1
======== CHANNEL f1 ========
SFO1 500.3030896 MHz
NUC1 1H
P1 15.00 usec
PLW1 7.99830008 W
F2 - Processing parameters
SI 65536
SF 500.3000133 MHz
WDW EM
SSB 0
LB 0.30 Hz
GB 0
PC 1.00
8.25
8.20
ppm
1.97
1.00
5.17
2.09
1.05
2.11
9.51
3.26
ppm

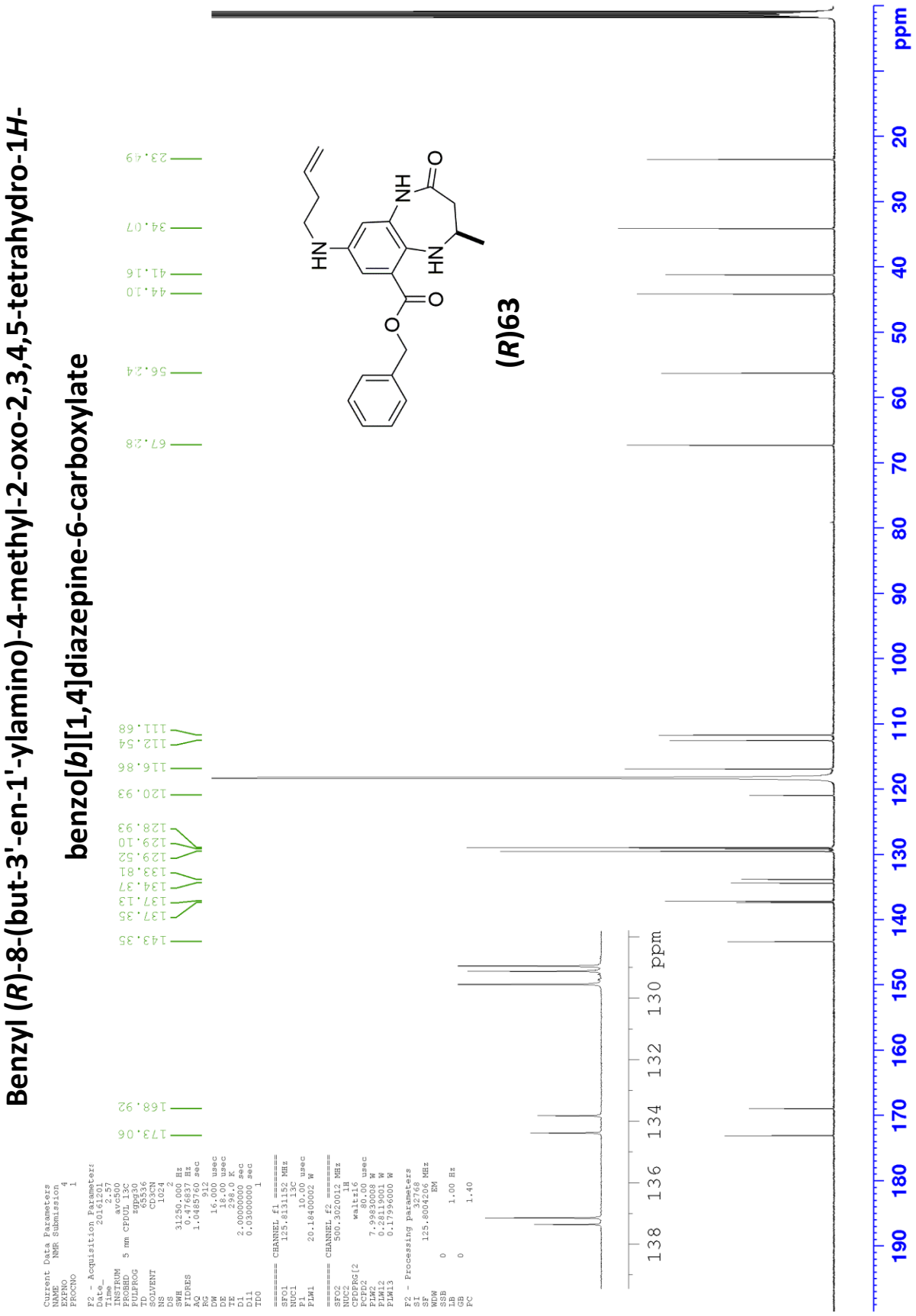
Benzyl (*R*)-2-((4'-(*tert*-butoxy)-4'-oxobutan-2'-yl)amino)-5-iodo-3-nitrobenzoate



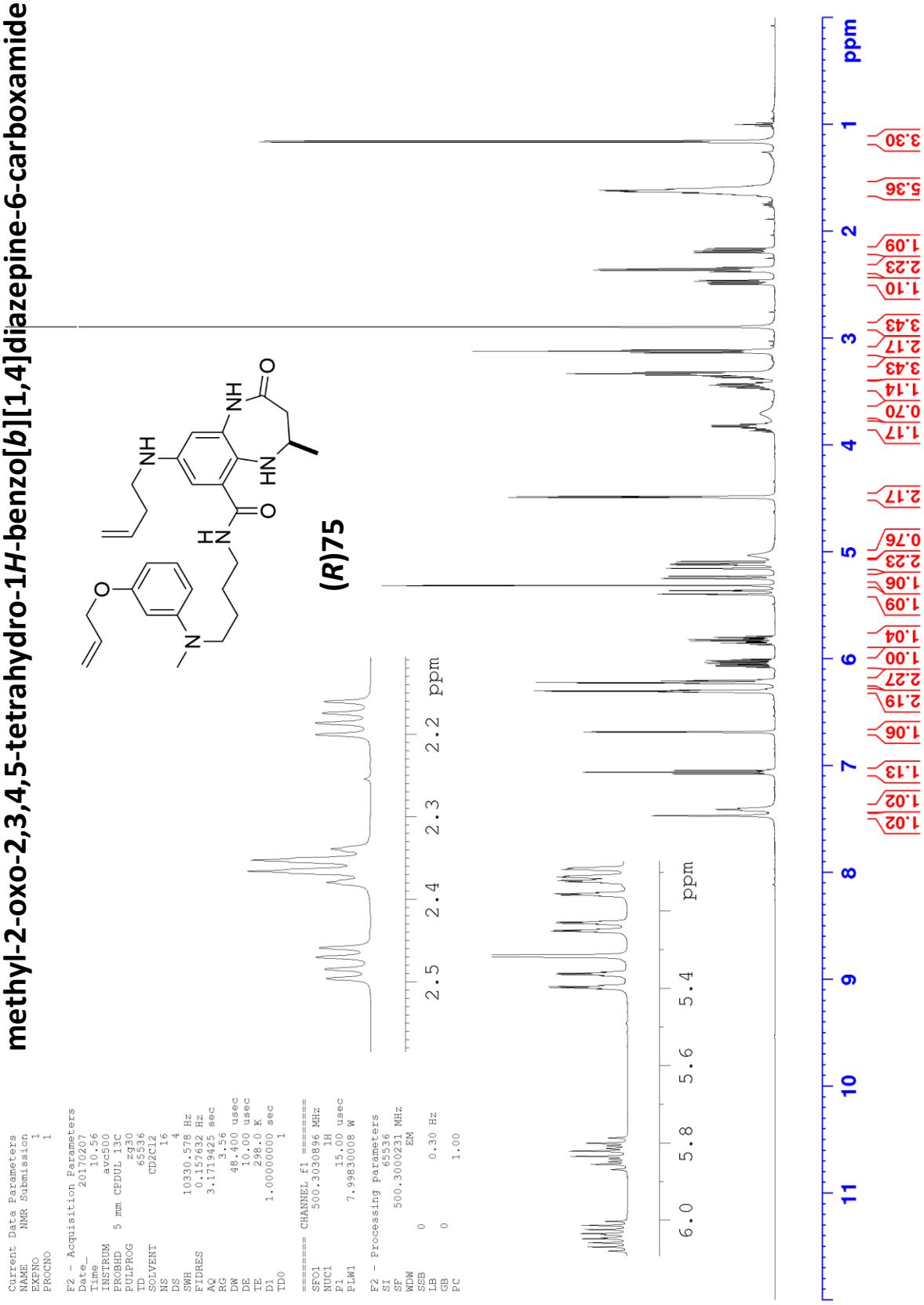

Benzyl (R)-5-(but-3''-en-1''-ylamino)-2-((4'-(tert-butoxy)-4'-oxobutan-2'-yl)amino)-3-nitrobenzoate
(R)74
HN
NO2
HN
O
O
O
O
Current Data Parameters
NAME NMR SUBMISSION ACETONITRILE
EXPNO 1
PROCNO 1
F2 - Acquisition Parameters
Date_ 20161117
Time 18.00
INSTRUM avc500
PROBHD 5 mm CPDUL 13C
PULPROG zg30
TD 65536
SOLVENT CD3CN
NS 16
DS 4
SWH 10330.578 Hz
FIDRES 0.157632 Hz
AQ 3.1719425 sec
RG 203
DW 48.400 usec
DE 10.00 usec
TE 298.0 K
D1 1.00000000 sec
TD0 1
======== CHANNEL f1 ========
SFO1 500.3030896 MHz
NUC1 1H
P1 15.00 usec
PLW1 7.99830008 W
F2 - Processing parameters
SI 65536
SF 500.3000160 MHz
WDW EM
SSB 0
LB 0.30 Hz
GB 0
PC 1.00
7.5
7.4
7.3
ppm
5.8
5.6
5.4
5.2
ppm
1.88
3.85
0.95
0.93
0.94
2.00
0.96
0.95
0.92
0.98
1.99
2.29
1.74
9.00
3.00
ppm


Benzyl (R)-5-(but-3''-en-1''-ylamino)-2-((4'-(tert-butoxy)-4'-oxobutan-2'-yl)amino)-3-nitrobenzoate
(R)74
Current Data Parameters
NAME NMR SUBMISSION ACET:NITRILE
EXPNO 4
PROCNO 1
F2 - Acquisition Parameters
Date_ 20161117
Time 19:15
INSTRUM avc500
PROBHD 5 mm CPDUL 13C
PULPROG zgpg30
TD 65536
SOLVENT CD3CN
NS 1024
DS 4
SWH 31250.000 Hz
FIDRES 0.476837 Hz
AQ 1.0485760 sec
RG 912
DW 16.000 usec
DE 6.00 usec
TE 298.0 K
D1 2.00000000 sec
D11 0.03000000 sec
TD0 1
======== CHANNEL f1 ========
SFO1 125.8131152 MHz
NUC1 13C
P1 10.00 usec
PLW1 20.18400002 W
======== CHANNEL f2 ========
SFO2 500.3020012 MHz
NUC2 1H
CPDPRG[2 waltz16
PCPD2 80.00 usec
PLW2 7.99810008 W
PLW12 0.28110001 W
PLW13 0.17996000 W
F2 - Processing parameters
SI 32768
SF 125.8004183 MHz
WDW EM
SSB 0
LB 1.00 Hz
GB 0
PC 1.40
171.30
167.92
141.95
141.65
136.90
136.87
136.12
129.57
129.30
129.25
123.49
122.67
117.06
112.67
81.13
67.96
52.20
44.41
43.97
33.84
28.06
21.22
HN
NO2
HN
O
O
O
O
O
140
135
130
ppm
190
180
170
160
150
140
130
120
110
100
90
80
70
60
50
40
30
20
ppm

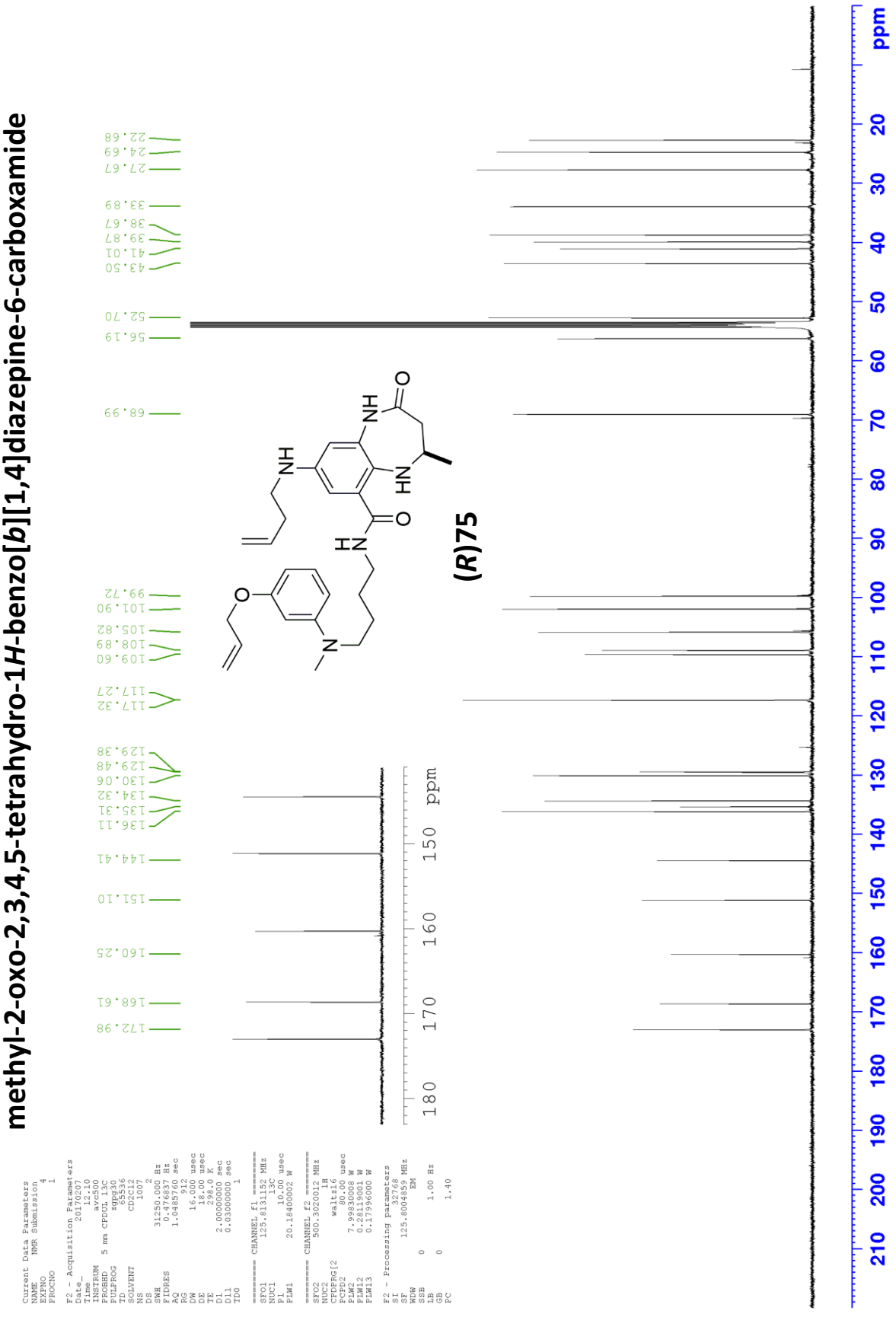

Benzyl (R)-8-(but-3'-en-1'-ylamino)-4-methyl-2-oxo-2,3,4,5-te
(R)63
Current Data Parameters
NAME NMR Submission
EXPNO 1
PROCNO 1
F2 - Acquisition Parameters
Date_ 20161201
Time_ 1.41
INSTRUM av600
PROBHD 5 mm CPDUL 13C
PULPROG zg30
TD 65536
SOLVENT CD3CN
NS 16
DS 4
SWH 10330.578 Hz
FIDRES 0.157632 Hz
AQ 3.1719425 sec
RG 3.2
DW 48.400 usec
DE 10.00 usec
TE 298.0 K
D1 1.00000000 sec
TD0 1
======== CHANNEL f1 ========
SFO1 500.3030896 MHz
NUC1 1H
P1 15.00 usec
PLW1 7.99830008 W
F2 - Processing parameters
SI 65536
SF 500.3000154 MHz
WDW EM
SSB 0
LB 0.30 Hz
GB 0
PC 1.00
ppm
0.97
5.00
1.00
1.03
0.85
0.99
2.11
1.02
0.99
0.86
1.02
2.04
1.05
2.08
1.01
3.11

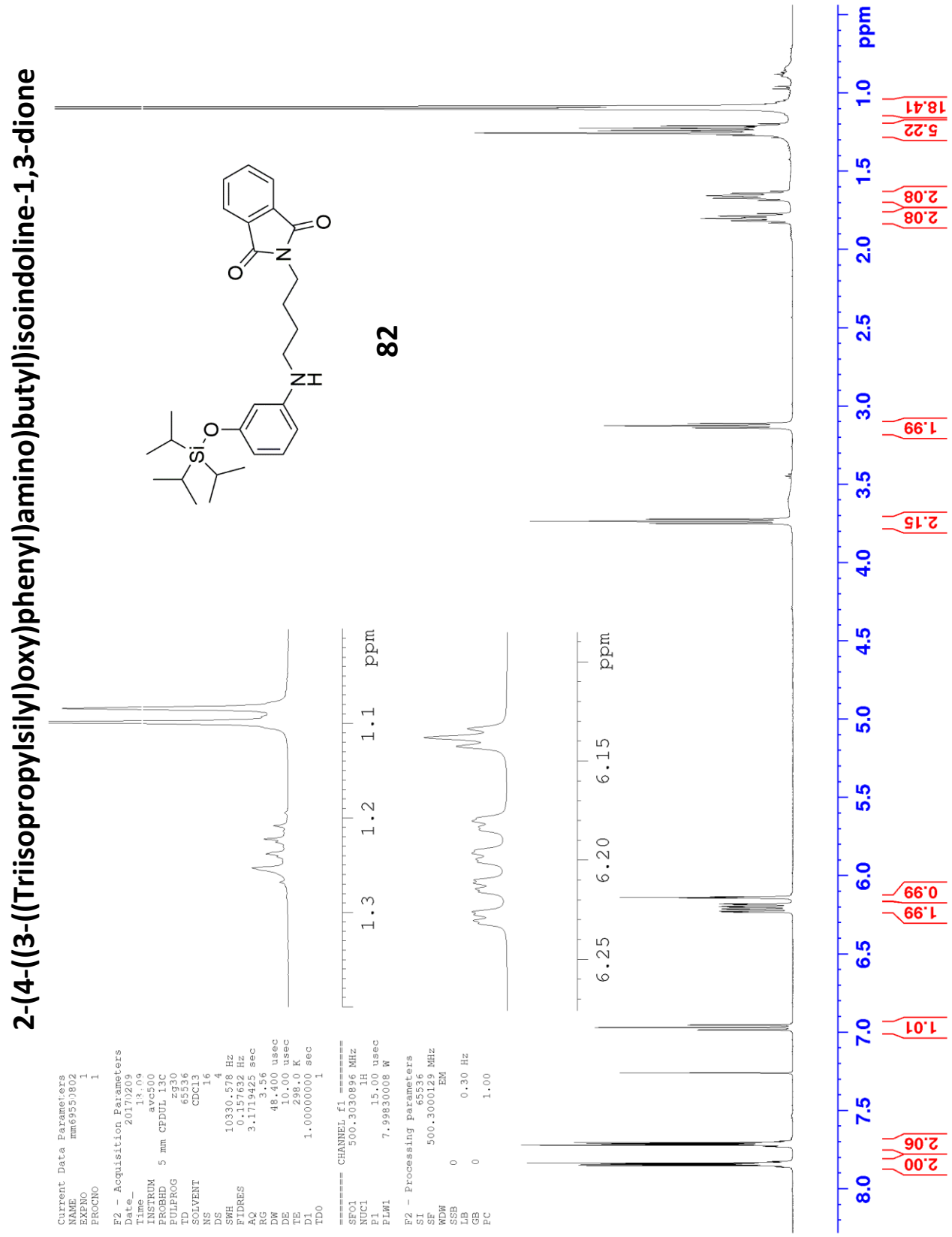

Benzyl (R)-8-(but-3'-en-1'-ylamino)-4-methyl-2-oxo-2,3,4,5-tetrahydro-1H-benzo[b][1,4]diazepine-6-carboxylate
(R)63
Current Data Parameters
NAME
EXPNO 4
PROCNO 1
F2 - Acquisition Parameters
Date_ 20161201
Time 2.57
INSTRUM spect
PROBHD 5 mm CPDUL 13C
PULPROG zgpg30
TD 65536
SOLVENT CD3CN
NS 1024
DS 2
SWH 31250.000 Hz
FIDRES 0.476837 Hz
AQ 1.04857600 sec
RG 912
DW 16.000 usec
DE 6.50 usec
TE 298.0 K
D1 2.00000000 sec
D11 0.03000000 sec
TD0 1
======== CHANNEL f1 ========
SFO1 125.81311152 MHz
NUC1 13C
P1 10.00 usec
PLW1 20.18400002 W
======== CHANNEL f2 ========
SFO2 500.3020012 MHz
NUC2 1H
CPDPRG[2 waltz16
PCPD2 80.00 usec
PLW2 7.99880004 W
PLW12 0.28119001 W
PLW13 0.17996000 W
F2 - Processing parameters
SI 32768
SF 125.8004706 MHz
WDW EM
SSB 0
LB 1.00 Hz
GB 0
PC 1.40
173.06
168.92
143.35
137.35
137.13
134.37
133.81
129.52
129.10
128.93
120.93
116.86
112.54
111.68
67.28
56.24
44.10
41.16
34.07
23.49
NH
NH
O
O
O
NH
138 136 134 132 130 ppm
190 180 170 160 150 140 130 120 110 100 90 80 70 60 50 40 30 20 ppm

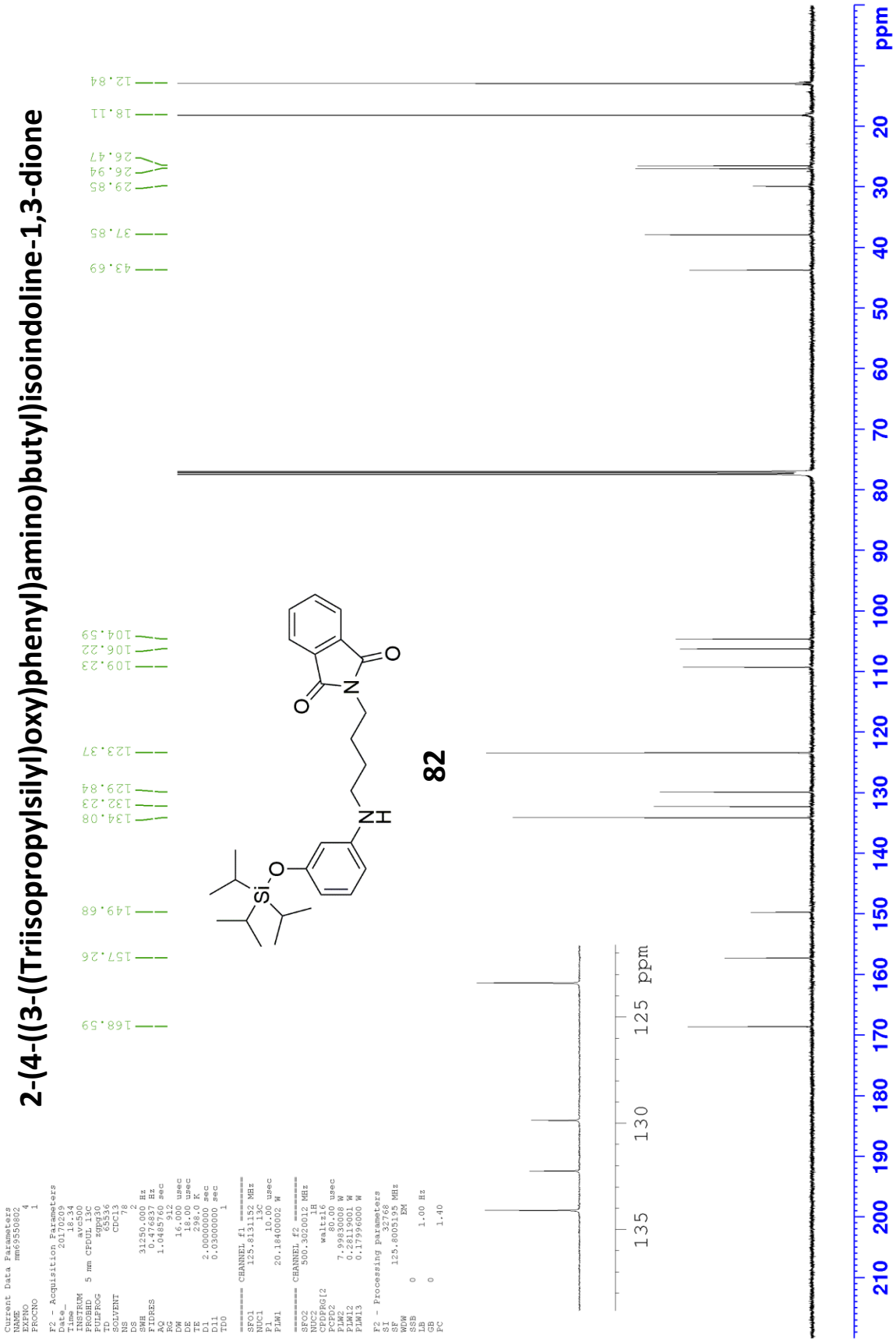
(*R*)-*N*-(4-((3-(Allyloxy)phenyl)(methyl)amino)butyl)-8-(but-3-en-1-ylamino)-4-methyl-2-oxo-2,3,4,5-tetrahydro-1*H*-benzo[*b*][1,4]diazepine-6-carboxamide

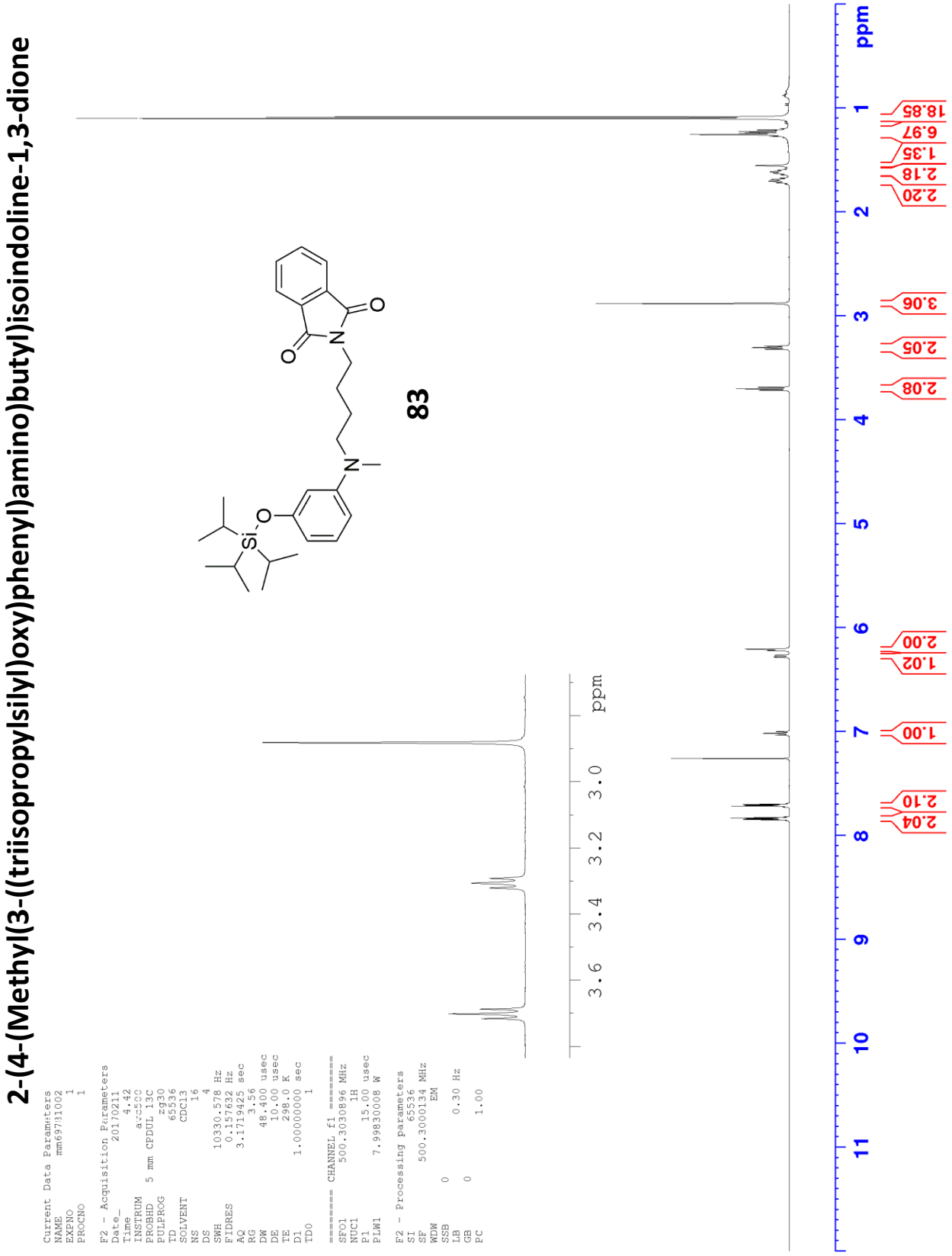


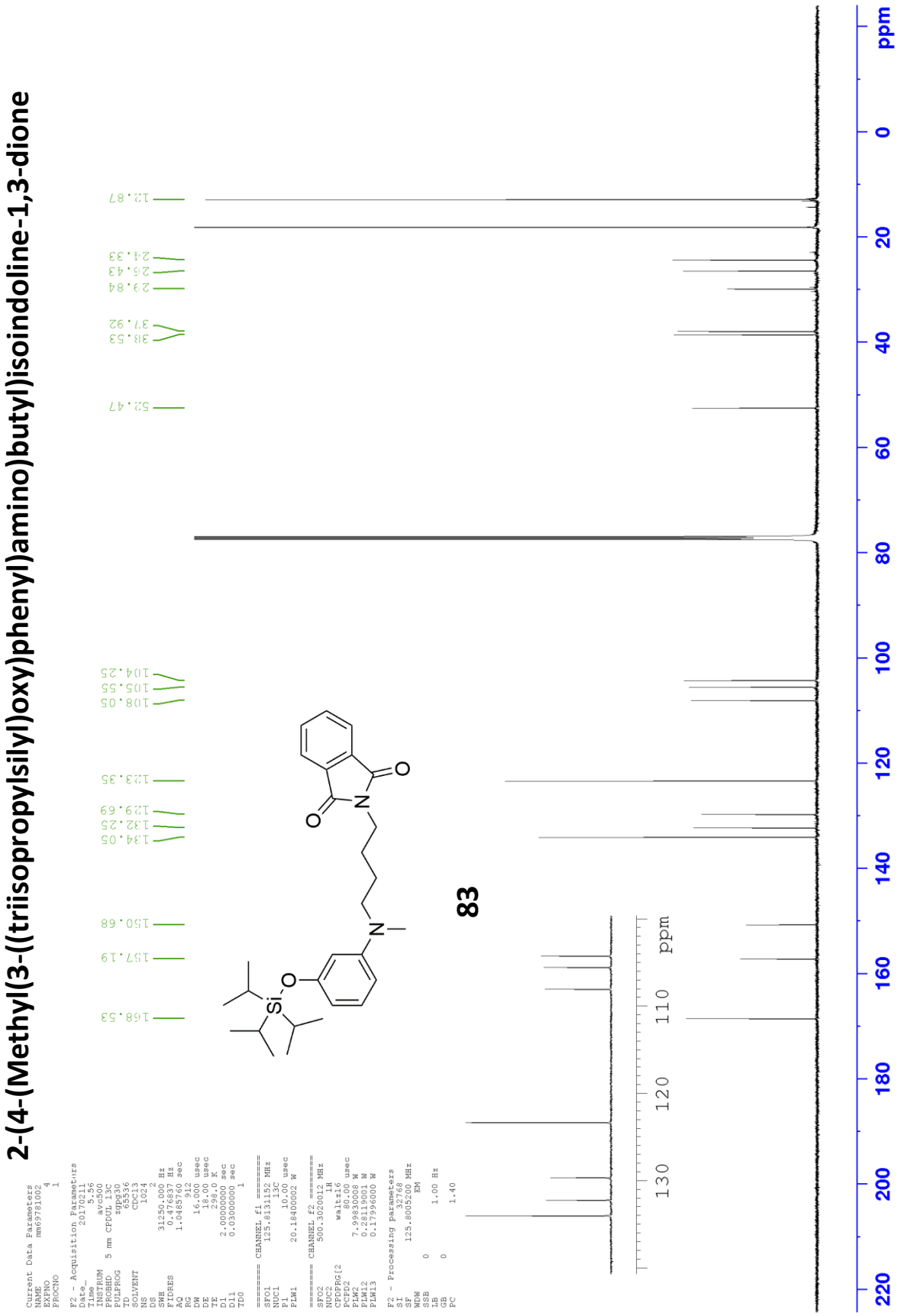
(*R*)-*N*-(4-((3-(Allyloxy)phenyl)(methyl)amino)butyl)-8-(but-3-en-1-ylamino)-4-methyl-2-oxo-2,3,4,5-tetrahydro-1*H*-benzo[*b*][1,4]diazepine-6-carboxamide

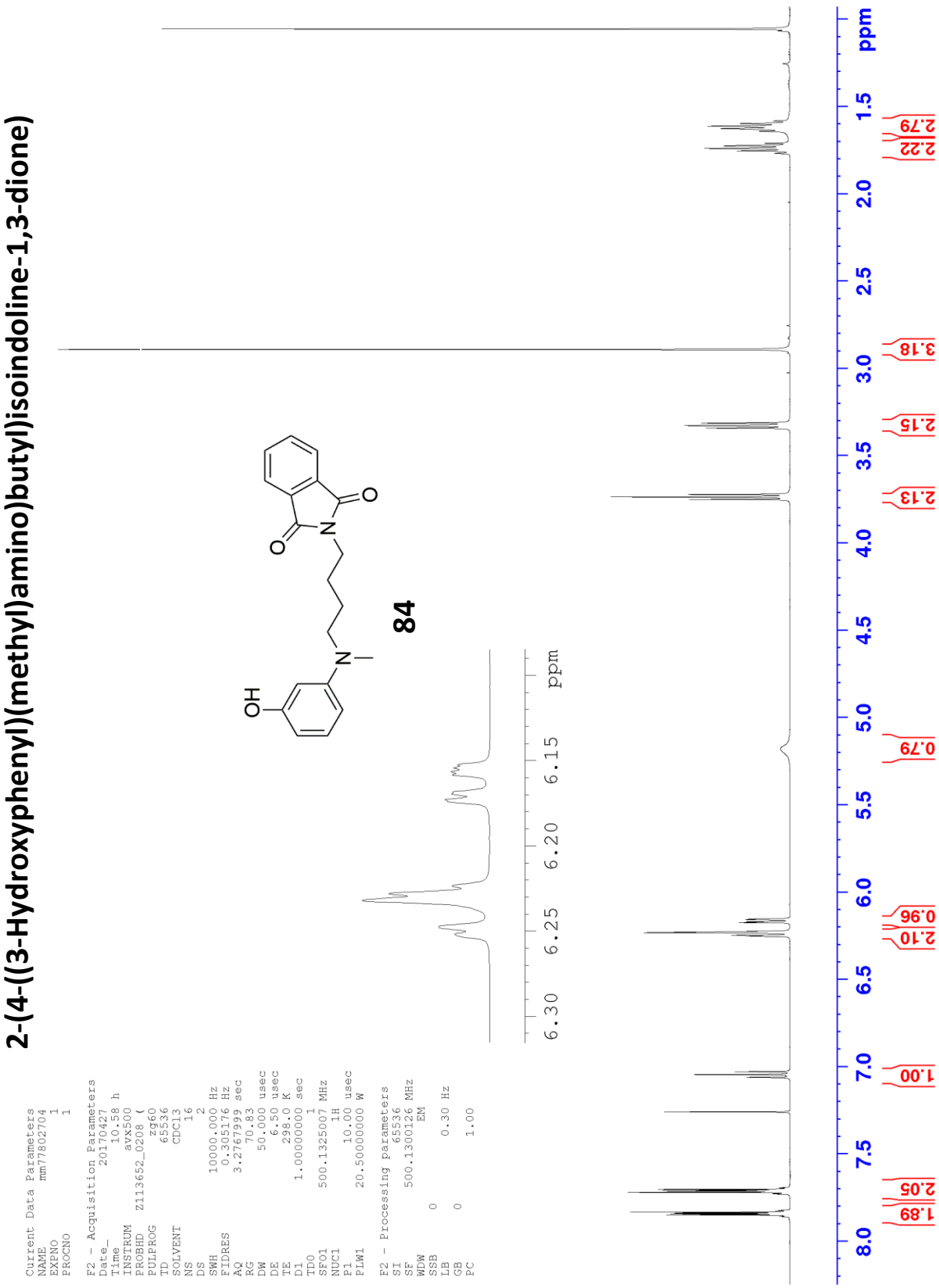


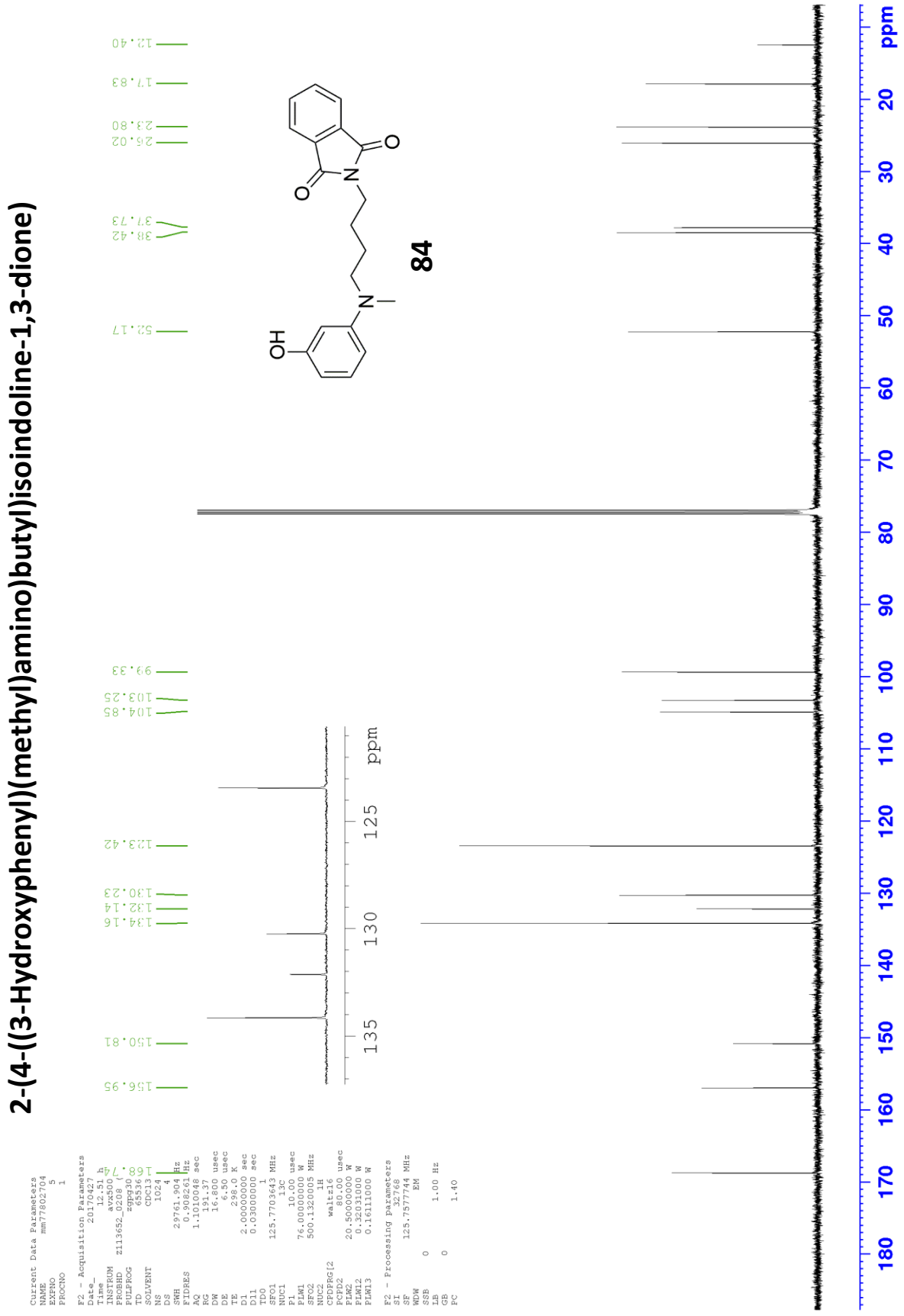

2-(4-((3-((Triisopropylsilyl)oxy)phenyl)amino)butyl)isoindoline-1,3-dione
82
Current Data Parameters
NAME mm6955)802
EXPNO 1
PROCNO 1
F2 - Acquisition Parameters
Date_ 2017)209
Time_ 13.09
INSTRUM avc500
PROBHD 5 mm CPDUL 13C
PULPROG zg30
TD 65536
SOLVENT CDC13
NS 16
DS 4
SWH 10330.578 Hz
FIDRES 0.157632 Hz
AQ 3.1719425 sec
RG 3.56
DW 48.400 usec
DE 10.00 usec
TE 298.0 K
D1 1.00000000 sec
TD0 1
======== CHANNEL f1 ========
SFO1 500.3030896 MHz
NUC1 1H
P1 15.00 usec
PLW1 7.99830008 W
F2 - Processing parameters
SI 65536
SF 500.3000129 MHz
WDW EM
SSB 0
LB 0.30 Hz
GB 0
PC 1.00
1.3 1.2 1.1 ppm
6.25 6.20 6.15 ppm
8.0 7.5 7.0 6.5 6.0 5.5 5.0 4.5 4.0 3.5 3.0 2.5 2.0 1.5 1.0 ppm
2.00
2.06
1.01
1.99
0.99
2.15
1.99
2.08
2.08
5.22
18.41

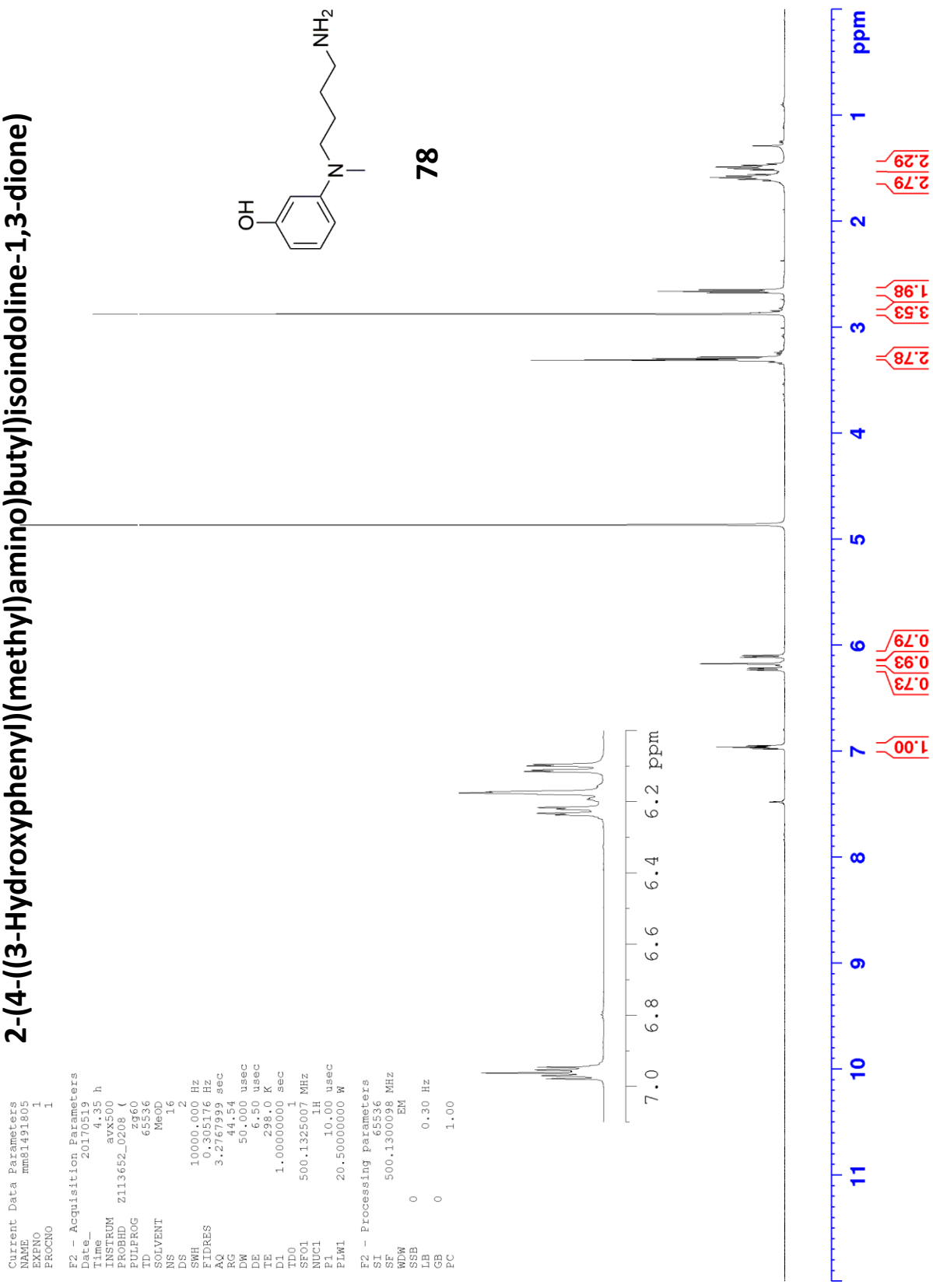

2-(4-((3-((Triisopropylsilyl)oxy)phenyl)amino)butyl)isoindoline-1,3-dione
82
Current Data Parameters
NAME mm69550802
EXPNO 4
PROCNO 1
F2 - Acquisition Parameters
Date_ 20170209
Time 18.34
INSTRUM avc500
PROBHD 5 mm CPDUL 13C
PULPROG zgpg30
TD 65536
SOLVENT CDCl3
NS 78
DS 2
SWH 31250.000 Hz
FIDRES 0.476837 Hz
AQ 1.0485760 sec
RG 912
DW 16.000 usec
DE 18.00 usec
TE 298.0 K
D1 2.00000000 sec
D11 0.03000000 sec
TD0 1
======== CHANNEL f1 ========
SFO1 125.8131152 MHz
NUC1 13C
P1 10.00 usec
PLW1 20.18400002 W
======== CHANNEL f2 ========
SFO2 500.3020012 MHz
NUC2 1H
CPDPRG[2 waltz16
PCPD2 80.00 usec
PLW2 7.99830008 W
PLW12 0.28119001 W
PLW13 0.17996000 W
F2 - Processing parameters
SI 32768
SF 125.8005195 MHz
WDW EM
SSB 0
LB 1.00 Hz
GB 0
PC 1.40
12.84
18.11
26.47
26.94
29.85
37.85
43.69
104.59
106.22
109.23
123.37
129.84
132.23
134.08
149.68
157.26
168.59
135
130
125 ppm
ppm

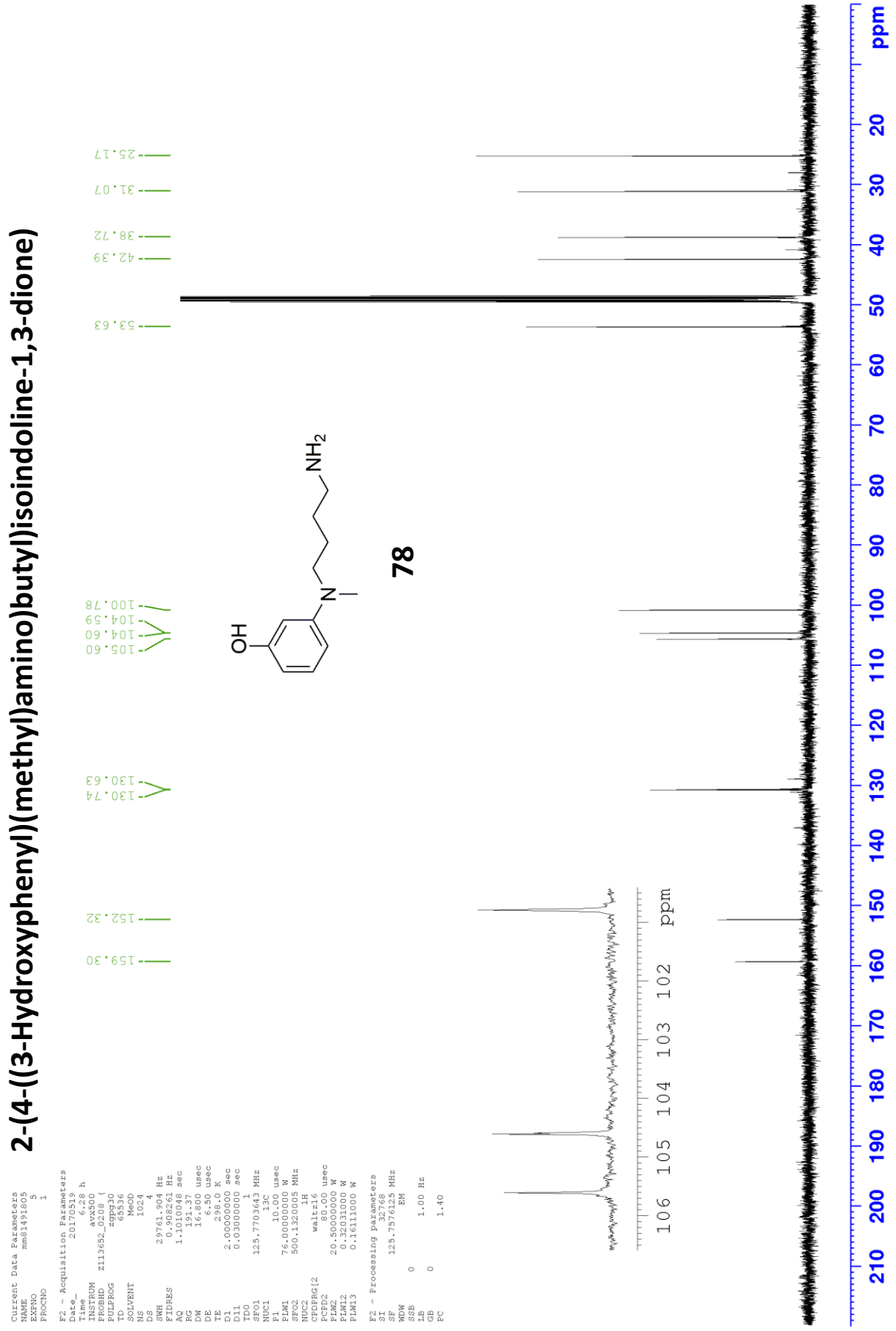

2-(4-(Methyl(3-((triisopropylsilyl)oxy)phenyl)amino)butyl)isoindoline-1,3-dione
83
Current Data Parameters
NAME mm697l1002
EXPNO 1
PROCNO 1
F2 - Acquisition Parameters
Date_ 20170211
Time 4.42
INSTRUM av-cccc
PROBHD 5 mm CPDUL 13C
PULPROG zg30
TD 65536
SOLVENT CDCl3
NS 16
DS 4
SWH 10330.578 Hz
FIDRES 0.157632 Hz
AQ 3.1719425 sec
RG 3.56
DW 48.400 usec
DE 10.00 usec
TE 298.0 K
D1 1.00000000 sec
TD0 1
======== CHANNEL f1 ========
SFO1 500.3030896 MHz
NUC1 1H
P1 15.00 usec
PLW1 7.99830008 W
F2 - Processing parameters
SI 65536
SF 500.3000134 MHz
WDW EM
SSB 0
LB 0.30 Hz
GB 0
PC 1.00
3.6 3.4 3.2 3.0 ppm
11 10 9 8 7 6 5 4 3 2 1 ppm
2.04
2.10
1.00
1.02
2.00
2.08
2.05
3.06
2.20
2.18
1.35
6.97
18.85


2-(4-(Methyl(3-((triisopropylsilyl)oxy)phenyl)amino)butyl)isoindoline-1,3-dione
83
ppm

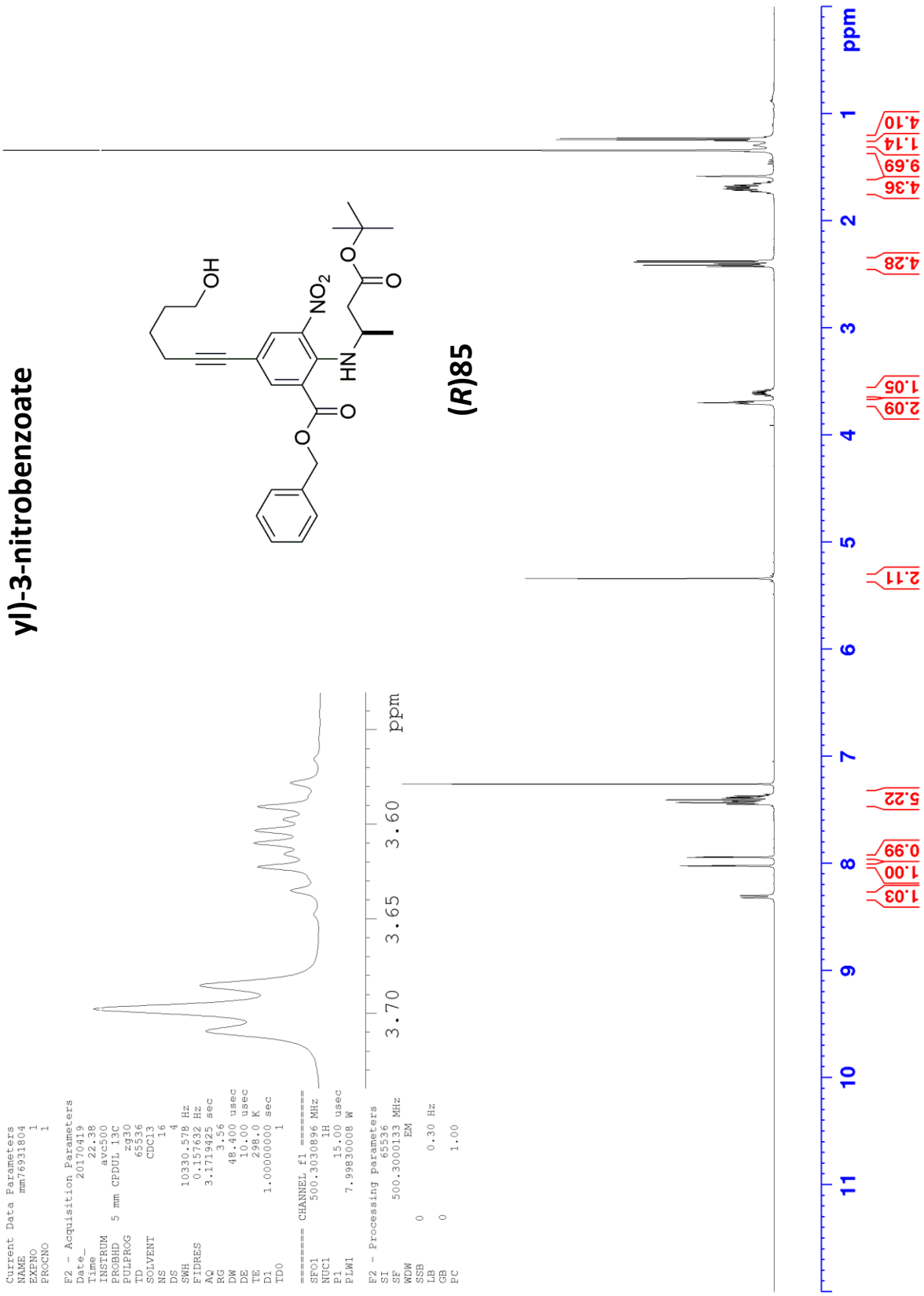

2-(4-((3-Hydroxyphenyl)(methyl)amino)butyl)isoindoline-1,3-dione)
84
OH
N
O
O
N
Current Data Parameters
NAME mm7802704
EXPNO 1
PROCNO 1
F2 - Acquisition Parameters
Date_ 20170427
Time_ 10.58 h
INSTRUM avx500
PROBHD Z113652_0208 (
PULPROG zg60
TD 65536
SOLVENT CDC13
NS 16
DS 2
SWH 10000.000 Hz
FIDRES 0.305176 Hz
AQ 3.2767999 sec
RG 70.83
DW 50.000 usec
DE 6.50 usec
TE 298.0 K
D1 1.00000000 sec
TD0 1
SFO1 500.1325007 MHz
NUC1 1H
P1 10.00 usec
PLW1 20.50000000 W
F2 - Processing parameters
SI 65536
SF 500.1300126 MHz
WDW EM
SSB 0
LB 0.30 Hz
GB 0
PC 1.00
6.30
6.25
6.20
6.15
ppm
8.0
7.5
7.0
6.5
6.0
5.5
5.0
4.5
4.0
3.5
3.0
2.5
2.0
1.5
ppm
1.89
2.05
1.00
2.10
0.96
0.79
2.13
2.15
3.18
2.22
2.79


2-(4-((3-Hydroxyphenyl)(methyl)amino)butyl)isoindoline-1,3-dione)
84
OH
N
O
ppm

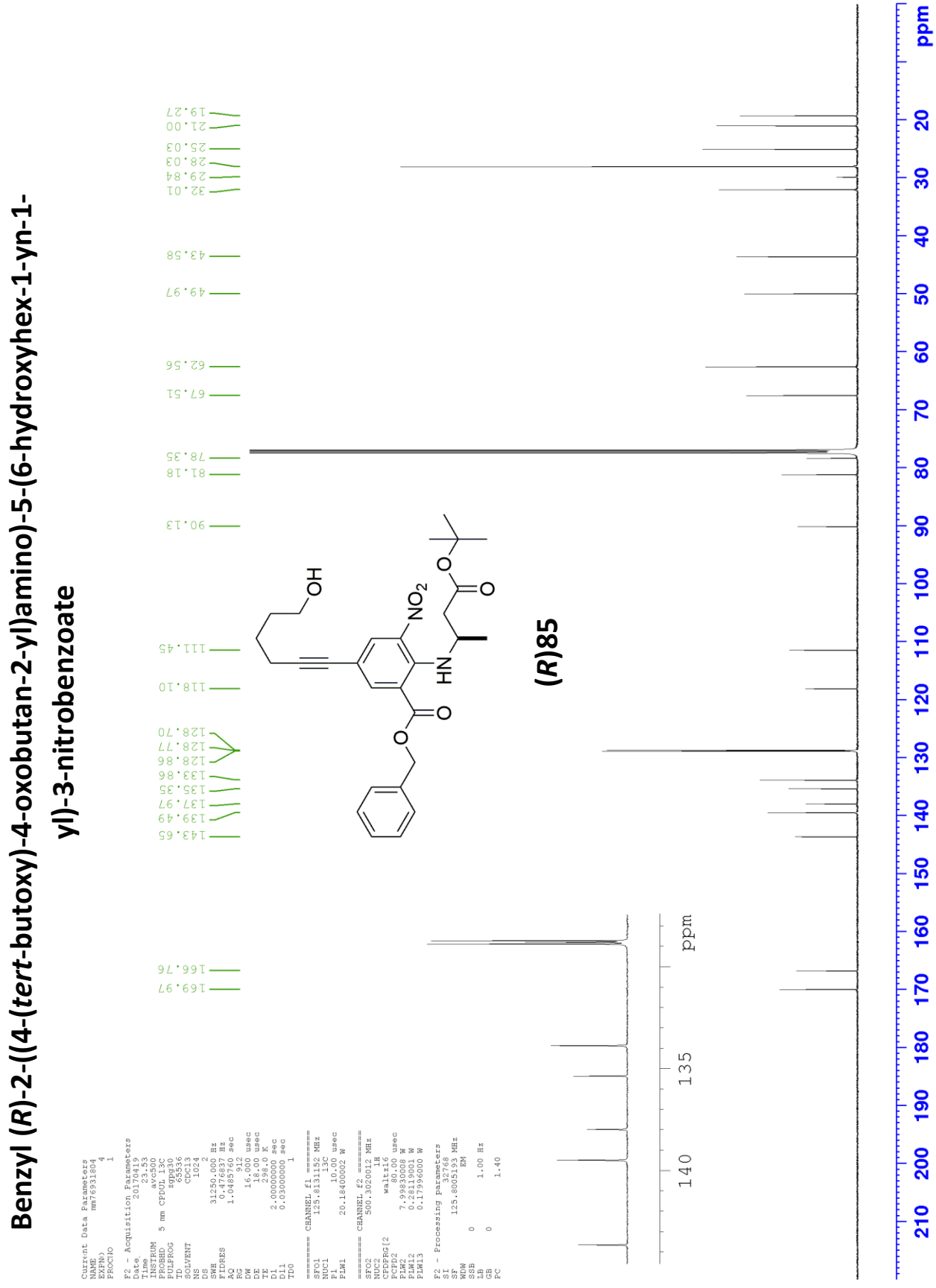

2-(4-((3-Hydroxyphenyl)(methyl)amino)butyl)isoindoline-1,3-dione)
78
OH
N
NH2
Current Data Parameters
NAME mm81491805
EXPNO 1
PROCNO 1
F2 - Acquisition Parameters
Date_ 20170519
Time 4.35 h
INSTRUM avx500
PROBHD Z113652_0208 (
PULPROG zg60
TD 65536
SOLVENT MeOD
NS 16
DS 2
SWH 10000.000 Hz
FIDRES 0.305176 Hz
AQ 3.2767999 sec
RG 44.54
DW 50.000 usec
DE 6.50 usec
TE 298.0 K
D1 1.00000000 sec
TD0 1
SFO1 500.1325007 MHz
NUC1 1H
P1 10.00 usec
PLW1 20.50000000 W
F2 - Processing parameters
SI 65536
SF 500.1300098 MHz
WDW EM
SSB 0
LB 0.30 Hz
GB 0
PC 1.00
7.0
6.8
6.6
6.4
6.2 ppm
ppm
1.00
0.73
0.93
0.79
2.78
3.53
1.98
2.78
2.79
2.29


2-(4-((3-Hydroxyphenyl)(methyl)amino)butyl)isoindoline-1,3-dione)
78
OH
N
NH2
159.30
152.32
130.74
130.63
105.60
104.60
104.59
100.78
53.63
42.39
38.72
31.07
25.17
106 105 104 103 102 ppm
210 200 190 180 170 160 150 140 130 120 110 100 90 80 70 60 50 40 30 20 ppm

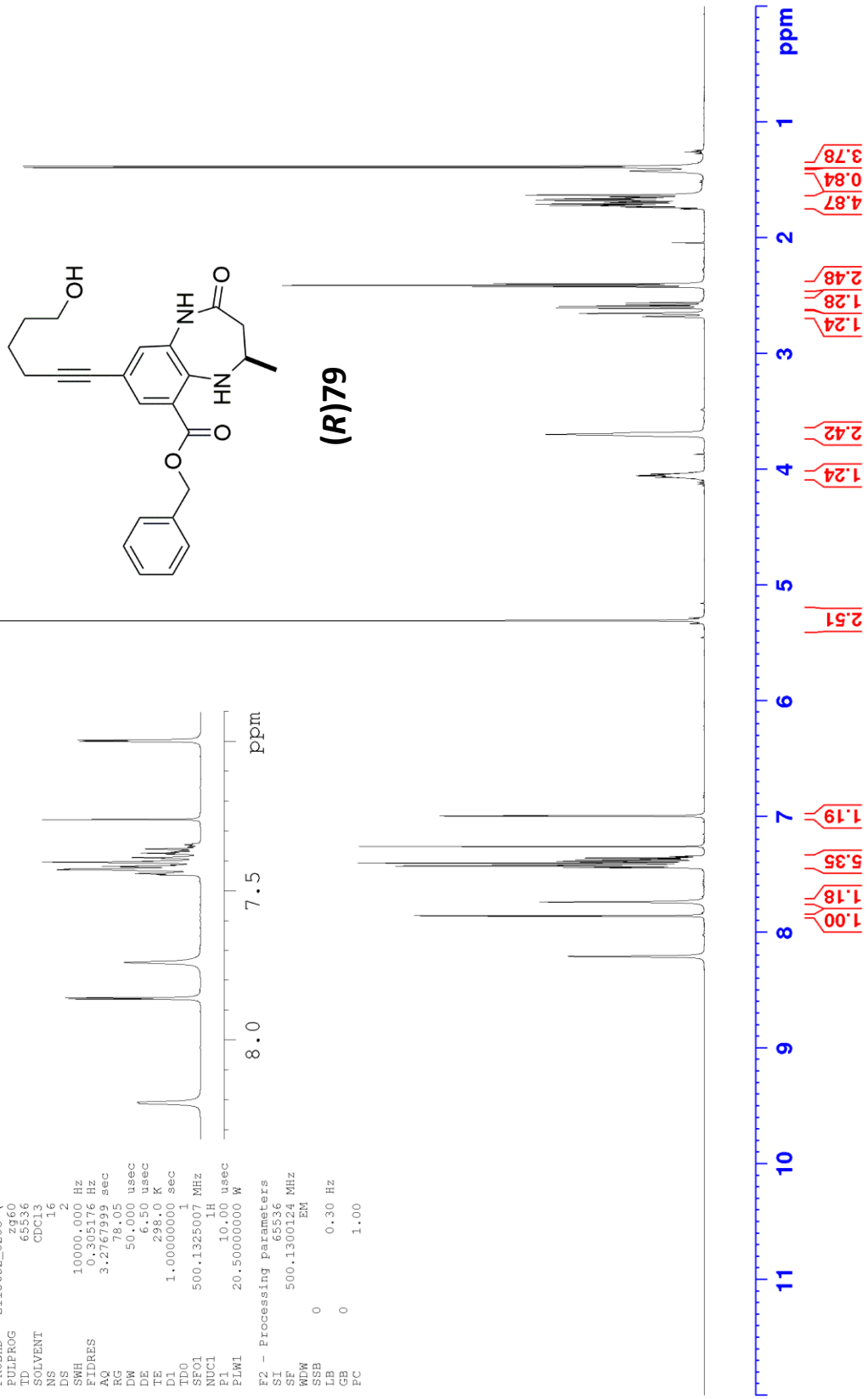
Benzyl (*R*)-2-((4-(*tert*-butoxy)-4-oxobutan-2-yl)amino)-5-(6-hydroxyhex-1-yn-1-yl)-3-nitrobenzoate

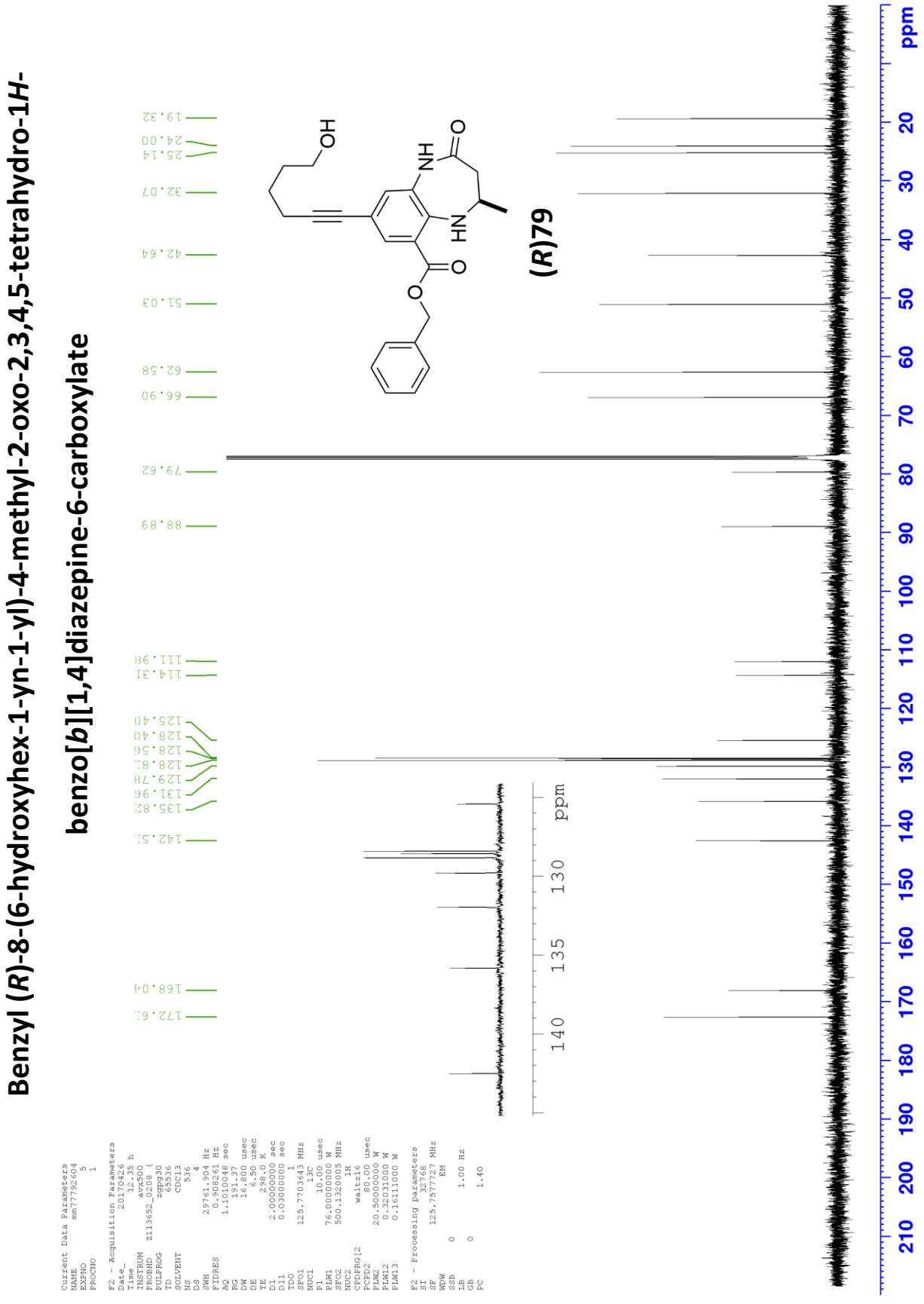


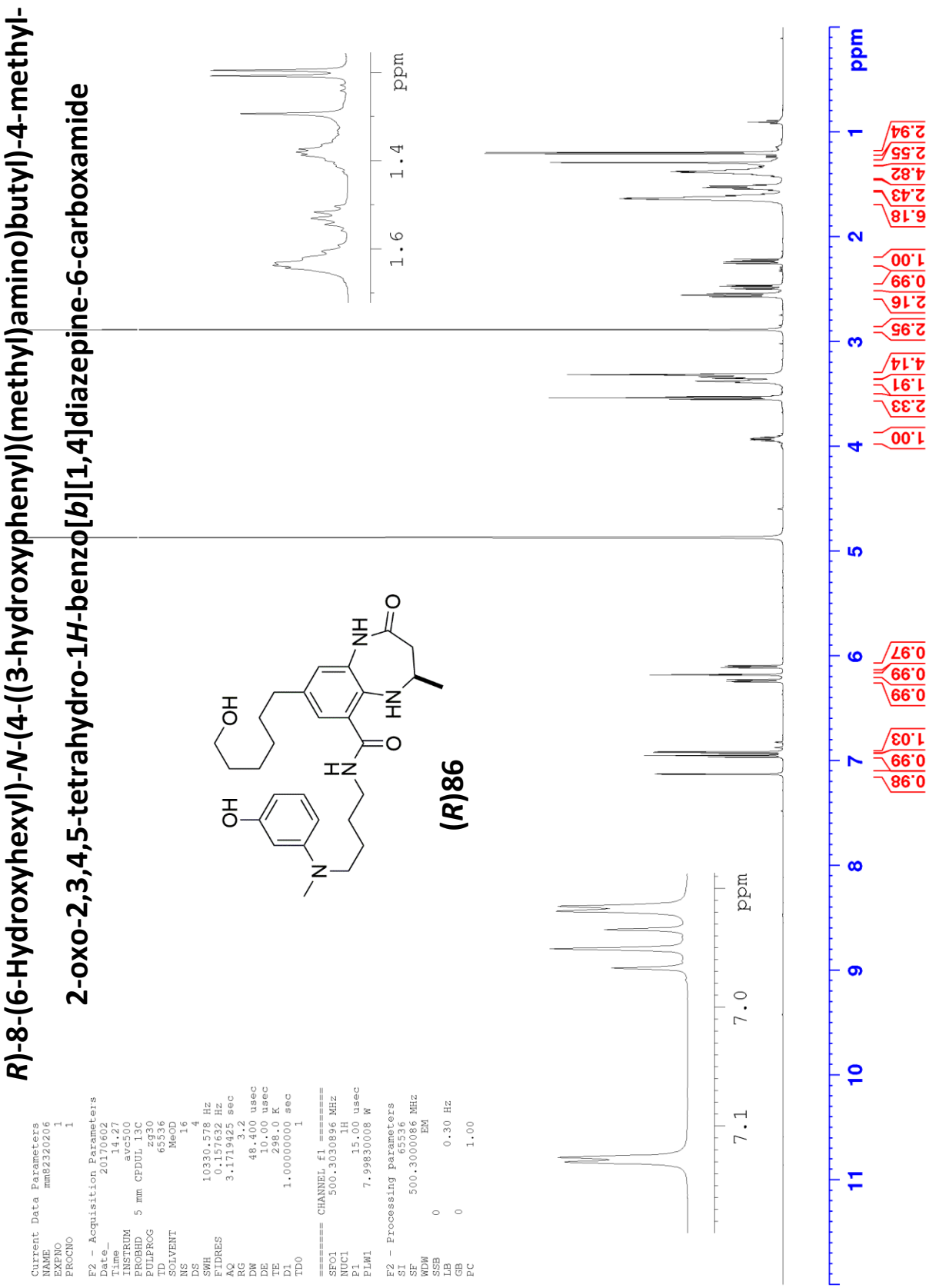
Benzyl (*R*)-2-((4-(*tert*-butoxy)-4-oxobutan-2-yl)amino)-5-(6-hydroxyhex-1-yn-1-yl)-3-nitrobenzoate

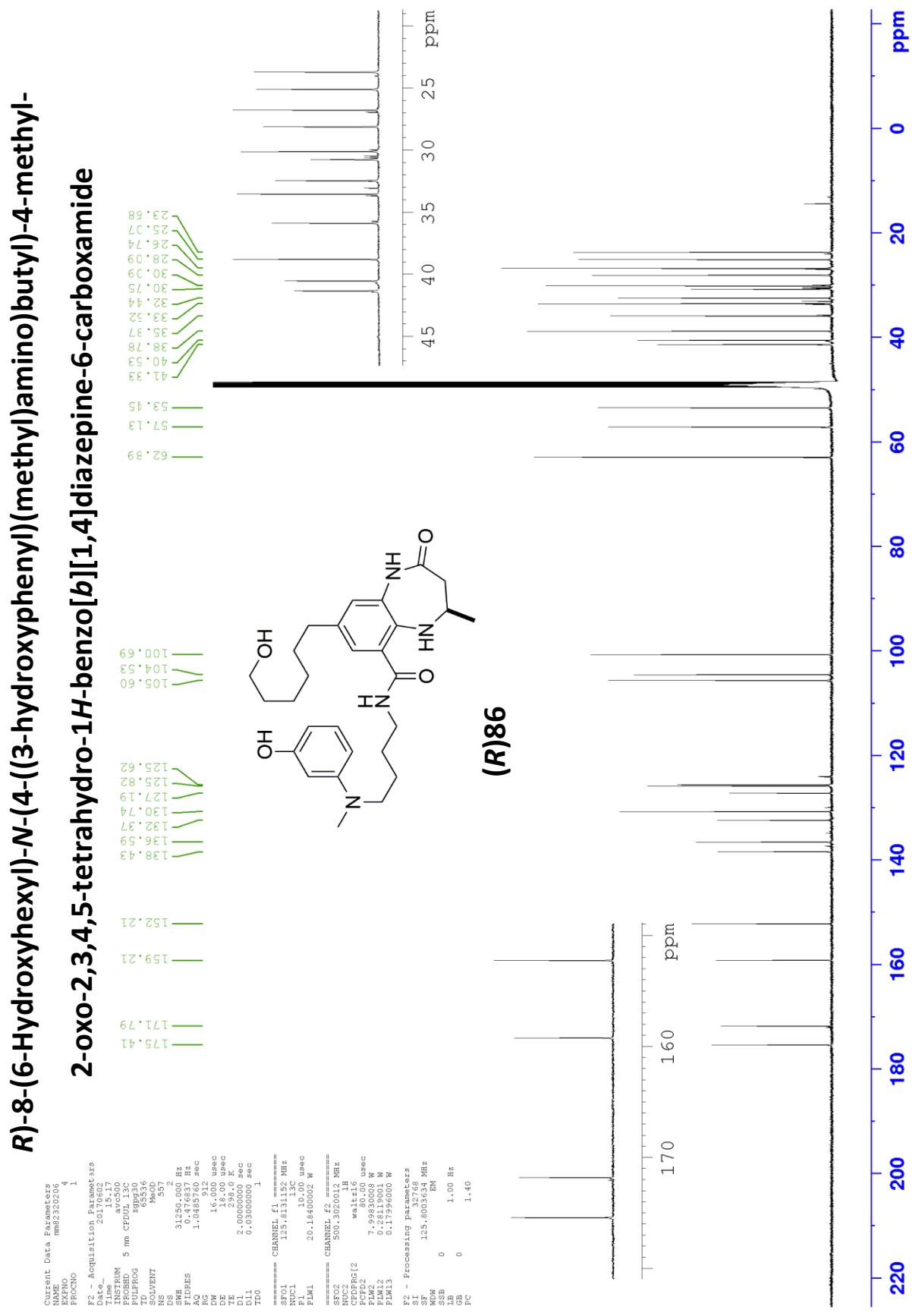


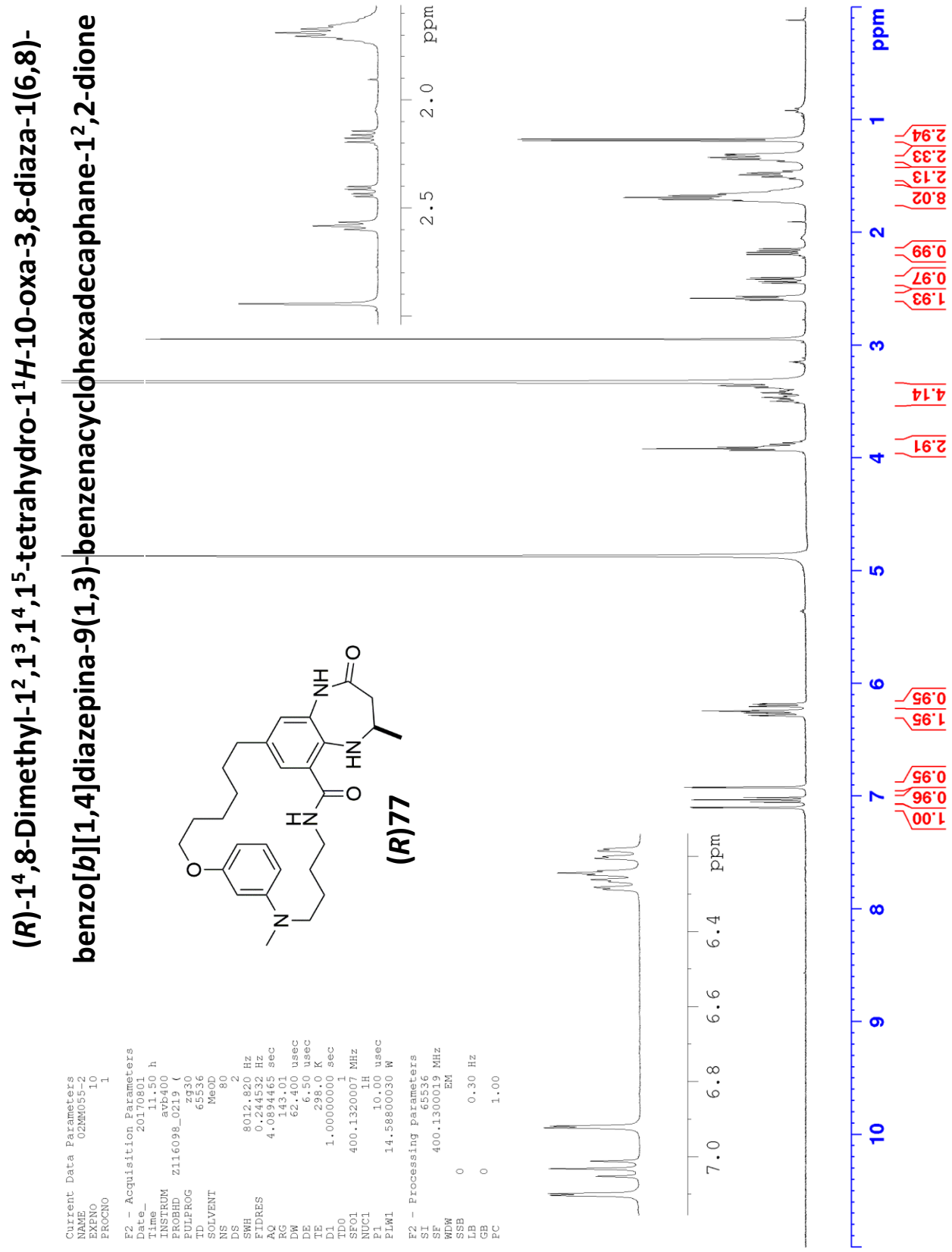
Benzyl (*R*)-8-(6-hydroxyhex-1-yn-1-yl)-4-methyl-2-oxo-2,3,4,5-tetrahydro-1*H*-benzo[*b*][1,4]diazepine-6-carboxylate



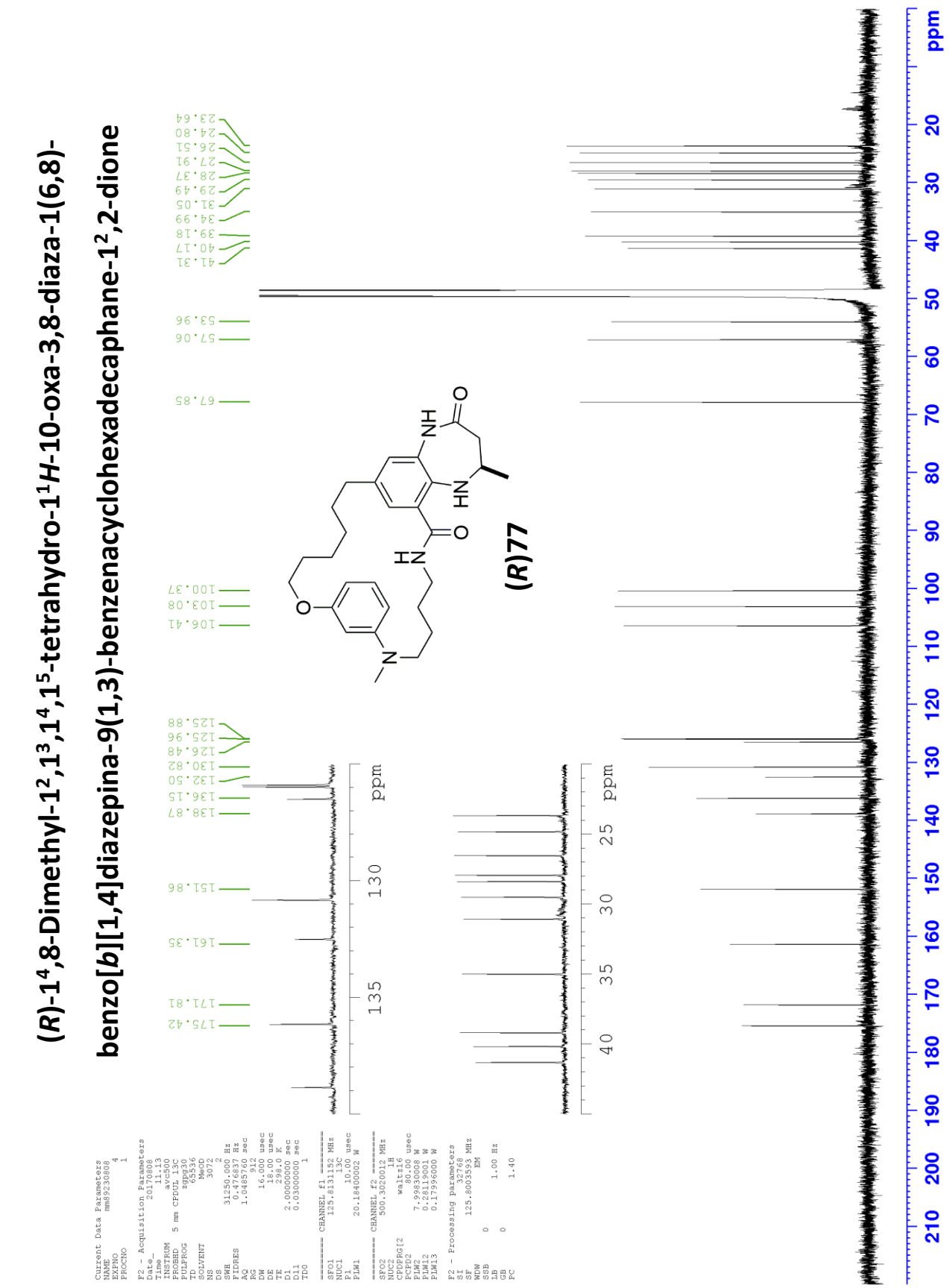

Benzyl (R)-8-(6-hydroxyhex-1-yn-1-yl)-4-methyl-2-oxo-2,3,4,5-tetrahydro-1H-benzo[b][1,4]diazepine-6-carboxylate
(R)79
OH
NH
O
NH
O
O
ppm

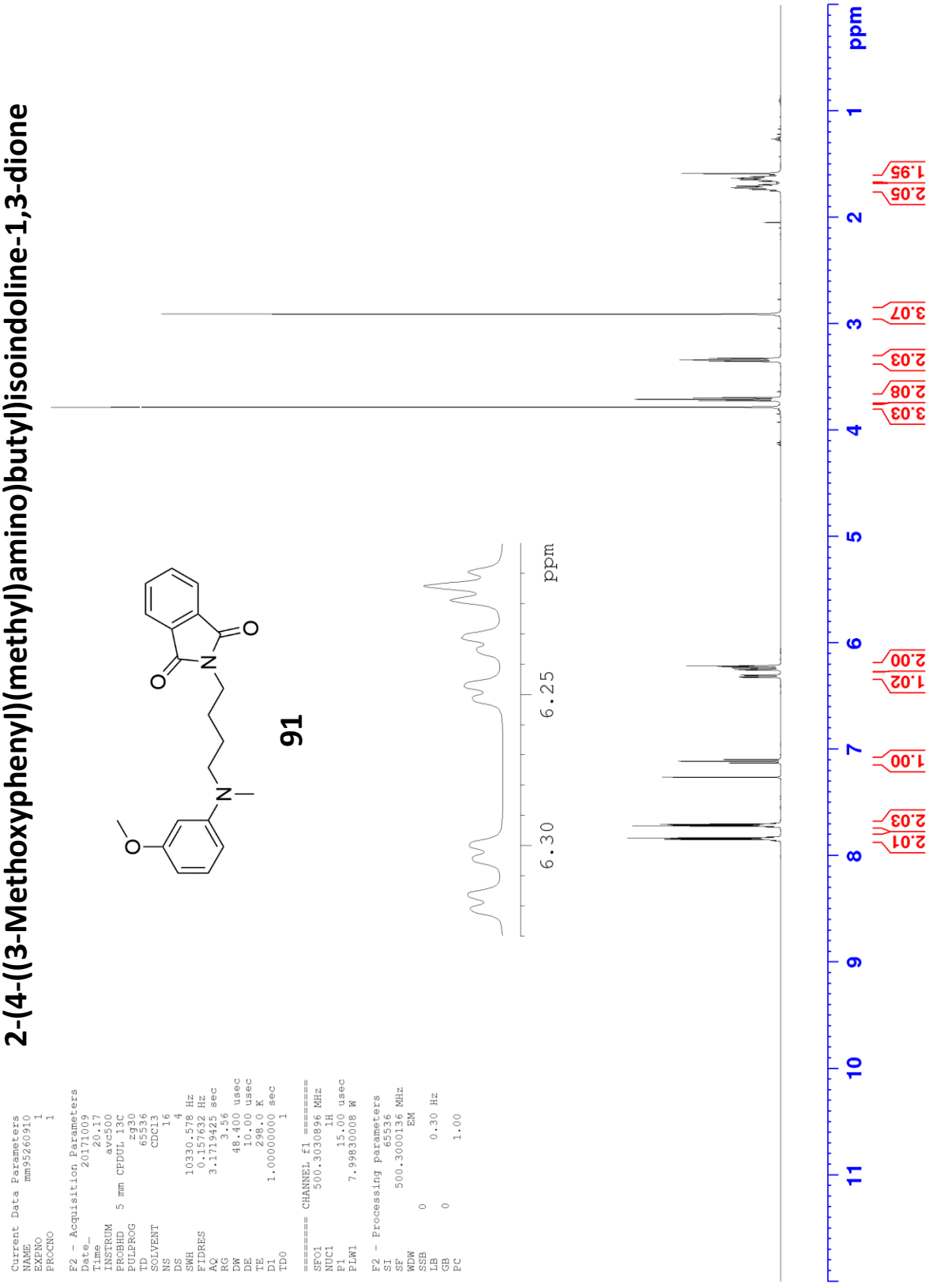

(R)-8-(6-Hydroxyhexyl)-N-(4-((3-hydroxyphenyl)(methyl)amino)butyl)-4-methyl-2-oxo-2,3,4,5-tetrahydro-1H-benzo[b][1,4]diazepine-6-carboxamide
(R)86
Current Data Parameters
NAME mm82320206
EXPNO 1
PROCNO 1
F2 - Acquisition Parameters
Date_ 20170602
Time 14.27
INSTRUM avc500
PROBHD 5 mm CPDUL 13C
PULPROG zg30
TD 65536
SOLVENT MeOD
NS 16
DS 4
SWH 10330.578 Hz
FIDRES 0.157632 Hz
AQ 3.1719425 sec
RG 3.2
DW 48.400 usec
DE 10.00 usec
TE 298.0 K
D1 1.00000000 sec
TD0 1
======== CHANNEL f1 ========
SFO1 500.3030896 MHz
NUC1 1H
P1 15.00 usec
PLW1 7.99830008 W
F2 - Processing parameters
SI 65536
SF 500.3000086 MHz
WDW EM
SSB 0
LB 0.30 Hz
GB 0
PC 1.00
ppm
0.98
1.03
0.99
0.99
0.97
1.00
2.33
1.91
4.14
2.95
2.16
0.99
1.00
6.18
2.43
4.82
2.55
2.94

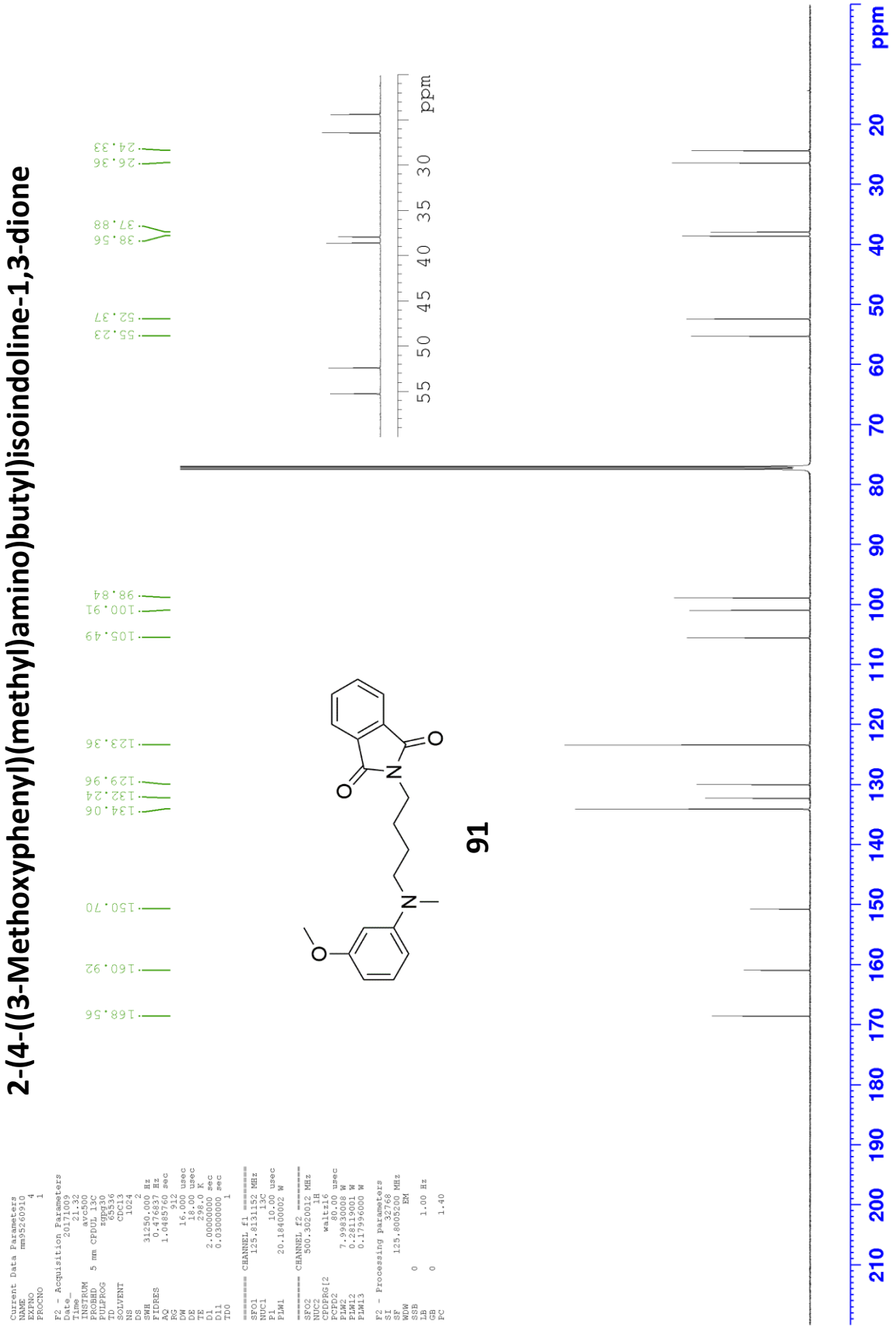

(R)-8-(6-Hydroxyhexyl)-N-(4-((3-hydroxyphenyl)(methyl)amino)butyl)-4-methyl-2-oxo-2,3,4,5-tetrahydro-1H-benzo[b][1,4]diazepine-6-carboxamide
(R)86
ppm


(R)-1⁴,8-Dimethyl-1²,1³,1⁴,1⁵-tetrahydro-1¹H-10-oxa-3,8-diaza-1(6,8)-benzo[b][1,4]diazepina-9(1,3)-benzenacyclohexadecaphane-1²,2-dione
(R)77
Current Data Parameters
NAME 02MM055-2
EXPNO 10
PROCNO 1
F2 - Acquisition Parameters
Date_ 20170801
Time 11.50 h
INSTRUM avb400
PROBHD Z116098_0219 (
PULPROG zg30
TD 65536
SOLVENT MeOD
NS 80
DS 2
SWH 8012.820 Hz
FIDRES 0.244532 Hz
AQ 4.0894465 sec
RG 143.01
DW 62.400 usec
DE 6.50 usec
TE 298.0 K
D1 1.00000000 sec
TD0 1
SFO1 400.1320007 MHz
NUC1 1H
P1 10.00 usec
PLW1 14.58800030 W
F2 - Processing parameters
SI 65536
SF 400.1300019 MHz
WDW EM
SSB 0
LB 0.30 Hz
GB 0
PC 1.00
ppm
1.00
0.96
0.95
1.95
0.95
2.91
4.14
1.93
0.97
0.99
8.02
2.13
2.33
2.94

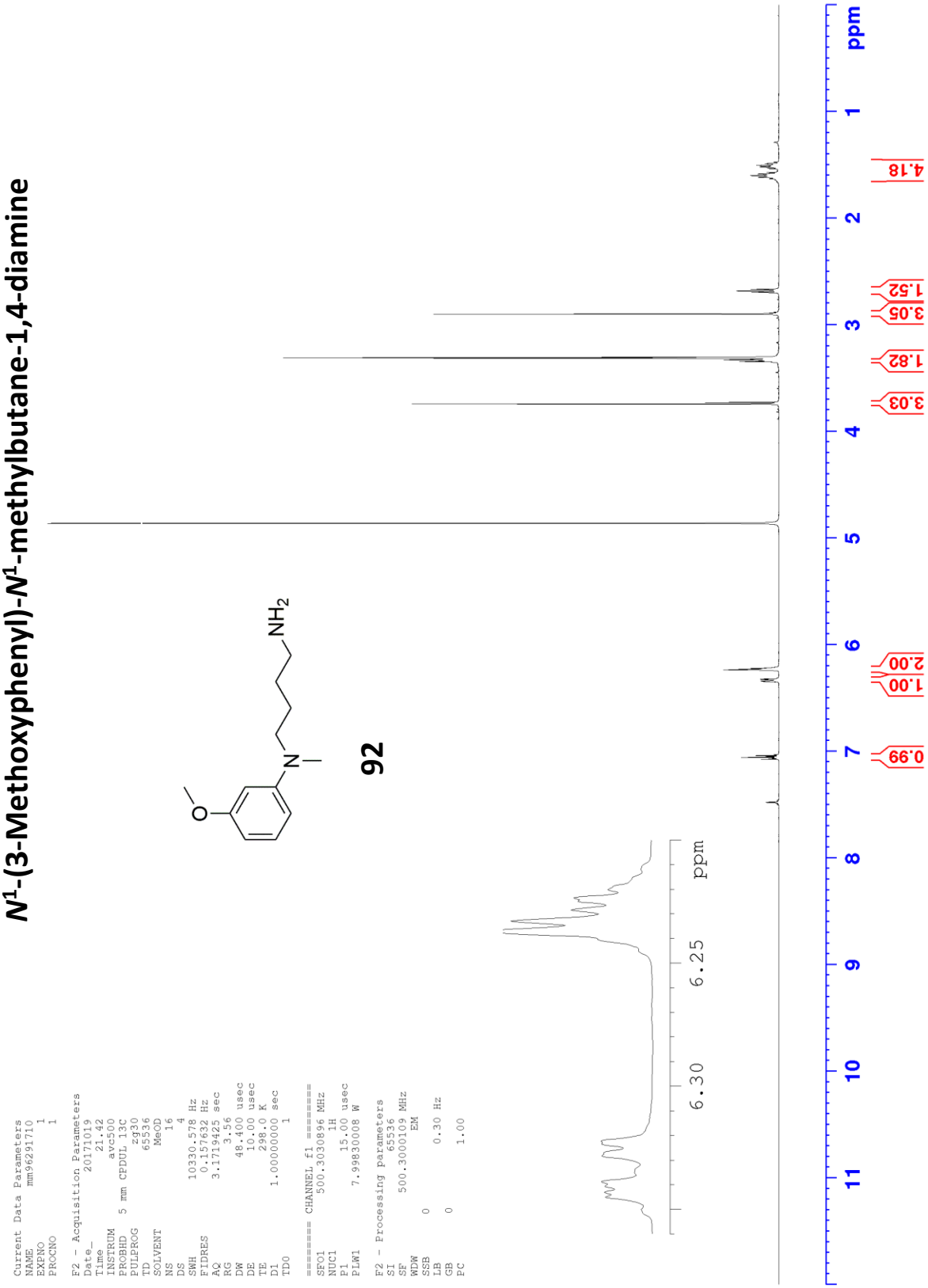
(*R*)-1^4,8-Dimethyl-1^2,1^3,1^4,1^5-tetrahydro-1^1*H*-10-oxa-3,8-diaza-1(6,8)-benzo[*b*][1,4]diazepina-9(1,3)-benzenacyclohexadecaphane-1^2,2-dione



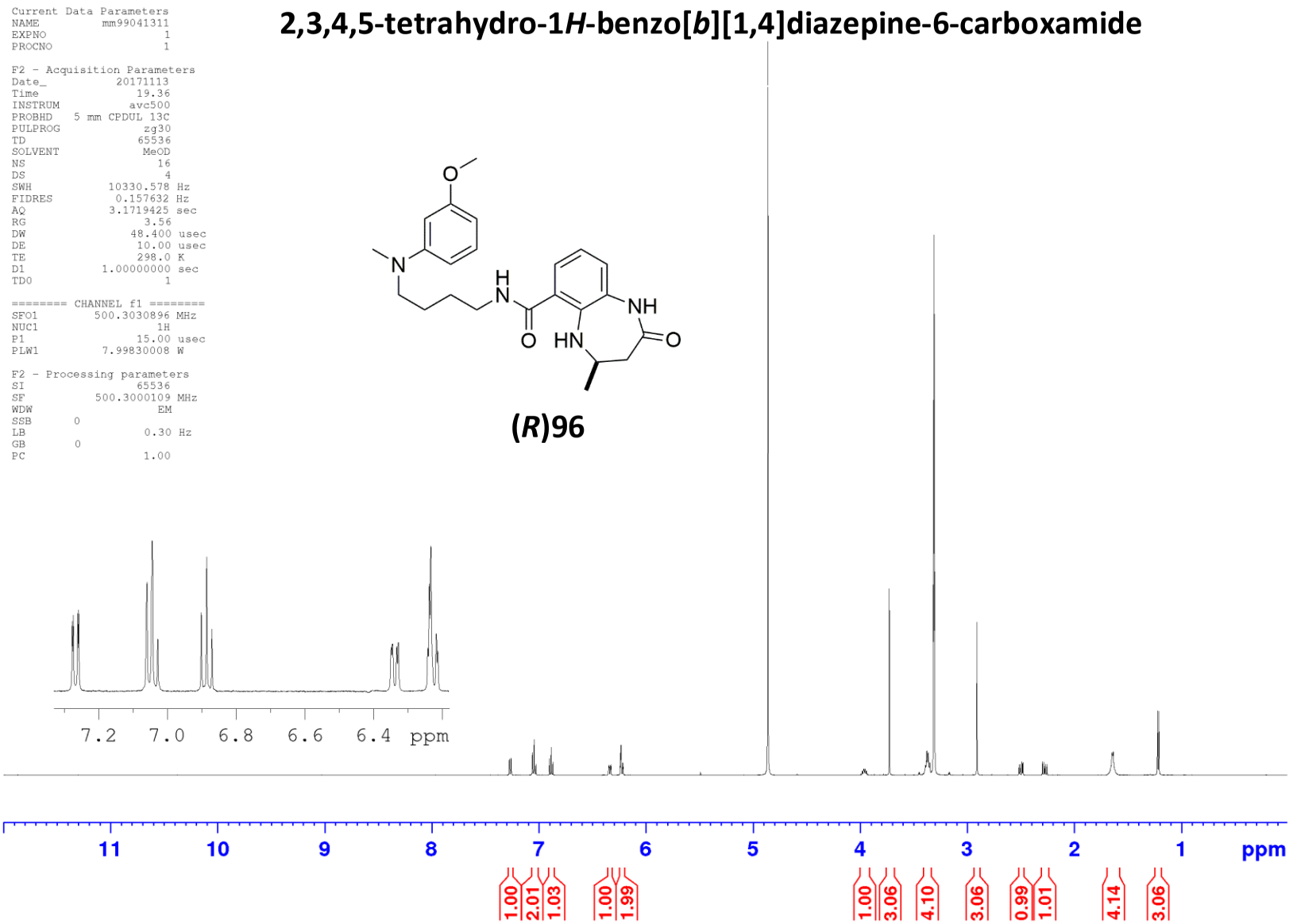

2-(4-((3-Methoxyphenyl)(methyl)amino)butyl)isoindoline-1,3-dione
Current Data Parameters
NAME mm9526091O
EXPNO 1
PROCNO 1
F2 - Acquisition Parameters
Date_ 20171009
Time 20.17
INSTRUM avc500
PROBHD 5 mm CPDUL 13C
PULPROG zg30
TD 65536
SOLVENT CDCl3
NS 16
DS 4
SWH 10330.578 Hz
FIDRES 0.157632 Hz
AQ 3.1719425 sec
RG 3.56
DW 48.400 usec
DE 10.00 usec
TE 298.0 K
D1 1.00000000 sec
TD0 1
======== CHANNEL f1 ========
SFO1 500.3030896 MHz
NUC1 1H
P1 15.00 usec
PLW1 7.99830008 W
F2 - Processing parameters
SI 65536
SF 500.3000136 MHz
WDW EM
SSB 0
LB 0.30 Hz
GB 0
PC 1.00
91
6.30
6.25
ppm
2.01
2.03
1.00
1.02
2.00
3.03
2.08
2.03
3.07
2.05
1.95
11
10
9
8
7
6
5
4
3
2
1
ppm


2-(4-((3-Methoxyphenyl)(methyl)amino)butyl)isoindoline-1,3-dione
91
Current Data Parameters
NAME mm95260910
EXPNO 4
PROCNO 1
F2 - Acquisition Parameters
Date_ 20171009
Time 21.32
INSTRUM av500
PROBHD 5 mm CPDUL 13C
PULPROG zgpg30
TD 65536
SOLVENT CDCl3
NS 1024
DS 2
SWH 31250.000 Hz
FIDRES 0.476837 Hz
AQ 1.0485760 sec
RG 203
DW 16.000 usec
DE 18.00 usec
TE 298.0 K
D1 2.00000000 sec
D11 0.03000000 sec
TD0 1
======== CHANNEL f1 ========
SFO1 125.8131152 MHz
NUC1 13C
P1 10.00 usec
PLW1 20.18400002 W
======== CHANNEL f2 ========
SFO2 500.3020612 MHz
NUC2 1H
CPDPRG2 waltz16
PCPD2 80.00 usec
PLW2 7.99830008 W
PLW12 0.28119001 W
PLW13 0.17996000 W
F2 - Processing parameters
SI 32768
SF 125.8005200 MHz
WDW EM
SSB 0
LB 1.00 Hz
GB 0
PC 1.40
168.56
160.92
150.70
134.06
132.24
129.96
123.36
105.49
100.91
98.84
55.23
52.37
38.56
37.88
26.36
24.33
ppm
55 50 45 40 35 30
210 200 190 180 170 160 150 140 130 120 110 100 90 80 70 60 50 40 30 20
ppm

N^1-(3-Methoxyphenyl)-N^1-methylbutane-1,4-diamine

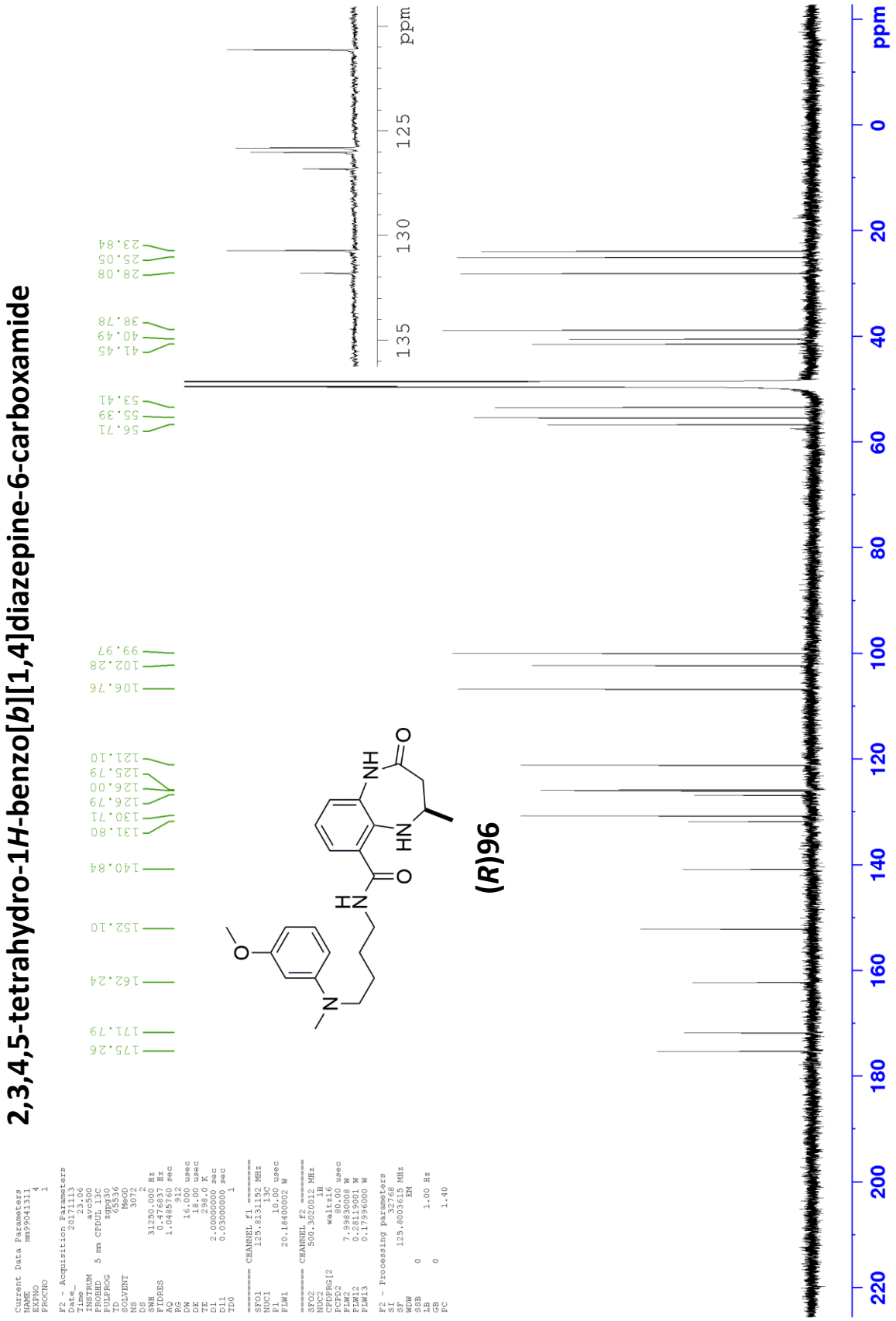


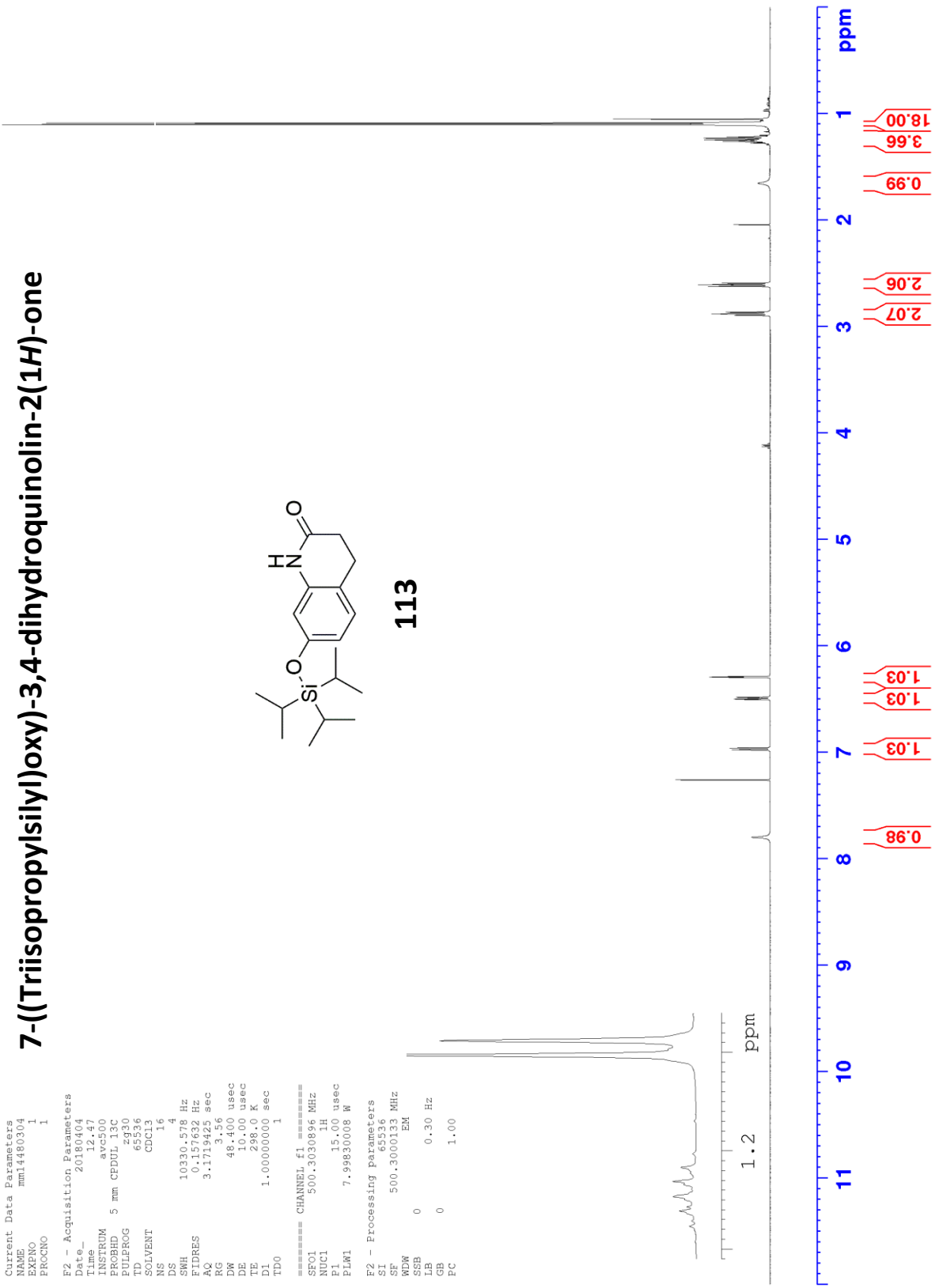
(*R*)-*N*-(3-((3-(*R*)-*N*-(4-((3-Methoxyphenyl)(methyl)amino)butyl)-4-methyl-2-oxo-2,3,4,5-tetrahydro-1*H*-benzo[*b*][1,4]diazepine-6-carboxamide

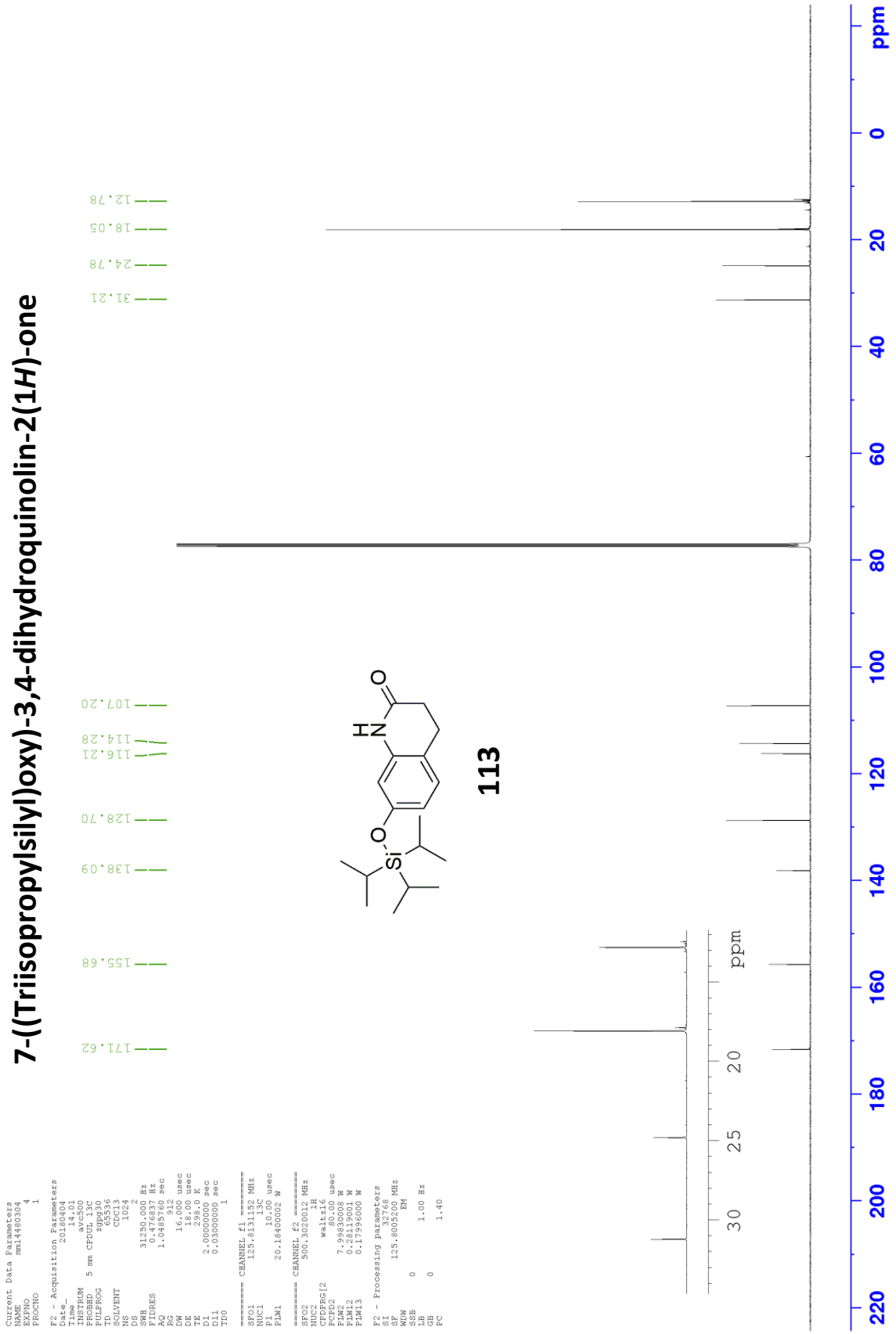


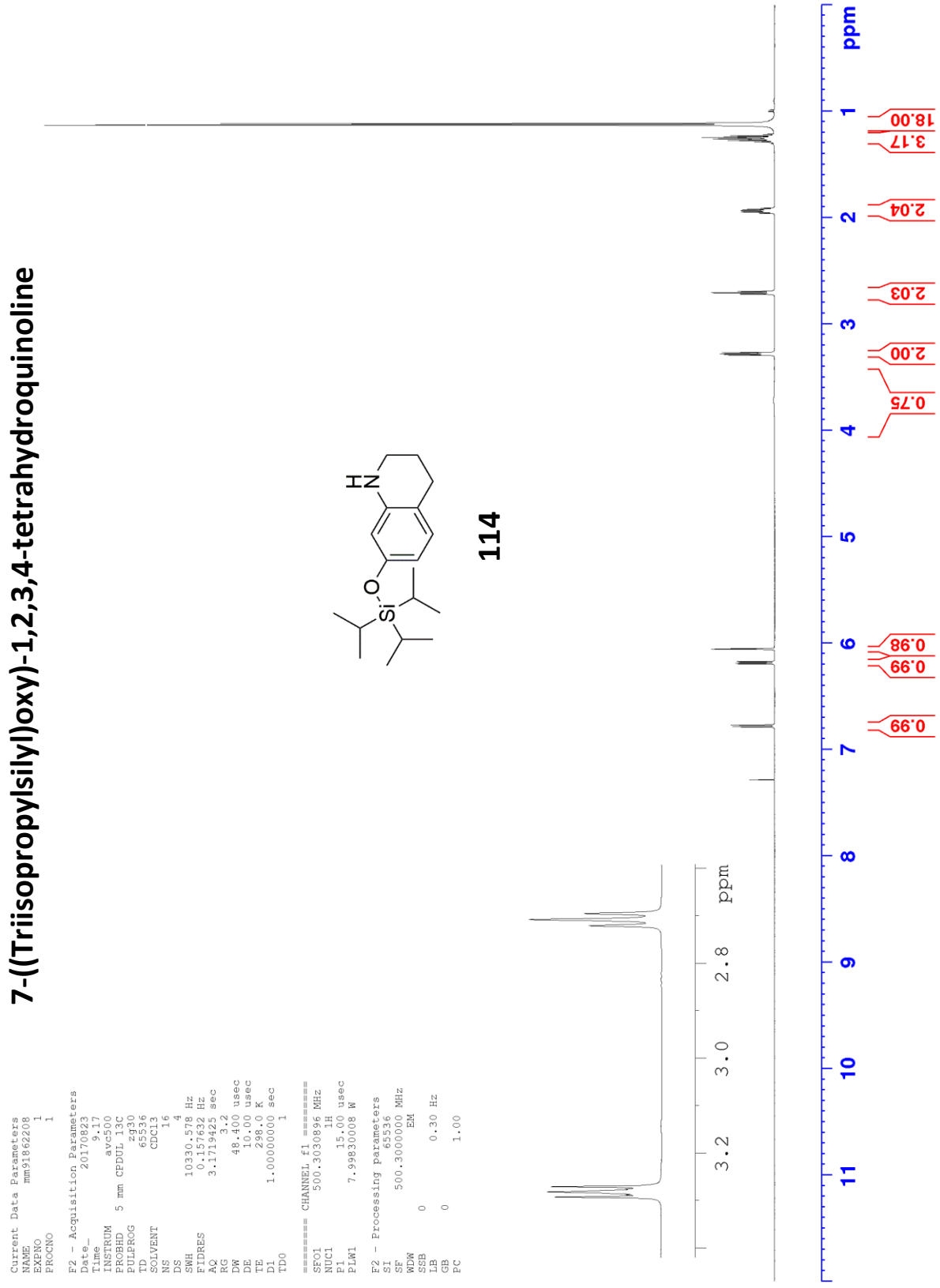
(*R*)96

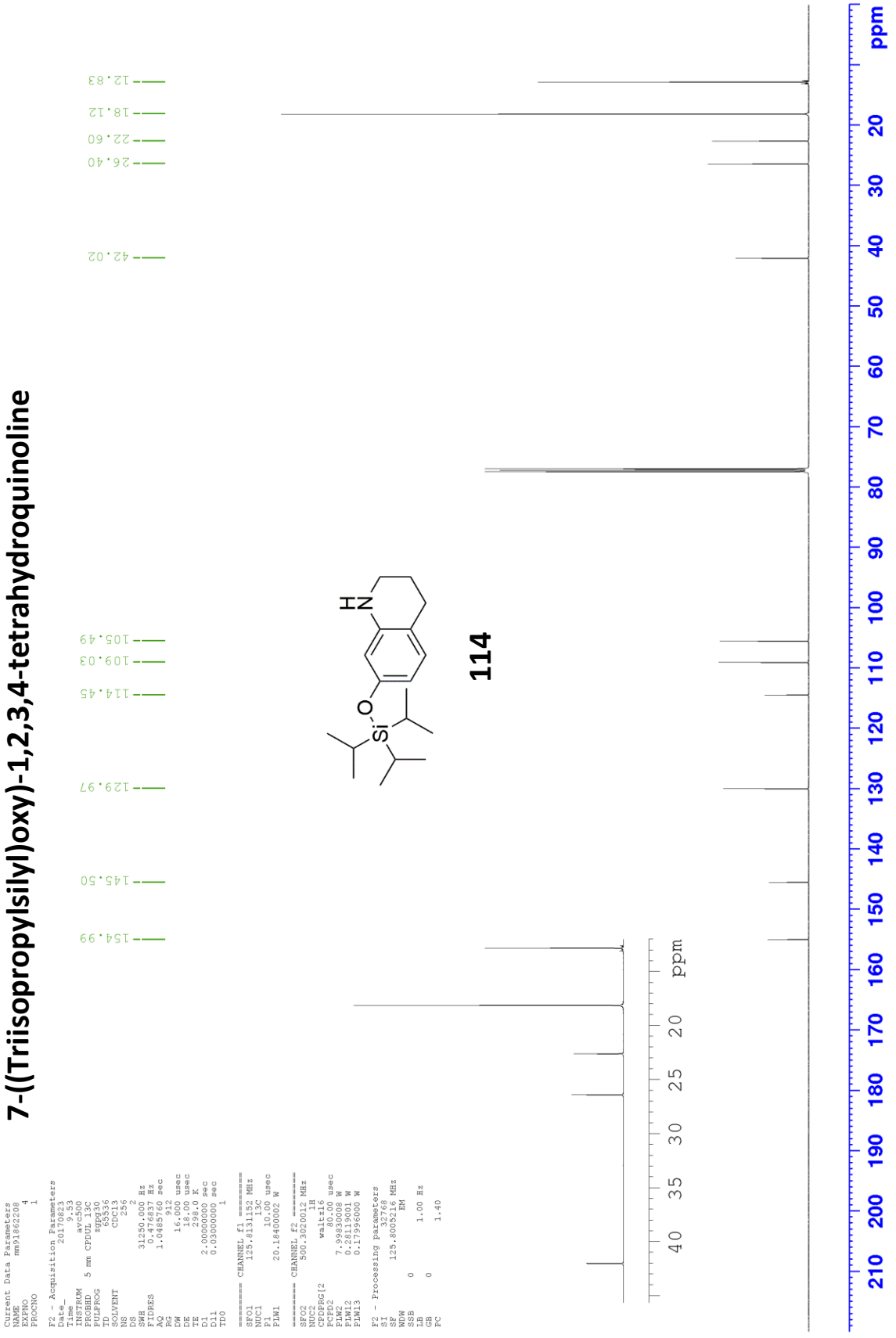
(*R*)-*N*-(3-((3-(*R*)-*N*-(4-((3-Methoxyphenyl)(methyl)amino)butyl)-4-methyl-2-oxo-2,3,4,5-tetrahydro-1*H*-benzo[*b*][1,4]diazepine-6-carboxamide

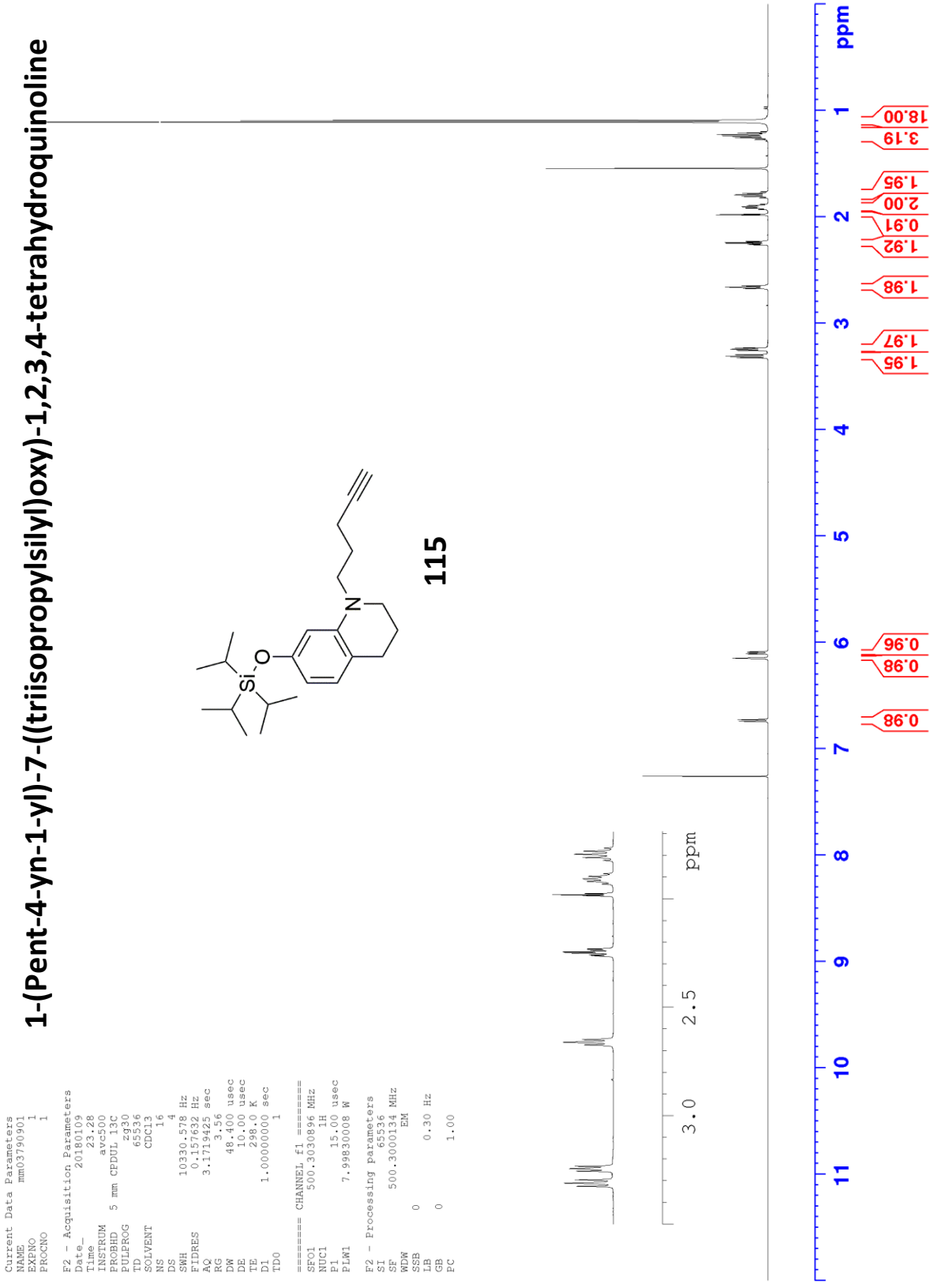


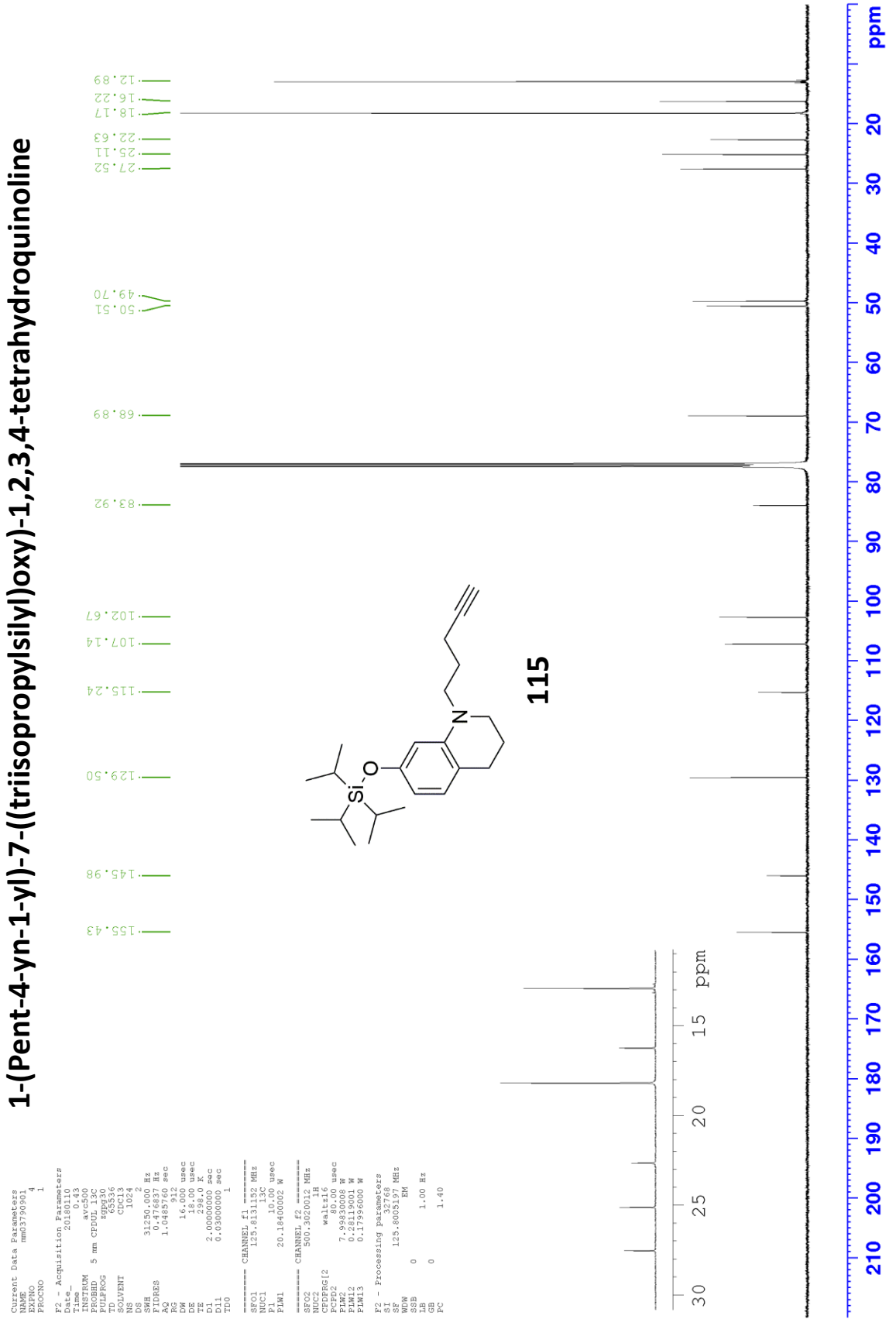

7-((Triisopropylsilyl)oxy)-3,4-dihydroquinolin-2(1H)-one
113
Current Data Parameters
NAME mm14480304
EXPNO 1
PROCNO 1
F2 - Acquisition Parameters
Date_ 20180404
Time 12.47
INSTRUM avc500
PROBHD 5 mm CPDUL 13C
PULPROG zg30
TD 65536
SOLVENT CDCl3
NS 16
DS 4
SWH 10330.578 Hz
FIDRES 0.157632 Hz
AQ 3.1719425 sec
RG 3.56
DW 48.400 usec
DE 10.00 usec
TE 298.0 K
D1 1.00000000 sec
TD0 1
======== CHANNEL f1 ========
SFO1 500.3030896 MHz
NUC1 1H
P1 15.00 usec
PLW1 7.99830008 W
F2 - Processing parameters
SI 65536
SF 500.3000133 MHz
WDW EM
SSB 0
LB 0.30 Hz
GB 0
PC 1.00
1.2
ppm
11
10
9
8
7
6
5
4
3
2
1
ppm
0.98
1.03
1.03
1.03
2.07
2.06
0.99
3.66
18.00

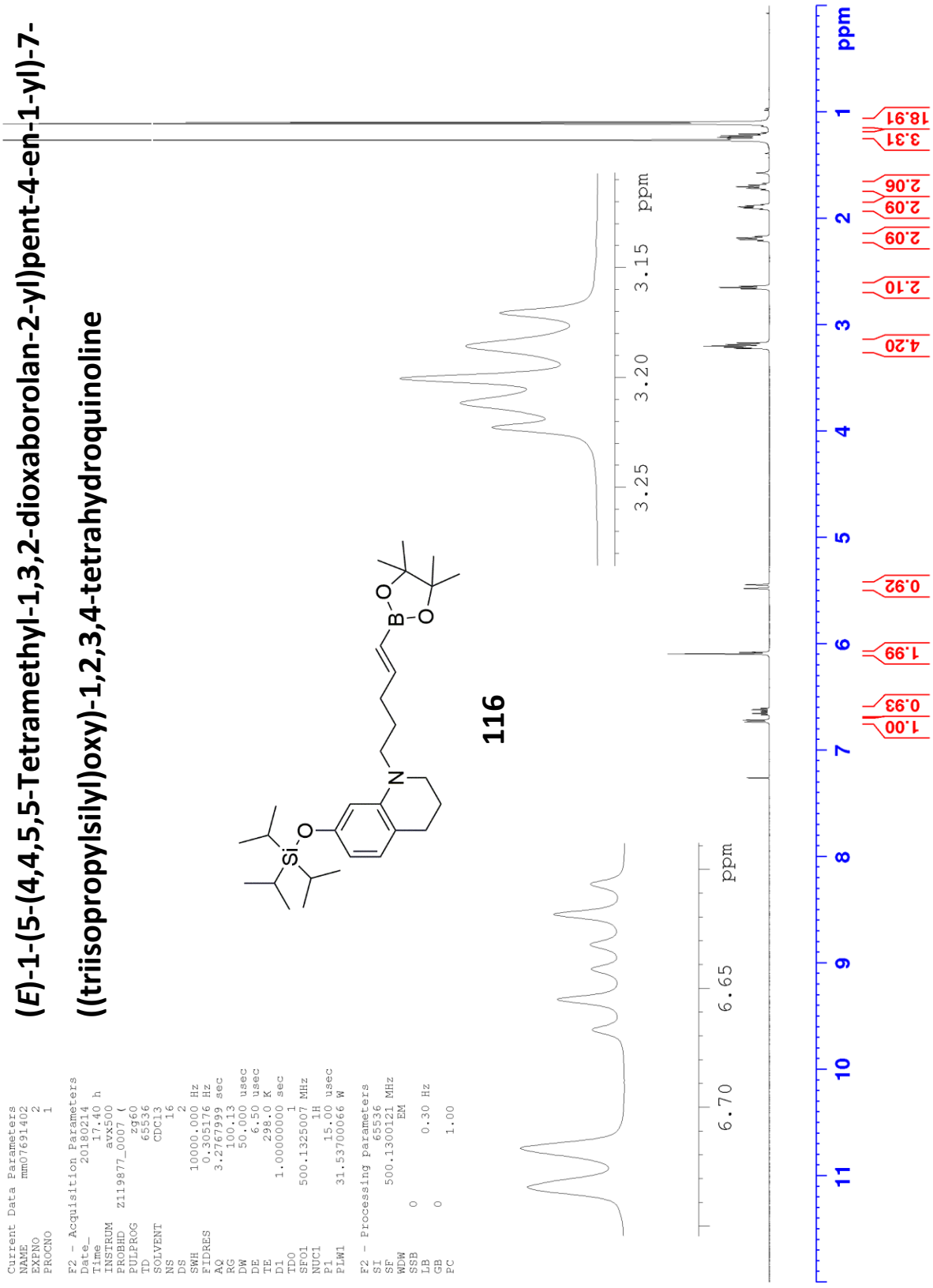

7-((Triisopropylsilyl)oxy)-3,4-dihydroquinolin-2(1H)-one
113
Current Data Parameters
NAME mm14480304
EXPNO 4
PROCNO 1
F2 - Acquisition Parameters
Date_ 20180404
Time 14.01
INSTRUM av600
PROBHD 5 mm CPDUL 13C
PULPROG zgpg30
TD 65536
SOLVENT CDCl3
NS 1024
DS 2
SWH 31250.000 Hz
FIDRES 0.476837 Hz
AQ 1.04857600 sec
RG 912
DW 16.000 usec
DE 18.00 usec
TE 298.0 K
D1 2.00000000 sec
D11 0.03000000 sec
TD0 1
======== CHANNEL f1 ========
SFO1 125.8131152 MHz
NUC1 13C
P1 10.00 usec
PLW1 20.18400002 W
======== CHANNEL f2 ========
SFO2 500.3020012 MHz
NUC2 1H
CPDPRG[2 waltz16
PCPD2 100.00 usec
PLW2 7.99830008 W
PLW12 0.28119001 W
PLW13 0.17996000 W
F2 - Processing parameters
SI 32768
SF 125.8005200 MHz
WDW EM
SSB 0
LB 1.00 Hz
GB 0
PC 1.40
171.62
155.68
138.09
128.70
116.21
114.28
107.20
31.21
24.78
18.05
12.78
ppm
220
200
180
160
140
120
100
80
60
40
20
0


7-((Triisopropylsilyl)oxy)-1,2,3,4-tetrahydroquinoline
114
Current Data Parameters
NAME mm91862208
EXPNO 1
PROCNO 1
F2 - Acquisition Parameters
Date_ 20170823
Time 9.17
INSTRUM avc500
PROBHD 5 mm CPDUL 13C
PULPROG zg30
TD 65536
SOLVENT CDCl3
NS 16
DS 4
SWH 10330.578 Hz
FIDRES 0.157632 Hz
AQ 3.1719425 sec
RG 3.2
DW 48.400 usec
DE 10.00 usec
TE 298.0 K
D1 1.00000000 sec
TD0 1
======== CHANNEL f1 ========
SFO1 500.3030896 MHz
NUC1 1H
P1 15.00 usec
PLW1 7.99830008 W
F2 - Processing parameters
SI 65536
SF 500.3000000 MHz
WDW EM
SSB 0
LB 0.30 Hz
GB 0
PC 1.00
3.2
3.0
2.8
ppm
ppm
18.00
3.17
2.04
2.03
2.00
0.75
0.98
0.99
0.99

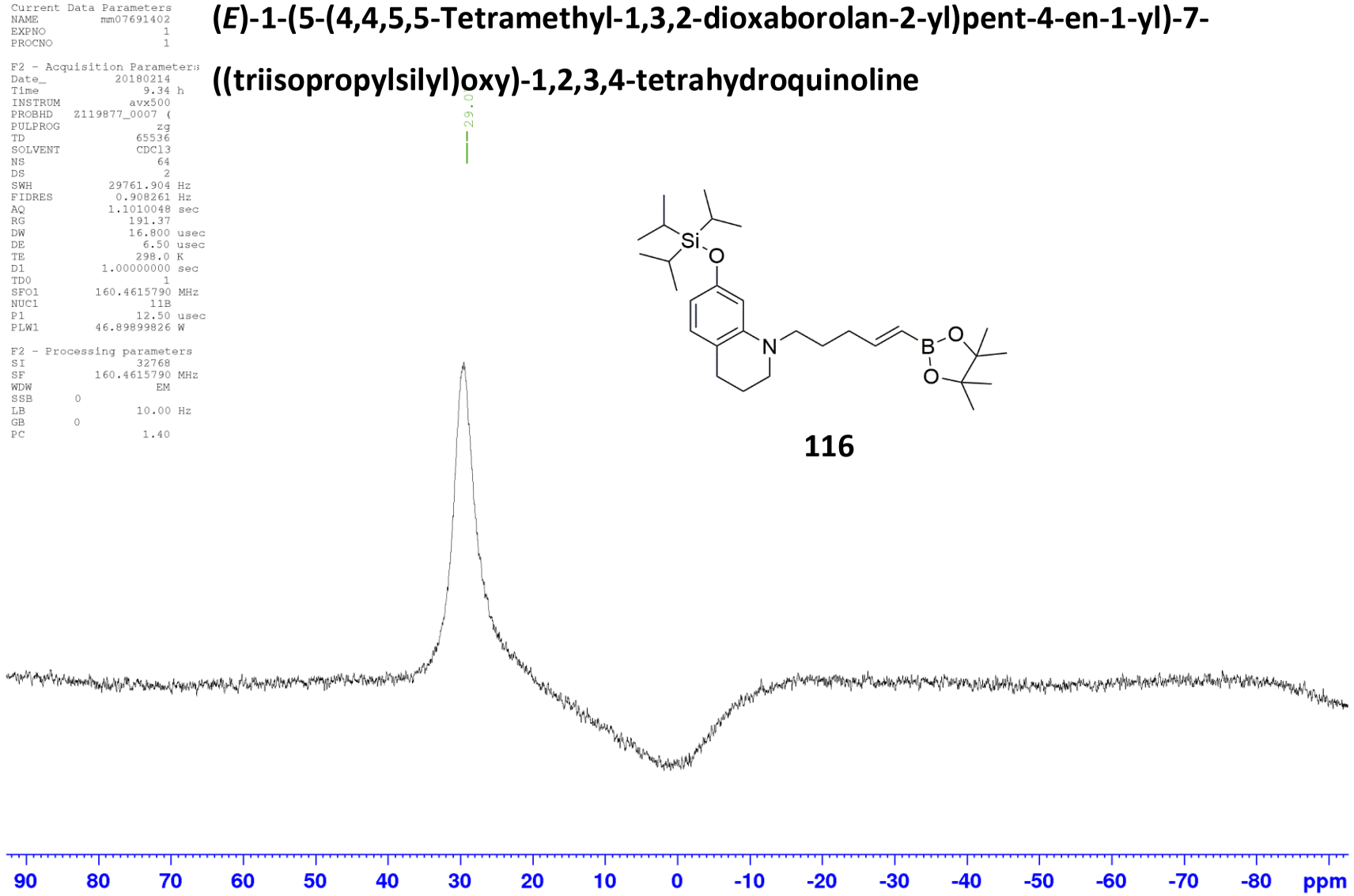

7-((Triisopropylsilyl)oxy)-1,2,3,4-tetrahydroquinoline
114
154.99
145.50
129.97
114.45
109.03
105.49
42.02
26.40
22.60
18.12
12.83
ppm


1-(Pent-4-yn-1-yl)-7-((triisopropylsilyl)oxy)-1,2,3,4-tetrahydroquinoline
115
Current Data Parameters
NAME mm03790901
EXPNO 1
PROCNO 1
F2 - Acquisition Parameters
Date_ 20180109
Time 23.28
INSTRUM avc500
PROBHD 5 mm CPDUL 13C
PULPROG zg30
TD 65536
SOLVENT CDCl3
NS 16
DS 4
SWH 10330.578 Hz
FIDRES 0.157632 Hz
AQ 3.1719425 sec
RG 3.56
DW 48.400 usec
DE 10.00 usec
TE 298.0 K
D1 1.00000000 sec
TD0 1
======== CHANNEL f1 ========
SFO1 500.3030896 MHz
NUC1 1H
P1 15.00 usec
PLW1 7.99830008 W
F2 - Processing parameters
SI 65536
SF 500.3000134 MHz
WDW EM
SSB 0
LB 0.30 Hz
GB 0
PC 1.00
3.0
2.5
ppm
11
10
9
8
7
6
5
4
3
2
1
ppm
0.98
0.98
0.96
1.95
1.97
1.98
1.92
0.91
2.00
1.95
3.19
18.00


1-(Pent-4-yn-1-yl)-7-((triisopropylsilyl)oxy)-1,2,3,4-tetrahydroquinoline
115
12.89
16.22
18.17
22.63
25.11
27.52
49.70
50.51
68.89
83.92
102.67
107.14
115.24
129.50
145.98
155.43
ppm

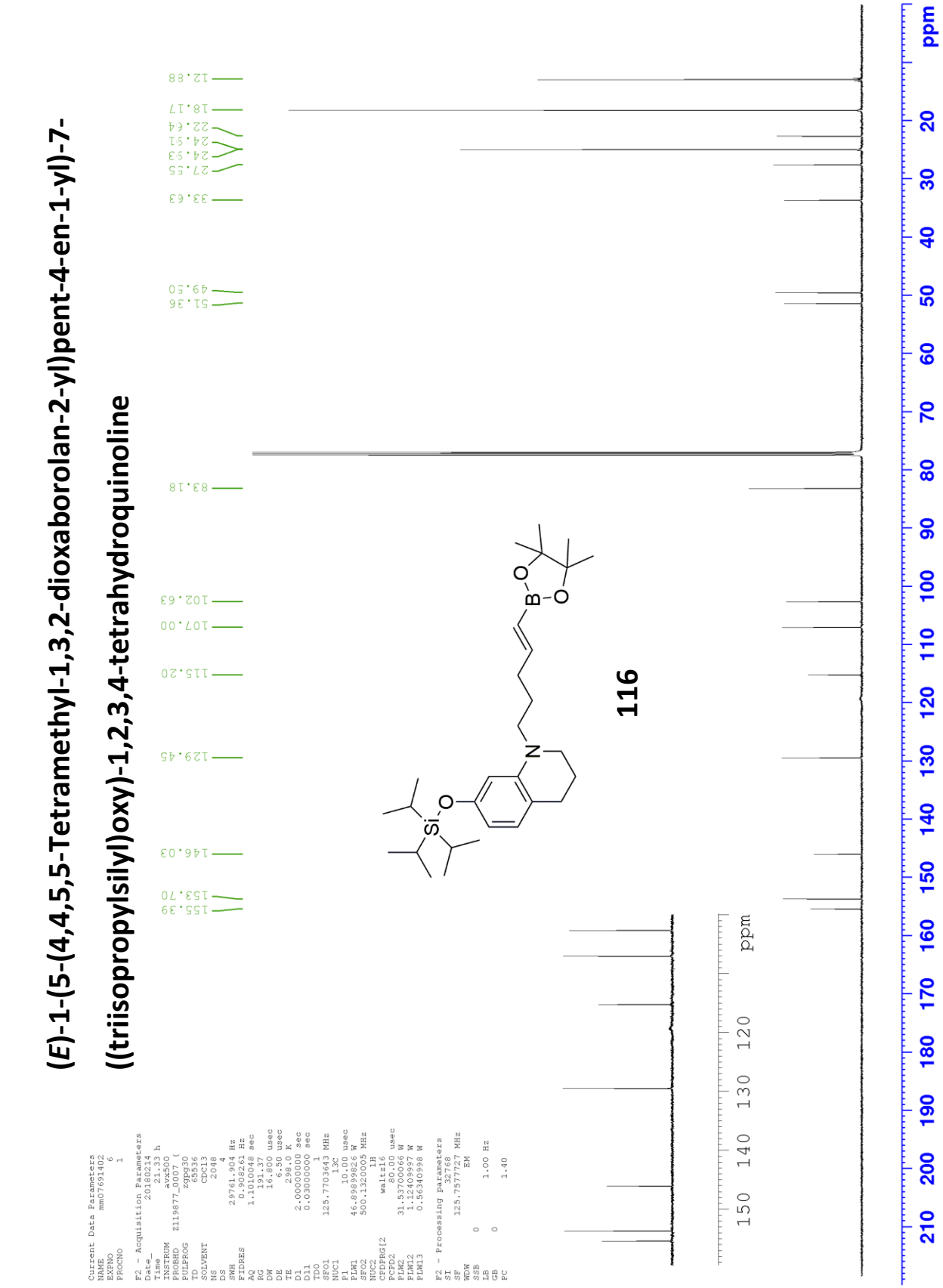

(E)-1-(5-(4,4,5,5-Tetramethyl-1,3,2-dioxaborolan-2-yl)pent-4-en-1-yl)-7-((triisopropylsilyl)oxy)-1,2,3,4-tetrahydroquinoline
116
Current Data Parameters
NAME mm07691402
EXPNO 2
PROCNO 1
F2 - Acquisition Parameters
Date_ 20180214
Time 17.40 h
INSTRUM avx500
PROBHD Z119877_0007 (
PULPROG zg60
TD 65536
SOLVENT CDCl3
NS 16
DS 2
SWH 10000.000 Hz
FIDRES 0.305176 Hz
AQ 3.2767999 sec
RG 100.13
DW 50.000 usec
DE 6.50 usec
TE 298.0 K
D1 1.00000000 sec
TD0 1
SFO1 500.1325007 MHz
NUC1 1H
P1 15.00 usec
PLW1 31.53700066 W
F2 - Processing parameters
SI 65536
SF 500.1300121 MHz
WDW EM
SSB 0
LB 0.30 Hz
GB 0
PC 1.00
6.70
6.65
ppm
3.25
3.20
3.15
ppm
1.00
0.93
1.99
0.92
2.10
4.20
2.09
2.09
2.06
3.31
18.91
ppm

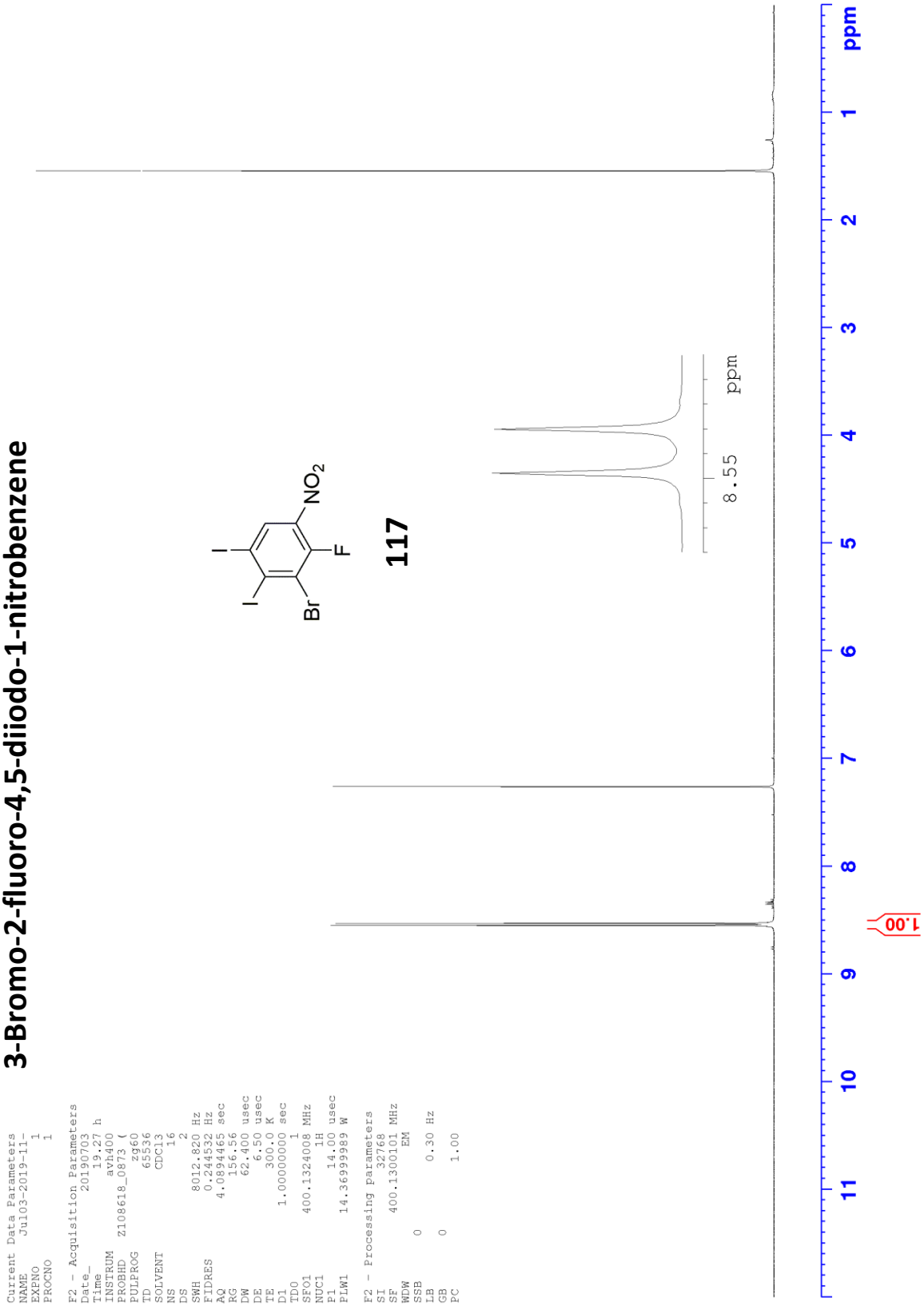
(*E*)-1-(5-(4,4,5,5-Tetramethyl-1,3,2-dioxaborolan-2-yl)pent-4-en-1-yl)-7-((triisopropylsilyl)oxy)-1,2,3,4-tetrahydroquinoline

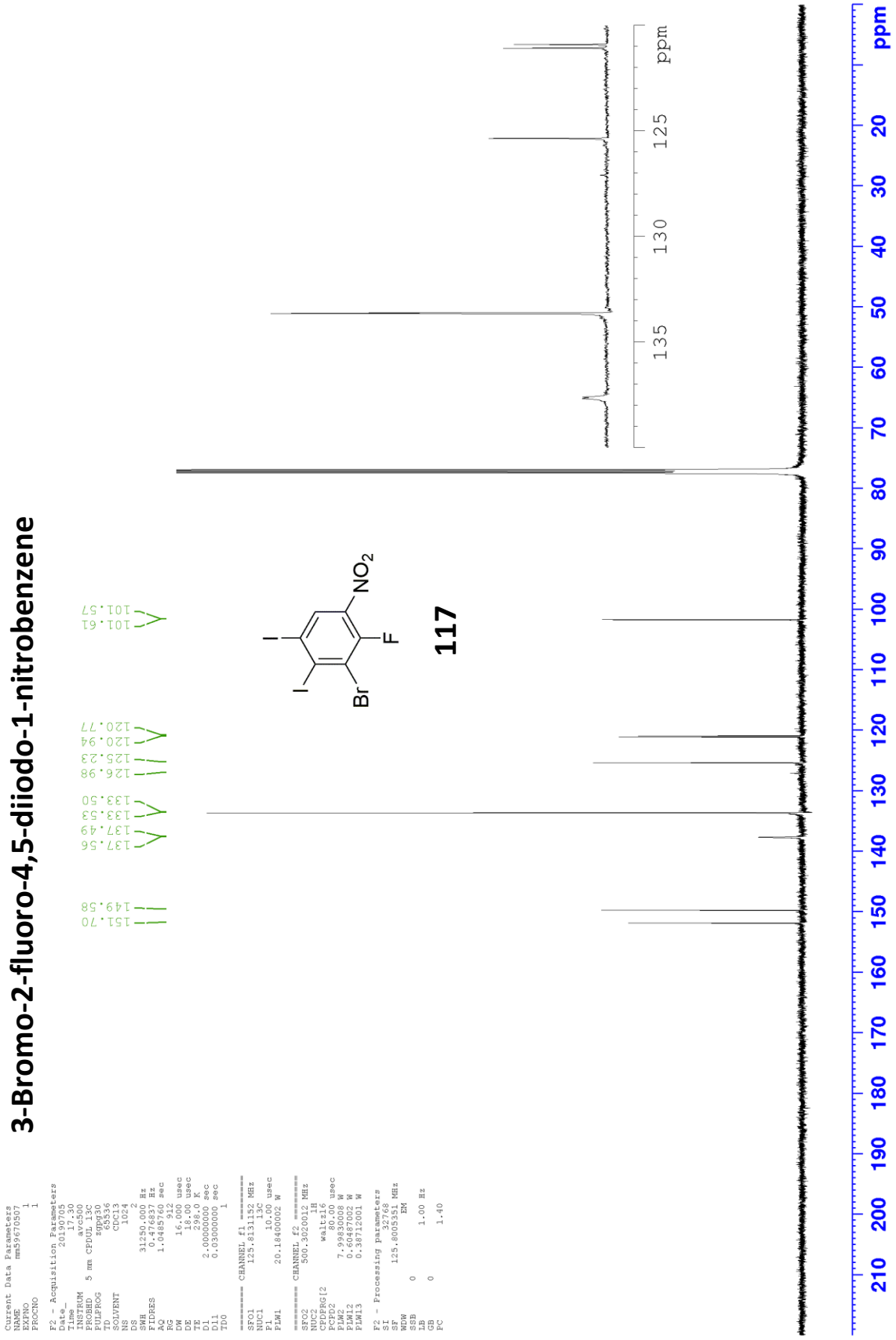


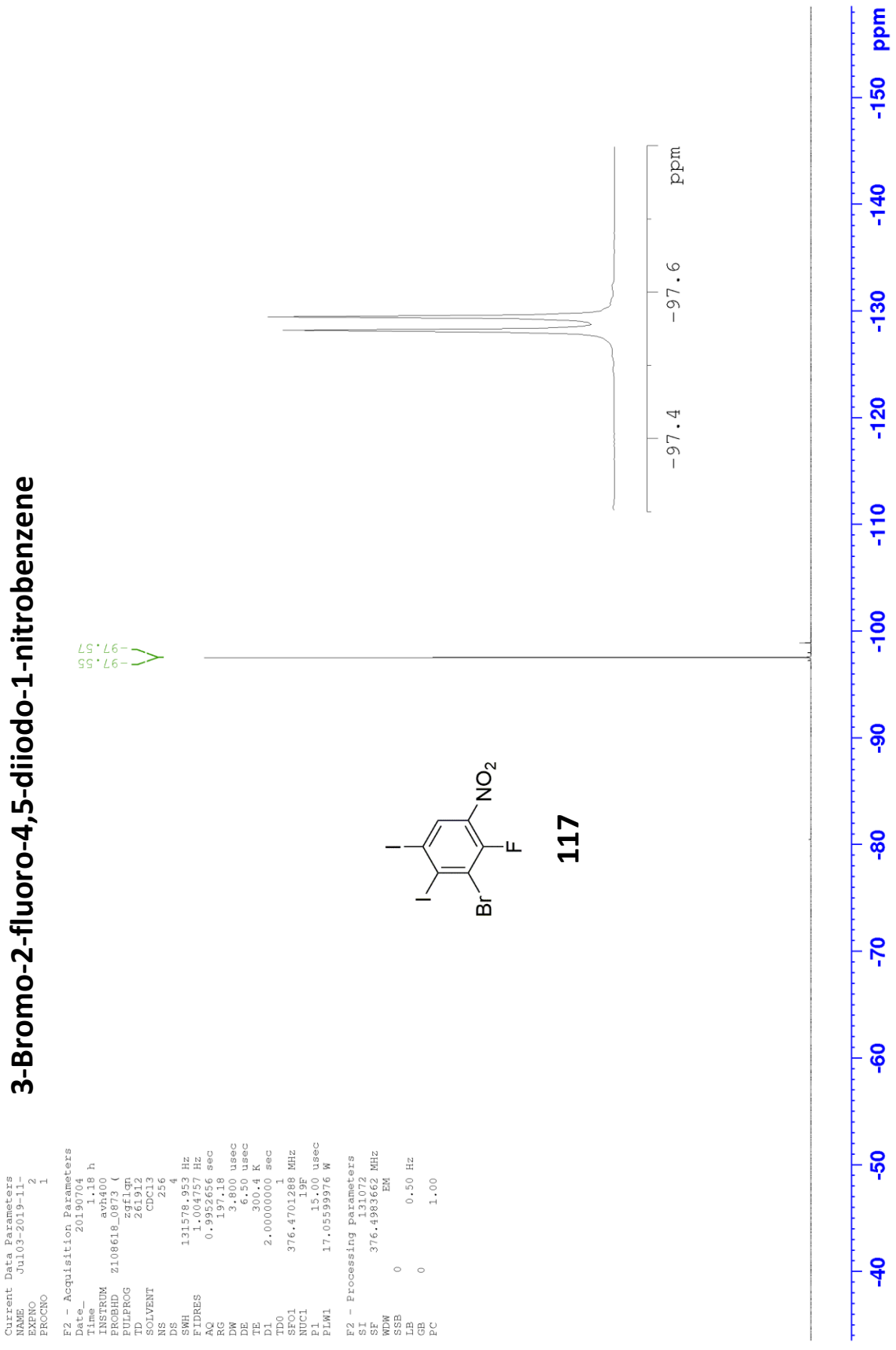
116

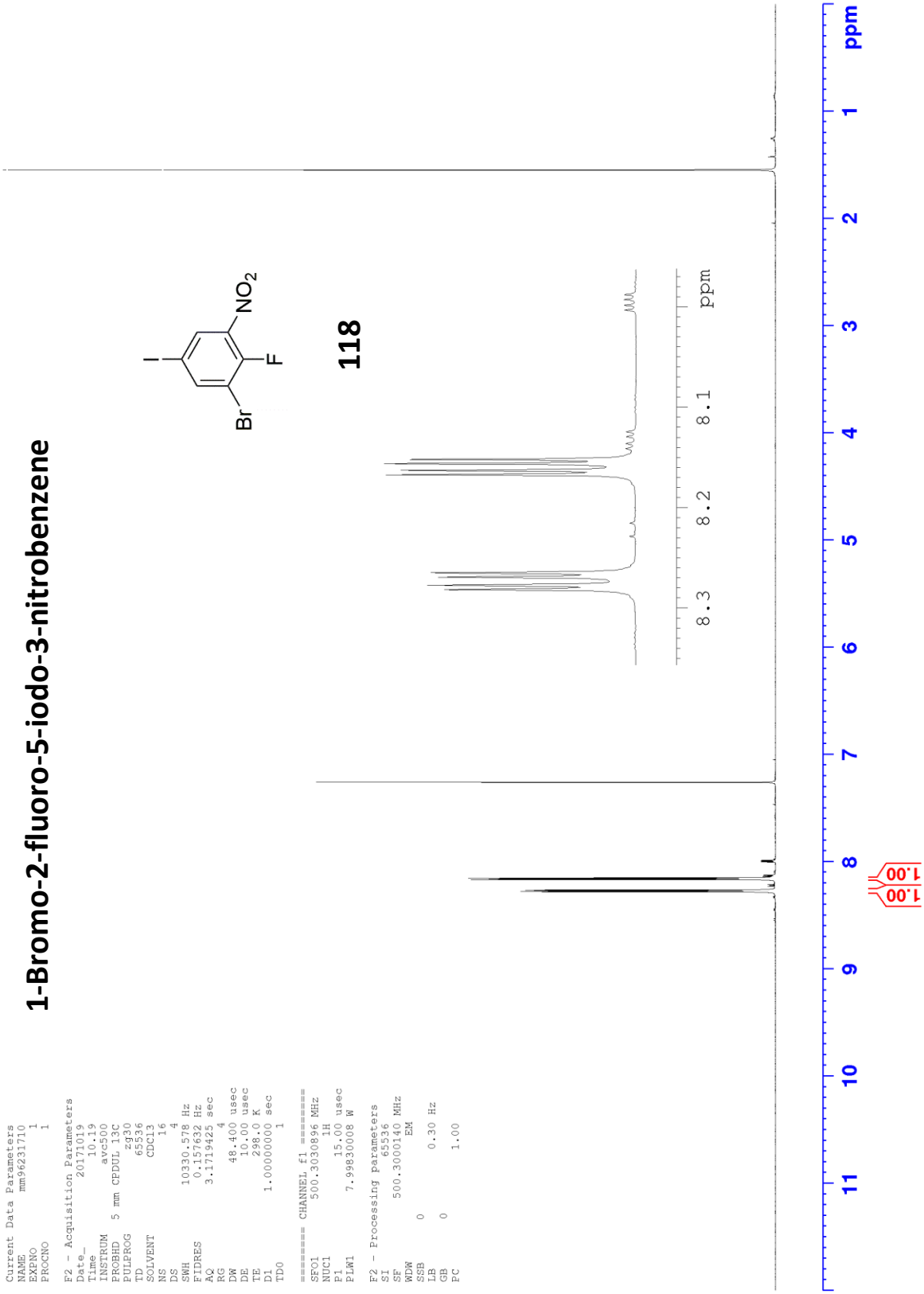
(*E*)-1-(5-(4,4,5,5-Tetramethyl-1,3,2-dioxaborolan-2-yl)pent-4-en-1-yl)-7-((triisopropylsilyl)oxy)-1,2,3,4-tetrahydroquinoline

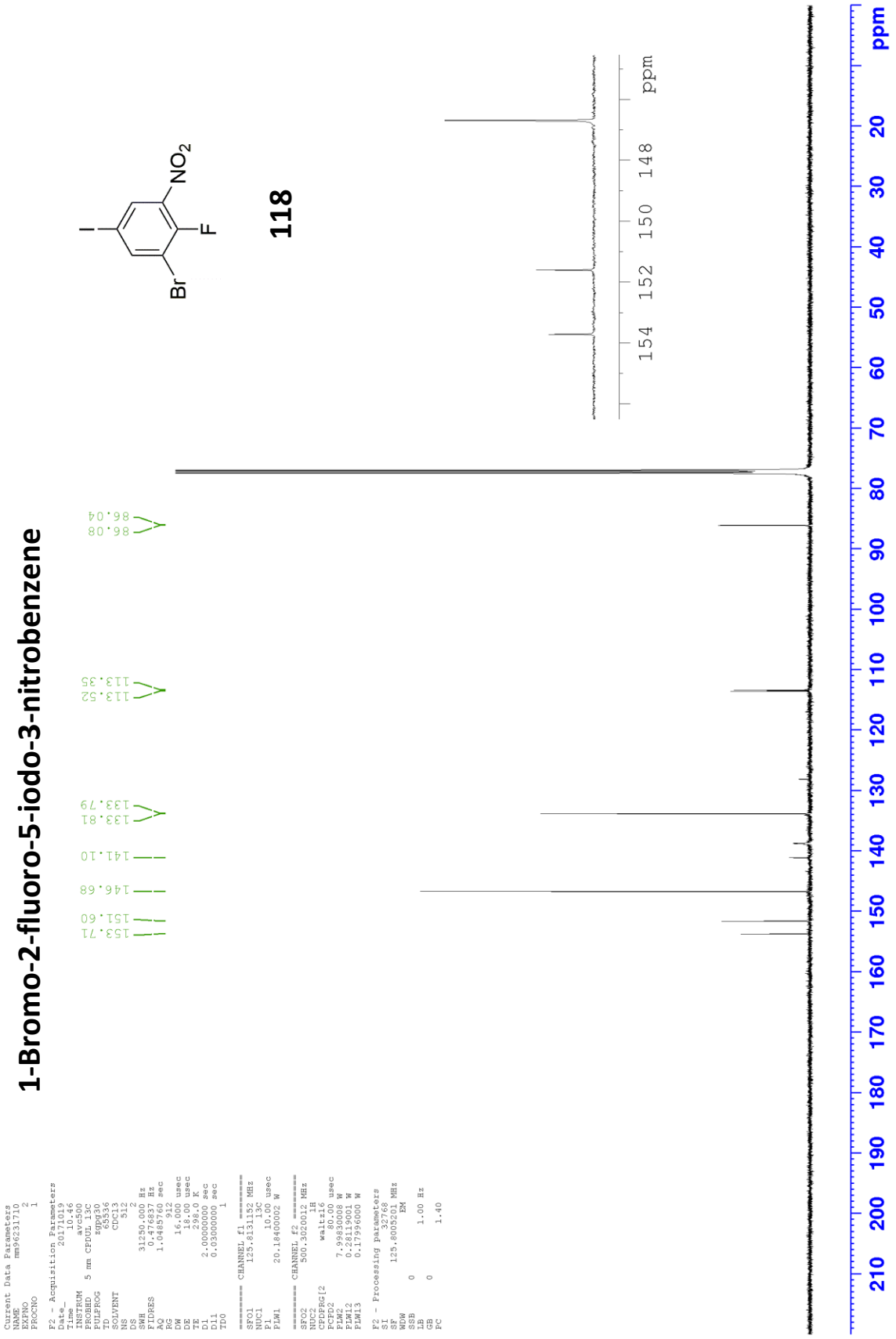


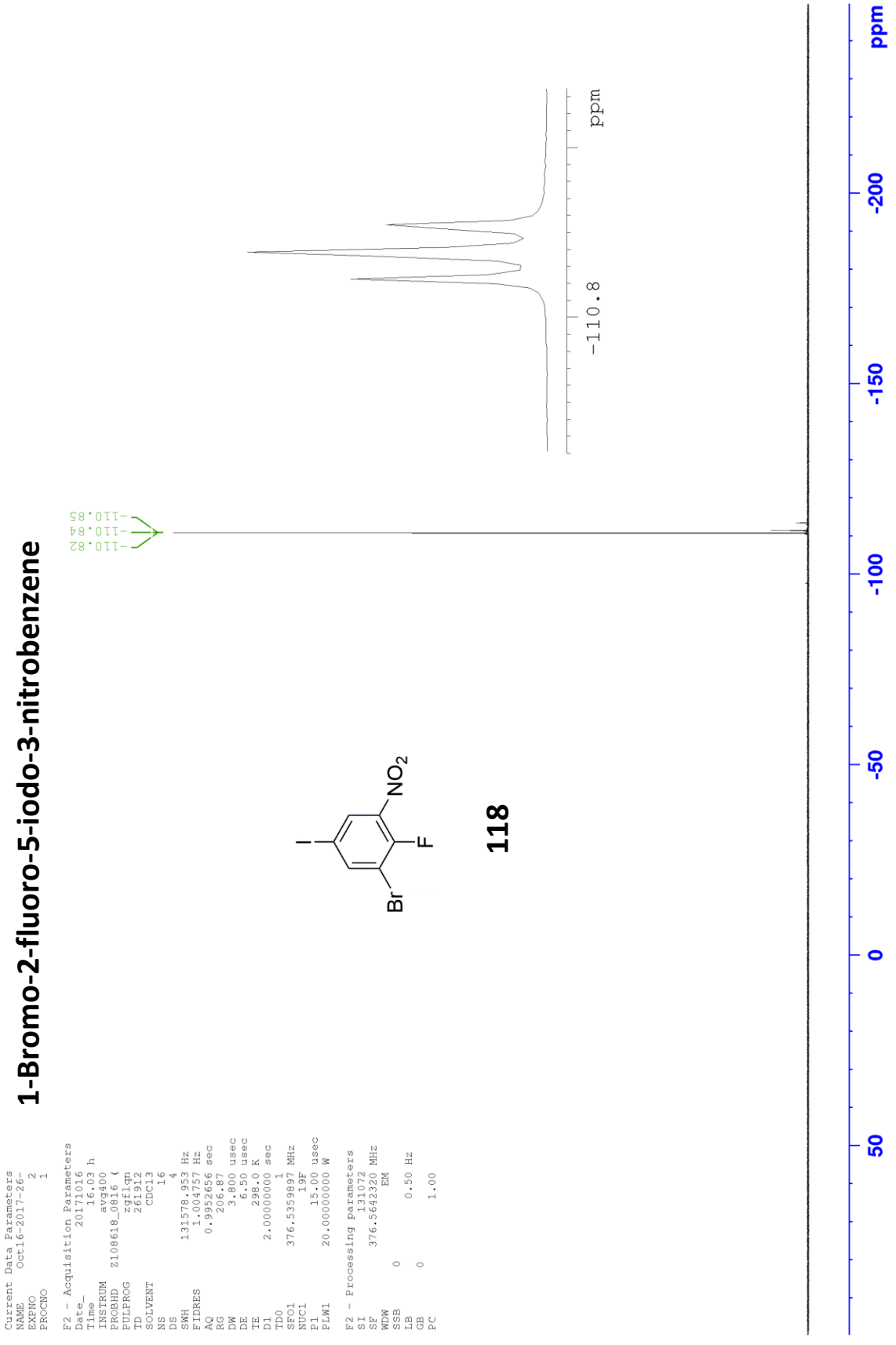

3-Bromo-2-fluoro-4,5-diiodo-1-nitrobenzene
117
8.55
ppm
1.00
Current Data Parameters
NAME Ju103-2019-11-
EXPNO 1
PROCNO 1
F2 - Acquisition Parameters
Date_ 20190703
Time_ 19.27 h
INSTRUM avb400
PROBHD Z108618_0873 (
PULPROG zg60
TD 65536
SOLVENT CDCl3
NS 16
DS 2
SWH 8012.820 Hz
FIDRES 0.2445532 Hz
AQ 4.0894465 sec
RG 156.56
DW 62.400 usec
DE 6.50 usec
TE 300.0 K
D1 1.00000000 sec
TD0 1
SFO1 400.1324008 MHz
NUC1 1H
P1 14.00 usec
PLW1 14.36999989 W
F2 - Processing parameters
SI 32768
SF 400.1300101 MHz
WDW EM
SSB 0
LB 0.30 Hz
GB 0
PC 1.00
11
10
9
8
7
6
5
4
3
2
1
ppm


3-Bromo-2-fluoro-4,5-diiodo-1-nitrobenzene
117
Br
I
I
F
NO2
101.61
101.57
120.77
120.94
125.23
126.98
133.50
133.53
137.49
137.56
149.58
151.70
135
130
125
ppm
210
200
190
180
170
160
150
140
130
120
110
100
90
80
70
60
50
40
30
20
ppm

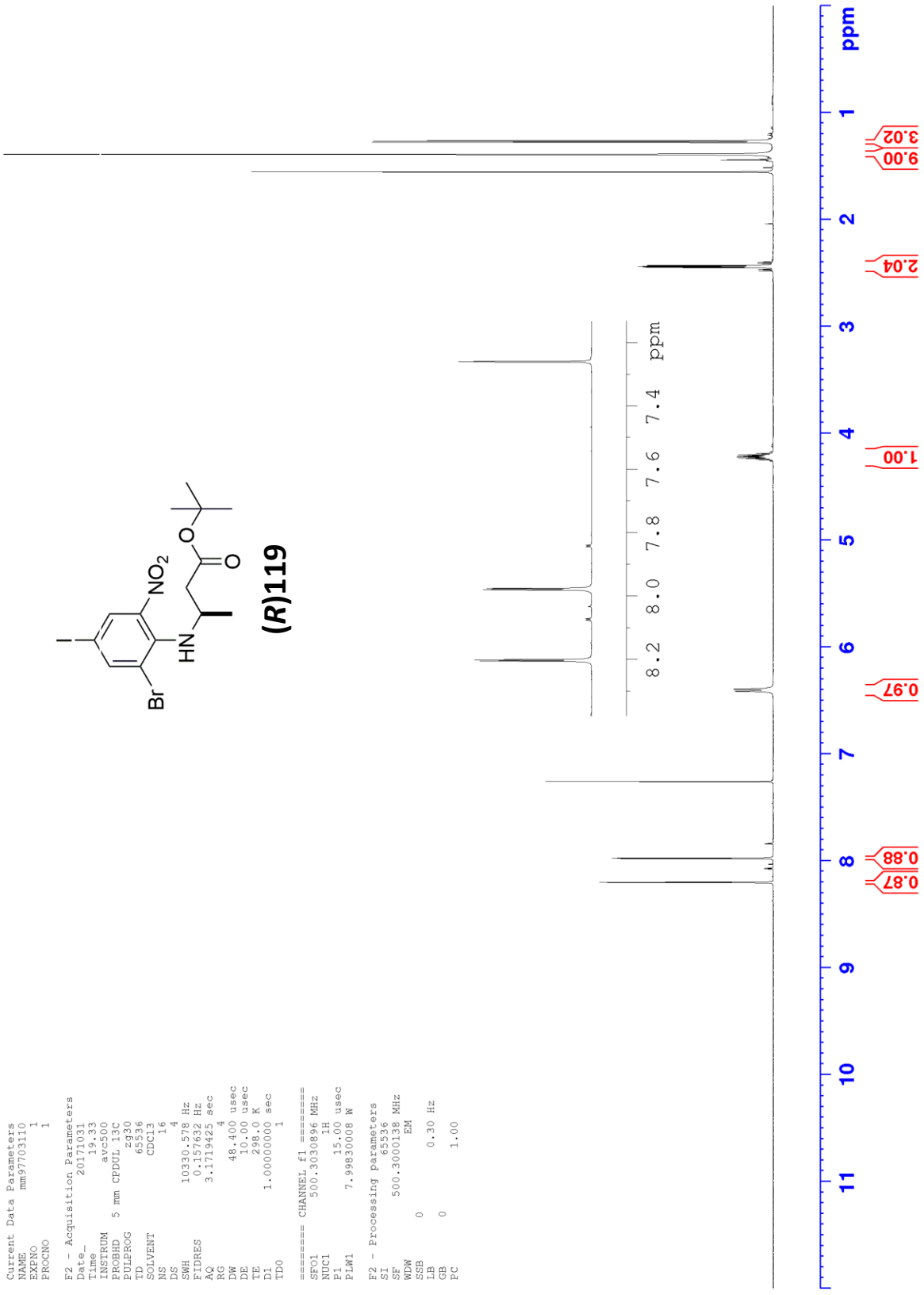

3-Bromo-2-fluoro-4,5-diiodo-1-nitrobenzene
Current Data Parameters
NAME Jul03-2019-11-
EXPNO 2
PROCNO 1
F2 - Acquisition Parameters
Date_ 20190704
Time 1.18 h
INSTRUM avh400
PROBHD Z108618_0873 (
PULPROG zgflqn
TD 261912
SOLVENT CDCl3
NS 256
DS 4
SWH 131578.953 Hz
FIDRES 1.004757 Hz
AQ 0.995656 sec
RG 197.18
DW 3.800 usec
DE 6.50 usec
TE 300.4 K
D1 2.00000000 sec
TD0 1
SFO1 376.4701288 MHz
NUC1 19F
P1 15.00 usec
PLW1 17.05599976 W
F2 - Processing parameters
SI 131072
SF 376.4983662 MHz
WDW EM
SSB 0
LB 0.50 Hz
GB 0
PC 1.00
-97.57
-97.55
-97.4
-97.6
ppm
-40
-50
-60
-70
-80
-90
-100
-110
-120
-130
-140
-150
ppm
NO2
F
I
I
Br
117


1-Bromo-2-fluoro-5-iodo-3-nitrobenzene
118
NO2
I
F
Br
ppm
8.3
8.2
8.1
1.00
1.00
Current Data Parameters
NAME mm96231710
EXPNO 1
PROCNO 1
F2 - Acquisition Parameters
Date_ 20171019
Time_ 10.19
INSTRUM ave500
PROBHD 5 mm CPDUL 13C
PULPROG zg30
TD 65536
SOLVENT CDCl3
NS 16
DS 4
SWH 10330.578 Hz
FIDRES 0.157632 Hz
AQ 3.1719425 sec
RG 4
DW 48.400 usec
DE 10.00 usec
TE 298.0 K
D1 1.00000000 sec
TD0 1
======== CHANNEL f1 ========
SFO1 500.3030896 MHz
NUC1 1H
P1 15.00 usec
PLW1 7.99830008 W
F2 - Processing parameters
SI 65536
SF 500.3000140 MHz
WDW EM
SSB 0
LB 0.30 Hz
GB 0
PC 1.00


1-Bromo-2-fluoro-5-iodo-3-nitrobenzene
118
NO2
F
Br
I
153.71
151.60
146.68
141.10
133.81
133.79
113.52
113.35
86.08
86.04
154 152 150 148 ppm
210 200 190 180 170 160 150 140 130 120 110 100 90 80 70 60 50 40 30 20 ppm
Current Data Parameters
NAME mm96231710
EXPNO 2
PROCNO 1
F2 - Acquisition Parameters
Date_ 20171019
Time 10:46
INSTRUM av500
PROBHD 5 mm CPDUL 13C
PULPROG zgpg30
TD 65536
SOLVENT CDCl3
NS 512
DS 2
SWH 31250.000 Hz
FIDRES 0.476837 Hz
AQ 1.0485760 sec
RG 912
DW 16.000 usec
DE 18.00 usec
TE 298.0 K
D1 2.00000000 sec
D11 0.03000000 sec
TD0 1
======== CHANNEL f1 ========
SFO1 125.8131152 MHz
NUC1 13C
P1 10.00 usec
PLW1 20.18400002 W
======== CHANNEL f2 ========
SFO2 500.3020012 MHz
NUC2 1H
CPDPRG[2 waltz16
PCPD2 80.00 usec
PLW2 7.99830008 W
PLW12 0.28119001 W
PLW13 0.17996000 W
F2 - Processing parameters
SI 32768
SF 125.8005201 MHz
WDW EM
SSB 0
LB 1.00 Hz
GB 0
PC 1.40


1-Bromo-2-fluoro-5-iodo-3-nitrobenzene
118
Br
F
I
NO2
-110.82
-110.84
-110.85
-110.8
ppm
50
0
-50
-100
-150
-200
ppm

tert-Butyl (*R*)-3-((2-bromo-4-iodo-6-nitrophenyl)amino)butanoate

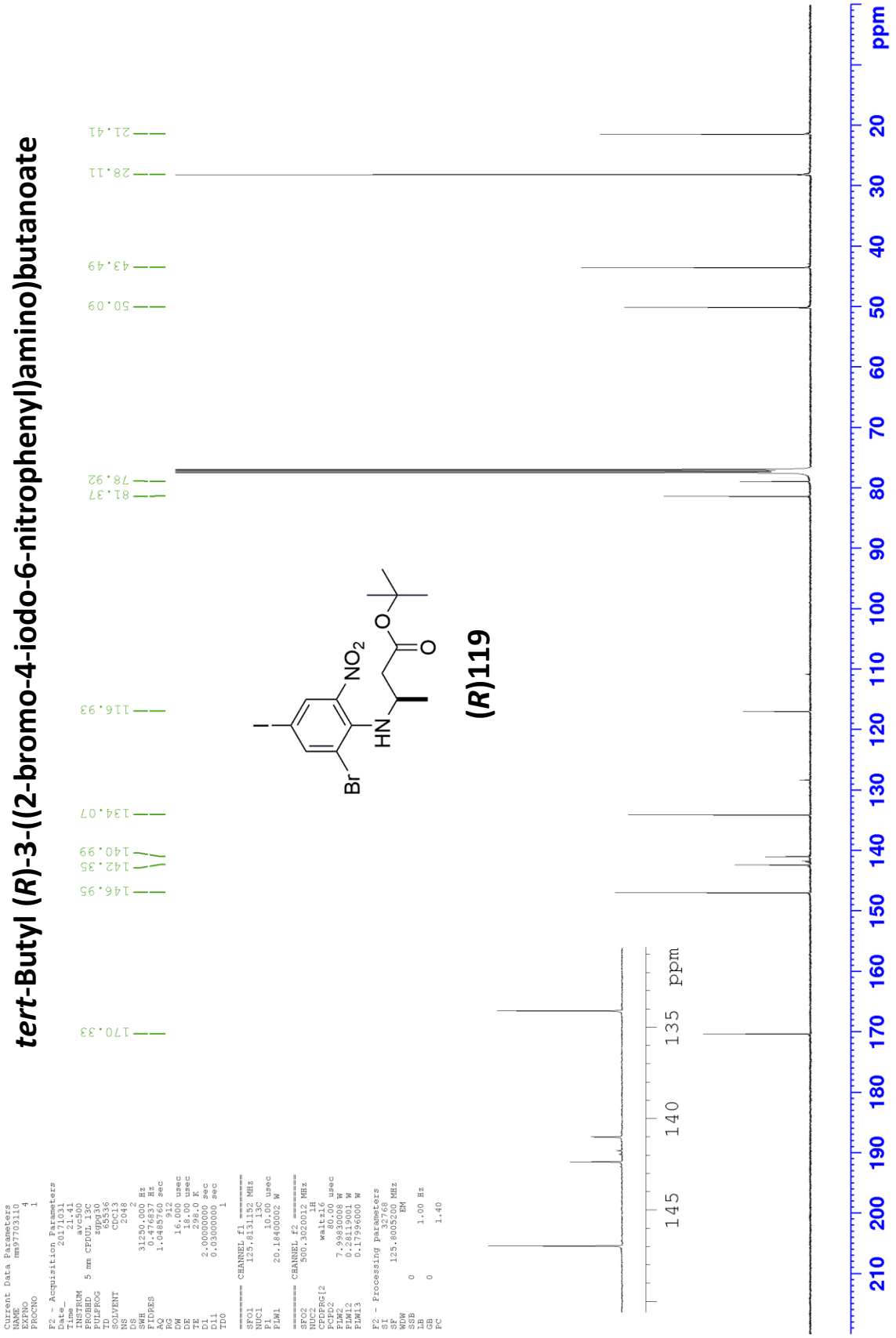



```
Current Data Parameters
NAME        mm97703110
EXPNO              1
PROCNO             1

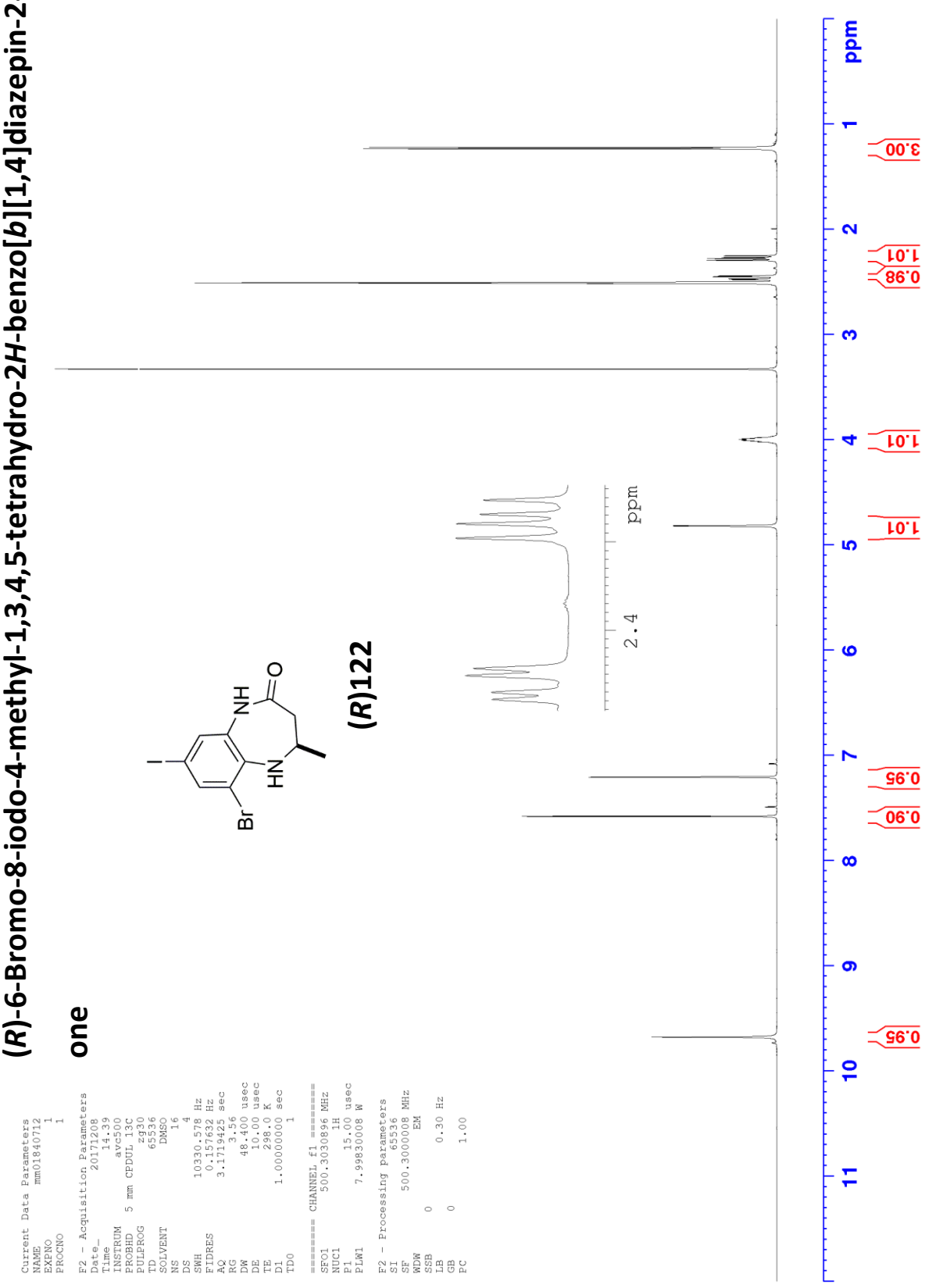
F2 - Acquisition Parameters
Date_        20171031
Time             19.33
INSTRUM         avc500
PROBHD   5 mm CPDUL 13C
PULPROG          zg30
TD              65536
SOLVENT         CDCl3
NS                 16
DS                  4
SWH         10330.578 Hz
FIDRES       0.157632 Hz
AQ           3.1719425 sec
RG                  4
DW             48.400 usec
DE             10.00 usec
TE             298.0 K
D1          1.00000000 sec
TD0                 1

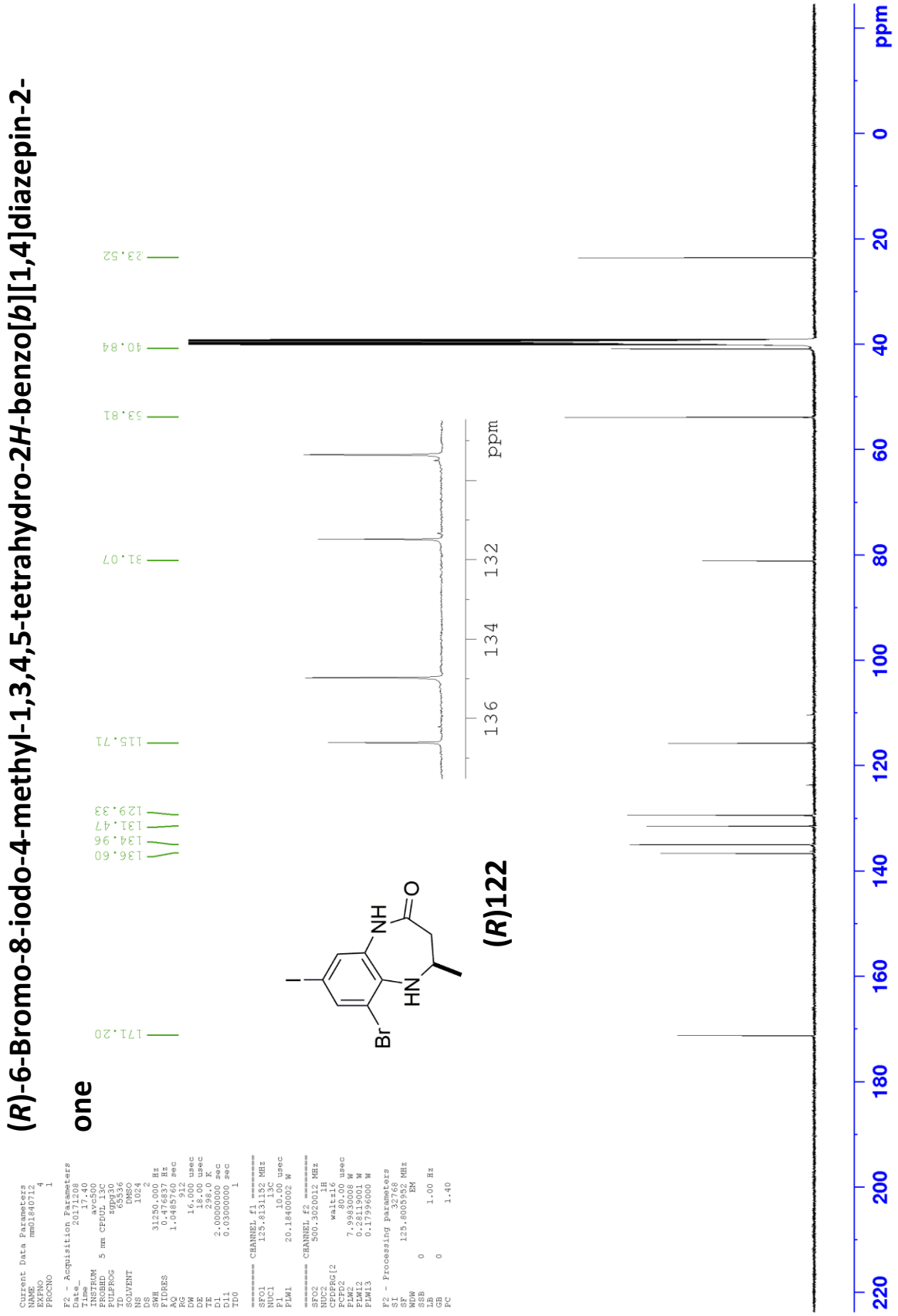
======== CHANNEL f1 ========
SFO1        500.3030896 MHz
NUC1               1H
P1              15.00 usec
PLW1        7.99830008 W

F2 - Processing parameters
SI              65536
SF          500.3000138 MHz
WDW                EM
SSB             0
LB              0.30 Hz
GB              0
PC              1.00
```

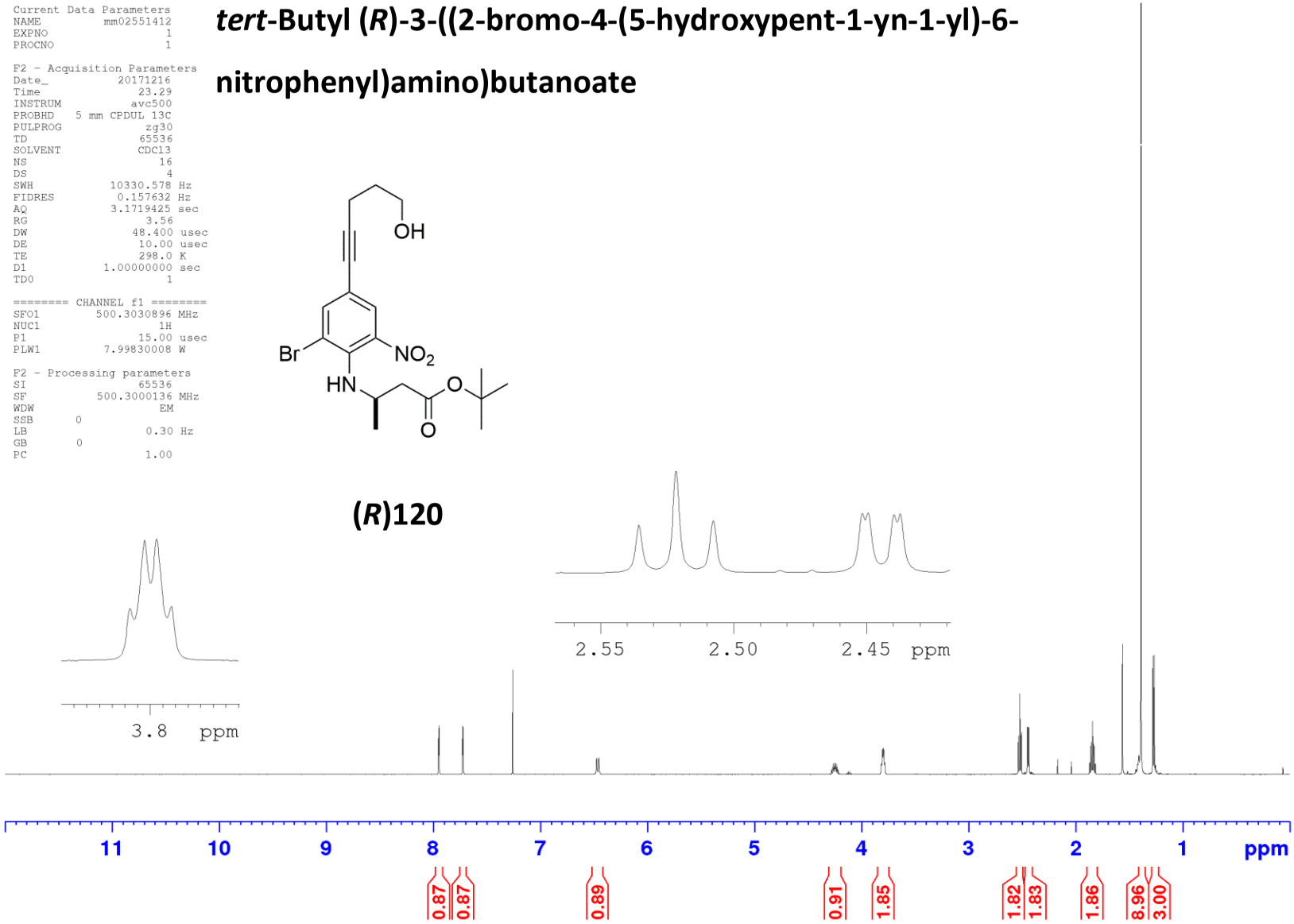

tert-Butyl (R)-3-((2-bromo-4-iodo-6-nitrophenyl)amino)butanoate
(R)119
170.33
146.95
142.35
140.99
134.07
116.93
81.37
78.92
50.09
43.49
28.11
21.41
ppm

(*R*)-6-Bromo-8-iodo-4-methyl-1,3,4,5-tetrahydro-2*H*-benzo[*b*][1,4]diazepin-2-one

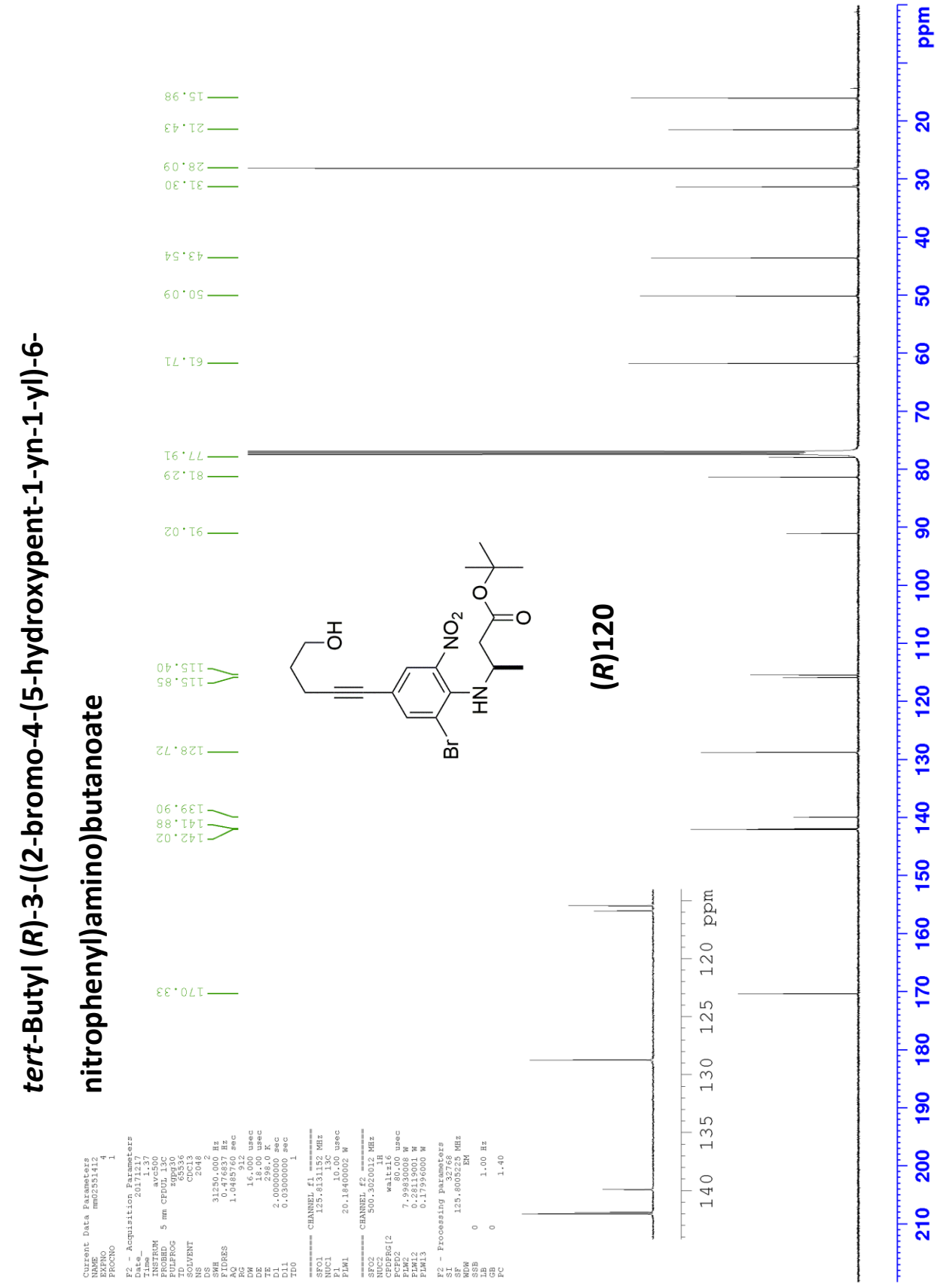



(R)-6-Bromo-8-iodo-4-methyl-1,3,4,5-tetrahydro-2H-benzo[b][1,4]diazepin-2-one
(R)122
Br
NH
HN
O
ppm
136
134
132
171.20
136.60
134.96
131.47
129.33
115.71
81.07
53.81
40.84
23.52
220
200
180
160
140
120
100
80
60
40
20
0

tert-Butyl (*R*)-3-((2-bromo-4-(5-hydroxypent-1-yn-1-yl)-6-nitrophenyl)amino)butanoate



***tert*-Butyl (*R*)-3-((2-bromo-4-(5-hydroxypent-1-yn-1-yl)-6-nitrophenyl)amino)butanoate**



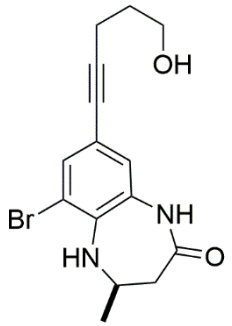
tert-(*R*)-6-Bromo-8-(6-hydroxyhex-1-yn-1-yl)-4-methyl-1,3,4,5-tetrahydro-2*H*-benzo[*b*][1,4]diazepin-2-one

```
Current Data Parameters
NAME          mm02541412
EXPNO                  1
PROCNO                 1

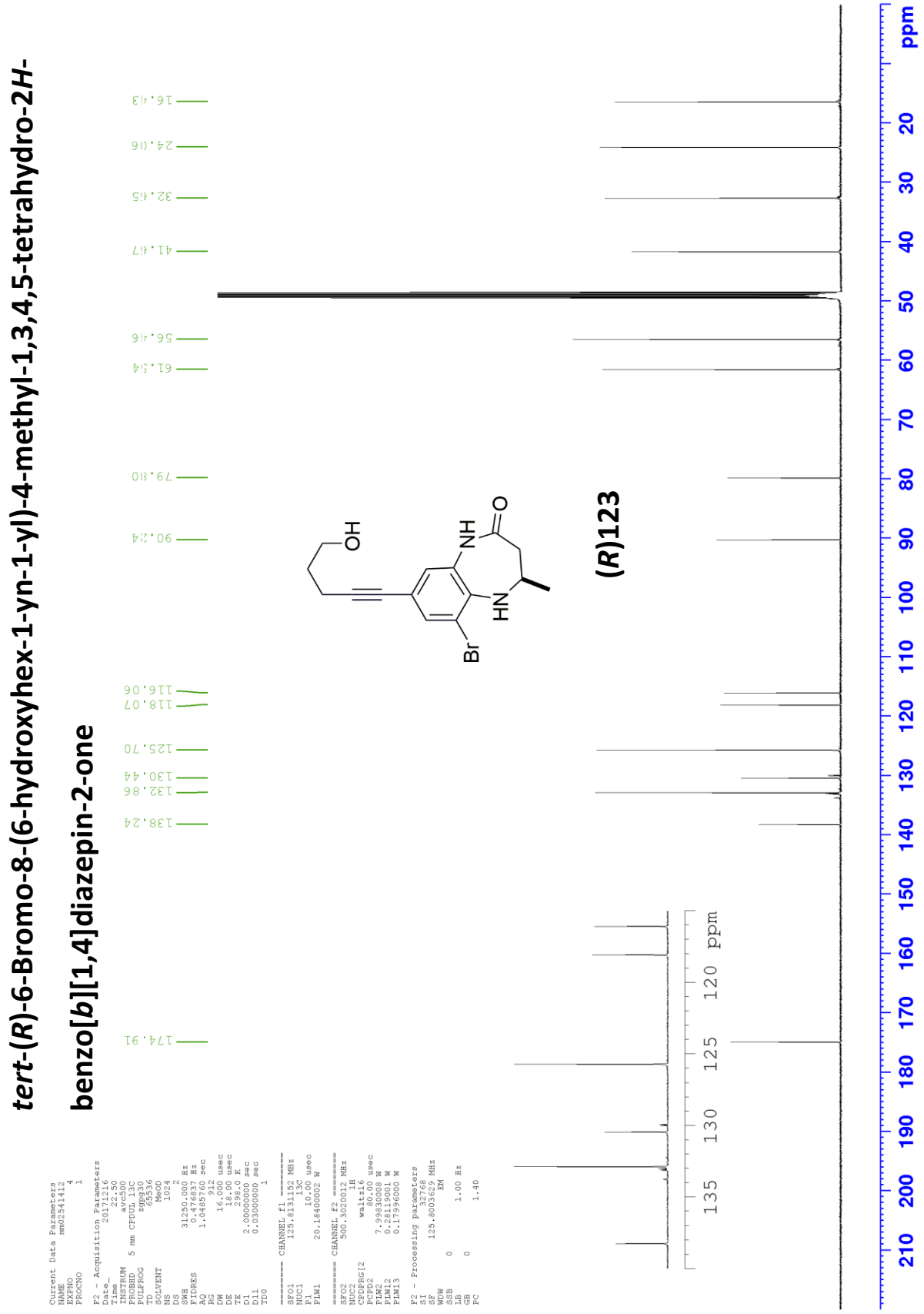
F2 - Acquisition Parameters
Date_           20171216
Time              21.35
INSTRUM          avc500
PROBHD   5 mm CPDUL 13C
PULPROG            zg30
TD                65536
SOLVENT            MeOD
NS                   16
DS                    4
SWH           10330.578 Hz
FIDRES         0.157632 Hz
AQ            3.1719425 sec
RG                 3.56
DW               48.400 usec
DE               10.00 usec
TE               298.0 K
D1            1.00000000 sec
TD0                    1

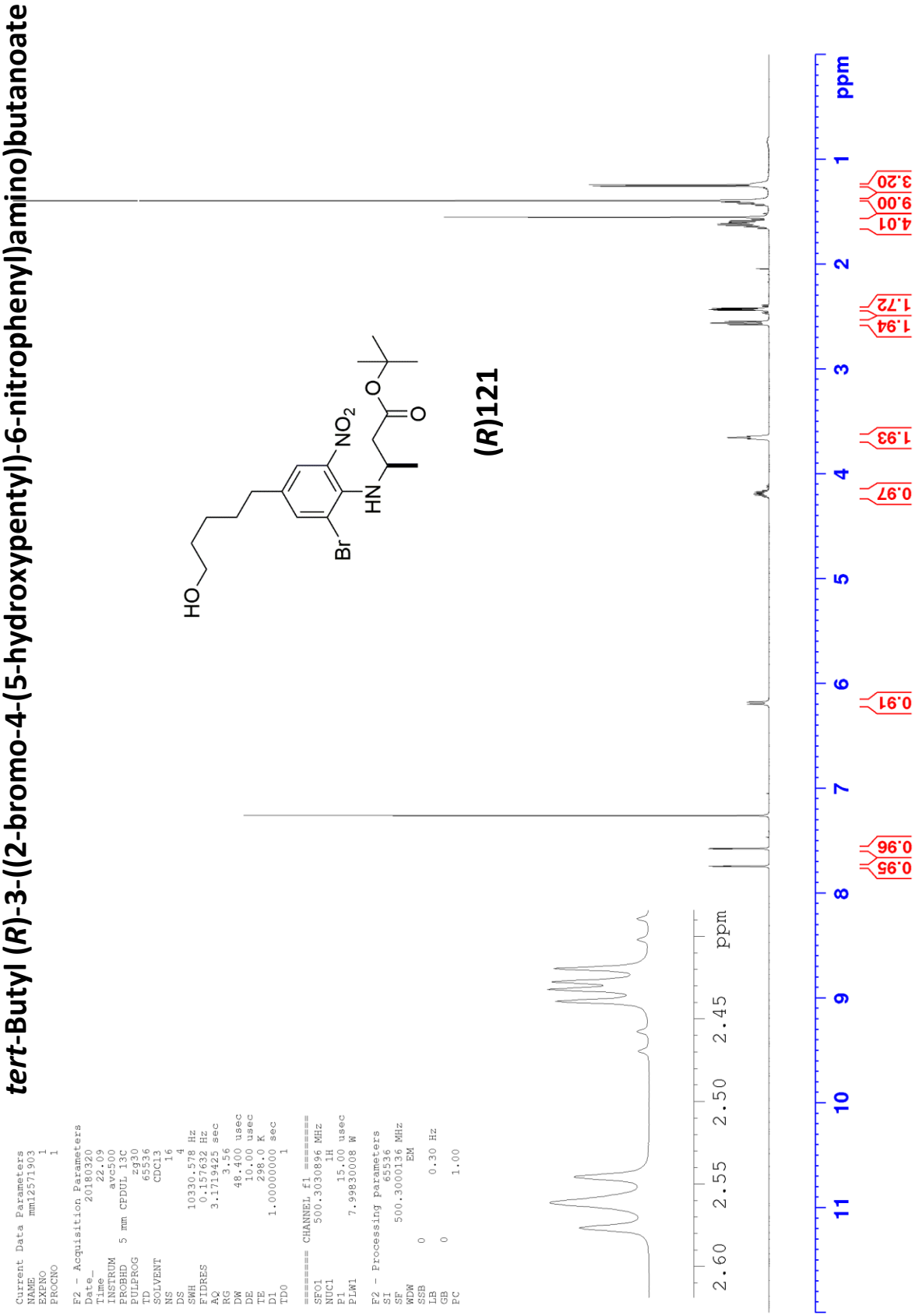
======== CHANNEL f1 ========
SFO1         500.3030896 MHz
NUC1                   1H
P1                15.00 usec
PLW1          7.99830008 W

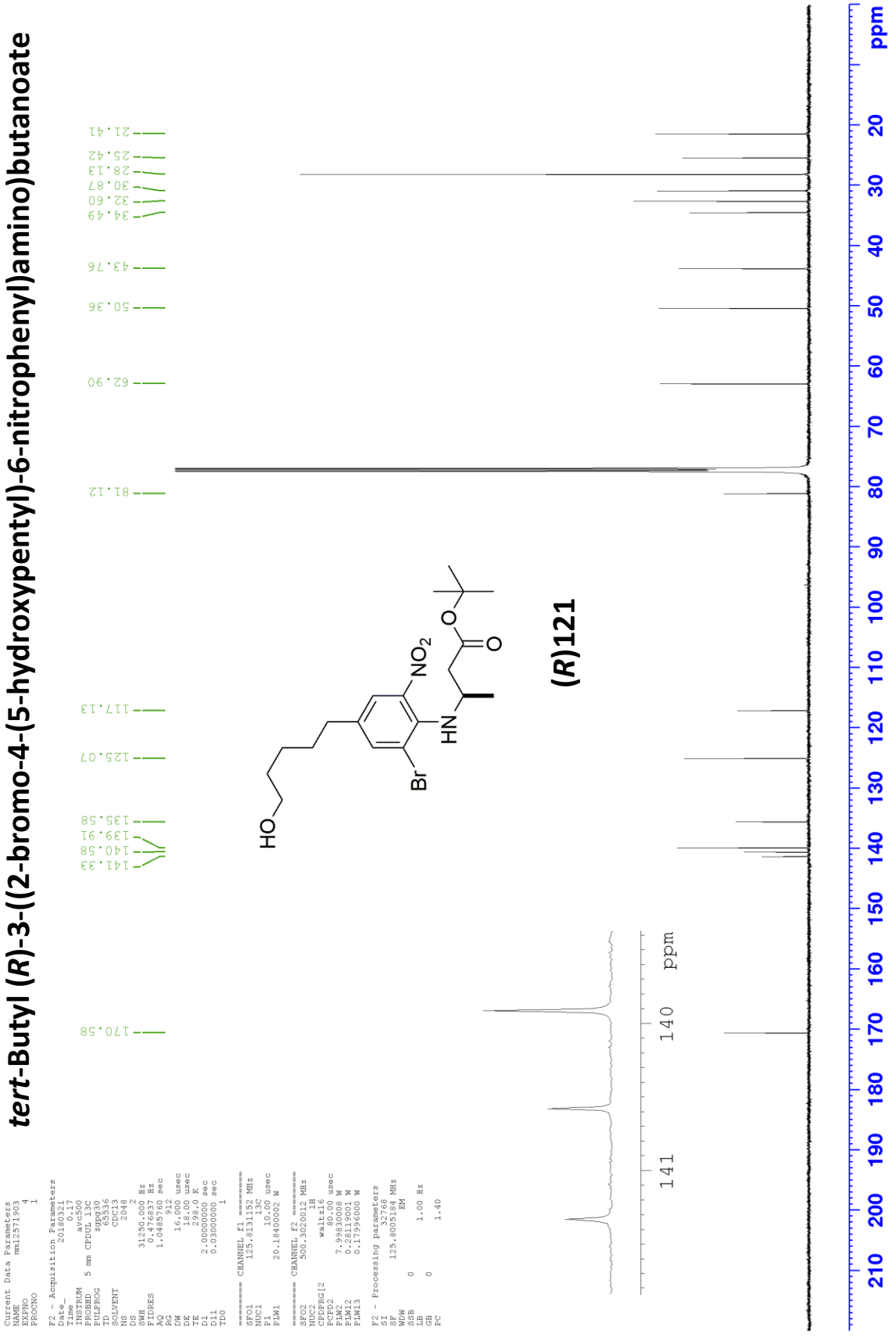
F2 - Processing parameters
SI                 65536
SF            500.3000065 MHz
WDW                   EM
SSB       0
LB                 0.30 Hz
GB        0
PC                 1.00
```

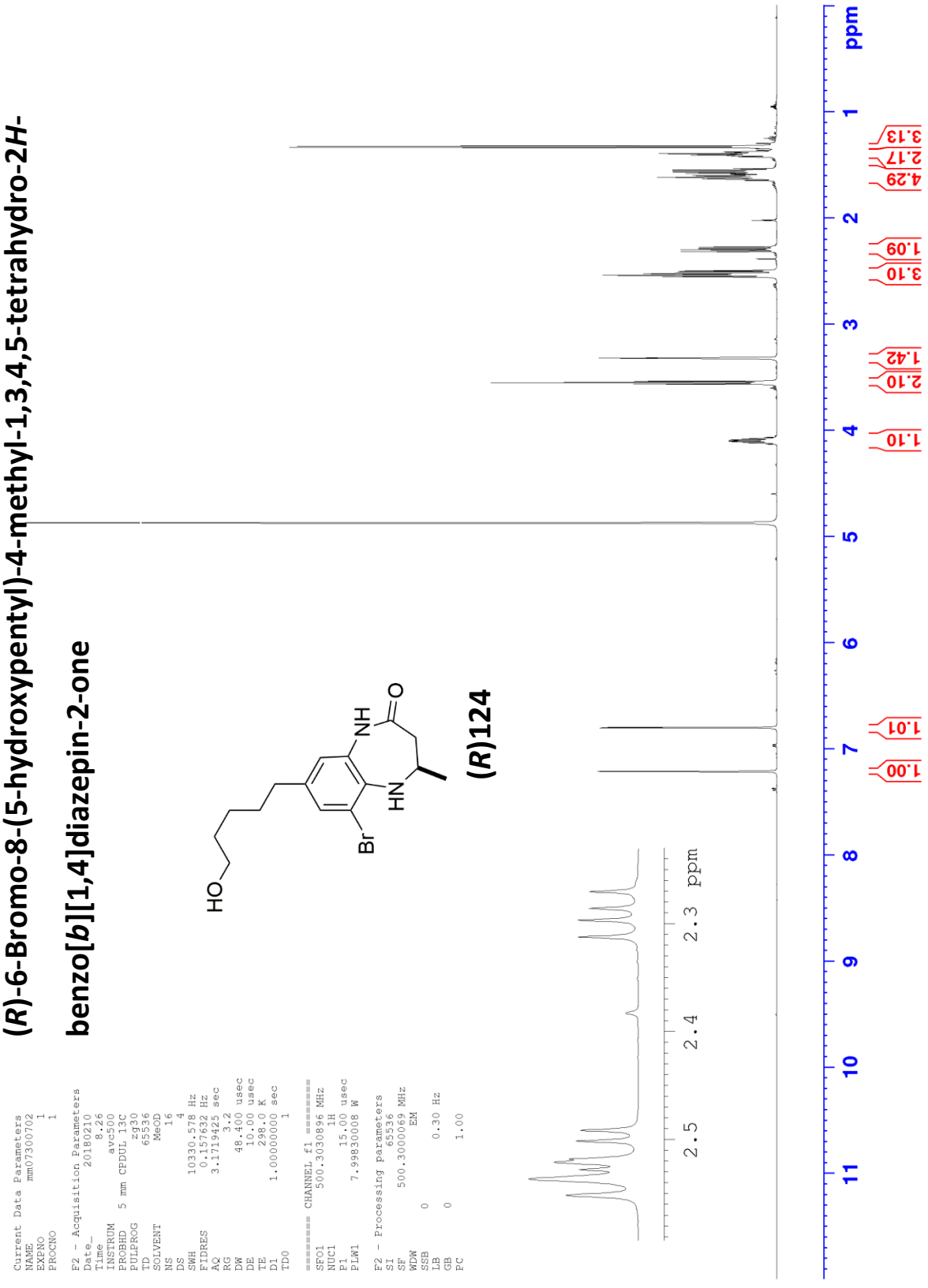


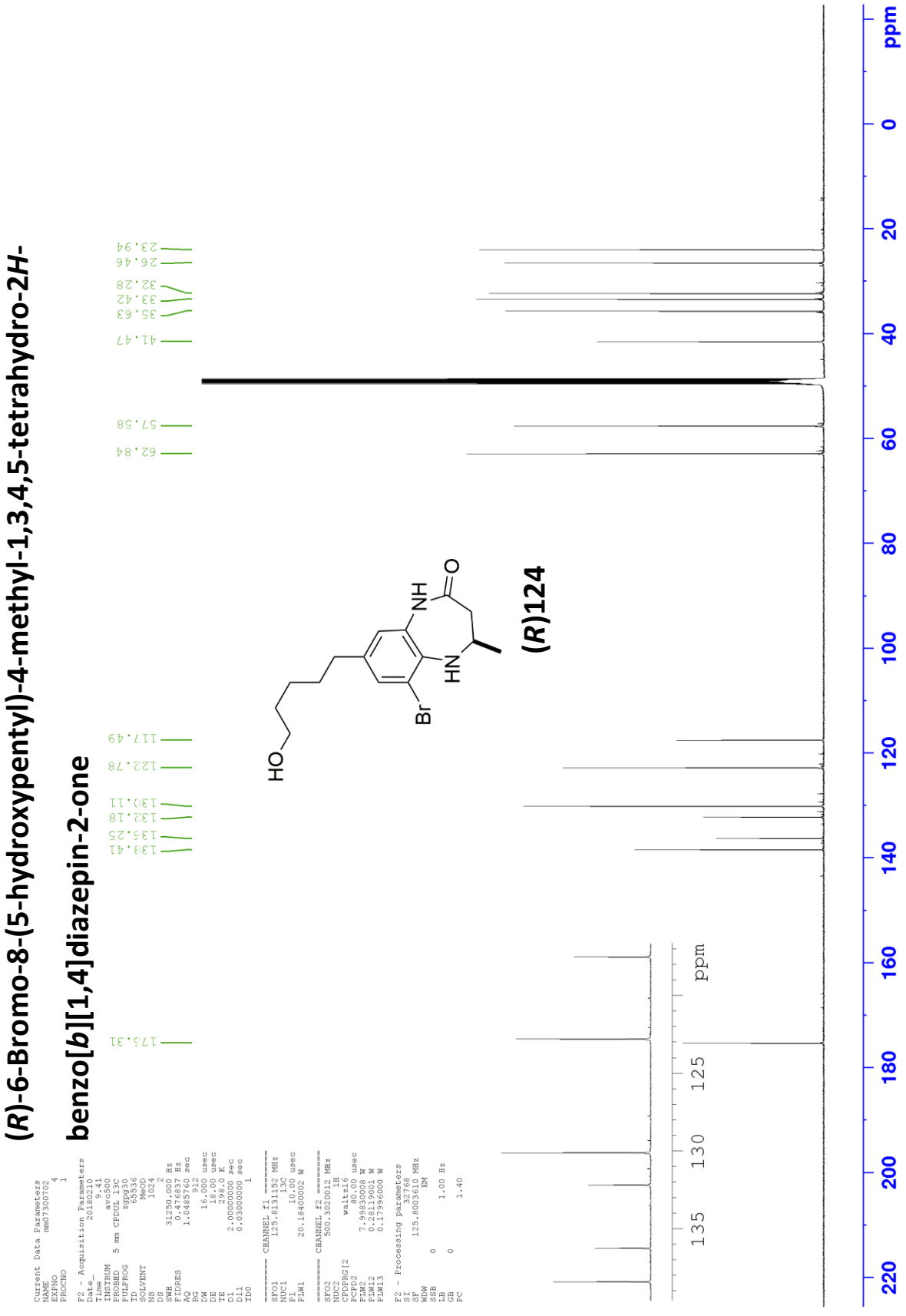
(*R*)123

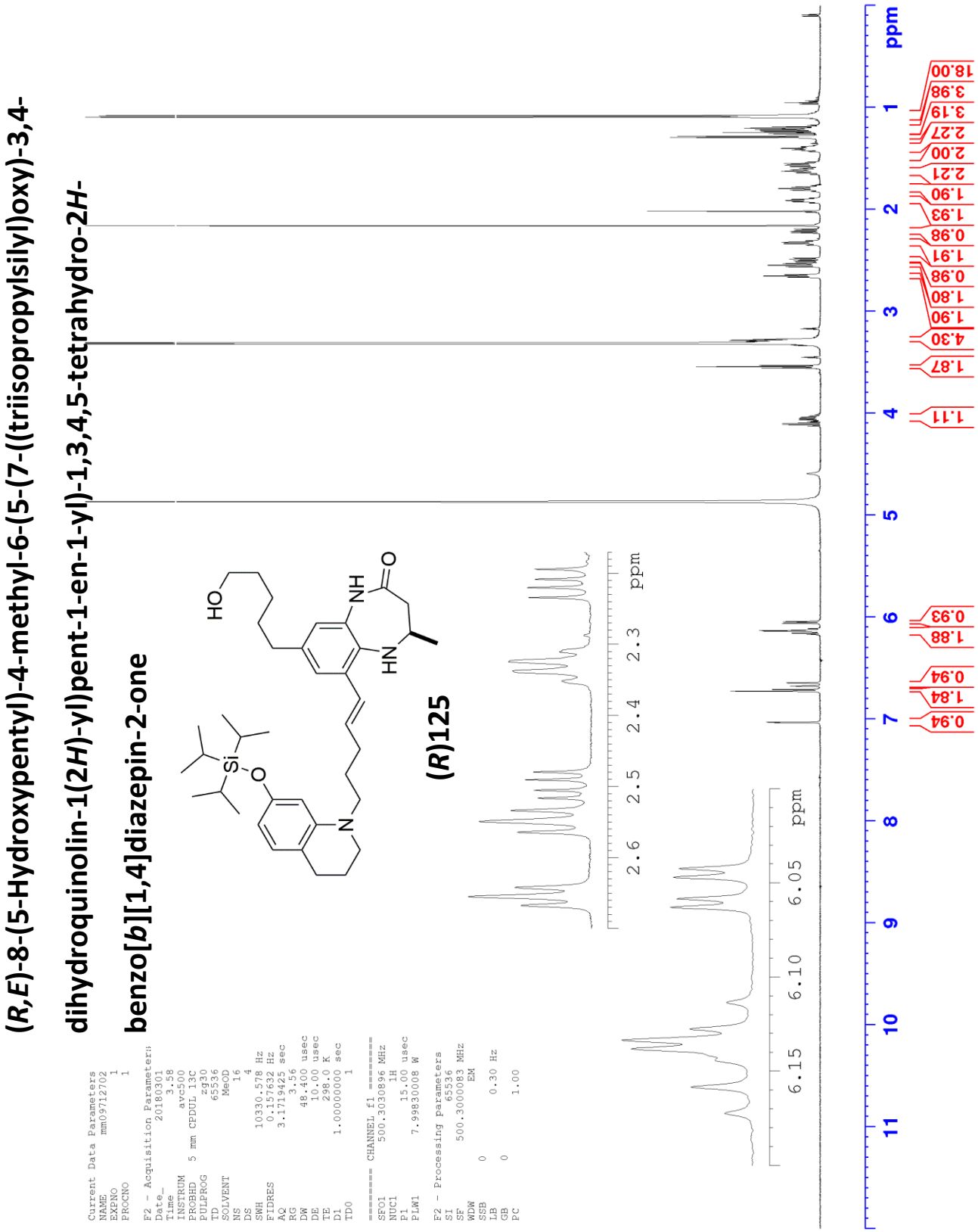

tert-(R)-6-Bromo-8-(6-hydroxyhex-1-yn-1-yl)-4-methyl-1,3,4,5-tetrahydro-2H-benzo[b][1,4]diazepin-2-one
(R)123
OH
NH
O
HN
Br
174.91
138.24
132.86
130.44
125.70
118.07
116.06
90.24
79.80
61.54
56.46
41.67
32.65
24.06
16.43
135 130 125 120 ppm
210 200 190 180 170 160 150 140 130 120 110 100 90 80 70 60 50 40 30 20 ppm


tert-Butyl (R)-3-((2-bromo-4-(5-hydroxypentyl)-6-nitrophenyl)amino)butanoate
(R)121
HO
Br
HN
NO2
O
O
Current Data Parameters
NAME mm12571903
EXPNO 1
PROCNO 1
F2 - Acquisition Parameters
Date_ 20180320
Time 22.09
INSTRUM avc500
PROBHD 5 mm CPDUL 13C
PULPROG zg30
TD 65536
SOLVENT CDCl3
NS 16
DS 4
SWH 10330.578 Hz
FIDRES 0.157632 Hz
AQ 3.1719425 sec
RG 3.56
DW 48.400 usec
DE 10.00 usec
TE 298.0 K
D1 1.00000000 sec
TD0 1
======== CHANNEL f1 ========
SFO1 500.3030896 MHz
NUC1 1H
P1 15.00 usec
PLW1 7.99830008 W
F2 - Processing parameters
SI 65536
SF 500.3000136 MHz
WDW EM
SSB 0
LB 0.30 Hz
GB 0
PC 1.00
2.60
2.55
2.50
2.45
ppm
11
10
9
8
7
6
5
4
3
2
1
ppm
0.95
0.96
0.91
0.97
1.93
1.94
1.72
4.01
9.00
3.20

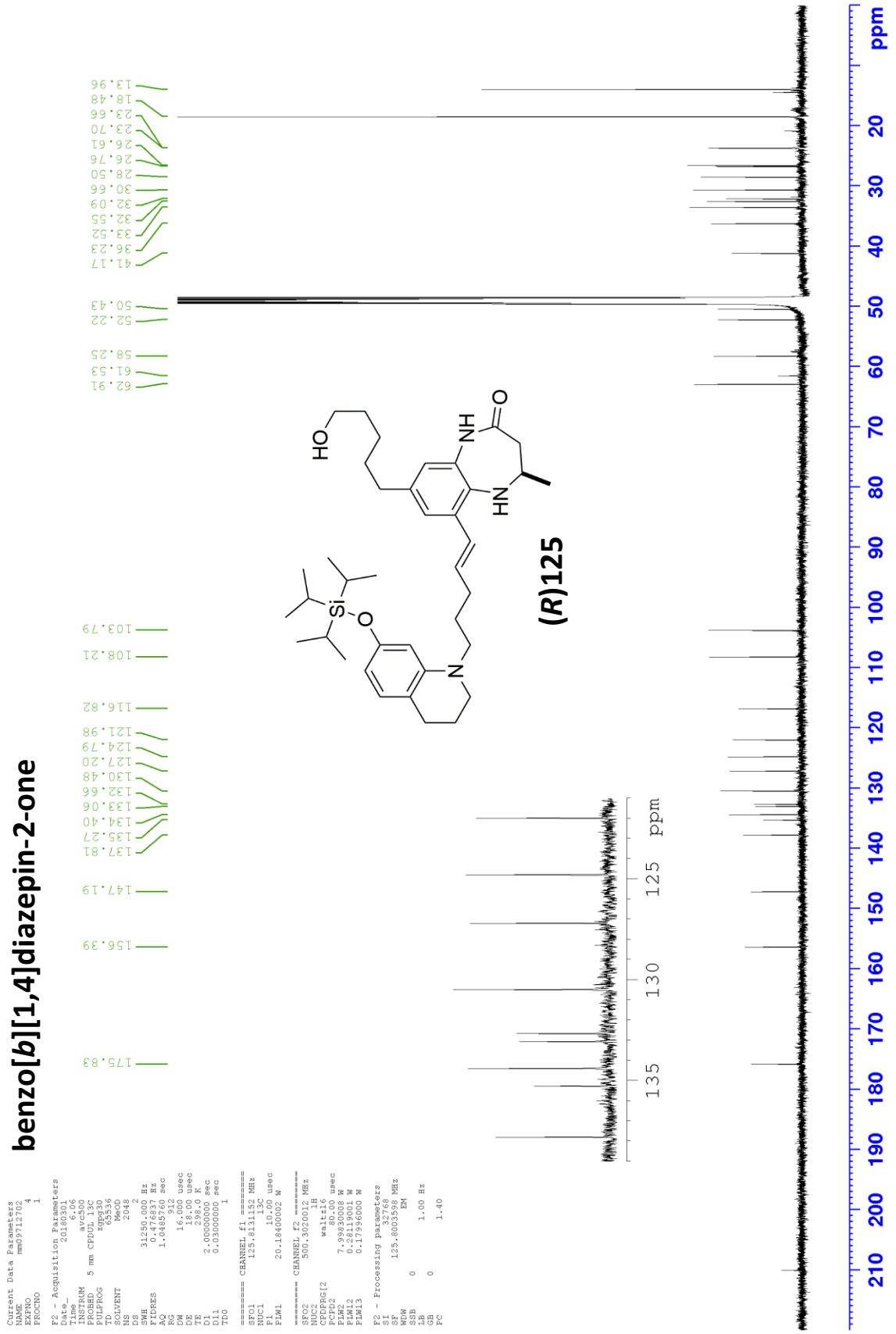

tert-Butyl (R)-3-((2-bromo-4-(5-hydroxypentyl)-6-nitrophenyl)amino)butanoate
(R)121
Current Data Parameters
NAME mm12571903
EXPNO 4
PROCNO 1
F2 - Acquisition Parameters
Date_ 20180321
Time 0.17
INSTRUM avc500
PROBHD 5 mm CPDUL 13C
PULPROG zgpg30
TD 65536
SOLVENT CDCl3
NS 2048
DS 2
SWH 31250.000 Hz
FIDRES 0.476837 Hz
AQ 1.0485760 sec
RG 912
DW 16.000 usec
DE 18.00 usec
TE 298.0 K
D1 2.00000000 sec
D11 0.03000000 sec
TD0 1
SFO1 125.8113152 MHz
NUC1 13C
P1 10.00 usec
PLW1 20.18400002 W
SFO2 500.3020012 MHz
NUC2 1H
CPDPRG[2 waltz16
PCPD2 80.00 usec
PLW2 7.99830008 W
PLW12 0.29819001 W
PLW13 0.17996000 W
F2 - Processing parameters
SI 32768
SF 125.8005164 MHz
WDW EM
SSB 0
LB 1.00 Hz
GB 0
PC 1.40
170.58
141.33
140.58
139.91
135.58
125.07
117.13
81.12
62.90
50.36
43.76
34.49
32.60
30.87
28.13
25.42
21.41
HO
Br
NO2
HN
O
O
141
140
ppm
210 200 190 180 170 160 150 140 130 120 110 100 90 80 70 60 50 40 30 20
ppm


(R)-6-Bromo-8-(5-hydroxypentyl)-4-methyl-1,3,4,5-tetrahydro-2H-
benzo[b][1,4]diazepin-2-one
(R)124
Current Data Parameters
NAME mm07300702
EXPNO 1
PROCNO 1
F2 - Acquisition Parameters
Date_ 20180210
Time 8.26
INSTRUM avc500
PROBHD 5 mm CPDUL 13C
PULPROG zg30
TD 65536
SOLVENT MeOD
NS 16
DS 4
SWH 10330.578 Hz
FIDRES 0.157632 Hz
AQ 3.1719425 sec
RG 3.2
DW 48.400 usec
DE 10.00 usec
TE 298.0 K
D1 1.00000000 sec
TD0 1
======== CHANNEL f1 ========
SFO1 500.3030896 MHz
NUC1 1H
P1 15.00 usec
PLW1 7.99830008 W
F2 - Processing parameters
SI 65536
SF 500.3000069 MHz
WDW EM
SSB 0
LB 0.30 Hz
GB 0
PC 1.00
HO
NH
O
HN
Br
2.5
2.4
2.3 ppm
1.00
1.01
1.10
2.10
1.42
3.10
1.09
4.29
2.17
3.13
ppm

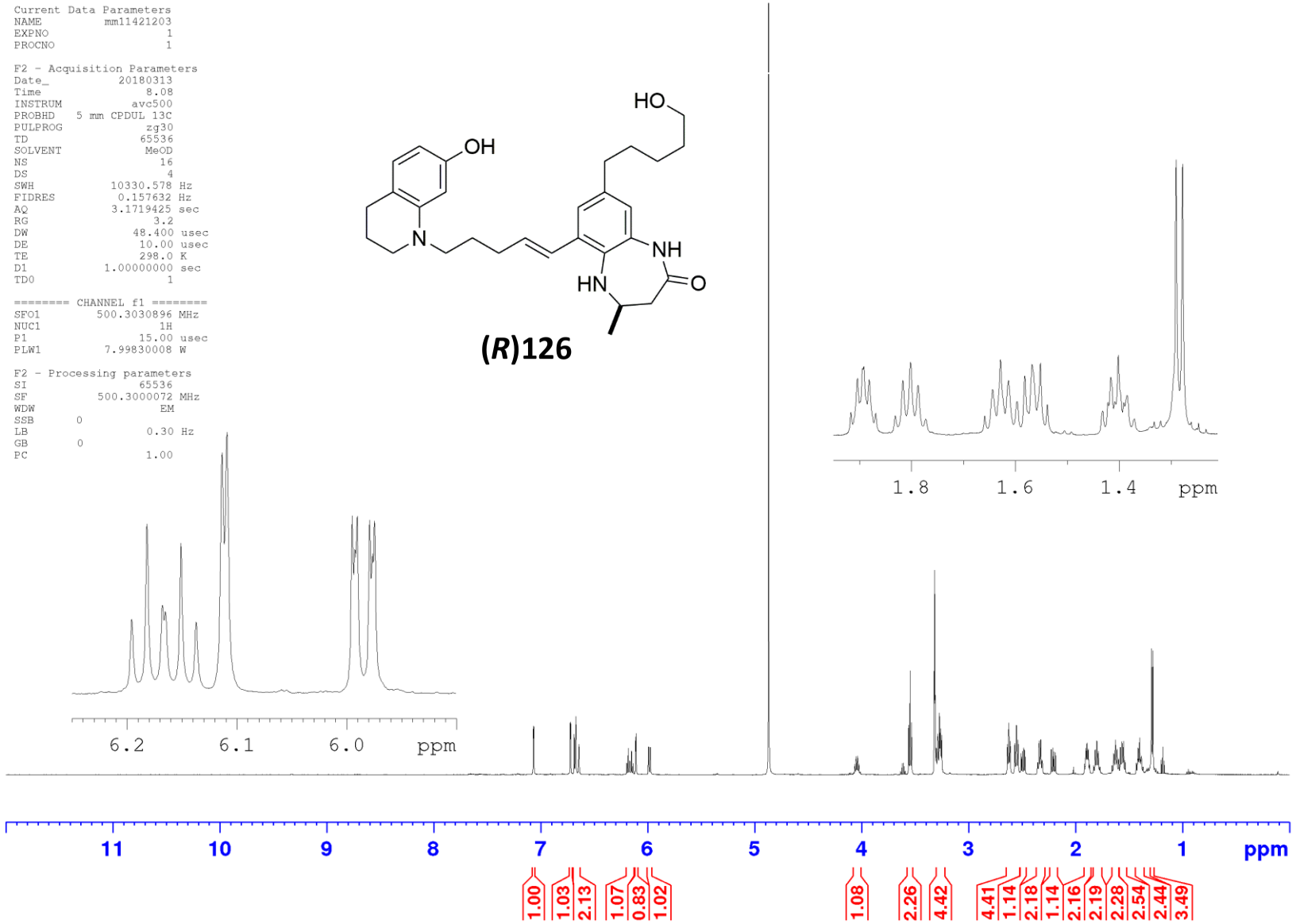

(R)-6-Bromo-8-(5-hydroxypentyl)-4-methyl-1,3,4,5-tetrahydro-2H-benzo[b][1,4]diazepin-2-one
(R)124
175.31
138.41
135.25
132.18
130.11
122.78
117.49
62.84
57.58
41.47
35.63
33.42
32.28
26.46
23.94
HO
Br
NH
HN
O
ppm


(R,E)-8-(5-Hydroxypentyl)-4-methyl-6-(5-(7-((triisopropylsilyl)oxy)-3,4-dihydroquinolin-1(2H)-yl)pent-1-en-1-yl)-1,3,4,5-tetrahydro-2H-benzo[b][1,4]diazepin-2-one
(R)125
Current Data Parameters
NAME mm09712702
EXPNO 1
PROCNO 1
F2 - Acquisition Parameters
Date_ 20180301
Time 3.58
INSTRUM avc500
PROBHD 5 mm CPDUL 13C
PULPROG zg30
TD 65536
SOLVENT MeOD
NS 16
DS 4
SWH 10330.578 Hz
FIDRES 0.157632 Hz
AQ 3.1719425 sec
RG 3.56
DW 48.400 usec
DE 10.00 usec
TE 298.0 K
D1 1.00000000 sec
TD0 1
======== CHANNEL f1 ========
SFO1 500.3030896 MHz
NUC1 1H
P1 15.00 usec
PLW1 7.99830008 W
F2 - Processing parameters
SI 65536
SF 500.3000083 MHz
WDW EM
SSB 0
LB 0.30 Hz
GB 0
PC 1.00
HO
Si
O
N
NH
O
HN
6.15
6.10
6.05
ppm
2.6
2.5
2.4
2.3
ppm
0.94
1.84
0.94
1.88
0.93
1.11
1.87
4.30
1.90
1.80
0.98
1.91
0.98
1.93
1.90
2.21
2.00
2.27
3.19
3.98
18.00
ppm

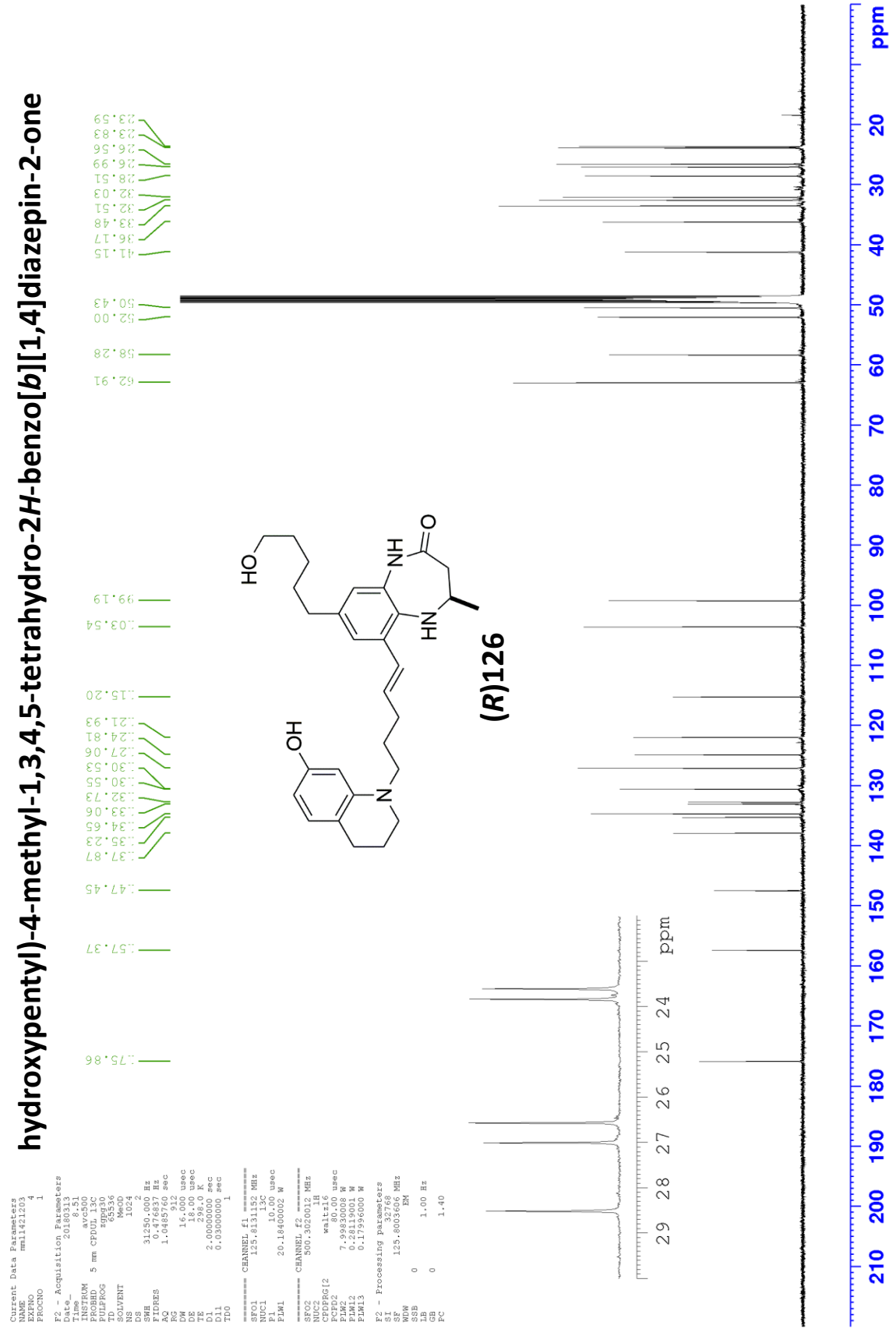
(*R*,*E*)-8-(5-Hydroxypentyl)-4-methyl-6-(5-(7-((triisopropylsilyl)oxy)-3,4-dihydroquinolin-1(2*H*)-yl)pent-1-en-1-yl)-1,3,4,5-tetrahydro-2*H*-benzo[*b*][1,4]diazepin-2-one

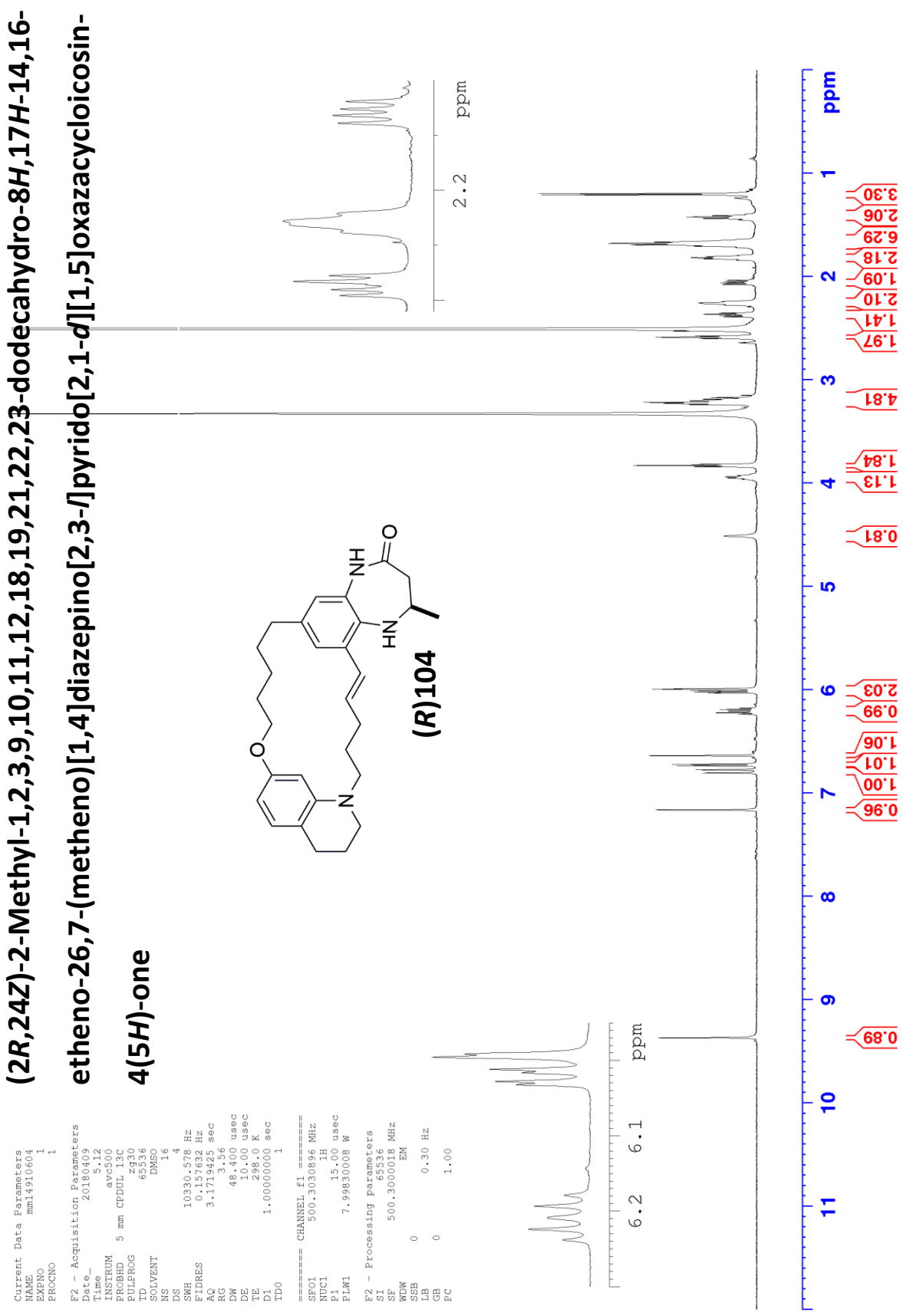


(*R,E*)-6-(5-(7-Hydroxy-3,4-dihydroquinolin-1(2*H*)-yl)pent-1-en-1-yl)-8-(5-hydroxypentyl)-4-methyl-1,3,4,5-tetrahydro-2*H*-benzo[*b*][1,4]diazepin-2-one

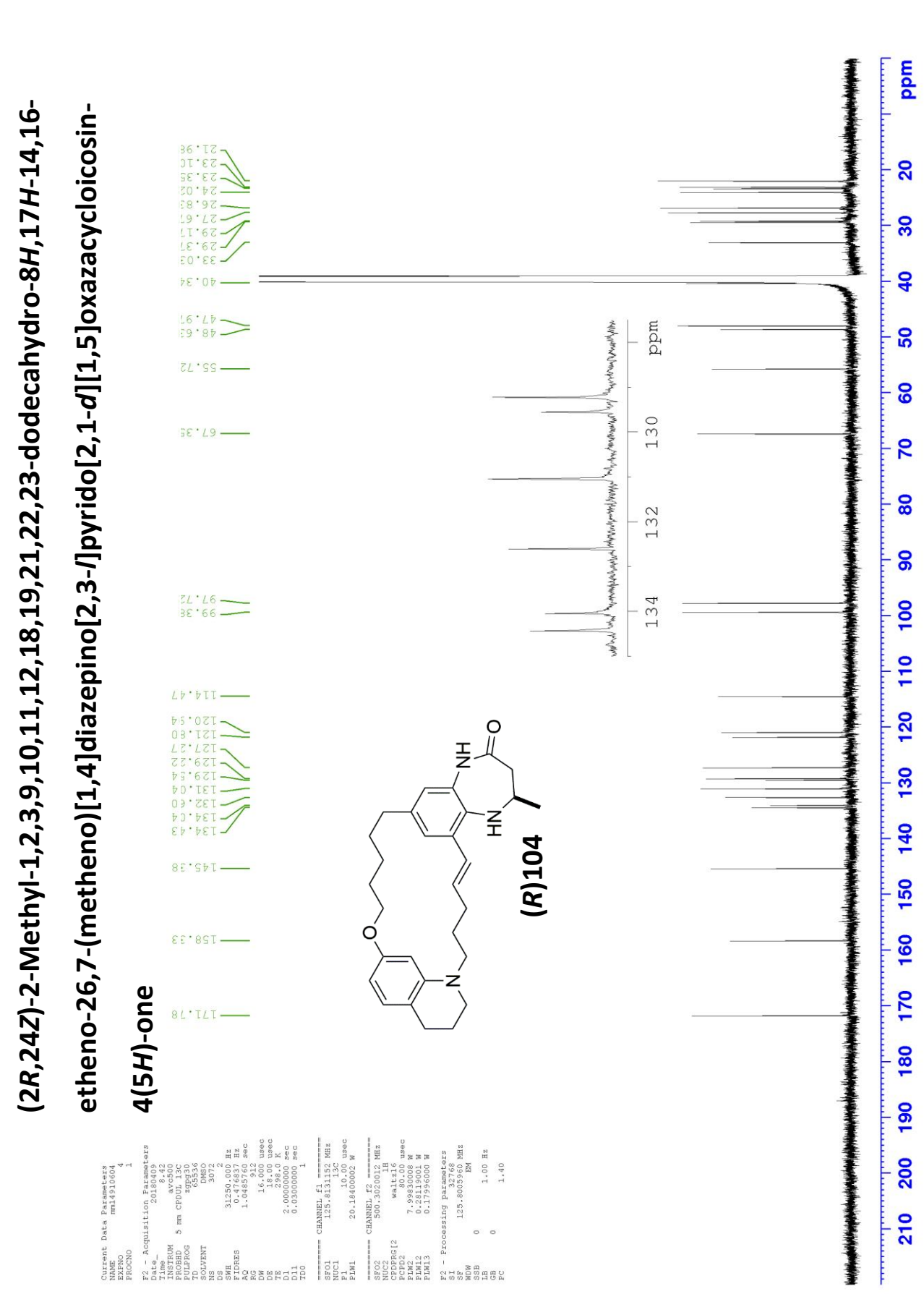


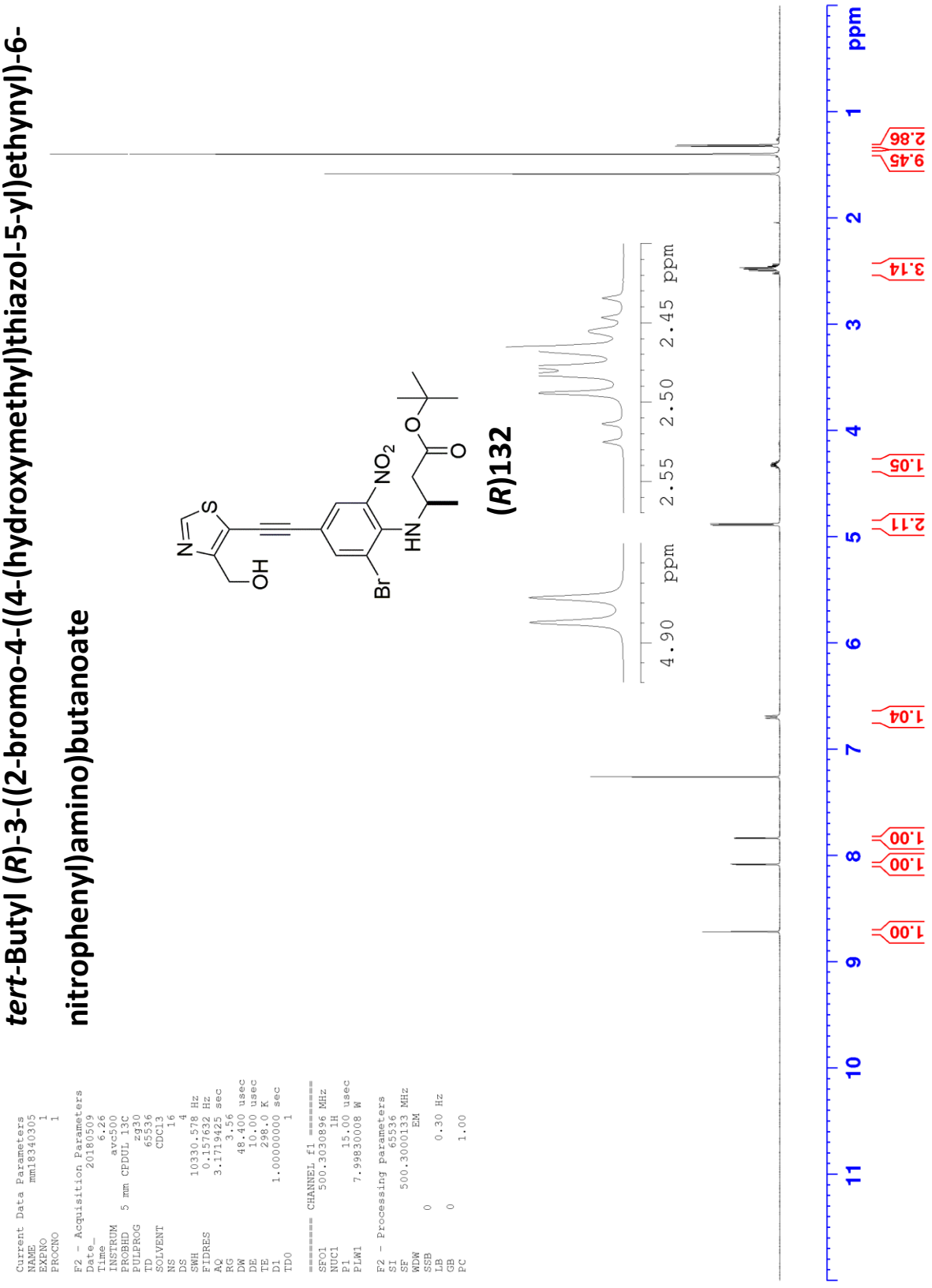
(*R*,*E*)-6-(5-(7-Hydroxy-3,4-dihydroquinolin-1(2*H*)-yl)pent-1-en-1-yl)-8-(5-hydroxypentyl)-4-methyl-1,3,4,5-tetrahydro-2*H*-benzo[*b*][1,4]diazepin-2-one

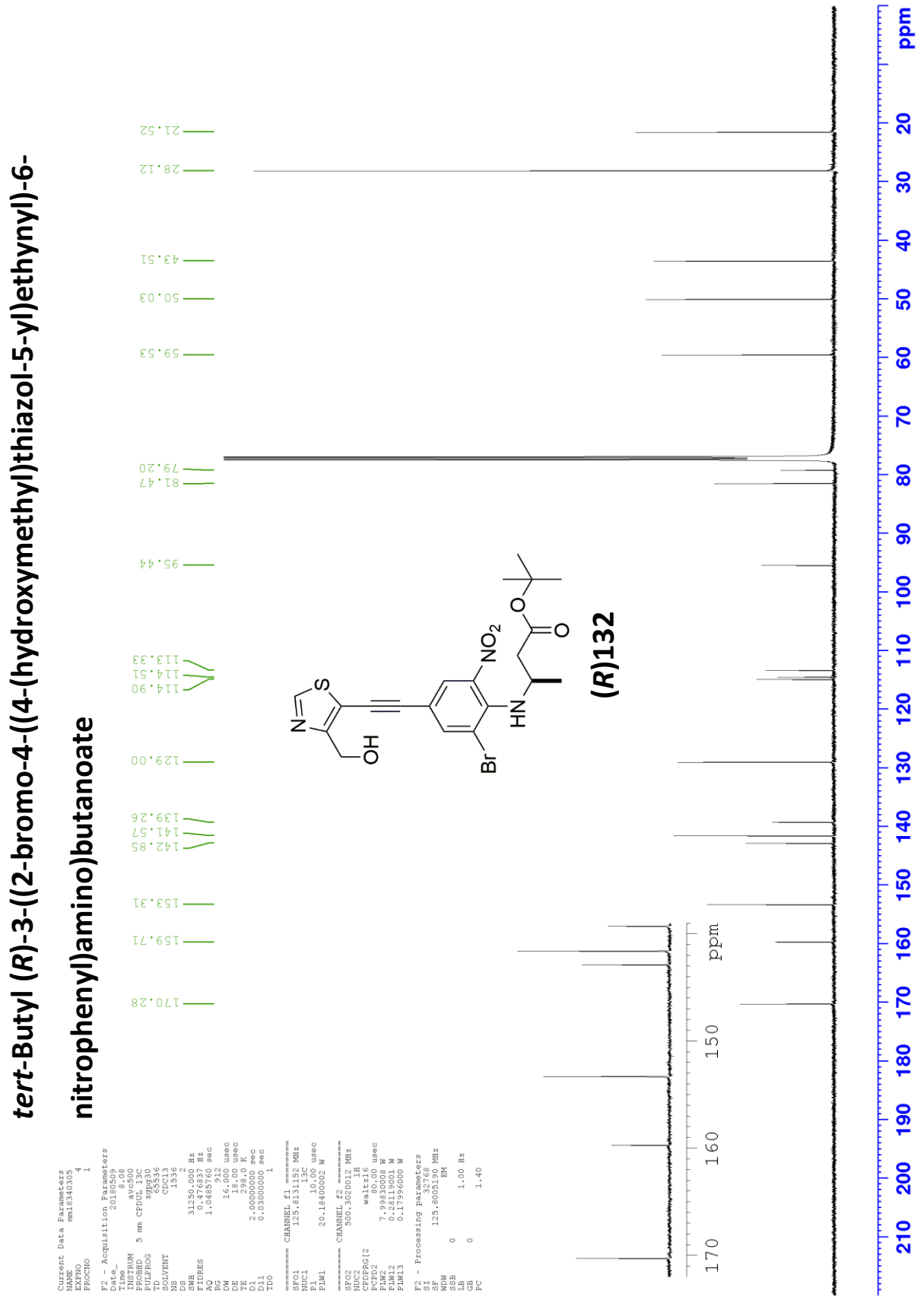


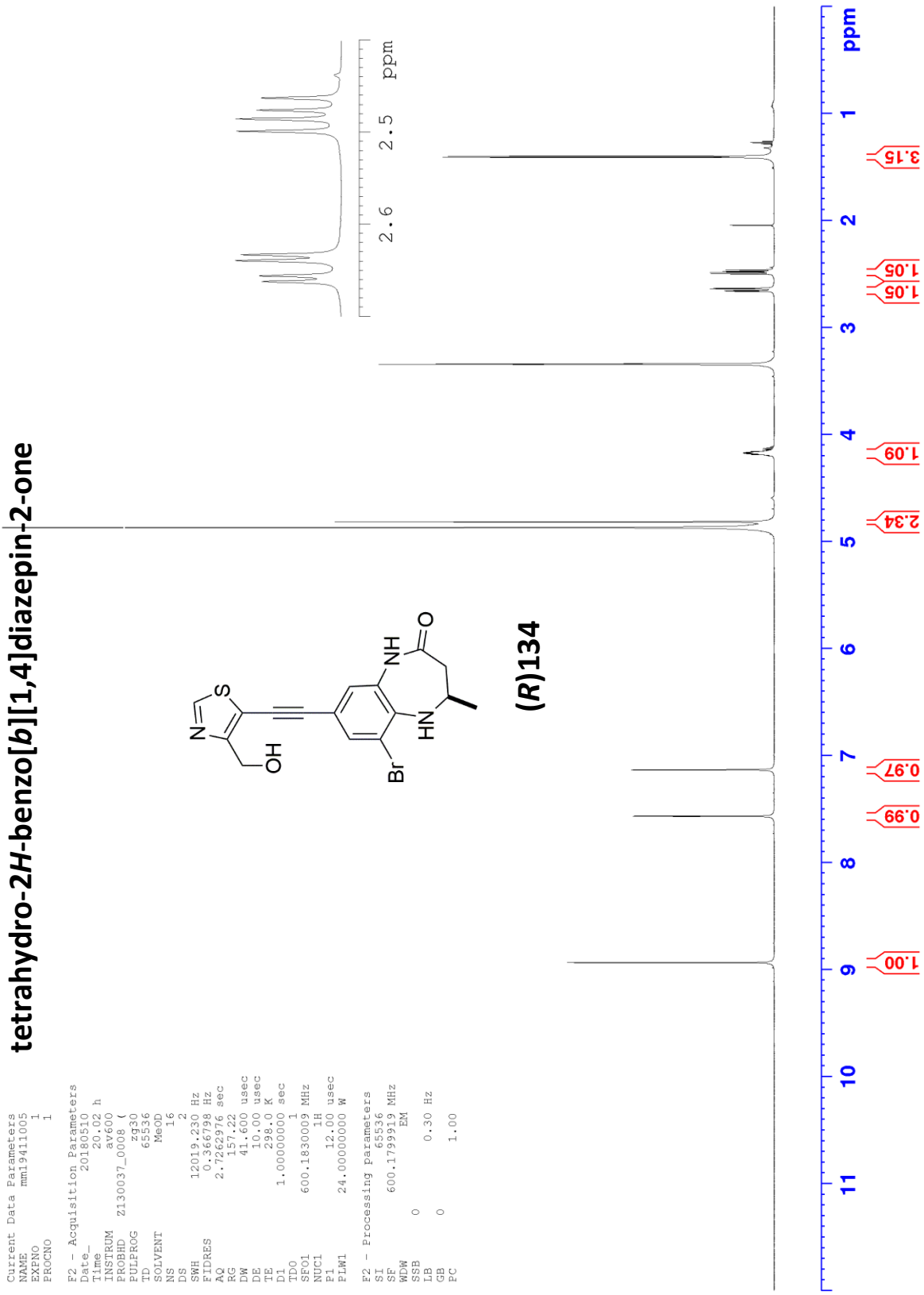

(2R,24Z)-2-Methyl-1,2,3,9,10,11,12,18,19,21,22,23-dodecahydro-8H,17H-14,16-etheno-26,7-(metheno)[1,4]diazepino[2,3-l]pyrido[2,1-d][1,5]oxazacycloicosin-4(5H)-one
(R)104
Current Data Parameters
NAME mm14910604
EXPNO 1
PROCNO 1
F2 - Acquisition Parameters
Date_ 20180409
Time_ 5.12
INSTRUM avc500
PROBHD 5 mm CPDUL 13C
PULPROG zg30
TD 65536
SOLVENT DMSO
NS 16
DS 4
SWH 10330.578 Hz
FIDRES 0.157632 Hz
AQ 3.1719425 sec
RG 3.56
DW 48.400 usec
DE 10.00 usec
TE 298.0 K
D1 1.00000000 sec
TD0 1
======== CHANNEL f1 ========
SFO1 500.3030896 MHz
NUC1 1H
P1 15.00 usec
PLW1 7.99830008 W
F2 - Processing parameters
SI 65536
SF 500.3000018 MHz
WDW EM
SSB 0
LB 0.30 Hz
GB 0
PC 1.00
6.2
6.1
ppm
2.2
ppm
11
10
9
8
7
6
5
4
3
2
1
ppm
0.89
0.96
1.00
1.01
1.06
0.99
2.03
0.81
1.13
1.84
4.81
1.97
1.41
2.10
1.09
2.18
6.29
2.06
3.30

(2*R*,24*Z*)-2-Methyl-1,2,3,9,10,11,12,18,19,21,22,23-dodecahydro-8*H*,17*H*-14,16-etheno-26,7-(metheno)[1,4]diazepino[2,3-*l*]pyrido[2,1-*d*][1,5]oxazacycloicosin-4(5*H*)-one

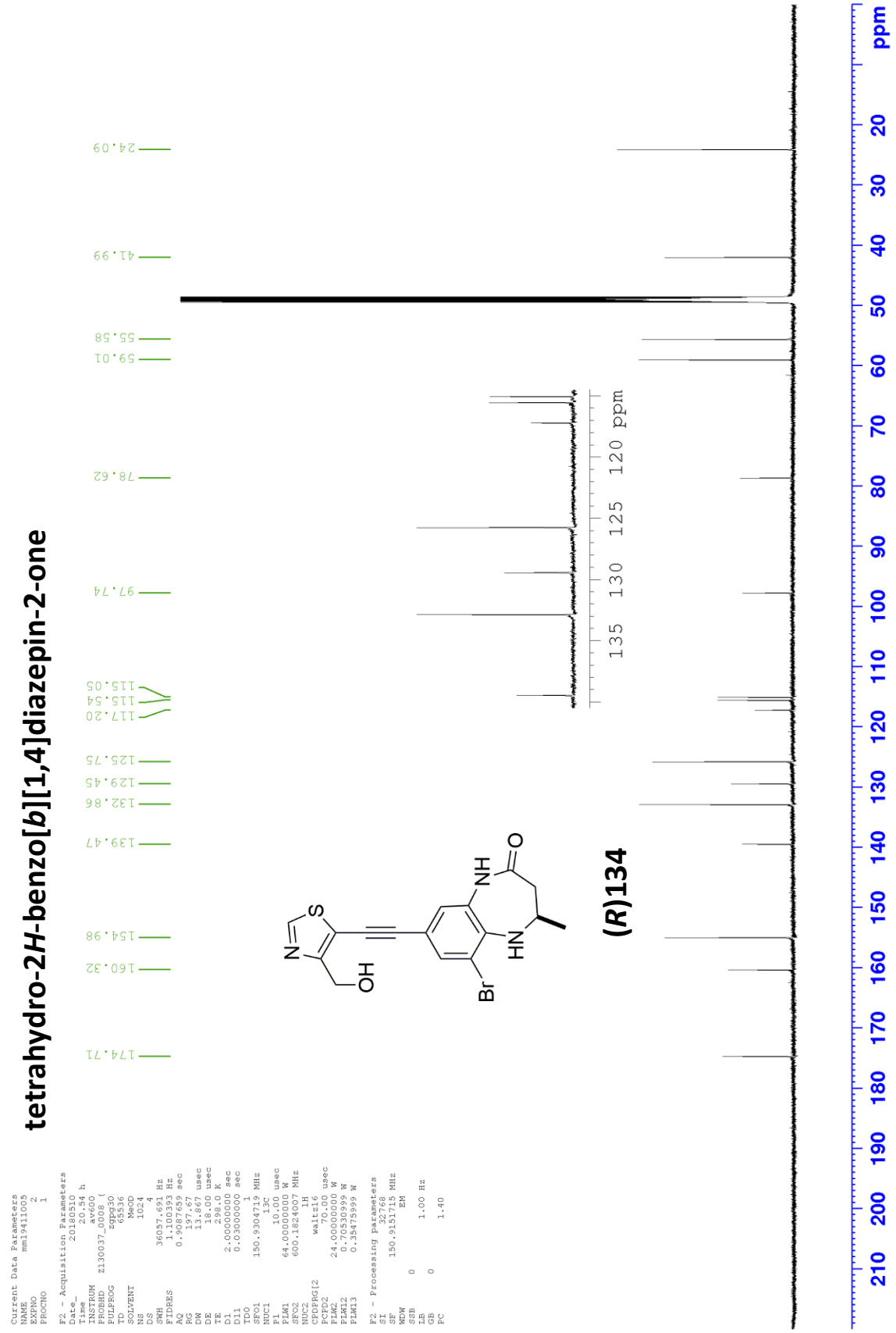


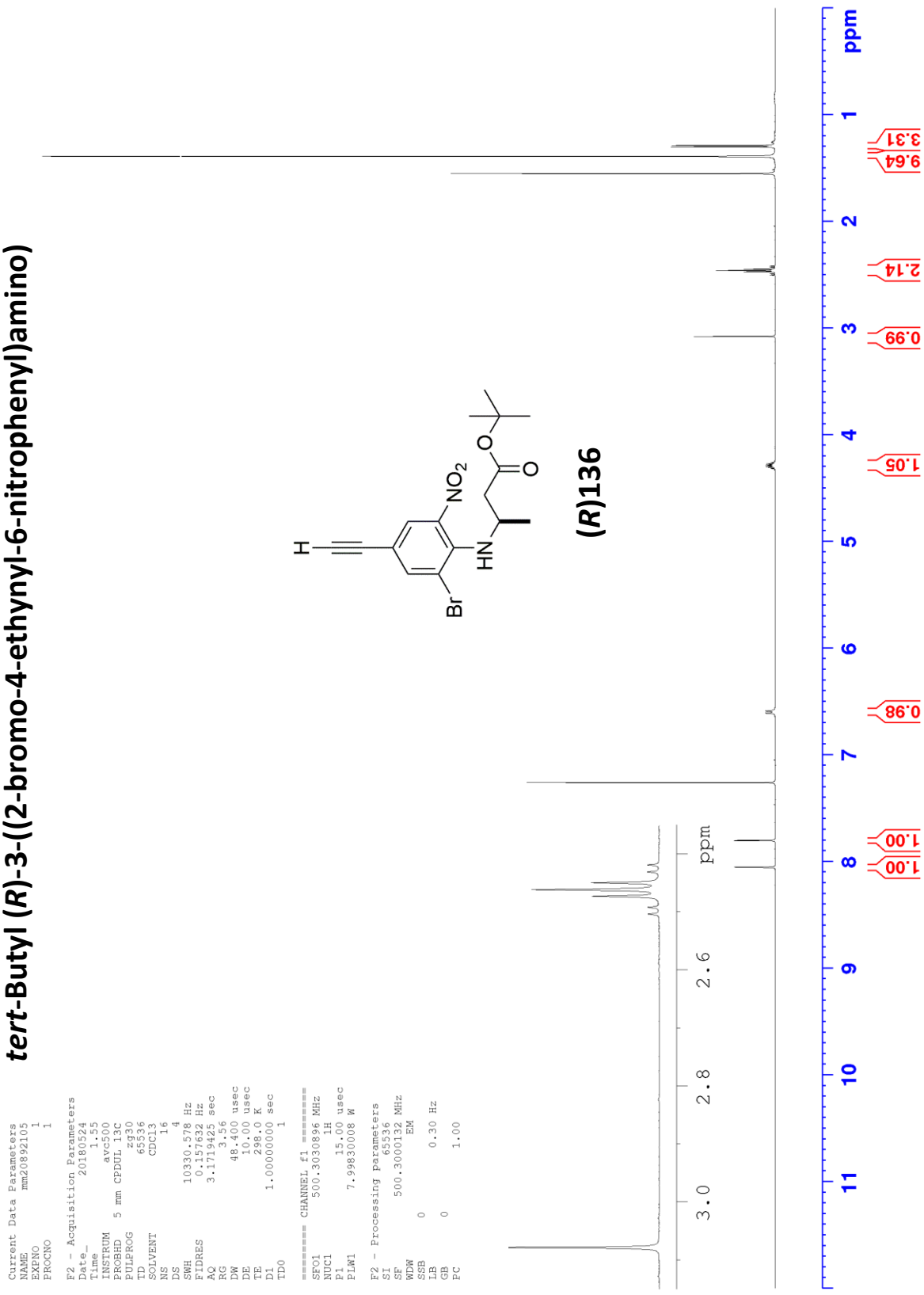

tert-Butyl (R)-3-((2-bromo-4-((4-(hydroxymethyl)thiazol-5-yl)ethynyl)-6-nitrophenyl)amino)butanoate
(R)132
Current Data Parameters
NAME mm18340305
EXPNO 1
PROCNO 1
F2 - Acquisition Parameters
Date_ 20180509
Time 6.26
INSTRUM avc500
PROBHD 5 mm CPDUL 13C
PULPROG zg30
TD 65536
SOLVENT CDCl3
NS 16
DS 4
SWH 10330.578 Hz
FIDRES 0.157632 Hz
AQ 3.1719425 sec
RG 3.56
DW 48.400 usec
DE 10.00 usec
TE 298.0 K
D1 1.00000000 sec
TD0 1
======== CHANNEL f1 ========
SFO1 500.3030896 MHz
NUC1 1H
P1 15.00 usec
PLW1 7.99830008 W
F2 - Processing parameters
SI 65536
SF 500.3000133 MHz
WDW EM
SSB 0
LB 0.30 Hz
GB 0
PC 1.00
4.90 ppm
2.55
2.50
2.45 ppm
ppm
1.00
1.00
1.00
1.04
1.05
2.11
3.14
9.45
2.86

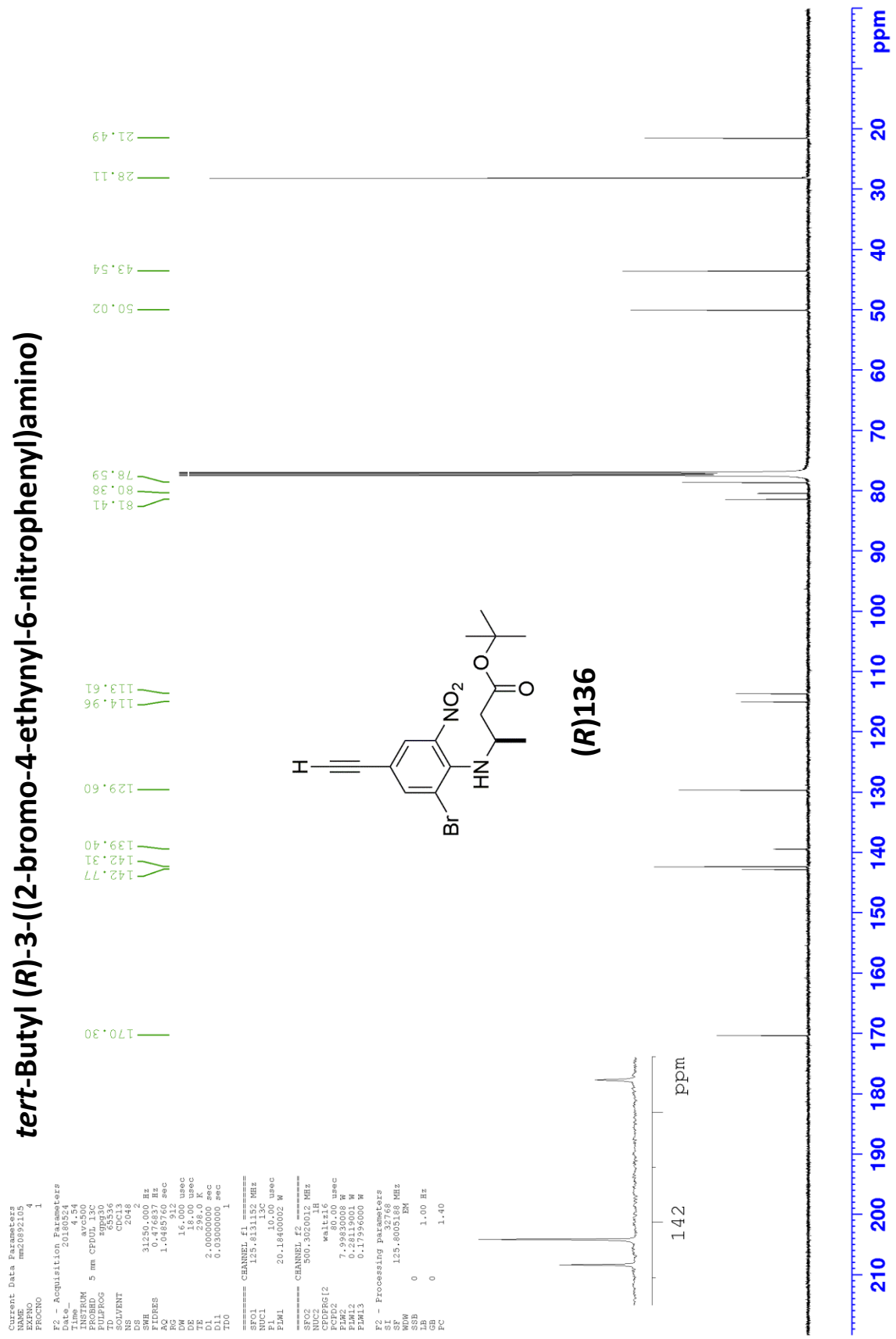

tert-Butyl (R)-3-((2-bromo-4-((4-(hydroxymethyl)thiazol-5-yl)ethynyl)-6-nitrophenyl)amino)butanoate
(R)132
Current Data Parameters
NAME mm18340305
EXPNO 4
PROCNO 1
F2 - Acquisition Parameters
Date_ 20180509
Time 8.08
INSTRUM avc500
PROBHD 5 mm CPDUL 13C
PULPROG zgpg30
TD 65536
SOLVENT CDCl3
NS 1536
DS 2
SWH 31250.000 Hz
FIDRES 0.476837 Hz
AQ 1.0485760 sec
RG 912
DW 16.000 usec
DE 18.00 usec
TE 298.0 K
D1 2.00000000 sec
D11 0.03000000 sec
TD0 1
======== CHANNEL f1 ========
SFO1 125.6131152 MHz
NUC1 13C
P1 10.00 usec
PLW1 20.18400002 W
======== CHANNEL f2 ========
SFO2 500.3020012 MHz
NUC2 1H
CPDPRG[2 waltz16
PCPD2 80.00 usec
PLW2 7.99800008 W
PLW12 0.28119001 W
PLW13 0.17996000 W
F2 - Processing parameters
SI 32768
SF 125.8005190 MHz
WDW EM
SSB 0
LB 1.00 Hz
GB 0
PC 1.40
170.28
159.71
153.31
142.85
141.57
139.26
129.00
114.90
114.51
113.33
95.44
81.47
79.20
59.53
50.03
43.51
28.12
21.52
ppm

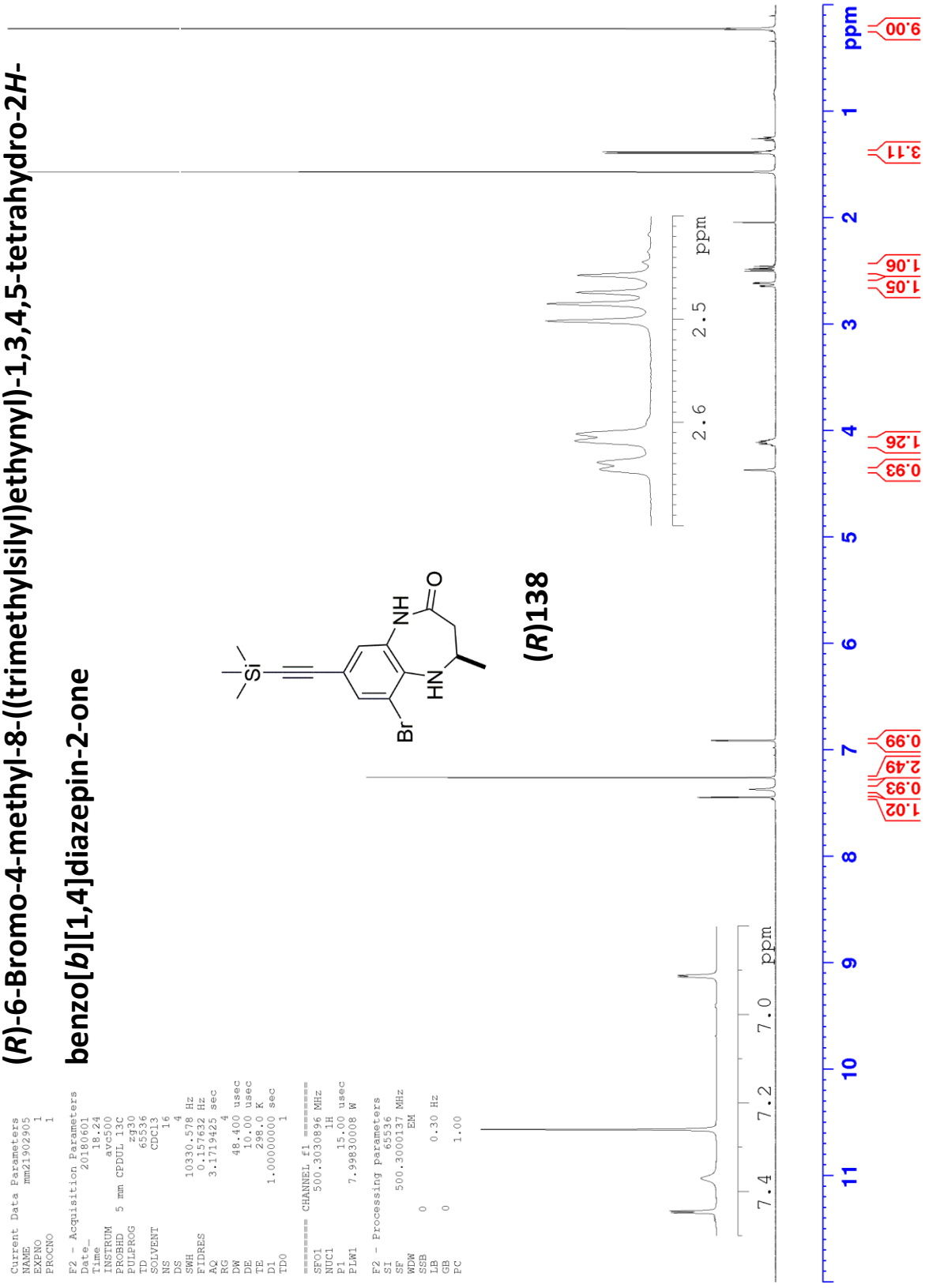

(R)-6-Bromo-8-((4-(hydroxymethyl)thiazol-5-yl)ethynyl)-4-methyl-1,3,4,5-tetrahydro-2H-benzo[b][1,4]diazepin-2-one
(R)134
Current Data Parameters
NAME nm19411005
EXPNO 1
PROCNO 1
F2 - Acquisition Parameters
Date_ 20180510
Time 20.02 h
INSTRUM av600
PROBHD Z130037_0008 (
PULPROG zg30
TD 65536
SOLVENT MeOD
NS 16
DS 2
SWH 12019.230 Hz
FIDRES 0.366798 Hz
AQ 2.7262976 sec
RG 157.22
DW 41.600 usec
DE 10.00 usec
TE 298.0 K
D1 1.00000000 sec
TD0 1
SFO1 600.1830009 MHz
NUC1 1H
P1 12.00 usec
PLW1 24.00000000 W
F2 - Processing parameters
SI 65536
SF 600.1799919 MHz
WDW EM
SSB 0
LB 0.30 Hz
GB 0
PC 1.00
2.6
2.5
ppm
1.00
0.99
0.97
1.09
2.34
1.05
1.05
3.15
ppm

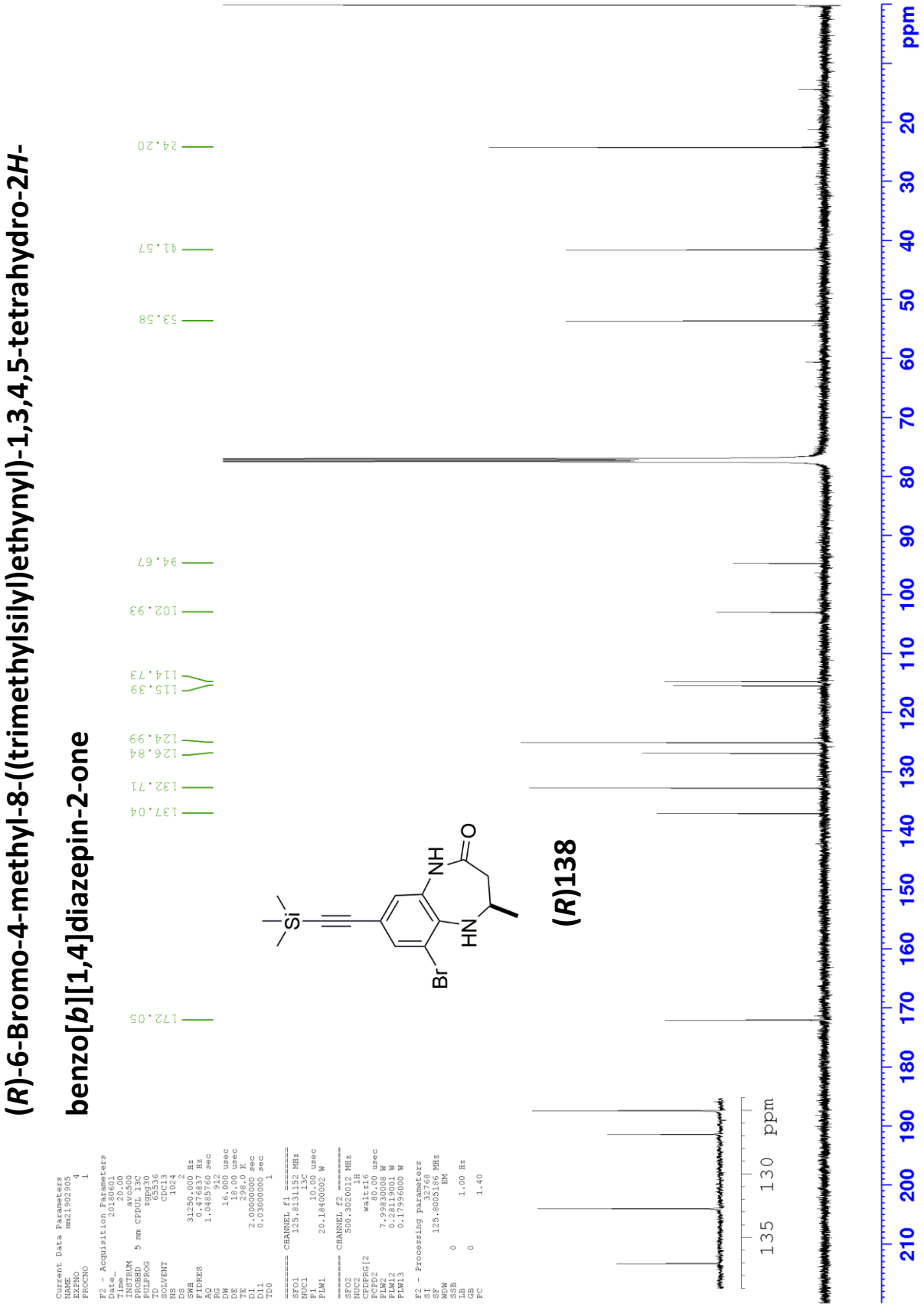
(*R*)-6-Bromo-8-((4-(hydroxymethyl)thiazol-5-yl)ethynyl)-4-methyl-1,3,4,5-tetrahydro-2*H*-benzo[*b*][1,4]diazepin-2-one

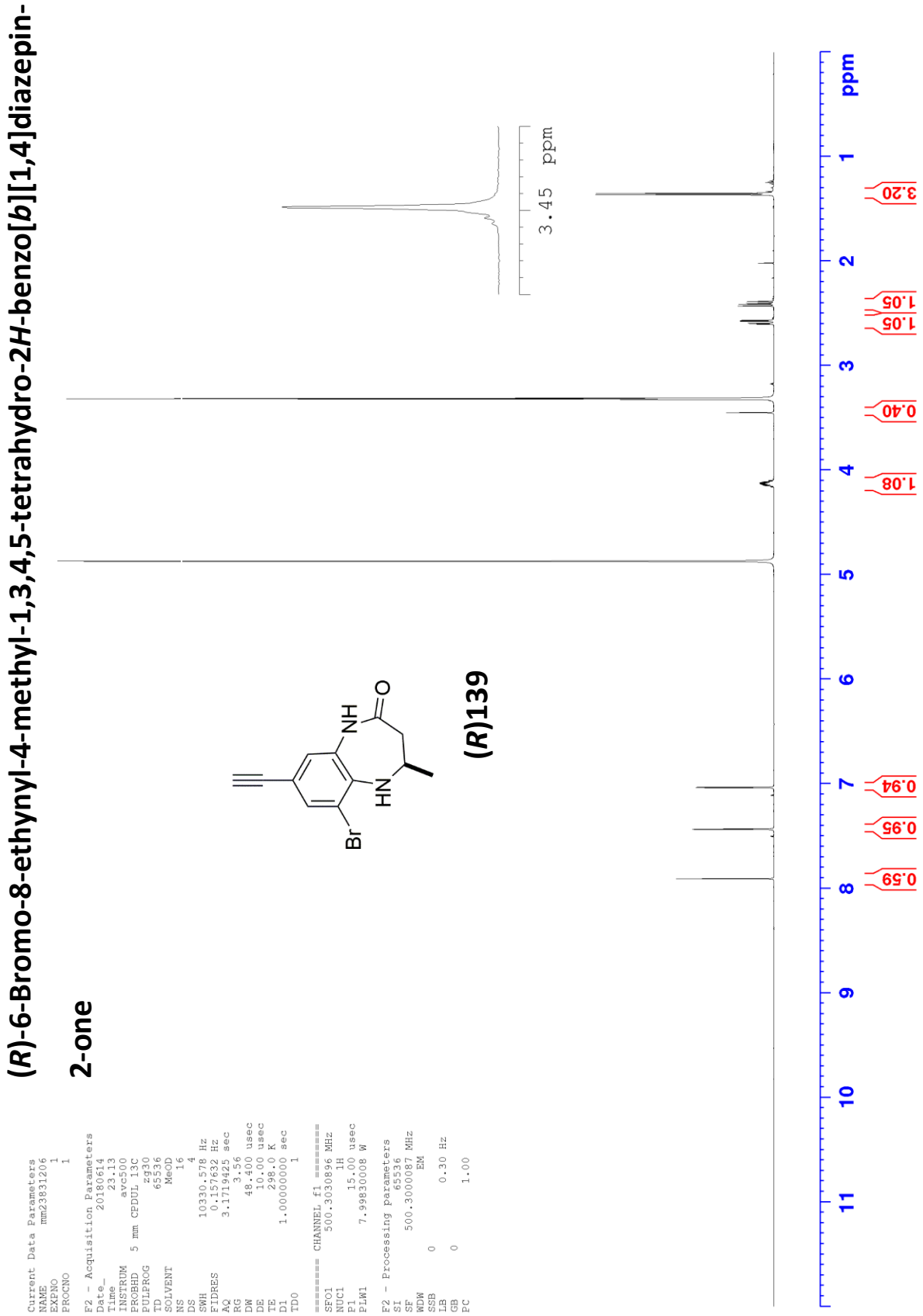


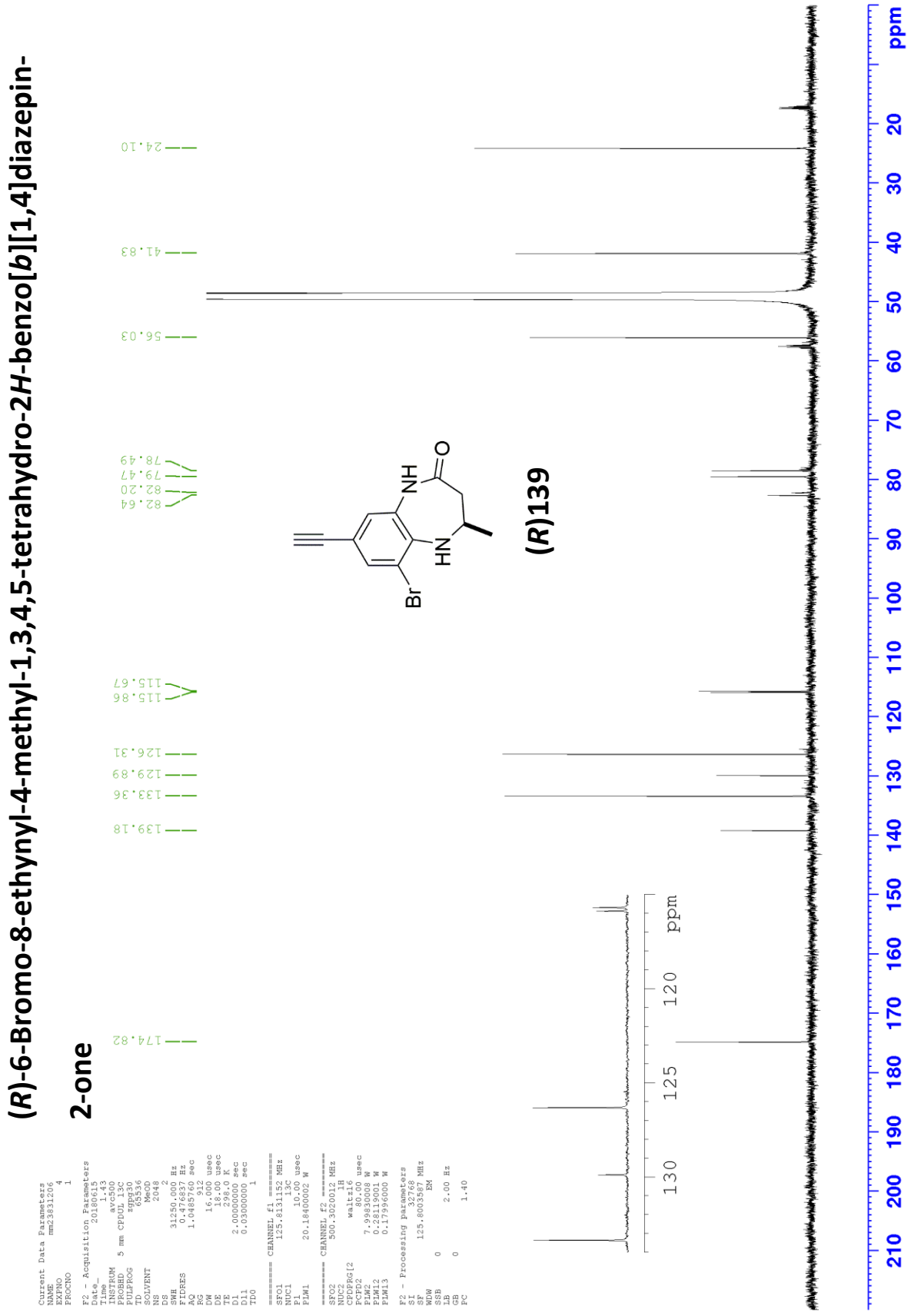

tert-Butyl (R)-3-((2-bromo-4-ethynyl-6-nitrophenyl)amino)
(R)136
Current Data Parameters
NAME mm20892105
EXPNO 1
PROCNO 1
F2 - Acquisition Parameters
Date_ 20180524
Time 1.55
INSTRUM av-500
PROBHD 5 mm CPDUL 13C
PULPROG zg30
TD 65536
SOLVENT CDCl3
NS 16
DS 4
SWH 10330.578 Hz
FIDRES 0.157632 Hz
AQ 3.1719425 sec
RG 3.56
DW 48.400 usec
DE 10.00 usec
TE 298.0 K
D1 1.00000000 sec
TD0 1
======== CHANNEL f1 ========
SFO1 500.3030896 MHz
NUC1 1H
P1 15.00 usec
PLW1 7.99830008 W
F2 - Processing parameters
SI 65536
SF 500.3000132 MHz
WDW EM
SSB 0
LB 0.30 Hz
GB 0
PC 1.00
ppm
3.0
2.8
2.6
11
10
9
8
7
6
5
4
3
2
1
ppm
1.00
1.00
0.98
1.05
0.99
2.14
9.64
3.31

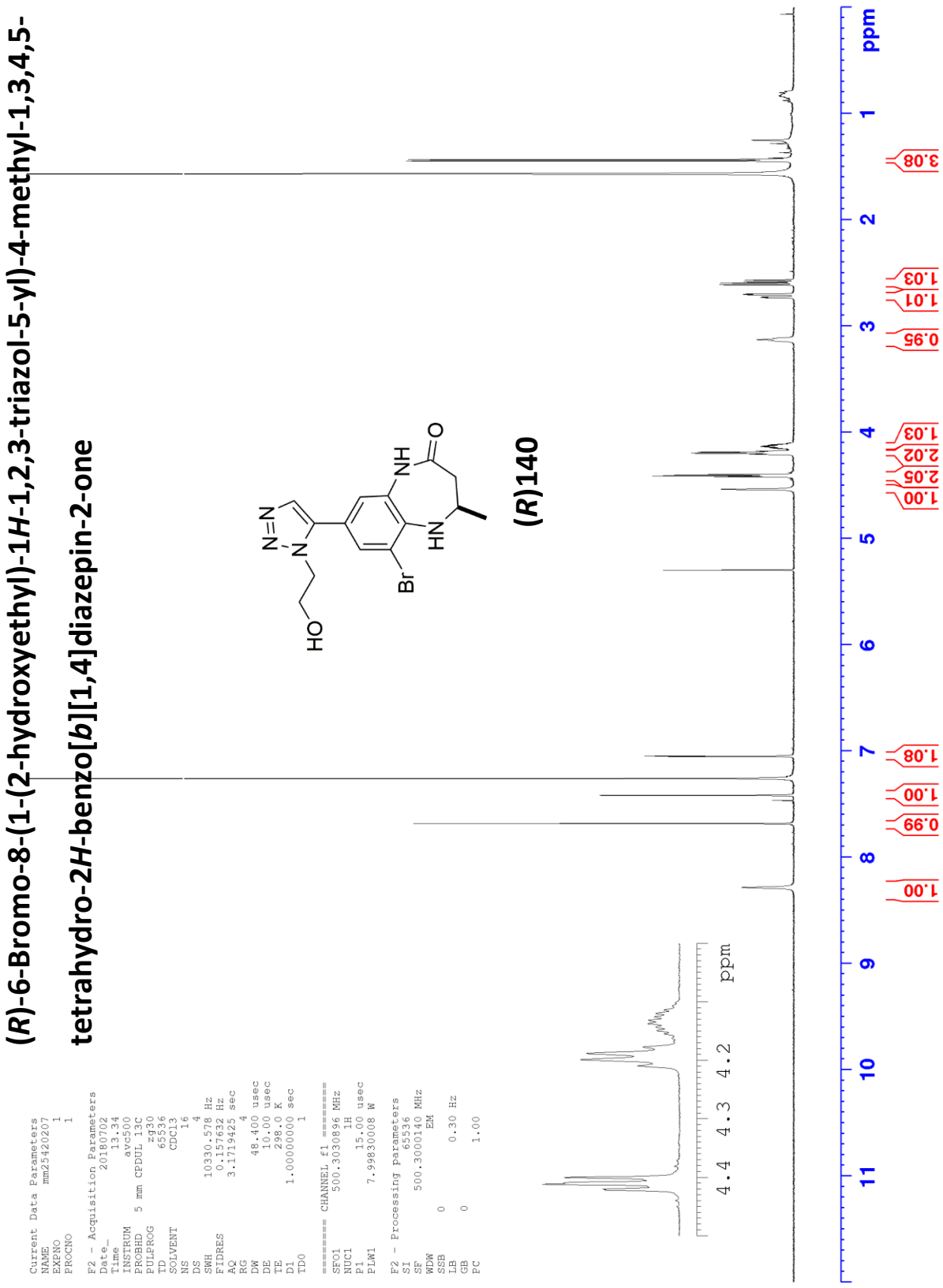

tert-Butyl (R)-3-((2-bromo-4-ethynyl-6-nitrophenyl)amino)
(R)136
Current Data Parameters
NAME mm20892105
EXPNO 4
PROCNO 1
F2 - Acquisition Parameters
Date_ 20180524
Time 4.54
INSTRUM av500
PROBHD 5 mm CPDUL 13C
PULPROG zgpg30
TD 65536
SOLVENT CDCl3
NS 2048
DS 2
SWH 31250.000 Hz
FIDRES 0.476837 Hz
AQ 1.0485760 sec
RG 203.2
DW 16.000 usec
DE 18.00 usec
TE 298.0 K
D1 2.00000000 sec
D11 0.03000000 sec
TD0 1
======== CHANNEL f1 ========
SFO1 125.8131152 MHz
NUC1 13C
P1 10.00 usec
PLW1 20.18400002 W
======== CHANNEL f2 ========
SFO2 500.3020012 MHz
NUC2 1H
CPDPRG[2 waltz16
PCPD2 80.00 usec
PLW2 7.99830008 W
PLW12 0.28119001 W
PLW13 0.17996000 W
F2 - Processing parameters
SI 32768
SF 125.8005188 MHz
WDW EM
SSB 0
LB 1.00 Hz
GB 0
PC 1.40
170.30
142.77
142.31
139.40
129.60
114.96
113.61
81.41
80.38
78.59
50.02
43.54
28.11
21.49
142
ppm
ppm

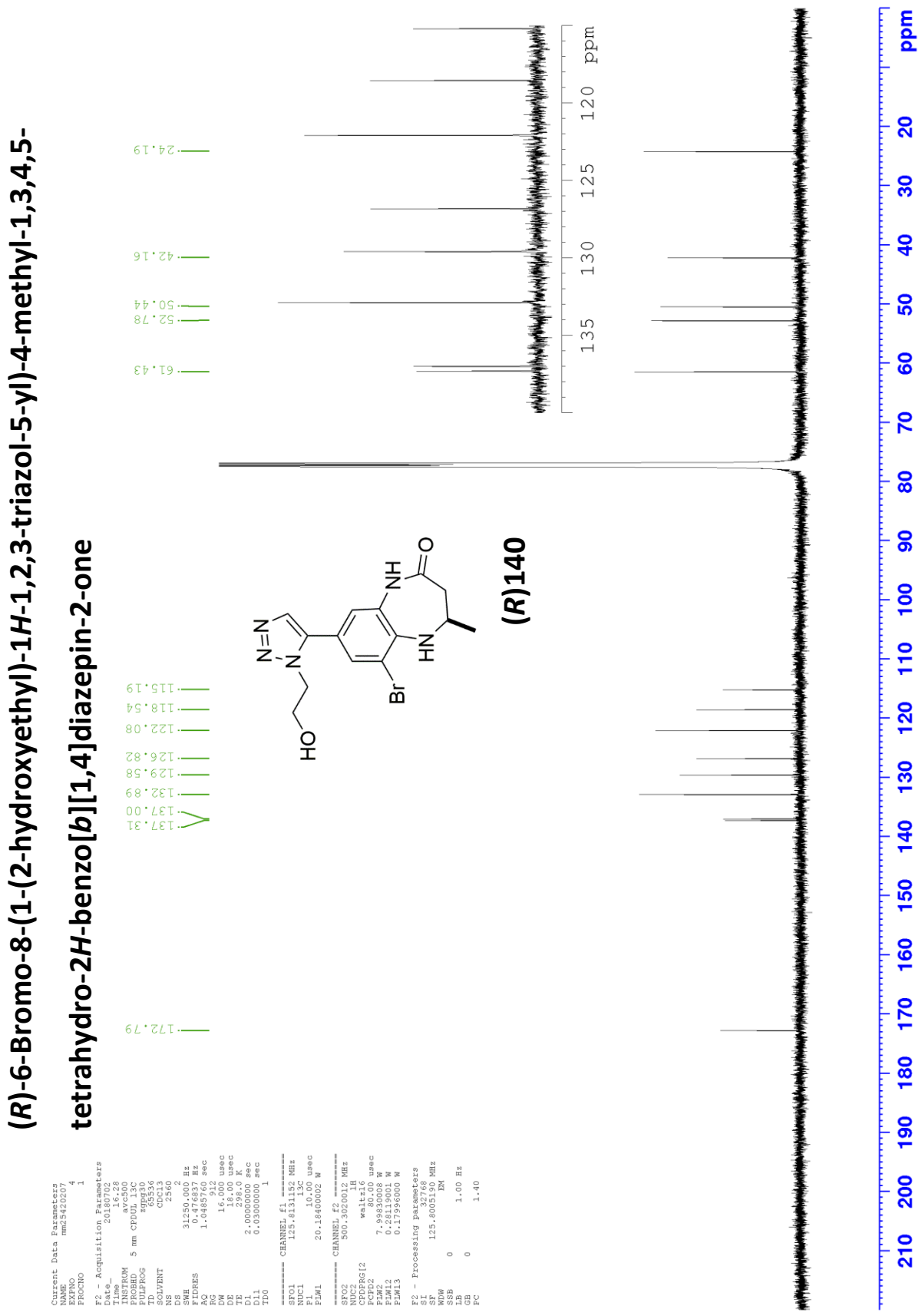

(R)-6-Bromo-4-methyl-8-((trimethylsilyl)ethynyl)-1,3,4,5-tetrahydro-2H-benzo[b][1,4]diazepin-2-one
(R)138
Br
NH
HN
O
Si
ppm
9.00
3.11
1.05
1.06
0.93
1.26
1.02
0.93
2.49
0.99


(R)-6-Bromo-4-methyl-8-((trimethylsilyl)ethynyl)-1,3,4,5-tetrahydro-2H-benzo[b][1,4]diazepin-2-one
(R)138
Si
NH
O
HN
Br
172.05
137.04
132.71
126.84
124.99
115.39
114.73
102.93
94.67
53.58
41.57
24.20
135 130 ppm
ppm

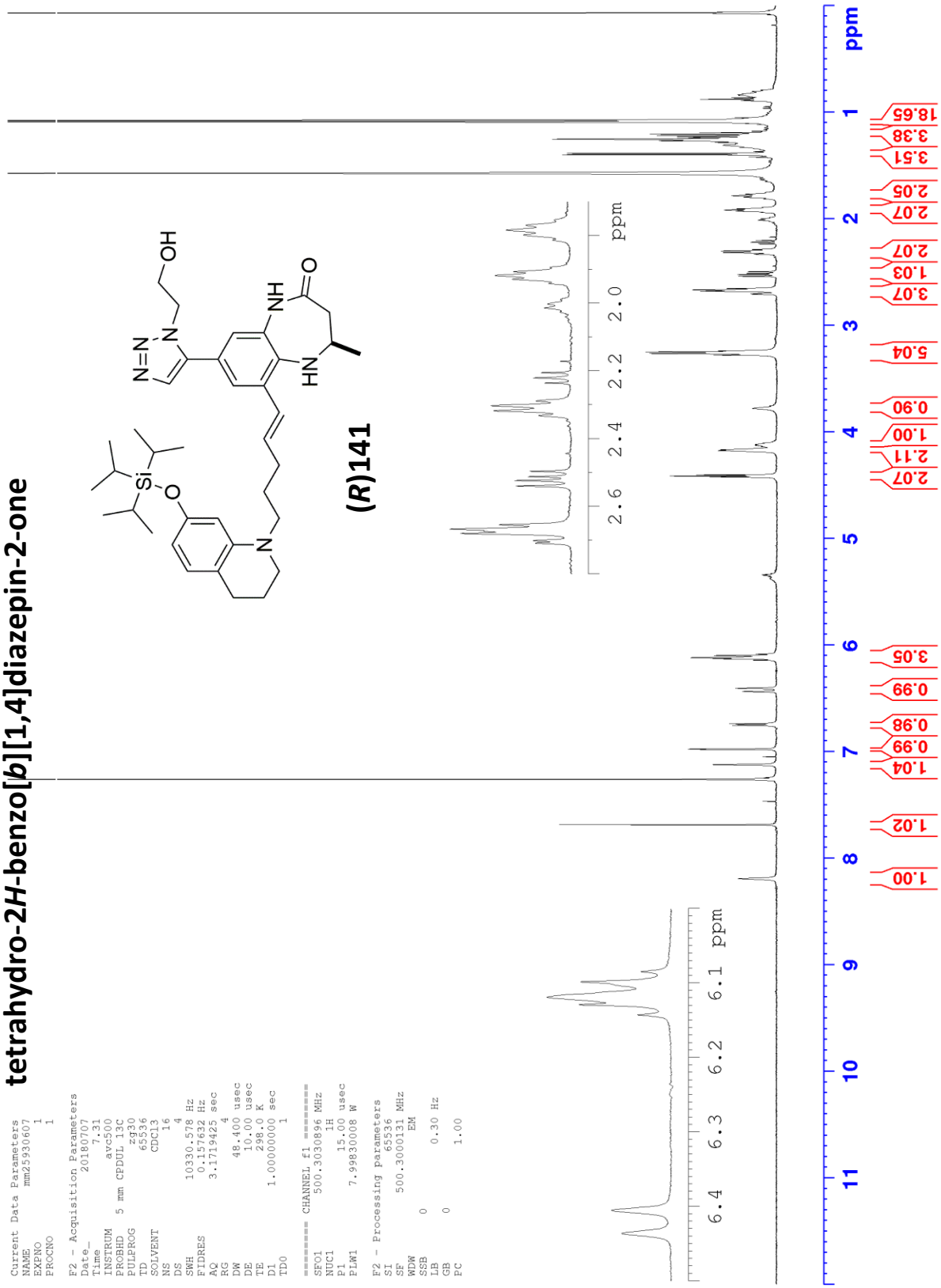

(R)-6-Bromo-8-ethynyl-4-methyl-1,3,4,5-tetrahydro-2H-benzo[b][1,4]diazepin-2-one
(R)139
Br
NH
HN
O
3.45 ppm
0.59
0.95
0.94
1.08
0.40
1.05
1.05
3.20
ppm
Current Data Parameters
NAME mm23831206
EXPNO 1
PROCNO 1
F2 - Acquisition Parameters
Date_ 20180614
Time 23.13
INSTRUM avc500
PROBHD 5 mm CPDUL 13C
PULPROG zg30
TD 65536
SOLVENT MeOD
NS 16
DS 4
SWH 10330.578 Hz
FIDRES 0.157632 Hz
AQ 3.1719425 sec
RG 3.56
DW 48.400 usec
DE 10.00 usec
TE 298.0 K
D1 1.00000000 sec
TD0 1
======== CHANNEL f1 ========
SFO1 500.3030896 MHz
NUC1 1H
P1 15.00 usec
PLW1 7.99830008 W
F2 - Processing parameters
SI 65536
SF 500.3000087 MHz
WDW EM
SSB 0
LB 0.30 Hz
GB 0
PC 1.00


(R)-6-Bromo-8-ethynyl-4-methyl-1,3,4,5-tetrahydro-2H-benzo[b][1,4]diazepin-2-one
(R)139
Br
NH
HN
O
174.82
139.18
133.36
129.89
126.31
115.86
115.67
82.64
82.20
79.47
78.49
56.03
41.83
24.10
ppm

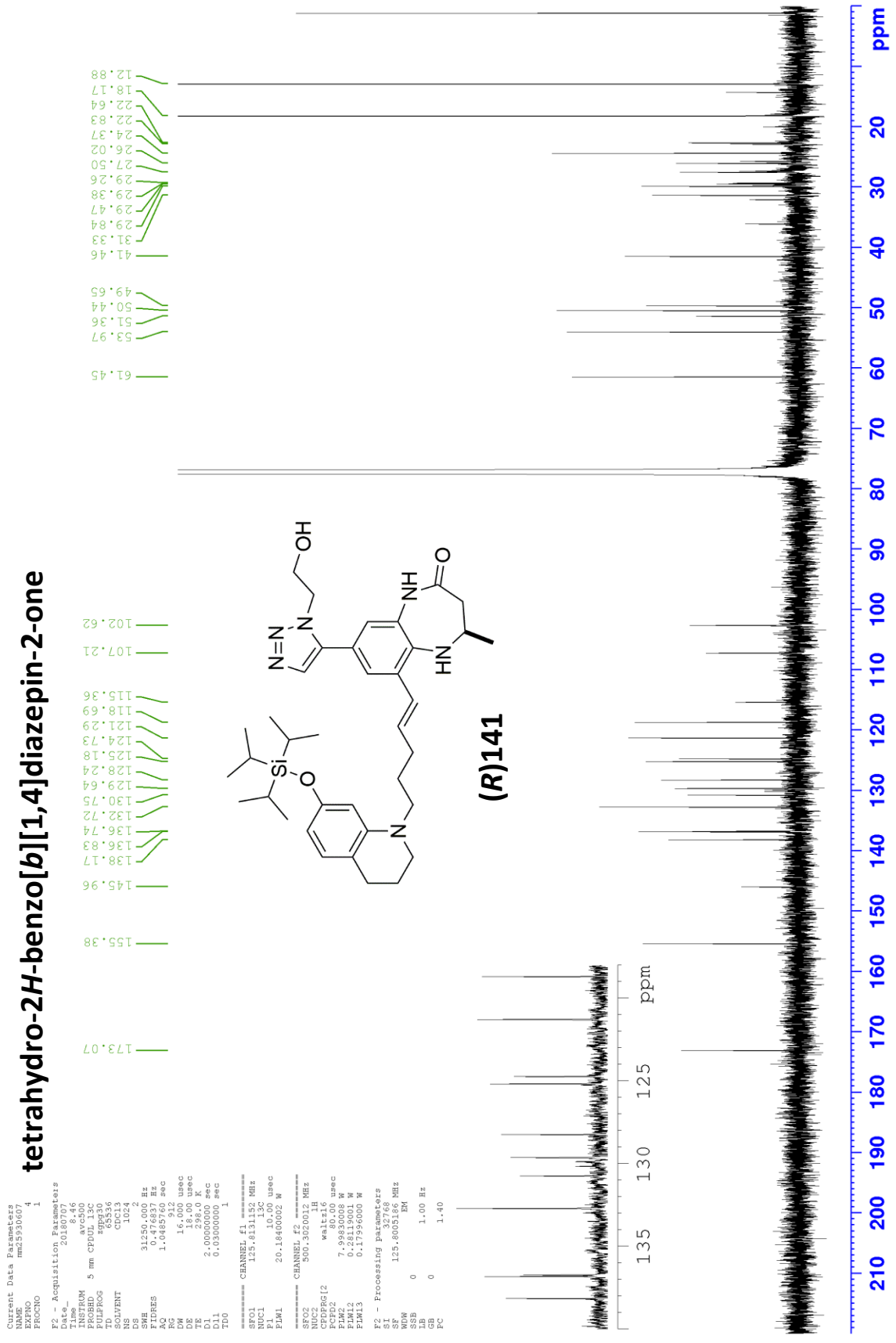

(R)-6-Bromo-8-(1-(2-hydroxyethyl)-1H-1,2,3-triazol-5-yl)-4-methyl-1,3,4,5-tetrahydro-2H-benzo[b][1,4]diazepin-2-one
(R)140
Current Data Parameters
NAME mm25420207
EXPNO 1
PROCNO 1
F2 - Acquisition Parameters
Date_ 20180702
Time 13.34
INSTRUM ave500
PROBHD 5 mm CPDUL 13C
PULPROG zg30
TD 65536
SOLVENT CDCl3
NS 16
DS 4
SWH 10330.578 Hz
FIDRES 0.157632 Hz
AQ 3.1719425 sec
RG 4
DW 48.400 usec
DE 10.00 usec
TE 298.0 K
D1 1.00000000 sec
TD0 1
======== CHANNEL f1 ========
SFO1 500.3030896 MHz
NUC1 1H
P1 15.00 usec
PLW1 7.99830008 W
F2 - Processing parameters
SI 65536
SF 500.3000140 MHz
WDW EM
SSB 0
LB 0.30 Hz
GB 0
PC 1.00
ppm
1.00
0.99
1.00
1.08
1.00
2.05
2.02
1.03
0.95
1.01
1.03
3.08


(R)-6-Bromo-8-(1-(2-hydroxyethyl)-1H-1,2,3-triazol-5-yl)-4-methyl-1,3,4,5-tetrahydro-2H-benzo[b][1,4]diazepin-2-one
(R)140
Current Data Parameters
NAME mm25420207
EXPNO 4
PROCNO 1
F2 - Acquisition Parameters
Date_ 20180702
Time 16.28
INSTRUM av500
PROBHD 5 mm CPDUL 13C
PULPROG zgpg30
TD 65536
SOLVENT CDCl3
NS 256
DS 2
SWH 31250.000 Hz
FIDRES 0.476837 Hz
AQ 1.0485760 sec
RG 202
DW 16.000 usec
DE 18.00 usec
TE 298.0 K
D1 2.00000000 sec
D11 0.03000000 sec
TD0 1
======== CHANNEL f1 ========
SFO1 125.8131152 MHz
NUC1 13C
P1 10.00 usec
PLW1 20.18400002 W
======== CHANNEL f2 ========
SFO2 500.3020012 MHz
NUC2 1H
CPDPRG[2 waltz16
PCPD2 80.00 usec
PLW2 7.99830008 W
PLW12 0.28119001 W
PLW13 0.17996600 W
F2 - Processing parameters
SI 32768
SF 125.8005190 MHz
WDW EM
SSB 0
LB 1.00 Hz
GB 0
PC 1.40
172.79
137.31
137.00
132.89
129.58
126.82
122.08
118.54
115.19
61.43
52.78
50.44
42.16
24.19
135 130 125 120 ppm
210 200 190 180 170 160 150 140 130 120 110 100 90 80 70 60 50 40 30 20 ppm

(*R*,*E*)-8-(1-(2-Hydroxyethyl)-*1H*-1,2,3-triazol-5-yl)-4-methyl-6-(5-((triisopropylsilyl)oxy)-3,4-dihydroquinolin-1(2*H*)-yl)pent-1-en-1-yl)-1,3,4,5-tetrahydro-2*H*-benzo[*b*][1,4]diazepin-2-one

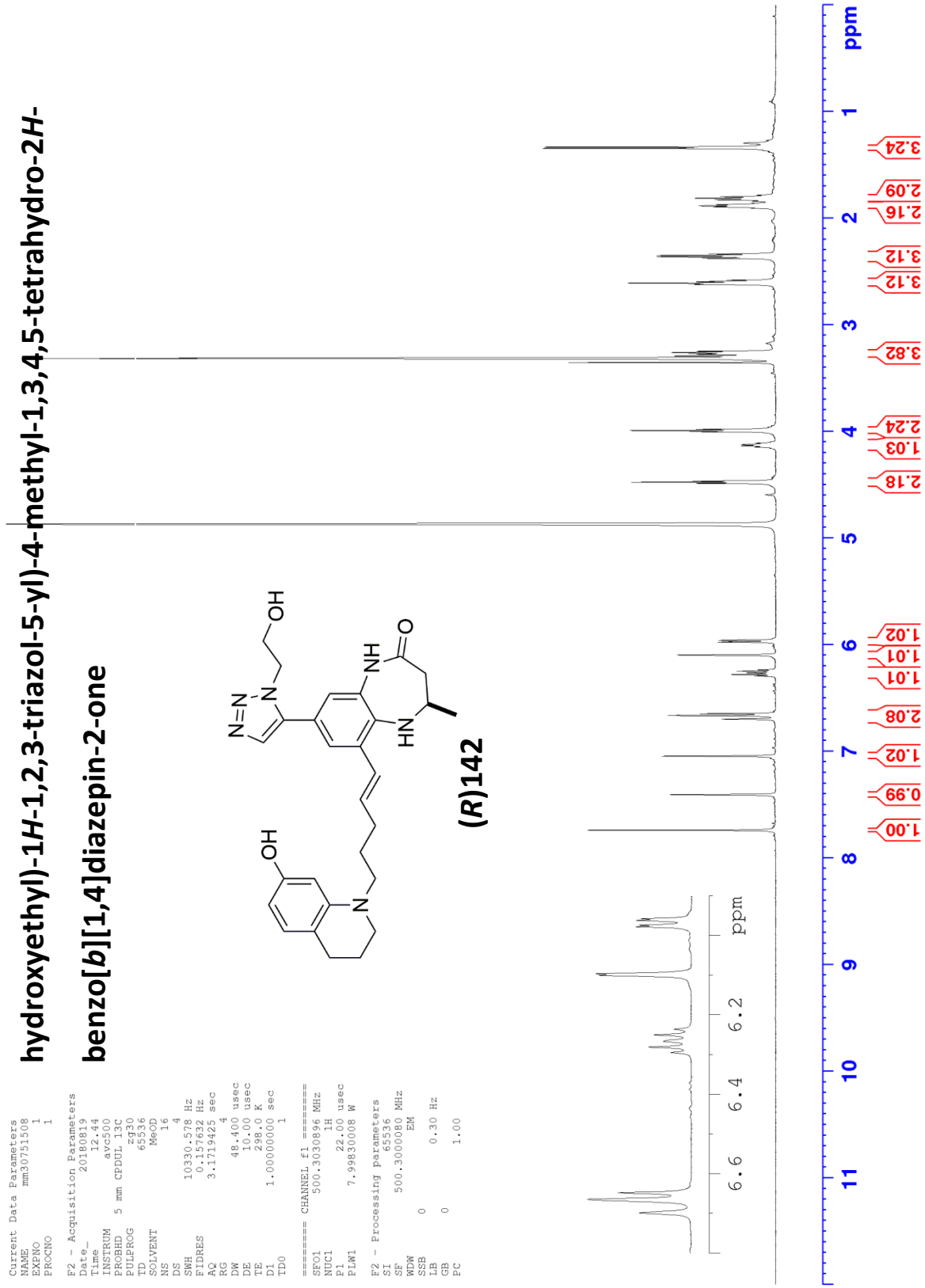


(*R*,*E*)-8-(1-(2-Hydroxyethyl)-1*H*-1,2,3-triazol-5-yl)-4-methyl-6-(5-(7-((triisopropylsilyl)oxy)-3,4-dihydroquinolin-1(2*H*)-yl)pent-1-en-1-yl)-1,3,4,5-tetrahydro-2*H*-benzo[*b*][1,4]diazepin-2-one

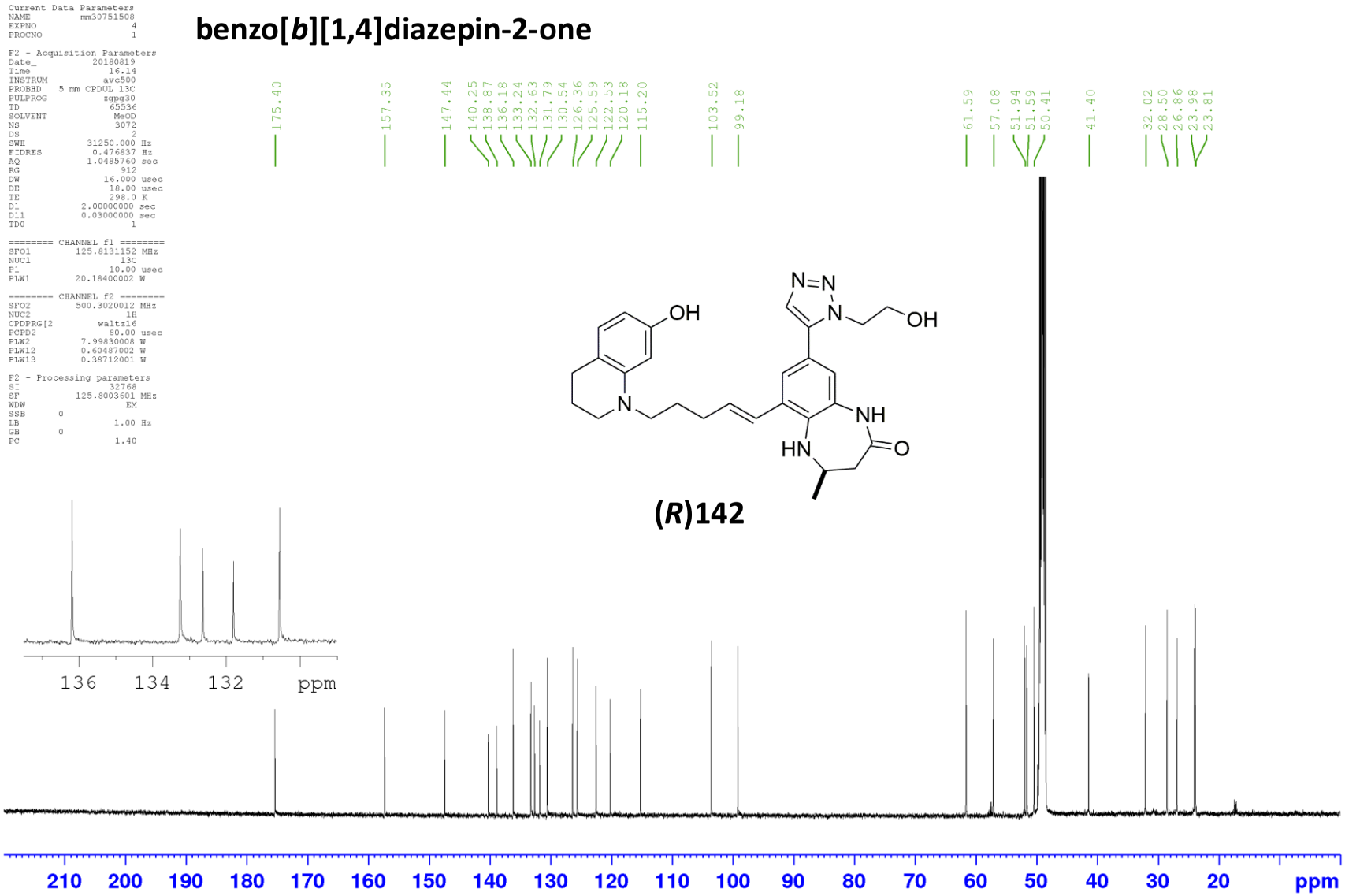


(*R*,*E*)-6-(5-(7-Hydroxy-3,4-dihydroquinolin-1(2*H*)-yl)pent-1-en-1-yl)-8-(1-(2-hydroxyethyl)-1*H*-1,2,3-triazol-5-yl)-4-methyl-1,3,4,5-tetrahydro-2*H*-benzo[*b*][1,4]diazepin-2-one

(*R*)142

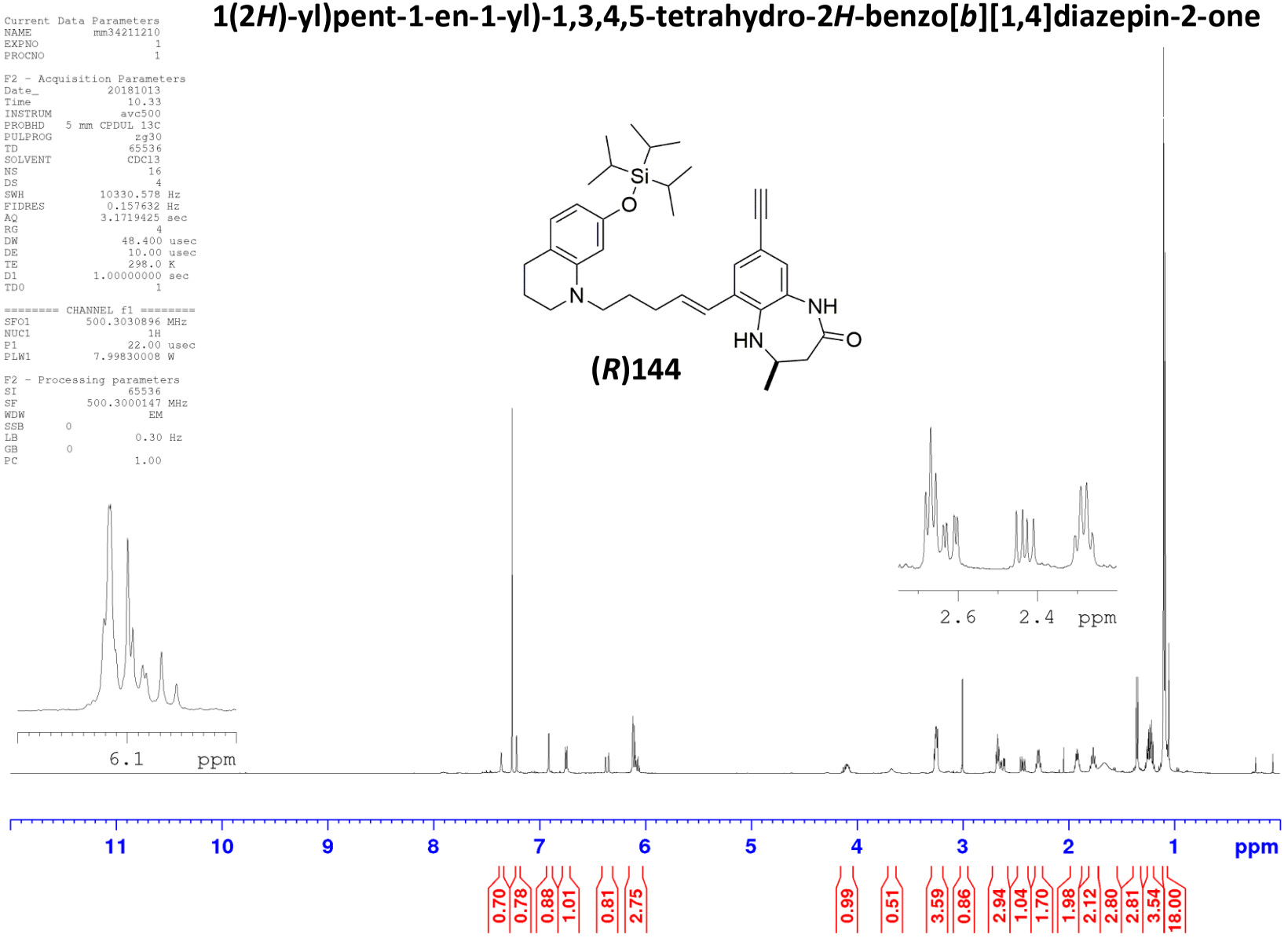


(*R*,*E*)-6-(5-(7-Hydroxy-3,4-dihydroquinolin-1(2*H*)-yl)pent-1-en-1-yl)-8-(1-(2-hydroxyethyl)-1*H*-1,2,3-triazol-5-yl)-4-methyl-1,3,4,5-tetrahydro-2*H*-benzo[*b*][1,4]diazepin-2-one

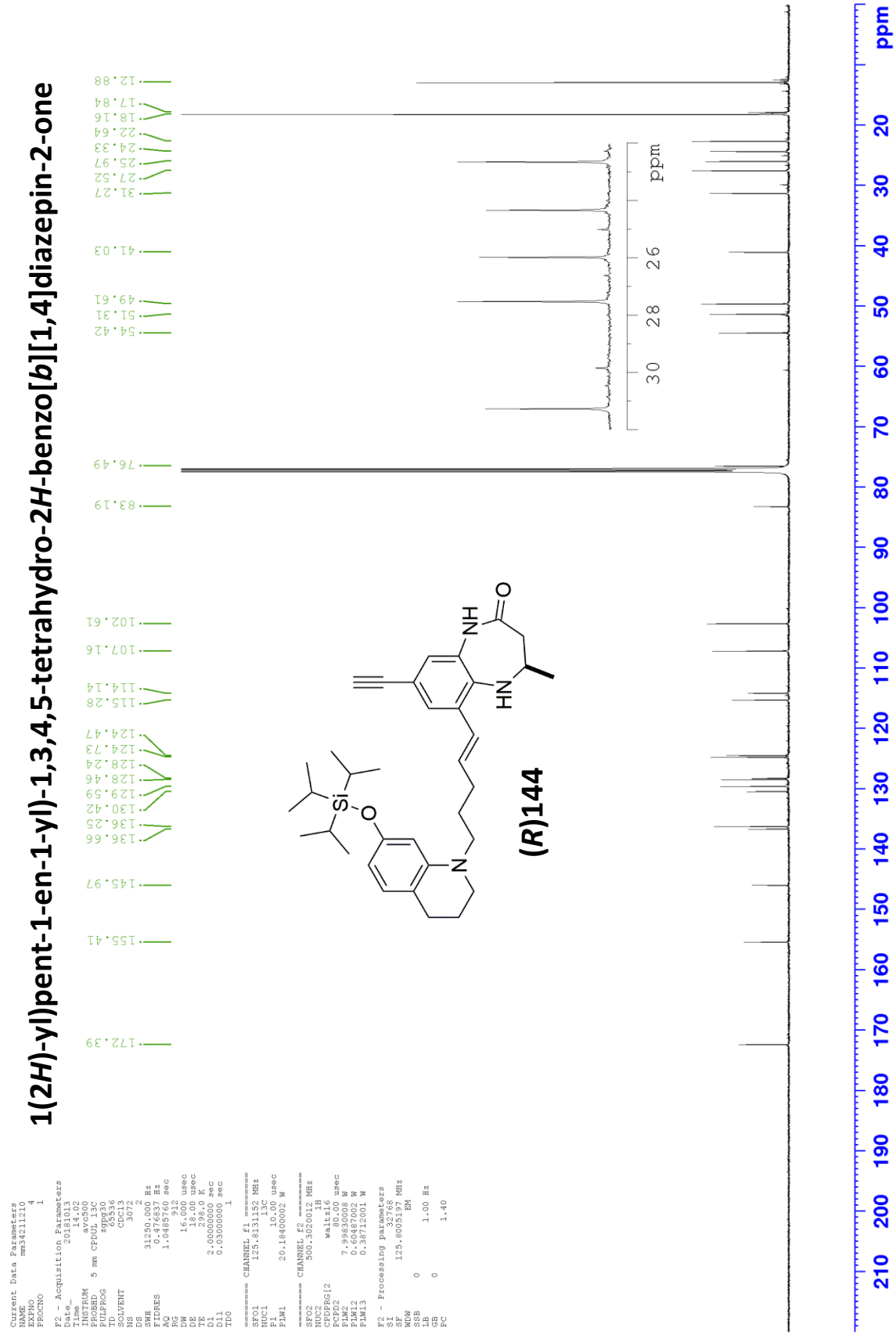


(*R*)142

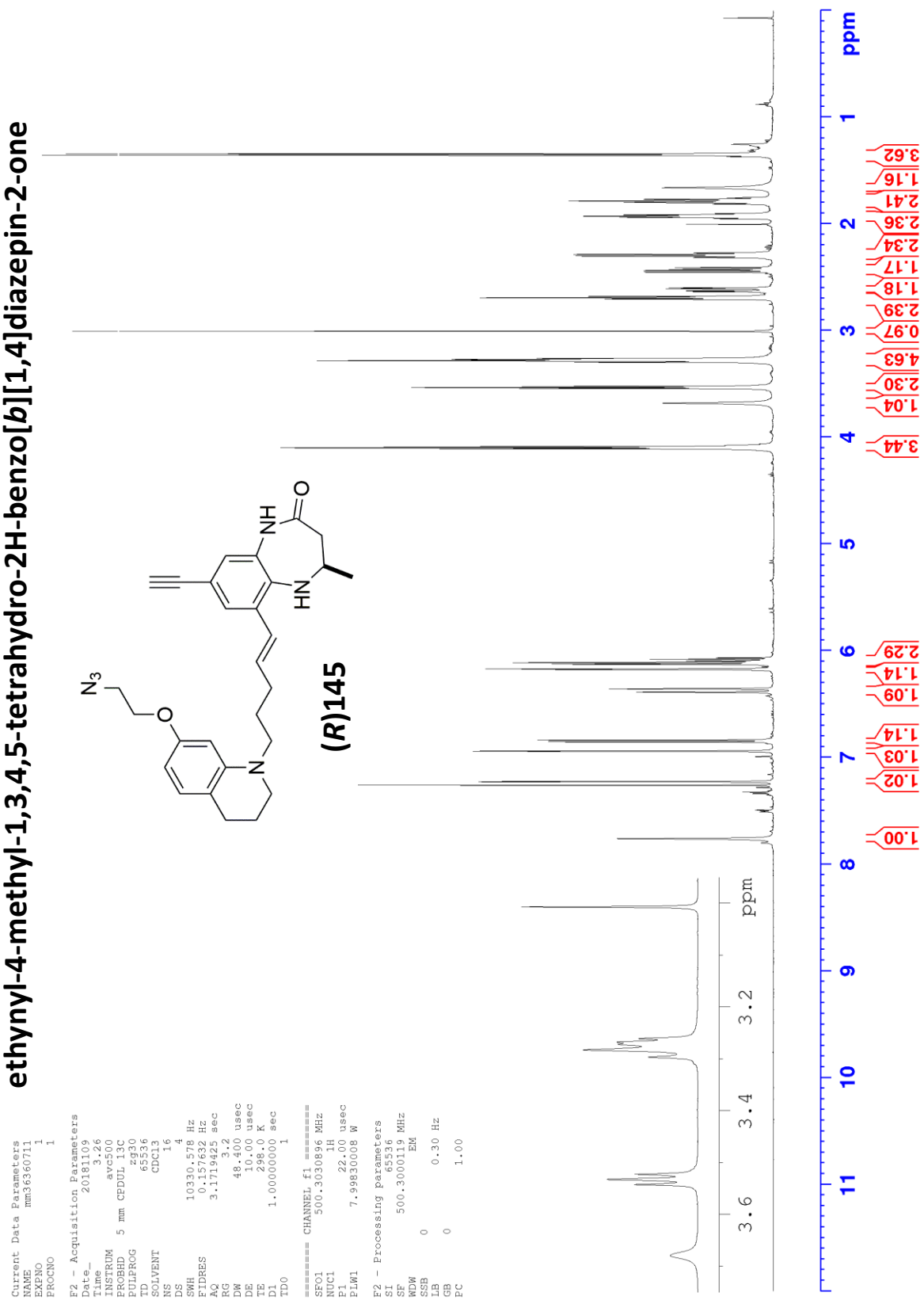
(*R*,*E*)-8-Ethynyl-4-methyl-6-(5-(7-((triisopropylsilyl)oxy)-3,4-dihydroquinolin-1(2*H*)-yl)pent-1-en-1-yl)-1,3,4,5-tetrahydro-2*H*-benzo[*b*][1,4]diazepin-2-one



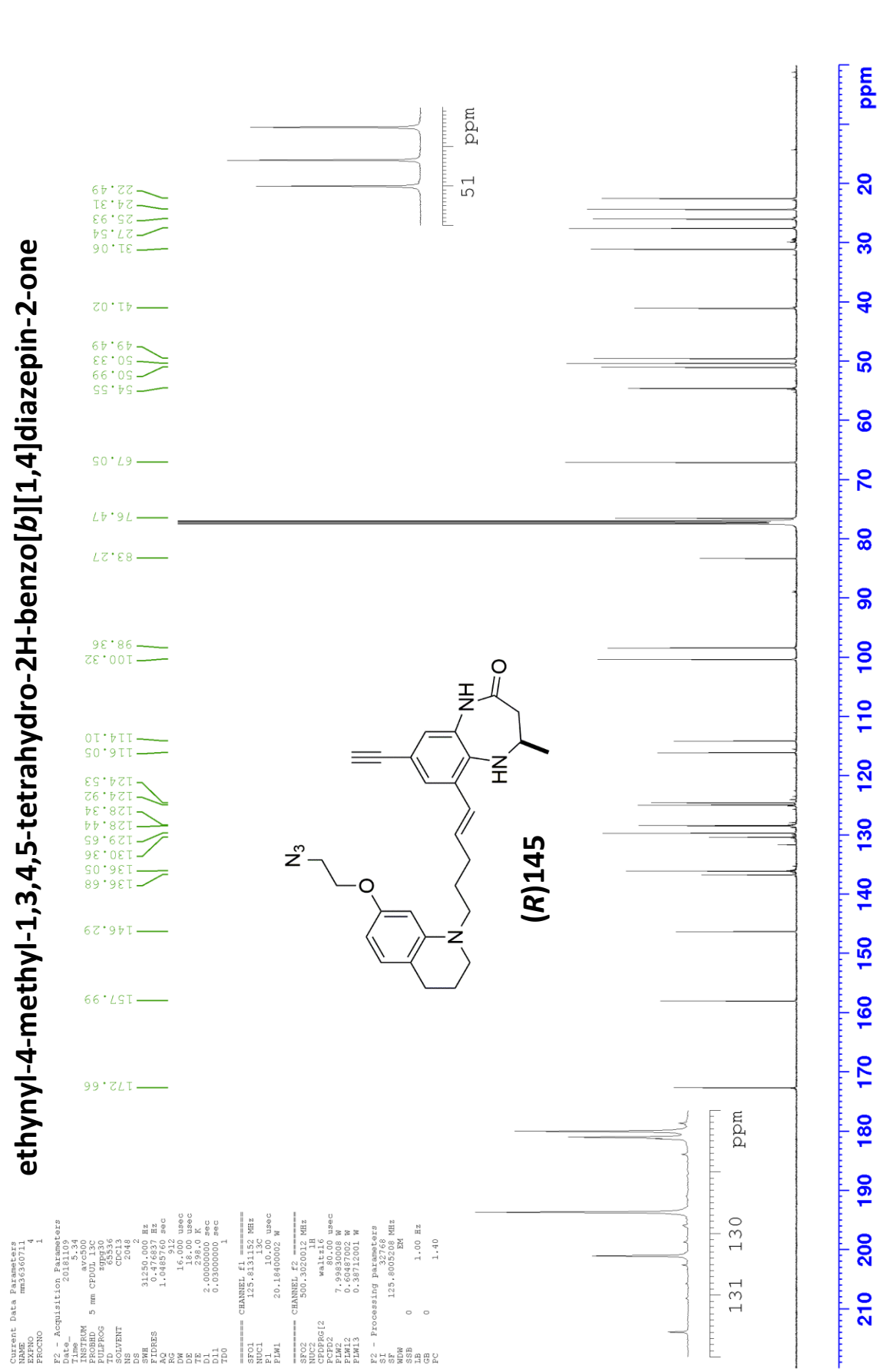
(*R*,*E*)-8-Ethynyl-4-methyl-6-(5-(7-((triisopropylsilyl)oxy)-3,4-dihydroquinolin-1(2*H*)-yl)pent-1-en-1-yl)-1,3,4,5-tetrahydro-2*H*-benzo[*b*][1,4]diazepin-2-one

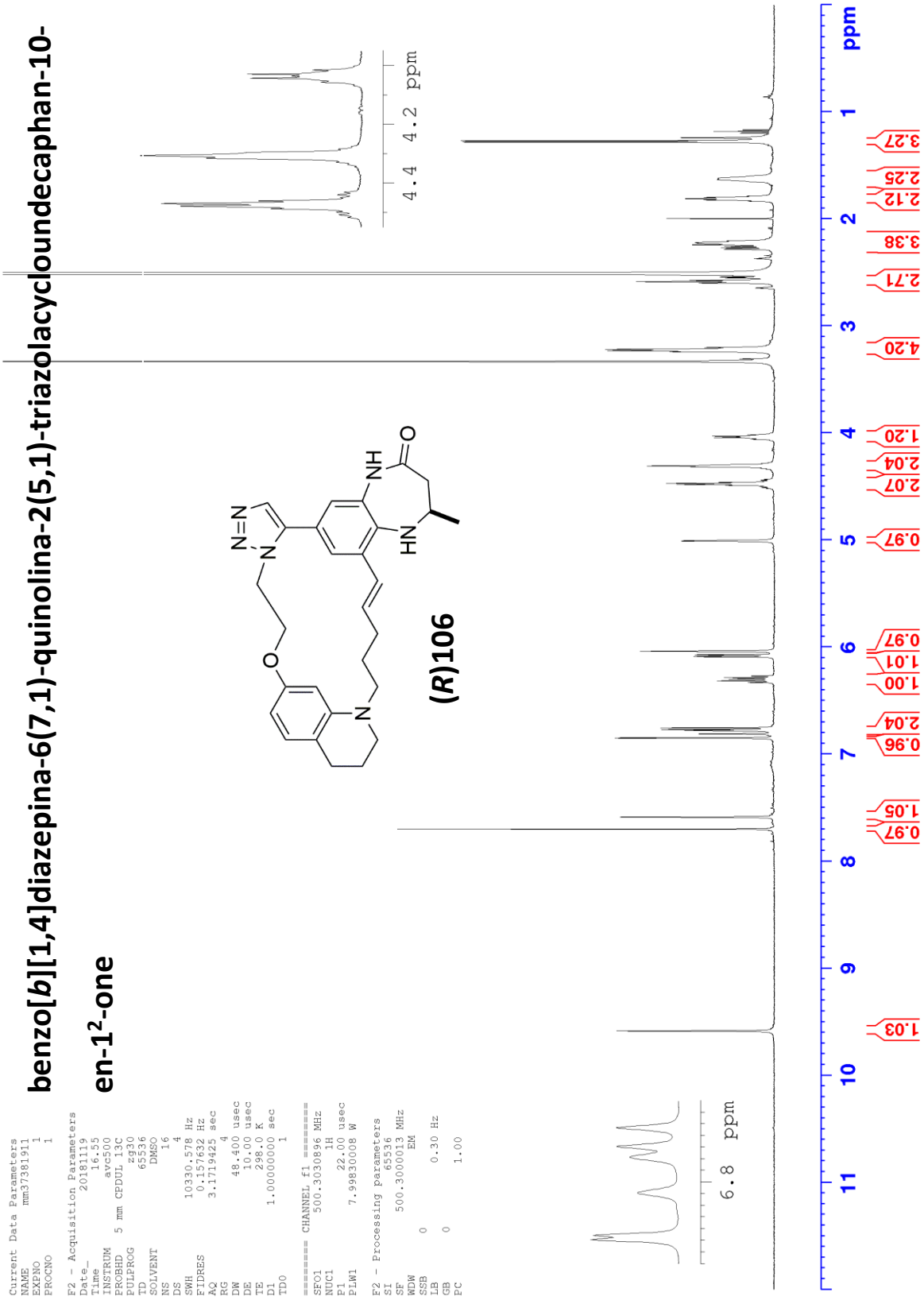


(*R*,*E*)-6-(5-(7-(2-Azidoethoxy)-3,4-dihydroquinolin-1(2*H*)-yl)pent-1-en-1-yl)-8-ethynyl-4-methyl-1,3,4,5-tetrahydro-2H-benzo[*b*][1,4]diazepin-2-one

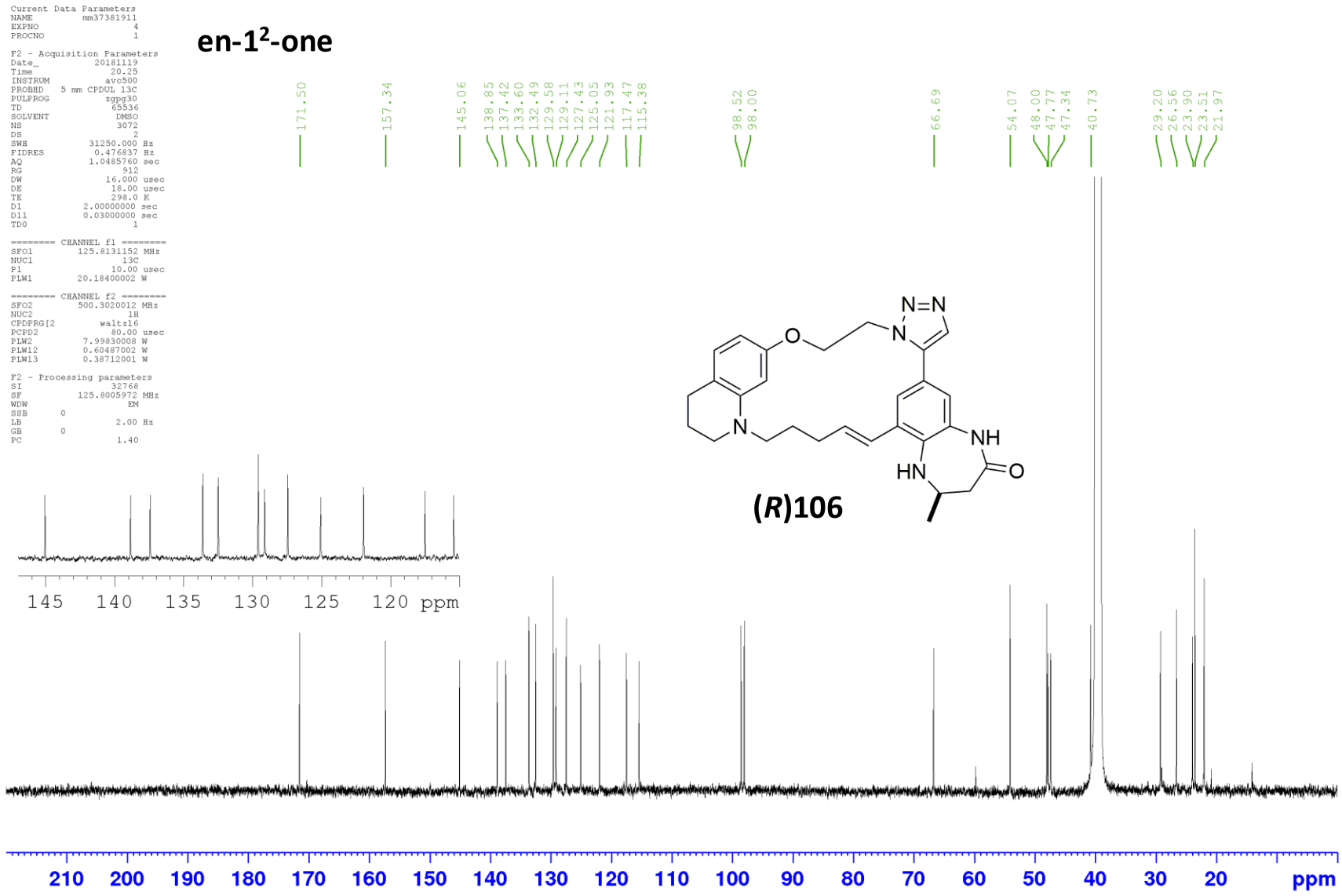


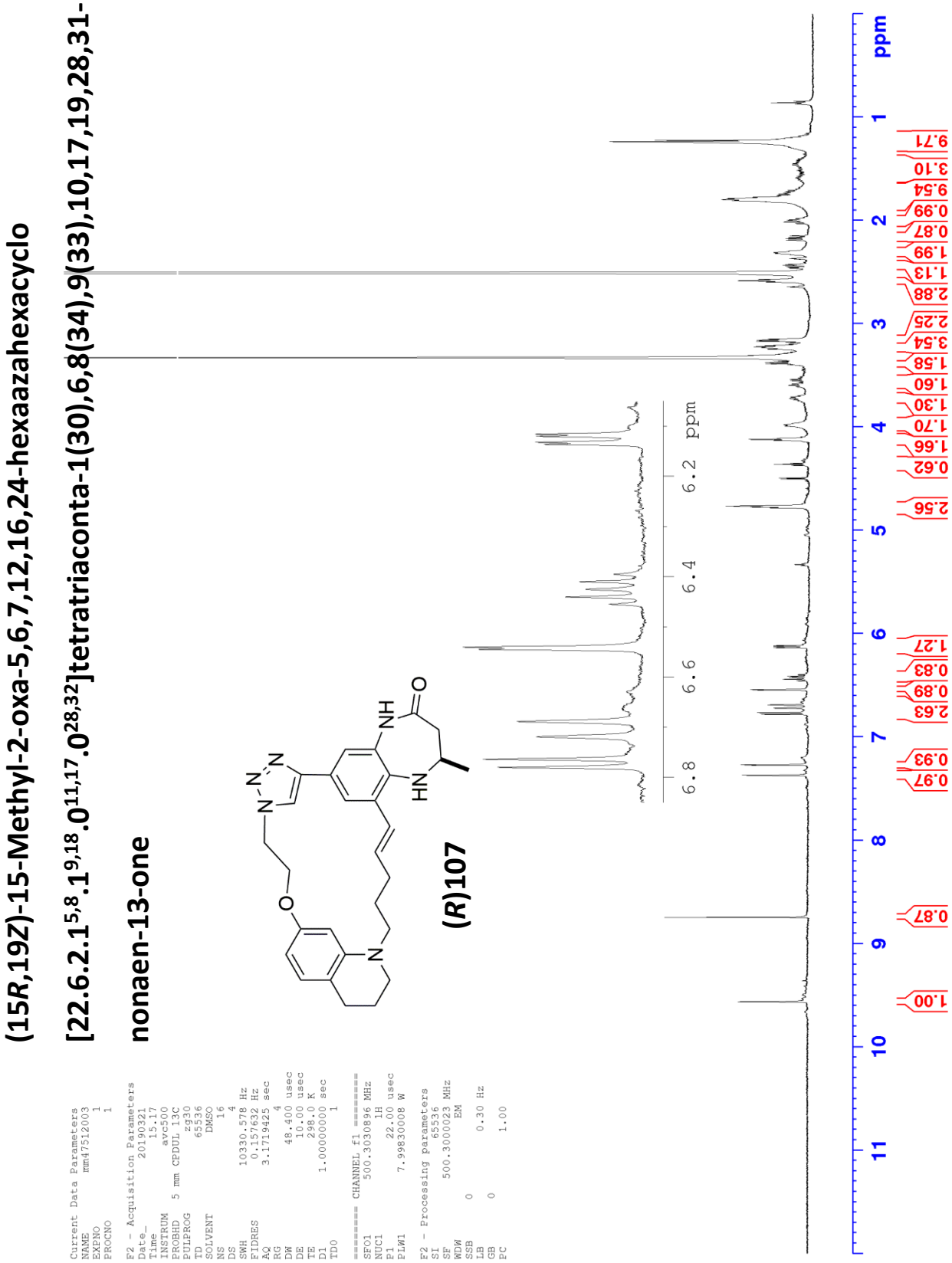
(*R*,*E*)-6-(5-(7-(2-Azidoethoxy)-3,4-dihydroquinolin-1(2*H*)-yl)pent-1-en-1-yl)-8-ethynyl-4-methyl-1,3,4,5-tetrahydro-2H-benzo[*b*][1,4]diazepin-2-one



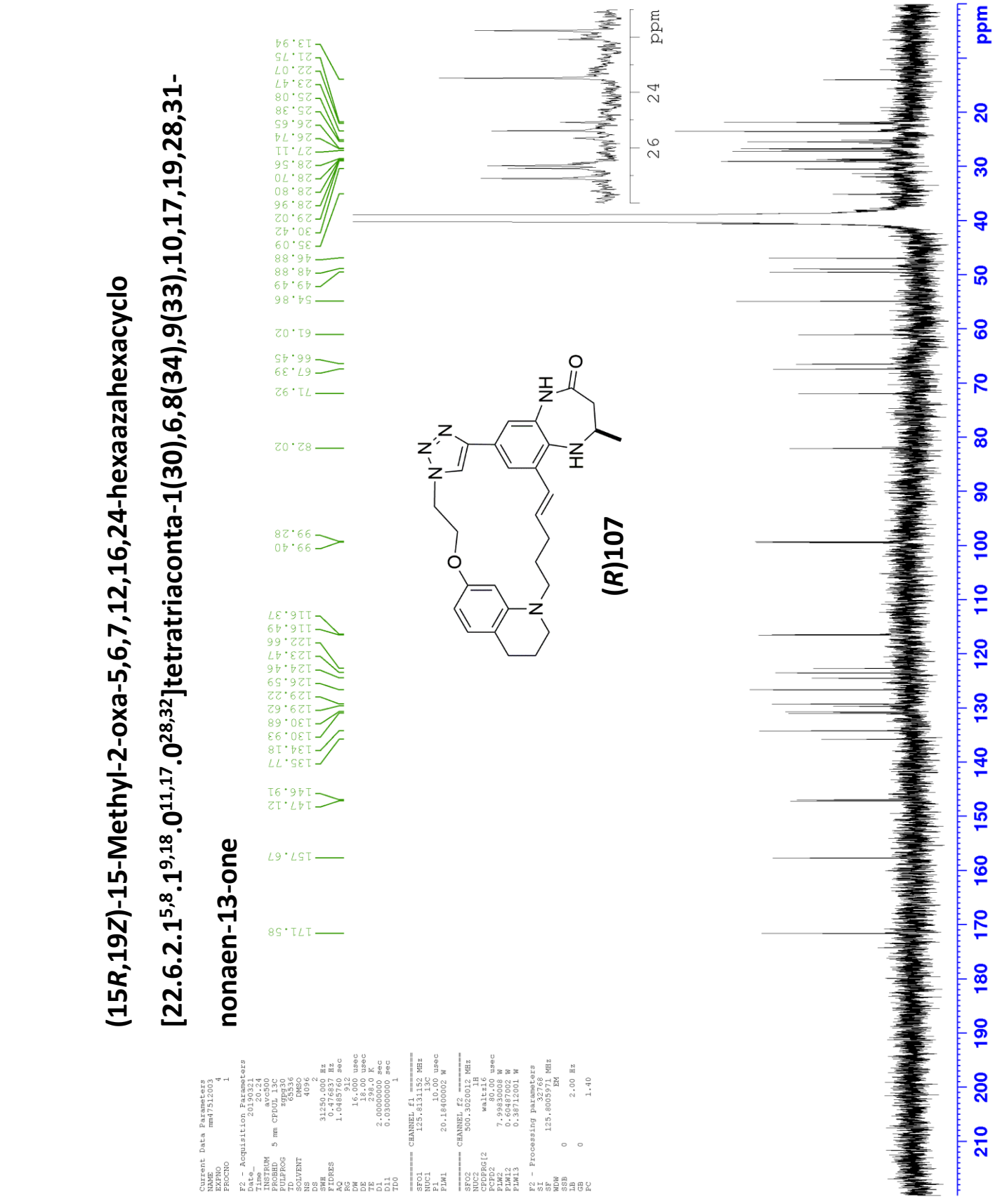

(R,E)-1⁴-Methyl-1²,1³,1⁴,1⁵,6¹,6²,6³,6⁴-octahydro-1¹H,2¹H-5-oxa-1(8,6)-benzo[b][1,4]diazepina-6(7,1)-quinolina-2(5,1)-triazolacycloundecaphan-10-en-1²-one
(R)106
Current Data Parameters
NAME mm37381911
EXPNO 1
PROCNO 1
F2 - Acquisition Parameters
Date_ 20181119
Time 16.55
INSTRUM avc500
PROBHD 5 mm CPDUL 13C
PULPROG zg30
TD 65536
SOLVENT DMSO
NS 16
DS 4
SWH 10330.578 Hz
FIDRES 0.157632 Hz
AQ 3.1719425 sec
RG 4
DW 48.400 usec
DE 10.00 usec
TE 298.0 K
D1 1.00000000 sec
TD0 1
======== CHANNEL f1 ========
SFO1 500.3030896 MHz
NUC1 1H
P1 22.00 usec
PLW1 7.99830008 W
F2 - Processing parameters
SI 65536
SF 500.3000013 MHz
WDW EM
SSB 0
LB 0.30 Hz
GB 0
PC 1.00
4.4 4.2 ppm
6.8 ppm
ppm
1.03
0.97
1.05
0.96
2.04
1.00
1.01
0.97
2.07
2.04
1.20
4.20
2.71
3.38
2.12
2.25
3.27

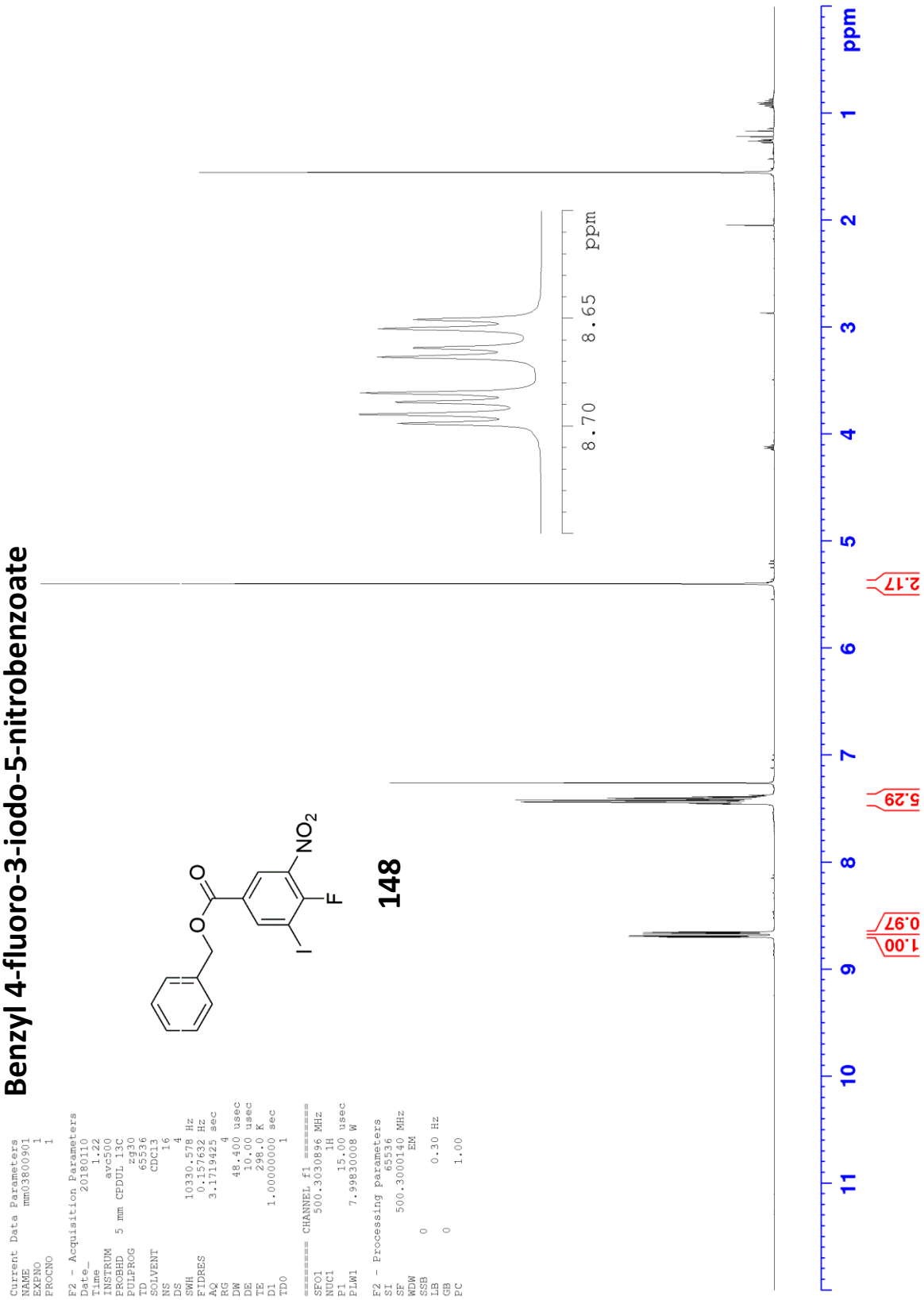
(*R*,*E*)-1^4-Methyl-1^2,1^3,1^4,1^5,6^1,6^2,6^3,6^4-octahydro-1^1*H*,2^1*H*-5-oxa-1(8,6)-benzo[*b*][1,4]diazepina-6(7,1)-quinolina-2(5,1)-triazolacycloundecaphan-10-en-1^2-one

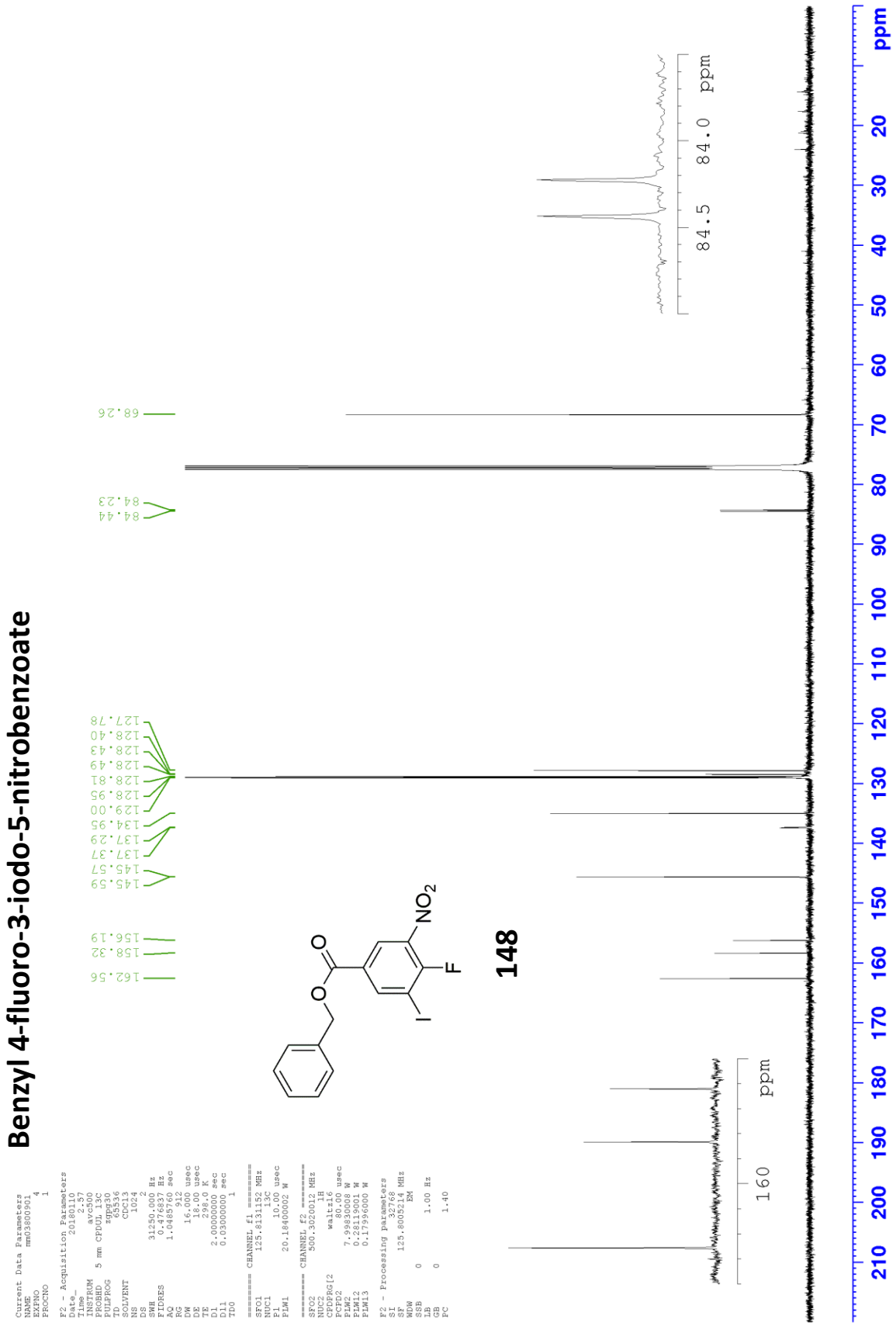


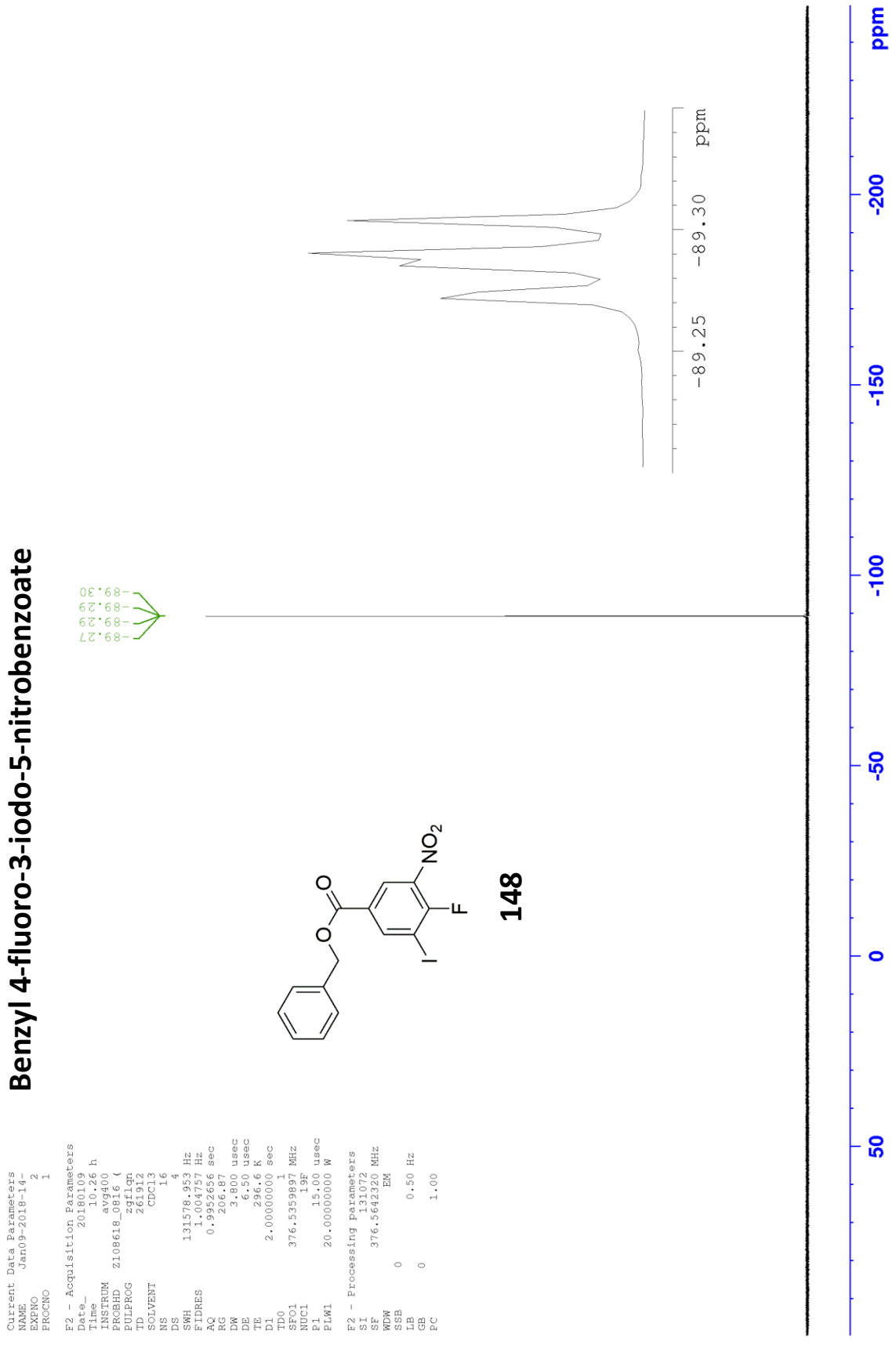

(15R,19Z)-15-Methyl-2-oxa-5,6,7,12,16,24-hexaazahexacyclo
[22.6.2.1^5,8.1^9,18.0^11,17.0^28,32]tetratriaconta-1(30),6,8(34),9(33),10,17,19,28,31-
nonaen-13-one
(R)107
Current Data Parameters
NAME mm47512003
EXPNO 1
PROCNO 1
F2 - Acquisition Parameters
Date_ 20190321
Time 15.17
INSTRUM avc500
PROBHD 5 mm CPDUL 13C
PULPROG zg30
TD 65536
SOLVENT DMSO
NS 16
DS 4
SWH 10330.578 Hz
FIDRES 0.157632 Hz
AQ 3.1719425 sec
RG 4
DW 48.400 usec
DE 10.00 usec
TE 298.0 K
D1 1.00000000 sec
TD0 1
======== CHANNEL f1 ========
SFO1 500.3030896 MHz
NUC1 1H
P1 22.00 usec
PLW1 7.99830008 W
F2 - Processing parameters
SI 65536
SF 500.3000023 MHz
WDW EM
SSB 0
LB 0.30 Hz
GB 0
PC 1.00
6.8
6.6
6.4
6.2
ppm
1.00
0.87
0.97
0.93
2.63
0.89
0.83
1.27
2.56
0.62
1.66
1.70
1.30
1.60
1.58
3.54
2.25
2.88
1.13
1.99
0.87
0.99
9.54
3.10
9.71
11
10
9
8
7
6
5
4
3
2
1
ppm

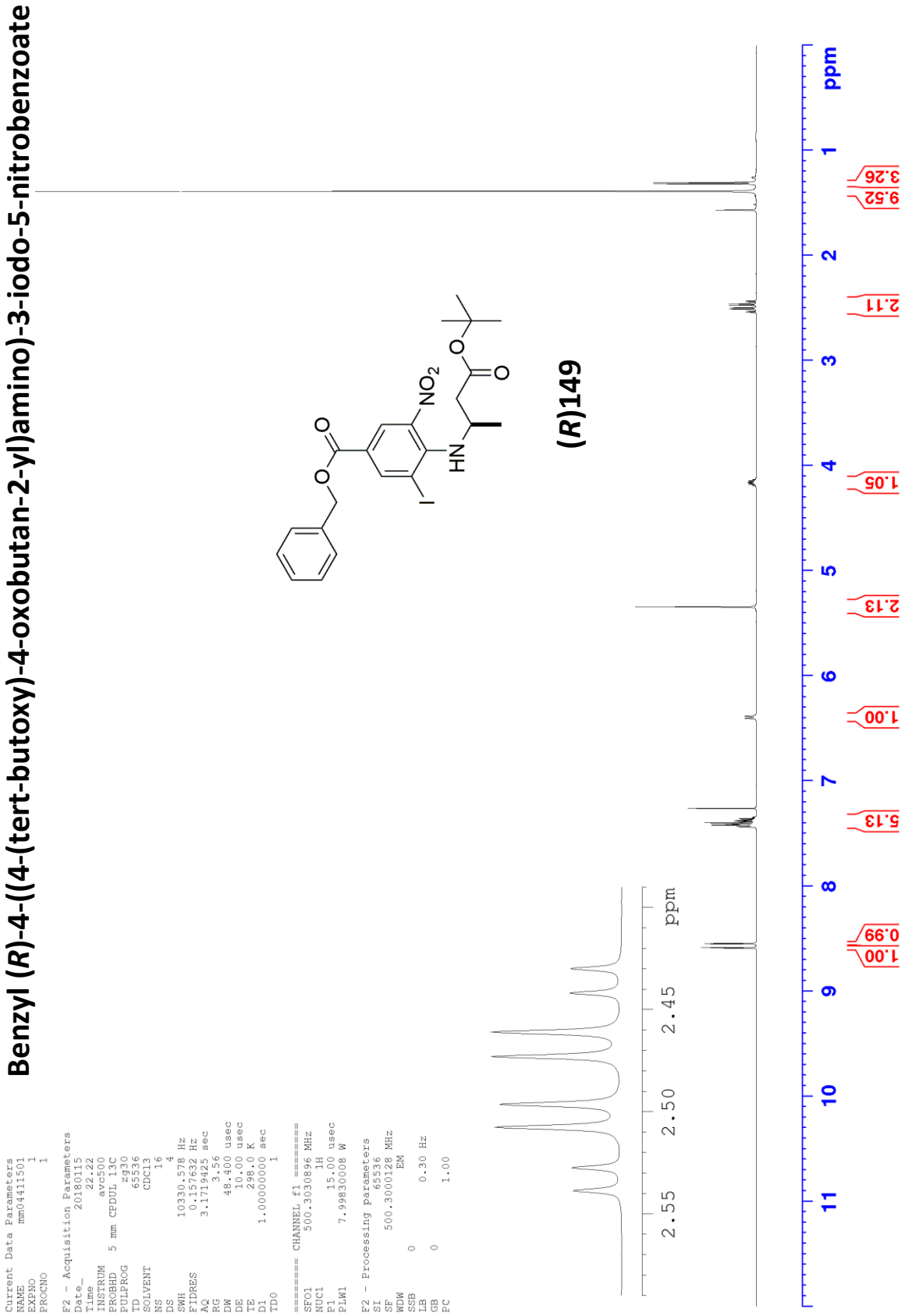
(15*R*,19*Z*)-15-Methyl-2-oxa-5,6,7,12,16,24-hexaazahexacyclo [22.6.2.2.1^{5,8}.1^{9,18}.0^{11,17}.0^{28,32}]tetratriaconta-1(30),6,8(34),9(33),10,17,19,28,31-nonaen-13-one

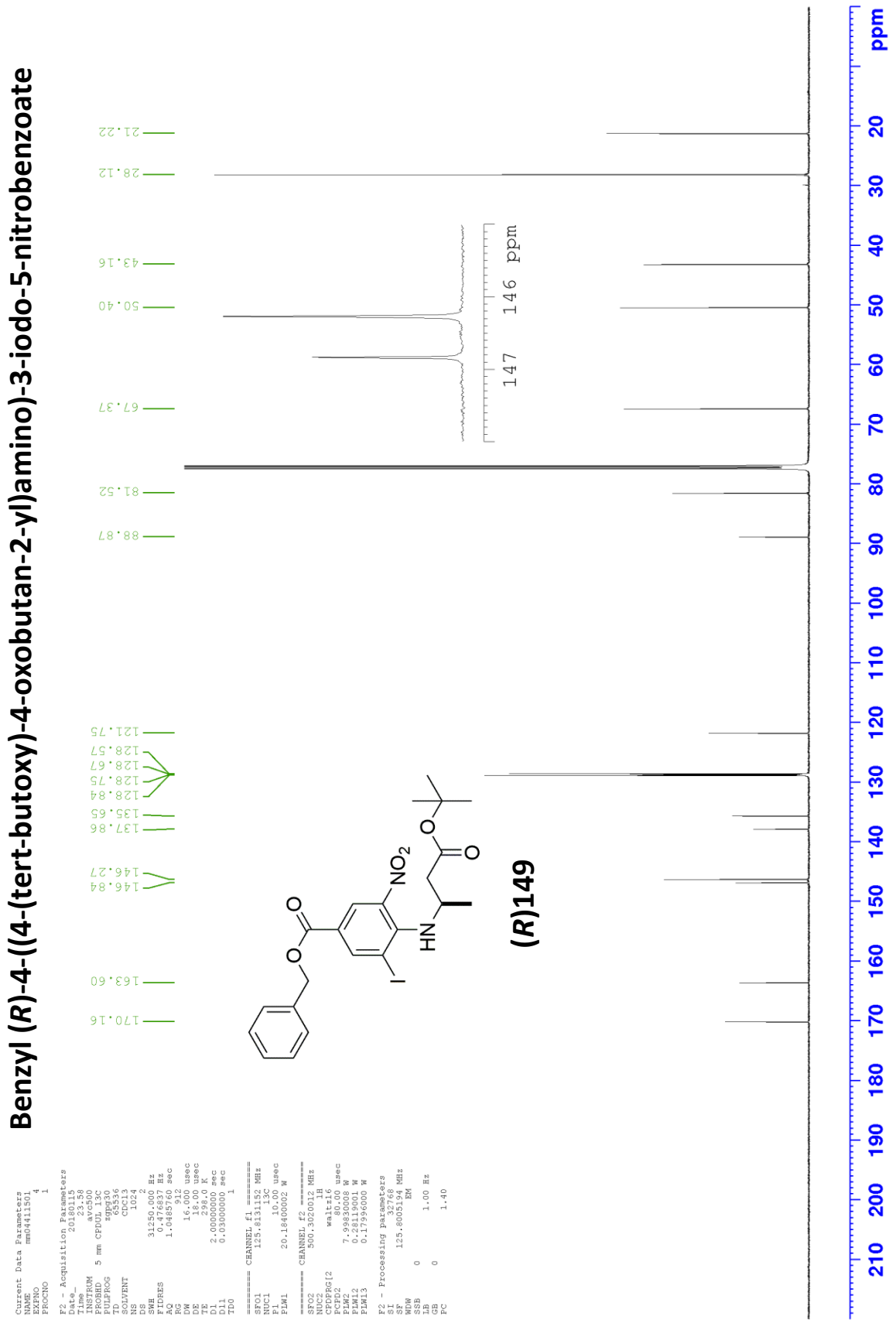


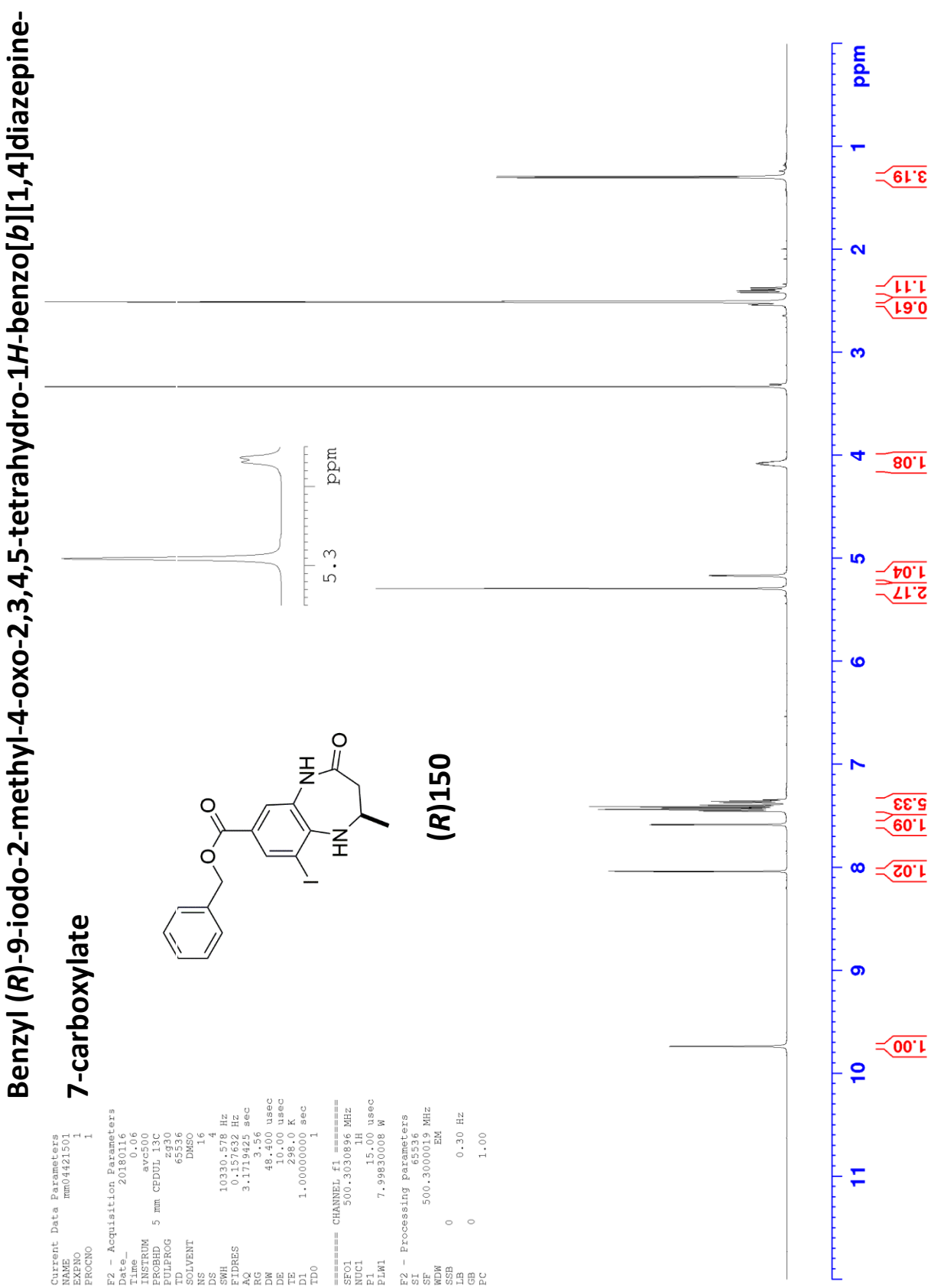

Benzyl 4-fluoro-3-iodo-5-nitrobenzoate
148
Current Data Parameters
NAME mm03800901
EXPNO 1
PROCNO 1
F2 - Acquisition Parameters
Date_ 20180110
Time 1.22
INSTRUM avc500
PROBHD 5 mm CPDUL 13C
PULPROG zg30
TD 65536
SOLVENT CDCl3
NS 16
DS 4
SWH 10330.578 Hz
FIDRES 0.157632 Hz
AQ 3.1719425 sec
RG 4
DW 48.400 usec
DE 10.00 usec
TE 298.0 K
D1 1.00000000 sec
TD0 1
======== CHANNEL f1 ========
SFO1 500.3030896 MHz
NUC1 1H
P1 15.00 usec
PLW1 7.99830008 W
F2 - Processing parameters
SI 65536
SF 500.3000140 MHz
WDW EM
SSB 0
LB 0.30 Hz
GB 0
PC 1.00
8.70
8.65
ppm
2.17
5.29
1.00
0.97
ppm

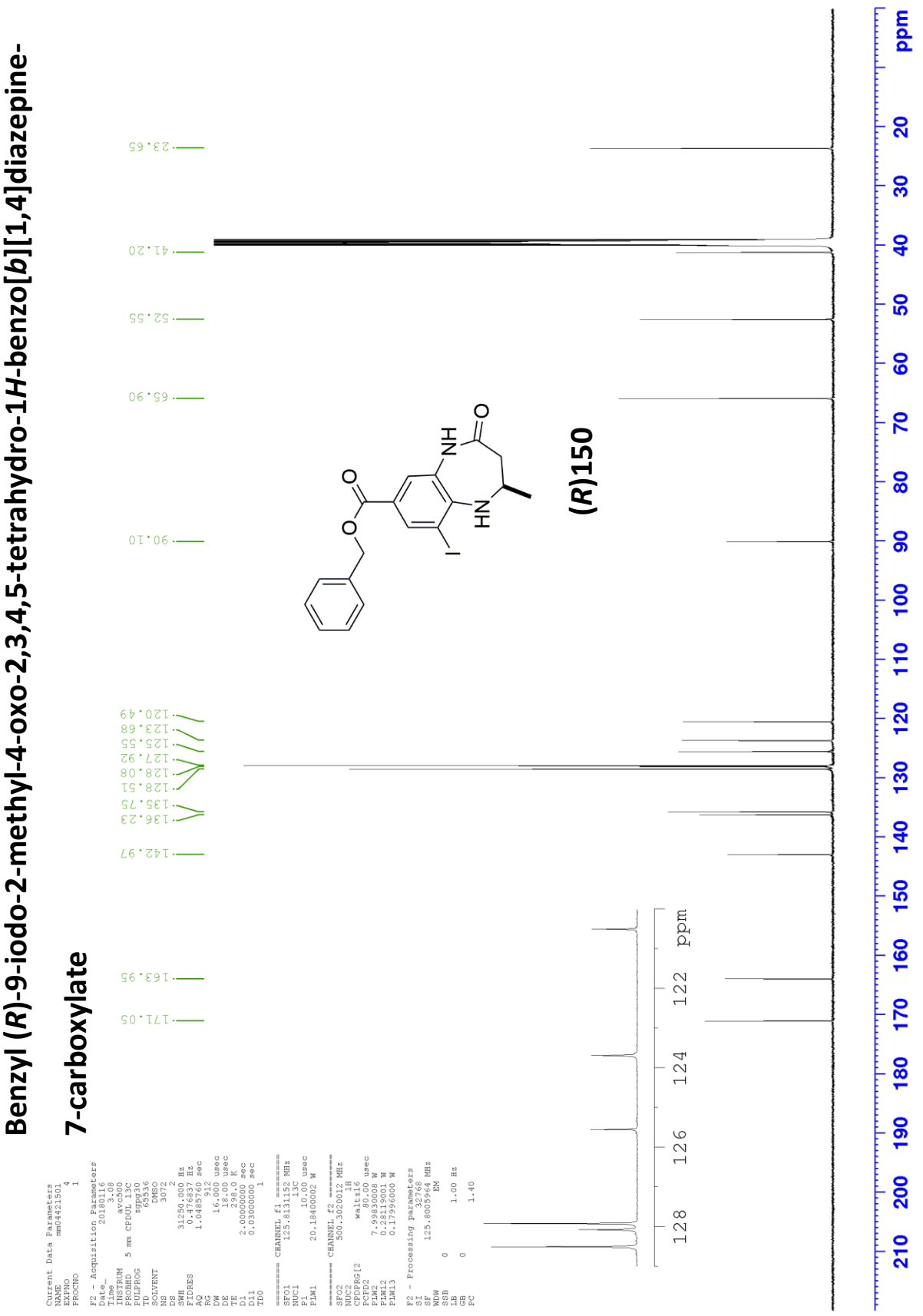

Benzyl 4-fluoro-3-iodo-5-nitrobenzoate
148
Current Data Parameters
NAME mm03800901
EXPNO 4
PROCNO 1
F2 - Acquisition Parameters
Date_ 20180110
Time 2.57
INSTRUM avc500
PROBHD 5 mm CPDUL 13C
PULPROG zgpg30
TD 65536
SOLVENT CDCl3
NS 1024
DS 2
SWH 31250.000 Hz
FIDRES 0.476837 Hz
AQ 1.0485760 sec
RG 912
DW 16.000 usec
DE 18.00 usec
TE 298.0 K
D1 2.00000000 sec
D11 0.03000000 sec
TD0 1
======== CHANNEL f1 ========
SFO1 125.8131132 MHz
NUC1 13C
P1 10.00 usec
PLW1 20.18400002 W
======== CHANNEL f2 ========
SFO2 500.3020012 MHz
NUC2 1H
CPDPRG[2 waltz16
PCPD2 80.00 usec
PLW2 7.99830008 W
PLW12 0.21810001 W
PLW13 0.17996000 W
F2 - Processing parameters
SI 32768
SF 125.8005214 MHz
WDW EM
SSB 0
LB 1.00 Hz
GB 0
PC 1.40
162.56
158.32
156.19
145.59
145.57
137.37
137.29
134.95
129.00
128.95
128.81
128.49
128.43
128.40
127.78
84.44
84.23
68.26
84.5
84.0
ppm
160
ppm
ppm


Benzyl 4-fluoro-3-iodo-5-nitrobenzoate
148
Current Data Parameters
NAME Jan09-2018-14-
EXPNO 2
PROCNO 1
F2 - Acquisition Parameters
Date_ 20180109
Time 10.26 h
INSTRUM avg400
PROBHD 2108618_0816 (
PULPROG zgflqn
TD 261912
SOLVENT CDCl3
NS 16
DS 4
SWH 131578.953 Hz
FIDRES 1.004757 Hz
AQ 0.9952656 sec
RG 206.87
DW 3.800 usec
DE 6.50 usec
TE 296.6 K
D1 2.00000000 sec
TD0 1
SFO1 376.5359897 MHz
NUC1 19F
P1 15.00 usec
PLW1 20.00000000 W
F2 - Processing parameters
SI 131072
SF 376.5642320 MHz
WDW EM
SSB 0
LB 0.50 Hz
GB 0
PC 1.00
-89.27
-89.29
-89.29
-89.30
-89.25
-89.30
ppm
50
0
-50
-100
-150
-200
ppm

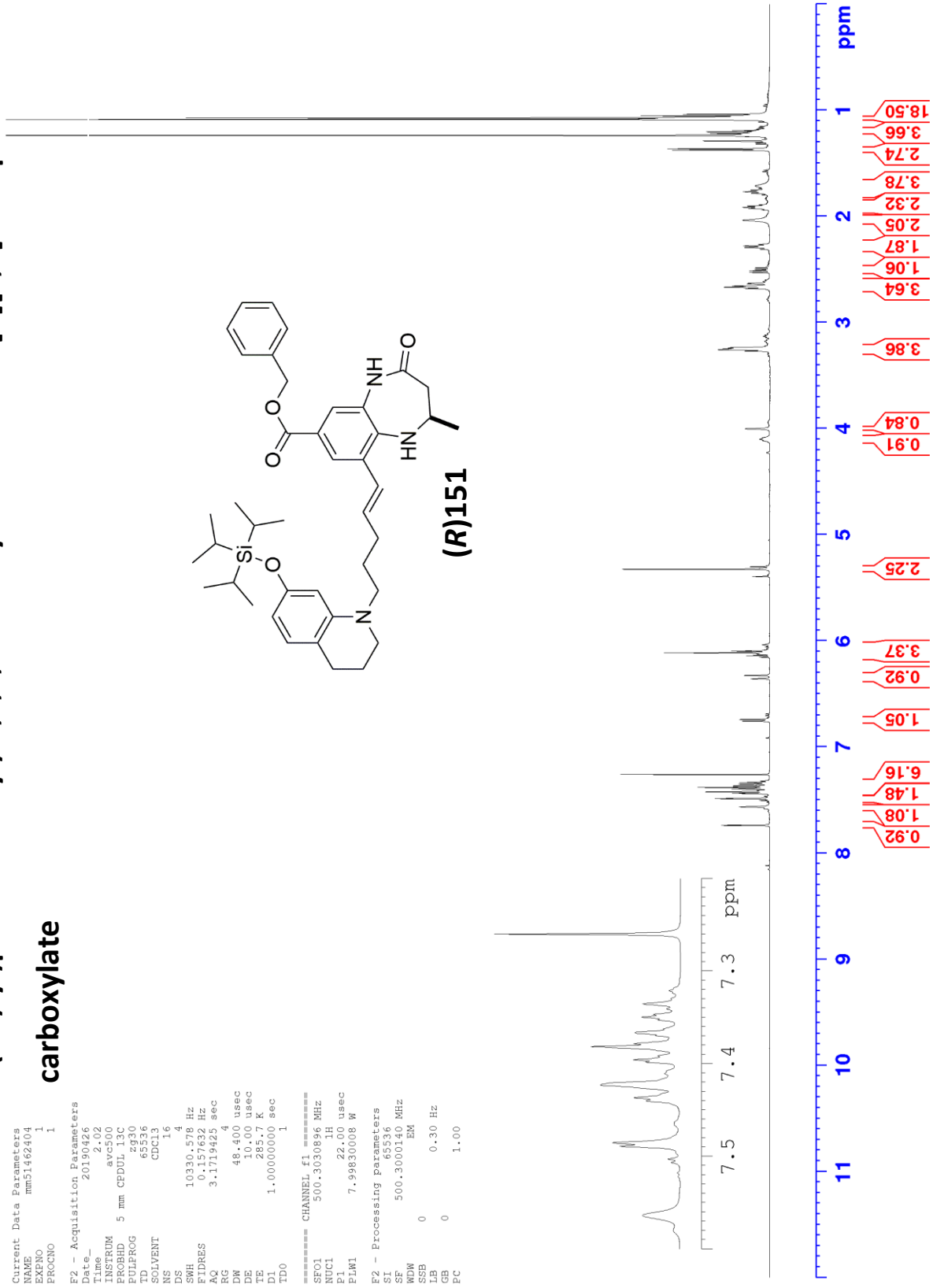

Benzyl (R)-4-((4-(tert-butoxy)-4-oxobutan-2-yl)amino)-3-iodo-5-nitrobenzoate
(R)149
Current Data Parameters
NAME mm04411501
EXPNO 1
PROCNO 1
F2 - Acquisition Parameters
Date_ 20180115
Time 22.22
INSTRUM avc500
PROBHD 5 mm CPDUL 13C
PULPROG zg30
TD 65536
SOLVENT CDCl3
NS 16
DS 4
SWH 10330.578 Hz
FIDRES 0.157632 Hz
AQ 3.1719425 sec
RG 3.56
DW 48.400 usec
DE 10.00 usec
TE 298.0 K
D1 1.00000000 sec
TD0 1
======== CHANNEL f1 ========
SFO1 500.3030896 MHz
NUC1 1H
P1 15.00 usec
PLW1 7.99830008 W
F2 - Processing parameters
SI 65536
SF 500.3000128 MHz
WDW EM
SSB 0
LB 0.30 Hz
GB 0
PC 1.00
2.55
2.50
2.45
ppm
11
10
9
8
7
6
5
4
3
2
1
ppm
1.00
0.99
5.13
1.00
2.13
1.05
2.11
9.52
3.26


Benzyl (R)-4-((4-(tert-butoxy)-4-oxobutan-2-yl)amino)-3-iodo-5-nitrobenzoate
(R)149
Current Data Parameters
NAME mm04411501
EXPNO 4
PROCNO 1
F2 - Acquisition Parameters
Date_ 20180115
Time 23.58
INSTRUM spect
PROBHD 5 mm CPDUL 13C
PULPROG zgpg30
TD 65536
SOLVENT CDCl3
NS 1024
DS 2
SWH 31250.000 Hz
FIDRES 0.476837 Hz
AQ 1.04885760 sec
RG 912
DW 16.000 usec
DE 18.00 usec
TE 298.0 K
D1 2.00000000 sec
D11 0.03000000 sec
TD0 1
======== CHANNEL f1 ========
SFO1 125.8131152 MHz
NUC1 13C
P1 10.00 usec
PLW1 20.18400002 W
======== CHANNEL f2 ========
SFO2 500.3020012 MHz
NUC2 1H
CPDPRG[2 waltz16
PCPD2 80.00 usec
PLW2 7.99830008 W
PLW12 0.28119001 W
PLW13 0.17996000 W
F2 - Processing parameters
SI 32768
SF 125.8005194 MHz
WDW EM
SSB 0
LB 1.00 Hz
GB 0
PC 1.40
170.16
163.60
146.84
146.27
137.86
135.65
128.84
128.75
128.67
128.57
121.75
88.87
81.52
67.37
50.40
43.16
28.12
21.22
147
146 ppm
ppm

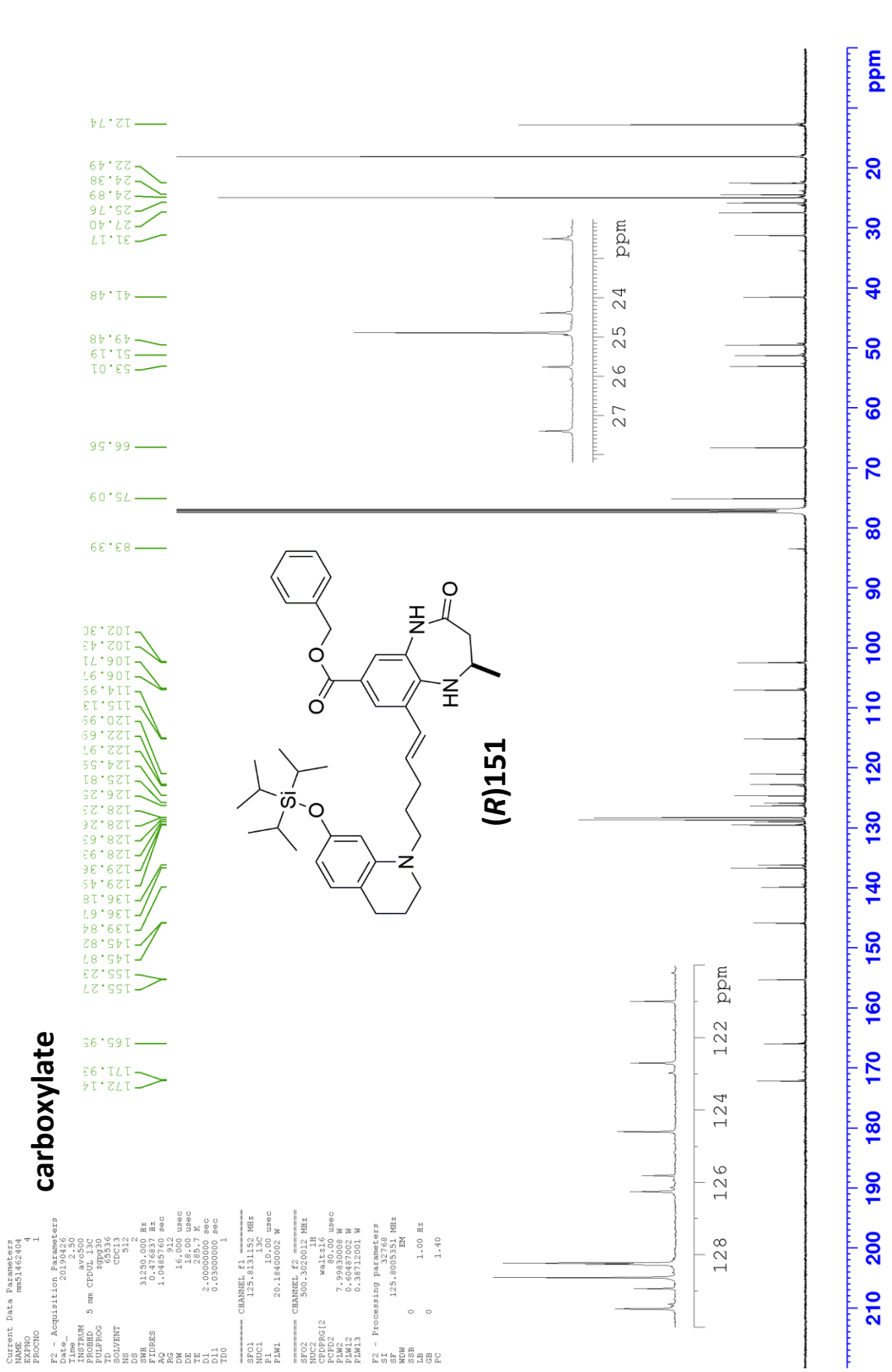

Benzyl (R)-9-iodo-2-methyl-4-oxo-2,3,4,5-tetrahydro-1H-benzo[b][1,4]diazepine-
7-carboxylate
(R)150
Current Data Parameters
NAME mm04421501
EXPNO 1
PROCNO 1
F2 - Acquisition Parameters
Date_ 20180116
Time 0.06
INSTRUM avc500
PROBHD 5 mm CPDUL 13C
PULPROG zg30
TD 65536
SOLVENT DMSO
NS 16
DS 4
SWH 10330.578 Hz
FIDRES 0.157632 Hz
AQ 3.1719425 sec
RG 3.56
DW 48.400 usec
DE 10.00 usec
TE 298.0 K
D1 1.00000000 sec
TD0 1
======== CHANNEL f1 ========
SFO1 500.3030896 MHz
NUC1 1H
P1 15.00 usec
PLW1 7.99830008 W
F2 - Processing parameters
SI 65536
SF 500.3000019 MHz
WDW EM
SSB 0
LB 0.30 Hz
GB 0
PC 1.00
5.3
ppm
1.00
1.02
1.09
5.33
1.04
2.17
1.08
0.61
1.11
3.19
11
10
9
8
7
6
5
4
3
2
1
ppm


Benzyl (R)-9-iodo-2-methyl-4-oxo-2,3,4,5-tetrahydro-1H-benzo[b][1,4]diazepine-7-carboxylate
(R)150
Current Data Parameters
NAME mm0421501
EXPNO 4
PROCNO 1
F2 - Acquisition Parameters
Date_ 20181116
Time 3.18
INSTRUM avc500
PROBHD 5 mm CPDUL 13C
PULPROG zgpg30
TD 65536
SOLVENT DMSO
NS 3072
DS 2
SWH 31250.000 Hz
FIDRES 0.476837 Hz
AQ 1.048832 sec
RG 912
DW 16.000 usec
DE 18.00 usec
TE 298.0 K
D1 2.00000000 sec
D11 0.03000000 sec
TD0 1
SFO1 125.8131152 MHz
NUC1 13C
P1 10.00 usec
PLW1 20.18400002 W
SFO2 500.3020012 MHz
NUC2 1H
CPDPRG[2 waltz16
PCPD2 80.00 usec
PLW2 7.99830008 W
PLW12 0.28119001 W
PLW13 0.17996000 W
F2 - Processing parameters
SI 32768
SF 125.8005964 MHz
WDW EM
SSB 0
LB 1.00 Hz
GB 0
PC 1.40
171.05
163.95
142.97
136.23
135.75
128.51
128.08
127.92
125.55
123.68
120.49
90.10
65.90
52.55
41.20
23.65
128
126
124
122
ppm
210
200
190
180
170
160
150
140
130
120
110
100
90
80
70
60
50
40
30
20
ppm

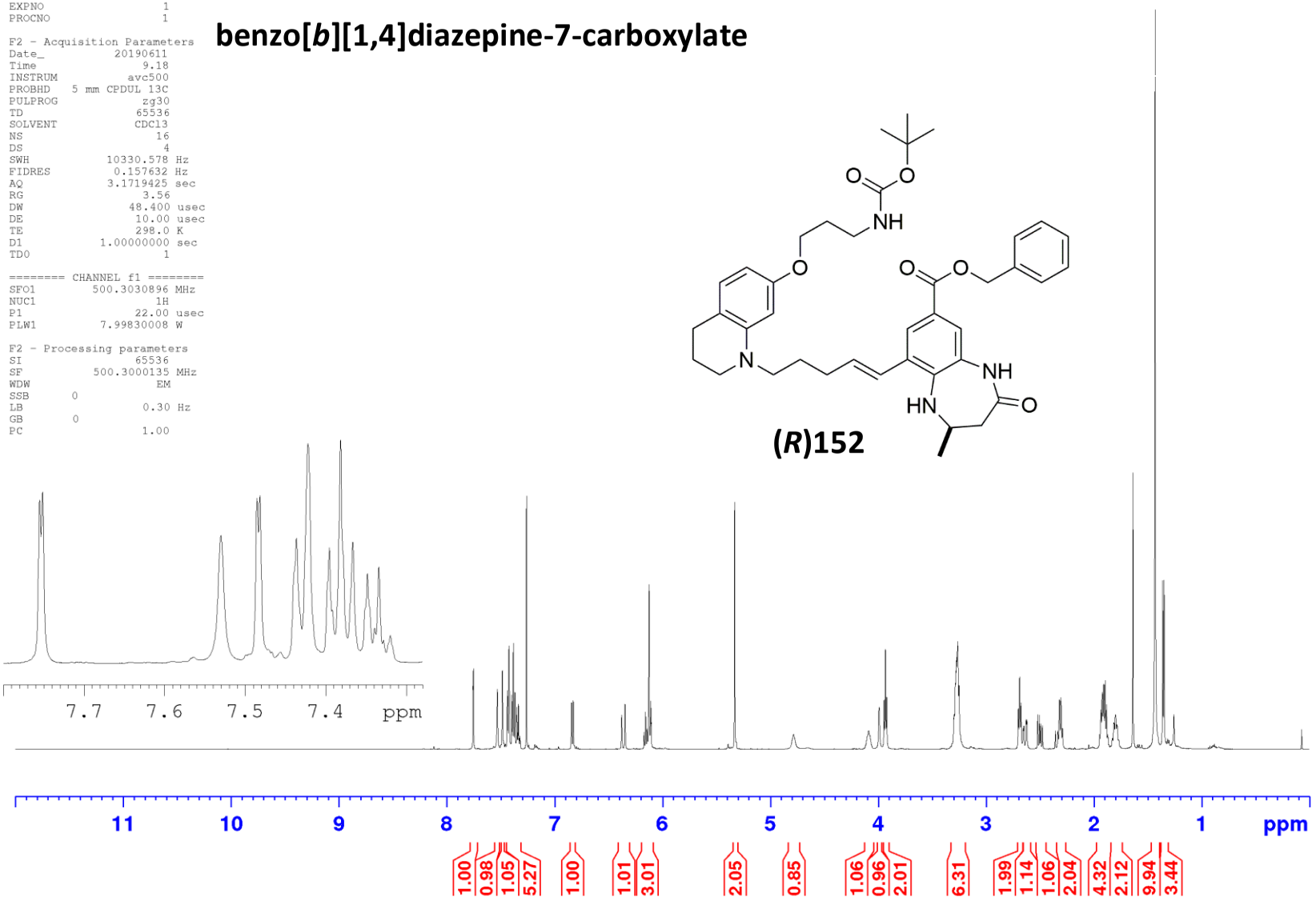
Benzyl (*R*,*E*)-2-methyl-4-oxo-9-(5-(7-((triisopropylsilyl)oxy)-3,4-dihydroquinolin-1(2*H*)-yl)pent-1-en-1-yl)-2,3,4,5-tetrahydro-1*H*-benzo[*b*][1,4]diazepine-7-carboxylate



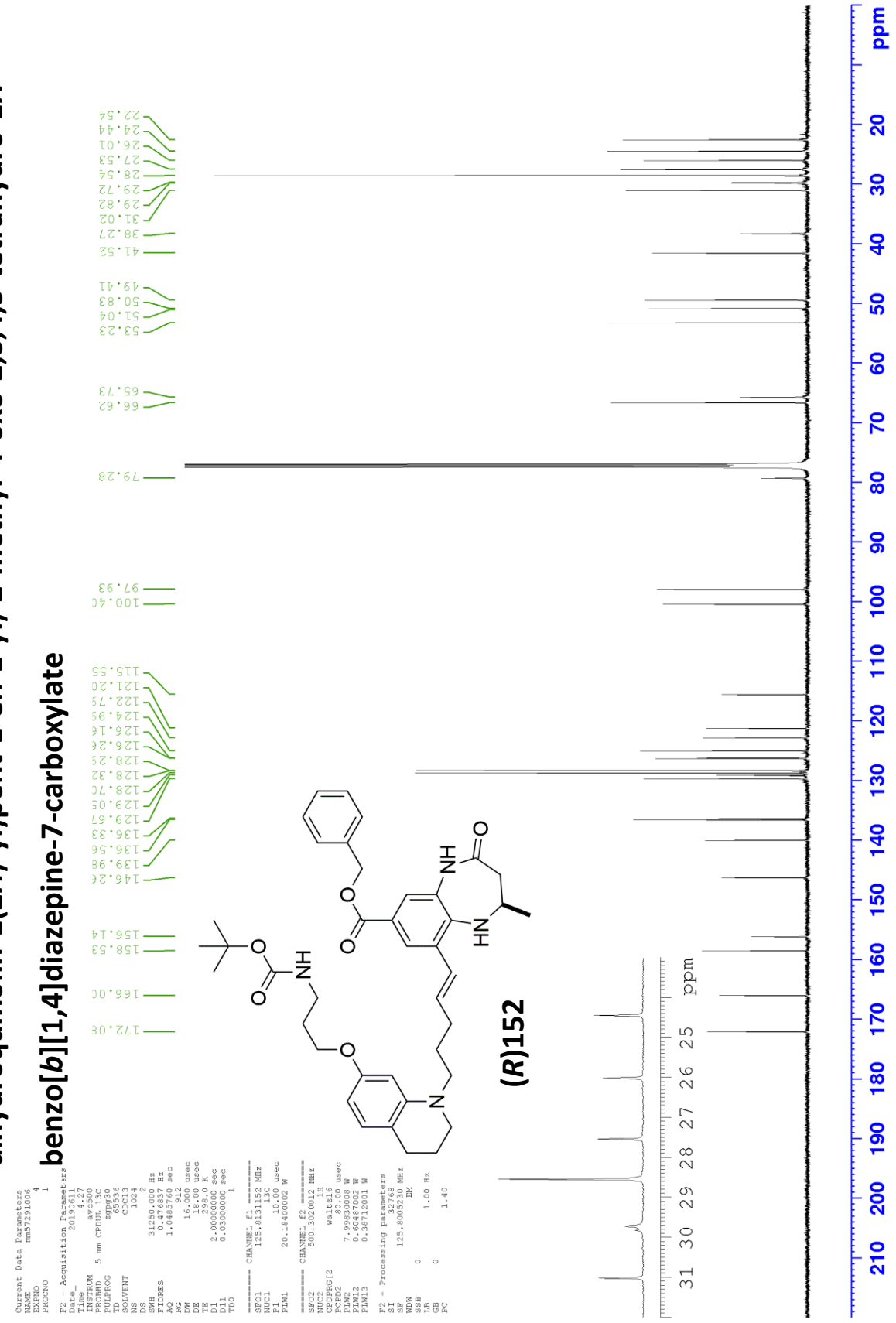
Benzyl (*R*,*E*)-2-methyl-4-oxo-9-(5-(7-((triisopropylsilyl)oxy)-3,4-dihydroquinolin-1(2*H*)-yl)pent-1-en-1-yl)-2,3,4,5-tetrahydro-1*H*-benzo[*b*][1,4]diazepine-7-carboxylate



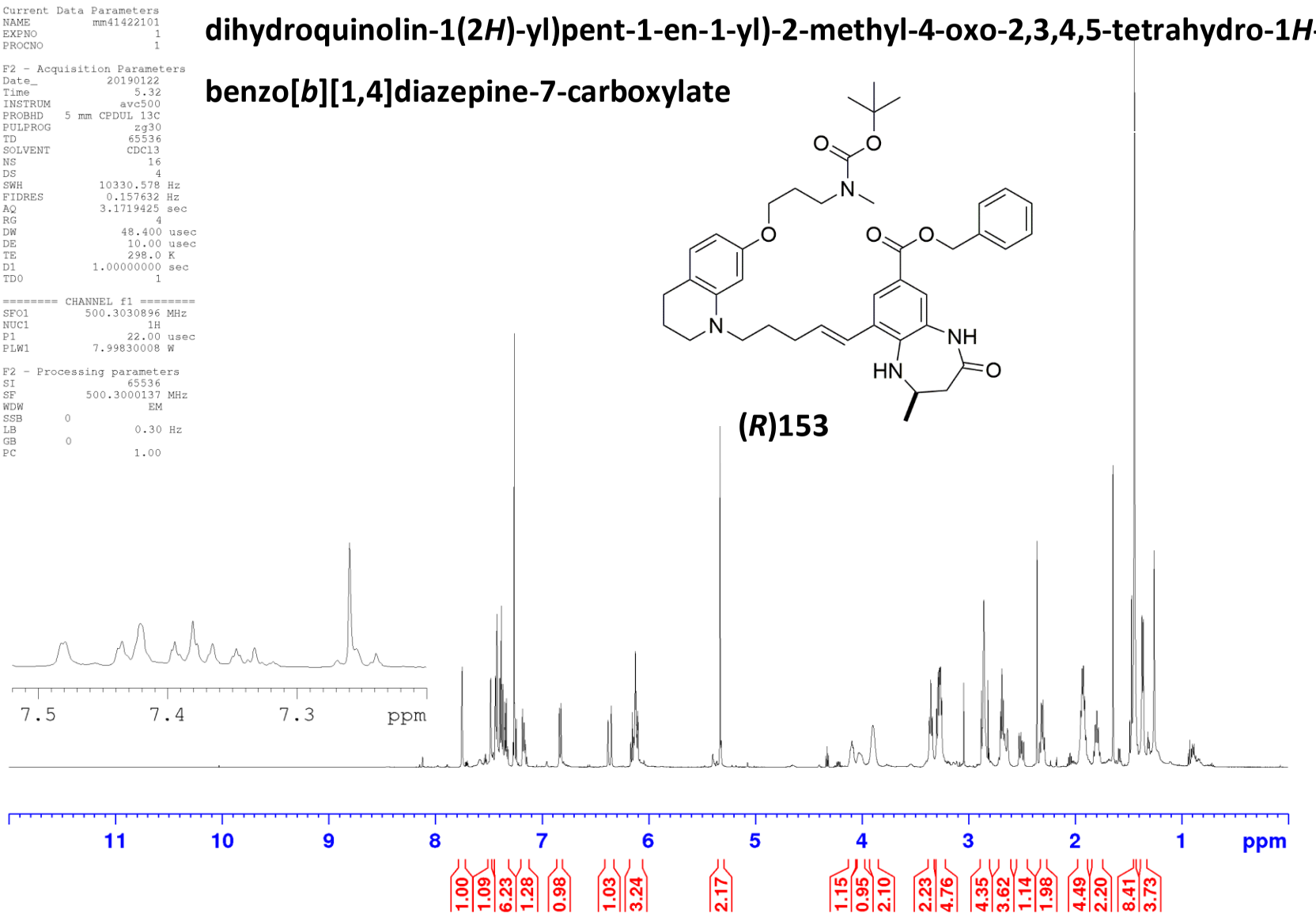
Benzyl (*R*,*E*)-9-(5-(7-(3-((*tert*-butoxycarbonyl)amino)propoxy)-3,4-dihydroquinolin-1(2*H*)-yl)pent-1-en-1-yl)-2-methyl-4-oxo-2,3,4,5-tetrahydro-1*H*-benzo[*b*][1,4]diazepine-7-carboxylate



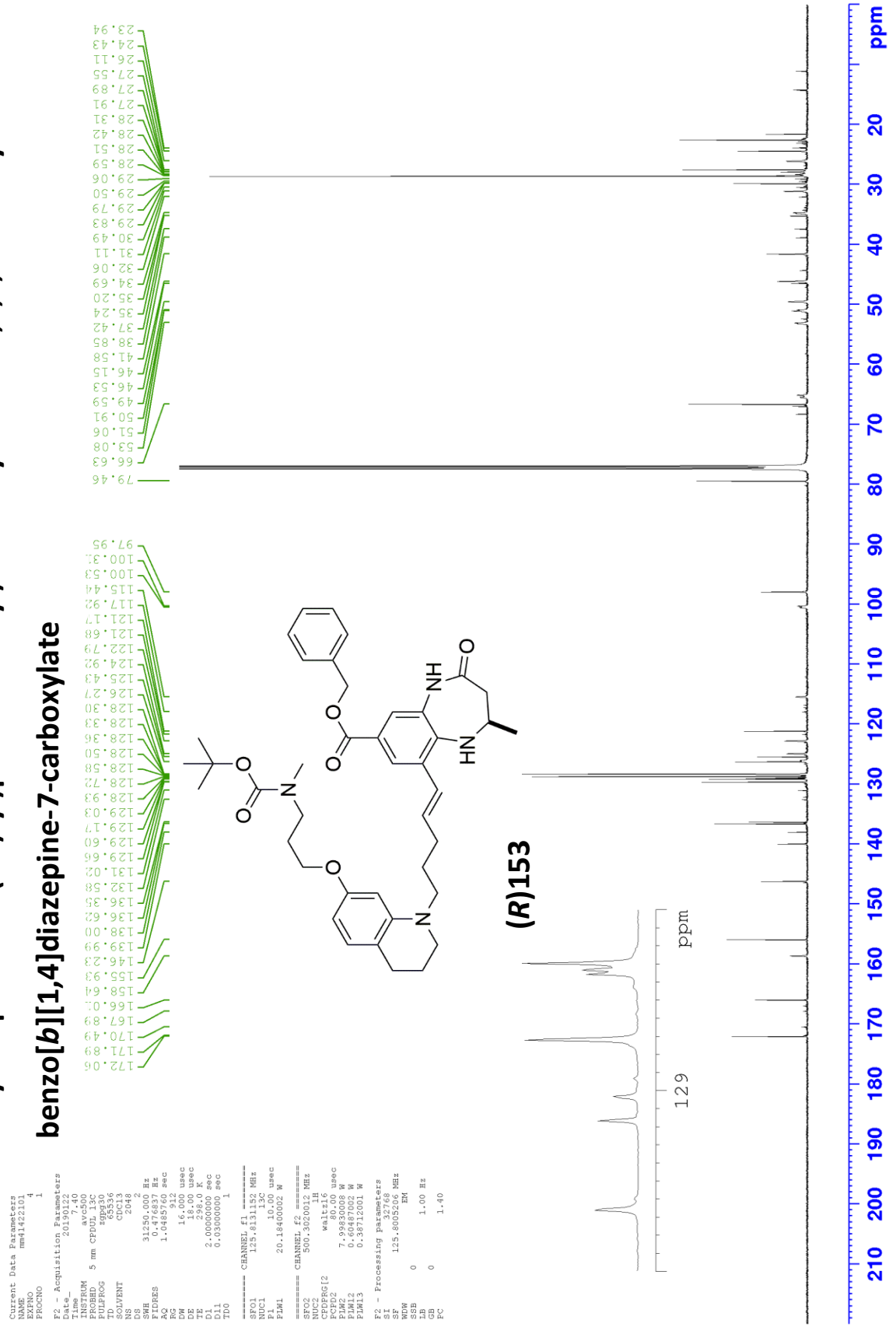
Benzyl (*R*,*E*)-9-(5-(7-(3-((*tert*-butoxycarbonyl)amino)propoxy)-3,4-dihydroquinolin-1(2*H*)-yl)pent-1-en-1-yl)-2-methyl-4-oxo-2,3,4,5-tetrahydro-1*H*-benzo[*b*][1,4]diazepine-7-carboxylate



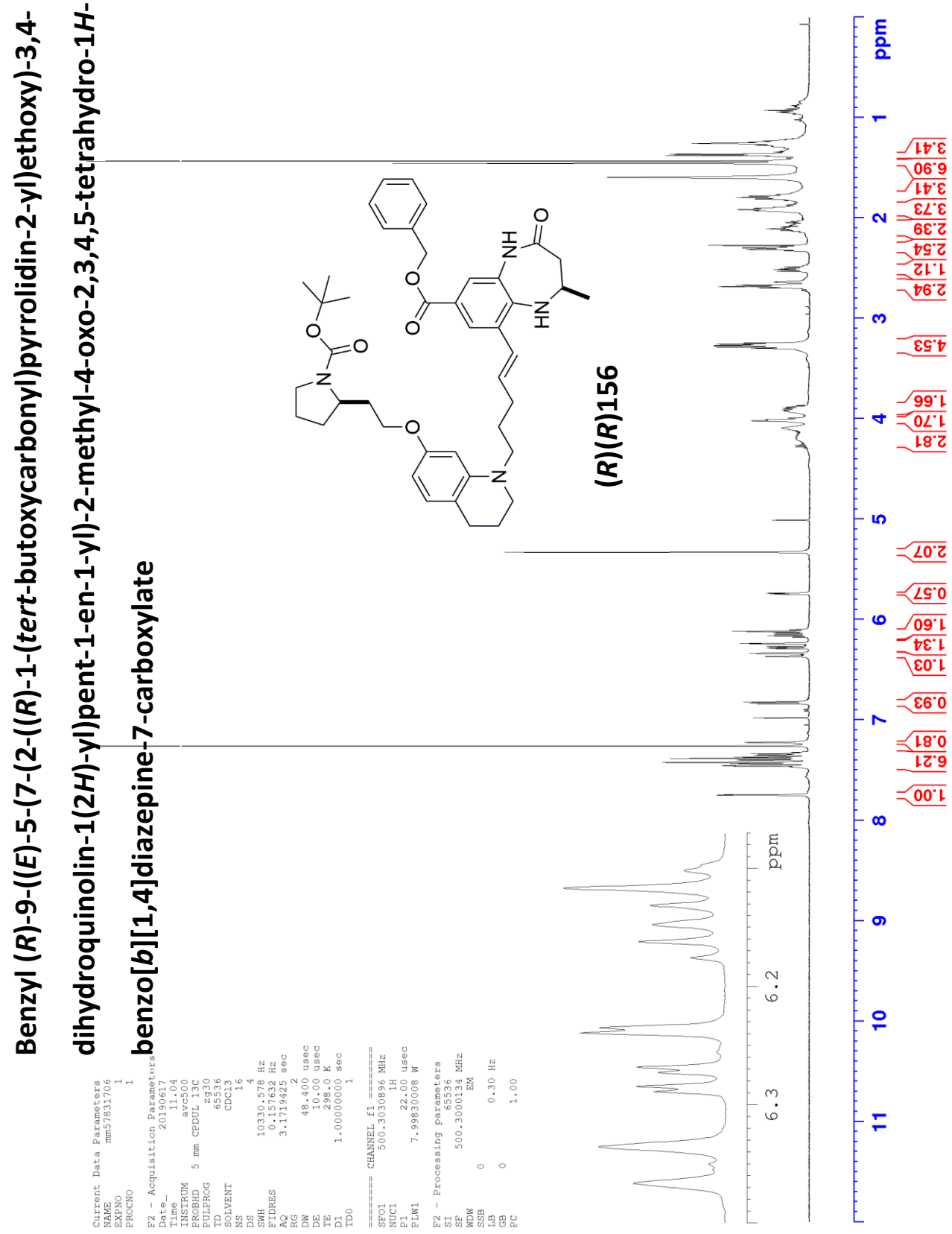
Benzyl (*R,E*)-9-(5-(7-(3-((*tert*-butoxycarbonyl)(methyl)amino)propoxy)-3,4-dihydroquinolin-1(2*H*)-yl)pent-1-en-1-yl)-2-methyl-4-oxo-2,3,4,5-tetrahydro-1*H*-benzo[*b*][1,4]diazepine-7-carboxylate



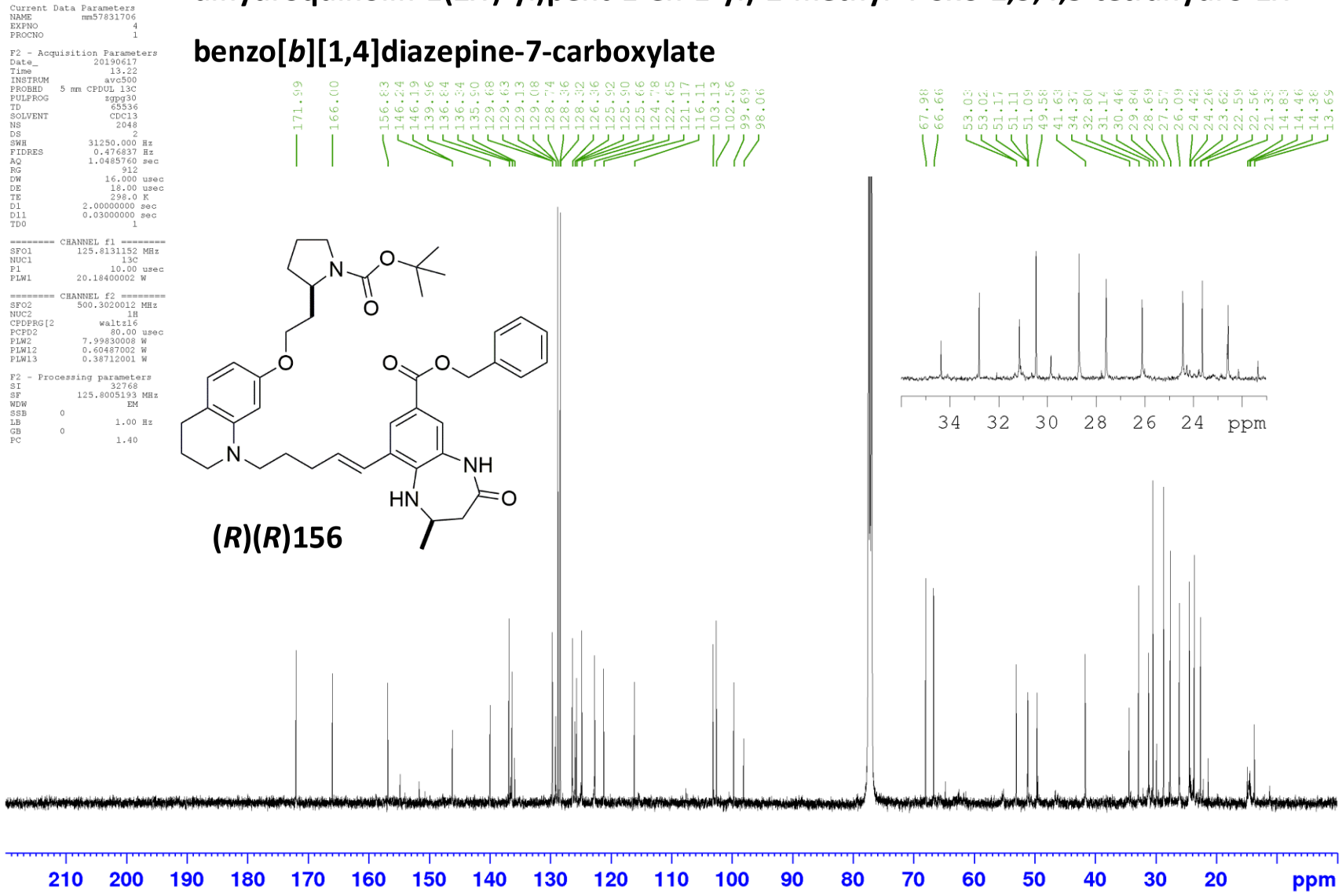
Benzyl (*R*,*E*)-9-(5-(7-(3-((*tert*-butoxycarbonyl)(methyl)amino)propoxy)-3,4-dihydroquinolin-1(2*H*)-yl)pent-1-en-1-yl)-2-methyl-4-oxo-2,3,4,5-tetrahydro-1*H*-benzo[*b*][1,4]diazepine-7-carboxylate



Benzyl (*R*)-9-((*E*)-5-(7-(2-((*R*)-1-(*tert*-butoxycarbonyl)pyrrolidin-2-yl)ethoxy)-3,4-dihydroquinolin-1(2*H*)-yl)pent-1-en-1-yl)-2-methyl-4-oxo-2,3,4,5-tetrahydro-1*H*-benzo[*b*][1,4]diazepine-7-carboxylate

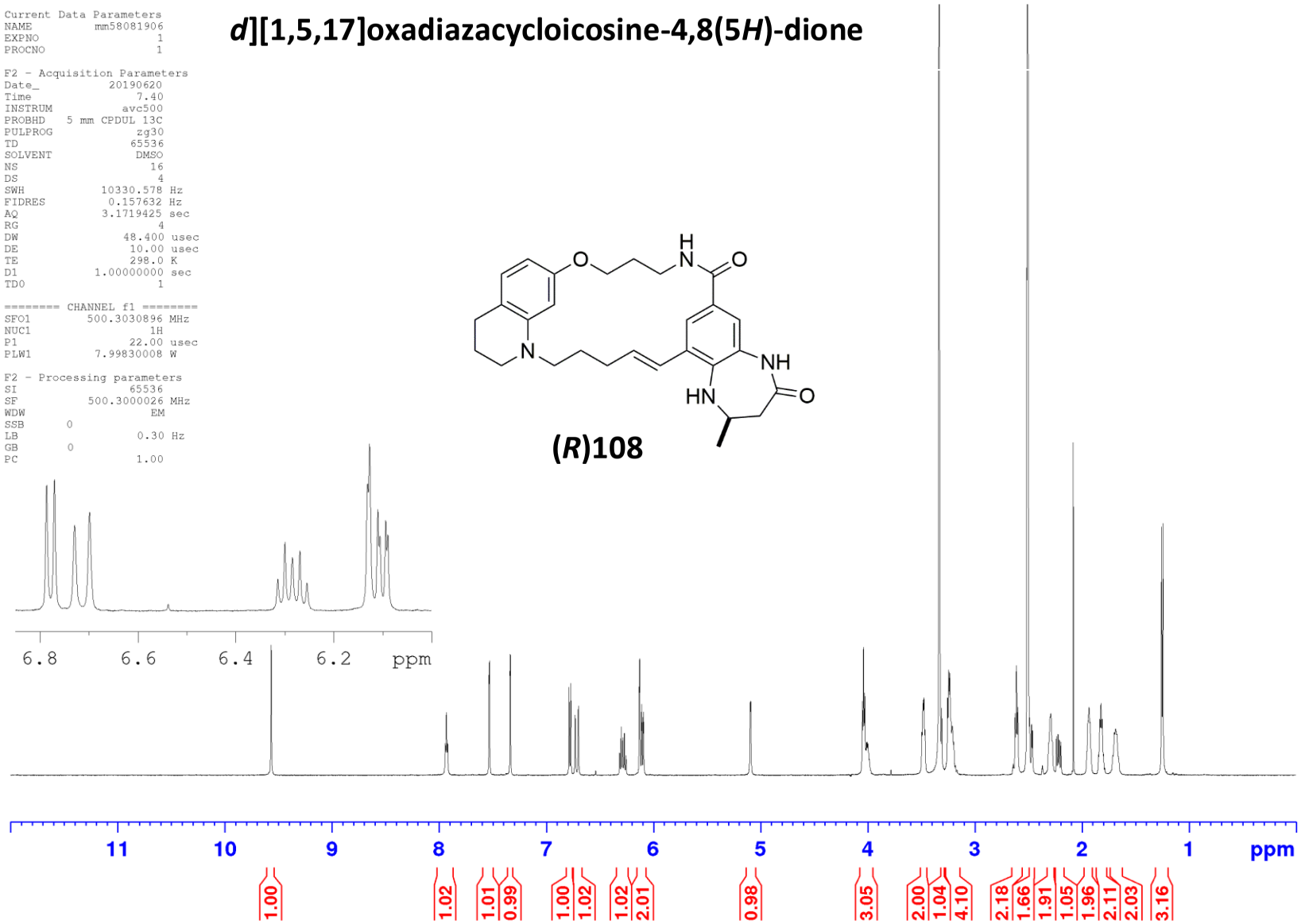


Benzyl (*R*)-9-((*E*)-5-(7-(2-((*R*)-1-(*tert*-butoxycarbonyl)pyrrolidin-2-yl)ethoxy)-3,4-dihydroquinolin-1(2*H*)-yl)pent-1-en-1-yl)-2-methyl-4-oxo-2,3,4,5-tetrahydro-1*H*-benzo[*b*][1,4]diazepine-7-carboxylate



(*R*)(*R*)156

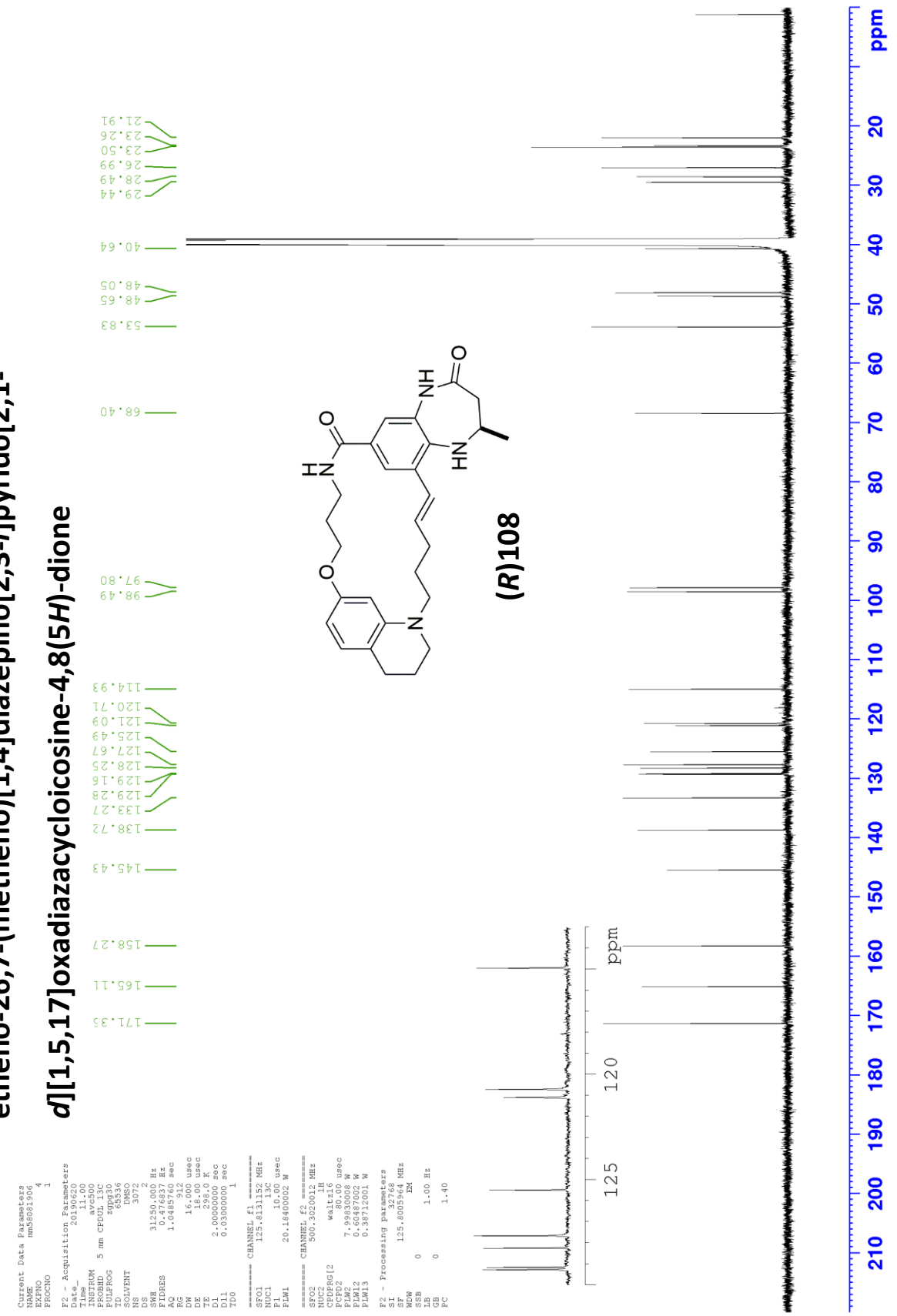
(2*R*,24*Z*)-2-Methyl-1,2,3,9,10,11,12,18,19,21,22,23-dodecahydro-8*H*,17*H*-14,16-etheno-26,7-(metheno)[1,4]diazepino[2,3-*l*]pyrido[2,1-*d*][1,5,17]oxadiazacycloicosine-4,8(5*H*)-dione



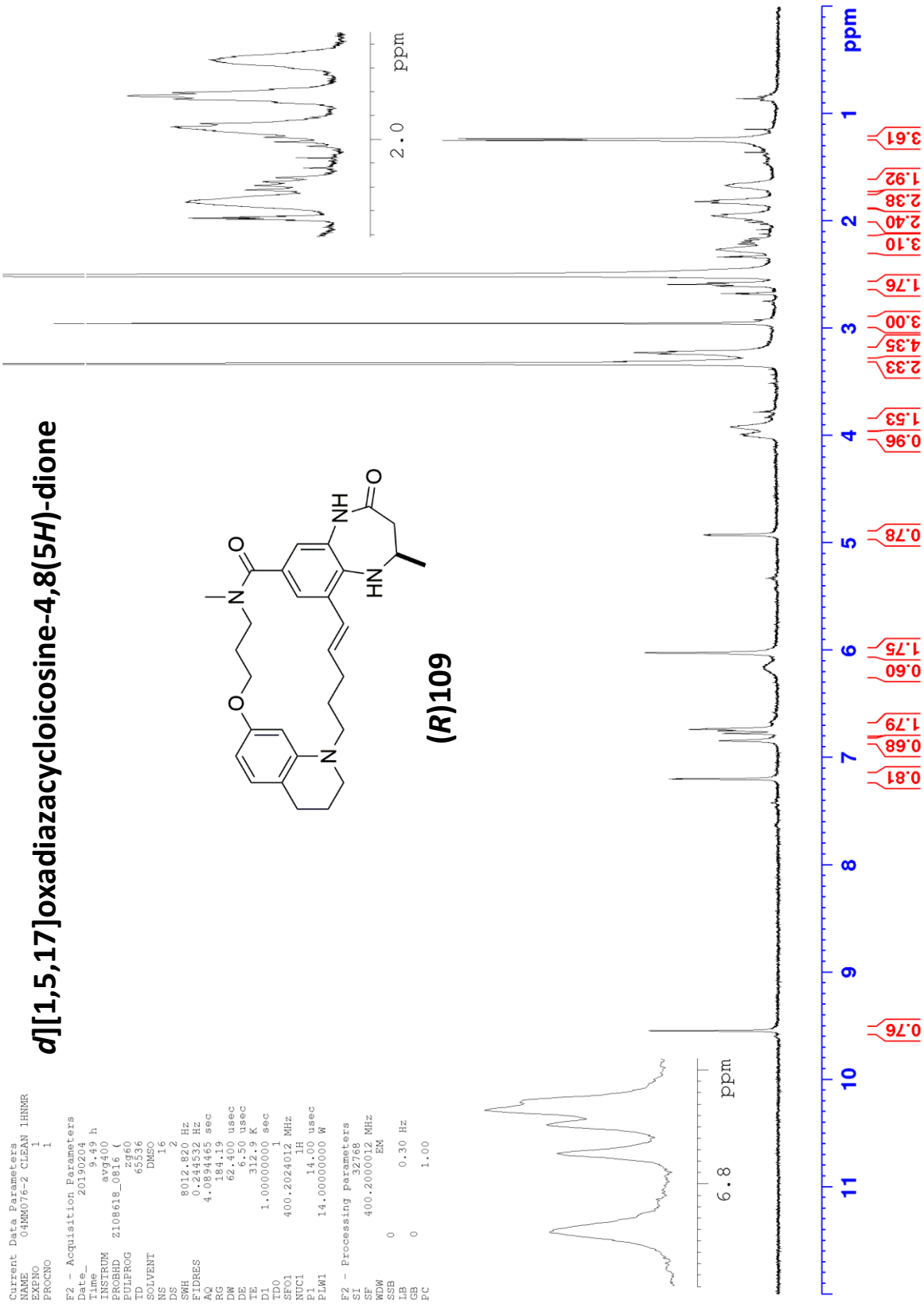
(*R*)108

(2*R*,24*Z*)-2-Methyl-1,2,3,9,10,11,12,18,19,21,22,23-dodecahydro-8*H*,17*H*-14,16-etheno-26,7-(metheno)[1,4]diazepino[2,3-*l*]pyrido[2,1-*d*][1,5,17]oxadiazacycloicosine-4,8(5*H*)-dione

(*R*)108

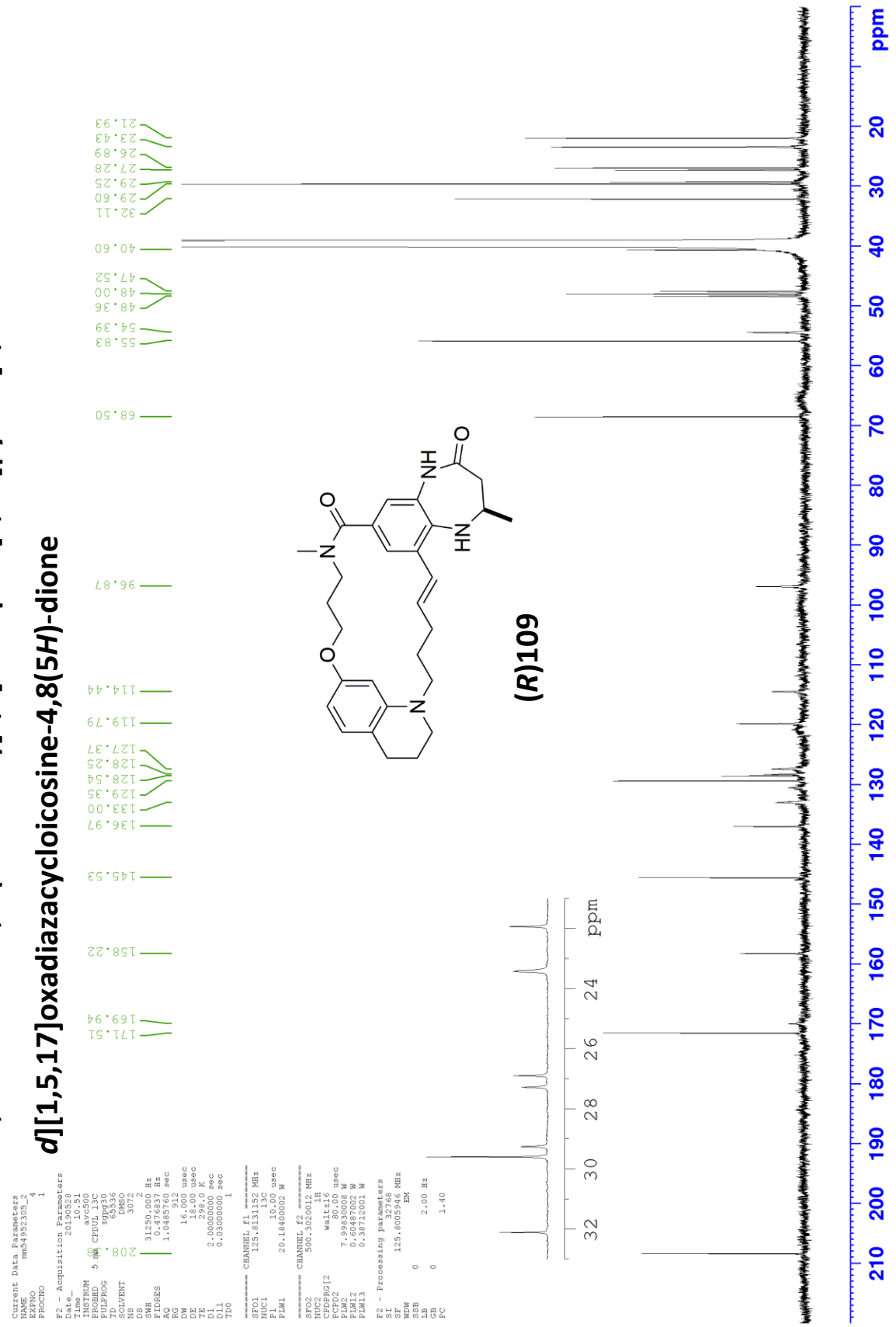


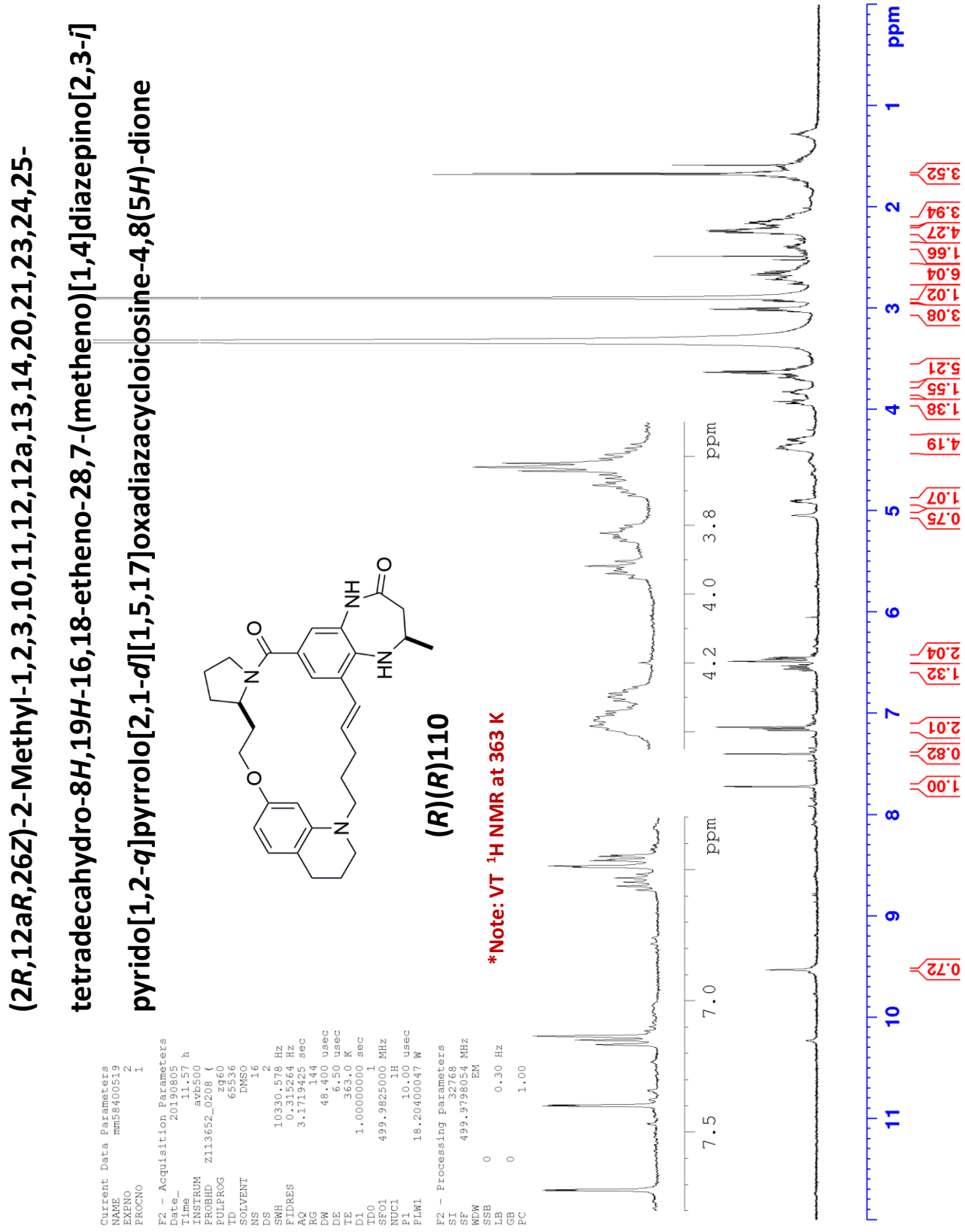
(2*R*,24*Z*)-2,9-Dimethyl-1,2,3,9,10,11,12,18,19,21,22,23-dodecahydro-8*H*,17*H*-14,16-etheno-26,7-(metheno)[1,4]diazepino[2,3-*l*]pyrido[2,1-*d*][1,5,17]oxadiazacycloicosine-4,8(5*H*)-dione



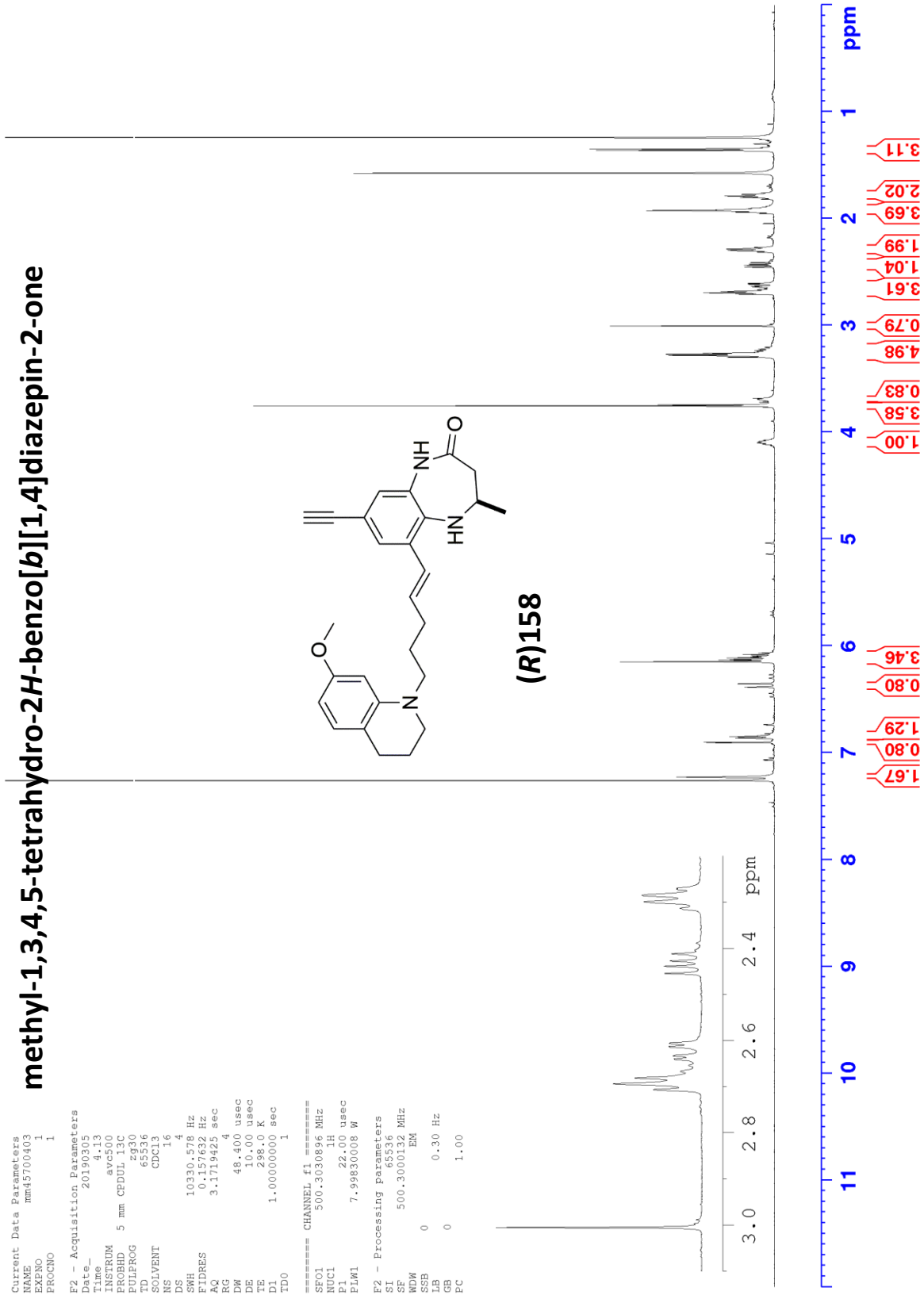
(*R*)109

(2*R*,24*Z*)-2,9-Dimethyl-1,2,3,9,10,11,12,18,19,21,22,23-dodecahydro-8*H*,17*H*-14,16-etheno-26,7-(metheno)[1,4]diazepino[2,3-*l*]pyrido[2,1-*d*][1,5,17]oxadiazacycloicosine-4,8(5*H*)-dione

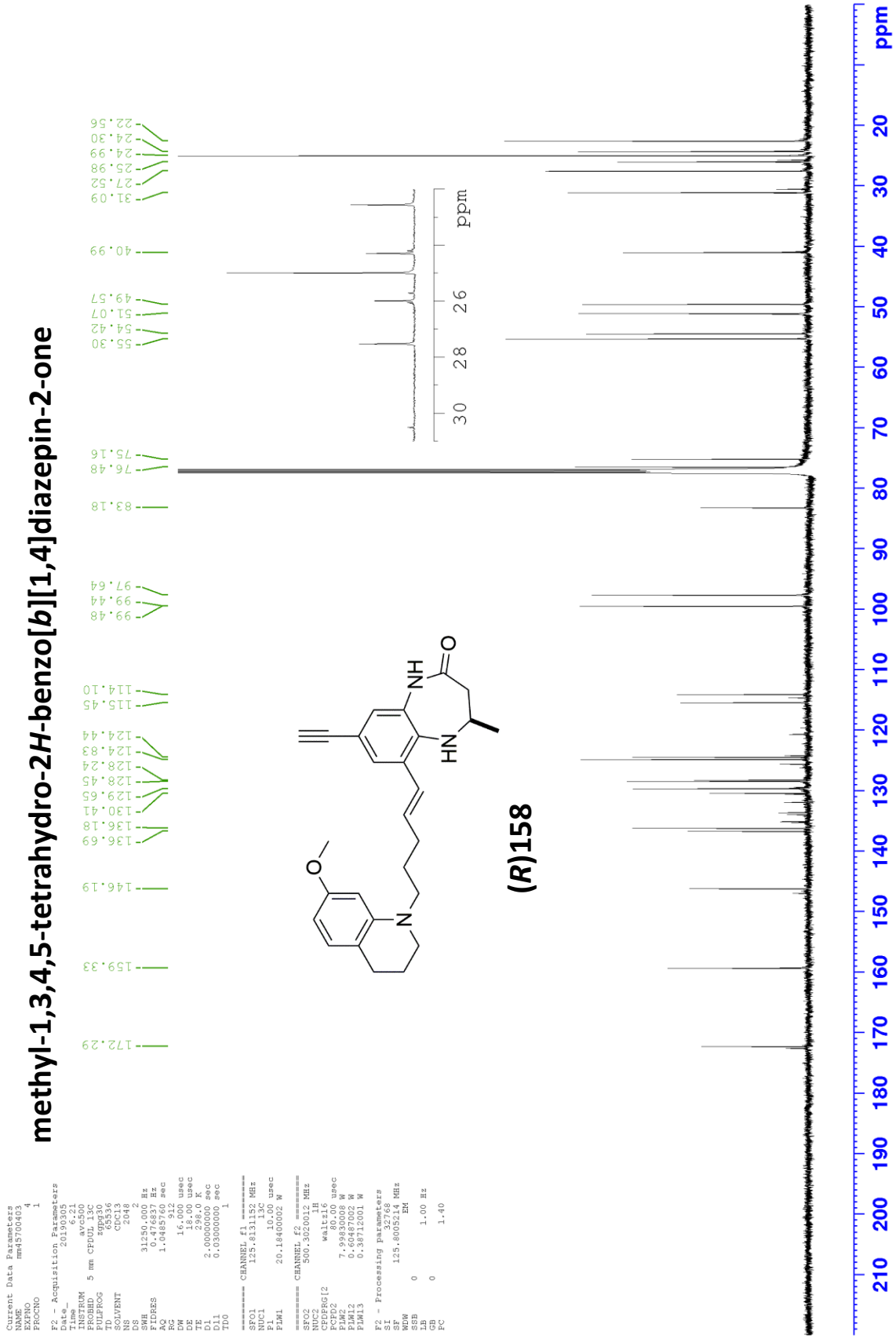



(2R,12aR,26Z)-2-Methyl-1,2,3,10,11,12,12a,13,14,20,21,23,24,25-tetradecahydro-8H,19H-16,18-etheno-28,7-(metheno)[1,4]diazepino[2,3-i]pyrido[1,2-q]pyrrolo[2,1-d][1,5,17]oxadiazacycloicosine-4,8(5H)-dione
(R)(R)110
*Note: VT 1H NMR at 363 K
Current Data Parameters
NAME mm58400519
EXPNO 2
PROCNO 1
F2 - Acquisition Parameters
Date_ 20190805
Time 11.57 h
INSTRUM avb500
PROBHD Z113652_0208 (
PULPROG zg60
TD 65536
SOLVENT DMSO
NS 16
DS 2
SWH 10330.578 Hz
FIDRES 0.315264 Hz
AQ 3.1719425 sec
RG 144
DW 48.400 usec
DE 6.50 usec
TE 363.0 K
D1 1.00000000 sec
TD0 1
SFO1 499.9825000 MHz
NUC1 1H
P1 10.00 usec
PLW1 18.20400047 W
F2 - Processing parameters
SI 32768
SF 499.9798054 MHz
WDW EM
SSB 0
LB 0.30 Hz
GB 0
PC 1.00
7.5
7.0
4.2
4.0
3.8
ppm
0.72
1.00
0.82
2.01
1.32
2.04
4.19
1.07
0.75
5.21
1.55
1.38
3.08
1.02
6.04
1.66
4.27
3.94
3.52

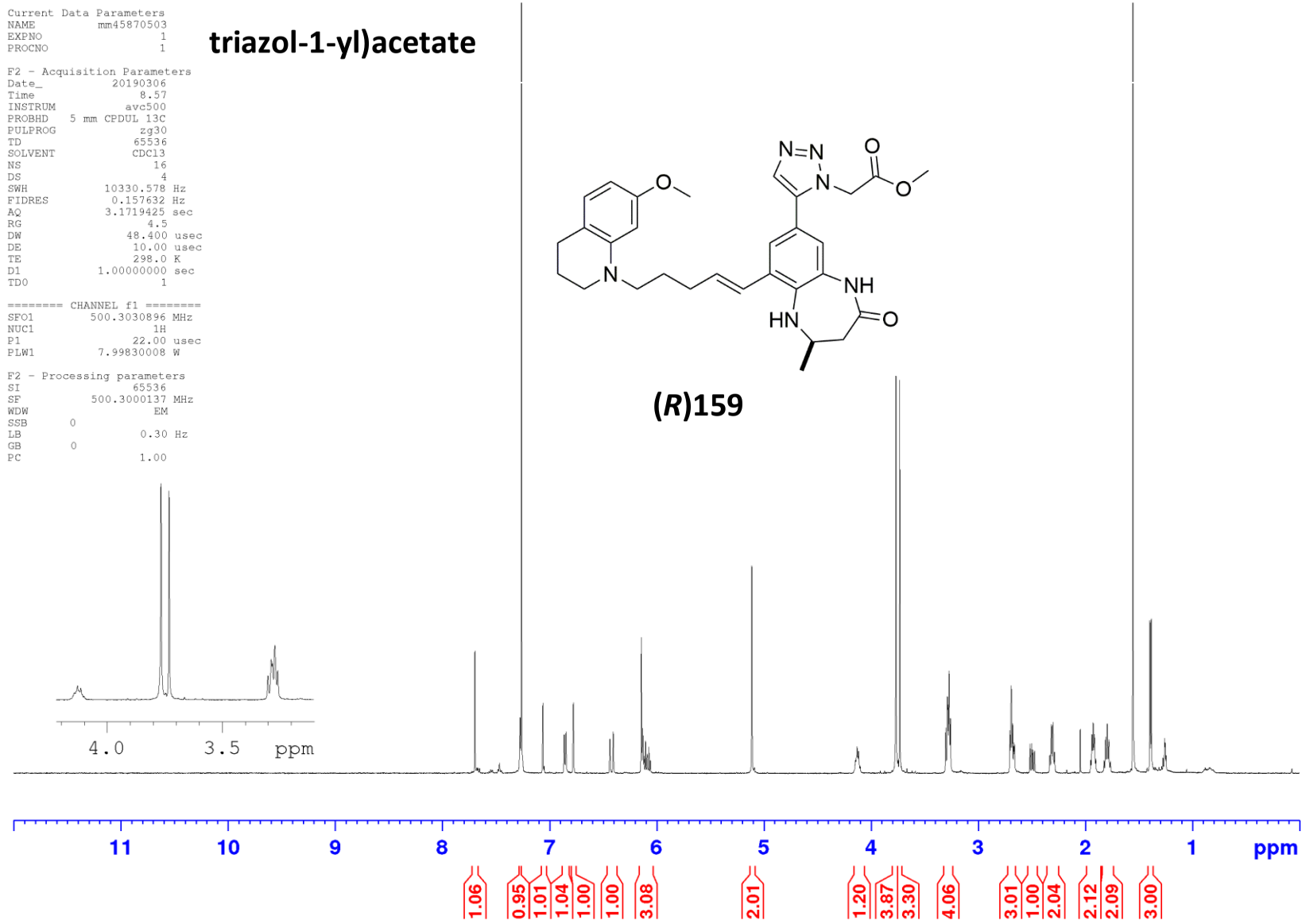
(*R,E*)-8-Ethynyl-6-(5-(7-methoxy-3,4-dihydroquinolin-1(2*H*)-yl)pent-1-en-1-yl)-4-methyl-1,3,4,5-tetrahydro-2*H*-benzo[*b*][1,4]diazepin-2-one



(*R*,*E*)-8-Ethynyl-6-(5-(7-methoxy-3,4-dihydroquinolin-1(2*H*)-yl)pent-1-en-1-yl)-4-methyl-1,3,4,5-tetrahydro-2*H*-benzo[*b*][1,4]diazepin-2-one

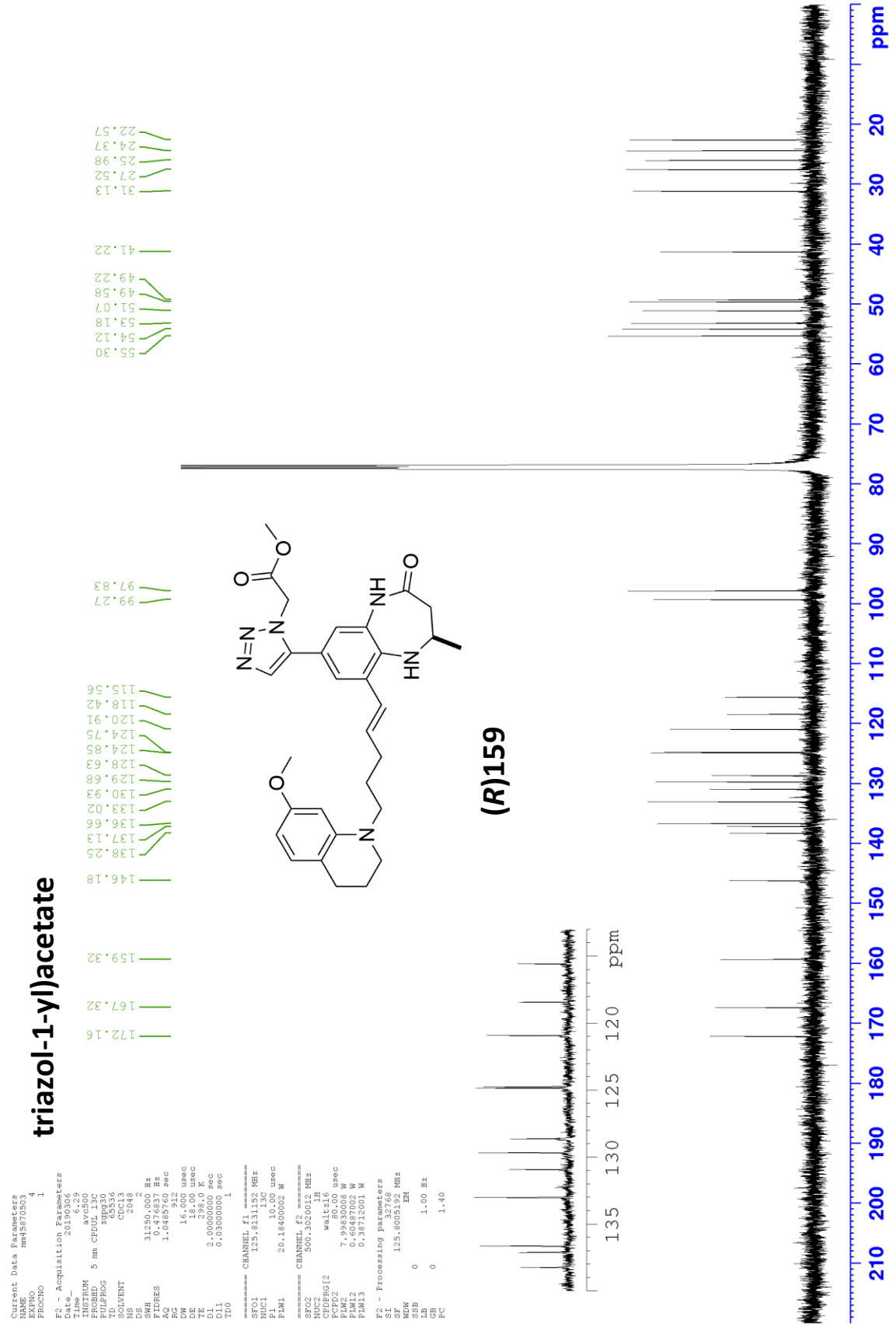


Methyl (*R,E*)-2-(5-(9-(5-(7-methoxy-3,4-dihydroquinolin-1(2*H*)-yl)pent-1-en-1-yl)-2-methyl-4-oxo-2,3,4,5-tetrahydro-1*H*-benzo[*b*][1,4]diazepin-7-yl)-1*H*-1,2,3-triazol-1-yl)acetate

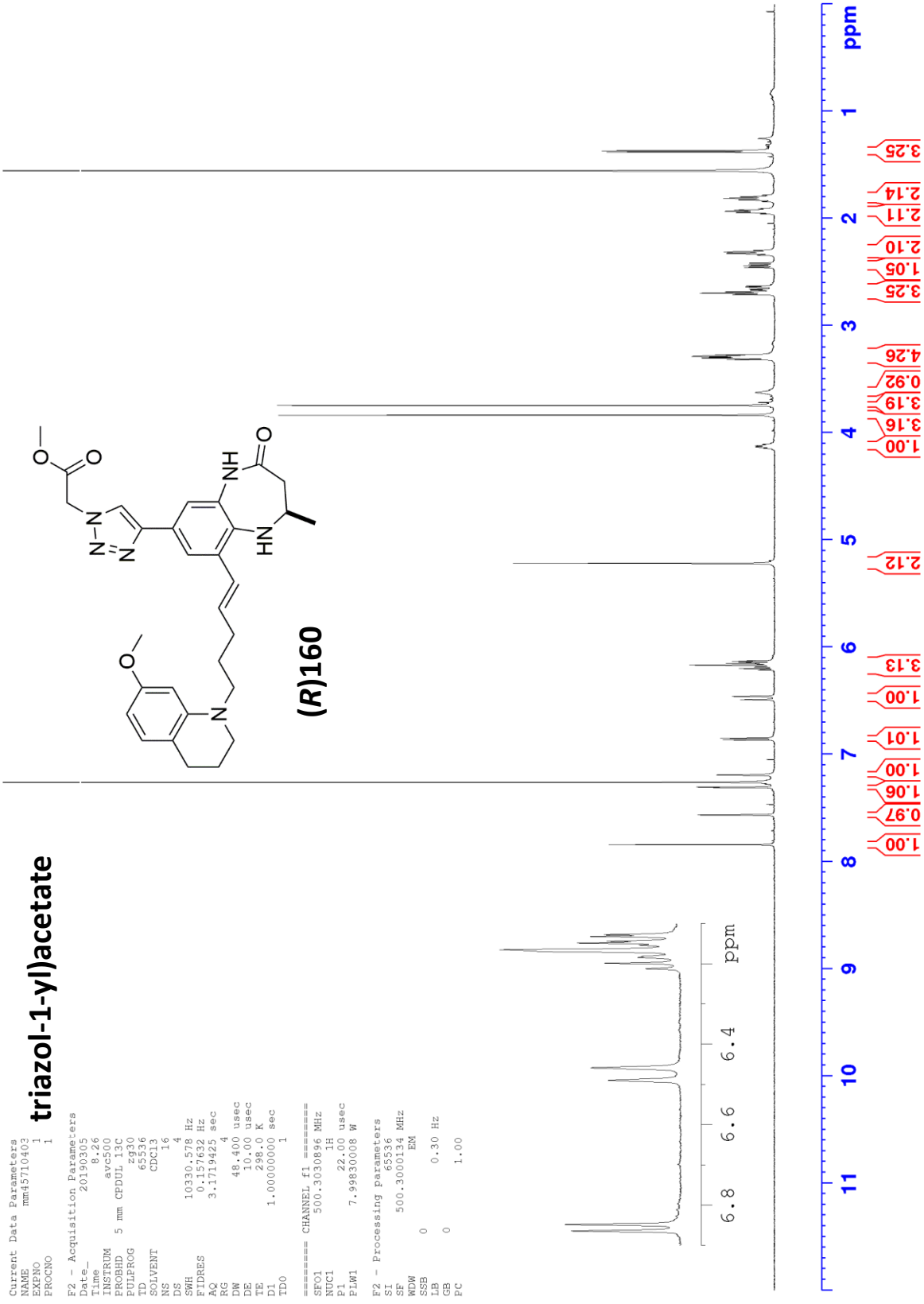


(*R*)159

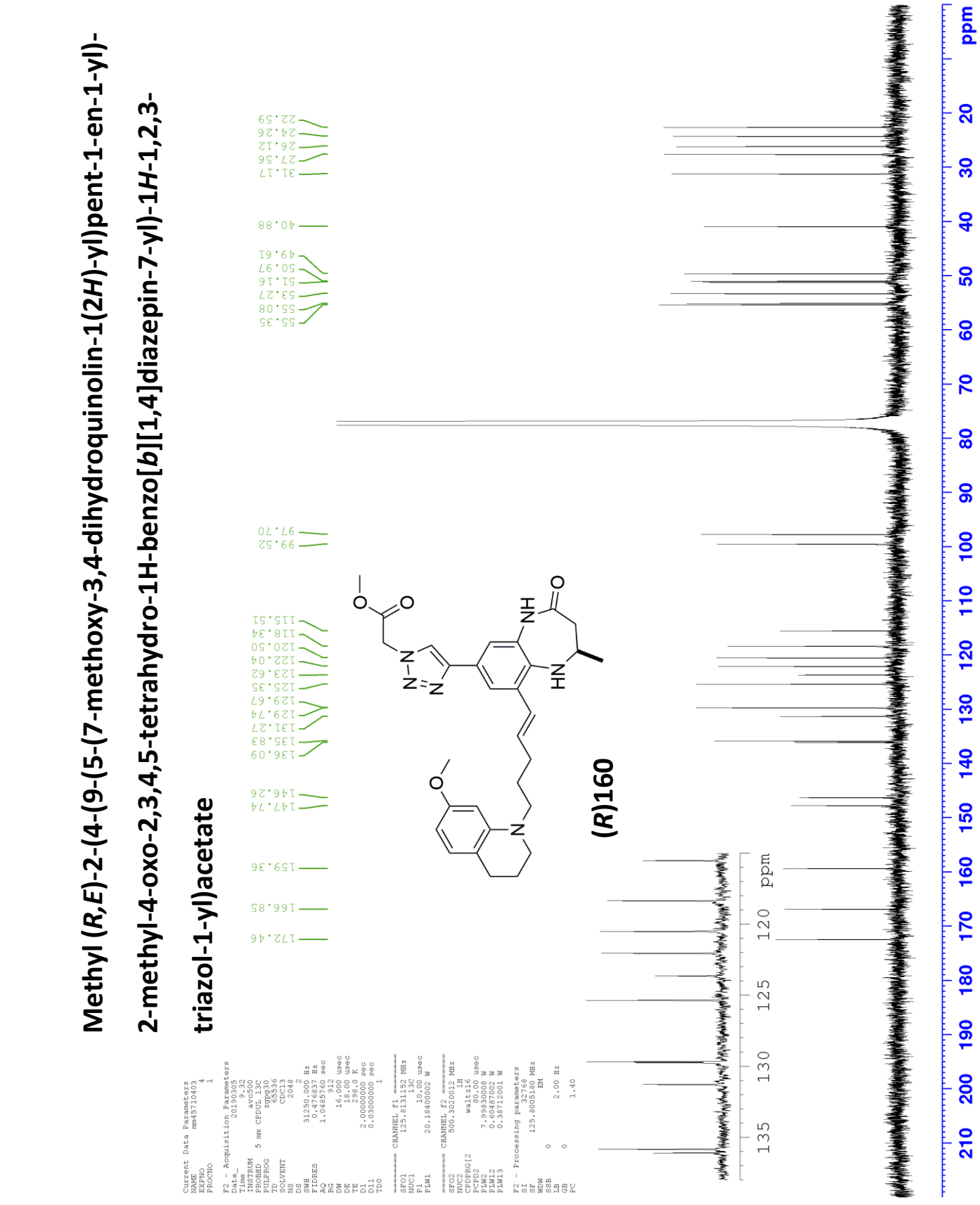
Methyl (*R*,*E*)-2-(5-(9-(5-(7-methoxy-3,4-dihydroquinolin-1(2*H*)-yl)pent-1-en-1-yl)-2-methyl-4-oxo-2,3,4,5-tetrahydro-1*H*-benzo[*b*][1,4]diazepin-7-yl)-1*H*-1,2,3-triazol-1-yl)acetate



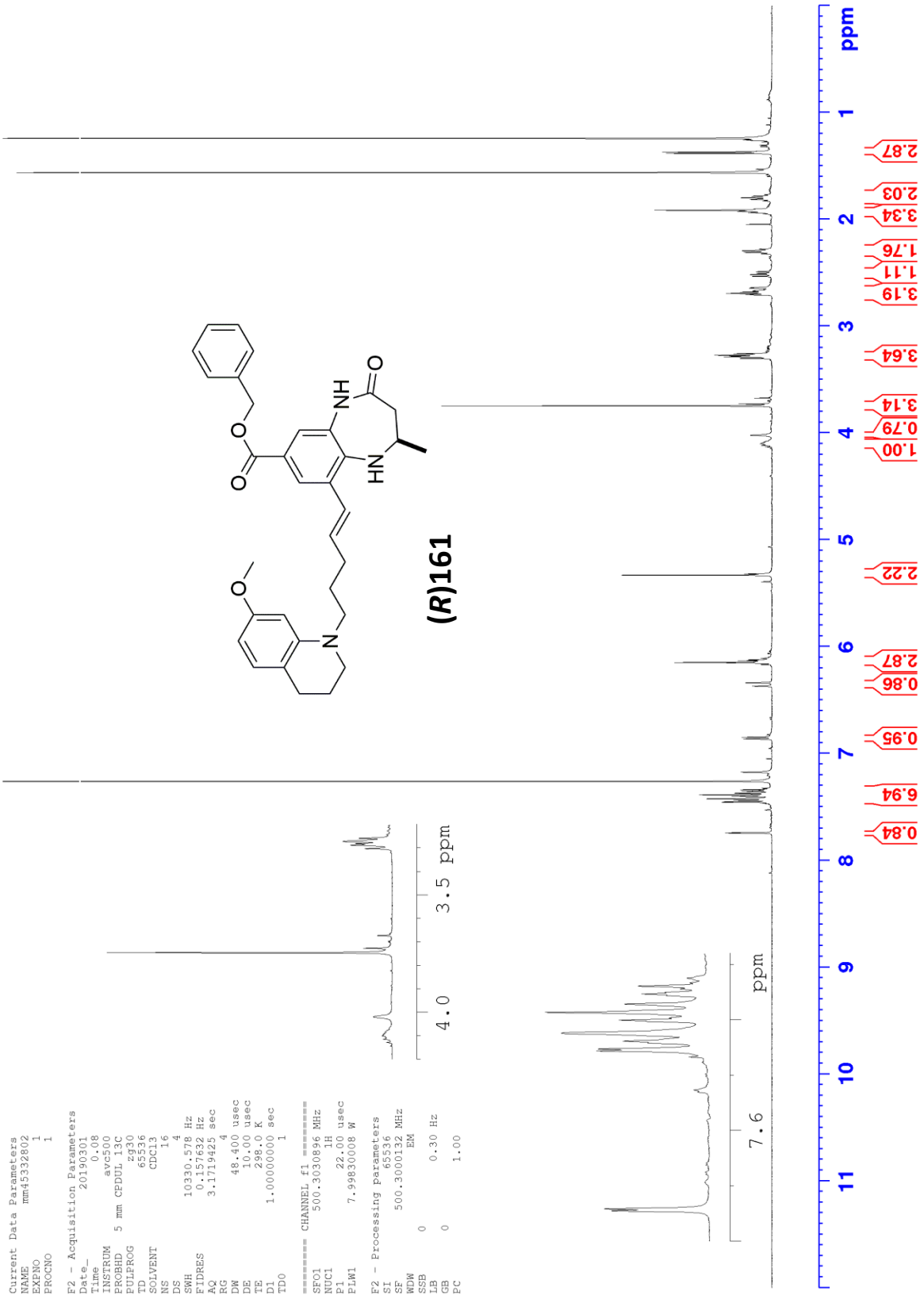
Methyl (*R*,*E*)-2-(4-(9-(5-(7-methoxy-3,4-dihydroquinolin-1(2*H*)-yl)pent-1-en-1-yl)-2-methyl-4-oxo-2,3,4,5-tetrahydro-1H-benzo[*b*][1,4]diazepin-7-yl)-1*H*-1,2,3-triazol-1-yl)acetate

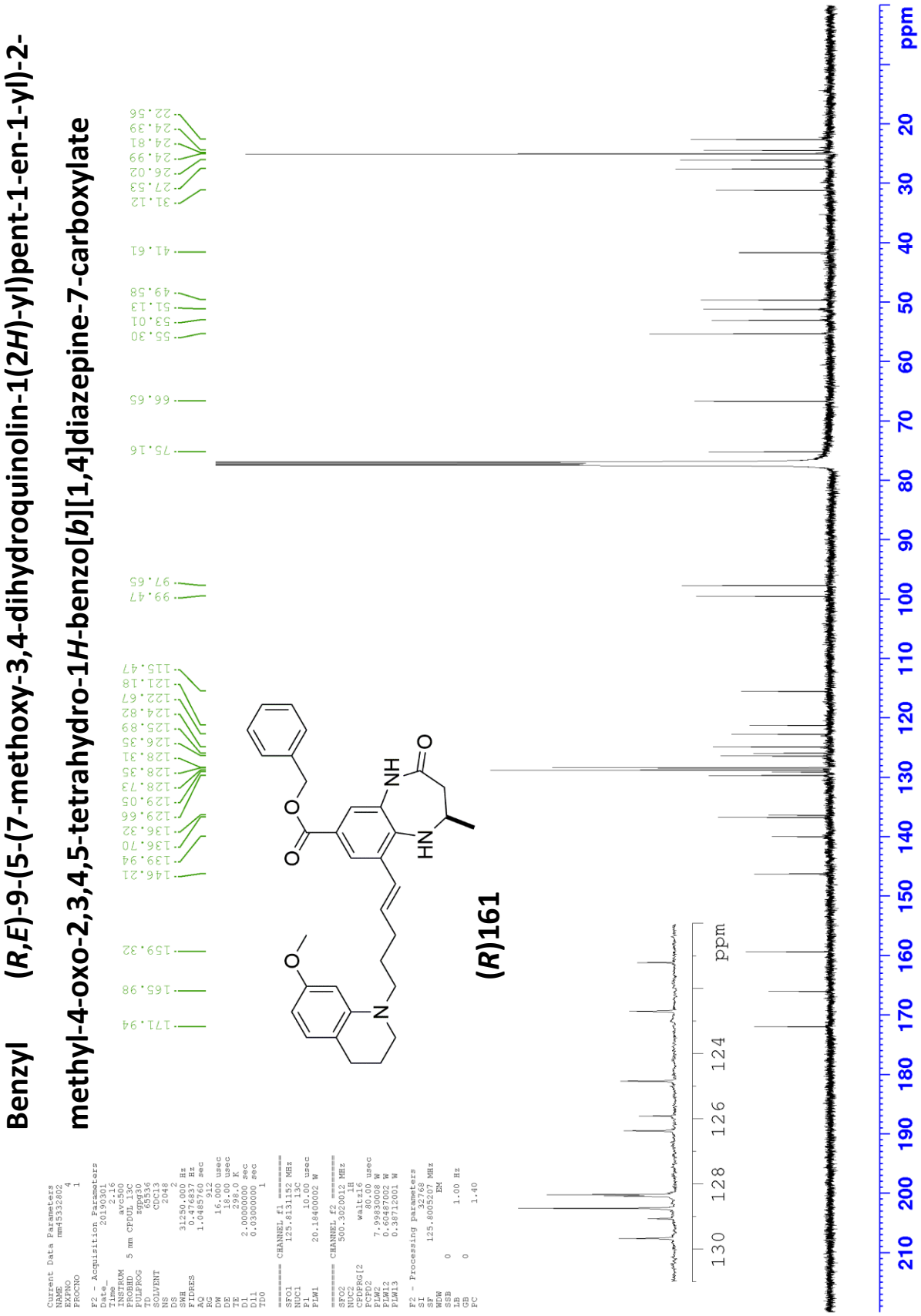


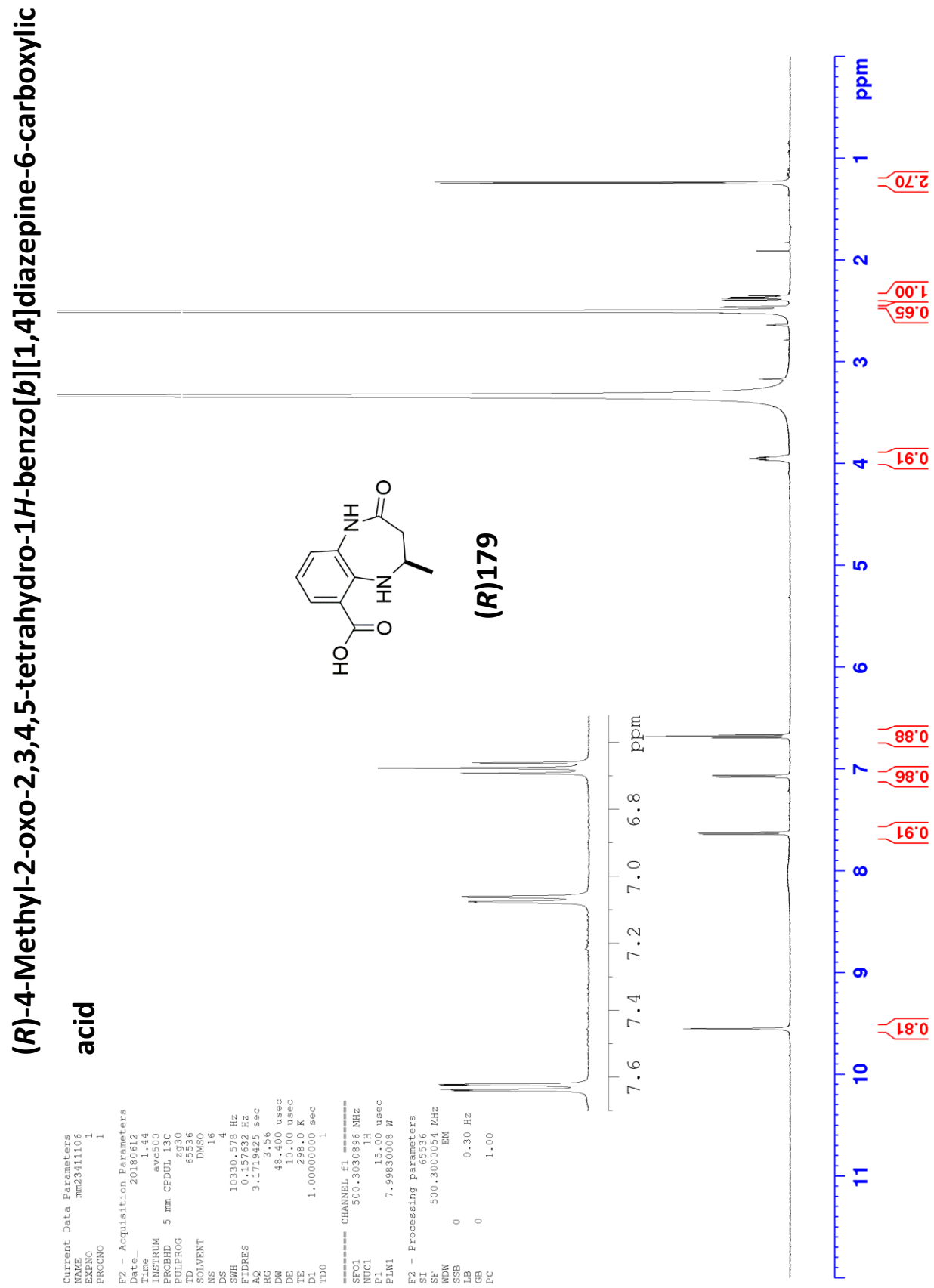
Methyl (*R*,*E*)-2-(4-(9-(5-(7-methoxy-3,4-dihydroquinolin-1(2*H*)-yl)pent-1-en-1-yl)-2-methyl-4-oxo-2,3,4,5-tetrahydro-1H-benzo[*b*][1,4]diazepin-7-yl)-1*H*-1,2,3-triazol-1-yl)acetate

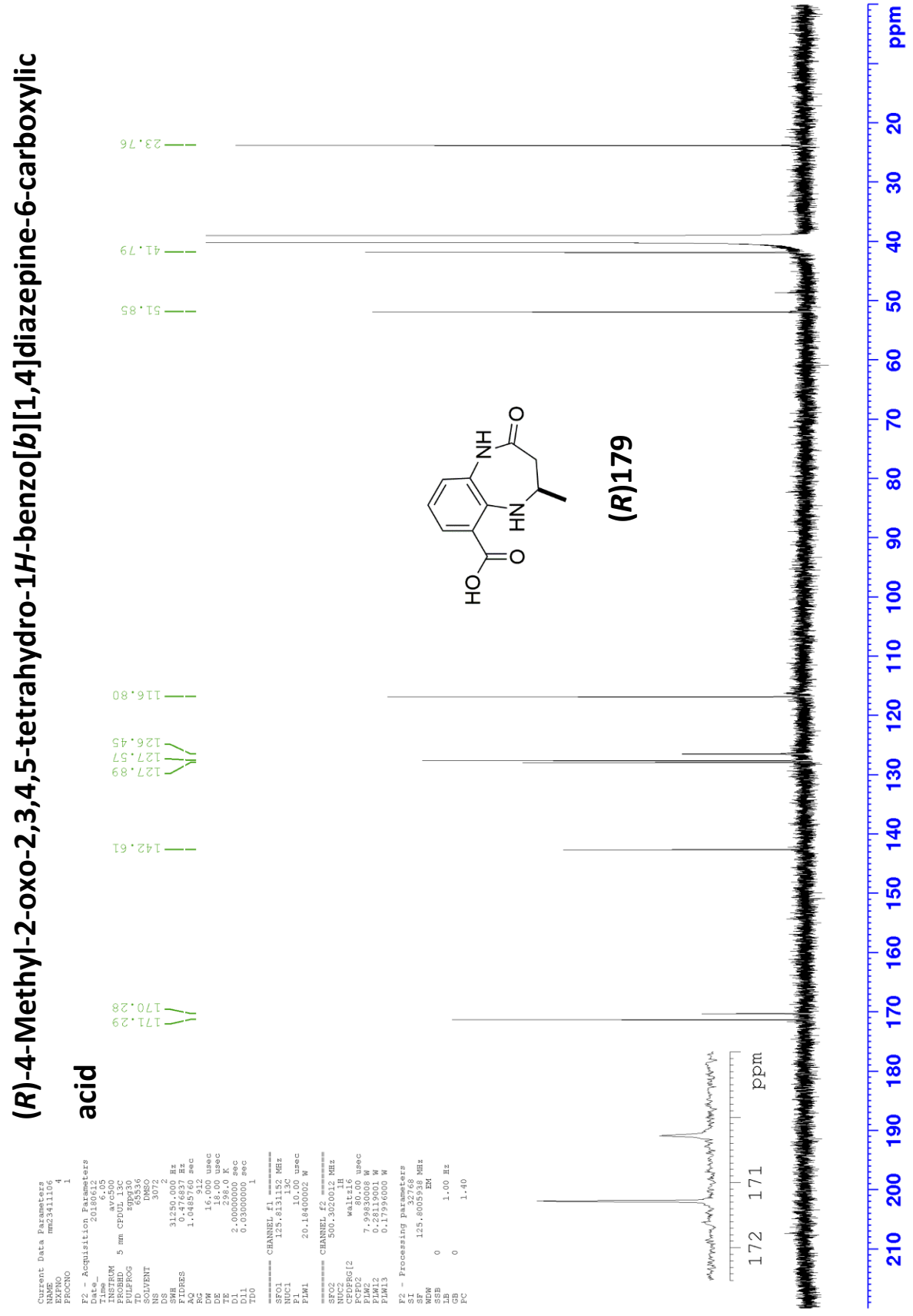


Benzyl (*R*,*E*)-9-(5-(7-methoxy-3,4-dihydroquinolin-1(2*H*)-yl)pent-1-en-1-yl)-2-methyl-4-oxo-2,3,4,5-tetrahydro-1*H*-benzo[*b*][1,4]diazepine-7-carboxylate

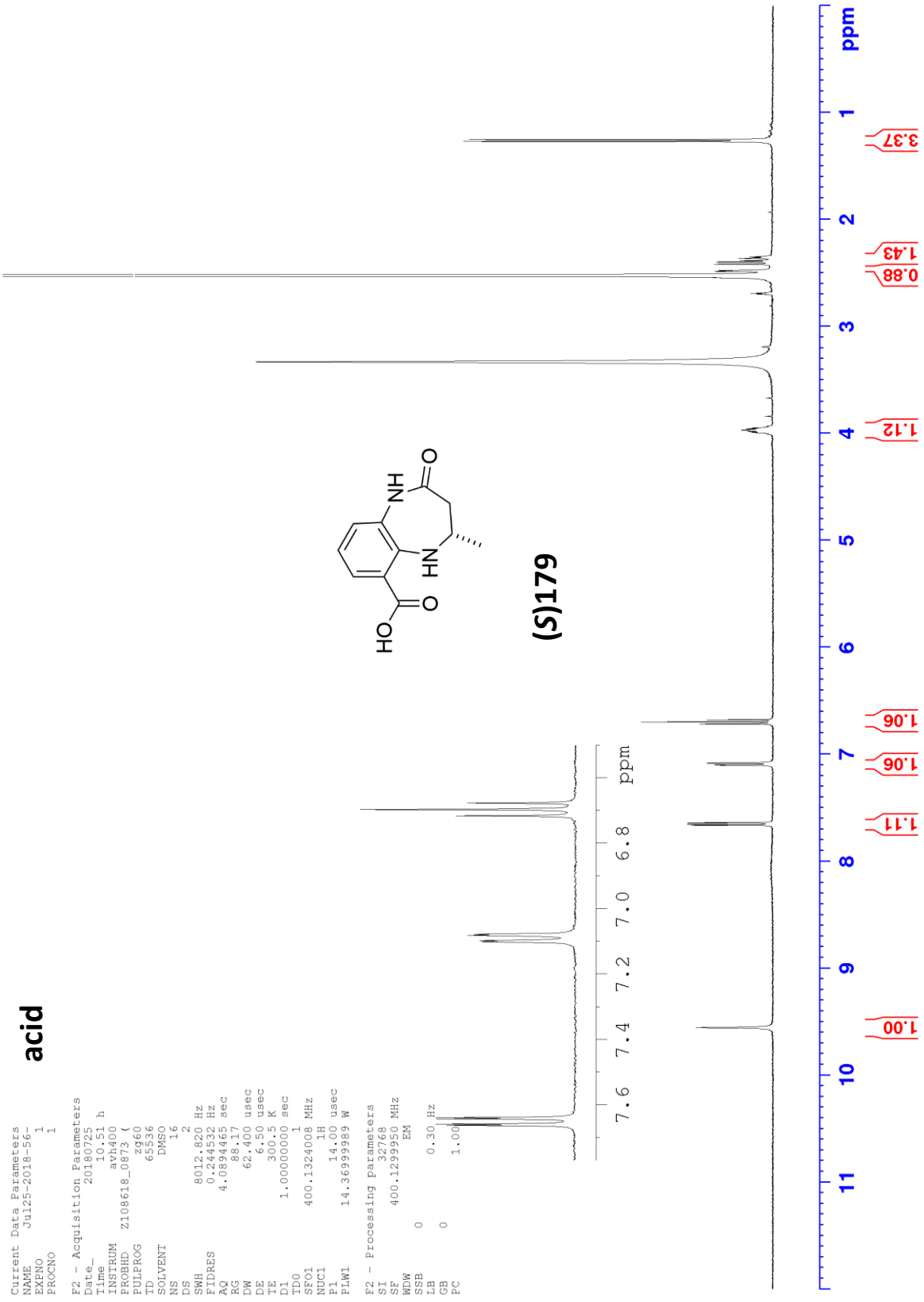


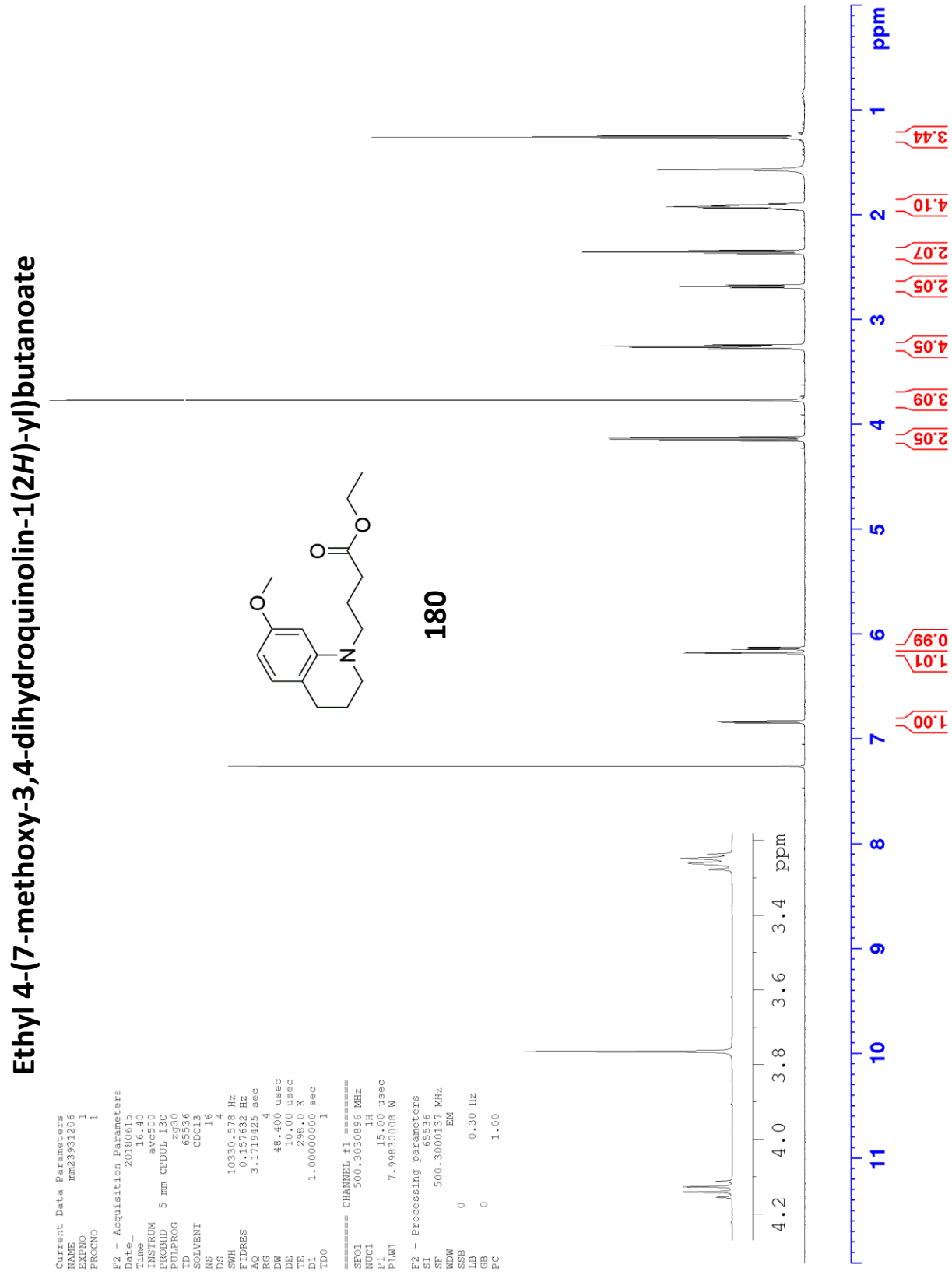

Benzyl (R,E)-9-(5-(7-methoxy-3,4-dihydroquinolin-1(2H)-yl)pent-1-en-1-yl)-2-methyl-4-oxo-2,3,4,5-tetrahydro-1H-benzo[b][1,4]diazepine-7-carboxylate
(R)161
ppm

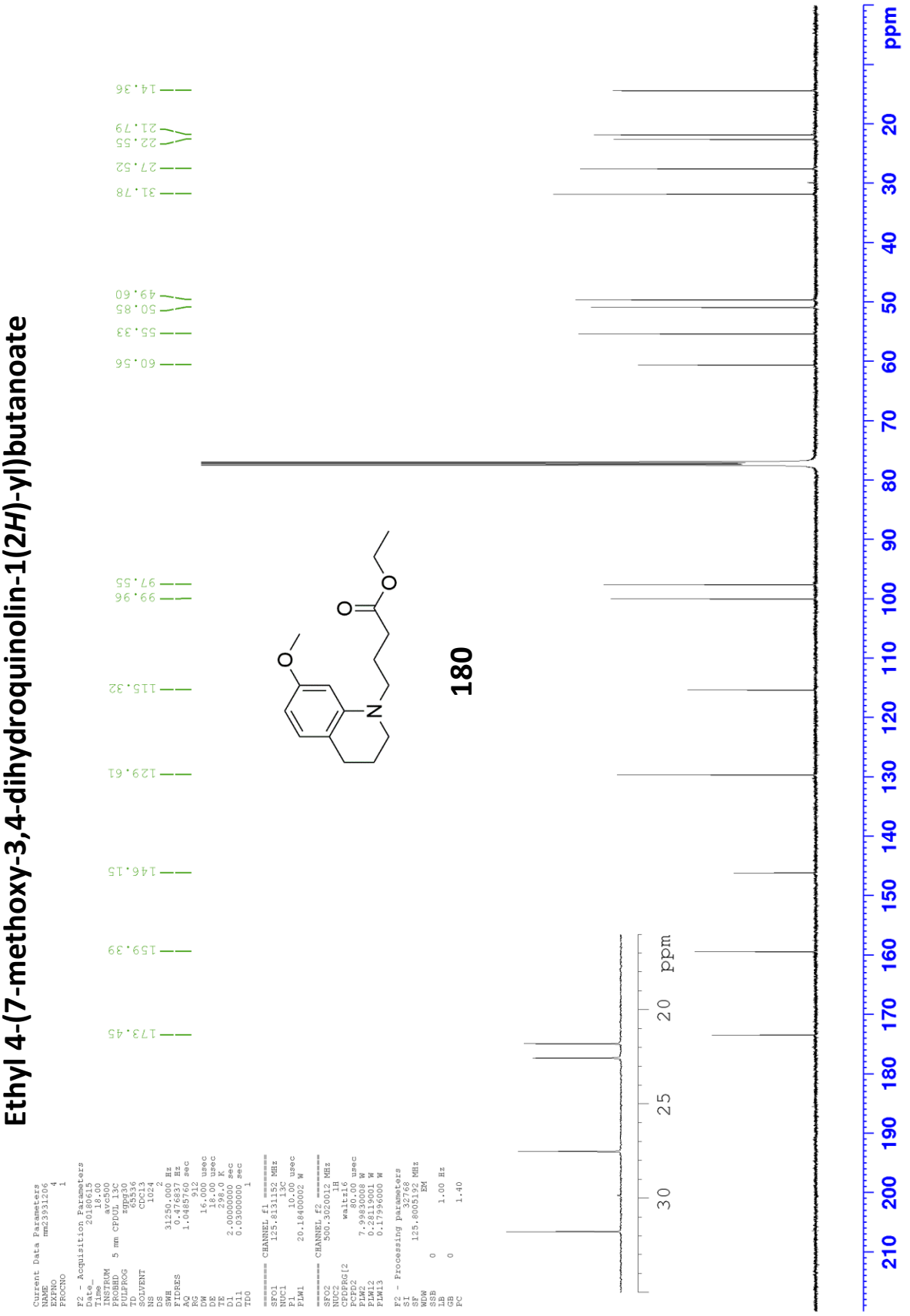

(R)-4-Methyl-2-oxo-2,3,4,5-tetrahydro-1H-benzo[b][1,4]diazepine-6-carboxylic acid
(R)179
Current Data Parameters
NAME mm23411106
EXPNO 1
PROCNO 1
F2 - Acquisition Parameters
Date_ 20180612
Time_ 1.44
INSTRUM av500
PROBHD 5 mm CPDUL 13C
PULPROG zg30
TD 65536
SOLVENT DMSO
NS 16
DS 4
SWH 10330.578 Hz
FIDRES 0.157632 Hz
AQ 3.1719425 sec
RG 3.56
DW 48.400 usec
DE 10.00 usec
TE 298.0 K
D1 1.00000000 sec
TD0 1
======== CHANNEL f1 ========
SFO1 500.3030896 MHz
NUC1 1H
P1 15.00 usec
PLW1 7.99830008 W
F2 - Processing parameters
SI 65536
SF 500.3000054 MHz
WDW EM
SSB 0
LB 0.30 Hz
GB 0
PC 1.00
7.6
7.4
7.2
7.0
6.8
ppm
0.81
0.91
0.86
0.88
0.91
2.70
0.65
1.00
ppm

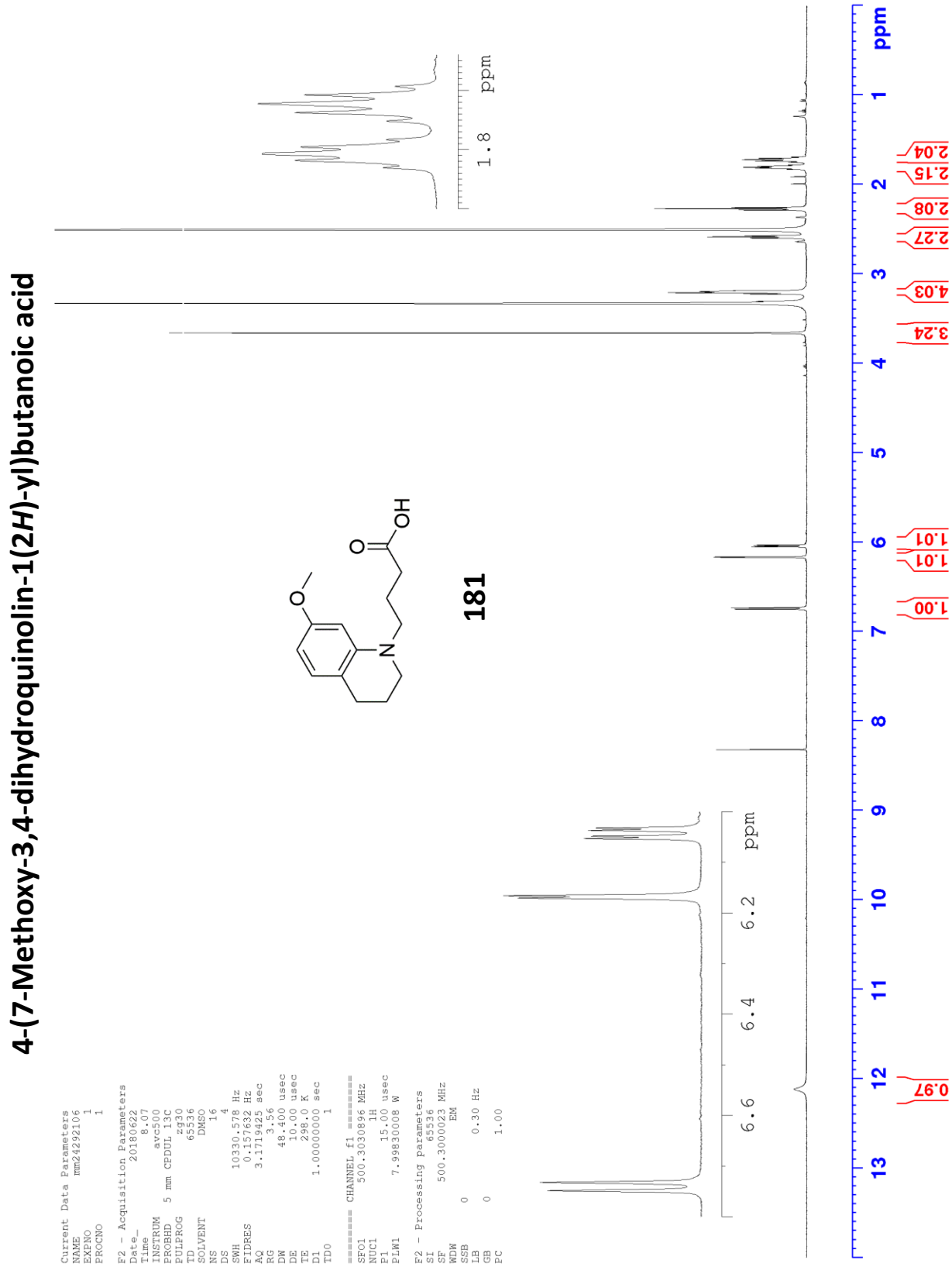

(R)-4-Methyl-2-oxo-2,3,4,5-tetrahydro-1H-benzo[b][1,4]diazepine-6-carboxylic acid
(R)179
23.76
41.79
51.85
116.80
126.45
127.57
127.89
142.61
170.28
171.29
ppm

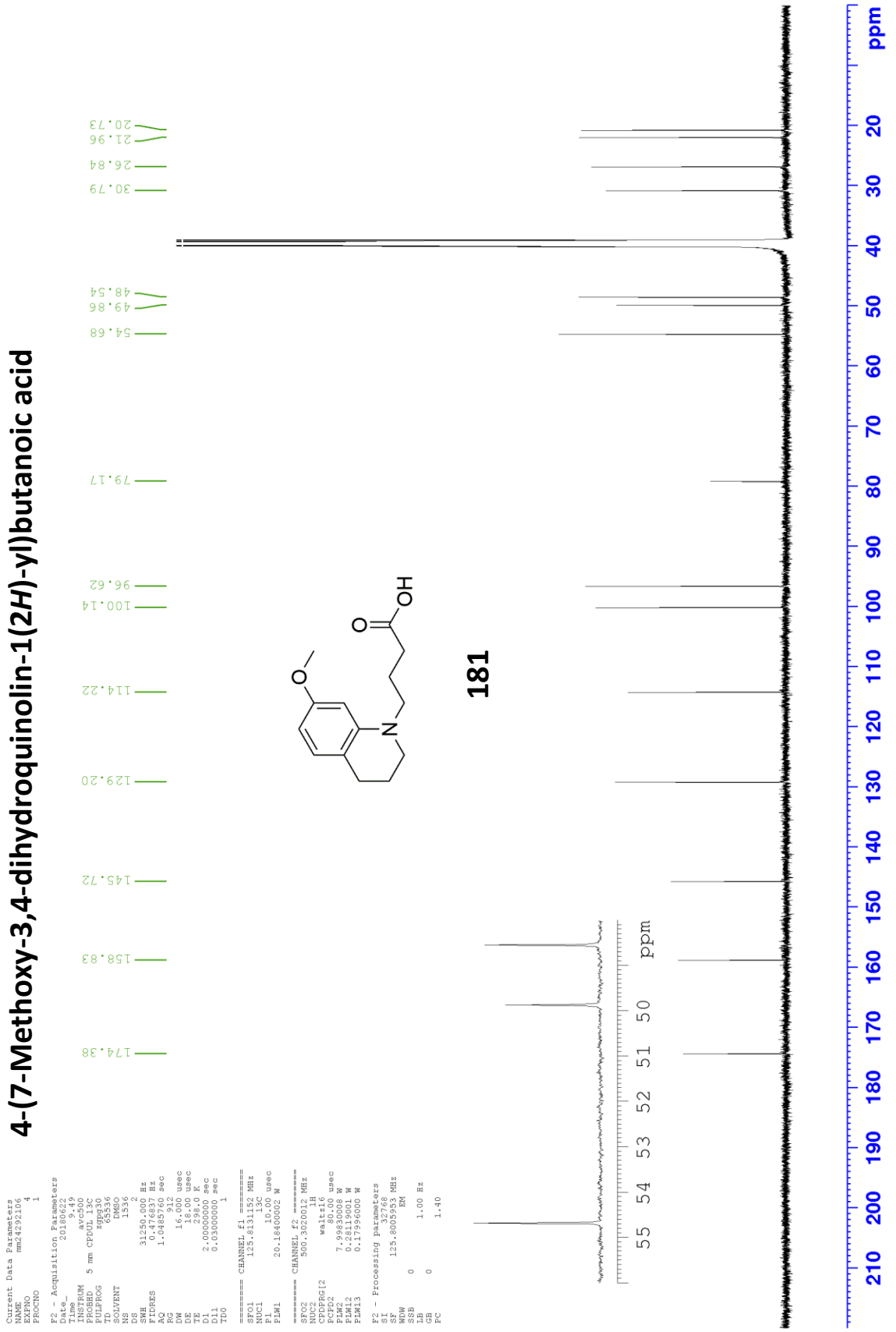
(*S*)-4-Methyl-2-oxo-2,3,4,5-tetrahydro-1*H*-benzo[*b*][1,4]diazepine-6-carboxylic acid

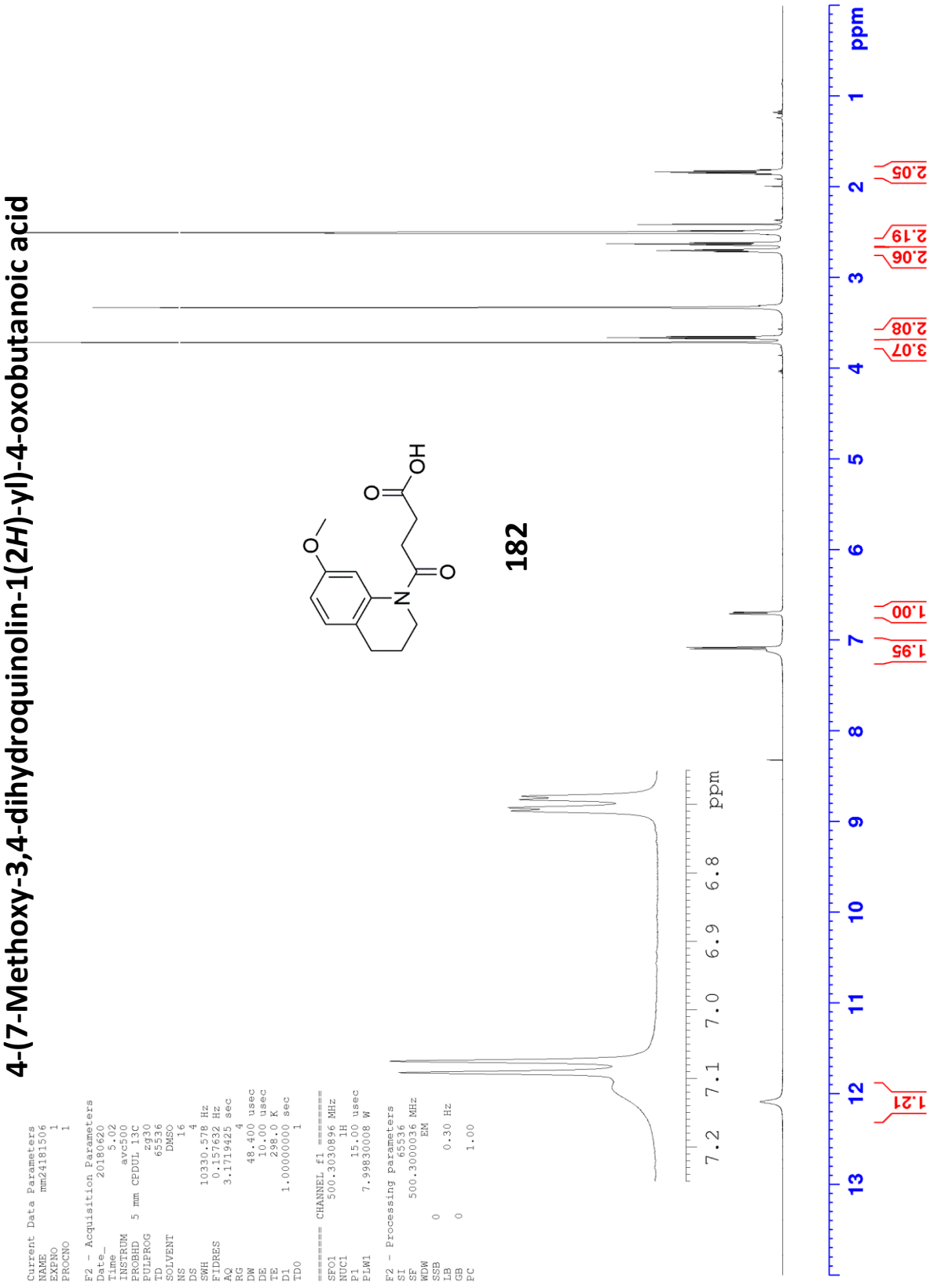


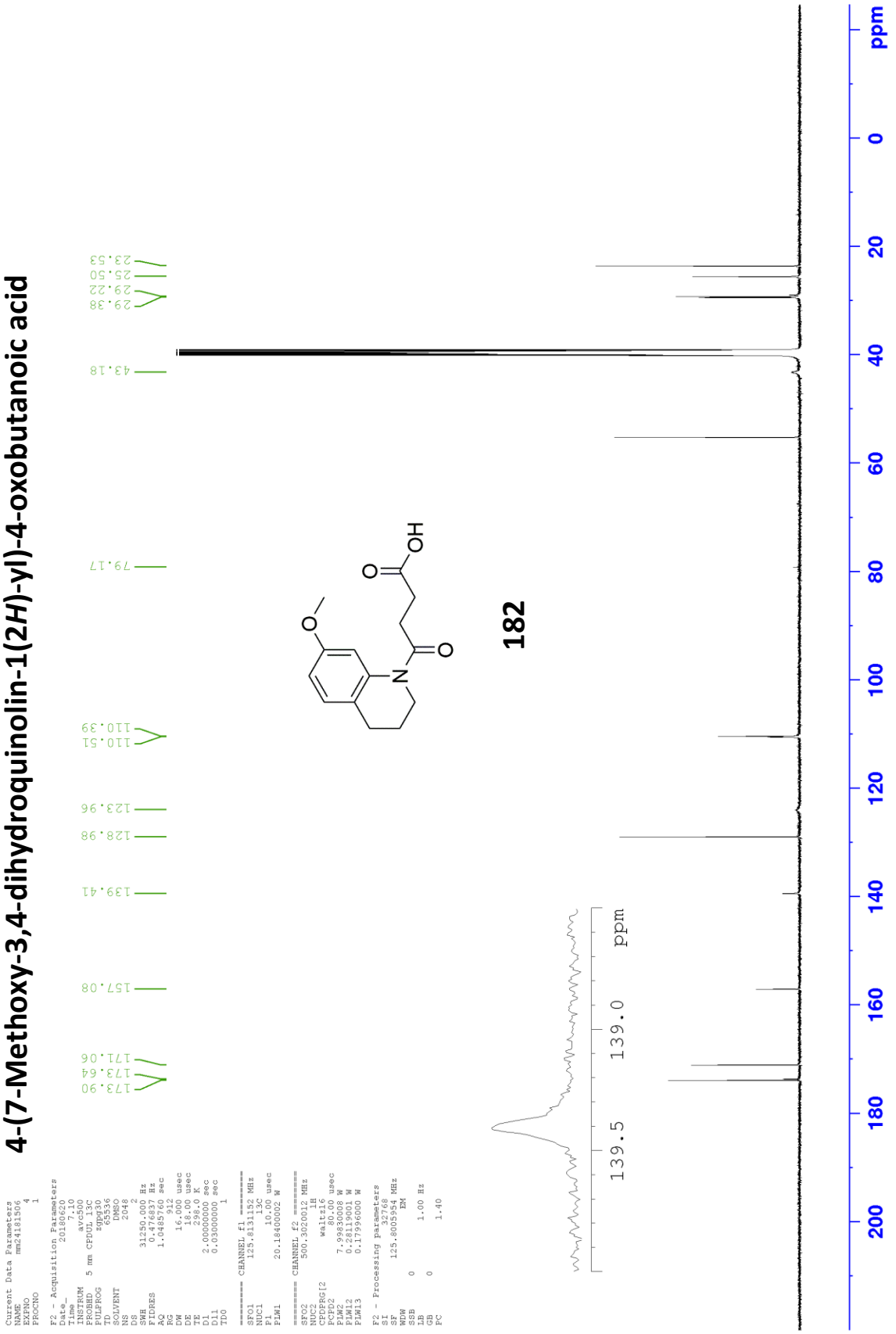

Ethyl 4-(7-methoxy-3,4-dihydroquinolin-1(2H)-yl)butanoate
180
Current Data Parameters
NAME mm23931206
EXPNO 1
PROCNO 1
F2 - Acquisition Parameters
Date_ 20180615
Time 16.40
INSTRUM avc500
PROBHD 5 mm CPDUL 13C
PULPROG zg30
TD 65536
SOLVENT CDCl3
NS 16
DS 4
SWH 10330.578 Hz
FIDRES 0.157632 Hz
AQ 3.1719425 sec
RG 4
DW 48.400 usec
DE 10.00 usec
TE 298.0 K
D1 1.00000000 sec
TD0 1
======== CHANNEL f1 ========
SFO1 500.3030896 MHz
NUC1 1H
P1 15.00 usec
PLW1 7.99830008 W
F2 - Processing parameters
SI 65536
SF 500.3000137 MHz
WDW EM
SSB 0
LB 0.30 Hz
GB 0
PC 1.00
4.2 4.0 3.8 3.6 3.4 ppm
ppm
1.00
0.99
1.01
2.05
3.09
4.05
2.05
2.07
4.10
3.44

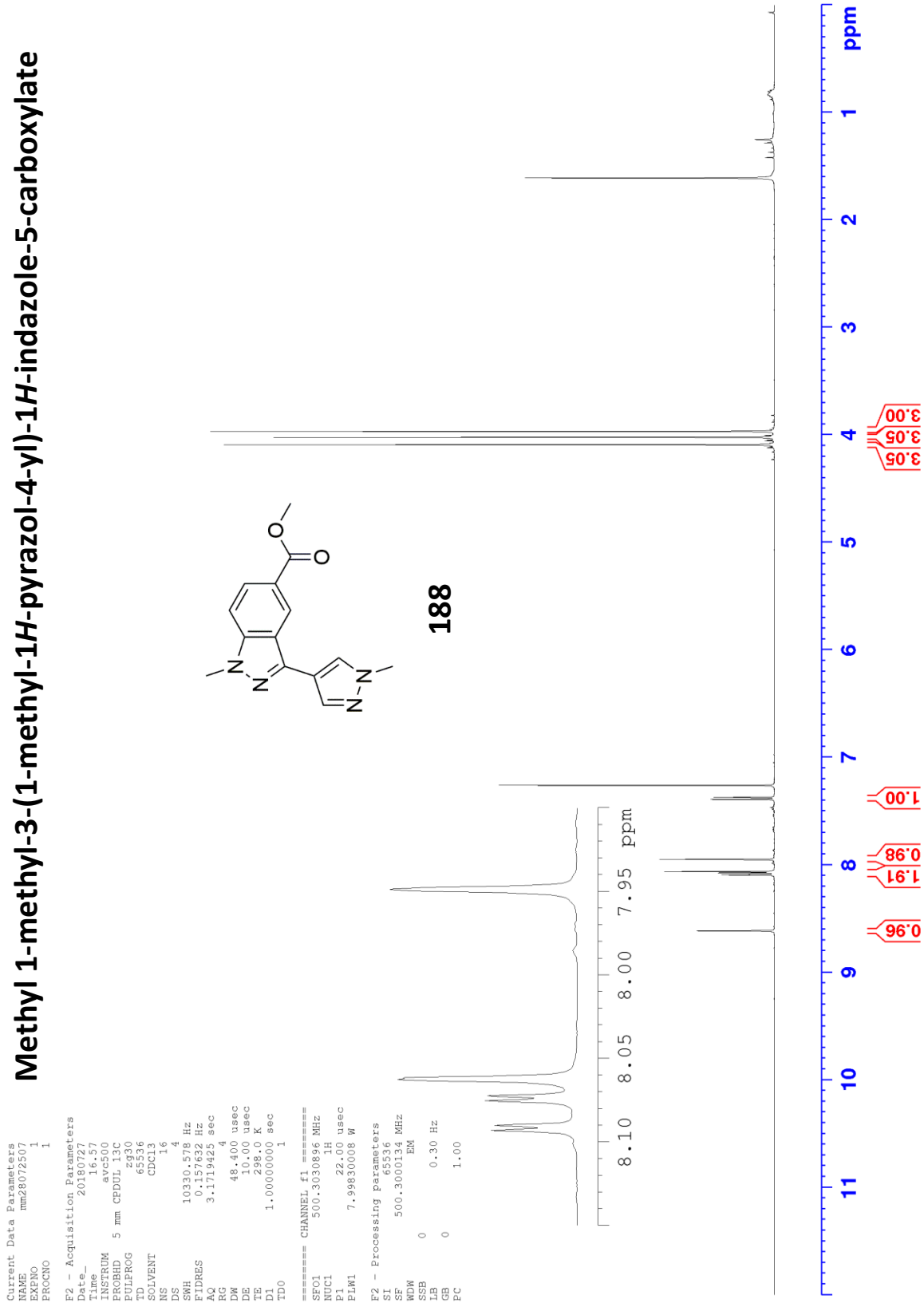

Ethyl 4-(7-methoxy-3,4-dihydroquinolin-1(2H)-yl)butanoate
180
173.45
159.39
146.15
129.61
115.32
99.96
97.55
60.56
55.33
50.85
49.60
31.78
27.52
22.55
21.79
14.36
ppm

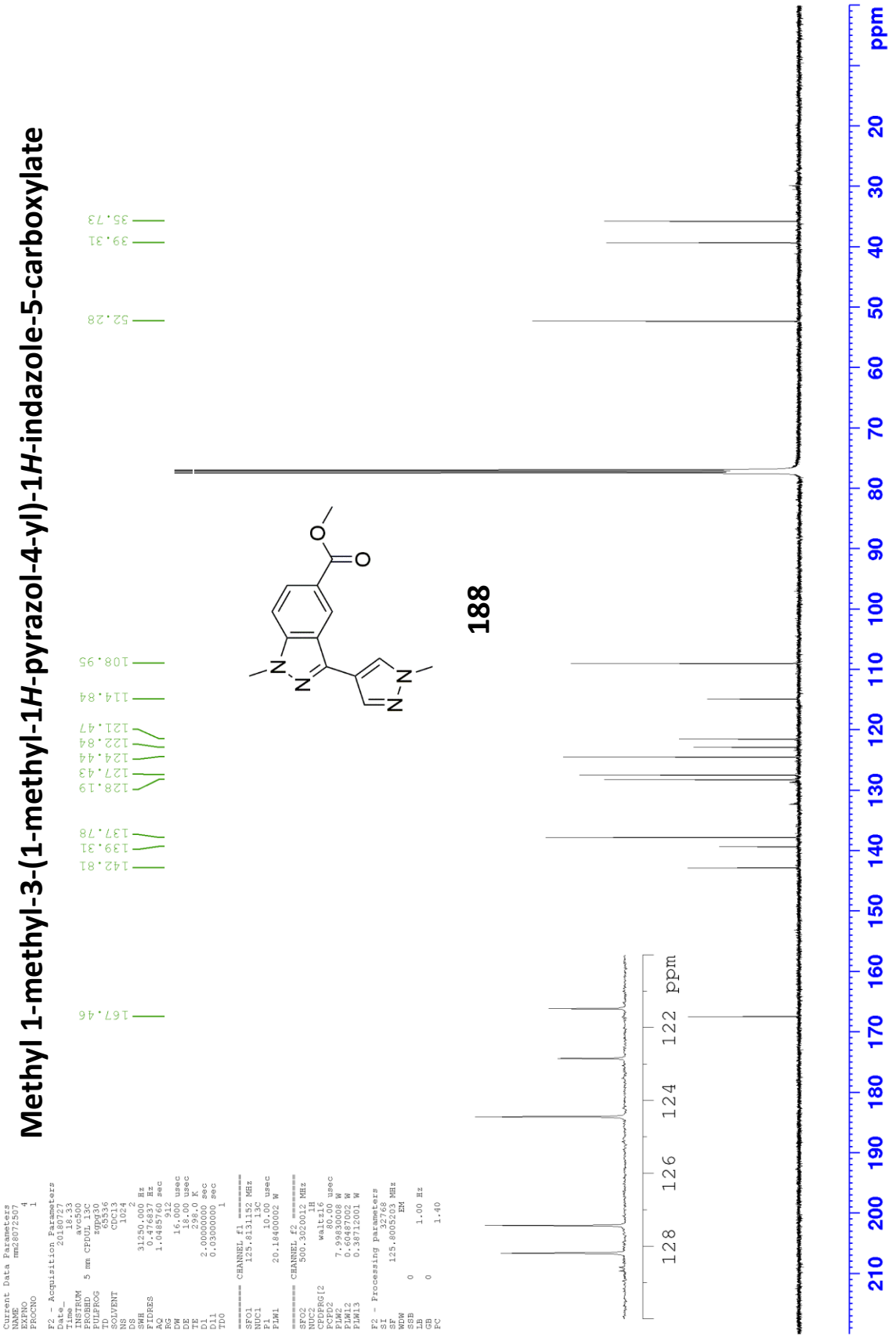

4-(7-Methoxy-3,4-dihydroquinolin-1(2H)-yl)butanoic acid
181
Current Data Parameters
NAME mm24292106
EXPNO 1
PROCNO 1
F2 - Acquisition Parameters
Date_ 20180622
Time 8.07
INSTRUM av-500
PROBHD 5 mm CPDUL 13C
PULPROG zg30
TD 65536
SOLVENT DMSO
NS 16
DS 4
SWH 10330.578 Hz
FIDRES 0.157632 Hz
AQ 3.1719425 sec
RG 3.56
DW 48.400 usec
DE 10.00 usec
TE 298.0 K
D1 1.00000000 sec
TD0 1
======== CHANNEL f1 ========
SFO1 500.3030896 MHz
NUC1 1H
P1 15.00 usec
PLW1 7.99830008 W
F2 - Processing parameters
SI 65536
SF 500.3000023 MHz
WDW EM
SSB 0
LB 0.30 Hz
GB 0
PC 1.00
1.8 ppm
6.6
6.4
6.2
ppm
0.97
1.01
1.01
1.00
3.24
4.03
2.27
2.08
2.15
2.04
ppm

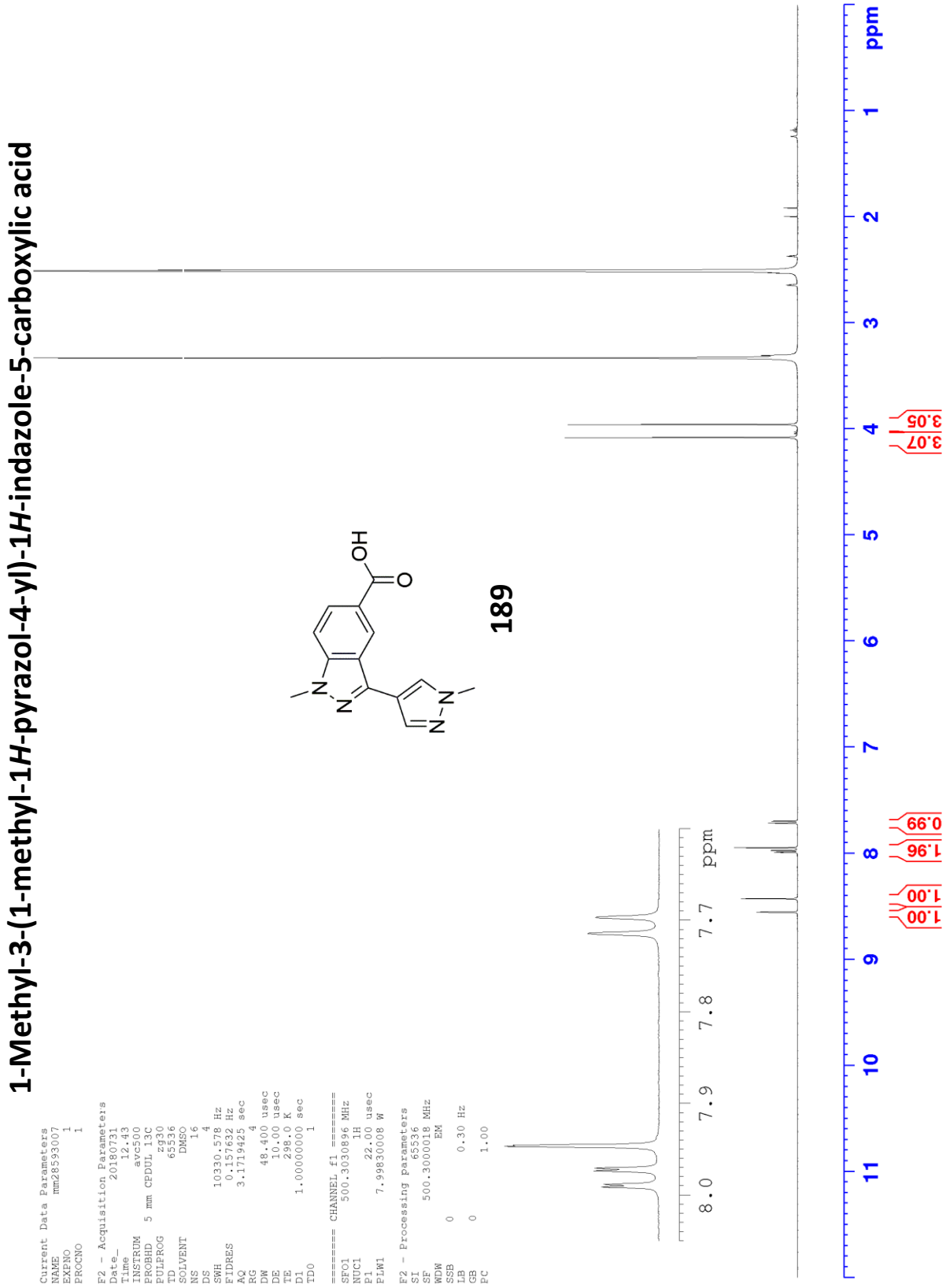

4-(7-Methoxy-3,4-dihydroquinolin-1(2H)-yl)butanoic acid
181
Current Data Parameters
NAME nm24292106
EXPNO 4
PROCNO 1
F2 - Acquisition Parameters
Date_ 20180622
Time 9.40
INSTRUM avc500
PROBHD 5 mm CPDUL 13C
PULPROG zgpg30
TD 65536
SOLVENT DMSO
NS 152
DS 2
SWH 31250.000 Hz
FIDRES 0.476837 Hz
AQ 1.0485760 sec
RG 32
DW 16.000 usec
DE 18.00 usec
TE 298.0 K
D1 2.00000000 sec
D11 0.03000000 sec
TD0 1
======== CHANNEL f1 ========
SFO1 125.8131152 MHz
NUC1 13C
P1 10.00 usec
PLW1 20.18400002 W
======== CHANNEL f2 ========
SFO2 500.3020012 MHz
NUC2 1H
CPDPRG2 waltz16
PCPD2 80.00 usec
PLW2 7.99830008 W
PLW12 0.28119001 W
PLW13 0.17996000 W
F2 - Processing parameters
SI 32768
SF 125.8005953 MHz
WDW EM
SSB 0
LB 1.00 Hz
GB 0
PC 1.40
174.38
158.83
145.72
129.20
114.22
100.14
96.62
79.17
54.68
49.86
48.54
30.79
26.84
21.96
20.73
55 54 53 52 51 50 ppm
210 200 190 180 170 160 150 140 130 120 110 100 90 80 70 60 50 40 30 20 ppm

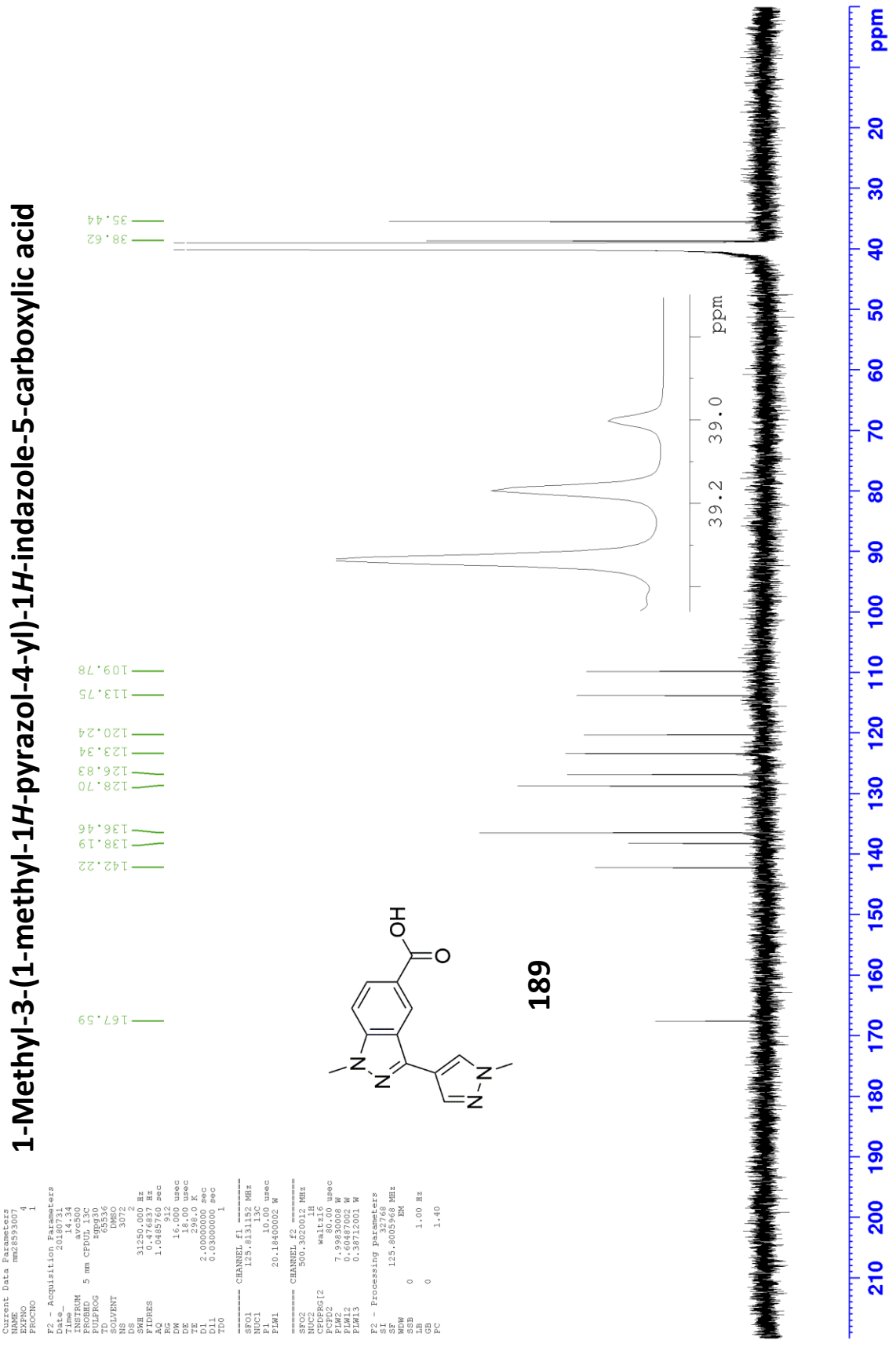

4-(7-Methoxy-3,4-dihydroquinolin-1(2H)-yl)-4-oxobutanoic acid
182
Current Data Parameters
NAME mm24181506
EXPNO 1
PROCNO 1
F2 - Acquisition Parameters
Date_ 20180620
Time 5.02
INSTRUM avc500
PROBHD 5 mm CPDUL 13C
PULPROG zg30
TD 65536
SOLVENT DMSO
NS 16
DS 4
SWH 10330.578 Hz
FIDRES 0.157632 Hz
AQ 3.1719425 sec
RG 4
DW 48.400 usec
DE 10.00 usec
TE 298.0 K
D1 1.00000000 sec
TD0 1
======== CHANNEL f1 ========
SFO1 500.3030896 MHz
NUC1 1H
P1 15.00 usec
PLW1 7.99830008 W
F2 - Processing parameters
SI 65536
SF 500.3000036 MHz
WDW EM
SSB 0
LB 0.30 Hz
GB 0
PC 1.00
7.2
7.1
7.0
6.9
6.8
ppm
1.21
2.05
2.19
2.06
3.07
2.08
1.00
1.95
ppm

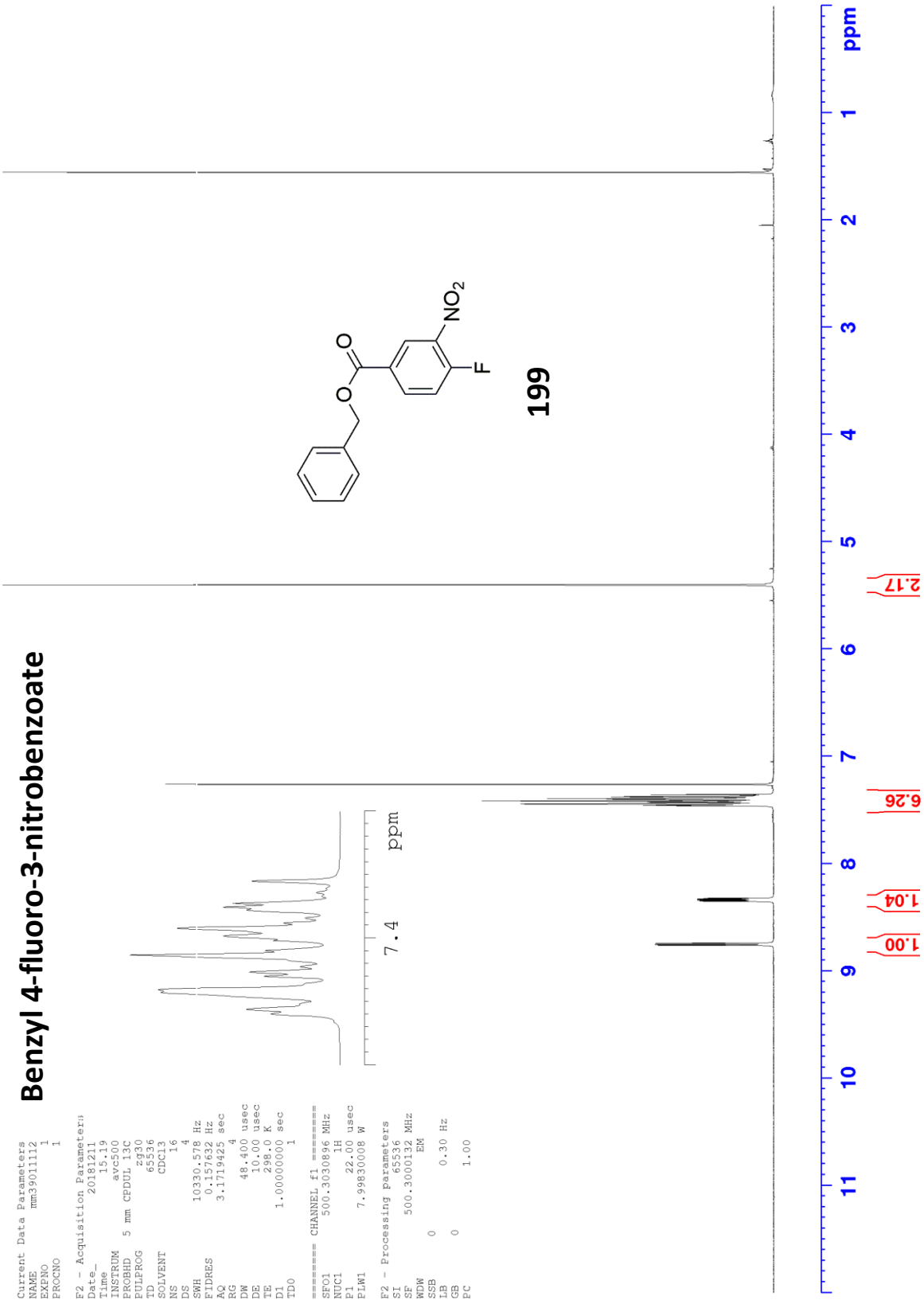

4-(7-Methoxy-3,4-dihydroquinolin-1(2H)-yl)-4-oxobutanoic acid
182
Current Data Parameters
NAME mm24181506
EXPNO 4
PROCNO 1
F2 - Acquisition Parameters
Date_ 20180620
Time 7.10
INSTRUM av-500
PROBHD 5 mm CPDUL 13C
PULPROG zgpg30
TD 65536
SOLVENT DMSO
NS 2048
DS 4
SWH 31250.000 Hz
FIDRES 0.476837 Hz
AQ 1.0485760 sec
RG 512
DW 16.000 usec
DE 18.00 usec
TE 298.0 K
D1 2.00000000 sec
D11 0.03000000 sec
TD0 1
CHANNEL f1
SFO1 125.8131152 MHz
NUC1 13C
P1 10.00 usec
PLW1 20.18400002 W
CHANNEL f2
SFO2 500.3020012 MHz
NUC2 1H
CPDPRG[2 waltz16
PCPD2 80.00 usec
PLW2 7.99830008 W
PLW12 0.28119001 W
PLW13 0.17996000 W
F2 - Processing parameters
SI 32768
SF 125.8005954 MHz
WDW EM
SSB 0
LB 1.00 Hz
GB 0
PC 1.40
173.90
173.64
171.06
157.08
139.41
128.98
123.96
110.51
110.39
79.17
43.18
29.38
29.22
25.50
23.53
139.5
139.0
ppm
200
180
160
140
120
100
80
60
40
20
0
ppm

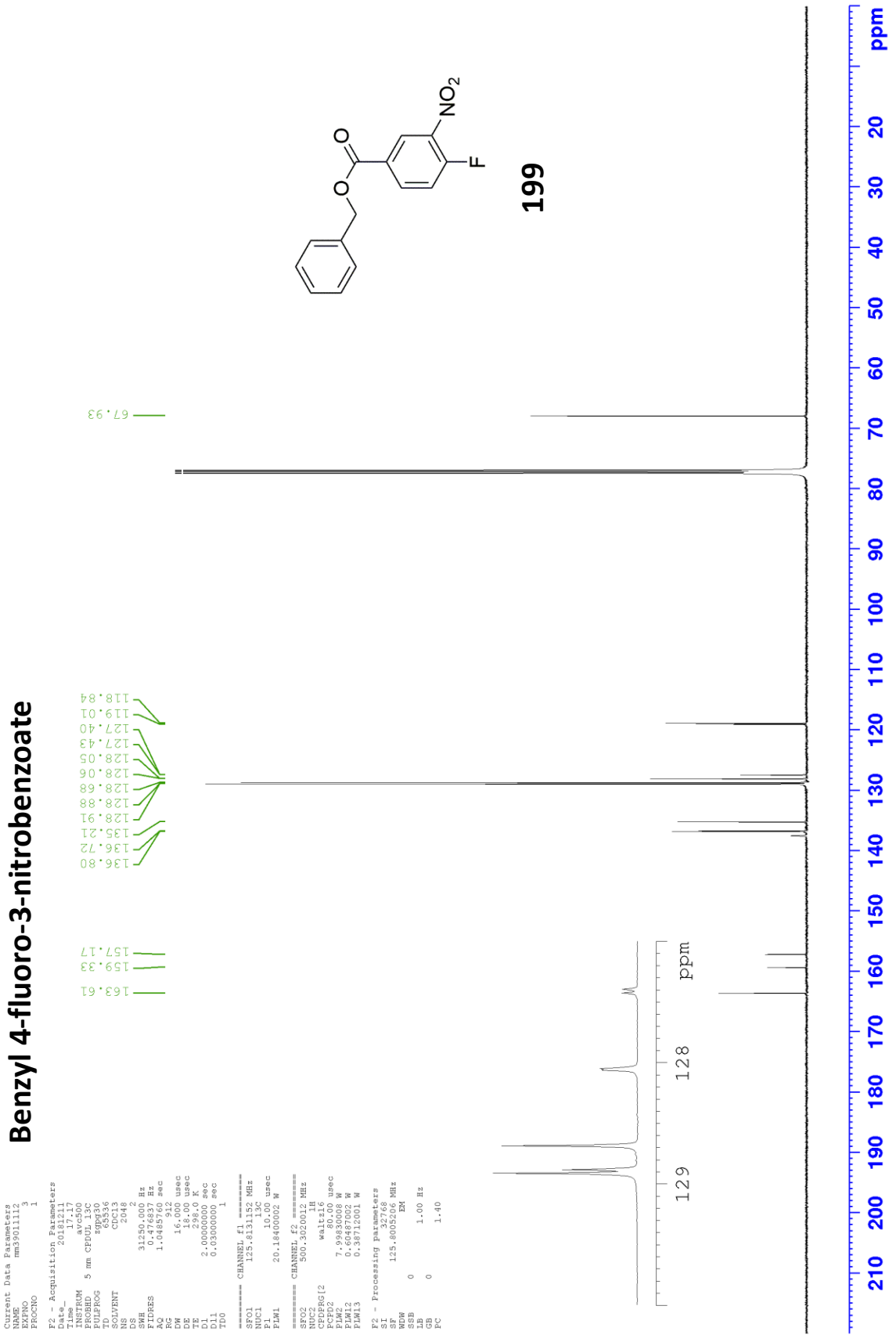

Methyl 1-methyl-3-(1-methyl-1H-pyrazol-4-yl)-1H-indazole-5-carboxylate
188
Current Data Parameters
NAME mm28072507
EXPNO 1
PROCNO 1
F2 - Acquisition Parameters
Date_ 20180727
Time 16.57
INSTRUM avc500
PROBHD 5 mm CPDUL 13C
PULPROG zg30
TD 65536
SOLVENT CDCl3
NS 16
DS 4
SWH 10330.578 Hz
FIDRES 0.157632 Hz
AQ 3.1719425 sec
RG 4
DW 48.400 usec
DE 10.00 usec
TE 298.0 K
D1 1.00000000 sec
TD0 1
======== CHANNEL f1 ========
SFO1 500.3030896 MHz
NUC1 1H
P1 22.00 usec
PLW1 7.99830008 W
F2 - Processing parameters
SI 65536
SF 500.3000134 MHz
WDW EM
SSB 0
LB 0.30 Hz
GB 0
PC 1.00
8.10
8.05
8.00
7.95 ppm
0.96
1.91
0.98
1.00
3.05
3.05
3.00
11
10
9
8
7
6
5
4
3
2
1
ppm

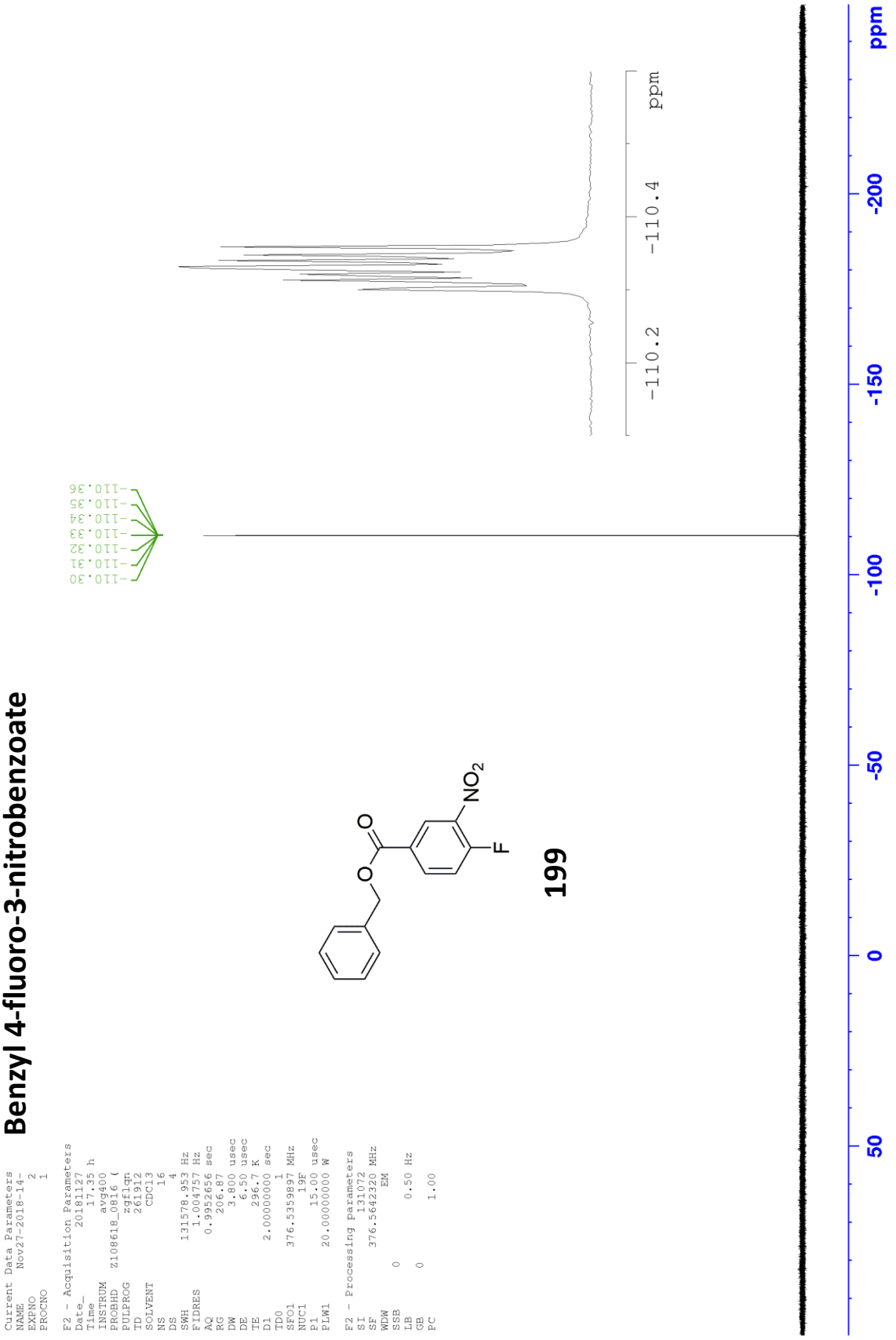

Methyl 1-methyl-3-(1-methyl-1H-pyrazol-4-yl)-1H-indazole-5-carboxylate
188
167.46
142.81
139.31
137.78
128.19
127.43
124.44
122.84
121.47
114.84
108.95
52.28
39.31
35.73
ppm

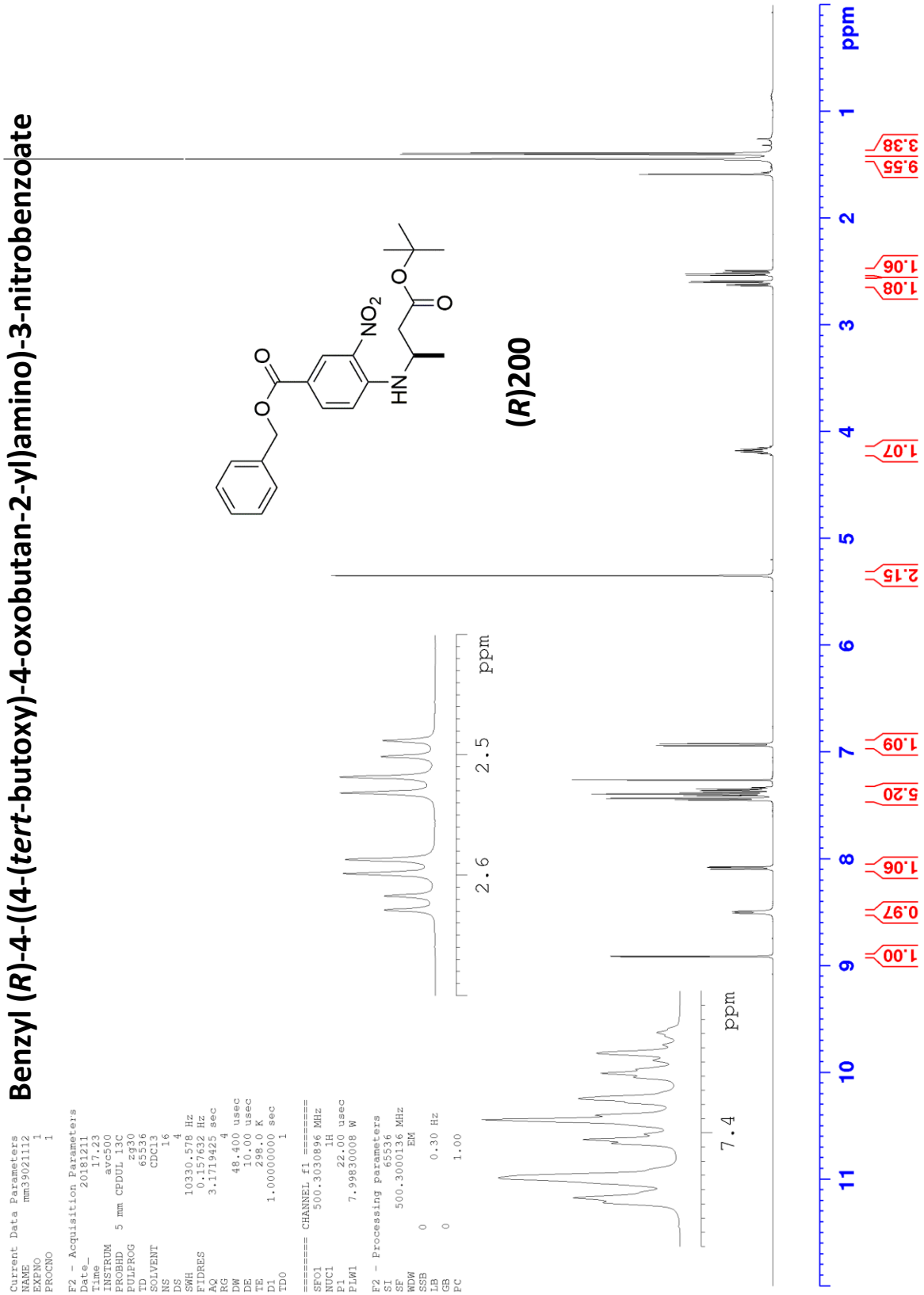

1-Methyl-3-(1-methyl-1H-pyrazol-4-yl)-1H-indazole-5-carboxylic acid
189
Current Data Parameters
NAME mm28593007
EXPNO 1
PROCNO 1
F2 - Acquisition Parameters
Date_ 20180731
Time 12.43
INSTRUM avc500
PROBHD 5 mm CPDUL 13C
PULPROG zg30
TD 65536
SOLVENT DMSO
NS 16
DS 4
SWH 10330.578 Hz
FIDRES 0.157632 Hz
AQ 3.1719425 sec
RG 4
DW 48.400 usec
DE 10.00 usec
TE 298.0 K
D1 1.00000000 sec
TD0 1
======== CHANNEL f1 ========
SFO1 500.3030896 MHz
NUC1 1H
P1 22.00 usec
PLW1 7.99830008 W
F2 - Processing parameters
SI 65536
SF 500.3000018 MHz
WDW EM
SSB 0
LB 0.30 Hz
GB 0
PC 1.00
8.0
7.9
7.8
7.7
ppm
1.00
1.00
0.99
1.96
3.07
3.05
ppm

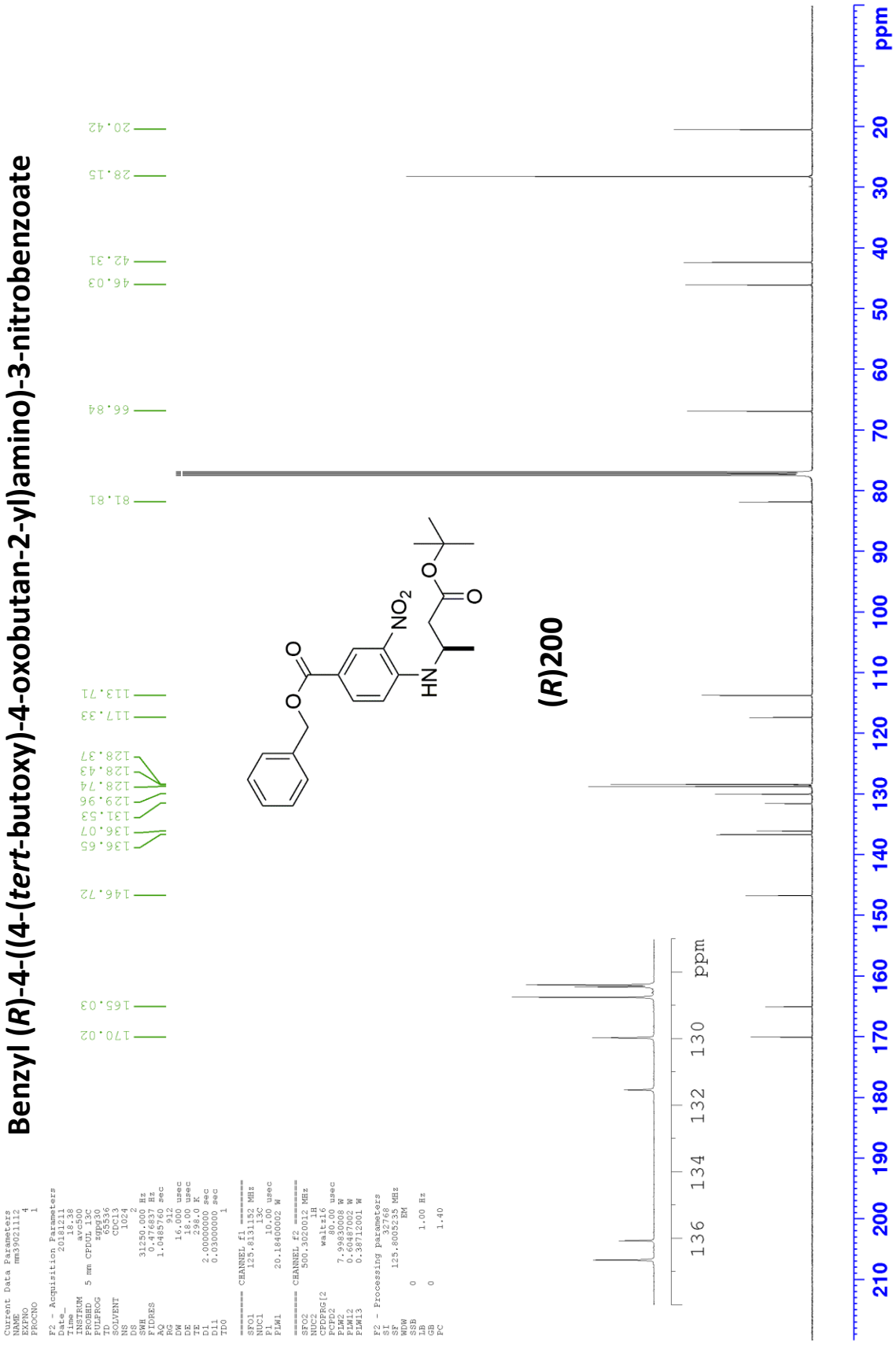

1-Methyl-3-(1-methyl-1H-pyrazol-4-yl)-1H-indazole-5-carboxylic acid
189
167.59
142.22
138.19
136.46
128.70
126.83
123.34
120.24
113.75
109.78
38.62
35.44
39.2
39.0
ppm
210 200 190 180 170 160 150 140 130 120 110 100 90 80 70 60 50 40 30 20 ppm

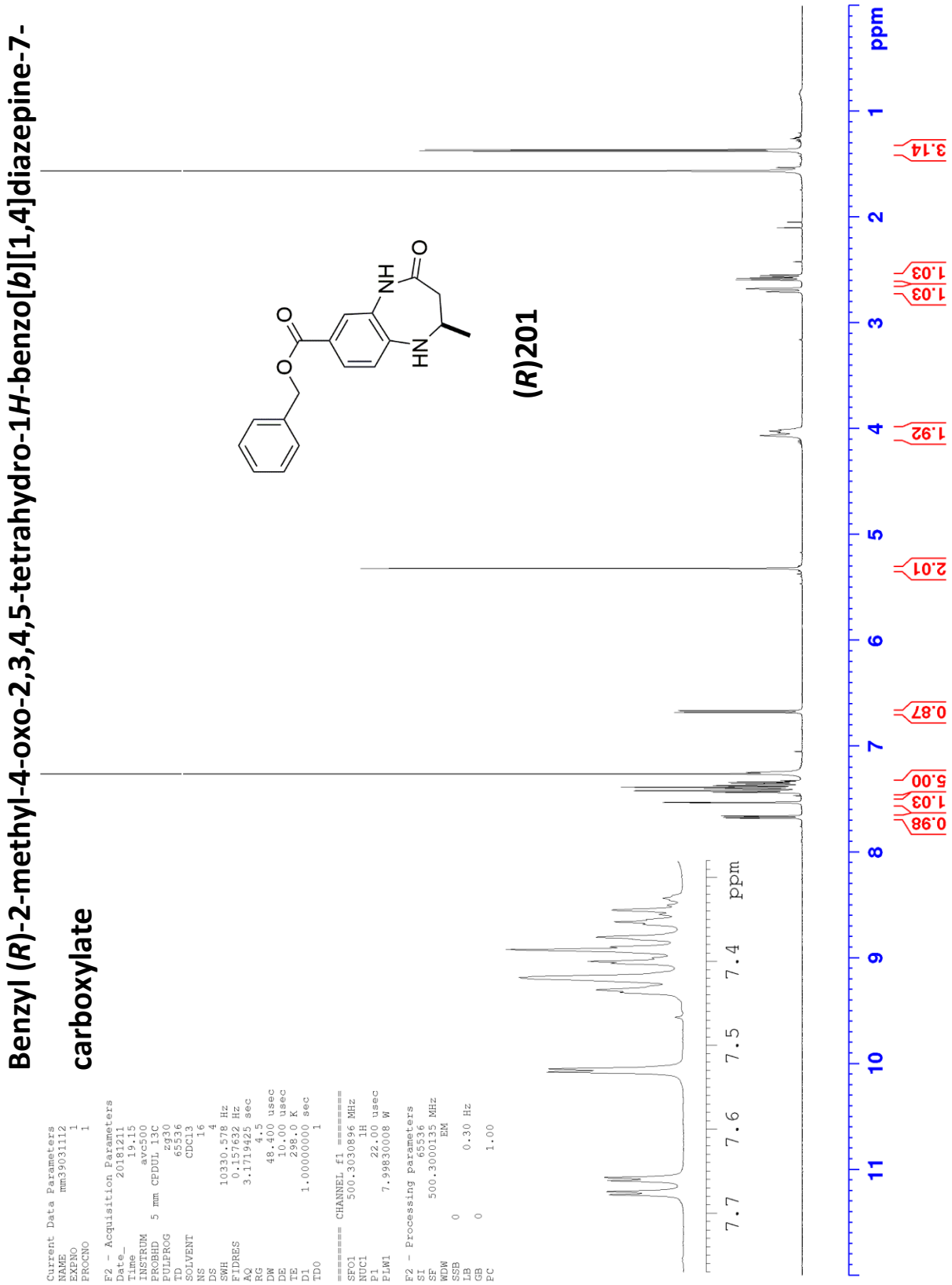

Benzyl 4-fluoro-3-nitrobenzoate
199
Current Data Parameters
NAME mm39011112
EXPNO 1
PROCNO 1
F2 - Acquisition Parameters
Date_ 20181211
Time_ 15.19
INSTRUM avc500
PROBHD 5 mm CPDUL 13C
PULPROG zg30
TD 65536
SOLVENT CDCl3
NS 16
DS 4
SWH 10330.578 Hz
FIDRES 0.157632 Hz
AQ 3.1719425 sec
RG 4
DW 48.400 usec
DE 10.00 usec
TE 298.0 K
D1 1.00000000 sec
TD0 1
======== CHANNEL f1 ========
SFO1 500.3030896 MHz
NUC1 1H
P1 22.00 usec
PLW1 7.99830008 W
F2 - Processing parameters
SI 65536
SF 500.3000132 MHz
WDW EM
SSB 0
LB 0.30 Hz
GB 0
PC 1.00
7.4
ppm
2.17
6.26
1.04
1.00
ppm

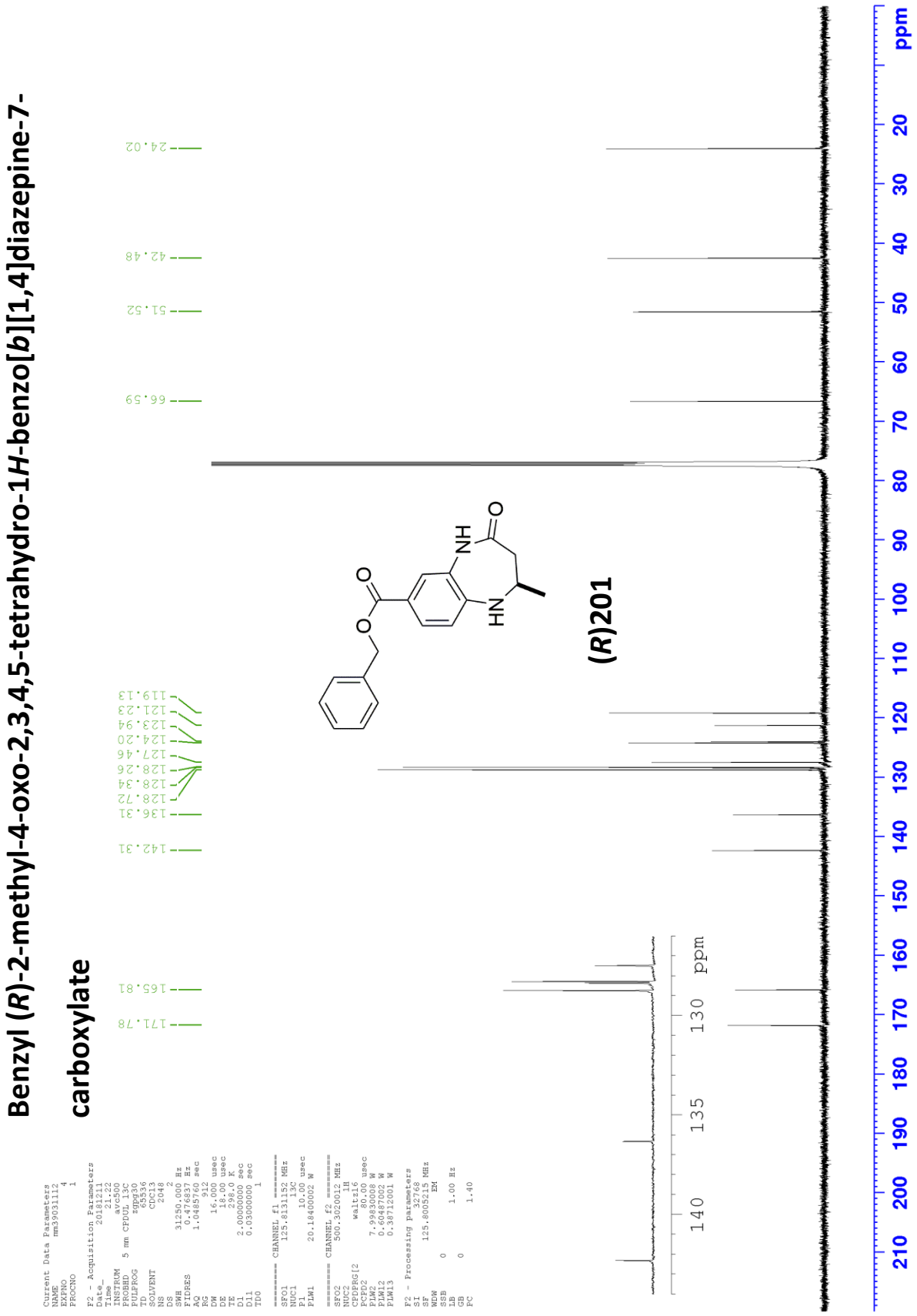

Benzyl 4-fluoro-3-nitrobenzoate
199
NO2
F
O
O
Current Data Parameters
NAME mm39011112
EXPNO 3
PROCNO 1
F2 - Acquisition Parameters
Date_ 20181211
Time 17:17
INSTRUM av500
PROBHD 5 mm CPDUL 13C
PULPROG sgpg30
TD 65536
SOLVENT CDCl3
NS 2048
DS 2
SWH 31250.000 Hz
FIDRES 0.476837 Hz
AQ 1.0485760 sec
RG 912
DW 16.000 usec
DW 18.00 usec
TE 298.0 K
D1 2.00000000 sec
D11 0.03000000 sec
TD0 1
======== CHANNEL f1 ========
SFO1 125.8131152 MHz
NUC1 13C
P1 10.00 usec
PLW1 20.18400002 W
======== CHANNEL f2 ========
SFO2 500.3020012 MHz
NUC2 1H
CPDPRG[2 waltz16
PCPD2 80.00 usec
PLW2 7.99830008 W
PLW12 0.60487002 W
PLW13 0.38712001 W
F2 - Processing parameters
SI 32768
SF 125.8005206 MHz
WDW EM
SSB 0
LB 1.00 Hz
GB 0
PC 1.40
163.61
159.33
157.17
136.80
136.72
135.21
128.91
128.88
128.68
128.06
128.05
127.43
127.40
119.01
118.84
67.93
129
128
ppm
210 200 190 180 170 160 150 140 130 120 110 100 90 80 70 60 50 40 30 20 ppm

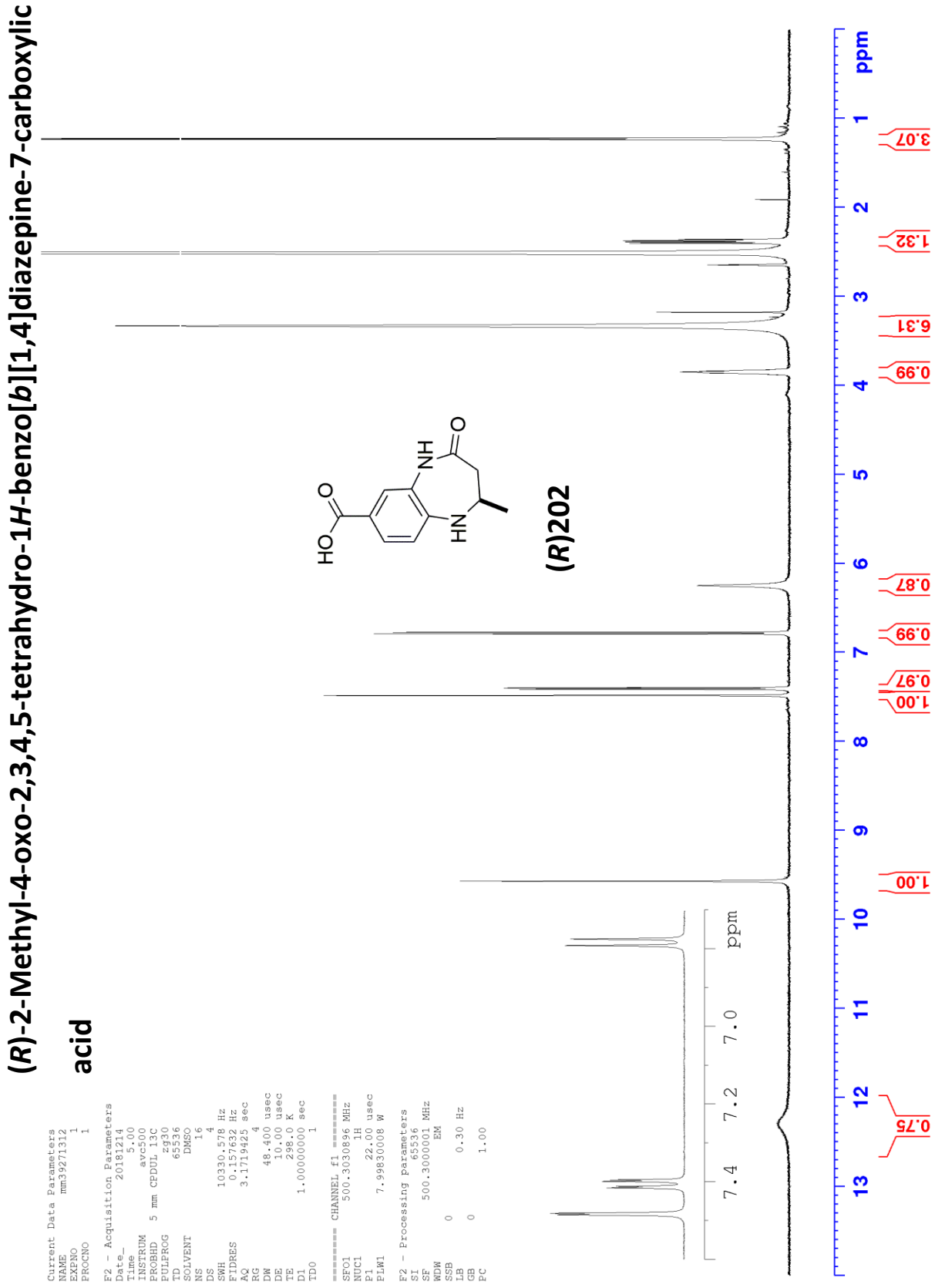

Benzyl 4-fluoro-3-nitrobenzoate
199
Current Data Parameters
NAME Nov27-2018-14-
EXPNO 2
PROCNO 1
F2 - Acquisition Parameters
Date_ 20181127
Time_ 17.35 h
INSTRUM avg400
PROBHD Z108618_0816 (
PULPROG zgflqn
TD 261912
SOLVENT CDCl3
NS 16
DS 4
SWH 131578.953 Hz
FIDRES 1.004757 Hz
AQ 0.9952656 sec
RG 206.87
DW 3.800 usec
DE 6.50 usec
TE 296.7 K
D1 2.00000000 sec
TD0 1
SFO1 376.5359897 MHz
NUC1 19F
P1 15.00 usec
PLW1 20.00000000 W
F2 - Processing parameters
SI 131072
SF 376.5642320 MHz
WDW EM
SSB 0
LB 0.50 Hz
GB 0
PC 1.00
-110.30
-110.31
-110.32
-110.33
-110.34
-110.35
-110.36
-110.2
-110.4
ppm
50
0
-50
-100
-150
-200
ppm


Benzyl (R)-4-((4-(tert-butoxy)-4-oxobutan-2-yl)amino)-3-nitrobenzoate
(R)200
Current Data Parameters
NAME mm39021112
EXPNO 1
PROCNO 1
F2 - Acquisition Parameters
Date_ 20181211
Time 17:23
INSTRUM avc500
PROBHD 5 mm CPDUL 13C
PULPROG zg30
TD 65536
SOLVENT CDCl3
NS 16
DS 4
SWH 10330.578 Hz
FIDRES 0.157632 Hz
AQ 3.17719425 sec
RG 4
DW 48.400 usec
DE 10.00 usec
TE 298.0 K
D1 1.00000000 sec
TD0 1
======== CHANNEL f1 ========
SFO1 500.3030896 MHz
NUC1 1H
P1 22.00 usec
PLW1 7.99830008 W
F2 - Processing parameters
SI 65536
SF 500.3000136 MHz
WDW EM
SSB 0
LB 0.30 Hz
GB 0
PC 1.00
NO2
HN
O
ppm
7.4
2.6
2.5
1.00
0.97
1.06
5.20
1.09
1.07
2.15
1.08
1.06
9.55
3.38


Benzyl (R)-4-((4-(tert-butoxy)-4-oxobutan-2-yl)amino)-3-nitrobenzoate
(R)200
Current Data Parameters
NAME mm390211112
EXPNO 4
PROCNO 1
F2 - Acquisition Parameters
Date_ 20181211
Time 16:38
INSTRUM av600
PROBHD 5 mm CPDUL 13C
PULPROG zgpg30
TD 65536
SOLVENT CDCl3
NS 1024
DS 2
SWH 31250.000 Hz
FIDRES 0.476837 Hz
AQ 1.0485760 sec
RG 812
DW 16.000 usec
DE 18.00 usec
TE 298.0 K
D1 2.00000000 sec
D11 0.03000000 sec
TD0 1
CHANNEL f1
SFO1 125.8131152 MHz
NUC1 13C
P1 10.00 usec
PLW1 20.18400002 W
CHANNEL f2
SFO2 500.3020012 MHz
NUC2 1H
CPDPRG[2 waltz16
PCPD2 80.00 usec
PLW2 7.99830008 W
PLW12 0.60487002 W
PLW13 0.38712001 W
F2 - Processing parameters
SI 32768
SF 125.8005235 MHz
WDW EM
SSB 0
LB 1.00 Hz
GB 0
PC 1.40
170.02
165.03
146.72
136.65
136.07
131.53
129.96
128.74
128.43
128.37
117.33
113.71
81.81
66.84
46.03
42.31
28.15
20.42
O
O
NO2
HN
O
O
136 134 132 130 ppm
210 200 190 180 170 160 150 140 130 120 110 100 90 80 70 60 50 40 30 20 ppm

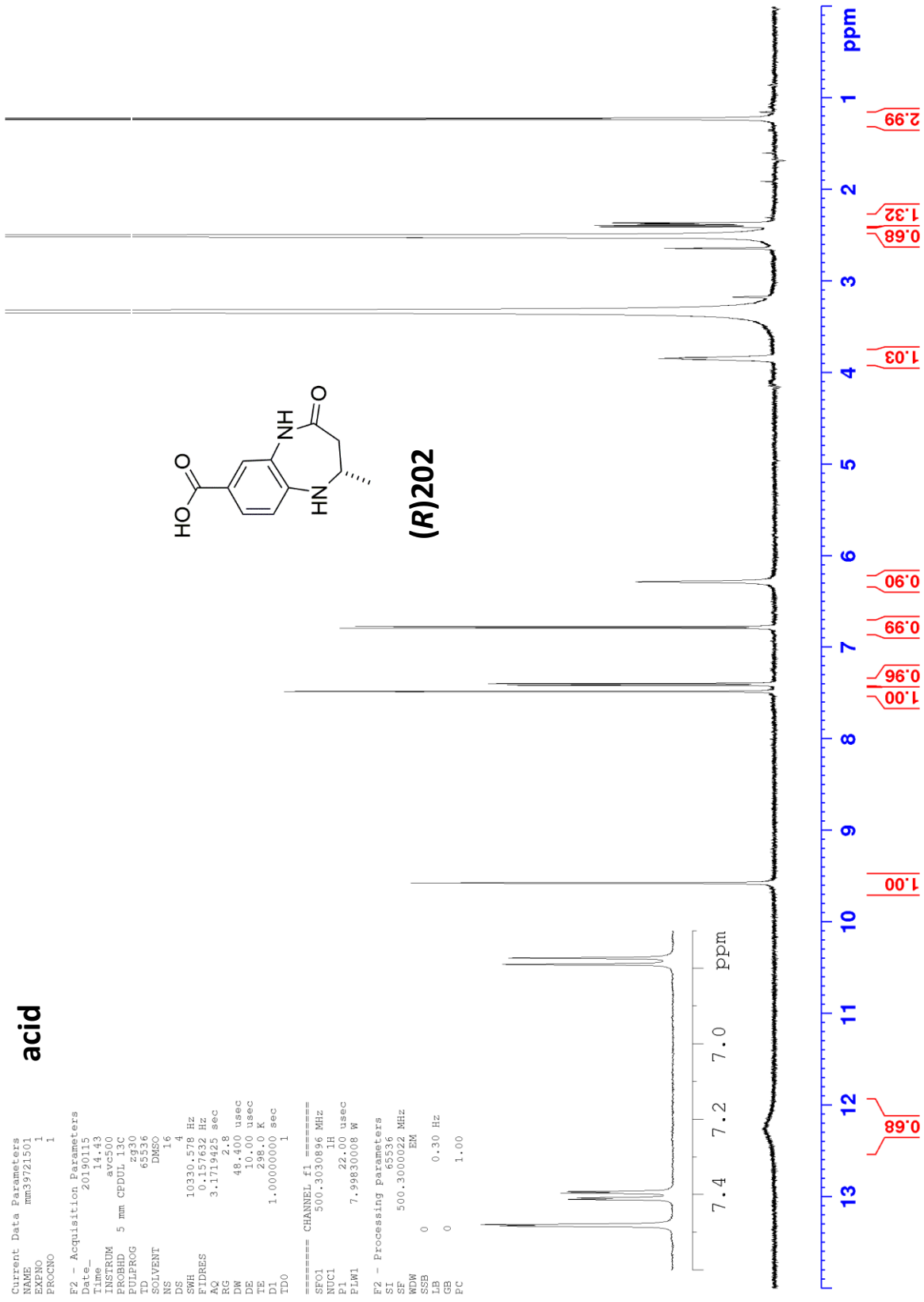

Benzyl (R)-2-methyl-4-oxo-2,3,4,5-tetrahydro-1H-benzo[b][1,4]diazepine-7-carboxylate
(R)201
Current Data Parameters
NAME mm3903112
EXPNO 1
PROCNO 1
F2 - Acquisition Parameters
Date_ 20181211
Time 19.15
INSTRUM avc500
PROBHD 5 mm CPDUL 13C
PULPROG zg30
TD 65536
SOLVENT CDCl3
NS 16
DS 4
SWH 10330.578 Hz
FIDRES 0.157632 Hz
AQ 3.1719425 sec
RG 4.5
DW 48.400 usec
DE 10.00 usec
TE 298.0 K
D1 1.00000000 sec
TD0 1
======== CHANNEL f1 ========
SFO1 500.3030896 MHz
NUC1 1H
P1 22.00 usec
PLW1 7.99830008 W
F2 - Processing parameters
SI 65536
SF 500.3000135 MHz
WDW EM
SSB 0
LB 0.30 Hz
GB 0
PC 1.00
7.7
7.6
7.5
7.4
ppm
11
10
9
8
7
6
5
4
3
2
1
ppm
0.98
1.03
5.00
0.87
2.01
1.92
1.03
1.03
3.14


Benzyl (R)-2-methyl-4-oxo-2,3,4,5-tetrahydro-1H-benzo[b][1,4]diazepine-7-carboxylate
(R)201
Current Data Parameters
NAME nm39031112
EXPNO 4
PROCNO 1
F2 - Acquisition Parameters
Date_ 20181211
Time 21.22
INSTRUM av500
PROBHD 5 mm CPDUL 13C
PULPROG zgpg30
TD 65536
SOLVENT CDCl3
NS 2048
DS 4
SWH 31250.000 Hz
FIDRES 0.476837 Hz
AQ 1.0485760 sec
RG 202
DW 16.000 usec
DE 18.00 usec
TE 298.0 K
D1 2.00000000 sec
D11 0.03000000 sec
TD0 1
SFO1 125.8131152 MHz
NUC1 13C
P1 10.00 usec
PLW1 20.18400002 W
SFO2 500.3020012 MHz
NUC2 1H
CPDPRG[2 waltz16
PCPD2 80.00 usec
PLW2 7.99830008 W
PLW12 0.60487002 W
PLW13 0.38712001 W
F2 - Processing parameters
SI 32768
SF 125.8005215 MHz
WDW EM
SSB 0
LB 1.00 Hz
GB 0
PC 1.40
171.78
165.81
142.31
136.31
128.72
128.34
128.26
127.46
124.20
123.94
121.23
119.13
66.59
51.52
42.48
24.02
140
135
130
ppm
210 200 190 180 170 160 150 140 130 120 110 100 90 80 70 60 50 40 30 20 ppm


(R)-2-Methyl-4-oxo-2,3,4,5-tetrahydro-1H-benzo[b][1,4]diazepine-7-carboxylic acid
(R)202
Current Data Parameters
NAME mm39271312
EXPNO 1
PROCNO 1
F2 - Acquisition Parameters
Date_ 20181214
Time 5.00
INSTRUM avc500
PROBHD 5 mm CPDUL 13C
PULPROG zg30
TD 65536
SOLVENT DMSO
NS 16
DS 4
SWH 10330.578 Hz
FIDRES 0.157632 Hz
AQ 3.1719425 sec
RG 4
DW 48.400 usec
DE 10.00 usec
TE 298.0 K
D1 1.00000000 sec
TD0 1
======== CHANNEL f1 ========
SFO1 500.3030896 MHz
NUC1 1H
P1 22.00 usec
PLW1 7.99830008 W
F2 - Processing parameters
SI 65536
SF 500.3000001 MHz
WDW EM
SSB 0
LB 0.30 Hz
GB 0
PC 1.00
7.4
7.2
7.0
ppm
1.00
0.75
1.32
6.31
0.99
0.87
0.99
0.97
1.00
3.07

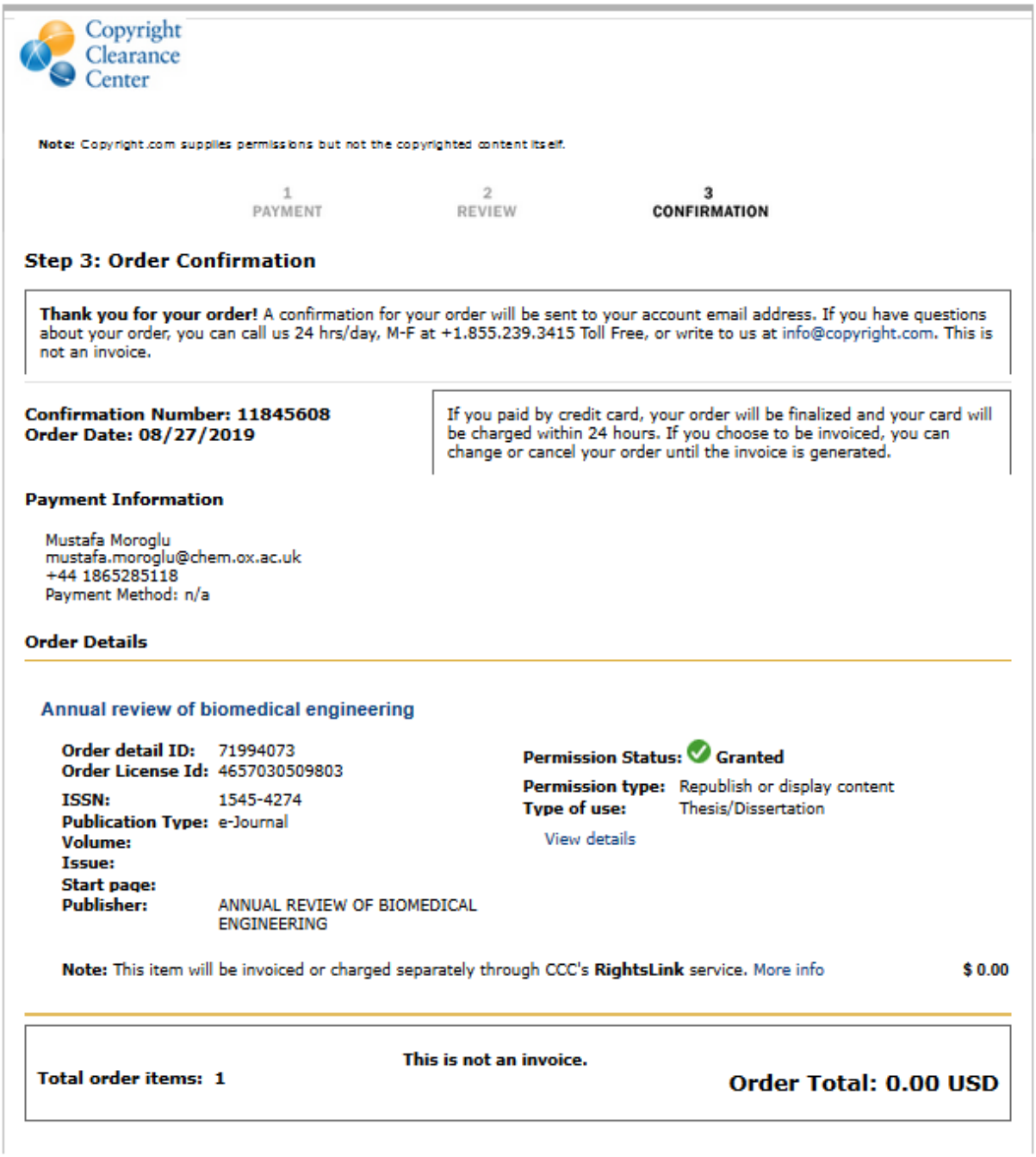

(R)-2-Methyl-4-oxo-2,3,4,5-tetrahydro-1H-benzo[b][1,4]diazepine-7-carboxylic acid
(R)202
Current Data Parameters
NAME mm392713l2_2
EXPNO 4
PROCNO 1
F2 - Acquisition Parameters
Date_ 20181214
Time 14.30
INSTRUM av500
PROBHD 5 mm CPDUL 13C
PULPROG zgpg30
TD 65536
SOLVENT DMSO
NS 3072
DS 2
SWH 31250.000 Hz
FIDRES 0.476837 Hz
AQ 1.0485760 sec
RG 912
DW 16.000 usec
DE 18.00 usec
TE 298.0 K
D1 2.00000000 sec
D11 0.03000000 sec
TD0 1
SFO1 125.8131152 MHz
NUC1 13C
P1 10.00 usec
PLW1 20.18400002 W
SFO2 500.3020012 MHz
NUC2 1H
CPDPRG[2 waltz16
PCPD2 80.00 usec
PLW2 7.99830008 W
PLW12 0.60487002 W
PLW13 0.38712001 W
F2 - Processing parameters
SI 32768
SF 125.7993397 MHz
WDW EM
SSB 0
LB 1.00 Hz
GB 0
PC 1.40
181.13
177.11
152.94
135.82
134.04
133.75
128.08
60.53
52.57
33.34
136 134 132 130 ppm
210 200 190 180 170 160 150 140 130 120 110 100 90 80 70 60 50 40 30 20 ppm

(*S*)-2-Methyl-4-oxo-2,3,4,5-tetrahydro-1*H*-benzo[*b*][1,4]diazepine-7-carboxylic acid



H Permissions for reprinted/adapted figures

Figure 1.1 *Overview of chromosome structure and post-translational modifications.*



Copyright Clearance Center

Note: Copyright.com supplies permissions but not the copyrighted content itself.

1 PAYMENT 2 REVIEW 3 CONFIRMATION

Step 3: Order Confirmation

Thank you for your order! A confirmation for your order will be sent to your account email address. If you have questions about your order, you can call us 24 hrs/day, M-F at +1.855.239.3415 Toll Free, or write to us at info@copyright.com. This is not an invoice.

Confirmation Number: 11845608
Order Date: 08/27/2019

If you paid by credit card, your order will be finalized and your card will be charged within 24 hours. If you choose to be invoiced, you can change or cancel your order until the invoice is generated.

Payment Information

Mustafa Moroglu
mustafa.moroglu@chem.ox.ac.uk
+44 1865285118
Payment Method: n/a

Order Details

Annual review of biomedical engineering

Order detail ID: 71994073
Order License Id: 4657030509803
ISSN: 1545-4274
Publication Type: e-Journal
Volume:
Issue:
Start page:
Publisher: ANNUAL REVIEW OF BIOMEDICAL ENGINEERING

Permission Status: Granted
Permission type: Republish or display content
Type of use: Thesis/Dissertation
View details

Note: This item will be invoiced or charged separately through CCC's **RightsLink** service. More info **$ 0.00**

Total order items: 1

This is not an invoice.

Order Total: 0.00 USD

Figure 1.3 *Structure-based phylogenetic tree of the human bromodomain family.*

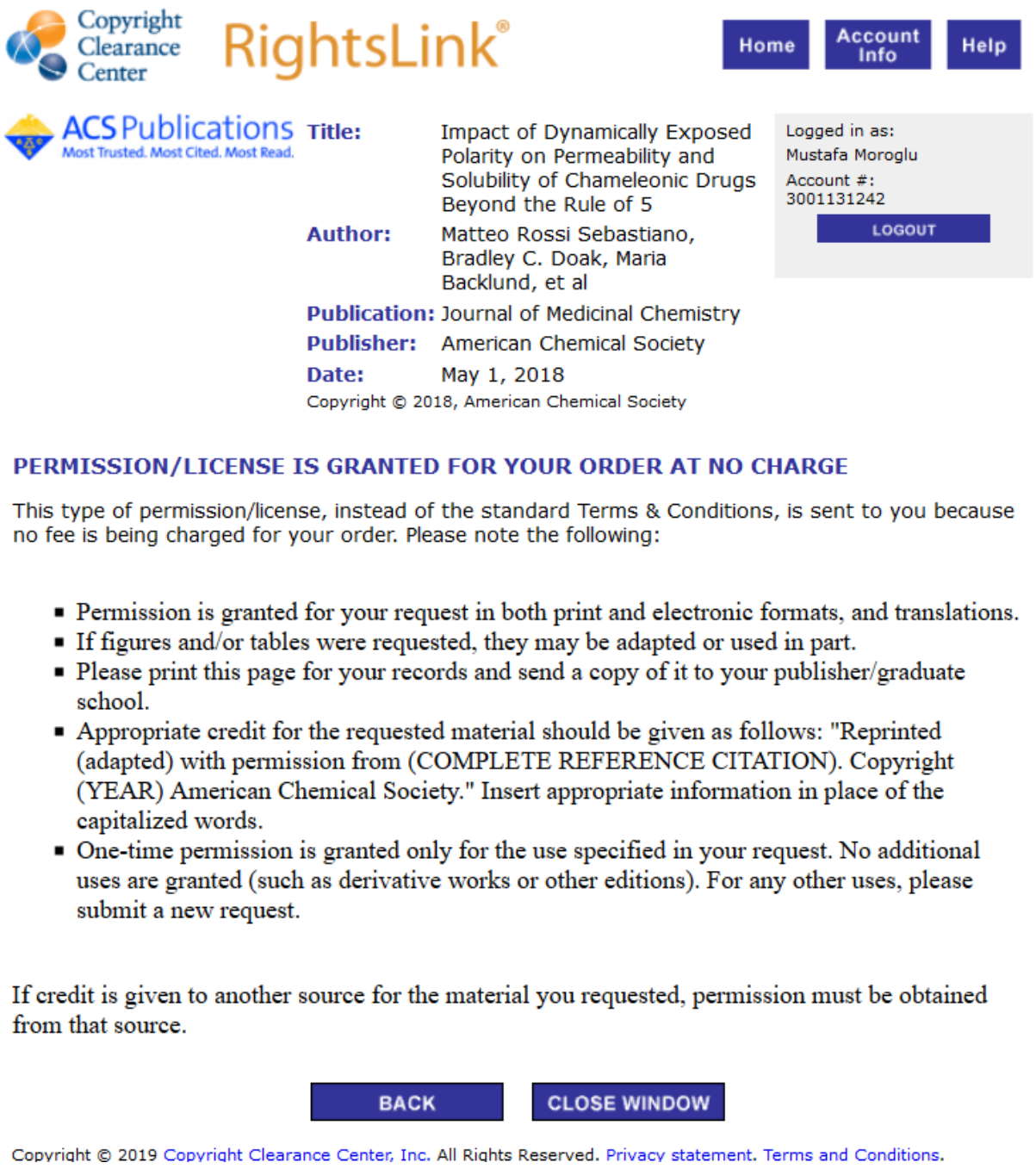
SPRINGER NATURE LICENSE
TERMS AND CONDITIONS

Aug 28, 2019

This Agreement between Mustafa Moroglu ("You") and Springer Nature ("Springer Nature") consists of your license details and the terms and conditions provided by Springer Nature and Copyright Clearance Center.

License Number	4657571384840
License date	Aug 28, 2019
Licensed Content Publisher	Springer Nature
Licensed Content Publication	Nature Reviews Molecular Cell Biology
Licensed Content Title	Functions of bromodomain-containing proteins and their roles in homeostasis and cancer
Licensed Content Author	Takao Fujisawa, Panagis Filippakopoulos
Licensed Content Date	Jan 5, 2017
Licensed Content Volume	18
Licensed Content Issue	4
Type of Use	Thesis/Dissertation
Requestor type	academic/university or research institute
Format	print and electronic
Portion	figures/tables/illustrations
Number of figures/tables /illustrations	1
High-res required	no
Will you be translating?	no
Circulation/distribution	<501
Author of this Springer Nature content	no
Title	Development of small molecule CREBBP bromodomain ligands using medicinal chemistry-based approaches
Institution name	University of Oxford
Expected presentation date	Oct 2019
Portions	Figure 1.2
Requestor Location	Mustafa Moroglu Chemistry Research Laboratory 12 Mansfield Road Oxford, OX1 3TA United Kingdom Attn: Mustafa Moroglu
Total	0.00 GBP

Figure 1.15 *Conformational changes in telithromycin in crystal structures that display minimum (PDB: 1YIJ) and maximum (PDB: 1P9X) solvent accessible 3D PSA.*



Copyright Clearance Center RightsLink®

Home | Account Info | Help

ACS Publications Most Trusted. Most Cited. Most Read.

Logged in as: Mustafa Moroglu
Account #: 3001131242
LOGOUT

Title: Impact of Dynamically Exposed Polarity on Permeability and Solubility of Chameleonic Drugs Beyond the Rule of 5

Author: Matteo Rossi Sebastiano, Bradley C. Doak, Maria Backlund, et al

Publication: Journal of Medicinal Chemistry

Publisher: American Chemical Society

Date: May 1, 2018

Copyright © 2018, American Chemical Society

PERMISSION/LICENSE IS GRANTED FOR YOUR ORDER AT NO CHARGE

This type of permission/license, instead of the standard Terms & Conditions, is sent to you because no fee is being charged for your order. Please note the following:

- Permission is granted for your request in both print and electronic formats, and translations.
- If figures and/or tables were requested, they may be adapted or used in part.
- Please print this page for your records and send a copy of it to your publisher/graduate school.
- Appropriate credit for the requested material should be given as follows: "Reprinted (adapted) with permission from (COMPLETE REFERENCE CITATION). Copyright (YEAR) American Chemical Society." Insert appropriate information in place of the capitalized words.
- One-time permission is granted only for the use specified in your request. No additional uses are granted (such as derivative works or other editions). For any other uses, please submit a new request.

If credit is given to another source for the material you requested, permission must be obtained from that source.

BACK | CLOSE WINDOW

Copyright © 2019 Copyright Clearance Center, Inc. All Rights Reserved. Privacy statement. Terms and Conditions.

Figure 1.16 *1D NMR conformation analysis showing relative conformational populations.*

Copyright Clearance Center RightsLink®

Home | Account Info | Help

ACS Publications
Most Trusted. Most Cited. Most Read.

Title: Discovery of Pyrazolo[1,5-a]pyrimidine B-Cell Lymphoma 6 (BCL6) Binders and Optimization to High Affinity Macrocyclic Inhibitors
Author: William McCoull, Roman D. Abrams, Erica Anderson, et al
Publication: Journal of Medicinal Chemistry
Publisher: American Chemical Society
Date: May 1, 2017
Copyright © 2017, American Chemical Society

Logged in as:
Mustafa Moroglu
Account #:
3001131242
LOGOUT

PERMISSION/LICENSE IS GRANTED FOR YOUR ORDER AT NO CHARGE

This type of permission/license, instead of the standard Terms & Conditions, is sent to you because no fee is being charged for your order. Please note the following:

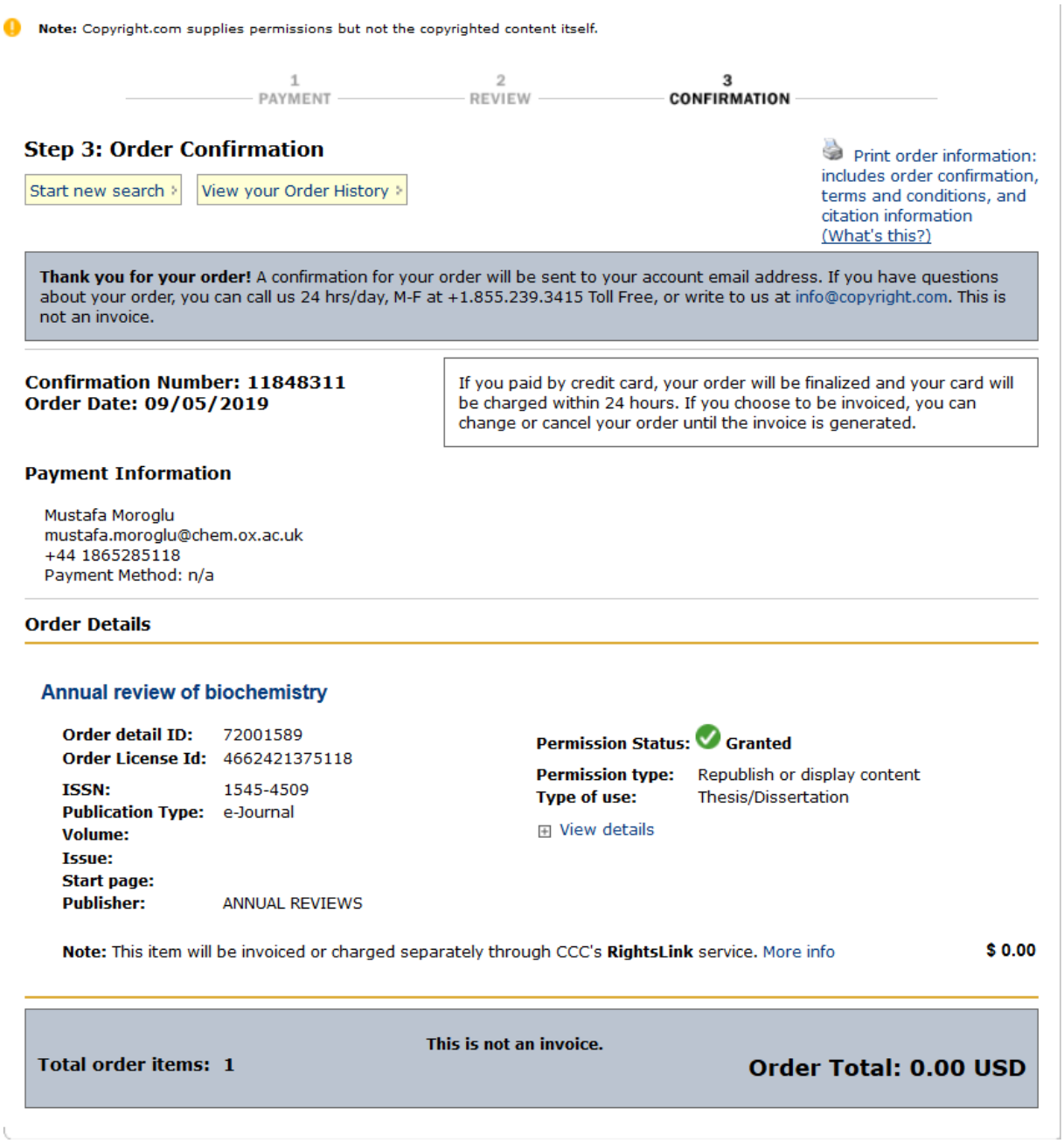
- Permission is granted for your request in both print and electronic formats, and translations.
- If figures and/or tables were requested, they may be adapted or used in part.
- Please print this page for your records and send a copy of it to your publisher/graduate school.
- Appropriate credit for the requested material should be given as follows: "Reprinted (adapted) with permission from (COMPLETE REFERENCE CITATION). Copyright (YEAR) American Chemical Society." Insert appropriate information in place of the capitalized words.
- One-time permission is granted only for the use specified in your request. No additional uses are granted (such as derivative works or other editions). For any other uses, please submit a new request.

If credit is given to another source for the material you requested, permission must be obtained from that source.

BACK | CLOSE WINDOW

Copyright © 2019 Copyright Clearance Center, Inc. All Rights Reserved. Privacy statement. Terms and Conditions.
Comments? We would like to hear from you. E-mail us at customercare@copyright.com

Figure 1.23 *Schematic representation of (A) antibody phage display libraries and DNA-encoded chemical libraries and (B) and screening procedures with DNA-encoded chemical libraries.*



Note: Copyright.com supplies permissions but not the copyrighted content itself.

1 PAYMENT — 2 REVIEW — 3 CONFIRMATION

Step 3: Order Confirmation

Start new search | View your Order History

Print order information: includes order confirmation, terms and conditions, and citation information (What's this?)

Thank you for your order! A confirmation for your order will be sent to your account email address. If you have questions about your order, you can call us 24 hrs/day, M-F at +1.855.239.3415 Toll Free, or write to us at info@copyright.com. This is not an invoice.

Confirmation Number: 11848311
Order Date: 09/05/2019

If you paid by credit card, your order will be finalized and your card will be charged within 24 hours. If you choose to be invoiced, you can change or cancel your order until the invoice is generated.

Payment Information

Mustafa Moroglu
mustafa.moroglu@chem.ox.ac.uk
+44 1865285118
Payment Method: n/a

Order Details

Annual review of biochemistry

Order detail ID:	72001589
Order License Id:	4662421375118
ISSN:	1545-4509
Publication Type:	e-Journal
Volume:	
Issue:	
Start page:	
Publisher:	ANNUAL REVIEWS

Permission Status: Granted
Permission type: Republish or display content
Type of use: Thesis/Dissertation
View details

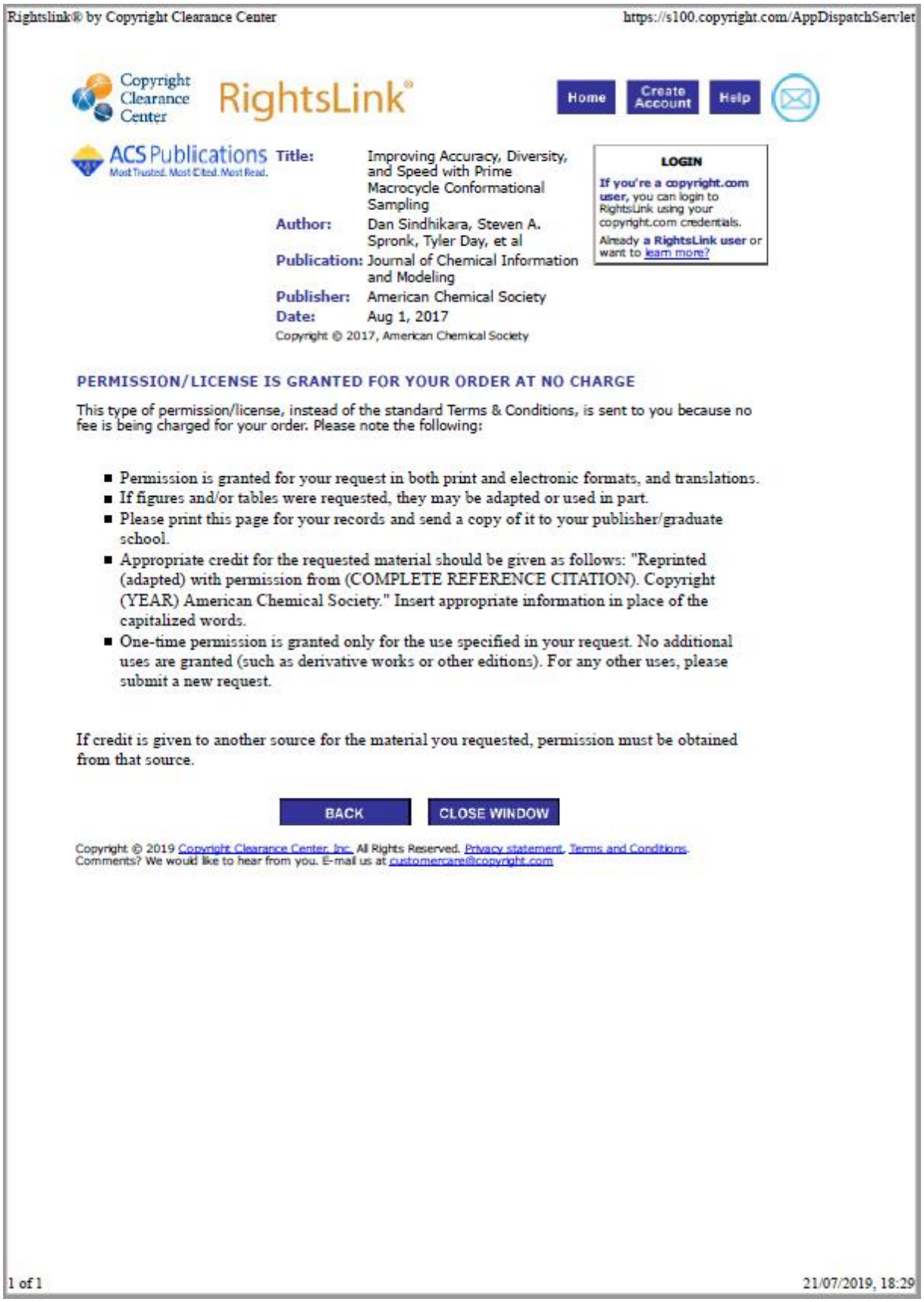
Note: This item will be invoiced or charged separately through CCC's **RightsLink** service. More info **$ 0.00**

Total order items: 1

This is not an invoice.

Order Total: 0.00 USD

Figure 4.3 *Prime MCS workflow summary diagram.*



Rightslink® by Copyright Clearance Center https://s100.copyright.com/AppDispatchServlet

Copyright Clearance Center RightsLink®

Home | Create Account | Help

ACS Publications Most Trusted. Most Cited. Most Read.

Title: Improving Accuracy, Diversity, and Speed with Prime Macrocycle Conformational Sampling
Author: Dan Sindhikara, Steven A. Spronk, Tyler Day, et al
Publication: Journal of Chemical Information and Modeling
Publisher: American Chemical Society
Date: Aug 1, 2017
Copyright © 2017, American Chemical Society

LOGIN
If you're a copyright.com user, you can login to RightsLink using your copyright.com credentials.
Already a RightsLink user or want to learn more?

PERMISSION/LICENSE IS GRANTED FOR YOUR ORDER AT NO CHARGE

This type of permission/license, instead of the standard Terms & Conditions, is sent to you because no fee is being charged for your order. Please note the following:

- Permission is granted for your request in both print and electronic formats, and translations.
- If figures and/or tables were requested, they may be adapted or used in part.
- Please print this page for your records and send a copy of it to your publisher/graduate school.
- Appropriate credit for the requested material should be given as follows: "Reprinted (adapted) with permission from (COMPLETE REFERENCE CITATION). Copyright (YEAR) American Chemical Society." Insert appropriate information in place of the capitalized words.
- One-time permission is granted only for the use specified in your request. No additional uses are granted (such as derivative works or other editions). For any other uses, please submit a new request.

If credit is given to another source for the material you requested, permission must be obtained from that source.

BACK CLOSE WINDOW

Copyright © 2019 Copyright Clearance Center, Inc. All Rights Reserved. Privacy statement. Terms and Conditions.
Comments? We would like to hear from you. E-mail us at customercare@copyright.com

1 of 1 21/07/2019, 18:29